



UNIVERSITAT DE  
BARCELONA

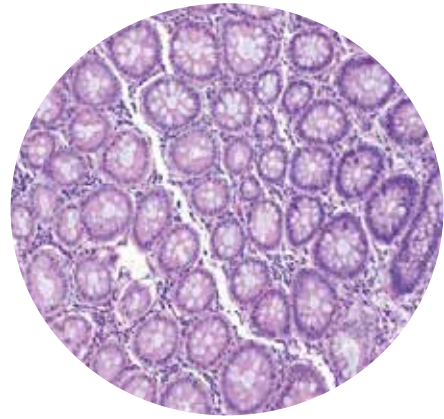
## Study of a custom panel of CXC chemokines in the serum from metastatic CRC patients as predictive and/or prognostic biomarkers

Sara Cabrero de las Heras

**ADVERTIMENT.** La consulta d'aquesta tesi queda condicionada a l'acceptació de les següents condicions d'ús: La difusió d'aquesta tesi per mitjà del servei TDX ([www.tdx.cat](http://www.tdx.cat)) i a través del Dipòsit Digital de la UB ([diposit.ub.edu](http://diposit.ub.edu)) ha estat autoritzada pels titulars dels drets de propietat intel·lectual únicament per a usos privats emmarcats en activitats d'investigació i docència. No s'autoritza la seva reproducció amb finalitats de lucre ni la seva difusió i posada a disposició des d'un lloc aliè al servei TDX ni al Dipòsit Digital de la UB. No s'autoritza la presentació del seu contingut en una finestra o marc aliè a TDX o al Dipòsit Digital de la UB (framing). Aquesta reserva de drets afecta tant al resum de presentació de la tesi com als seus continguts. En la utilització o cita de parts de la tesi és obligat indicar el nom de la persona autora.

**ADVERTENCIA.** La consulta de esta tesis queda condicionada a la aceptación de las siguientes condiciones de uso: La difusión de esta tesis por medio del servicio TDR ([www.tdx.cat](http://www.tdx.cat)) y a través del Repositorio Digital de la UB ([diposit.ub.edu](http://diposit.ub.edu)) ha sido autorizada por los titulares de los derechos de propiedad intelectual únicamente para usos privados enmarcados en actividades de investigación y docencia. No se autoriza su reproducción con finalidades de lucro ni su difusión y puesta a disposición desde un sitio ajeno al servicio TDR o al Repositorio Digital de la UB. No se autoriza la presentación de su contenido en una ventana o marco ajeno a TDR o al Repositorio Digital de la UB (framing). Esta reserva de derechos afecta tanto al resumen de presentación de la tesis como a sus contenidos. En la utilización o cita de partes de la tesis es obligado indicar el nombre de la persona autora.

**WARNING.** On having consulted this thesis you're accepting the following use conditions: Spreading this thesis by the TDX ([www.tdx.cat](http://www.tdx.cat)) service and by the UB Digital Repository ([diposit.ub.edu](http://diposit.ub.edu)) has been authorized by the titular of the intellectual property rights only for private uses placed in investigation and teaching activities. Reproduction with lucrative aims is not authorized nor its spreading and availability from a site foreign to the TDX service or to the UB Digital Repository. Introducing its content in a window or frame foreign to the TDX service or to the UB Digital Repository is not authorized (framing). Those rights affect to the presentation summary of the thesis as well as to its contents. In the using or citation of parts of the thesis it's obliged to indicate the name of the author.



Study of a custom  
panel of CXC  
chemokines in the  
serum from metastatic  
CRC patients as  
predictive and/or  
prognostic biomarkers

**SARA CABRERO DE LAS HERAS**





UNIVERSITAT DE  
BARCELONA

UNIVERSITY OF BARCELONA  
FACULTY OF MEDICINE AND HEALTH SCIENCES  
PHD PROGRAMME IN BIOMEDICINE

# Study of a custom panel of CXC chemokines in the serum from metastatic CRC patients as predictive and/or prognostic biomarkers

**SARA CABRERO DE LAS HERAS**

Resistance, chemotherapy, and predictive biomarkers group  
Germans Trias i Pujol Research Institute

February 2023

Thesis manuscript submitted by Sara Cabrero de las Heras applying  
for PhD expedition from University of Barcelona

A handwritten signature in black ink, appearing to read 'Eva Martínez Balibrea'.

**Dr. Eva Martínez Balibrea**  
Director

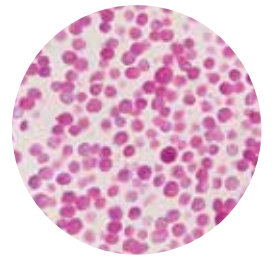
A handwritten signature in black ink, appearing to read 'Francesc Viñals'.

**Dr. Francesc Viñals**  
Tutor

A handwritten signature in black ink, appearing to read 'Sara Cabrero de las Heras'.

**Sara Cabrero de las Heras**  
Author

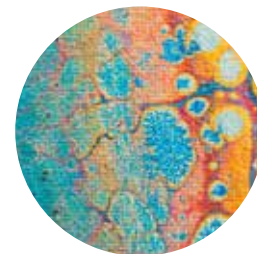




“Yo creo que nada sucede por casualidad,  
¿Sabes? Que, en el fondo, las cosas tienen un  
plan secreto aunque nosotros  
no lo entendamos”

- *La sombra del viento, Carlos Ruiz Zafón*





# Aknowledgments

**En mi humilde opinión, la parte de agradecimientos es esencial, pues una tesis NUNCA es de una sola persona. Por eso no me lo he tomado a la ligera y os he dedicado a todos unas palabras. Ya sabéis que soy (un poco) sensible. Espero que me sintáis cuando leáis lo que os dedico aquí.**

**GRACIAS.**

Me gustaría empezar agradeciéndolo a los **pacientes** y en especial (aunque no tuviese cáncer de colon) a Elena Huelva. Ella, con su actitud y trabajo dedicado a visibilizar una situación que sufren millones de personas, me ha inspirado, acompañado y dado muchas fuerzas a lo largo de esta tesis. Entender que todo este trabajo vale la pena, que no lo haces por ti, si no por los pacientes. Todas esas personitas anónimas que te acompañan día a día... y no nos engañemos, quien sabe si tú o alguien de tu familia en un futuro. La investigación es absolutamente necesaria y aunque poco reconocida, es preciosa. Por todos los pacientes que han aceptado participar en este estudio y que me han permitido llevar a cabo esta tesis. De vosotros surgió mi motivación por continuar en el mundo de la investigación traslacional. Granito a granito, llegarán las mejoras en los tratamientos y si me permitís soñar un poco... quien sabe si la cura (algún día). Hay que pensar a lo grande. Gracias de corazón.

*"Mis ganas ganan" - Elena Huelva*

Mi carrera de biología (en mi Madrid) me llevó a Ámsterdam. Ámsterdam me trajo a Barcelona. Barcelona me trajo al laboratorio de **Eva** y ella, apostando por mi cuando no sabía ni por dónde empezar, me ha guiado y permitido que hoy, tenga esta tesis terminada y, por ende, si todo va bien, sea Doctora.

Retrocediendo en el tiempo hasta 2011-12, no sin cierta morriña, me recuerdo caminando por los pasillos de la facultad de Biología de la Complutense. En las puertas de los despachos de los profesores, no podía evitar fijarme en las placas "**Dr. Carlos Vicente Córdoba**". Ese prefijo, el título de Dr me hacía tenerles aún más respeto, yo solo pensaba, "que gente tan inteligente, trabajadora y dedicada". De entre tantos buenos profesionales que me he cruzado durante todo este camino (doctores y no doctores), hago mención a mi profesor Carlos porque él me enseñó mucho de la ciencia, a entenderla y quererla como es, siempre desde su humildad y gratitud. Gracias Carlos, siempre te voy a recordar.

Como comentaba al inicio, es precisamente de esta gratitud, donde nace este apartado de la tesis. Me parece mentira haber llegado a este punto. Siento que estos cinco años han volado, pero a la vez me han cundido y me han permitido aprender mucho, especialmente de los errores. Para una persona competitiva y persistente como yo, el doctorado ha sido una prueba de fuego. Lleno de intentos, los cuales, la mayoría de las veces no salían bien. Pero ha sido de los fracasos de lo que más he aprendido. Pues me ayudaban a avanzar un poquito cada día y valorar los aciertos y las buenas decisiones con mucho más entusiasmo. Exprimiéndolos lo más posible y aplicando este aprendizaje al trabajo y a la vida. Un doctorado es mucho más que una tesis. Un doctorado es una lección de vida.

Todo este aprendizaje y gratitud, me lleva a todos vosotros, con quienes he compartido mis fracasos y aciertos, mis días buenos y malos, mis audios eternos y videollamadas en pijama, confinamientos, risas, miedos e inseguridades. Todo.

A mi familia. Lo más bonito y grande que tengo. Por acompañarme en esta aventura llamada vida. Por vuestros consejos y dedicación. No he podido estar mejor acompañada. Gracias a todos. En especial a mis **abuelos** (qué SUERTE la mía), a **Mabel y Pablo** (por TANTO), a **Yoli**, Yolanda Cabrero, por tu dedicación en esta tesis, con tu grandísima profesionalidad y tiempo empleado. La Sara creativa nació contigo, Marta y tus padres en Morales, me encanta haber podido aprender de ti una vez más con esta tesis. Mención de honor a mis padres, **papis**, sin vuestra ayuda, apoyo incondicional, confianza y amor, no hubiese llegado ni a primero de la ESO. Soy quien soy, porque me habéis acompañado en mi crecimiento personal y profesional. Vuestro orgullo, es mi orgullo. Os quiero.

A mi chico, **Martí**. Gracias por ser tú. Gracias por quererme y ayudarme a ser un poquito mejor cada día. Por aprender el uno del otro, por tu paciencia y tiempo dedicado a esta tesis. Por ser mi diseñador y artista del Photoshop e InDesign favorito. Porque tú eres mi compañero de vida de elección. Y me hace feliz. Cada día un poquito más. Gracias. Gracias también a tu familia, por ayudarme, animarme y creer en mi desde el principio. Tener lejos a mi familia no es fácil y habéis hecho de domingos tristes, días geniales. Gracias por acompañarme junto a vuestro hijo y hermano, por transmitirme toda vuestra fuerza para terminar esta tesis.

A **Baloo**, el niño peludo de la familia. Gracias por no separarte de mí ni un momento mientras escribía esta tesis. Por obligarme a salir y darme mimitos. Has llegado hace muy poquito y ya no sabemos vivir sin ti. Gracias por tu amor incondicional.

Gracias **Eva**, como he mencionado arriba has sido una gran guía y mentora durante todo ese camino. Gracias por confiar en mí y en mis capacidades para llevar adelante este proyecto. Algo que todos compartimos es que tu despacho siempre tiene la puerta abierta para nosotros, para hablar de ciencia (la mayoría de las veces), pero no siempre. Para mí has sido (y eres) mucho más que una jefa. Gracias por todo.

A todos/as los/as oncólogos/as, enfermeros/as y clínicos/as que han participado en este proyecto. Sin duda ha sido un reto para todos, pero la comunicación siempre ha sido nuestro fuerte. Gracias por haber hecho lo posible para que esto saliera y dedicarle tiempo a la "chica citokinas". Mención especial a Xavi Hernandez y Cristina Bugés. Xavi, no tenías por qué y has aportado muchísimo a nivel clínico a este proyecto. Siempre con la mejor de tus sonrisas. Muchísimas gracias. Cris, mil gracias por toda tu implicación en este proyecto. Gracias por ayudarme con las bases de datos, mirando la información de los pacientes y contestando whatsapps e emails cuando estabas de vacaciones. Gracias.

A mi estadísticas de confianza, **Anna** y **Andrea**. Aunque ha sido en la última etapa.. vaya etapa! Muchas gracias por estar siempre disponibles, vuestras explicaciones y grandísimo trabajo dedicado a esta tesis. Sois las mejores.

A mis **desayunos con amor**, **Crist**, qué hubiese hecho sin ti tantos y tantos días. Qué suerte la mía que acabases en nuestro laboratorio y poder llamarte AMIGA, gracias por quererme (y aguantarme) como soy, por tu apoyo incondicional y también, por tu dedicación a esta tesis de la que hoy estoy tan orgullosa. **Tania**, mi Tania, otra personita más que me llevo para siempre. Esa energía cautivadora y ganas de vivir te hacen única y lo mejor es que se contagia. Eres magia amiga, gracias por acompañarme todo este tiempo y alegrarme la existencia. **Cris M**, tú siempre tan responsable y centrada, me has llevado por la buena vida y aquí me tienes, con una tesis bajo el brazo. Eres muy bonita y especial Cris. Ay como te hemos echado de menos amiga, gracias por estar siempre disponible para ayudarme y acompañarme a por chocolate. **Carmeta**, nuestra niña, el pollito que ha crecido y ahora es toda una científica con una tesis en el horno. Gracias por tu sonrisa y cariño hacia mí siempre. Tu sinceridad y compañía han sido claves para mí en muchos momentos, gracias baby. **Carla**, bienvenida al labo baby. Pese a tus idas y venidas, te has hecho un sitito en nuestro "molt honorable" grupo de desayunos. Eres un amor además de MUY inteligente y válida para este mundo científico. Muchísimas gracias por quedarte conmigo hasta altas horas de la tarde, divagando, llorando de risa y sin duda, produciendo material científico de calidad. Te deseo todo lo mejor en tu aventura PhD, que empieza ahora. Eres mi mejor sucesora. **María**, mi compi de Comité, que fácil es hablar contigo y sentirme apoyada. Ha sido una suerte coincidir en este arduo camino, lo has hecho todo más fácil. Aprovecho tu mención para agradeceros a ti a **Bea** vuestro apoyo a nivel científico. Ha sido un placer discutir y contar con vuestra ayuda. Gracias.

A mi labo, **RCPB-B-ARGO**, gracias a todos por vuestra compañía, apoyo y ayuda en tantos y tantos momentos a lo largo de estos años. Ha sido una SUERTE para mí formar parte de este grupo. Desde que **Vicenç** me enseñó a po-

ner “Abad” hasta hoy han pasado muchas cosas y personas por él. Gracias a todos porque he aprendido mucho con todos. Vicenç, “mi supervisor de máster”, como solía llamarte, contigo me inicié en el mundo de los cultivos celulares y mira hasta donde he llegado. Gracias por toda tu ayuda y tiempo empleado en mí. Me hace especial ilusión mencionar que además de dentro del labo, junto con **Vero** (y **Lucky, Paulita** aún no estaba en este mundo) me ayudasteis mucho. Estar lejos de casa para mí nunca ha sido fácil y vosotros me ofrecisteis la vuestra desde el primer día. Me habéis acompañado en esta aventura y ayudado mucho, gracias. **Sara B**, former member but still a great friend. Thank you VERY MUCH for our discussions and your determination, you have been a great example for me, teaching me many things, especially time management. I have missed your energy and good advice in the lab. But I know you are always there for me, as I am there for you. LovU. **Marta D**, Martoni, mi compi de mesa, voy a echar de menos nuestras conversaciones y confianza. Hemos compartido muchas frustraciones y alegrías. Especialmente lo primero puedo afirmar que ha ayudado a que, en lugar de tirarnos de los pelos, hayamos tenido salud mental. Eres una super mami, doctora por partida doble y mi médico de confianza. Gracias por todo. **Ferrán**, has sido un gran compañero de risas, viajes (Mallorca, esquí y PROCUREs) y en el labo, en especial con el CRISPR ¡Qué hubiese hecho sin ti! Además de un solete de persona serás el siguiente en doctorarte (junto con Carmeta y Marta) y no me extraña porque eres un buen científico. Valdrá la pena, ya verás. **Anna**, la famosa Annete, la “otra” jefa (como nos gusta llamarte). No estabas en el labo y tanto Eva como Crist te mencionaban tanto que casi te conocía, y no me extraña ¡porque vaya tía! Tu sonrisa, energía, siempre animada, con ganas de aprender, y tus preguntas “brillantes” (como yo digo), porque vaya visión tienes... han sido un gran ejemplo y motivación para mí. Espero poder seguir aprendiendo y compartir más momentos con las chicas y contigo. Gracias por todo Anna. Adrià, gracias por estar y ser siempre tan atento. Porque desde tu llegada nos haces la vida en el laboratorio a todos mucho más fácil, con tus conocimientos, experiencia previa y forma de ser aportas MUCHO. Gracias Adrià. **María S**, pese a toda tu carga laboral e ir de un lado a otro, siempre estás pendiente de todos nosotros y nuestros proyectos. Con palabras de ánimo y una sonrisa que dedicarnos. Me encantó compartir el viaje de esquí para así conocernos un poquito más. Gracias por ser así, porque he aprendido mucho de ti y contigo. **Marta C**, eres una pura sangre, tremendamente sincera, única y genial. Ha sido un placer coincidir contigo en esta última etapa en el labo. Gracias por tu energía, tus palabras de ánimo y preocuparte por mí. Lo vas a petar como estudiante del doctorado. ¡Ya verás! Muchos ánimos y cuenta conmigo para lo que necesites. Maria F, ¡Qué personita tan dulce y agradable!. Gracias por dedicarme siempre una sonrisa y tiempo para enviarme un whatsapp y ver como estaba, por tus ánimos y fuerzas. Me quedo con ganas de conocerte un poquito más. Eres un sol.

A mis **IGTP Girls, Vero, Núria, Sara B** ¡Qué suerte la mía! Qué bien me lo pasaba cuando íbamos a comer todas juntas con los chicos y no parábamos de reírnos. Preparando el vídeo de la tesis de Vicenç/Bystrup, tomando cafés, paseando por Barcelona/Badalona, vuestros peques, TODO. Siento que somos las cuatro muy diferentes, pero a la vez coincidimos en muchas cosas. Hemos sabido entendernos y ayudarnos siempre, en muchos momentos, duros y fantásticos. Gracias chicas, espero que esto dure siempre. **Núria**, como diría mi madre, “la mami”, tu personalidad es absolutamente única. No se que pasa con la gente de neurociencias, pero vuestros cerebros privilegiados, pese a ser difíciles de seguir a veces, son absolutamente desternillantes. Me

ha encantado conocerte, escucharte y vivir estos años contigo. He aprendido MUCHO de tu experiencia personal y profesional. Echaré mucho de menos ir por el IGTP mar y verte super concentrada con tus imágenes y WB junto a **Marc**, otra personita estupenda que me llevo de estos años. Estar en el Odyssey y escucharte decir “que taaaalll” ... gracias por ser tú, eres extraordinaria. **Vero**... que decir de “lo nuestro” jajajaja. En muchos momentos te he sentido como a una hermana. Mi tiempo en el labo, ha sido aún más largo que esta tesis y me has cuidado, escuchado, aconsejado, incluso dejado que me equivocase para estar ahí para mí una y MIL veces. Como decía arriba, junto a Vicenç, habéis sido mi casa.

Mis **GTCA**, mis madrileñas/toledanas por excelencia. ¡Y pensar que todo esto empezó con vosotras! Tantas y tantas horas de clase, prácticas, alumnario, PARANINFO, viajes y locuras varias. Sois magia chicas, todas y cada una de vosotras, crecer con vosotras es de lo más bonito que tengo y espero teneros toda mi vida. Pese a la distancia y nuestros compromisos hemos sabido mantenernos en contacto y no solo esto, si no esta amistad tan bonita. Gracias por animarme, por creer en mí, por quererme como soy y por todo vuestro apoyo. Pensar en vosotras me da muchas fuerzas a seguir en el mundillo de la biología. Por seguir acompañándonos y celebrando éxitos y fracasos. Os ADORO.

A mis amigas del alma, **Claudia, Victoria, Carmen y Karla**. Sin duda seréis las madrinas de mis hijos (si es que tengo cuatro). Sois las que mejor me conocéis, las personas que tengo más presente en mi día a día, con mis aciertos y errores. Vosotras me dais la mano cada vez que me caigo y habéis estado a mi lado SIEMPRE. No todo el mundo tiene unas amigas tan fuertes y maravillosas como vosotras de referente. La palabra orgullo se queda corta cuando pienso en vosotras, ¡espero que podamos seguir celebrando la vida! Soy hija única, pero tengo cuatro angelitos en mi camino que se comportan como hermanas. Gracias por no soltarme nunca de la mano, por creer en mí, por admirarnos y respetarnos mutuamente, sois mi familia de elección. **Claudia**, mi tat, esa personita fiel y preciosa que me alegra el corazón y la vida. Desde que nos conocimos en el Santo Ángel, supimos que estábamos hechas la una para la otra. Nuestra conexión es muy especial. Gracias por acompañarme, aguantarme en la distancia, por todos tus buenos consejos, animarme y hacerme sentir única. Siempre práctica, ayudándome a desenredar los líos que voy creando y encontrándome en el camino para no perder de vista lo importante, como mientras escribía la tesis, animándome a pensar en mi futuro, profesional y personal. Te entiendo, y te quiero. **Victoria**, mi opositora, tu vida nunca ha sido fácil y siempre le has plantado cara. Eres toda una luchadora y ejemplo de superación e inspiración para mí. Desde que nos miramos en ese ascensor supimos que íbamos a ser amigas. Por desgracia, siempre ha habido distancia entre nosotras, pero cuando nos vemos, aprovechamos el tiempo juntas como nadie. Gracias por tu apoyo incondicional y fuerza que me han animado la vida y en especial ahora, en la escritura de esta tesis. Te quiero millones. **Carmen**, la persona con más personalidad que conozco. Tan tuya y de los demás que asombra a quien te conoce. Eres un torbellino de alegría y fuerza que acompañan allá donde vas. Gracias por enseñarme a quererme como soy. Gracias por ser tú. Te quiero amigui. **Karli**, mi otra mitad en Barcelona. Quién me iba a decir a mí que esa super valiente recién llegada de Chile me iba a robar el corazón para siempre. La vida me fascina y contigo en ella mucho más. Gracias por ser mi mayor aliada y compañera de aventuras. Mi animadora personal, apoyo, confidente y estilista. Tú sonrisa inunda

cualquier habitación para hacerla más bonita y a mí, me haces ser mejor día a día. Gracias mi Karli, te quiero.

**My Amsterdam people**, I still remember our introduction week, how you all were so determined towards your PhD. I had no clue what that was. Spending that year with you all, taught me a lot, your wisdom, previous experience, and kindness helped me grow (personal and professionally) and open a HUGE window of hope, regarding science, in my life. Our friendship, **Adrienne, Lorena, Inez, Andrea, Ziva...** is great. Long distance relationships are not easy but we manage to keep in touch and stay close. Hopefully, our kids will also learn (not necessary science) and run in this life together. I love you all.

Mi grupi **terraceo**, la terreta y Esparraguera están muy bien representados en este grupo. Yo, llegando tarde al tercer día de clase con mi carpeta de Tous y gabardina, demostré ser un outlier desde el principio, pero me habéis sabido aceptar como nadie. He aprendido, compartido y reído tanto con vosotros... siempre con la cervecita en la mano. Doy gracias a la UPF por ponerme en mi camino y llenarlo de risas, amor, momentos geniales y amistad. Somos una pequeña piña de (buena) gente random que se quiere mucho. Espero que sigamos creciendo juntos amigos. Os quiero.

A mis chicos favoritos, **Fernandito y Joselu**, sois los mejores copilotos que he tenido nunca. Gracias por compartir conmigo vuestro tiempo y espacio personal, alegrando mis mañanas y tardes con vuestras historias, canciones favoritas y cafés/croissants. Compartir es vivir y con vosotros, la vida ha sido mucho más fácil estos años. Gracias, chicos.

A mi **PhD Committee...** ay cuánto he aprendido y crecido con vosotros. Gracias por dejarme formar parte de este equipo y demostrarnos todo lo que podemos hacer juntos. El buen ambiente, calidad humana, buenas ideas, discusiones enriquecedoras, networking y diversión, nunca han faltado en nuestras reuniones. Lo vais a seguir petando babies. Gracias por vuestro apoyo y todo lo que me habéis enseñado. Me lo llevo para siempre.

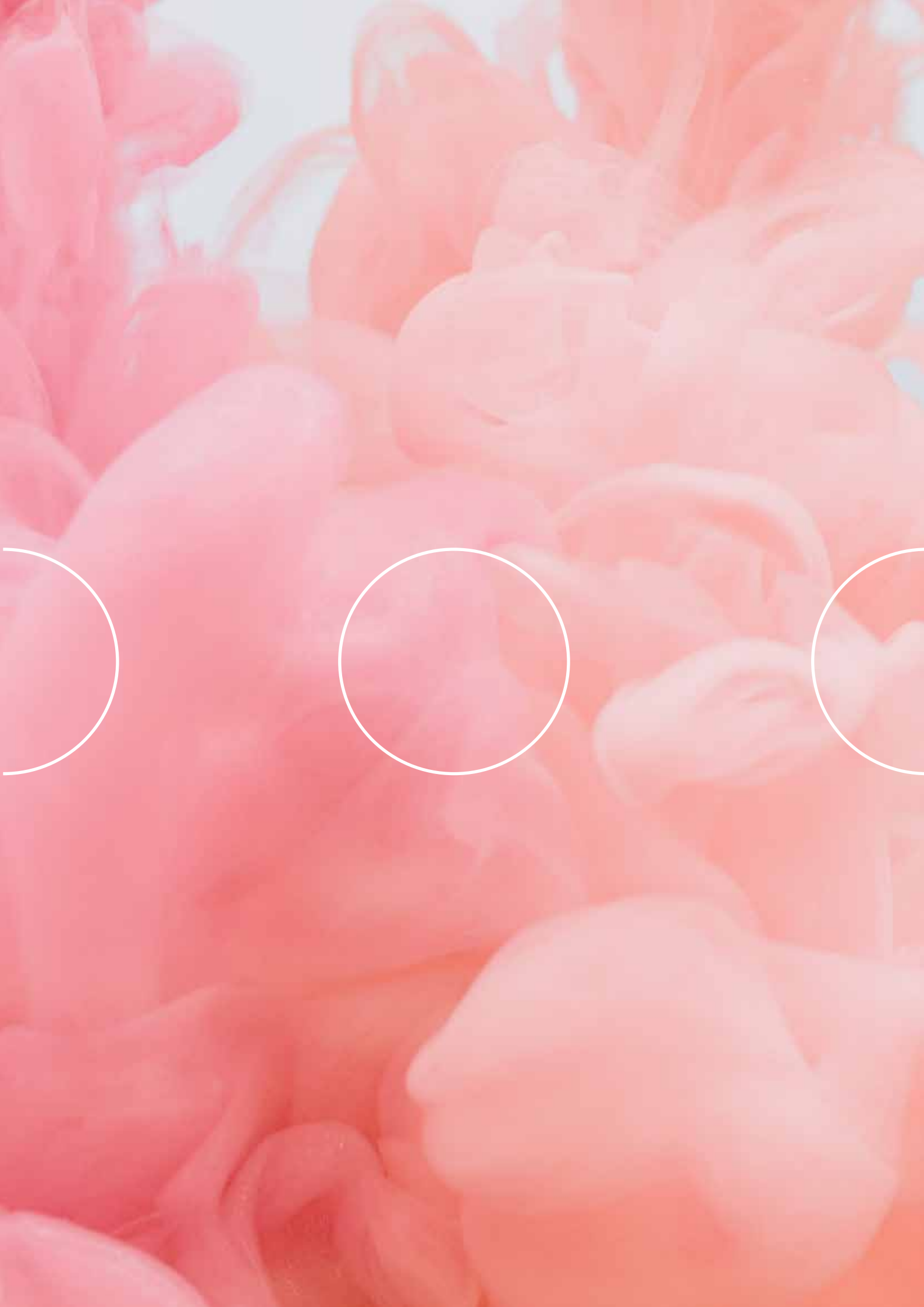
A mi **Zamora** y sus zamoranos, a mi **Madrid** y sus madrileños. No todo el mundo tiene la suerte de considerarse “Zamorana-Madrileña” como me gusta decir a mí. A veces es complicado porque tengo el corazón dividido, pero “qué bonita la vida”. Gracias a ambas ciudades y a mi gente, qué suerte poder tener personitas tan maravillosas en las dos con las que reencontrarme y sentir que vuelvo a casa. La Catedral, la Puerta de Alcalá, Santa Clara y Serrano, escuchar el Merlú o ver la Sierra de Guadarrama y el Pirulí desde la ventana mi habitación, la Bocca di Baco o el Bar Vlazquez... podría continuar indefinidamente, pero ¿Por qué escoger cuando lo tengo todo? Gracias.

Por último, gracias **Barcelona** y a todas y cada una de las personas del **Campus Can Ruti** que me han ayudado de mil formas a lo largo de estos años y no he podido mencionar en esta tesis... son muchas las páginas de agradecimientos, y se me iba de las manos. Ya lo sabía, pero escribir todo esto me ha ayudado aún más a darme cuenta de lo afortunada que soy por haberme rodeado de todos vosotros, personas únicas que me han dado un trocito de su corazón. Prometo cuidároslo bien. Espero que hagáis lo mismo con el mío. Gracias.



“Yo soy de los que piensan como Nobel que la humanidad extraerá más bien que mal de los nuevos descubrimientos”.

*Marie Curie*



# Abbreviations



<b>5-FU</b>	5-Fluorouracil
<b>ABC</b>	ATP-binding cassette
<b>ACS</b>	American Cancer Society
<b>AJCC</b>	American Joint Committee on Cancer
<b>AKT</b>	Protein kinase B
<b>ATCC</b>	American Type Culture Collection
<b>APCs</b>	Antigen-presenting cells
<b>APC</b>	Adenomatous polyposis coli gene
<b>BER</b>	Base excision repair system
<b>BB</b>	Beva Bevacizumab
<b>BV</b>	Brilliant violet
<b>BRAF</b>	v-Raf murine sarcoma viral homolog B
<b>C</b>	Cysteine
<b>CA</b>	Carbohydrate antigen 19-9
<b>CAFs</b>	Cancer-associated fibroblasts
<b>CAPOX</b>	Capecitabine plus OXA
<b>CAR-T</b>	Chimeric antigen Receptor T cells
<b>CCL</b>	CC chemokine ligand
<b>CCR</b>	CC chemokine receptor
<b>cDC1s</b>	Conventional type 1 dendritic cells
<b>CEA</b>	Carcinoembryonic antigen
<b>CIMP</b>	CPG island methylator phenotype
<b>CIN</b>	Chromosomal instability
<b>CMS</b>	Consensus molecular subtype
<b>COVID-19</b>	Coronavirus disease 2019
<b>CpG</b>	Island Cytosine-Guanine dinucleotide group island
<b>CRC</b>	Colorectal Cancer
<b>CRISPR</b>	Clustered regularly interspaced palindromic repeats
<b>CT</b>	Computed tomography
<b>CTCs</b>	Circulating tumor cells
<b>CtDNA</b>	Circulating tumor DNA
<b>CTLA-4</b>	Cytotoxic T-lymphocyte-associated protein 4
<b>CXCL</b>	CXC chemokine ligand
<b>CXCR</b>	CXC chemokine receptor
<b>DCs</b>	Dendritic cells
<b>DFS</b>	Disease-free survival
<b>DNA</b>	Deoxyribonucleic acid
<b>dTMP</b>	Deoxythymidine monophosphate
<b>dUMP</b>	Deoxyuridine monophosphate
<b>EGFR</b>	Epithelial growth factor receptor
<b>ELR</b>	Glutamic-leucine-arginine motif
<b>EMT</b>	Epithelial to mesenchymal transition
<b>FACS</b>	Fluorescent activated cell sorter
<b>FAP</b>	Familial adenomatous polyposis
<b>FDA</b>	Food and drug administration

<b>FDR</b>	False discovery rate
<b>FOBT</b>	Fecal occult-blood testing
<b>FOLFIRI</b>	Leucovorin/5-fluorouracil plus irinotecan
<b>FOLFOX</b>	Leucovorin/5-fluorouracil plus oxaliplatin
<b>FVS</b>	Fixable viability stain
<b>GCO</b>	Global Cancer Observatory
<b>gMDSCs</b>	Granulocytic myeloid-derived suppressor cells
<b>GSEA</b>	Gene set enrichment analysis
<b>GTPase</b>	GTPase guanosine triphosphate hydrolase
<b>HDI</b>	Human development index
<b>HER2</b>	Human epidermal growth factor receptor 2
<b>HR</b>	Hazard ratios
<b>IARC</b>	International Agency for Research on Cancer
<b>ICI</b>	Immune checkpoint inhibitors
<b>IgG</b>	Immunoglobulin G
<b>IHC</b>	Immunohistochemistry
<b>IQR</b>	Interquartile range
<b>IL</b>	Interleukin
<b>ILCs</b>	Innate lymphoid cells
<b>INF</b>	Interferon
<b>KM</b>	Kaplan-Meier
<b>KRAS</b>	Kirsten rat sarcoma virus
<b>LAT</b>	Local ablative treatments
<b>LOH</b>	Loss of heterozygosis
<b>LS</b>	Lynch Syndrome
<b>MAP</b>	MYH-associated polyposis
<b>MAPK</b>	Mitogen-activated protein kinase
<b>mCRC</b>	metastatic CRC
<b>MEK</b>	Mitogen-activated protein kinase
<b>mMDSCs</b>	Monocytic myeloid-derived suppressor cells
<b>MHC-I</b>	Major histocompatibility complex I
<b>MMR</b>	Mismatch repair
<b>MRI</b>	Magnetic resonance imaging
<b>MSS</b>	Microsatellite status stability
<b>MSI</b>	Microsatellite status instability
<b>MSI-H</b>	Highly MSI
<b>NER</b>	Nucleotide excision repair
<b>NF-<math>\kappa</math>B</b>	Nuclear factor kappa light chain enhancer of activated B cells
<b>NIH</b>	National Institutes of Health
<b>NK</b>	Natural killer cells
<b>NKT</b>	Natural killer T cells
<b>NOLBL</b>	Non labeled
<b>NRAS</b>	Neuroblastoma RAS viral oncogene homolog
<b>NSCLC</b>	Non-small cell lung cancer
<b>OS</b>	Overall survival
<b>OXA</b>	Oxaliplatin
<b>PBS</b>	Phosphate buffered serum
<b>PCR</b>	Polymerase chain reaction
<b>PD-1</b>	Programmed cell death protein 1
<b>PD-L1</b>	Programmed death ligands 1
<b>PD-L2</b>	Programmed death ligands 2
<b>pDCs</b>	Plasmacytoid dendritic cells
<b>PE</b>	Phycoerythrin

<b>PFS</b>	Progression-free survival
<b>PI3K</b>	Phosphatidylinositol 3-kinase
<b>PJS</b>	Peutz-Jeghers syndrome
<b>PKB</b>	Protein kinase B
<b>PRC2</b>	Polycomb repressive complex 2
<b>RNA</b>	Ribonucleic acid
<b>RT</b>	Room temperature
<b>SARS-CoV-2</b>	Severe acute respiratory syndrome coronavirus 2
<b>SgRNA</b>	Short guide RNA
<b>SiRNA</b>	Small interfering RNA
<b>SMAD4</b>	Mothers against decapentaplegic homolog 4
<b>STAT3</b>	Signal transducer and activator of transcription 3
<b>STR</b>	Short tandem repeat
<b>TAA</b>	Tumor-associated antigens
<b>TAMs</b>	Tumor-associated macrophages
<b>TCGA</b>	The Cancer Genome Atlas
<b>TCR</b>	T cell receptor
<b>TFH</b>	T follicular helper cells
<b>TGF-<math>\beta</math></b>	Transforming growth factor-beta
<b>TGF<math>\beta</math>R2</b>	Transforming growth factor-beta receptor II
<b>TH</b>	T helper cells
<b>TIBs</b>	Tumor-infiltrating B cells
<b>TLS</b>	Tertiary lymphoid structures
<b>TMA</b>	Tumor microarray
<b>TMB</b>	Tumor mutational burden
<b>TME</b>	Tumor microenvironment
<b>TNF-<math>\alpha</math></b>	Tumor necrosis factor
<b>TP53</b>	Tumor protein P53
<b>Tregs</b>	Treg regulatory T cells
<b>TS</b>	Thymidylate synthase
<b>UICC</b>	International Union for Cancer Control
<b>VEGF</b>	Vascular endothelial growth factor
<b>VEGFR</b>	Vascular endothelial growth factor receptor
<b>WT</b>	Wild type





# Table of contents

## **01 INTRODUCTION / PÁG 23**

---

### **1. Colorectal Cancer / p. 23**

- 1.1. Incidence and Mortality / p. 23
- 1.2. CRC Prognosis / p. 24
- 1.3. Risk Factors / p. 24
- 1.4. CRC Pathophysiology / p. 25
  - 1.4.1. Microsatellite Instability (MSI) / p. 26
  - 1.4.2. Chromosomal Instability (CIN) / p. 27
  - 1.4.3. CPG Island Methylator Phenotype (CIMP) / p. 27
  - 1.4.4. Other Molecular Abnormalities / p. 27
- 1.5. Diagnosis and Staging / p. 28
  - 1.5.1. Screening and detection / p. 28
  - 1.5.2. Tumor Staging / p. 29
  - 1.5.3. Consensus Molecular Subtypes / p. 29
- 1.6. CRC Management / p. 31
  - 1.6.1. Surgery / p. 31
  - 1.6.2. Metastatic Disease Management / p. 32
  - 1.6.3. Types of Treatments / p. 33
  - 1.6.4. Treatment Resistance / p. 36
  - 1.6.5. Prognostic and Predictive Biomarkers in CRC / p. 37

### **2. Cancer and Immunity / p. 38**

- 2.1. Immunoediting: immunosurveillance, equilibrium, escape and the immune contexture / p. 40
- 2.2. Chemokines in Cancer and Immunity / p. 42
  - 2.2.1. Chemokines Structure / p. 42
  - 2.2.2. Chemokines Promoting Pro-tumoral Immunity / p. 43
  - 2.2.3. Chemokines Promoting Anti-tumoral Immunity / p. 46
  - 2.2.4. The CXC family of Chemokines / p. 48
  - 2.2.5. CXC Chemokines and Their Receptors Role in CRC / p. 49
  - 2.2.6. Therapeutic Strategies Targeting CXC Chemokines in Cancer / p. 52

## **02 HYPOTHESIS AND OBJECTIVES / p. 55**

---

## **03 MATERIALS AND METHODS / p. 59**

---

### **1. Study Design, Participating Hospitals, and Inclusion Criteria / p. 59**

### **2. Sample Collection, Processing, and Storage / p. 61**

- 2.1. Serum samples processing / p. 62
- 2.2. Tissue Microarray (TMA) / p. 62

### **3. Immunohistochemistry / p. 63**

### **4. Luminex® Analysis of Serum Samples / p. 64**

### **5. CXCL13 *in silico* Analysis / p. 65**

### **6. Validation Studies / p. 66**

### **7. Statistical Methods / p. 69**

## **04 RESULTS / p. 73**

---

### **Objective 1 / p. 73**

- 1.1. Patients' inclusion and their clinicopathological and molecular characteristics / p. 73
- 1.2. Clinicopathological and molecular characteristics association with outcome / p. 76

### **Objective 2 / p. 79**

- 2.1. CXC chemokines distribution and principal component analysis (PCA) of our CXC Luminex® panel / p. 79
- 2.2. Time-point dynamics of CXC chemokines along the treatment / p. 82
- 2.3. Multidimensional analysis of CXC PRET levels association with clinicopathological and molecular patients' features / p. 87
- 2.4. Association of PRET, EVAR and PROG CXC chemokines levels with patients' clinicopathological and molecular characteristics and with response to treatment / p. 88
- 2.5. CXC chemokines serum levels and their association with OS and PFS / p. 96
  - 2.5.1. CXC chemokines serum levels and their association with OS and PFS in all patients / p. 96
    - 2.5.1.1 Basal CXC levels and their association with OS and PFS / p. 96
    - 2.5.1.2 Dynamic changes of CXC levels between PRET and EVAR samples and their association with OS and PFS / p. 98
  - 2.5.2 CXC chemokines serum levels and their association with OS and PFS in patients who did not undergo radical surgery during the study / p. 103
    - 2.5.2.1 Basal CXC levels and their association with OS and PFS in non-operated patients / p. 103
    - 2.5.2.2. Dynamic changes of CXC levels between PRET and EVAR samples and their association with OS and PFS in non-operated patients / p. 105
- 2.6. Analysis of the specificity and sensitivity of CXCL13 as a prognostic biomarker: ROC Curve / p. 107

**Objective 3 / p. 109**

- 3.1. Study of CD20, CD3 and Vimentin in primary CRC tumors, presence of TLS and their correlation to CXCL13 serum levels / p. 109
- 3.2. CXCL13 *in silico* analysis. Study of CXCL13 gene expression and its correlation with immune-cells infiltration, TLS and survival metastases from CRC patients / p. 112

**Objective 4 / p. 115**

4. Study of CXCL13 serum levels in a healthy controls cohort / p. 115

**Objective 5 / p. 116**

5. Study of serum CXCL13 as a prognostic marker in an independent cohort of mCRC patients / p. 116

**05 DISCUSSION / p. 121**

---

**06 CONCLUSIONS / p. 131**

---

**07 BIBLIOGRAPHY / p. 133**

---

**08 ANNEXES / p. 157**

---

**Annex I:** Review / p. 158

**Annex II:** Newsletter (e.g. November 2019) / p. 173

**Annex III:** Luminex-Biorad user manual / p. 174

**Annex IV:** PRET CXC chemokines serum levels in patients with known immune system alterations vs. patients with non-reported alterations / p. 215

**Annex V:** CXC chemokines distribution at EVAR and PROG time-points / p. 218

**Annex VI:** PRET, EVAR and PROG CXC chemokines serum levels association with response to treatment and patients' clinicopathological and molecular characteristics / p. 222

**Annex VII:** CXC chemokines serum levels at EVAR and PROG time-points association with survival / p. 248

**Annex VIII:** CXC chemokines dynamic changes along PRET-PROG and EVAR-PROG association with survival / p. 265



# Introduction



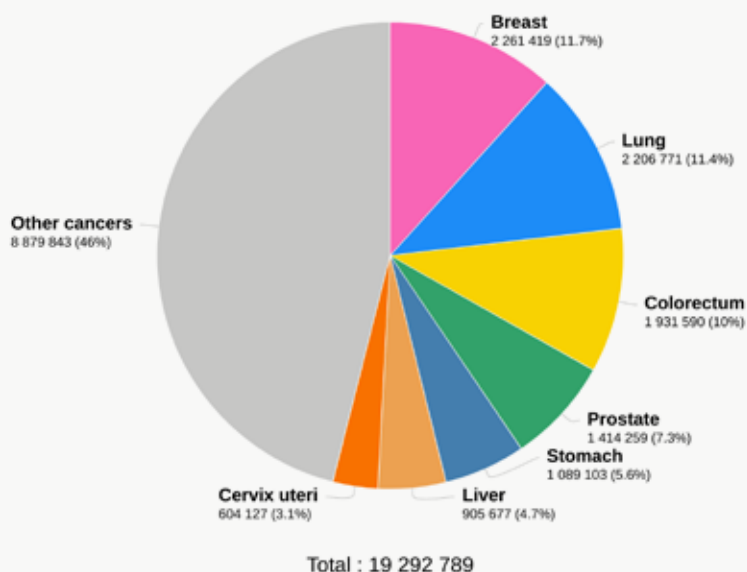
## 1. COLORECTAL CANCER

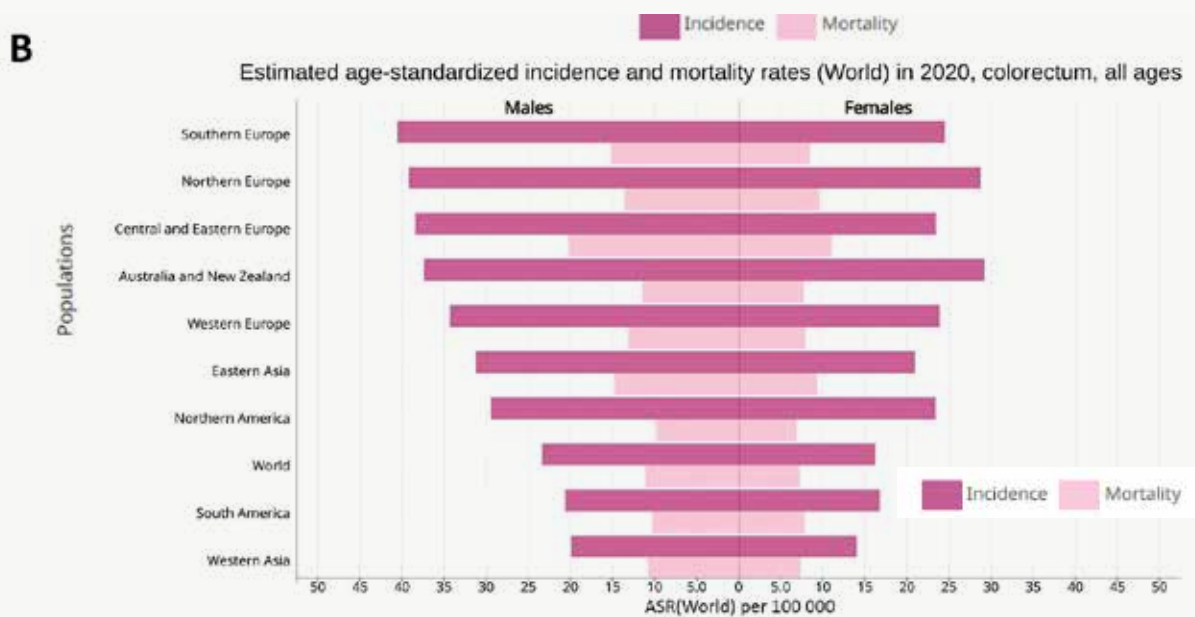
### 1.1. INCIDENCE AND MORTALITY

Colorectal cancer (CRC) is the third most common cancer in both sexes and represents the second cause of cancer-related deaths worldwide, with 935.173 in 2020 (**Figure 1A**). It is the second-and third-most common cancer in women and men, respectively. A total of 864.000 women (9.4% of all new cancer cases) and 1.07 million men (10.6% of new cancer cases) were diagnosed with CRC worldwide. The age-standardized incidence rate (ASR<sub>i</sub>) of CRC is higher in men (23.4 per 100.000 individuals) than in women (16.2 per 100.000) and varies depending on the world region, happening more than half of the cases in the more-developed ones (Europe, Australia, and New Zealand) (**Figure 1B**, in dark pink). Similarly happens with the age-standardized mortality rate (ASR<sub>m</sub>), which is higher in men (20.2 per 100.000) than in women (11.0 per 100.000) and so in more-developed countries (**Figure 1B**, light pink)<sup>1</sup>. These variations are associated with different socioeconomic levels. For instance, CRC mortality which depends on the tumor's stage at the moment of diagnosis is influenced by the level of healthcare in each country, which translates into the availability of population to screening programs<sup>2,3</sup>.

A

Estimated number of new cases in 2020, World, both sexes, all ages





**Figure 1. Incidence and mortality statistics of CRC in 2020. A.** Cancer-related death cases in both sexes worldwide. **B.** Age-standardized incidence and mortality rates of CRC in the world divided by sex. Source<sup>1</sup>.

All these estimates do not consider the possible consequences of severe acute respiratory syndrome coronavirus 2 (SARS-CoV-2), the virus responsible for coronavirus disease 2019 (COVID-19). Even though it remains unclear, reduced access to healthcare systems and delays in diagnosis and associated treatments may have caused a provisional decline in the incidence followed by increases in the diagnosis of advanced-stage and mortality<sup>4,5</sup>.

## 1.2. CRC PROGNOSIS

The American Cancer Society (ACS)<sup>6</sup> official statistics stands that the 5-year overall survival (OS) is approximately 90% for those patients with localized CRC (stage I, IIA, and IIB), 71% for patients with regional cancer (stage IIC and III) and it decreases to 14% for patients with advanced disease (stage IV). Delayed diagnosis is mostly due to the lengthy silent nature of the disease, 90% of cases are diagnosed after symptoms appear, either by colonoscopy (~80%) or emergent surgery (~10%). To mitigate this, the ACS decreased the prescribed age for screening initiation for individuals at average risk from 45 to 50 years in 2018<sup>3</sup>. Early screenings, such as fecal occult blood testing (FOBT), have reduced advanced-stage diagnosis by lowering CRC-related deaths (by 20–30%)<sup>7</sup>. This data highlights the importance of early CRC diagnosis. The earlier the diagnosis the higher the chances to survive CRC.

## 1.3. RISK FACTORS

Risk factors in CRC are known to be genetic and environmental. Most CRCs are sporadic, around 75% of patients do not have any family history and their lifetime risk of developing CRC is 3–5%, increasing with age. The median age at diagnosis is 68 in men and 72 in women<sup>6,7</sup>. However, in patients with a first-degree relative with CRC diagnosed between 50–70 years, the risk rises to 20%<sup>6</sup>. In addition, around 15% of sporadic CRCs are micro-

satellite unstable (MSI), resulting from hypermethylation of the MLH1 promoter<sup>8</sup>. Also, there are predisposing conditions to CRC such as inflammatory bowel disease (ulcerative colitis, Crohn's disease) and cigarette smoke among others.

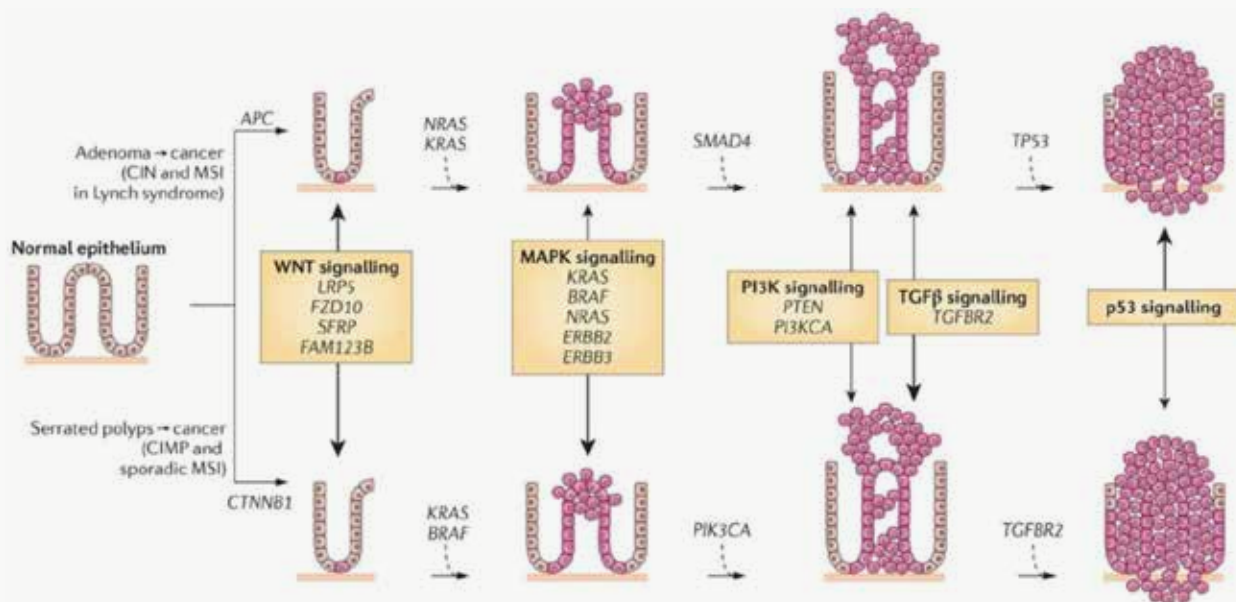
On the other hand, 5–10% of CRC cases arise from hereditary diseases (pre-cancerous conditions) typically classified as Lynch syndrome (LS) (or hereditary nonpolyposis CRC) or polyposis syndromes<sup>7</sup>, in which polyps evolve into carcinogenesis. LS represents 2–4% of CRCs and is characterized by a mutation in one allele of the DNA mismatch repair (MMR) genes, MLH1 and MSH2 (90%), or MSH6 (10%) and PMS2 (rare). Polyposis syndromes classification depends on the predominant type of polyp, adenomatous (familial adenomatous polyposis [FAP]), hamartomatous (Peutz-Jeghers syndrome [PJS]), and serrated. FAP is the second most common hereditary syndrome and represents 1% of all CRCs. Most patients show a big number of adenomas at a young age caused by mutations in the APC gene, strongly related to the Wnt pathway. Even though the way CRC carcinogenesis arises differs among the syndromes, most are caused by a single germline mutation causing genetic instability and therefore a CRC risk<sup>7,8</sup>.

CRC may be considered as a geographic socioeconomic development marker<sup>3</sup>. It has been reported that 16–71% of cases in Europe and the United States are caused by lifestyle factors. Incidence grows uniformly with increasing human development index (HDI), which can be translated into lifestyle factors such as diet<sup>6,7</sup>. Increased intake of red and processed meat, sedentary life together with excess body weight raises CRC risk by an estimated 1.16-fold per 100g increase of daily intake. On the contrary, in some high-incidence countries, CRC prevalence has declined based on a better-quality food intake (milk, fresh fruit, whole grains, vegetables, fiber, and vitamin D among others). Population healthier habits decrease its risk to approximately 10% per daily intake of 10g fiber, 300mg calcium, or 200mL milk together with 30 minutes of daily physical activity<sup>3,6</sup>. The multiple environmental factors related to colorectal carcinogenesis are likely reflected in the CRC heterogeneity, which has favored more in-depth research in the 'molecular pathological epidemiology' field. Based on studying the associations between environmental and genetic factors and tumor molecular characteristics and progression. Also, there are many hypotheses regarding the correlation between colonic microbiota and CRC, which may as well shed some light on the field<sup>6</sup>.

#### **1.4 CRC PATHOPHYSIOLOGY**

CRC malignancy originates from either the colon or the rectum. Since both cancers share many biological and clinical features, they are often combined<sup>9</sup>.

The most frequent CRC form is adenocarcinoma (up to 90% CRC cases), originating in colorectal mucosa epithelial cells. Over 95% of tumoral gland formation is present in well-differentiated adenocarcinomas, whereas only 50–95% in moderately differentiated or <50% in poorly differentiated adenocarcinomas. Being moderately differentiated the most frequent diagnosis (around 70%). In addition, the left colon is more frequently affected than the right colon (5:1)<sup>9</sup>.



**Figure 2. From polyp to CRC.** CRC development sequences described, show how the normal epithelium progresses to CRC together with the molecular and genetic players involved. Both sequences include how an aberrant crypt focus promotes the formation of early and advanced polyps that further progress into early and advanced CRC. The top sequence is the “classic” one, in which tubular adenomas end up in adenocarcinomas. The bottom pathway also called “alternative” affects serrated polyps and their progression to serrated CRC. This represents 15% of sporadic CRC tumors. The model proposed by Fearon and Vogelstein in 1990. Figure from<sup>3</sup>.

It has been demonstrated that CRC develops after the epithelial cells acquire several hallmarks of cancer<sup>10</sup> by accumulating gene mutations and epigenetic alterations, which take over 10-15 years to occur. Typically, CRC develops (**Figure 2**, top scheme) when dysplastic adenomas appear, which are the most common precursor forms of premalignant lesions. Chromosomal instability (CIN) is characterized by APC gene mutations occurring in almost 70% of all non-hereditary CRC adenomas, an early event in this carcinogenesis process resulting in CRC. The adenoma-carcinoma process is promoted by the accumulation of mutations, the activation of oncogenes, and the inactivation of tumor suppressor genes. However, around 15% of sporadic CRCs, are known as serrated polyps and develop from different molecular pathways (**Figure 2**, lower scheme), depending on where they arise, right or left colon. In the right colon, they usually present MSI and CPG island methylator phenotype (CIMP), while in the left colon, the polyps are microsatellite stable (MSS) and carry mutations in Kirsten rat sarcoma virus (KRAS), some also present an attenuated pattern of CIMP<sup>3,11,12</sup>. Therefore, this adenoma-to-carcinoma process can be caused by one or a combination of the main molecular pathways described: MSI, CIN, and CIMP<sup>6,13</sup>. The molecular characteristics of these pathways are used in the clinics for diagnosing and managing CRC patients.

#### 1.4.1 Microsatellite instability (MSI)

Microsatellites are small (1-6 base pairs) DNA-repeating segments in the entire genome (representing around 3% of the human genome). As a result of their repeated structure, they present a high mutation rate, usually repaired by the MMR machinery. When there are deficiencies in the DNA MMR (dMMR) genes (MLH1, MLH3, MSH2, MSH3, MSH6, PMS1, PMS2 and ATPases) it results in a strong mutator phenotype, with broad disparate lengths of microsatellites, known as MSI<sup>14-16</sup>. Fifteen percent of CRC patients harbor MSI tumors, where only 3% associate with LS and the other 12% is mainly caused by

the sporadic hypermethylation of the MLH1 MMR gene promoter; therefore, about 85% of patients are classified as MSS. MSI tumors tend to accumulate driver mutations in other genes, commonly in the transforming growth factor-beta receptor II (TGF- $\beta$ R2) and v-Raf murine sarcoma viral homolog B (BRAF)<sup>14,17</sup>. Regarding MSI CRC tumors, it has been reported that they tend to arise in the proximal colon, present immune infiltration of lymphocytes and are poorly differentiated. These MSI CRC tumors are more frequently diagnosed in stage II and rather uncommon in metastatic tumors, in fact when diagnosed at an early stage, patients present a better prognosis than others without MSI, while when diagnosed at a late stage, the prognosis is poor<sup>18,19</sup>.

#### **1.4.2 Chromosomal instability (CIN)**

60-70% of sporadic CRC cases present CIN, which is characterized by chromosomal number imbalances (aneuploidy) and heterozygosity loss (LOH). Mainly caused by defects in telomere stability together with chromosomal segregation and DNA response damage. Along with these abnormalities, CIN tumors show an accumulation of mutations in specific tumor suppressor genes such as the Tumor protein P53 (TP53), APC, or mothers against decapentaplegic homolog 4 (SMAD4) as well as in oncogenes such as KRAS. Also, the accumulation of mutations in Phosphatidylinositol 3-kinase (PI3K) is known to induce CRC initiation through the activation of critical pathways<sup>13,14</sup>. The CIN CRC model of carcinogenesis proposed by Fearon and Vogelstein in 1990<sup>20</sup> (**Figure 2**, top) is still widely accepted for tumor progression. It describes how the APC gene inactivation results in hyperactivation of the Wnt signaling pathway, a key-initiating event. Likewise, epigenetic changes in  $\beta$ -catenin display the same result. Both cause uncontrolled cell proliferation and differentiation leading to adenoma progression. Further mutations in KRAS, TP53 and others, result in carcinoma development<sup>3,13,14</sup>.

#### **1.4.3 CPG Island methylator phenotype (CIMP)**

One deeply studied epigenetic mechanism that regulates gene expression is DNA methylation. It consists of the covalent addition of a methyl group (CH<sub>3</sub>) to the carbon 5 of the cytosine ring of CpG islands (Cytosine-Guanine dinucleotide group) present in gene promoter regions<sup>21</sup>. Global DNA hypomethylation and localized promoter hypermethylation are common epigenetic events that occur in cancer<sup>14</sup>. 20-30% of all CRCs comprise the CIMP phenotype, it is usually associated with female gender and older age. Mutations in the BRAF V600E gene seem to be an early event in CIMP tumors, which strongly correlate with MLH1 hypermethylation. CIMP represents most MSI-positive/CIN-negative CRCs, where 33% of CIMP-positive tumors exhibit chromosomal abnormalities<sup>13,14,20</sup>. Estimating the methylation status of specific genes may be useful in clinical practice, particularly, of the serrated lesions associated with a CIMP signature, for which diagnostic and pathological interpretation remains challenging. Nevertheless, CIMP tumors are heterogeneous and the value of CIMP genes hypermethylation as prognostic biomarkers remains controversial<sup>21,22</sup>.

#### **1.4.4 Other molecular abnormalities**

Nearly 80% of all CRCs express or overexpress the epithelial growth factor receptor gene (EGFR). Its overexpression is associated with decreased survival and risk of metastases<sup>3</sup>. EGFR is a transmembrane receptor that belongs to a family of four related proteins (EGFR, HER2, HER3 and HER4). After EGF or other ligands bind to a single chain, it forms a dimer and activates a signaling cascade<sup>23</sup>. EGFR signaling involves two main axes. One is the KRAS-RAF-MAPK signaling pathway, where KRAS belongs to the oncogenes family of KRAS, HRAS, and NRAS. When active, it recruits the serine protein BRAF, initiating the cytoplasmic phosphorylation cascade that leads to transcription factors activation. The alternative axis comprises membrane localization of

PI3K, promoting protein kinase B (AKT) activation, which represents a parallel signaling. Both axes are closely related and interconnected, as PI3K can also be activated via RAS proteins<sup>24</sup>. These signaling cascades may result in cancer-cell proliferation, apoptosis blockade, invasion and metastasis, as well as tumor-induced neovascularization<sup>23</sup>. KRAS and BRAF are the most important oncogenes in CRC. It is estimated that KRAS mutations are present in 42% of CRCs, while BRAF mutations are found in around 10% of the cases. Importantly, both mutations are mutually exclusive in CRC<sup>24</sup>. KRAS protein regulates numerous signaling pathways such as PI3K/AKT, mitogen-activated protein kinase (MEK) or extracellular regulated protein kinases (ERK) among others, as a membrane-bound regulatory protein (G protein). It belongs to the GTPase family of proteins, binding guanine nucleotides, functioning through the guanosine diphosphate (GDP)/triphosphate (GTP) binary switch<sup>25</sup>. In CRC, most RAS-activating mutations happen in codons 12, 13, and 61, being G12D, G12V, and G13D the most frequent<sup>17,26</sup>. These mutations in 12 and 13 are known to cause constitutive activation of the GTPase, outbreking possible anti-EGFR effects<sup>27</sup>. BRAF's typical activating mutation is V600E, which consists of a substitution of a central amino acid in the kinase domain. V600E is necessary to keep RAF in the inactive conformation. The human epidermal growth factor receptor 2 (HER2) belongs to the EGFR family of receptors, controlling epithelial cell growth, and its amplification, short variant modulations, or both, are present in approximately 5% of metastatic CRC (mCRC) patients<sup>28</sup>. On the other hand, mutations in tumor suppressor genes are also relevant in CRC. Around 54% of patients have p53 dysfunction<sup>17</sup>. p53 is an essential regulator of DNA damage, apoptosis, proliferation, and stress response, thus, it plays a crucial role in cancer progression. When there are damaged cells during the cell cycle, p53 is the regulator that stops it, avoiding cells from entering apoptosis. If there are mutations in TP53, it does not behave as a tumor suppressor gene but as an oncogene, promoting a more aggressive phenotype<sup>29</sup>. The adenomatous polyposis coli gene (APC) is another important tumor suppressor gene in CRC and its mutations are present in 75% of sporadic CRC patients<sup>17</sup>. APC gene mutation is, as previously mentioned, an early event in CRC. When mutated, there is constitutive activation of the canonical Wnt signaling which causes dysregulation of differentiation, survival, cell proliferation, and apoptosis<sup>30</sup>.

## **1.5. DIAGNOSIS AND STAGING**

### **1.5.1 Screening and detection**

CRC is usually diagnosed after a patient is exhibiting a series of symptoms such as change in bowel habits, diarrhea, constipation, feeling that the bowel does not empty completely or weight loss with no known explanation among others, or after a screening program result, mainly consisting of a colonoscopy or a fecal occult blood test. Colonoscopies are very certain and efficient in determining the location of the tumor or tumors. Other analyses, which are becoming more sensitive and promising, take advantage of the DNA present in epithelial cells, also found in stool samples. It allows the identification of tumor-specific changes, such as mutations in KRAS, APC gene, or other typical CRC mutations. Pathologists are essential in CRC diagnosis. Besides testing MSI, BRAF, and KRAS mutations, the histopathological study is still basic to determine patients' stage, prognostic, and predictive parameters as well as tumor characterization<sup>18</sup>. Lately, circulating tumor mRNA, microRNA, and cytokeratin are under study as potential diagnostic markers. Furthermore, distant metastases diagnosis is an important aspect of mCRC. The most common locations are the liver and lungs, being liver the most frequent one, which explains why liver imaging by computed tomography (CT) is recommended in all CRC patients as well as magnetic resonance imaging (MRI)<sup>3,8,11</sup>. Lately, pathologists are paying special attention to tumor budding. If pre-

sent, it is considered an indicator of an aggressive tumor, closely related to epithelial to mesenchymal transition (EMT) in the tumor microenvironment (TME)<sup>31,32</sup>. It consists of single or small tumor cell clusters that are detached from the tumor<sup>33</sup>.

### 1.5.2 Tumor staging

The degree or extent of the CRC at diagnosis is crucial to determine patients' treatment and outcome. Tumor staging categories are clinicians' major tools to measure patients' prognosis and help them to decide which is the most appropriate treatment or even if it is worth enrolling a patient in a clinical trial. The TNM system is the most extensively staging system used, by the American Joint Committee on Cancer (AJCC) and the International Union for Cancer Control (UICC). It establishes the invasion of the primary tumor (T), regional lymph nodal metastasis (N), and distant metastases (M) (**Table 1**). A conclusive staging is usually done after surgery with a histopathological study. The staging system is frequently updated to prevail relevant to clinical practice<sup>34</sup>.

CRC TUMOR STAGING SYSTEM		
AJCC STAGE	TNM STAGE	TNM STAGE CRITERIA
Stage 0	Tis N0 M0	Tis: Tumor confined to mucosa; cancer-in-situ
Stage I	T1 N0 M0	T1: Tumor invades submucosa
Stage I	T2 N0 M0	T2: Tumor invades muscularis propria
Stage II-A	T3 N0 M0	T3: Tumor invades subserosa or beyond (without other organs involved)
Stage II-B	T4 N0 M0	T4: Tumor invades adjacent organs or perforates the visceral peritoneum
Stage III-A	T1-2 N1 M0	N1: Metastasis to 1-3 regional lymph nodes. T1 or T2
Stage III-B	T3-4 N1 M0	N1: Metastasis to 1-3 regional lymph nodes. T3 or T4
Stage III-C	Any T, N2 M0	N2: Metastasis to 4 or more regional lymph nodes. Any T
Stage IV	Any T, any N, M1	M1: Distant metastasis. Any T, any N

**Table 1. AJCC tumor staging system for CRC.** Tumor (T), nodes (N), metastasis (M)<sup>6</sup>

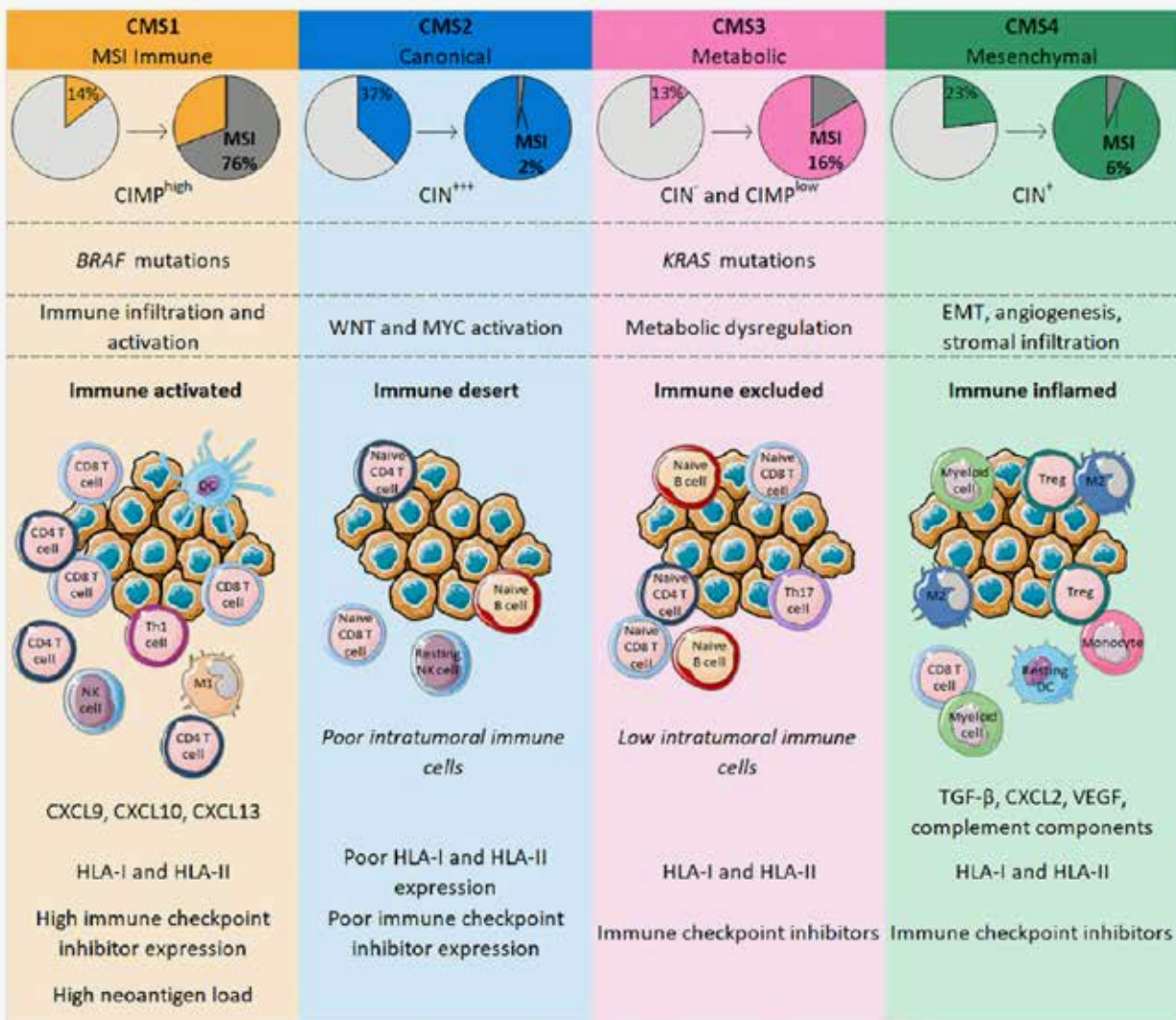
### 1.5.3 Consensus molecular subtypes

CRC cancer heterogeneity regarding clinical and molecular characteristics as well as response to treatment and prognosis, has highlighted the necessity of better classifying it into more robust subtypes. Over the years, different groups have put lots of effort into the definition of CRC subtypes<sup>35-40</sup>. The international CRC Subtyping Consortium was created in 2014 to unify the existing classifications and described the well-known four consensus molecular subtypes (CMS1 to CMS4) in 2015<sup>41</sup>, summarized in **Figure 3**<sup>42</sup>.

#### • CMS1 (MSI Immune subtype)

CMS1 represents 14% of all CRCs. It includes hypermutated tumors, which have a high CIMP signature and BRAF mutations and comprises most MSI tumors (76%). CMS1 is remarkably infiltrated with immune cells, T helper 1 (T<sub>H</sub>1), T follicular helper (TFH) cells, natural killer (NK) cells, activated lymphocytes, M1 macrophages, and dendritic cells (DCs). Accordingly, CMS1 tumors present high expression of genes involved in human leukocyte antigen (HLA) class I and class II families, related to antigen presentation and processing, also genes responsible for T cell chemotaxis like chemokine CXC ligand 9 (CXCL9) and CXCL10, as well as CXCL13, more related to B cell chemotaxis<sup>42,43</sup>. However, this CMS has a poor survival rate after relapse, which

has been demonstrated to correlate with BRAF mutations and MSI<sup>44,45</sup>. Also, these tumors are known to express immune checkpoint molecules such as the programmed death ligand 1 (PD-L1), cytotoxic T-lymphocyte-associated protein 4 (CTLA-4), and LAG3 by which they can escape immune surveillance<sup>42</sup>.



**Figure 3. CRC tumors classification into four CMSs.** The table displays the main characteristics of the CMSs, reflecting most of their significant biological differences in gene expression and intra-tumoral immune phenotype. Image from<sup>42</sup>

- **CMS2 (Canonical subtype)**

CMS2 subtype is known as the “canonical” and it includes 37% of all CRC cases. These tumors display epithelial markers, a high ratio of CIN and hyperactivation of the signaling pathways WNT and MYC<sup>41</sup>. CMS2 is the so-called “immune desert” because of the slight amount of intra-tumoral monocytes, myeloid cells, and lymphocytes. The modest number of immune cells present, are naïve T or B cells and resting NK cells, which are not able to participate in antitumor immunity. In consonance with this, they present poor expression of genes encoding for T cell activation, chemotaxis, and antigen presentation as well as of PD-1 and PD-L1<sup>42</sup>.

- **CMS3 (Metabolic subtype)**

CMS3 corresponds to only 13% of all CRCs. It is also known as the “metabolic” subtype

due to extensive alterations in many metabolic pathways. They often present KRAS gene mutations and low CIN and CIMP status. In addition, there is expression of HLA I and II, and although enriched in PD-1 expressing cells as well as T<sub>H</sub>17 and naive B and T cells, there is no active immune microenvironment, thus, are considered “immune excluded”<sup>42</sup>.

- **CMS4 (Mesenchymal subtype)**

CMS4 represents 23% of all CRC tumors. It is characterized by CIN status and EMT phenotype associated with the TGF- $\beta$  pathway, stromal infiltration, and angiogenesis<sup>41</sup>. CMS4 tumors are highly infiltrated by CD8<sup>+</sup> and CD4<sup>+</sup> T cells as well as by myeloid cells, resting DCs, monocytes, and activated NK and DCs. Despite this immune infiltration, these cells are at lower levels than in CMS1 tumors, while Treg infiltration is higher. This immune landscape favors tumor growth by immunosuppression and angiogenesis through factors like TGF- $\beta$ , CXCL2, and vascular endothelial growth factor (VEGF) that are typically secreted by Tregs, endothelial cells, and fibroblasts, which are abundant in CMS4 tumors. Even if immunosuppressive factors are present, HLA I and II and immune checkpoints are still expressed<sup>42</sup>. Moreover, patients with CMS4 tumors are commonly diagnosed at advanced stages (stages III and IV) with worse overall and relapse-free survival ratios<sup>41</sup>.

Still, due to mixed features, 13% of CRCs cannot clearly be classified into any CMS. This may be due to a transition phenotype or intratumoral heterogeneity<sup>41</sup>.

Patients' prognostic is different according to tumors' molecular subtype being those harboring CMS1 and CMS4 tumors are the ones with the best and worst prognoses, respectively. Nowadays, the translation of the CMS classifier into preclinical models presents a lot of potential, especially regarding drug discovery and sensitivity studies<sup>46,47</sup>. This is encouraging many groups to keep up their continued efforts to improve the CMS system translation into the clinics<sup>48</sup>. Classifying patients based on their molecular characteristics may offer different subgroups, each, prone to receive new treatments together with candidate targetable pathways<sup>47,48</sup>. Kwon et al, demonstrated retrospectively that the CMS can be used as a prognostic factor for stage III CRC patients that received FOLFOX as adjuvant chemotherapy<sup>49</sup>. Also, Louis Vermeulen's lab established an immunohistochemical-classifier based on FRMD6, ZEB1, HTR2B and CDX2 staining. These markers in combination with cytokeratin and MSI profile, facilitate patients' classification into the four CMS<sup>50</sup>. These findings highlight the great potential of CMS clinically, although there is a need for greater confidence in the CMS classification<sup>45</sup>.

## **1.6 CRC MANAGEMENT**

Since this project is aimed at the study of possible biomarkers in the setting of mCRC, this section will be focused only on metastatic disease. Over the last decade, the completed clinical trials have demonstrated an improvement in the survival of mCRC patients, mainly due to the advances toward an accurate diagnosis and staging, better surgical approaches as well as a more personalized treatment by using biological therapies targeting specific tumor features<sup>51,52</sup>.

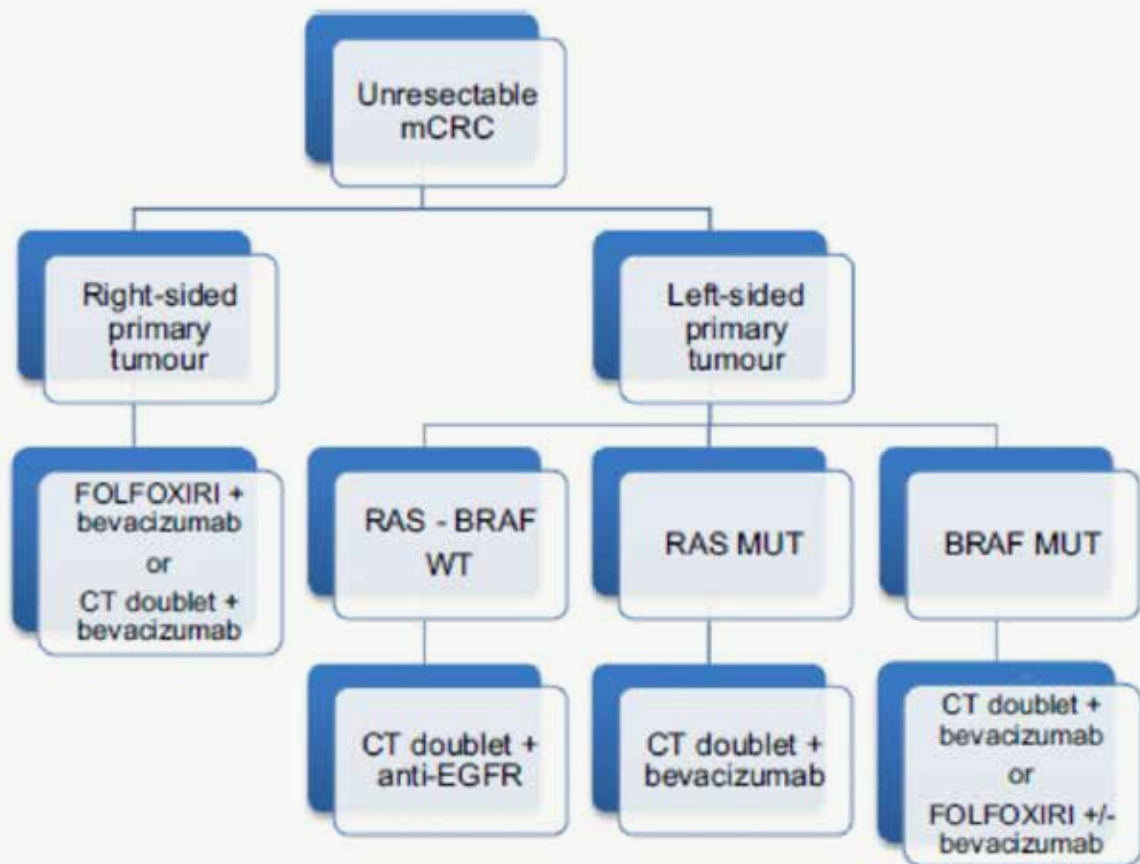
### **1.6.1. Surgery**

In the context of stage IV metastatic CRC, primary tumor removal depends on the patient's symptomatology. When the tumor causes a perforation or complete bowel obstruction or severe bleeding, resection is indicated. If it's asymptomatic, it will depend on the resectability of the metastases. If this is the case, it is more common when the

metastatic site is the liver<sup>53</sup>. Only 10-20% of CRC patients diagnosed with liver metastases are candidates for metastasis resection from the beginning. In some situations, with good responses to systemic chemotherapy, the option of resection appears. The criteria for potentially curative resection are based on the absence of tumor at margins, a minimum of 20-40% liver remnant, and functional vascular inflow and vascular/biliary outflow<sup>54</sup>. Unlike the liver, lung metastases barely are the only site of disease spreading. Therefore, a pulmonary metastasectomy usually depends on the therapy outcome of the other metastatic sites<sup>55</sup>. Patients with peritoneal metastases are usually the ones with the worst prognosis, although they can receive cytoreductive surgery which consists of the removal of all visible tumors. Cytoreductive surgery and hyperthermic intra-peritoneal chemotherapy are the standard care in peritoneal malignancies<sup>56,57</sup>.

### 1.6.2. Metastatic disease management

Around 20% of CRC patients are diagnosed with metastatic disease, while almost 50% of patients will develop metastasis after a primary tumor in the colon or rectum was diagnosed. The most frequent site of distant disease is the liver (50%), followed by the lungs (20%), peritoneum, and pelvic abdominal lymph nodes, which are usually combined with liver metastasis<sup>51,58,59</sup>. In the last decades, the survival of metastatic patients has improved to a median OS of 30 months<sup>60,61</sup>. This is due to the implementation of new treatments, the improvement in surgical procedures, and the accessibility to some local ablative treatments (LAT). Factors such as patient characteristics or the tumor's molecular profile may influence the choice of a successful first-line treatment<sup>51,58</sup> **Figure 4.**



**Figure 4.** First-line treatment algorithm for unresectable mCRC<sup>58</sup>.

The chemotherapeutic first-line treatment backbone combinations are the intravenous FOLFOX or FOLFIRI (leucovorin/5-fluorouracil plus irinotecan) regimens. The addition of targeted therapies has improved patients' clinical outcomes. They consist of monoclonal antibodies such as bevacizumab (anti-VEGFA) and cetuximab/panitumumab (anti-EGFR) (see section 1.6.5). At the time of first-line treatment failure, which happens to approximately two-thirds of patients, a second line is offered. It consists of a shift of the backbone given in the first line, and most of the time, a change in the targeted therapy. If the patient progresses to the second line of treatment a third line can be given, exploring new treatment combinations always aiming at improving the patient's performance status and overall quality of life<sup>5,11,62</sup>. Recently, the approach of rechallenging a tumor with a previously given treatment after its withdrawal has shown promising results, like with the anti-EGFR targeted therapy. The idea is to target again a possible clonal population of KRAS-wild type (WT) cells that expanded during the withdrawal<sup>63</sup>.

### **1.6.3 Types of treatments:**

#### **DRUGS USED IN FIRST-LINE AND ONWARDS:**

##### **Cytotoxic chemotherapeutic agents**

Chemotherapy consists of a systemic treatment aimed at stopping proliferation and promoting death of cancer cells. However, its effects are non-specific as they also target dividing normal cells, which leads to many side effects, such as neutropenia, diarrhea, neurologic damage, or immunosuppression among others<sup>3</sup>. As previously mentioned in paragraph 1.6.4, the main chemotherapeutic drugs used in CRC treatments are fluoropyrimidines (mainly 5-FU), irinotecan, and OXA<sup>64</sup>.

##### **- Fluoropyrimidines**

5-Fluorouracil (5-FU) is an inhibitor of the enzyme thymidylate synthase (TS). Since it was developed in the 1950s, it represents the base for both adjuvant and metastatic chemotherapy in CRC treatment. TS enzyme methylates deoxyuridine monophosphate (dUMP) to form deoxythymidine monophosphate (dTMP) thus representing an important enzyme in thymidine de novo synthesis which is essential in the replication and repair of DNA<sup>65,66</sup>. When TS is inhibited by 5-FU active metabolites, there is a deficit of the nucleotide thymidine, blocking DNA synthesis and leading to apoptosis in rapidly dividing cancer cells. To enhance its effects, 5-FU is often administered in combination with folinic acid (leucovorin)<sup>65,67</sup>. Capecitabine is a pro-drug that once absorbed is converted into enzymatically active 5-FU. In the case of elderly mCRC patients who are unsuitable to receive combination treatment, it is given as an alternative to intravenous 5-FU. Both drugs revealed equal survival rates in combination with other cytotoxic agents<sup>64,68</sup>.

##### **- Oxaliplatin**

OXA is a platinum drug. These compounds are the most widely used chemotherapeutics in the treatment of diverse types of cancers. They are characterized by the formation of DNA adducts through inter- and intra-strand cross-linking, and chelate formation, inhibiting DNA synthesis, replication, and transcription processes and ultimately causing cell death. Cell sensitivity to OXA is influenced by the cellular capacity on repairing these adducts. Some of the mechanisms involved in OXA resistance are: a decrease in cellular uptake/increase in cellular efflux or alterations in DNA repair pathways (base excision repair [BER] system, nucleotide excision repair [NER], double-strand breaks repair and DNA MMR mechanisms among others) have been

identified<sup>67,69,70</sup>. OXA was approved in the early 2000s, and in combination with 5-FU and leucovorin, improved CRC patients' survival<sup>71</sup>.

- Irinotecan

Irinotecan is a Camptothecin derivative (a natural compound from a Chinese ornamental tree) that inhibits topoisomerase I. After injection, Irinotecan is rapidly hydrolyzed into its active metabolite SN38, in the liver and plasma. SN38 binds to the DNA-Topo I complex, inhibiting cell replication and producing double-stranded cleavage within the molecule, thus causing cell death. These processes occur during the DNA synthesis phase (S phase) and irinotecan is therefore considered to be a cycle-specific drug<sup>72</sup>. Irinotecan was approved for CRC treatment in the late 1990s, right before OXA, and in combination with 5-FU and Leucovorin, FOLFIRI, is part of the standard of care today in CRC.

### Targeted drugs

Besides chemotherapy, biological targeted agents are used in the mCRC treatment. These targeted therapies, unlike chemotherapy, are specific agents directed to a subset of patients with defined biological cancer features. They include monoclonal antibodies against EGFR (cetuximab and panitumumab) and against VEGF (bevacizumab). There are more biological agents that target these pathways, however, cetuximab, panitumumab, and Bevacizumab are the only ones approved (to date) for first-line mCRC treatment<sup>51</sup>.

- Monoclonal antibodies against EGFR (cetuximab and panitumumab)

Overexpression of EGFR is a hallmark of many epithelial cancers, including CRC<sup>73</sup>. This feature is associated with reduced survival and increased risk of metastases. Both cetuximab and panitumumab, block this receptor and have proven their efficacy in patients that did not respond to chemotherapy combinations<sup>3,27,51</sup>. They are indicated in first-line mCRC patients combined with chemotherapy in KRAS WT tumors<sup>74</sup>: KRAS is a downstream effector of the EGFR pathway and when it is mutated (42% of CRC patients), it is constitutively active and evades the anti-EGFR effect. Moreover, before the administration of either of the monoclonal antibodies, the National comprehensive cancer network guidelines, recommend genotyping not only for KRAS but also for neuroblastoma RAS viral oncogene homolog (NRAS) and BRAF<sup>75</sup>.

- Monoclonal antibodies against VEGF-A (bevacizumab)

VEGF-A is a key glycoprotein that binds the VEGFR in the cell membrane and stimulates signaling cascades promoting vascular permeability, endothelial cell proliferation, and angiogenesis. The high metabolic rate of growing tumors makes them highly dependent on nutrients and oxygen which is facilitated by the generation of new vessels, a process called angiogenesis<sup>76,77</sup>. Bevacizumab (Beva) binds to circulating VEGF-A avoiding its binding to VEGFR and its further activation. That is why these drugs are called antiangiogenics. They reduce vascular growth subsequently limiting the blood supply to the tumor and ultimately, its growth. Several studies have demonstrated that the addition of Beva to both combinations of FOLFIRI and FOLFOX, improves progression-free survival (PFS) in mCRC patients<sup>76,78-80</sup>.

Guidelines regarding first-line treatment extent, recommend following patient's personal situation, toxicities and disease aggressiveness. Based on these, stop-and-go as well as intermittent treatment and maintenance treatment (5-FU with or without Beva) have emerged as individualized strategies openly discussed with the patient.

## Immunotherapy with checkpoint inhibitors

At this point, immunotherapy emerges aiming to improve or re-establish the immune system's ability to fight the disease. Due to its ability to target neoantigens, the adaptive immune system plays a much more significant part in the immune response to cancer cells. Based on this, diverse methods of immunotherapy have been developed, always seeking to get a better adaptive immune function against cancer. Some immune therapies are vaccines, monoclonal antibodies that target immune checkpoints and cytokine administration<sup>81,82</sup>. Also, prognosis and outcome are associated with the presence and type of tumor-infiltrating immune cells. Thus, infiltration of cytotoxic and effector memory T cells correlates with better survival of cancer patients<sup>83,84</sup>.

Usually, malignant cells present abnormal antigens on the surface by the major histocompatibility complex-I (MHC-I) leading to recognition and attack by the immune system. However, cancer cells may develop the ability to downregulate MHC-I molecules that together with other strategies lead to the omission by the immune system. For instance, cancer cells may also express PD-L1 and PD-L2 on the cell surface, which are ligands of T cell immune checkpoint receptors, PD-1. Their binding results in the inactivation and exhaustion of T cells<sup>85</sup>. Another important checkpoint exists between antigen-presenting cells (APCs) and T cells, namely CTLA-4. CTLA-4 is expressed on activated T cells, and inhibits directly the T-cell receptor (TCR), causing a reduced ability to interact with the APCs and therefore blocking the downstream cascade (T-cell maturation, proliferation and effector function)<sup>86</sup>. Immunotherapy's goal consists of trying to reawaken the anti-tumor response from the immune system, by blocking these interactions and avoiding tumors' escape from T cell detection, favoring tumor clearance, and immunosurveillance<sup>85,87</sup>.

In general terms, CRC is considered a cold tumor, with very little immune infiltration; in consequence, these therapies have proved unsuccessful in the majority of patients. However, a subgroup (around 4-5%) of mCRC patients whose tumors are characterized by a high mutational burden, MSI-H or dMMR have been shown to benefit from immune checkpoint inhibitors. In this context, there is a phase III trial, the Keynote-177 (NCT02563002), which is active, although not recruiting. It is an international, open-label, randomized study in dMMR/MSI-H mCRC patients that compared pembrolizumab monotherapy to a control group receiving standard chemotherapy as first-line treatment. The PFS resulted in 16.5 months vs. 8.2 months respectively. Additionally, with a less restrictive and simpler administration schedule than chemotherapy, patients treated with pembrolizumab displayed a better quality of life. Pembrolizumab was also associated with reduced mortality (HR=0.74; p=0.036), although it did not reach statistical significance criteria ( $p \leq 0.0246$ )<sup>88,89</sup>. Together with Pembrolizumab, Nivolumab, another PD-1 blocker, and Ipilimumab a CTLA-4 inhibitor, have shown beneficial effects in these MSI-H patients<sup>51,88,90-92</sup>. Pembrolizumab is approved in first-line treatment and Nivolumab and Ipilimumab in refractory disease in dMMR/MSI-H metastatic patients<sup>74,93-95</sup>.

### DRUGS SPECIFICALLY USED FROM SECOND-LINE TREATMENT ONWARDS:

Second-line treatment is approximately administered to two-thirds of mCRC patients and will depend on the previous treatment, organ functions and patient performance status scale (ECOG). In these settings, aflibercept (recombinant fusion protein that binds to VEGF-A and B preventing VEGFR activation) or small-molecule-based kinase inhibitors such as regorafenib and ramucirumab that target multiple pro-angiogenic growth factors have shown good results in chemorefractory mCRC<sup>51,58,85</sup>. As the knowle-

dge about tumor molecular abnormalities increases, new treatment possibilities arise, especially in second-line treatments and beyond<sup>46,58</sup>. For instance, some tumors harbor HER2 amplifications (3% of the cases) and BRAF V600E mutations (10% of the cases) that can be treated with anti-HER2 or -BRAF V600E drugs, respectively. For instance, interesting results have been reported from clinical trials targeting HER2 amplifications, with trastuzumab-lapatinib and trastuzumab-pertuzumab therapies<sup>51</sup>. Also, recent evidence has proven that in BRAF-mutated patients, a triple regimen of EGFR, BRAF, and MEK inhibitors (encorafenib, binimetinib, and cetuximab) offered significantly better survival benefit<sup>96</sup>.

#### **1.6.4 Treatment resistance**

Despite the advances in the clinical management of CRC patients, the 5-year survival rate in the metastatic disease is hardly above 12%. This is mostly due to the development of resistance to (almost all) treatments<sup>97,98</sup>. The Pharmacokinetics of the drugs is essential for systemic treatment since they must successfully reach the tumor cells. Impaired delivery of the drugs caused by alterations in processes such as absorption, distribution, metabolism, and excretion are needed to be taken into consideration<sup>99,100</sup>. Once the drugs reach the tumor cells, they can be intrinsically resistant or acquire resistance during treatment. Cancer cells may become resistant to a single drug or to a combination of drugs that share a similar mechanism of action, a phenomenon known as multidrug resistance. The main studied mechanisms of resistance consist of alterations in the transport of the drug across the plasma membrane or DNA repair, expression of growth factors, target molecules, and metabolic effects. Cellular transport of many drugs is done in part by the ATP-binding cassette (ABC) proteins. These ATP-dependent efflux pumps, lower the intracellular drug concentration keeping it below cell-killing levels<sup>100</sup>. Overexpression of ABC transporters, such as P-glycoprotein (Pgp, also known as ABCB1 or MDR1), is a known mechanism implicated in multidrug resistance (MDR), in vitro and in vivo<sup>101</sup>. In addition, this mechanism has a vast drug specificity, sustaining the MDR<sup>100</sup>. Another common mechanism of therapy resistance consists of defects in the apoptotic pathway. The p53 protein is an important regulator of apoptosis, inducing cell cycle G1 arrest, by preventing tumor cell replication after sensing genotoxic stress known as p53-mediated cell death. CRC tumors, often present mutations in p53, mostly resulting in a gain of function, a mechanism that has been related to resistance to DNA-damaging drugs<sup>100,102</sup>. Furthermore, the upregulation of alternative signaling pathways is another mechanism of resistance. In this regard, we reported in a previous work that CRC cell lines with acquired resistance to oxaliplatin had a hyperactivation of the NF- $\kappa$ B pathway<sup>103</sup>. As a consequence, these resistant cells overexpressed and secreted high amounts of some CXC chemokines including CXCL1, CXCL2, and CXCL8. Interestingly, the inhibition of this transcription factor with curcumin and the silencing of CXCL1 and CXCL8 genes resulted in the reversion of the resistance phenotype<sup>104</sup>.

In the case of targeted drugs, mutations in KRAS gene leads to constant activation of the RAS-RAF-MEK-ERK pathway, conferring resistance to anti-EGFR therapies. Recently, it has been described the emergence of mutations in RAS genes during cetuximab or panitumumab treatment as a mechanism of resistance acquisition. In fact, RAS WT patients may present one or more mutations in the MAPK pathways when resistance appears<sup>98</sup>. In this regard, some preclinical studies have shown how the addition of MEK inhibitors to anti-EGFR treatment reverts the acquired resistance to anti-EGFR drugs<sup>105</sup>. Also, when V600E mutation is present in the BRAF gene, cancerous cells are unresponsive to EGFR-directed therapies, which usually translates into worse survival<sup>24,28</sup>. Another known mechanism for CRC cells to become resistant to anti-EGFR therapies is through the HER2 pathway. The CRC cells take advantage of the HER2 pathway as a

sidestep signaling pathway, avoiding the anti-EGFR therapies<sup>28</sup>.

The identification and implementation of resistance biomarkers is aimed at improving treatment outcomes of CRC patients as they may help guide oncologists in choosing the best treatment schedules and avoiding treatments with non-effective drugs, thus saving money and patients from toxicity with no clinical benefit<sup>97,100</sup>.

### **1.6.5 Prognostic and predictive biomarkers in CRC**

The term biomarker is defined by the NIH as a biological molecule found in blood, other body fluids, or tissues that is a sign of a normal or abnormal process, or of a condition or disease<sup>106</sup>. In the past years, molecular and biological characterization of CRC has become essential in the management of this disease. Consequently, CRC-sensitive and specific biomarkers have arisen as crucial for CRC detection, prevention, diagnosis, and treatment. Nevertheless, their translation into the clinics is quite complex and all biomarkers must undergo clinical validation before Food and drug administration (FDA) approval<sup>95,107,108</sup>.

In clinical studies, when it comes to the evaluation of therapeutic benefits, discerning the prognostic and predictive value of biomarkers becomes a challenge. This complexity arises from the search for therapy effectiveness in patients displaying poor survival with standard treatments<sup>95</sup>. In CRC management, the prognostic-predictive tissue biomarkers used are MSI high, KRAS/NRAS, and BRAF mutations. In stage IV CRC MSI-high is considered a predictive marker of immunotherapy benefit<sup>93-95</sup>. As explained above, MSI-high tumors have a high mutational burden (TMB) which is a synonym of neoantigens and activated cytotoxic and lymphocyte infiltration, resulting in a strong antitumor immune response<sup>95,109</sup>.

As previously explained in section 1.6.5, patients that do not harbor any mutation in KRAS and NRAS genes may benefit from anti-EGFR addition to chemotherapy<sup>27,110,111</sup>. BRAF V600E mutations are a bad prognostic factor in stage III and IV CRC patients. At the same time, it is a predictive biomarker of response to BRAF inhibitors. Recently, the BEACON study showed that BRAF mutated mCRC patients could benefit from doublet or triplet BRAF, EGFR, and MEK inhibitors<sup>112</sup>. Several studies have shown that the sidedness of the tumor is also a prognostic-predictive marker<sup>113</sup>. RAS-WT right-sided CRCs present a worse prognosis than left-sided and do not show any benefit from anti-EGFR therapy; in this setting, a more aggressive treatment based on chemotherapy triplets could be used<sup>74,114</sup>. Along with these biomarkers, HER-2 amplification has lately emerged as a predictive biomarker of response to anti-HER2 therapies. In addition, these amplifications may also predict inefficacy and resistance development to anti-EGFR therapies<sup>115</sup>.

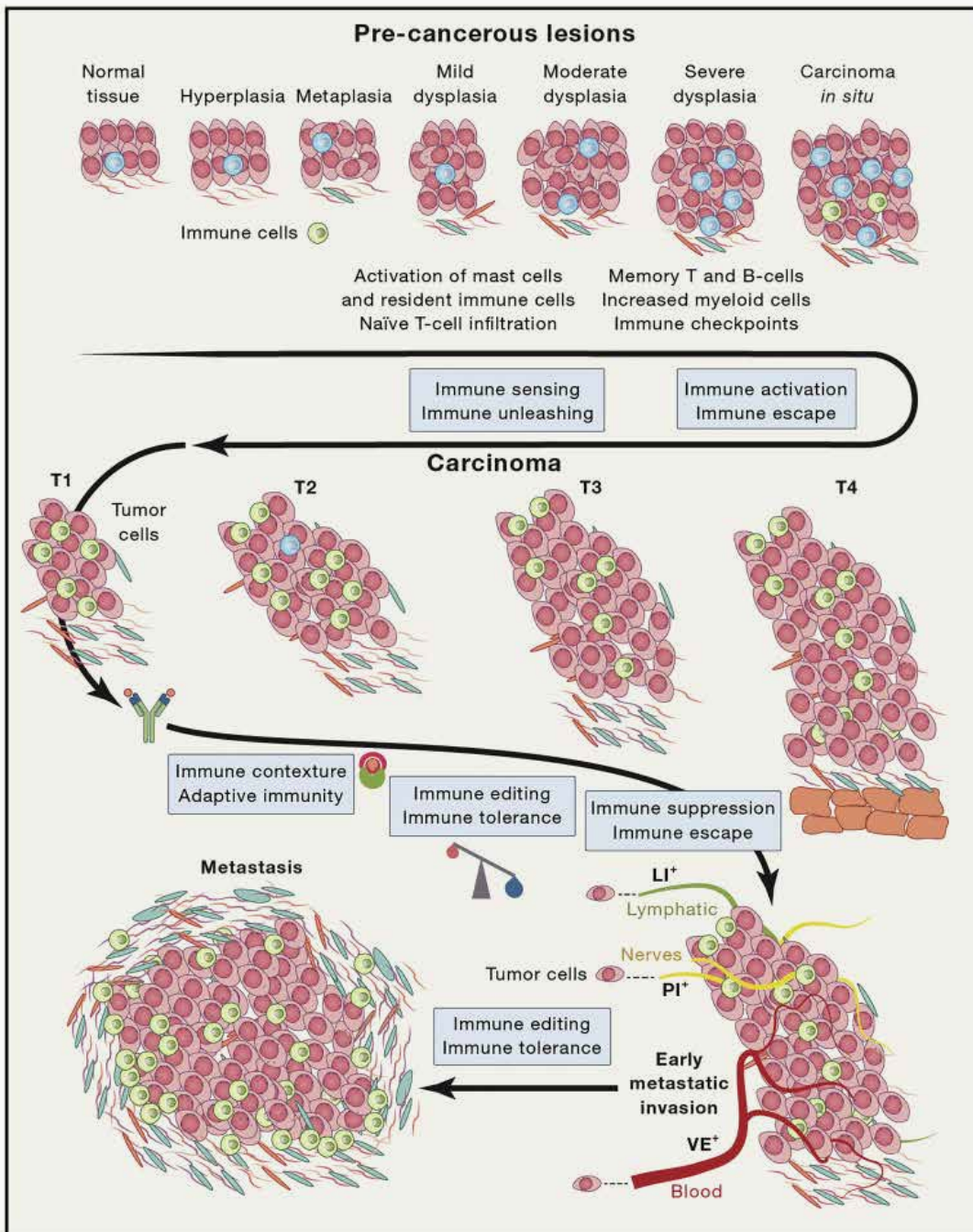
Although there has been a great advance in the use of biomarkers for CRC, new prospective studies are still necessary to validate new candidates. Blood tests are well established in clinical practice and therefore, blood-based markers seem convenient based on reproducibility, objectivity, and simple quantification, and are relatively low-priced. Unfortunately, blood-CRC biomarkers still show low sensitivity and specificities as is the case of the carcinoembryonic antigen (CEA), associated with other types of cancers, and carbohydrate antigen (CA) 19-9, which has shown inconsistent results in CRC diagnosis, treatment monitoring, and tumor surveillance<sup>58,116,117</sup>. A novel strategy consists of multivariate classification models, which measure numerous biomarkers and calculate the probability of having the disease. Interestingly, a panel of 15 diagnostic biomarkers did discriminate better between CRC patients and healthy subjects when compared

to single markers<sup>110</sup>. There are numerous additional biomarkers that show promising results but a few are being translated into the clinics. For instance, noninvasive biomarkers for early diagnosis such as circulating tumor cells (CTCs) and circulating tumor DNA (ctDNA). Both are easily isolated from patients' plasma or liquid biopsies and may add valuable information to advising clinical decisions<sup>118</sup>. Reece et al, demonstrated that ctDNA may help to assess surgical tumor clearance, choose an appropriate treatment, and monitor its response<sup>119-121</sup>. Although these results are very promising, their implementation will remain a challenge until there is a worldwide standardization of these methods and technology. Surely, these needs will be met, and liquid biopsy together with newly approved biomarkers will bring patients closer to an effective personalized treatment.

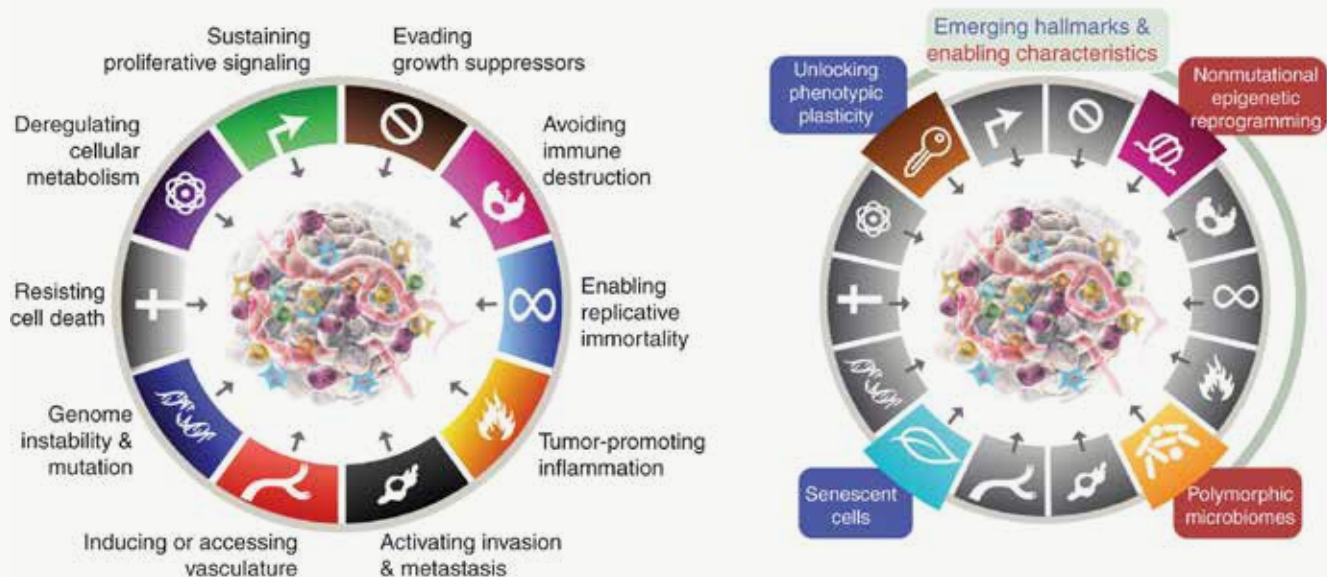
## 2. CANCER AND IMMUNITY

The first signs of the immune system's involvement in cancer control can be followed back over a century<sup>122</sup>. Yet, in the past two decades, definitive recognition of the tumor-immunology field arose. It was mainly due to the demonstration of two essential concepts that explained adaptive immunity's role in tumors: immunosurveillance and immunoediting<sup>123,124</sup>. The cancer immunosurveillance process functions as a potent tumor suppressor mechanism, although it is only one piece of the intricate relationship between the immune system and cancer<sup>123-125</sup>. In the event of an unsuccessful response to tumor elimination by the immune system, those tumors with diminished immunogenicity may arise, escaping immune recognition and elimination<sup>124,126</sup>. This duality of host-protective and tumor-promoting functions is named "cancer immunoediting" (see section 2.1)<sup>124,125,127</sup>. Together with the demonstration of these two concepts, numerous studies with encouraging results on how the immune system controls and contributes to disease progression, were obtained. Likewise, on its power to neutralize, counteract and possibly defeat the disease, for instance, the first FDA-approved vaccine against prostate cancer (2010), the first FDA-approved anti-CTLA-4 for melanoma in 2011 as well as anti-PD-1 as first-line treatment in lung cancer (2015)<sup>82</sup>. As a result of the numerous advances in the tumor immunology field, the definitive recognition was achieved with the Nobel Prize in Physiology or Medicine 2018 awarded to James P. Allison and Tasuku Honjo for their contributions to cancer therapy by the inhibition of T cells negative regulation. In fact, the action of innate and adaptive immunity affects the development of pre-cancerous and cancer stages **Figure 5**<sup>82</sup>.

Although the specific underlying mechanisms remain to be clarified, it is accepted that several immune and immune-derived factors have a role in the onset and progression of cancer. For instance, chronic inflammation acts as a niche-promoting carcinogenesis<sup>10,128</sup> and it is considered one of the 8 hallmarks of cancer (**Figure 6**, left)<sup>10</sup>. Pro-inflammatory and chemoattractant factors are released by malignant cells promoting immune cell infiltration<sup>129-131</sup> and reprogramming resident fibroblasts into cancer-associated fibroblasts (CAFs). These CAFs stimulate tumor cell growth and angiogenesis and recruit immune cells such as neutrophils, macrophages, and lymphocytes to the TME<sup>132-134</sup>, arranging the perfect setting for the disease<sup>135</sup>. Primary tumors' immune landscape depends on the tissue of origin, epigenetics, host's gut microbiome, genetic background and mutations as well as on the environmental conditions<sup>136-139</sup>. The combination of all these factors will determine the disease progression and the response to treatment<sup>140,141</sup>.



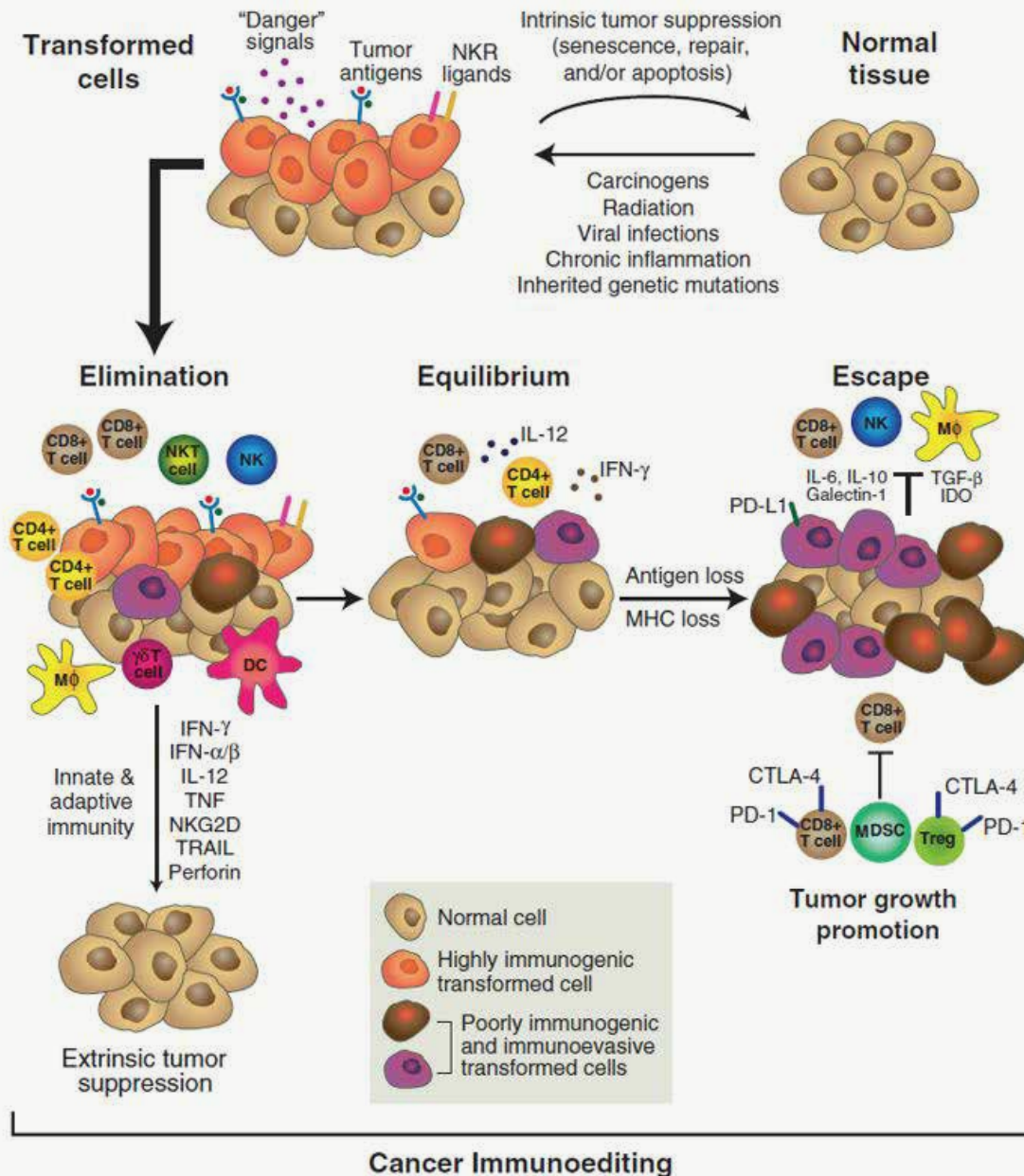
**Figure 5. Immune system role from pre-cancerous lesions to primary tumors and metastases:** Representation of the development of a primary tumor, from pre-malignant lesions and the corresponding immune contexture. Adaptive immunity regulates tumor growth although the tumor can evade immune recognition, via immune tolerance, suppression, and escape, favoring tumor progression and metastasis. Figure from<sup>82</sup>.



**Figure 6. The Hallmarks of Cancer:** There are eight Hallmarks of Cancer, since, along with the six (acquired capabilities) proposed in 2000<sup>142</sup>, the hallmarks “deregulating cellular metabolism” and “avoiding immune destruction” proposed in 2011 have been extensively validated<sup>10</sup>. The 2011 sequence also included two enabling characteristics “tumor-promoting inflammation”, which together with “genome instability and mutation,” were essential participants in the activation of the eight hallmarks for tumor growth and progression. Likewise, the figure on the right represents a proposal of four new possible emerging Hallmarks: there still are some extra features of this theoretic model that could be incorporated, if they can be extensively applied in all human cancers and are supported by an increasing number of publications. Figure from<sup>143</sup>

## 2.1. IMMUNOEDITING

The dynamic process by which the immune system can both limit and promote tumor development is called immunoediting. It consists of three phases termed elimination, equilibrium and escape (**Figure 7**). Immunosurveillance consists of the initial process in which immune cells recognize and destroy tumor cells. From the oncogenic transformation, cancer cells express neoantigens that are released at the time of tumor cell death. These neoantigens are captured by antigen-presenting cells, commonly type 1 dendritic cells (cDC1s)<sup>144</sup> driving priming and activation of T cell responses, possibly at the tertiary lymphoid structures (TLSs)<sup>145</sup>, always together with a cocktail of costimulatory signals and cytokines<sup>146</sup>. This represents a critical step, in which specific factors and parameters can bend the balance towards either anti-tumor effector T cells or pro-tumor Treg cells<sup>147</sup>.



**Figure 7. Cancer Surveillance and Immunoediting.** Cancer immunoediting involves three sequential stages: elimination, equilibrium, and escape. During elimination, innate and adaptive immunity collaborate to eradicate developing tumors. If fully completed, the host lives free of cancer and with elimination, immunoediting would be completed. However, some singular cancer cells may remain undetected, entering the equilibrium phase, which basically consists of avoiding cancer outgrowth by immunologic mechanisms. At this point, recognition or effector functions by innate immunity are not needed, only adaptive immunity. Again, concluded immunoediting would arise if the equilibrium phase is able to hamper the tumor outgrowth during the host lifetime. Nonetheless, there is constant pressure on the immune system caused by genetically unstable tumor cells which, after not being recognized, may then access the escape phase, where outgrowth is no longer prevented by immunity, causing within time clinically apparent disease. Figure slightly modified and adapted from<sup>123</sup>.

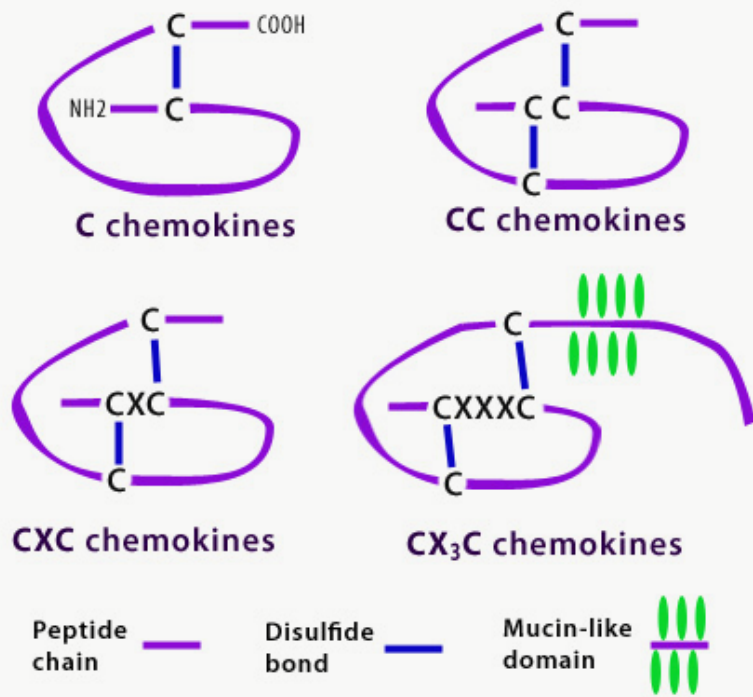
Elimination is followed by the equilibrium phase, in which the immune system repeatedly selects and/or promotes the appearance of tumor cells with the ability to survive the immune system's attack. This phase is characterized by constant proliferation and mutation that eventually favors tumor escape from the immune response<sup>82,123,125</sup>. This ability of tumor cells to coexist with the immune system and survive is another of the hallmarks of cancer<sup>143</sup>. Equilibrium is acknowledged to be the longest of the phases and could last for years<sup>81,82</sup>. The third phase of the immunoediting process is tumor escape or evasion. Cancer cells may grow and metastasize due to failing control and elimination by the immune system. This fact may be facilitated by the tumor-induced suppression of the immune system as well as by genetic acquisitions. One well-known mechanism is the expression of immune checkpoint molecules (PD-L1, PD-1, B7-H3 or Tim-3 among others) on the surface of cancer cells (like normal cells do); when these molecules bind to their corresponding proteins in effector T cells, the latter become anergic and unable to attack the tumor cells. This ability to evade immune attack is again considered a hallmark of cancer pathogenesis<sup>81,148</sup> (**Figure 7**).

The “immune contexture” concept is defined by the nature, immune functional orientation, density, and location of the tumor-immune infiltrate<sup>149</sup>. It was originally established in CRC, although over time its application has expanded to many different solid cancers<sup>150-152</sup>. This immune “contexture” was essential in the development of the Immunoscore. It is an immunohistochemistry (IHC)-based assay which defines hot (inflamed) and cold (non-inflamed) tumors together with prognostic information based on the presence/absence of CD3<sup>+</sup> and CD8<sup>+</sup> in specific regions (center and invasive margin) of the tumor<sup>141</sup>. A recent worldwide validation confirmed that the consensus Immunoscore holds prognostic value superior to that of the AJCC/UICC-TNM staging system<sup>153</sup>. Important players in that immune “contexture” are chemokines; these cytokines act as chemoattractants not only of the immune cells but also of the endothelial and tumor cells. Thus, they may influence the tumor-stroma interactions eventually affecting tumor cell growth, survival, migration, and angiogenesis, either suppressing or promoting cancer aggressiveness. Moreover, chemokines have also been associated with resistance to chemotherapy in CRC<sup>154</sup>, ovarian<sup>155</sup>, and breast cancer<sup>156</sup>, among others. Based on these and the fact that chemokines are the subject of study in this thesis, in the following sections we describe the different roles of chemokines in the tumor-stroma immune “contexture” and discuss their potential as therapeutic targets as well as their value as prognostic and/or predictive biomarkers in CRC.

## **2.2 CHEMOKINES IN CANCER AND IMMUNITY**

### **2.2.1 Chemokines structure**

Chemokines are a subfamily of chemotactic cytokines that are classified based on the position of the cysteine (C) residues on their primary amino acid sequence. There are four main subfamilies: CC, CXC, CX3C, and C. As shown in **Figure 8**, the cysteine amino acid residues are connected by disulfide bonds at the N-terminus within the mature protein, which corresponds to the chemokine ligand. These small proteins (8-10 kDa) exert their biological function by binding to their corresponding G-protein coupled receptors. This binding will modify the receptor's conformation and turn on the respective signaling pathway through the coupled G-protein activation. More than one ligand can bind to each receptor and vice versa<sup>157-159</sup>.



**Figure 8. C, CC, CXC, and CX<sub>3</sub>C chemokine's structure.** Chemokines usually contain four cysteines in conserved positions and the space between the two first ones, determines its kind. Cysteines grant the tertiary structure through the disulfide bonds. Figure from<sup>160</sup>

They are secreted proteins whose main function is to attract leukocytes and have crucial roles in cellular, immune, and physiological processes, including development. The latter may explain the reason why chemokines are so strongly conserved throughout evolution<sup>161,162</sup>. Chemokines may exhibit different roles in inflammatory bowel diseases, asthma, cancer, infections, arthritis and other disease processes. In the tumor microenvironment, tumor cells, immune cells, and stromal cells may secrete chemokines and express their corresponding receptors<sup>81,158,163-165</sup>. In turn, these chemokines may affect the migration of different immune cell subsets that will ultimately influence tumor fate.

### 2.2.2 Chemokines promoting pro-tumoral immunity

Some chemokines may favor tumor growth by promoting the migration of immune suppressor cells and endothelial cells among others to the tumor microenvironment. Historically, they have been named Angiogenic chemokines (**Figure 9**). In this case, the immune cells recruited may inhibit antitumor immune responses induced by other immune populations and may also promote and maintain cancer stemness and angiogenesis, leading to cancer progression. Angiogenic chemokines mainly attract monocytic and granulocytic myeloid-derived suppressor cells (MDSCs), IL-22 + CD4<sup>+</sup> T helper 22 (T<sub>H</sub>22) cells, IL-22 + innate lymphoid cells (ILCs), Treg cells, and plasmacytoid dendritic cells (pDCs)<sup>158,166</sup>.

#### - Recruitment of MDSCs.

MDSCs are a heterogeneous and immature (undifferentiated) cell population of myeloid origin. MDSCs play a role in tumor progression by downregulating antitumor immunity, mainly by impairing CD8<sup>+</sup> T cell responses and NK-mediated cytotoxicity. The immune suppressive effects of MDSCs may also empower the tumoral cells with stem celllike properties<sup>167-170</sup>. Monocytic MDSCs (mMDSCs) express CC chemokine receptor 2 (CCR2), CXC chemokine receptor 2 (CXCR2) and CXCR4 and can be recruited to the tumor microenvironment by the corresponding ligands CC ligand 2 (CCL2)<sup>171,172</sup>, CXC ligand 5 (CXCL5), and CXCL12, respectively. Granulocytic MDSCs (gMDSCs) present CXCR1 and CXCR2 which mediate their degranulation and migrating through the CXCR1/2-CXCL8 signaling pathway. Tregs and myeloid cells also secrete CXCL8, favoring the recruitment of neutrophils into the tumor microenvironment<sup>173</sup> and promoting tumor angiogenesis and boosting tumor progression and metastasis<sup>173,174</sup>.

#### - Recruitment of T<sub>H</sub>22 cells.

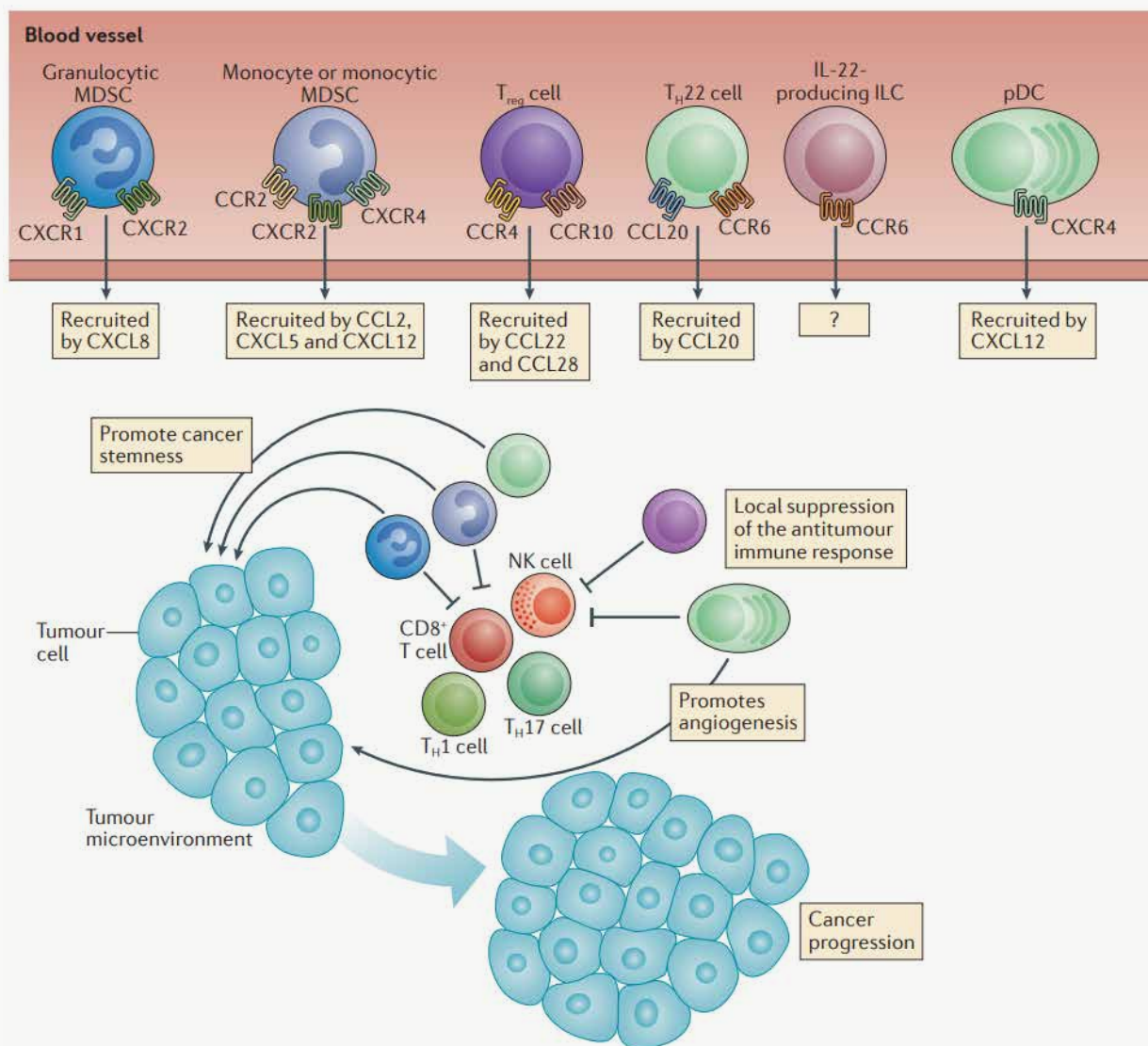
T<sub>H</sub>22 cells are a subset of CD4<sup>+</sup> T cells which under inflammatory conditions, overexpress IL-22 leading to pathological changes and tumor progression<sup>175</sup>. They express CCR6 and are therefore attracted by its ligand, CCL20 which is present in the tumor microenvironment<sup>176</sup>. T<sub>H</sub>22-derived IL-22 promotes the activation of signal transducer and activator of transcription 3 (STAT3) transcription factor, increasing the expression of histone H3 lysine 79 (H3K79) methyltransferase DOT1L<sup>176</sup> and of the H3K27 methyltransferase polycomb repressive complex 2 (PRC2). All together leads to increased proliferation, and stem expression of stemness genes such as NANOG, SOX2, and POU5F<sup>176,177</sup>.

#### - Recruitment of Treg cells.

Classical Tregs are CD4<sup>+</sup> CD25<sup>+</sup> FoxP3<sup>+</sup> T cells, which down-modulate T cell antitumor immunity by releasing soluble factors and by direct contact<sup>178</sup>. This T cell-mediated suppression may favor tumor growth and therefore is related to poor patient outcomes<sup>179,180</sup>. Treg cells express CCR4 and are chemoattracted to the tumor microenvironment in response to its ligand CCL22 which is mainly secreted by macrophages and tumor cells<sup>180</sup>. Tregs also express CCR10 and therefore migrate towards hypoxic regions from the tumor microenvironment that are enriched in CCR10 ligand, CCL28<sup>181</sup>. High amounts of Treg cells are commonly found in the bone marrow of patients with cancer<sup>182</sup> facilitating immunological tolerance and tumor metastasis to this site. In the tumor microenvironment, Treg cells have been reported to express inflammatory cytokines, like CXCL8<sup>183</sup> and IL17<sup>184</sup>, mediating T cell suppression and promoting inflammation.

#### - Recruitment of plasmacytoid DCs.

pDCs mainly inhabit and recirculate through lymphoid organs, where they represent 0.1%–0.5% of nucleated cells<sup>185</sup>. They express integrin  $\alpha$ 5 (VLA5) and CXCR4, the latter is responsible for their migration towards inflammatory sites such as tumors, where high levels of its ligand CXCL12 are found. pDCs act locally, promoting tumor angiogenesis and inflammation through the production of massive interferon I (INF-I) and proinflammatory chemokines such as CXCL4<sup>185,186</sup>. pDCs also induce Tregs to produce IL10 leading to increased tumor progression and immunological tolerance<sup>186-188</sup>.



**Figure 9. Pro-tumor effects of chemokines.** Among all immune cell populations, gMDSCs and mMDSCs, Treg cells, IL-22 + CD4<sup>+</sup> T<sub>H</sub>22 cells, IL-22 + ILCs and pDCs are some known to promote tumor growth. These cells are recruited to the tumor microenvironment in response to different chemokines. These pro-tumor immune cells are capable to inhibit antitumor immune responses, as well as advocating cancer progression along with angiogenesis and cancer stemness. Figure from<sup>158</sup>

### - Recruitment of macrophages.

Macrophages originate from bone-marrow derived monocytes and their main functions are killing microorganisms, removing dead cells and stimulating other immune cells. Tumor-associated macrophages (TAMs) are one of the main tumor-infiltrating immune cells and they are known to take part in the tumor microenvironment formation<sup>189</sup>. They express CCR2 and can be gathered at the tumor microenvironment by CCL2-CCR2 signaling pathway<sup>190</sup>. There is a positive correlation between CCL2 expression and the presence of TAMs which is usually associated with poor prognosis<sup>172</sup>. TAMs may promote tumor growth, invasion and metastasis, they express inhibitory B7 family members such as PD-L1 to inhibit TAA-specific effector T cells<sup>191-194</sup>. Furthermore, TAMs also favor chemoresistance<sup>195</sup> and boost cancer stemness and metastasis<sup>167,172,189</sup>.

### 2.2.3. Chemokines promoting anti-tumoral immunity

Those chemokines with anti-tumoral properties are called Angiostatic. They have been shown to recruit T CD8<sup>+</sup> cells, natural killer T (NKT) cells, T<sub>H</sub>1, and polyfunctional T<sub>H</sub>17 cells to the tumor microenvironment through chemokine-chemokine receptor signaling pathways (**Figure 10**).

#### - Recruitment of T<sub>H</sub>17 cells.

T<sub>H</sub>17 cells are CD4<sup>+</sup> T cells with an essential role in inflammation and autoimmune diseases. Regarding tumor immunity, T<sub>H</sub>17 has a dual function favoring but also inhibiting tumor growth<sup>196</sup>. They have high levels of CCR6, CXCR4, CD49 integrins and the C type lectin like receptor CD161<sup>197-200</sup> which favor their migration and accumulation within tumors and inflammatory tissues<sup>197,199,201,202</sup>. CXCL12, a ligand for CXCR4, and CCL20, a ligand for CCR6, are both present in the tumor microenvironment (TME), facilitating T<sub>H</sub>17 trafficking. Once in the TME, T<sub>H</sub>17 will further recruit NK cells, CD8<sup>+</sup> T cells, and DCs, favoring tumor regression<sup>197,199,202,203</sup>. CCR6-expressing cells, -such as macrophages, and B cells (discussed below), are also called up and once in the TME, they can initiate and broaden the effector immune cells locally, promoting tumor regression<sup>158</sup> **Figure 10**. CD8<sup>+</sup> T cells that are directed against specific TAAs, may induce anti-tumor immunity by secretion of effector cytokines and cytotoxic molecules such as granzyme B or perforin among others, promoting apoptosis of cancer cells<sup>83,84,158,197,204-206</sup>.

#### - Recruitment of myeloid DCs.

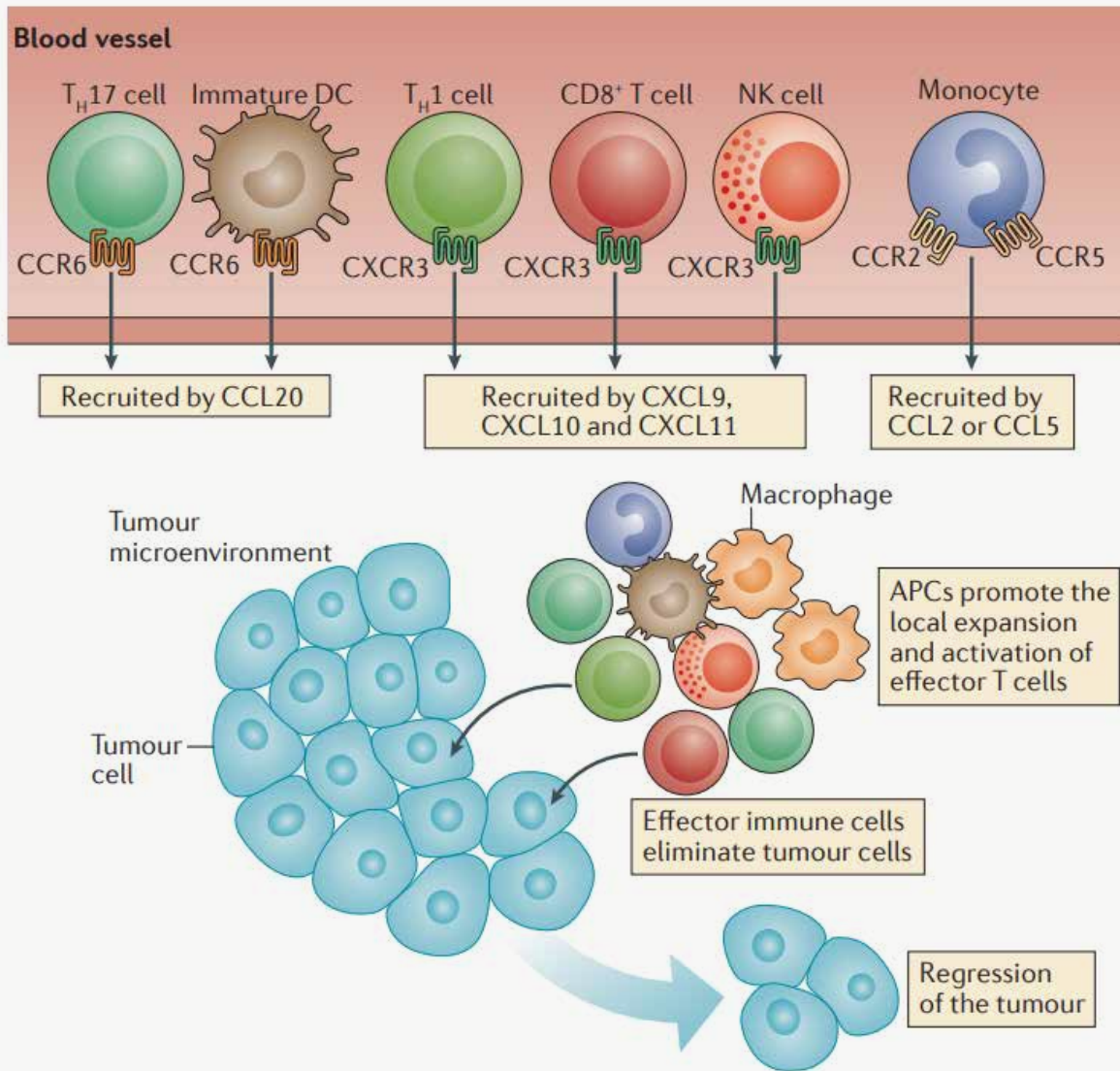
Myeloid DCs are a heterogeneous APCs population with proinflammatory or regulatory properties depending on the TME<sup>207</sup>. They express CCR6 and may migrate into tumors in response to CCL20 and induce tumor progression<sup>208,209</sup>. Nonetheless, CCL20 also promotes the maturation of DCs at the TME, resulting in the inhibition of tumor growth<sup>210</sup> through the priming and activation of TAA-specific effector T cells<sup>211</sup>.

#### - Recruitment of NK and NKT cells.

Both cell subsets are part of the innate immune system and share anti-tumor functions; however, they display distinct dynamics and distributions along the disease progression. Interestingly, at early cancer stages both have effector activity, while in later stages NKs become senescent while NKT cells are exhausted and therefore exhibit defective cytotoxic capacities<sup>212</sup>. NKT cells are divided into two subtypes based on the expression of their T cell receptor (TCR). Type I NKT cells present an invariant TCR $\alpha$ -chain (Va24 in humans) and type II NKT cells have diverse TCRs<sup>213</sup>. Type I NKT cells mainly have antitumor activities as they produce IFN $\gamma$  to activate more NK cells and CD8<sup>+</sup> T cells. Besides the IFN $\gamma$  mechanism, NKT cells also activate DCs to produce IL-12 favoring the antitumor activity<sup>214</sup>. Type II NKT cells are less known than Type I but they may recognize lipids by CD1d through their TCRs, and represent a different effector T cell population with both, protective and pathogenic immune-regulatory properties<sup>213-215</sup>. Most NKTs express non-lymphoid homing or inflammation-related chemokine receptors including CCR2, CCR5, and CXCR3<sup>216</sup>.

#### - Recruitment of T<sub>H</sub>1 immune cells.

T<sub>H</sub>1 cells are CD4<sup>+</sup> helper T cells that when active, as NKT type I, secrete IFN $\gamma$ , showing strong antitumoral effects in the TME<sup>217</sup>. These cells express CXCR3 whose ligands are CXCL9 and 10. Increased levels of CXCL9 and CXCL10 are associated with increased numbers of tumor-infiltrating immune cells and correlate with decreased levels of metastasis and a better outcome for patients<sup>83,84,204-206</sup>.



**Figure 10. Tumor immunity promotion by chemokines.** Recruitment of immune cells with antitumor activity, like CD8<sup>+</sup> T cells, T<sub>H</sub>1 cells, NK, and polyfunctional T<sub>H</sub>17 cells, via chemokine–chemokine receptor signaling pathways. Macrophages, DCs, and APCs migrate into the tumor microenvironment and may activate and expand other local effector immune cells, favoring the regression of the tumor. Figure from<sup>158</sup>

### - Recruitment of B cells.

The antitumoral role of tumor-infiltrating B lymphocytes (TIL-Bs) prevails controversial as they may exert different functions depending on their type and developmental state. Also, the majority of studies have focused on cellular response and the role of T cells, and, as a consequence, the clinical relevance is mostly associated with the T-cell lineage<sup>218–220</sup>. A useful marker to differentiate B cells is CD20, also known as B cell surface marker<sup>221</sup>. It is expressed in tumor-infiltrating B cells (TIBs) from early to late stages of differentiation (naive and memory B cells) and it is downregulated, as they differentiate into plasma cells (PCs)<sup>222</sup>. TIBs express CXCR4 and may be attracted to the tumor microenvironment by CXCL12. They can also be found in tumor-associated TLS being attracted by CXCL13<sup>223,224</sup>. When infiltrated in tumors they increase T cell responses by producing antibodies, cytokines, and chemokines, and may act as APCs, which has been associated with better survival<sup>225–227</sup>. Regulatory B cells<sup>228</sup> are a subset of B cells that are recruited into the TME and that also display different roles in tumor immunity

and tumorigenesis. Some studies have reported that regulatory B cells may negatively regulate tumor immunity and promote tumor progression via IL10, IL-35 and transforming growth factor $\beta$  (TGF- $\beta$ ), inducing tumor angiogenesis, decreasing CD4 and CD8 effector T cells response and recruiting tumorpromoting immune cells<sup>229-232</sup>.

To sum up, a wide variety of chemokines play a role in the recruitment of immune cells into the TME through the corresponding chemokine-chemokine receptor signaling. There, these immune cell populations are able to target both, tumor and stromal cells and either promote or abrogate tumor growth.

Given that this project is focused on the CXC family of chemokines, the following sections will review their roles in tumor growth and progression as well as in response and resistance to treatment, specifically in CRC.

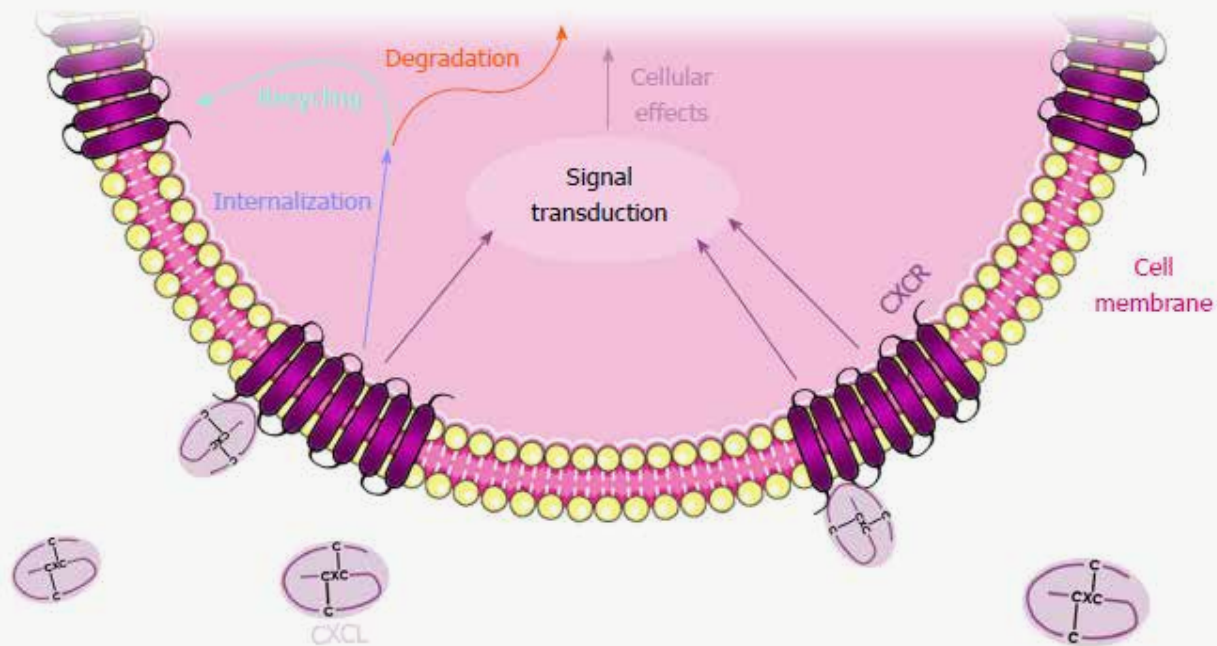
#### 2.2.4. The CXC family of chemokines

CXC chemokines are composed of 17 members of which CXCL15 is only present in mice and not in humans<sup>233</sup>. The CXC chemokines nomenclature is “CXCLx”, where the L refers to “ligand” and the x stands for a number. As explained before (see section 2.2.1), CXC chemokines share a common structure and chemotactic activity<sup>159</sup>. Interestingly, although CXCL17 is certainly chemotactic, from the structural point of view, it does not follow the classic CXC-type cysteine archetype and therefore, its belonging to the CXC family is discussed<sup>234</sup>.

OFFICIAL NAME	ALTERNATIVE NAME	RECEPTOR	EFFECT ON THE RECRUITMENT AND ACCUMULATION OF CELLS INTO THE TUMOR NICHE	EFFECT ON ANGIOGENESIS IN A TUMOR
CXCL1	GRO- $\alpha$	CXCR2	MDSC, MSC, TAN, Treg	Angiogenic
CXCL2	GRO- $\beta$	CXCR2	MDSC, TAN	Angiogenic
CXCL3	GRO- $\gamma$	CXCR2	TAN	Angiogenic
CXCL4	PF-4	CXCR3	TIL, Treg	Angiogenic
CXCL5	ENA-78	CXCR2	MDSC, TAN	Angiogenic
CXCL6	GCP-2	CXCR1, CXCR2	TAN	Angiogenic
CXCL7	NAP-2	CXCR2	TAN, TAM	Angiogenic
CXCL8	IL-8	CXCR1, CXCR2	MSC, TAM, TAN, MDSC	Angiogenic
CXCL9	MIG	CXCR3	TIL, Treg	Angiostatic
CXCL10	IP-10	CXCR3	TIL, Treg	Angiostatic
CXCL11	I-TAC	CXCR3, CXCR7	TIL, Treg	Angiostatic
CXCL12	SDF-1	CXCR4, CXCR7	MDSC, MSC, TAM, TAN, Treg	Angiogenic
CXCL13	BCA-1	CXCR3, CXCR5	MDSC, Treg	Angiostatic
CXCL14	-	Unkown	CAF, TIL	Angiostatic
CXCL16	-	CXCR6, mCXCL16	MSC, TAM, TIL, Treg	Angiogenic
CXCL17	VCC-1	CXCR8	MDSC	Angiogenic

**Table 2. List of human CXC chemokines, their CXCR binding receptors, and some of their angiogenic/angiostatic effects on selected cancer processes.** CAFs-cancer-associated fibroblasts; mCXCL16-transmembrane CXCL16; MSCs-mesenchymal stem cells; TANS-tumor-associated neutrophils. Table, slightly modified from<sup>233</sup>

CXC chemokines are classified as angiogenic or angiostatic depending on the presence (angiogenic) or absence (angiostatic) of the glutamic-leucine-arginine (ELR) motif at the N-terminal (**Table 2**). After binding to their corresponding CXCR, which in most cases is a 7-transmembrane G protein-coupled receptor, the latter is generally internalized by virtue of clathrin-mediated endocytosis, activating the coupled G protein, changing their conformation and initiating the corresponding signaling pathway<sup>159,235</sup>. Afterward is degraded or recycled into the plasma membrane (**Figure 11**). The unique exception is the CXCR7/ACKR3 which is classified as an atypical receptor as it is coupled to  $\beta$ -arrestins and not to the classic G protein<sup>236</sup>. As shown in **Table 2**, the same receptor can bind to different chemokines, and vice versa<sup>233</sup>.



**Figure 11. CXCL and CXCR regulatory mechanisms.** CXCL binding to the CXCR, which is located at the cellular membrane. Followed by CXCR internalization and signal transduction at the nucleus. Consequently, after the internalization, it gets degraded or recycled at the plasma membrane. Figure from<sup>159</sup>

### 2.2.5. CXC chemokines and their receptors role in CRC

Considering that chronic inflammation is one of the main risk factors for CRC<sup>158</sup>, countless pieces of evidence demonstrated that CXC chemokines and their receptors participate in most stages of CRC development. Also, there is scientific evidence regarding their possible role in response to therapy and chemoresistance. We published a review in 2018 that addressed most findings in the field (**Annex I**). In the following sections, the role of the different axes in CRC pathogenesis, as putative prognostic and/or predictive biomarkers and as drug target candidates are discussed<sup>159,237</sup>.

#### **CXCR1 and CXCR2 axes:**

The CXCR1/CXCR2 axis is the most extensively investigated pathway in cancer. CXCL1, 2, 3, 5, 6, 7, and 8 are all angiogenic chemokines, which share the same receptor, CXCR2. Several reports have demonstrated the upregulation of all these chemokines in CRC and their participation at different stages of the disease<sup>159,238-240</sup>. For instance, CXCL1 facilitates cell seeding and distant metastasis outgrowth<sup>241</sup>. It has been

reported to promote cancer cells' proliferation, migration, and invasion, as well as resistance to anticancer drugs and it has been proposed as a promising therapeutic target for mCRC<sup>159,242</sup>. However, further trials are needed to evaluate its potential translation to the clinics<sup>241,242</sup>. CXCL5 was found at higher levels in the serum and in FFPE tumors from CRC patients as compared to healthy controls<sup>238</sup>. CXCL7 promoted invasion and angiogenesis through the PI3K/AKT/mTOR signaling pathway and its overexpression correlated with worse prognosis in CRC patients<sup>240</sup>. CXCL8 (also known as IL-8) can be regulated by inflammatory signals, environmental and chemical stress, and by other stimuli such as steroid hormones<sup>243,244</sup>. It is mainly associated with neutrophil migration which promotes tumor growth, angiogenesis, motility, and invasion<sup>245,246</sup>. Tumor-derived CXCL8 will activate CXCR2-endothelial cells in the tumor vasculature promoting angiogenesis and at the same time attracting more neutrophils into the tumor site<sup>244</sup>. In vitro studies have shown that CXCL8-overexpressing CRC cell lines proliferated, migrated, and invaded more than control cell lines. When injected into immunodeficient mice they were able to develop a higher number of tumors that in turn were more vascularized as compared to controls<sup>247</sup>. CXCL1, CXCL2 and CXCL8 genes are transcribed by the NK- $\kappa$ B transcription factor; CRC cell lines with acquired resistance to oxaliplatin were shown to have this transcription factor hyperactivated, consequently leading to an overexpression of these 3 chemokines<sup>104</sup>. Several studies have demonstrated the metastatic potential of CXCL8 and its receptors, CXCR1/2<sup>248</sup>. Aiming a CXCL8-rich TME, a novel immunodeficient skin-specific CXCL8-expression transgenic mice model was generated in the study of Lee et al. When human and mouse CRC cells were subcutaneously injected, tumors were formed, and the CXCL8 present in the TME favored their growth, angiogenesis and increased cell extravasation to the lung and liver. In parallel, they also reported reduced colon cancer cell growth and metastasis development in a CXCR2-KO mice model<sup>249</sup>. In agreement, blocking CXCR1 and CXCR2 using an antagonist, resulted in increased tumor cell apoptosis and reduced metastasis<sup>250</sup>. Moreover, high serum levels of CXCL8 are associated with advanced CRC, distant metastases, and shorter CRC overall survival<sup>247,249</sup>.

### **CXCR4 and CXCR7 axes**

CXCR4 (Fusin) and its ligand CXCL12 (Stromal cell-derived factor 1) have a well-known role in metastasis development<sup>251-253</sup>. In CRC liver metastasis, CXCL12 is secreted by the Kupffer cells and by endothelial cells<sup>254</sup> and several studies have demonstrated that high CXCR4 expression in CRC patients is associated with liver metastasis<sup>255,256</sup>. In stage II-III CRC patients, overexpression of CXCR4 was strongly associated with earlier relapse. CXCR4 induced CRC cells clonogenic growth by releasing VEGF and upregulating the intercellular adhesion molecule 1 (ICAM-1)<sup>257</sup>. CXCR4 colocalizes with CRC stem cell markers like CD133 and CD44, which are associated with the epithelial-mesenchymal transition (EMT) process<sup>159</sup>. In 165 stage II-III CRC patients from the National Cancer Centre Hospital in Tokyo (Japan), high CXCL12 protein levels in the primary tumors, were associated with poor prognosis<sup>258</sup>. Also, increased mRNA levels of the receptor CXCR4 in primary CRC tissue have been associated with poor survival rates in stage IV CRC patients<sup>255</sup>. In addition, high concomitant expression of CXCR4 and VEGF proteins in primary CRC tissue predicted early distant relapse in stage II-III CRC patients<sup>257</sup>. Moreover, similar findings on CXCR4 association with tumor progression and low survival were reported from CXCR4 transcriptional levels in a systematic meta-analysis of 3794 stage I-IV CRC patients<sup>255,257,259,260</sup>. CXCR7 (ACKR3) also interacts with CXCL12, and when overexpressed in CRC cell lines, it induced angiogenesis through the activation of the AKT and ERK signaling pathways<sup>261</sup>. In addition, it was found to be overexpressed in metastatic lung tissue, together with CXCL12 when compared to primary lesions<sup>262</sup>. Moreover, substantially higher levels of CXCL12 were found in

malignant lung tissue when compared to benign tissue<sup>263</sup>.

### **CXCR3 axis**

Controversial results have been reported about the role of this axis in CRC. On one hand, CXCR3 and its ligands CXCL9 and CXCL10 were positively associated with lymph node metastasis and poor survival of CRC patients<sup>264</sup>. Moreover, levels of CXCL10 in serum from CRC patients increased according to the progression of the disease and correlated with the presence of distant metastases<sup>270</sup>. However, in a study cohort of 64 stage II and III CRC patients low levels of CXCL10 was an independent biomarker of prognosis and recurrence<sup>265</sup>. Other groups demonstrated that CXCL10 co-expression with its receptor CXCR3, predicted metastatic recurrence and therefore, poor CRC prognosis<sup>266</sup>. Nevertheless, the use of AMG487, a CXCR3 inhibitor, resulted in the inhibition of metastatic growth and implantation of CRC, in an in vivo model<sup>267</sup>.

### **CXCR5/CXCL13 axis**

The CXCL13 chemokine, originally known as BCA-1 (B cell-attracting chemokine 1), is secreted in B-cell areas of secondary lymphoid tissues (follicles of the spleen, tonsils, and lymph nodes). It is constitutively secreted by stromal cells<sup>268-271</sup>, and in humans, it is mainly produced by CD4<sup>+</sup> follicular helper T cells (TFH)<sup>272</sup>. Its associated receptor is CXCR5, although Jenh et al suggested that it could also bind to CXCR3 (**Table 2**). CXCL13 is the most important chemokine in controlling the migration of CXCR5-highly expressing B lymphocytes<sup>273-276</sup>. Nevertheless, it can also attract some T cell populations (such as TFH cells) and macrophages<sup>268,269,277</sup>. CXCL13 expression in lymphoid tissues guarantees the efficiency of naïve B cells in antigen presentation during emergent immune reactions<sup>278</sup> and abnormal signaling or expression of CXCL13/CXCR5 is usually associated with the onset of disease. The unusual expression of CXCL13 also promotes lymphoid neogenesis, also known as functional ectopic lymphoid structures or TLSs<sup>279-281</sup>. These TLSs are commonly found under chronic inflammation (infection, cancer, and autoimmune disease) in non-lymphoid tissues<sup>282</sup>, where they will induce local adaptive immune responses<sup>280,283</sup>. Friedman et al proposed a strategy that consisted of the induction of TLS formation in tumors treated with immunotherapy, aiming at better clinical outcomes and prognosis<sup>224</sup>. Unfortunately, the way TLSs are formed as well as their contribution to the tumor fate is not fully understood yet<sup>282</sup>. Bindea et al found increased levels of CXCL13 in human CRC tumors which activated TFH cells that in turn, increased intra-tumoral volume of B, TFH, T<sub>H</sub>1, cytotoxic, and memory T cells, generating a positive feedback loop<sup>284</sup>. Thus, both high numbers of CXCL13 and TFH cells may predict better survival in CRC patients<sup>285</sup>. In line with these results, low expression levels of CXCL13 in tumoral tissue from stage II CRC patients, have been described as a bad prognostic marker<sup>286,287</sup> and a CXCR5<sup>+</sup> CD8<sup>+</sup> T cells subset was shown to have anti-tumoral activity<sup>288</sup>. Nevertheless, other authors have reported contradictory results; for instance, Zhu et al<sup>289</sup> suggested that CXCL13 promotes proliferation, migration, and invasion of CRC via the PI3K/AKT pathway in CRC; also, increased CXCL13 in plasma from patients and high expression of CXCR5/CXCL13 in tumors, were associated to a worse prognosis in metastatic CRC<sup>290,291</sup>. Apparently, a possible explanation for these paradoxical results could be the influence of different factors, such as patients' molecular subtype, the treatments the patients received or the tumor stage, among others<sup>159</sup>.

### **CXCL16/CXCR6 axis**

CXCL16 is a particular chemokine as the CXCL16 gene is located in chromosome 17p13 which is different from the rest of CXCs<sup>292</sup> and shows little homology with them<sup>293</sup>. CXCL16 has the peculiarity of having a soluble and secreted domain (sCXCL16) and a transmembrane domain (mCXCL16)<sup>292</sup>. CXCL16 is cleaved by a disintegrin and metallo-

proteinase 10 (ADAM10)<sup>294-296</sup>. In the absence of ADAM10, ADAM17 may also cleave it<sup>297</sup>. sCXCL16 acts as a chemoattractant of cells that present the CXCR6 receptor<sup>292,293</sup>. In contrast, mCXCL16 is a transmembrane protein responsible for protein adhesion after binding to CXCR6<sup>298,299</sup>. mCXCL16 may also function as a membrane receptor by binding to either CXCR6<sup>300</sup> or sCXCL16<sup>301</sup> a mechanism known as reverse and inverse signaling, respectively<sup>302</sup>. Although it is classified as an angiostatic CXC chemokine, several reports have proven its activity as an angiogenic CXC in CRC<sup>159,303</sup>. Thus, CXCL16 expression has been found to be higher in colorectal tumors than in adjacent non-cancerous tissues or than in tissues from healthy subjects<sup>304,305</sup>. High CXCL16 levels were also observed in regional lymph nodes, which was associated with worse OS in CRC patients<sup>306</sup>. In a study with 314 CRC patients and 20 normal volunteers, the serum levels of CXCL16 were higher in patients than in healthy individuals, increased across the different tumor stages, and were associated with a poor prognosis<sup>307</sup>.

Considering all of the above and the fact that these small proteins can be found in the peripheral blood of CRC patients, it seems logical that they could serve as biomarkers in CRC.

Moreover, their clearly pro-tumoral role in some cases has generated interest in the pharmaceutical industry, which has developed several inhibitors. The most relevant drugs to date are summarized below.

### **2.2.6 Therapeutic strategies targeting CXC chemokines in cancer**

In the last years, growing evidence on the different effects that chemokines and their receptors have in the tumor inflammatory microenvironment has motivated the pharmaceutical industry towards efficient therapeutic approaches targeting CXC chemokines and their CXC receptors<sup>159,308</sup>. The main strategy would consist of complementing current cancer treatments to increase their effectiveness. Many of these therapeutic designs are aimed to block the CXC receptors and mostly consist of antibodies and small antagonist molecules<sup>158,308</sup>. **Table 3** summarizes the latest modulators that have entered clinical trials targeting the CXC/CXCR signaling axes in cancer.

Targeting the CXCR1/2 signaling axes

Several clinical trials are currently assessing the safety and efficacy of different CXCR1/2 antagonists in different tumor types (**Table 3**). In a phase I clinical trial of HER-2 negative metastatic breast cancer patients, the oral administration of a non-competitive CXCR1/2 antagonist (Reparixin) in combination with Paclitaxel, displayed a 30% of responsiveness (NCT02001974)<sup>309</sup>. Navarixin (MK-7123), with oral bioavailability, is currently being evaluated in advanced/metastatic solid tumors including CRC (NCT03473925). Also, the potential of CXCL5 as a biomarker is being tested in urothelial carcinoma (UC). The aim of the clinical study is to evaluate its expression in UC by IHC, determining its role in proliferation, migration and cancer spreading (NCT05139134).

#### **Targeting CXCL12/CXCR4 signaling axis**

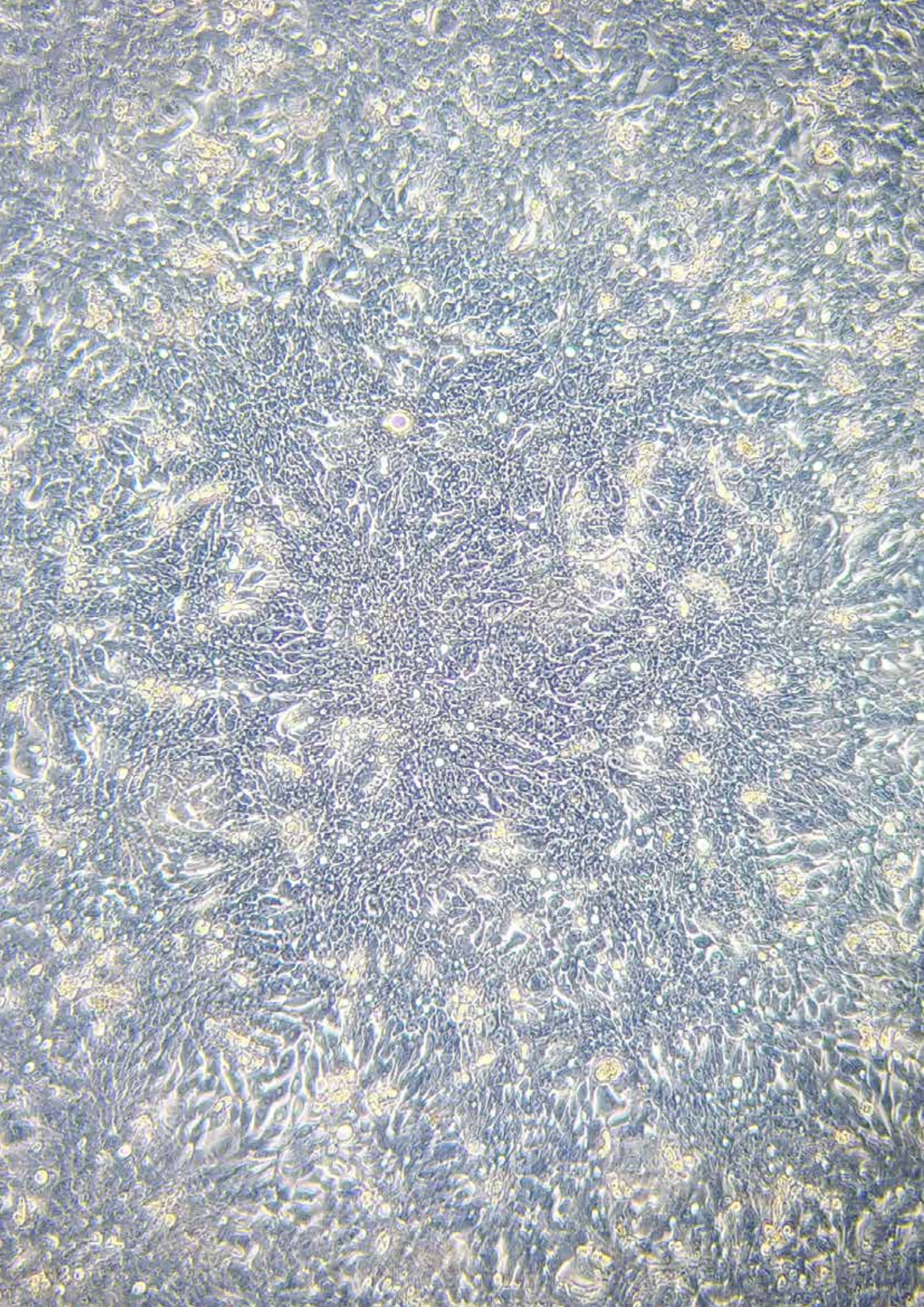
A phase I clinical trial (NCT03168139) evaluated the safety and tolerability of Olaptosed pegol, a CXCL12 inhibitor, and the changes in the TME induced by this drug as monotherapy in mCRC patients with liver metastasis. The treatment resulted safe for the participants and demonstrated an antitumoral effect. Another phase I trial (NCT02737072) testing LY2510924 in advanced solid tumors (colorectum, lung, breast, and prostate) resulted in a primary response rate of 20%. Additionally, the dose of 20mg/day was established based on the best tolerability and clinical safety<sup>310</sup>. Finally, a phase II trial

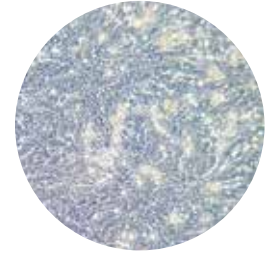
(NCT02907099) in metastatic pancreatic cancer studied the efficacy of the CXCR4 antagonist BL-8040 plus pembrolizumab. BL-8040 blocks some of the enzymes involved in tumor growth and increases T cell infiltration.

Several new CXC/CXCR therapeutic targets have been proposed, although not tested yet in clinical trials. All these research data aim to accelerate the translation of chemokine research into cancer precision medicine<sup>256,311,312</sup>.

TARGET	DRUG NAME	CONDITIONS	PHASE	STATUS	TRIAL NUMBER
<b>CXCL5</b>	Immunohistochemical expression of CXCL5	Urinary bladder urothelial carcinoma	Not Applicable	Recruiting	NCT05139134
<b>CXCR2</b>	AZD5069	Combination with enzalutamide in metastatic castration resistant prostate cancer	I/II	Active, not recruiting	NCT03177187
	Reparixin	Combination with Paclitaxel in metastatic Breast Cancer HER2 negative	I	Completed	NCT02001974
	Reparixin + PTX	Combination with Paclitaxel in metastatic Breast Cancer Triple-Negative (fRida)	II	Completed	NCT02370238
	AZD5069	Metastatic Pancreatic Ductal Adenocarcinoma	Ib/II	Completed	NCT02583477
	Navarixin	Combination with pembrolizumab advanced/metastatic solid tumors	II	Completed	NCT03473925
	CXCR2 ligands/CXCR2	Biological axis in pancreatic cancer	Not Applicable	Completed	NCT00851955
	CXCR2-transduced autologous tumor infiltrating lymphocytes	Metastatic melanoma	I/II	Active, not recruiting	NCT01740557
<b>CXCL12</b>	NOX-A12	Combination with irradiation in glioblastoma	I/II	Recruiting	NCT04121455
	NOX-A12	Combination with pembrolizumab in advanced colorectal and pancreatic cancer	I/II	Completed	NCT03168139
<b>CXCR4</b>	BL-8040	Combination with pembrolizumab in metastatic pancreatic adenocarcinoma	II	Active, not recruiting	NCT02907099
	LY2510924	Advanced solid tumors	I	Terminated	NCT02737072
	USL311	Solid tumors, relapsed/recurrent glioblastoma multiforme	I/II	Terminated	NCT02765165
<b>CXCR5</b>	CXCR5 modified EGFR CAR-T cells	Nonsmall cell lung cancer	I	Recruiting	NCT04153799 NCT05060796

**Table 3. Summary of the most recent clinical trials on CXC/CXCR in cancer.** Highlighted in light purple are those in CRC. Data from<sup>313</sup>





## 02

# Hypothesis and objectives

### HYPOTHESIS

Worldwide, CRC is the third most common cancer considering both sexes and represents the second most common cause of cancer-related death. CRC patients' survival is related to the tumor stage at the time of diagnosis. While treatment options rapidly increase for other types of cancer, only a few advances have been made in the treatment of CRC in the last decades. In the advanced disease, first-line treatment is based on the combination of chemotherapy (a fluoropyrimidine with oxaliplatin or irinotecan) plus an anti-EGFR antibody (cetuximab or panitumumab only in RAS WT patients) or an anti-angiogenic drug (Beva). In this setting, 5-year survival rates are less than 10%, being chemotherapy resistance the main reason for disease progression. Therefore, finding useful and reliable predictive and prognostic biomarkers, along with druggable targets is necessary, to optimize the efficacy of current and upcoming treatments. It has been proposed that serum levels of certain chemokines may be used as predictive markers of response to chemotherapy. CXC chemokines are a family of small cytokines (8 to 10 kDa), that signal through G-protein-coupled receptors, CXCRs. Secreted by tumor cells, leukocytes, fibroblasts, endothelial and epithelial cells, they chemoattract several cell types such as neutrophils and lymphocytes, fibroblasts, and eosinophils. All these cell populations have diverse effects on tumor progression, depending on which are being attracted to the tumor microenvironment by the CXC chemokines. Additionally, in CRC we reported that CRC cell lines with acquired resistance to oxaliplatin overexpressed and secreted high amounts of some CXC chemokines including CXCL1, CXCL2, and CXCL8, because of an acquired hyperactivation of the NF- $\kappa$ B pathway. Also, in an *in silico* series of 98 CRC MSS, stage II adenocarcinoma tissues, we observed that except for

CXCL12, all CXC chemokines showed significant overexpression in tumors as compared to adjacent normal tissues and that high expression of CXCL1, 2, 5, 6, and 8 correlated with worse disease-free survival.

Hence, considering all the above, together with the fact that CXC chemokines are secreted, and therefore can be easily detected in the blood of patients, we hypothesize that the CXC chemokine profile found in the serum of mCRC patients treated with OXA-based schedules as first-line treatment, may predict tumor response and/or prognosticate patients' outcomes, representing useful biomarkers in this disease. If our hypothesis is confirmed, our results may contribute to a better-personalized treatment and improved patient outcomes. To test our hypothesis, we propose the following objectives:

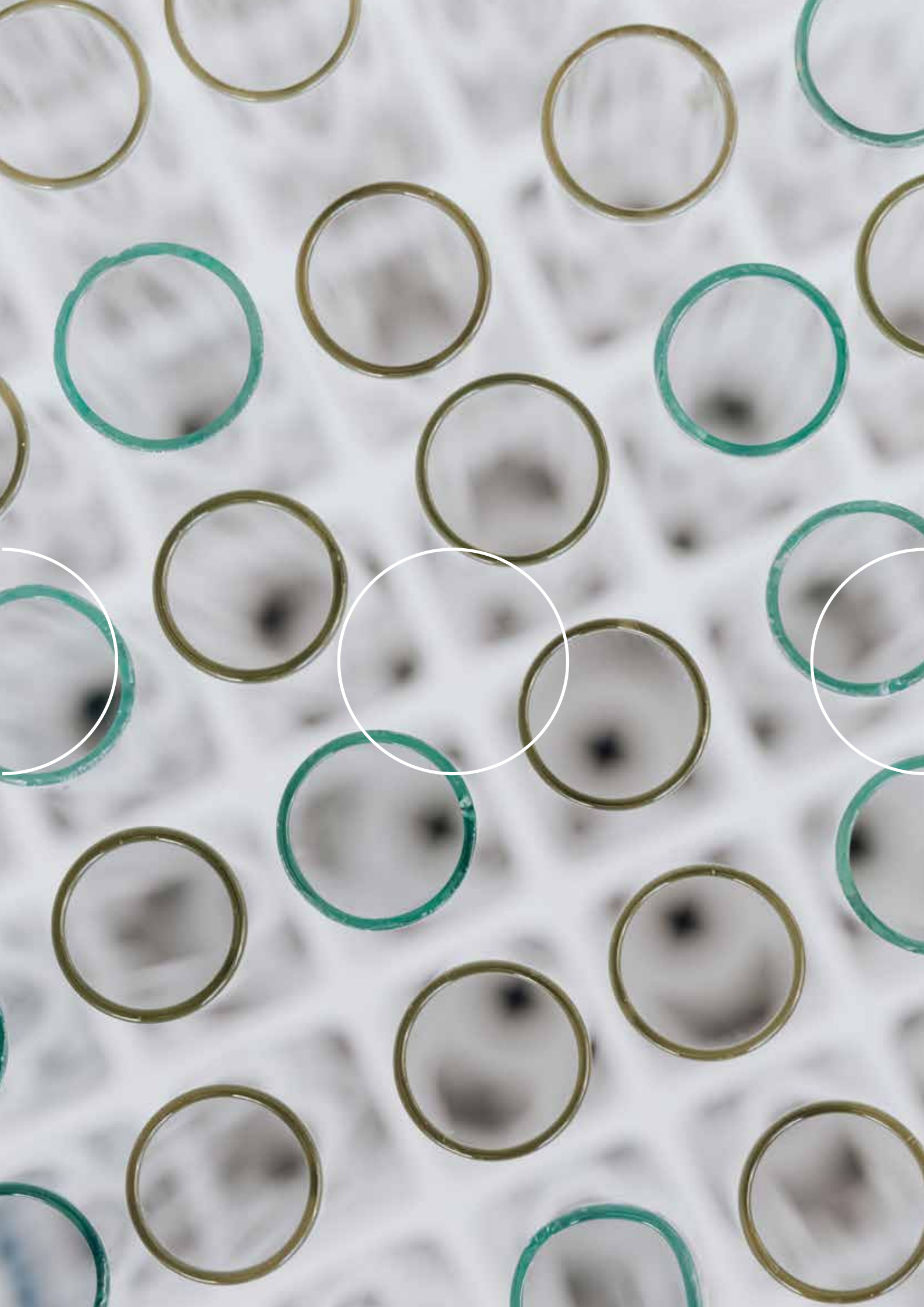
## OBJECTIVES

This project's main objective is to study the prognostic and/or predictive value of a panel of CXC chemokines in the serum of mCRC treated with OXA-based first-line treatments and to determine their applicability as biomarkers.

To achieve this goal, the specific aims of this thesis are:

- 1.** To obtain a collection of mCRC patients' serum samples: we will prospectively and consecutively collect serum samples from at least 100 mCRC patients that are going to receive an OXA-based-first-line treatment. Additionally, we will also collect these patients' primary tumors conserved in paraffin blocks. We will generate a database with relevant clinicopathological and molecular characteristics of the mCRC patients included in the study and will study their possible associations with outcome.
- 2.** To perform a Luminex-based study of a panel of eleven CXC chemokines in the mCRC patients' serum samples and to correlate the CXC levels with i) the patients' clinicopathological and molecular characteristics; ii) response to treatment; iii) overall survival and iv) progression-free survival.
- 3.** To study the expression of those CXC Chemokines with prognostic/predictive value in our patients' primary tumors by IHC staining or Nanostring® techniques. We will also evaluate other related factors. To perform an *in silico* analysis using publicly available transcriptomic data from CRC metastases.
- 4.** To analyze the serum levels of the resulting prognostic/predictive chemokines in a cohort of healthy controls and compare them to the levels obtained in our patients.
- 5.** To confirm our results in a similar independent cohort of patients.







## 03

# Materials and methods

### 1. STUDY DESIGN, PARTICIPATING HOSPITALS AND INCLUSION CRITERIA

This project consists of an experimental, longitudinal and prospective multicentric study, in which the main objective is to elucidate if levels of CXC chemokines found in patients' serum, may be prognostic or predictive biomarkers in mCRC. Five different hospitals from Catalonia have participated in the study: Dr. Josep Trueta Hospital (Girona), Vall d'Hebron Institute of Oncology (VHIO, Barcelona); Moises Broggi Hospital (Sant Joan Despí), Duran I Reynals Hospital (L'Hospitalet de Llobregat) and our institution, Germans Trias I Pujol University Hospital (Badalona) (**Table 4**). This study was coordinated by my thesis director Dr. Eva Martínez-Balibrea and myself. A Newsletter was used to update all collaborators monthly (**Annex II**). The study was approved by the Germans Trias I Pujol University Hospital Ethics Committee on the 22<sup>nd</sup> of July 2016 and with internal reference number IP-16-115.

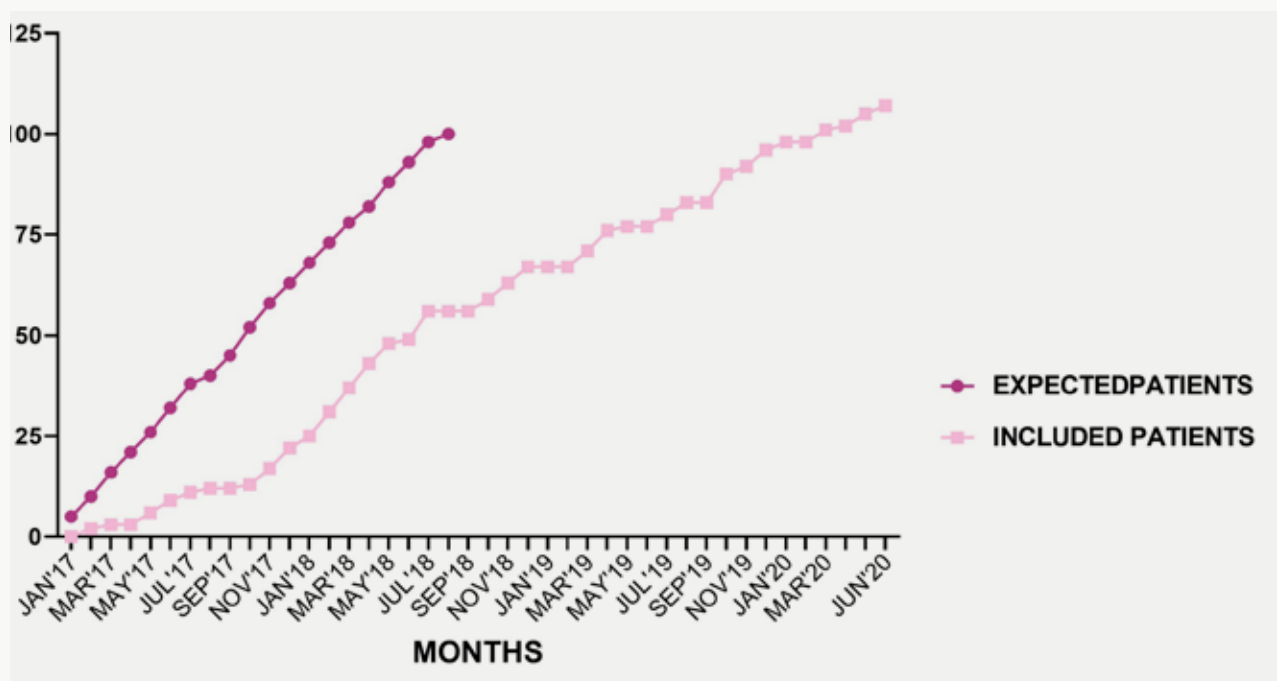
Calculation of the sample size in an exploratory study is complex but reaching the stipulated N to draw any conclusions with sufficient robustness was a requirement for us. To increase the probability of recruiting the minimum number of patients in the lesser time, we collaborated with five different hospitals (mentioned above). The estimated recruiting time was 18 months and the expected number of cases that each center could recruit can be found in **Table 4**. This was based on inclusion criteria, and an estimation of the number of mCRC cases each center treats per year.

PATIENTS INCLUDED IN THE STUDY		
PARTICIPATING HOSPITALS	EXPECTED PATIENTS	INCLUDED PATIENTS
DR. JOSEP TRUETA HOSPITAL	15	37
DURAN I REYNALS HOSPITAL	25	35
VALL D'HEBRON HOSPITAL	100	15
MOISES BROGGI HOSPITAL	15	13
GERMANS TRIAS I PUJOL UNIVERSITY HOSPITAL	30	7
<b>TOTAL OF PATIENTS</b>	<b>185</b>	<b>107</b>

**Table 4.** Participating hospitals and the number of patients expected and finally included in the study.

Taking all these into consideration, it was decided that the inclusion of 100 cases was feasible; we then calculated the magnitude of the differences that we would be able to detect taking into account that in the study 50% of the patients would respond and 50% would not. With a statistical power of 80%, the calculations showed that significant differences could be detected from 0.69 standard deviation units. The literature indicates that if differences can be detected with less than one standard deviation unit, the study has an adequate sample size and therefore this was set to 100 patients.

As can be depicted from **Figure 12**, patient inclusion took longer than expected, instead of 18 months, we finished including new patients after almost four years, by June 2020 with a final N of 107 patients. Patients' follow-up samples were taken along with the treatment, from November 2016 to April 2021. Among others, the main reasons for the delay were that previously treated patients with other regimens, and patients with alternative diseases and age over 80 years old were excluded from our study. Of course, the COVID-19 pandemic did not help and made us lose some of the follow-up samples.



**Figure 12.** Expected and included patient flow of our prolonged study.

The inclusion criteria were as follows: Patients with a diagnosed stage IV CRC, older than 18 years whose tumors harbored KRAS mutations or not, being candidates or not for metastasis resection and for first-line treatment with a fluoropyrimidine + oxaliplatin with or without Bevacizumab or Cetuximab/Panitumumab. All patients were properly informed and signed their corresponding informed consent. Also, the collection of clinical characteristics together with sample extractions, processing, and storage, have followed every standard local protocol.

Patients received one of the following chemotherapy regimens:

CHEMOTHERAPY	SYSTEMIC TREATMENT REGIMEN	FREQUENCY
<b>Oxaliplatin</b>		
<b>FOLFOX</b>	LV: 400mg/m <sup>2</sup> on day 1 + 5FU: 400mg/m <sup>2</sup> bolus on day 1, 5FU 2400mg/m <sup>2</sup> infusion on 46h + OXA: 85mg/m <sup>2</sup> on day 1	Every 2 weeks
<b>CAPOX</b>	Cape: 1000mg/m <sup>2</sup> every 12h oral day 1 to day 14 + OXA: 130mg/m <sup>2</sup> day 1	Every 3 weeks
<b>Bevacizumab</b>		
<b>FOLFOX-Bevacizumab</b>	Combined with FOLFOX regimen Beva: 5 mg/kg	Every 2 weeks
<b>CAPOX-Bevacizumab</b>	Combined with CAPOX regimen Beva: 7,5 mg/kg	Every 3 weeks
<b>Panitumumab</b>		
<b>FOLFOX-Panitumumab</b>	Combined with FOLFOX regimen + Pani: 6 mg/kg	Every 2 weeks
<b>Cetuximab</b>		
<b>FOLFOX-Cetuximab</b>	Combined with FOLFOX regimen + Cetux: 400 mg/m <sup>2</sup> first infusion, followed by 250 mg/m <sup>2</sup> or 500 mg/m <sup>2</sup> over 2h on day 1 (preferred)	Weekly or Every 2 weeks (preferred)
<b>CAPOX-Cetuximab</b>	Combined with CAPOX regimen + Cetux: 400 mg/m <sup>2</sup> first infusion, followed by 250 mg/m <sup>2</sup>	Weekly

**Table 5.** Systemic therapy regimens administered to the patients that participated in our study. From clinical practice guidelines (REF ICOPRAXIS & www.nccn.org/patients). LV: leucovorin; 5FU: 5-Fluorouracil; OXA: Oxaliplatin; Cape: Capecitabine; Beva: Bevacizumab; Pani: Panitumumab; Cetux: Cetuximab.

After four to six cycles of treatment, the response was evaluated in all patients, and the EVAR sample was extracted (median of 12 weeks). After the first EVAR, all patients that were stable (SD) or in partial/complete response (PR/CR) continued with the treatment cycles, while those that progressed stopped the treatment and were considered to receive second-line chemotherapy treatment +/- targeted therapy. All patients were treated until intolerable toxicity, withdrawal of consent, or death, whichever came first.

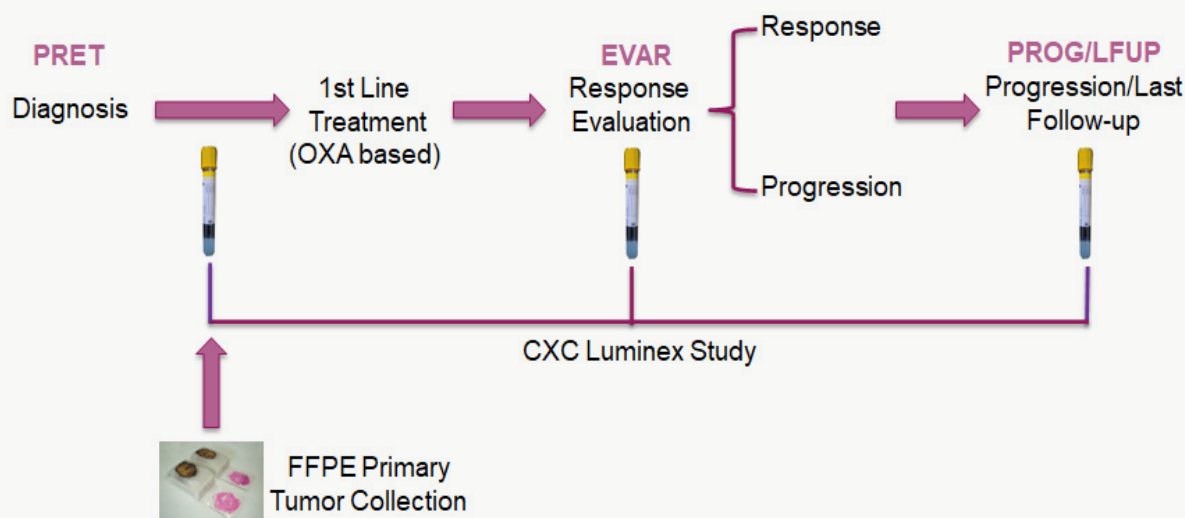
## 2. SAMPLE COLLECTION, PROCESSING AND STORAGE

Inclusion and follow-up of patients as well as sample collection was carried out during a total of 52 months (initially planned: 27 months).

Serum samples were obtained at different time-points of the disease (**Figure 13**). The first sample (PRET) was obtained before the first-line treatment. The second sample (EVAR) at the time of response evaluation, with a median time of 3 months (12 weeks) from the PRET sample extraction. The third sample (PROG/LFUP) was obtained at the time of tumor progression or end of the study. The median progression in these patients is about 9 months, so it was estimated that 50% would have progressed by the beginning of the third year. In the case of non-progression, a sample was also collected (LFUP) and patients were censored in the survival analysis in the last control date. In

those patients having a progressive disease at the first response evaluation (around 10%), only two samples were available.

In addition, a formalin-fixed and paraffin-embedded (FFPE) primary tumor sample was collected from each patient (according to availability) for a TMA elaboration and subsequent IHC expression analysis.



**Figure 13. Design of the study.** Time-points for the different serum and tumor samples.

## 2.1. Serum samples processing

One serum-separated tube (SST™ tube, BD Vacutiner®, BD) containing 5mL of whole blood was collected per patient and time-point (**Figure 13**). Patients' samples from our hospital, followed a circuit established by the oncology department, the biobank and our laboratory. The rest of the hospitals followed similar processing and storage conditions. Once the blood was collected, the SST tubes were inverted five times and allowed to clot for 30min at room temperature (RT) in the biochemistry department of Germans Trias I Pujol Hospital. Samples were picked up, labeled and delivered to our lab by the IGTP Biobank's personnel. The time between extraction and processing never was longer than 8hours.

The SST was centrifuged at 1000g for 15min at 4°C and subsequently, the serum was aliquoted into six aliquots of 500µL in Matrix™ 2D Barcoded Clear Polypropylene Open-Top Storage Tubes (Thermo Scientific) in a biological safety cabinet and stored in a Matrix 96-format 2D barcoded storage microplate (Thermo Scientific). Aliquots in the microplates were frozen down at -80°C in an ultra-low temperature freezer (-80°C) at the IGTP Biobank, to ensure serums' proper storage and preservation until their analysis.

## 2.2 Tissue Microarray (TMA)

One tissue microarray (TMA) was constructed from 26 primary tissue paraffin blocks of our mCRC patient's cohort (**Table 6**). The main reasons for such a low number of samples were the lack of availability and the poor quality and quantity of the tissue.

The shortage of material also explains why in some cases we were unable to make triplicates. Hematoxylin-eosin-stained slides of all primary tumors were reviewed to identify the most well-preserved areas at the pathology department of the Germans Trias I Pujol Hospital. Tissues corresponding to these areas were randomly sampled from the paraffin blocks, with no special preference for the different parts of the tumor (e.g., superficial zone vs. infiltrating border). Three cylindrical cores measuring 0.6mm in diameter were obtained from every donor using a TMA workstation MTA-1 (Beecher Instruments). Subsequently, immunohistochemistry procedures with specific antibodies were applied (see below 3. Immunohistochemistry).

FFPE BLOCKS INCLUDED IN THE STUDY	
PARTICIPATING HOSPITALS	FFPE BLOCKS INCLUDED
DR. JOSEP TRUETA HOSPITAL	13
DURAN I REYNALS HOSPITAL	3
VALL D'HEBRON HOSPITAL	0
MOISES BROGGI HOSPITAL	6
GERMANS TRIAS I PUJOL UNIVERSITY HOSPITAL	4
<b>TOTAL OF PATIENTS' FFPE BLOCKS</b>	<b>26</b>

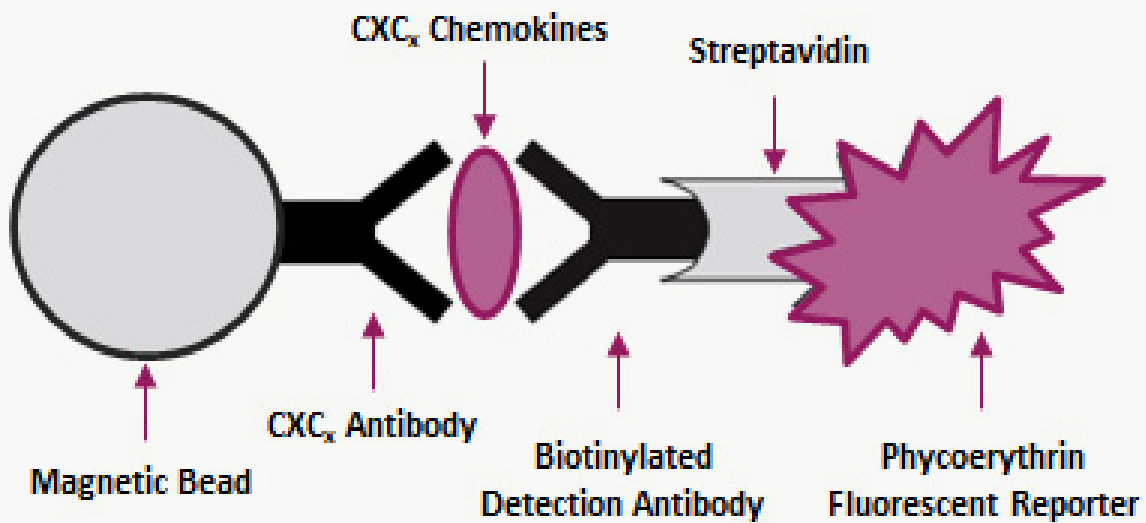
**Table 6.** Summary of all primary tissue blocks included in the TMA and the corresponding provider hospitals.

### 3. IMMUNOHISTOCHEMISTRY (IHC)

FFPE TMA sections were analyzed using standard IHC techniques. Immunostaining was performed automatically using an Autostainer Link48 machine (Dako Agilent, 5301 Stevens Creek Boulevard, Santa Clara, CA 95051, USA). The primary antibodies used were anti-vimentin (monoclonal mouse, ready-to-use, clone V9. Agilent Technologies), human anti-CD3 (rabbit polyclonal, ready-to-use. Agilent Technologies) and human anti-CD-20cy (monoclonal mouse, ready-to-use, clone L26. Agilent Technologies). Positive staining for anti-vimentin antibody was localized in the cytoplasm of stromal cells to assess the presence of stromal desmoplasia. Staining was semi-quantitatively assessed as 1 if less than 25% positivity was identified, 2 between 25 and 50%, and 3 more than 50%. Immunoreactivity in lymphocytes served as an internal anti-vimentin positive control. Positive staining for anti-human CD3 and anti-human CD20cy antibodies was localized to the lymphocyte membrane. CD3 staining was assessed as 1 if occasional lymphocytes were identified, 2 for groups of 5 to 10 lymphocytes, and 3 for groups of more than 10 lymphocytes. CD20 staining was assessed as 0 if no lymphocytes were observed, 1 for less than 5 and 2 for more than 5 lymphocytes. Slides were scanned at x40 magnification using an Ultra Fast scanner (Philips) to obtain an image of the entire slide.

#### 4. LUMINEX® ANALYSIS OF SERUM SAMPLES

Levels of a custom panel of CXC chemokines were analyzed in PRET, EVAR and PROG serum samples using a Bio-plex Pro™ Human Chemokine multiplex Assay (Bio-Plex Pro™ Human Chemokine Panel, 171-AK99MR2, Bio-Rad). This is an immunoassay based on magnetic beads that are covalently coupled to the antibodies directed against the desired biomarker and react if the sample contains the biomarker of interest. A biotinylated detection antibody is added, followed by a series of washes to remove unbound protein, to create the “sandwich” complex (**Figure 14**). Finally, to form the detection complex, a Streptavidin-phycoerythrin (SA-PE) conjugate is added to the sample. The Phycoerythrin serves as a fluorescent indicator, or reporter, which will be detected and measured in the Luminex® 200 reader.



**Figure 14.** Bio-Plex sandwich immunoassay.

In our study, the Bio-plex Pro™ Human Chemokine Assay was pre-coated with CXCL1, 2, 5, 6, 8, 9, 10, 11, 12, 13, and 16 antibodies, allowing us to detect all of them in a single well of a 96-well plate in approximately 4–5 hours. Reconstitution of the standards (lyophilized mixture of 40 standard analytes), thawing of serum samples and serial dilutions were prepared on ice following the manufacturer’s instructions. Samples were pre-diluted 10 times (1:10) in PBS. Prior to plating, standards and diluted samples were equilibrated to RT. When ready, we dispensed 50µL into the wells of the Bio-plex Pro 96 flat bottom plate (Bio-Rad), including 2 replicates per sample. All subsequent steps were taken following the manufacturer’s instructions (**Annex III**). Chemokine readings were performed in a Luminex® 200 equipment in the Cytometry department from the IGTP. The standard curve was constructed using a five-parametric logistic regression non-linear model using Xponent 3.1 (Luminex Inc.). Markers were grouped together according to the dilution factor after the cross-reactivity was checked across all analytes. Measurement values were interpolated to obtain the concentration of each metabolite (pg/mL) in the serum. During the experiment, intra-assay precision ranged from 2% to 4% and inter-assay precision ranged from 2% to 8%.

In order to measure serum levels from all our 104 patients' consecutive samples with the least possible variability, we performed two assays per day, for 3 consecutive days.

## 5. CXCL13 IN SILICO ANALYSIS

An *in silico* study was performed using the available transcriptomic data of liver metastasis samples from 119 mCRC patients treated by hepatic resection. Patients' outcome and systemic oncological treatment information were also available, data extracted from Eide et al., 2021 (<https://doi.org/10.1038/s41525-021-00223-7>) and Moosavi et al., 2021 (<https://doi.org/10.1186/s13073-021-00956-1>). Additionally, TLS genetic signatures data was extracted from Sautès-Fridman et al., 2019 (<https://doi.org/10.1038/s41568-019-0144-6>).

The aim of the study was to correlate CXCL13 genetic expression levels with immune and non-immune cell abundance, estimated using the MCP-counter algorithm published at (<https://doi.org/10.1186/s13059-016-1070-5>). We also studied the CXCL13 expression correlation with survival based on the mCRC patients' treatment as well as its correlation with TLS signatures and their association with patients' outcome. The cohort (**Table 7**) consisted of 119 liver metastases from mCRC, 15 naive patients and 104 had received OXA-based neoadjuvant treatment.

VARIABLES	ALL N = 119
	N (%)
<b>Sex</b>	
Male	71 (59.7%)
Female	48 (40.3%)
<b>Systemic oncological treatment prior to sampling of metastases</b>	
Neoadjuvant chemotherapy for this metastatic situation	104 (87.4%)
No previous systemic treatment (Naive)	15 (12.6%)
<b>KRAS and NRAS mutation</b>	
KRAS mut	50 (48.0%)
NRAS mut	7 (5.9%)
WT	62 (46.1%)

**Table 7.** Clinicopathological and molecular characteristics of patients from the *in silico* cohort. Other than these clinical information has not been provided by the authors.

The methodology used in each of the analyses is described below:

### - Database compilation

Gene expression data from the colorectal liver metastases, including clinicopathological annotations and patient survival data were downloaded from: GSE159216 (<https://www.ncbi.nlm.nih.gov/geo/query/acc.cgi?acc=GSE159216>)

### - Data processing

The raw intensity CEL files were background corrected, normalized, summarized at the gene level, and log<sub>2</sub> transformed using the robust multi-array average (RMA) method

implemented in the justRMA function in the affy package (<https://doi.org/10.1093/bioinformatics/btg405>) in R, using the custom Entrez CDF file (v22) from Brainarray (<https://doi.org/10.1186/1471-2105-8-48>).

Entrez IDs were converted to HGNC gene symbols using the biomaRt package (v 2.52.0) from Bioconductor (<https://doi.org/10.1038/nmeth.3252>).

## - Data analysis

### MCP-counter analysis

Gene expression was used to run MCP-Counter algorithm (<https://doi.org/10.1186/s13059-016-1070-5>) to estimate the population abundance of tissue-infiltrating immune and stromal cell populations.

### ssGSEA

MSS-like and MSI-like gene sets were retrieved from MsigDB (<http://www.gsea-msigdb.org/>) and gene signatures for the detection of tertiary lymphoid structures were available in Sautès-Fridman et al., 2019 (<https://doi.org/10.1038/s41568-019-0144-6>) Gene set scores were calculated using single sample Gene Set Enrichment Analysis (ssGSEA) implemented in the R package GSVA (v1.44.5) (<https://doi.org/10.1038/nature08460>)

## 6. VALIDATION STUDIES

### 6.1 Validation cohorts, samples processing and storage

#### • Healthy Controls Cohort:

Drs. Pilar Navarro and Neus Martínez-Bosh from the Barcelona Hospital del Mar kindly provided a total of 45 serum samples from healthy controls (HMar cohort). The 45 patients' median age at inclusion was 64.5 years old, of whom 60% were women, with no chronic or acute pathologies of note. These samples were collected between March and November 2022, under the approval of the Drug Research Ethics Committee of Parc de Salut Mar (CEIm-Parc de Salut Mar) (2017/7449/I and 2020/9067/I). All individuals signed an informed consent allowing the use of their samples for research purposes.

One serum BD Vacutainer containing 5mL of whole blood was collected per healthy individual and kept at 4°C. The time between extraction and processing never was longer than 8 hours. The tube was centrifuged for 10min 480g. The serum was aliquoted and stored at -80°C until its analysis.

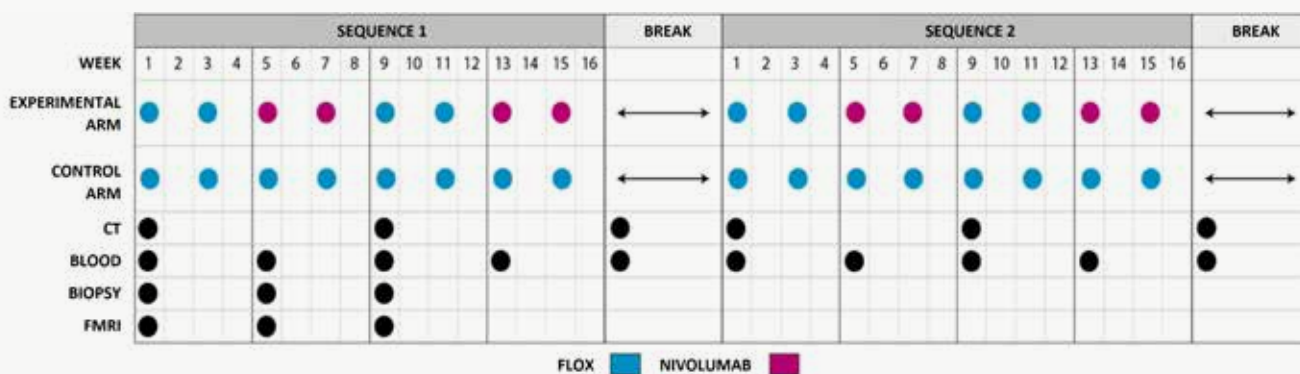
#### • mCRC Patients Cohort:

Dr. Sebastian Meltzer from the Akershus universitetssykehus (Oslo, Norway) kindly offered us to analyze a cohort of samples from mCRC patients who were enrolled in a randomized, controlled, ongoing phase II trial called METIMMOX (NCT03388190) (Oslo's cohort).

In the METIMMOX clinical trial, 80 patients were randomly assigned to receive either eight cycles of the oxaliplatin-based Nordic FLOX regimen Q2W (oxaliplatin 85mg/m<sup>2</sup> on day 1 and bolus 5-fluorouracil 500mg/m<sup>2</sup> and folinic acid 100 mg on days 1 and 2; control arm) or two cycles of FLOX Q2W before two cycles of nivolumab Q2W (240 mg flat dose) in a repeat sequential schedule to a total of eight cycles (experimental study arm). After eight treatment cycles, all patients proceeded to a treatment break until disease progression and reintroduction of a new treatment cycle. All patients were treated until the first confirmed disease progression on active therapy, intolerable toxicity, withdrawal of consent or death, whichever came first. The study was

approved by an independent ethics committee, the institutional review board, and the Norwegian Medicines Agency and was conducted in accordance with the Declaration of Helsinki. Written informed consent was required for study participation. The patient population has been thoroughly described in a previous paper (DOI: 10.1038/s41416-022-02004-0). In the current analysis, only the patients included in the study control arm were used.

Serial serum samples were collected monthly, at baseline and prior to every second treatment cycle, as shown in **Figure 15**. Specifically, samples were obtained at baseline (N = 36); and after 4 (N = 33), 8 (N = 28), 12 (N = 23) and 16 weeks (N = 17) last sample was obtained at end of treatment (N = 16).



**Figure 15.** Clinical trial scheme. Enrolled patients had computerized tomography (CT) scans of target and non-target lesions every 2 months until treatment failed. Patients were treated every two weeks in a go-and-stop manner, meaning that they had complete drug holidays after 4 months of treatment, until tumor progression and re-start of the same treatment. Blue dots correspond to FLOX and pink to Nivolumab treatment. Blood samples were collected every month (4 weeks), while biopsies and fMRI were during the first three months.

Patients were enrolled between the 29<sup>th</sup> of May 2018 and the 22<sup>nd</sup> of October 2021. From the original 40 patients allocated to the control arm, two were screening failures and two patients were withdrawn from the study shortly after inclusion due to the withdrawal of consent, leaving a total of 36 patients for analysis (patient and disease characteristics in **Table 8**). From these, a total of 19 patients left the study due to either toxicity or progression within the first 16 weeks of treatment, contributing to a falling number of serum samples available for analysis.

VARIABLES	ALL N = 36	VARIABLES	ALL N = 36
	N (%)		N (%)
<b>Age at Diagnosis</b>	65 (19%)		
<b>Sex</b>		<b>Radical Surgery</b>	
Male	22 (61%)	Yes	5 (14%)
Female	14 (39%)	No	31 (86%)
<b>Performance Status</b>		<b>Surgery</b>	
0	19 (53%)	No surgery	20 (56%)
1	17 (47%)	Only primary tumor	13 (36%)
2	0	Primary and metastasis	3 (8%)
<b>Primary Tumor Site</b>		<b>Resected Metastatic Organs</b>	
Colon	9 (25%)	Liver	5 (14%)
Rectum	9 (25%)	Lung	0
Unknown	18 (50%)	Peritoneum	0
<b>Metastatic Site</b>		<b>MSI/MSS</b>	
Liver	7 (19%)	MSI	0
Lung	0	MSS	36 (100%)
Liver+Lung	13 (36%)	Unknown	0
Other	16 (45%)		
<b>Oligo/Multiple Metastasis</b>		<b>BRAF and RAS mutation</b>	
<5 Metastasis	35 (97%)	BRAF mut	8 (22%)
≥5 Metastasis	1 (3%)	NRAS mut	4 (11%)
		KRAS mut	15 (42%)
		WT	9 (25%)
<b>First Line Treatment</b>		<b>Immune System Known Alterations</b>	
FLOX	36 (100%)	Autoimmune disease	
CT combined with targeted therapy	0	Patient with a transplant	
		Major surgery last month	
		Unknown	36 (100%)
<b>Second Line</b>		<b>Exitus</b>	
Yes	30 (83%)	Yes	34 (94%)
No	6 (17%)	No	2 (6%)
<b>Response Evaluation</b>		<b>Death Reason</b>	
CR/PR	21 (58%)	PD	35 (97%)
SD/PD	11 (42%)	Complications due to disease	35 (97%)
<b>Response Evaluation (Best)</b>		Non cancer related	0
Complete response (CR)	1 (3%)	Unknown	0
Partial response (PR)	20 (56%)	Complications treatment related	1 (3%)
Stable disease (SD)	8 (22%)		
Progressive disease (PD)	3 (8%)		
Censored before the first evaluation	4 (11%)		

**Table 8. Clinical, pathological, and molecular characteristics of patients from the Oslo Cohort.** FLOX ChT (5FU Bolus + Leucovorin + Oxaliplatin); CR: complete response; PR: partial response; SD: stable disease; PD: progressive disease; Surgery variable accounts for all patients that underwent any kind of surgery previous and during the trial.

Whole blood samples were collected in Vacuette® serum tubes, left at room temperature for at least 30min and centrifuged at 2200G for 10min. Further serum was aliquoted into 1mL vials and frozen and stored at -80°C until CXCL13 ELISA analysis.

## 6.2 ELISA assay for soluble CXCL13

ELISA assays to measure serum CXCL13 were performed by the principal investigators of the Oslo's and Hmar's cohorts, in their respective laboratories. In both cases, CXCL13 was analyzed with the Human CXCL13/BLC/BCA-1 Immunoassay Quantikine ELISA kit (R&D Systems). Serum samples were diluted 1:2 using the calibrator diluent (RD6-41) of the kit. Human CXCL13 standard was reconstituted in distilled water to further prepare serial dilutions as per the manufacturer's instructions. The procedure consists of a quantitative sandwich enzyme immunoassay technique. The supplied 96-well microplate is pre-coated with CXCL13 monoclonal antibody, into which standards and diluted samples were pipetted. While incubated, CXCL13 present in the sample is bound by the immobilized antibody. After serial washes with the 1:25 diluted washing buffer to avoid unbound substances unspecificities, an enzyme-linked monoclonal CXCL13 antibody was added to the wells. Followed by another round of washes, a substrate solution was added, and color developed in proportion to the amount of CXCL13 bound in the first step. Color development was stopped and the optical density (OD) was measured at 450nm and corrected at 540nm. The median value of two technical replicates was used for further analyses. The standard curve was generated by linearizing the OD values to the known human CXCL13 concentrations from the standards. Samples OD measurements were multiplied by the dilution factor (x2) and interpolated in the standard curve to obtain CXCL13 (pg/mL) concentration in the serum.

## 7. STATISTICAL METHODS

### Analysis of Luminex-based results:

Patients' characteristics were described with frequencies for categorical variables and median and interquartile range (IQR) for continuous ones. We used Principal Component Analysis (PCA) to explore dimensionality reduction and potential correlation between chemokines (CXCs). The Elbow method was used to choose the number of principal components on the scree plot. The dynamics of CXC levels at different time-points were studied using the paired Wilcoxon signed rank test. Association between clinical and demographical variables and chemokines values at each time-point were assessed using the Kruskal-Wallis test. To estimate overall survival (OS) the follow-up time (in months) was defined from the date of first treatment initiation to the date of death from any cause or last follow-up, whichever occurred first. Follow-up time for progression-free survival (PFS) was the time (in months) from the date of first treatment initiation to the date of progression, death from any cause or last follow-up whichever occurred first. For patients who underwent surgery after the first treatment initiation the follow-up time for PFS, was censored at the date of surgery. Median OS and median PFS were estimated with the Kaplan-Meier (KM) method and survival curves stratified by patient's characteristics were compared with the log-rank test. Univariate and multivariate Cox regression models were fitted to predict the risk of death and the risk of progression/death. Hazard ratios (HRs) and their 95% confidence intervals (CIs) were reported. For the study of the association between CXC and OS/PFS, the median cut-point for the CXC was selected. Moreover, Receiver operating characteristic (ROC) curves were used to determine optimal CXC thresholds for predicting mortality at 12 and 30 months after the first treatment initiation. CXC levels were log<sub>2</sub>-transformed and a heatmap was used to visualize the hierarchical clustering of variables using the Euclidean distance. All statistical analyses were performed with the R v. 4.1.2 statistical software.

#### CXCL13 *in silico* analysis:

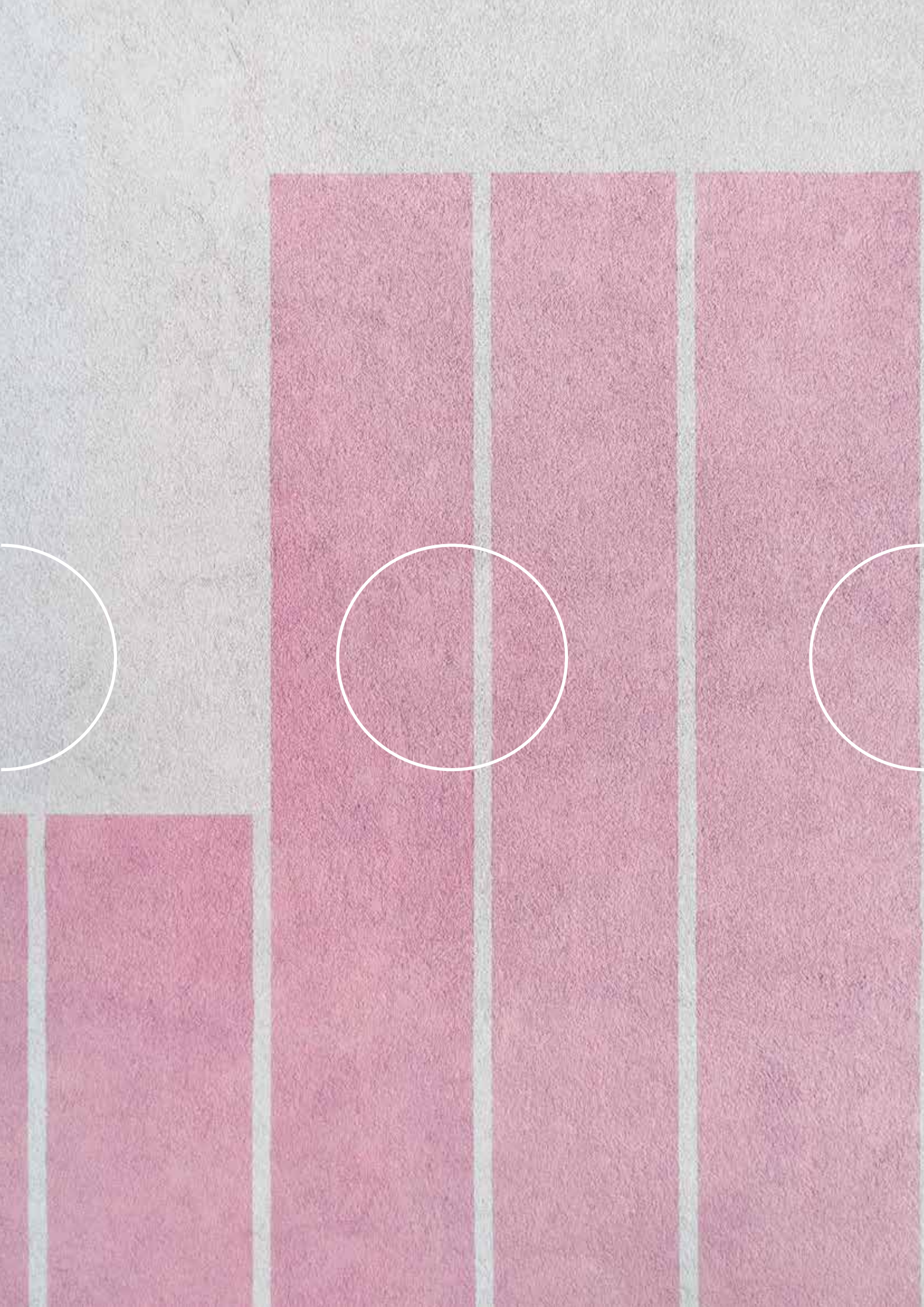
Spearman's correlation, Wilcoxon test and p-value adjustment were performed using the functions `cor`, `wilcoxon.test` and `p.adjust` in the R package `stats`. All p-values were two-sided. Adjustment of p-values was performed using Benjamini & Hochberg method. Kaplan–Meier and Cox proportional hazard analyses were performed using the R package `survival` (v3.4.0). Hazard ratios and Wald tests were calculated using the `cox.ph` function. Cox analyses were performed using gender as a covariate.

#### Validation studies:

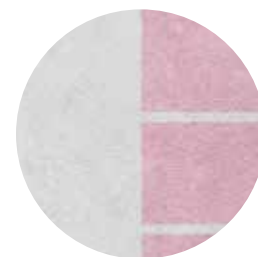
Analyses were performed using the IBM SPSS Statistics for Mac version 28 or GraphPad Prism version 9.5.0. All values are presented in median and interquartile range or number of events and percentage of the total number. Linear regression was calculated using Pearson's r-test. Correlations were calculated using Spearman's rho test, and differences between groups were analyzed using the Kruskal-Wallis test or Mann-Whitney U test when appropriate. Survival differences were assessed by the log-rank test and visualized using Kaplan-Meier curves, or Cox proportional hazard models presented as hazard ratio (HR) and 95% confidence intervals (95% CI). All tests were two-sided, and P values of less than 0.05 were considered statistically significant.

Response rate (RR) is defined as the percentage of patients with the best response (CR or PR) relative to the evaluable population in the sample, N = 104 patients. Overall survival (OS) is defined as the time a patient included in the study can survive from any cause after the disease is diagnosed. Progression-free survival (PFS) measures the time a patient can live without disease progression. The hazard ratio (HR) is the ratio of the probability of the event, in our study for OS the event is exitus and for PFS the event is progression.





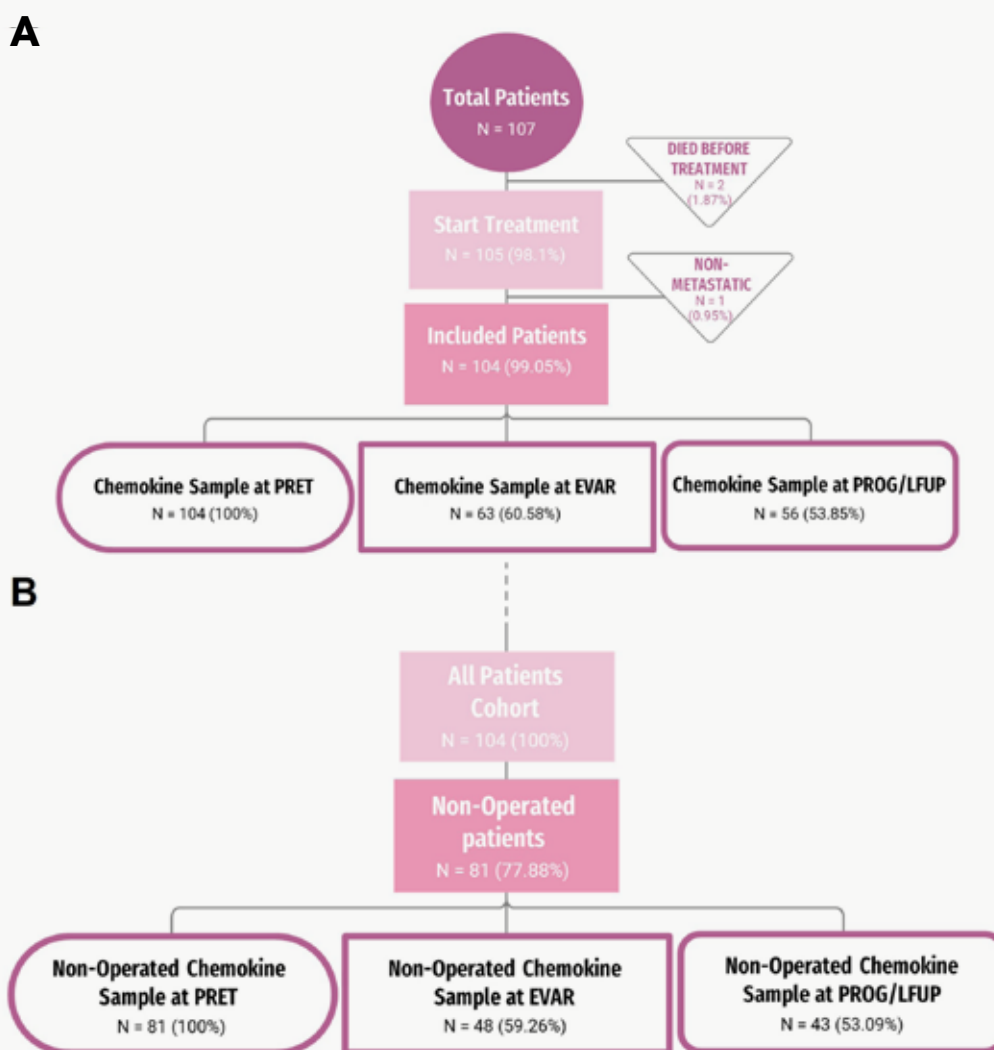
# 04 Results



## OBJECTIVE 1

### 1.1. Patients' inclusion and their clinicopathological and molecular characteristics

A total of 107 patients were included in this study. As it is shown in **Figure 16**, of the 107 patients included, 104 (97%) were suitable for analysis, while only 3 patients (3%) were non-evaluable: two died before the treatment started and one ended up not being metastatic. Along the treatment, after a median time of 12 weeks, 63 correlative samples were extracted at EVAR time-point, and finally, 43 correlative samples were obtained at PROG or end of study/ last follow-up (LFUP) time-point (**Figure 16.A**). Along the study, we will consider non-operated patients as a subcohort (N=81), therefore we also show the correlative samples at EVAR and PROG time-points that correspond to these non-operated patients (**Figure 16.B**).

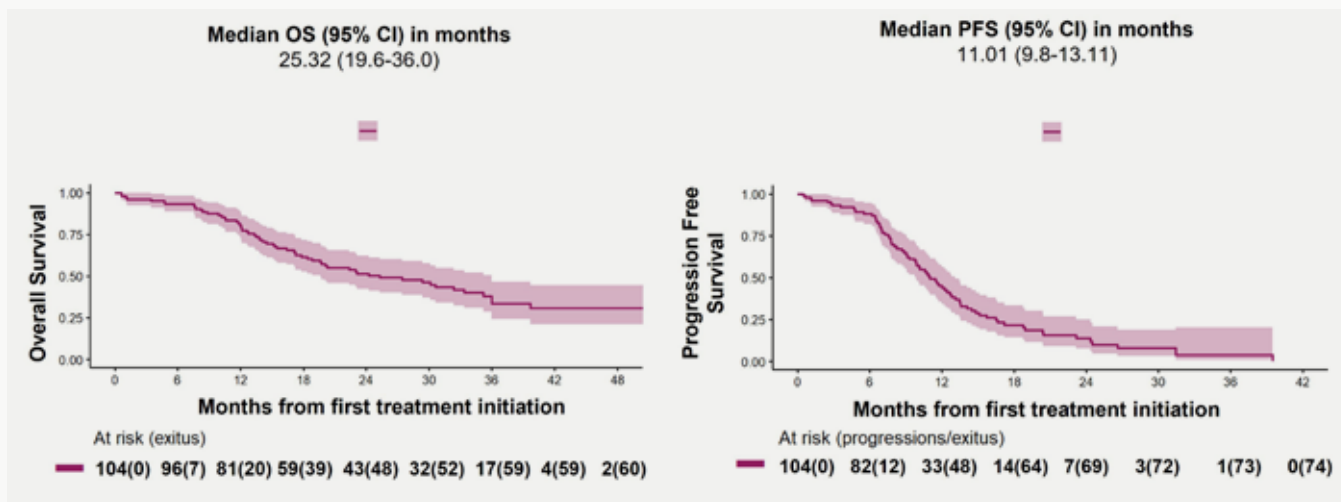


**Figure 16. Flowchart of patients and their corresponding time-point samples inclusion.** A: All cohort. B: Non-operated patients.

The most important clinical and pathologic features of the 104 patients included in this study are shown in **Table 9**. Our cohort's median OS was 25.32 months and the PFS was 11.01 months (**Figure 17**). The median age at diagnostic was 66.5 years old and 71.2% were men; the majority of patients (96.1%) presented a good performance status (0-1); the most frequent primary tumor localization was the colon (63.5%); regarding metastatic sites, 49% of the patients had metastasis in the liver followed by 10.6% in the lungs; nevertheless, 29.8% presented metastasis in both organs; 69.2% of patients presented multiple metastasis (defined by five or more metastases in the same or different organs); as planned, all patients received OXA-based first-line treatment, being FOLFOX alone or with Bevacizumab the most frequent schedules. The median start treatment date was 29th May 2018 (IQR: 17-Feb-18; 06-Apr-19), whereas the median last cycle administration date was 7<sup>th</sup> February 2019 (IQR: 15-09-18; 18-Dec-19). Also, the follow-up time mean was of 22.3 months (SD: 12.3). Patients' response rate was about 68% and 12 patients had a disease progression; of the 33 patients (31.7%) who underwent surgery during the study, 10 had surgery of the primary tumor (9.6%), 9 had surgery of the metastasis (8.7%) and 14 of the primary and metastasis (13.4%). Among them, 23 patients had radical surgery, which refers to patients that had surgery of either the metastasis alone or of the primary and metastasis (22.1%). Among all metastatic target sites, the liver was the main resected organ (78.3%). Regarding molecular features, 4.8% of the tumors were MSI; about half of the cases (52.9%) harbored mutations in RAS genes (8.7% NRAS, 44.2% KRAS) while as expected, a few cases (3.8%) were BRAF mutant. As CXC chemokines have a role in the immune system, we also considered possible related aspects that could influence the results; in this regard, we found that only 5.8% presented some alterations: 2 patients had an autoimmune disease, 1 patient had a transplant in the past and 3 patients had a major surgery previous to diagnosis. No statistically significant results were found when comparing the CXC PRET levels of these patients with the rest of the cohort. This analysis is shown in **Annex IV**. Almost 60% of the patients died during the study of which 65% died of disease progression, 20% because of disease complications, 1.7% for treatment-related complications and 13.3% because of other reasons (non-cancer related or unknown).

VARIABLES	ALL N = 104	VARIABLES	ALL N = 104
	N (%)		N (%)
<b>Age at Diagnosis [IQR]</b>	66.5 [58.8;73.0]	<b>Second Line</b>	
<b>Sex</b>		Yes	60 (47.7%)
Male	74 (71.2%)	No	44 (42.3%)
Female	30 (28.8%)		
<b>Performance Status</b>		<b>Surgery Along Disease</b>	
0	41 (39.4%)	No Surgery	60 (57.7%)
1	59 (56.7%)	Only Primary Tumor	21 (20.2%)
2	4 (3.8%)	Only Metastasis	9 (8.7%)
		Primary and Metastasis	14 (13.4%)
<b>Primary Tumor Site</b>		<b>Surgery During Study</b>	
Colon	66 (63.5%)	No Surgery During Study	71 (68.3%)
Rectum	38 (36.5%)	Only Primary Tumor	10 (9.6%)
		Only Metastasis	9 (8.7%)
		Primary and Metastasis	14 (13.4%)
<b>Metastatic Site</b>		<b>Radical Surgery</b>	
Liver	51 (49.0%)	Yes	23 (22.1%)
Lung	11 (10.6%)	No	81 (77.9%)
Liver + Lung	31 (29.8%)		
Other	11 (10.6%)		
<b>Oligo/Multiple Metastasis</b>		<b>Resected Metastatic Organs</b>	
< 5 Metastasis	32 (30.8%)	Liver	18 (78.3%)
≥ 5 Metastasis	72 (69.2%)	Lung	2 (8.7%)
		Peritoneum	3 (13%)
<b>First Line Treatment</b>		<b>MSI/MSS</b>	
FOLFOX	33 (31.7%)	MSI	5 (4.8%)
CAPOX	4 (3.9%)	MSS	75 (72.1%)
FOLFOX-Bevacizumab	38 (36.6%)	Unknown	24 (23.1%)
FOLFOX-Cetuximab	9 (8.7%)	<b>BRAF and RAS mutation</b>	
CAPOX-Bevacizumab	2 (1.9%)	BRAF mut	4 (3.8%)
CAPOX-Cetuximab	1 (1%)	NRAS mut	9 (8.7%)
FOLFOX-Panitumumab	17 (16.3%)	KRAS mut	46 (44.2%)
		WT	43 (41.3%)
		Unknown	2 (1.9%)
<b>First Line Treatment</b>		<b>Immune System Known Alterations</b>	
CT Alone	37 (35.6%)	Autoimmune Disease	2 (1.9%)
CT + Bevacizumab	40 (38.5%)	Patient with a Transplant	1 (1.0%)
CT + anti-EGFR	27 (26.0%)	Major Surgery Last Month	3 (2.9%)
		Unknown	98 (94.2%)
<b>Response Evaluation</b>		<b>Exitus</b>	
CR/PR	68 (65.4%)	Yes	60 (57.7%)
SD/PD	36 (34.6%)	No	44 (42.3%)
<b>Response Evaluation (Best)</b>		<b>Death Reason</b>	
Complete Response (CR)	1 (1%)	PD	39 (65.0%)
Partial Response (PR)	67 (64.4%)	Complications due to Disease	12 (20%)
Stable Disease (SD)	24 (23.1%)	Non cancer related	6 (10.0%)
Progressive Disease (PD)	12 (11.5%)	Unknown	2 (3.3%)
		Complications Treatment Related	1 (1.7%)

**Table 9. Clinical, pathological and molecular characteristics of patients.** Performance status (PS): 0: without limitations; 1: minimal limitations; 2: limitations. CT: chemotherapy (5FU/Capecitabine + Leucovorin + Oxaliplatin); anti-EGFR: Panitumumab, Cetuximab; CR: complete response; PR: partial response; SD: stable disease; PD: progressive disease. Surgery along disease variable accounts for all patients that underwent any kind of surgery previous and during our study.



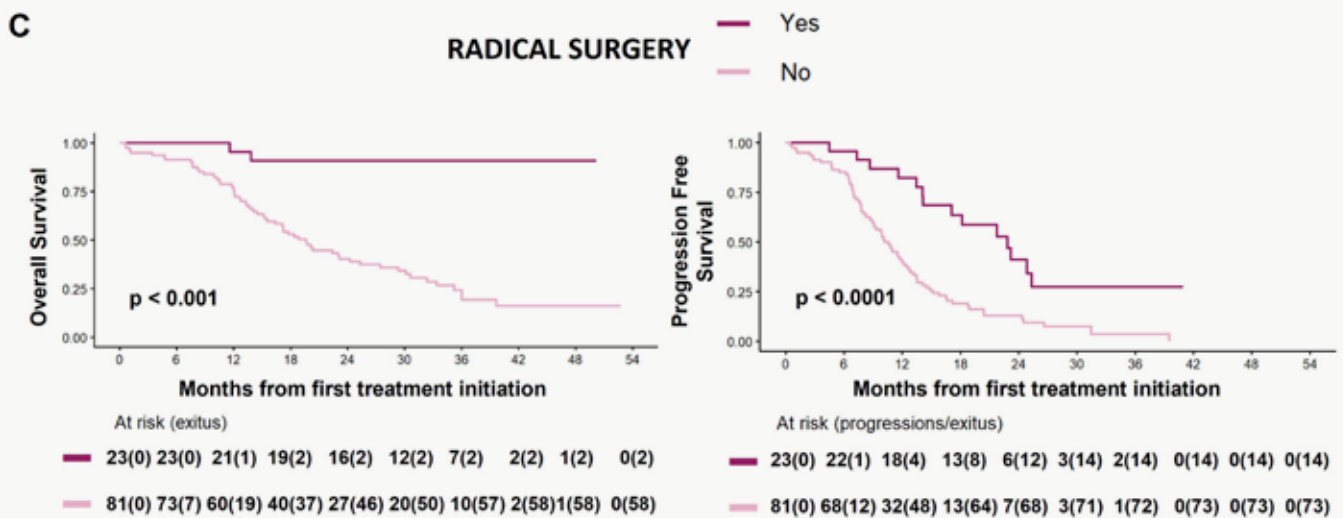
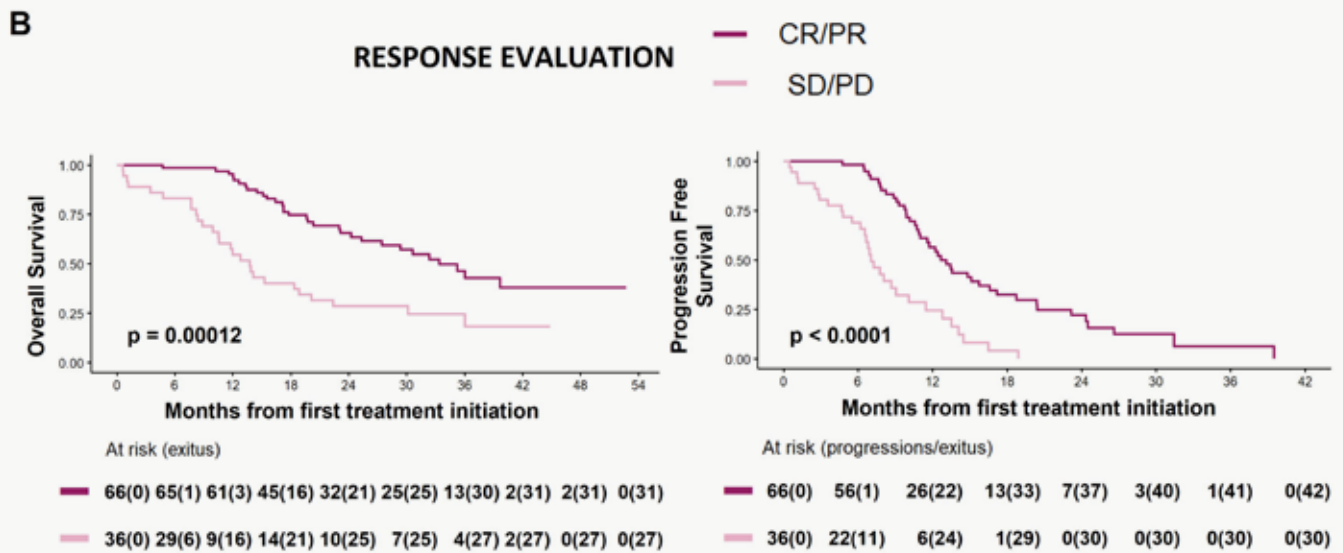
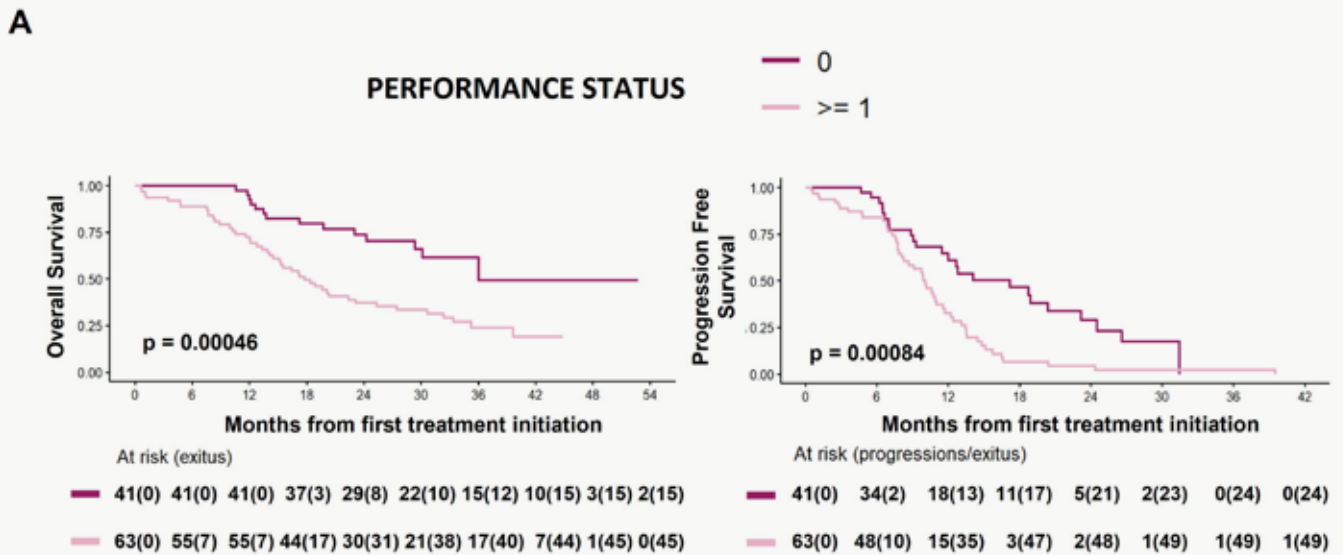
**Figure 17.** Kaplan-Meier plots corresponding to median OS and PFS of the cohort.

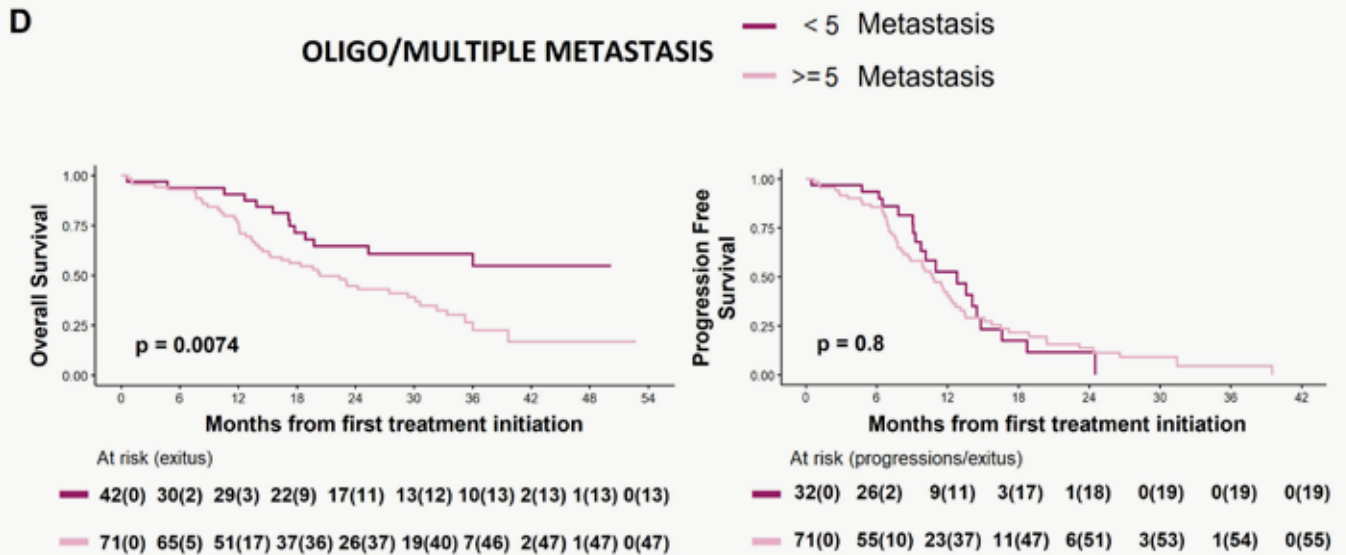
## 1.2. Clinicopathological and molecular characteristics association with outcome

We studied how the clinicopathological and molecular characteristics were associated with OS and PFS results are shown in **Table 10** and correspond to KM plots, **Figure 18**. Among all clinical variables, patients with a performance status (PS) of 1 or less, patients that did not respond to treatment or those that did not undergo a radical surgery during the study had statistically significant worse OS and PFS (Figures 18. A-C); patients with multiple metastasis had also statistically significant worse OS but not PFS (**Figure 18.D**). Among these variables, patients who underwent a radical surgery during our study had a clear benefit in terms of survival and PFS. Moreover, the fact of removing a more than possible source of chemokines can for sure affect our results. Therefore, radical surgery was specially taken into account in every further analysis in this study. This and the rest of the associated variables, together with age and sex, were considered in the multivariable models of our study.

VARIABLES N (%)	ALL N = 104	OVERALL SURVIVAL (OS)		PROGRESSION FREE SURVIVAL (PFS)	
		MEDIAN IN MONTHS (95% CI)	HR (95% CI, P VALUE)	MEDIAN IN MONTHS (95% CI)	HR (95% CI, P VALUE)
Age at Diagnosis [IQR]	66.5 [58.8;73.0]	-	1.02 (0.99-1.04, p=0.148)	-	1.00 (0.98-1.02, p=0.76)
Sex					
Male	74 (71.2%)	29.4 (19.7-NA)	1	11.5 (9.3-13.5)	1
Female	30 (28.8%)	20.3 (14.1-39.7)	1.24 (0.72-2.13, p=0.308)	11 (8.7-15.7)	1.27 (0.77-2.07, p=0.348)
Performance Status					
0	41 (39.4%)	36 (30.1-NA)	1	17.2 (12-24.5)	1
≥1	63 (60.6%)	17.8 (14.5-25.3)	2.66 (1.47-4.81, p=0.0005)	10.1 (8.3-11.7)	2.23 (1.33-3.73, p=0.0008)
Primary Tumor Site					
Colon	66 (63.5%)	22.4 (15.1-30.6)	1	10.6 (9.1-12.8)	1
Rectum	38 (36.5%)	36 (20.1-NA)	0.58 (0.34-1.01, p=0.054)	12.2 (10.1-18.7)	0.84 (0.52-1.38, p=0.498)
Metastatic Site					
Liver	51 (49.0%)	23 (18.4-NA)	1	10.2 (8.3-14.5)	1
Lung	11 (10.6%)	36 (36-NA)	0.49 (0.17-1.41, p=0.187)	14.1 (12.8-NA)	0.73 (0.34-1.55, p=0.408)
Liver + Lung	31 (29.8%)	23.1 (13.3-33.4)	1.45 (0.82-2.56, p=0.199)	10.9 (8.7-13.6)	1.20 (0.74-1.95, p=0.451)
Other	11 (10.6%)	20.3 (12.6-NA)	1.09 (0.45-2.61, p=0.853)	9.1 (6.5-NA)	0.93 (0.45-1.91, p=0.836)
Oligo/Multiple Metastasis					
< 5 Metastasis	32 (30.8%)	NA (19.7-NA)	1	12.8 (9.8-16.6)	1
≥ 5 Metastasis	72 (69.2%)	20.3 (15.3-30.6)	2.28 (1.23-4.24, p=0.007)	10.7 (8.7-12.7)	1.07 (0.63-1.82, p=0.801)
First Line Treatment					
Chemotherapy (CT)	37 (35.6%)	39.7 (17.1-NA)	1	9.1 (7.7-23.2)	1
CT + Bevacizumab	40 (38.5%)	23.1 (19.7-33.4)	1.49 (0.82-2.70, p=0.188)	12 (9.8-16.5)	0.82 (0.48-1.43, p=0.492)
CT + anti-EGFR	27 (26.0%)	30.6 (15.3-NA)	0.98 (0.48-2.00, p=0.950)	11.7 (10.2-15.1)	0.90 (0.48-1.69, p=0.743)
Response Evaluation					
CR/PR	64 (64%)	33.4 (25.3-NA)	1	12.7 (11-16.6)	1
SD/PD	36 (36%)	13.8 (10.5-22.4)	2.50 (1.5-4.18, p=0.0001)	7 (6.6-11.5)	3.29 (2.00-5.41, p<0.0001)
Radical Surgery					
Yes	23 (22.1%)	-	1	-	1
No	81 (77.9%)	19.6 (15.5-27.4)	2.95 (1.65-5.28, p<0.001)	10.6 (9.1-12.4)	2.95 (1.65-5.28, p<0.001)
MSI/MSS					
MSI	5 (4.8%)	17.8 (14.1-NA)	1	9.1 (6.6-NA)	1
MSS	75 (72.1%)	29.4 (22.4-39.7)	0.69 (0.25-1.92, p=0.473)	11.7 (9.8-14.1)	0.39 (0.15-1.01, p=0.052)
Unknown	24 (23.1%)	-	-	-	-
BRAF and KRAS mutation					
BRAF mut	4 (3.8%)	16.2 (11.6-NA)	1	9.1 (6.8-NA)	1
NRAS mut	9 (8.7%)	17.2 (7.5-NA)	1.53 (0.39-5.98, p=0.541)	9.1 (7.5-NA)	0.89 (0.23-3.4, p=0.865)
KRAS mut	46 (44.2%)	25.3 (17.8-36)	0.84 (0.26-2.79, p=0.782)	11.6 (8.9-14.8)	0.43 (0.13-1.43, p=0.168)
WT	43 (41.3%)	39.7 (20.1-NA)	0.52 (0.15-1.74, p=0.288)	12.8 (10.6-15.7)	0.43 (0.13-1.45, p=0.171)
Unknown	2 (1.9%)	-	-	-	-

**Table 10. Clinical and molecular characteristics and their association with OS and PFS.** Median OS and median PFS were estimated with the log-rank test. Univariate Cox regression hazard ratios (HR) and corresponding 95% confidence intervals (CIs) are shown. [IQR] interquartile range. In bold, all statistically significant results with p values under 0.05.





**Figure 18. Kaplan-Meier plots of indicated variables that were statistically associated with OS and/or PFS.** P value, HR and 95% CI according to univariate COX model.

## OBJECTIVE 2

### 2. 1. CXC chemokines distribution and principal component analysis (PCA) of our CXC Luminex® panel

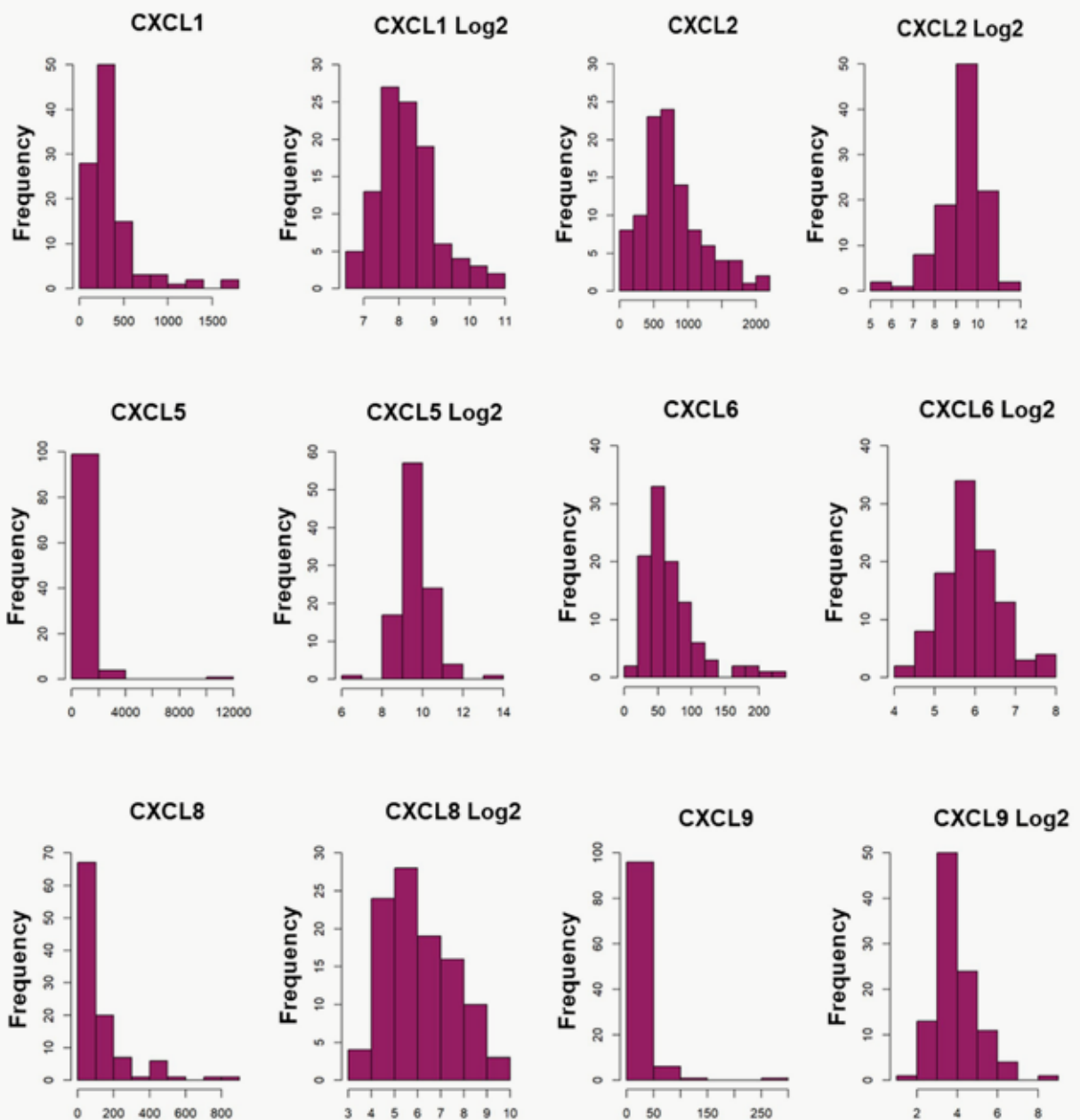
To study our chemokines distribution at each time-points, we analyzed each chemokine central tendency for all three time-points: PRET, EVAR and PROG, (**Figure 19.A.** corresponding to PRET levels, EVAR and PROG are shown in **Annex V**). Considering it and that the sample size is small, we choose the median as the cutoff point, as our chemokines did not follow a normal distribution. Normality tests were not necessary as the distribution graphs clearly show that CXC chemokines did not follow a normal distribution at any time-point.

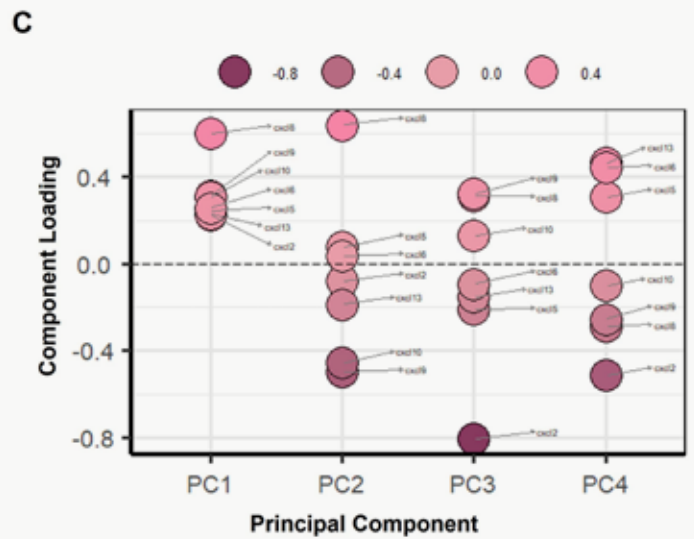
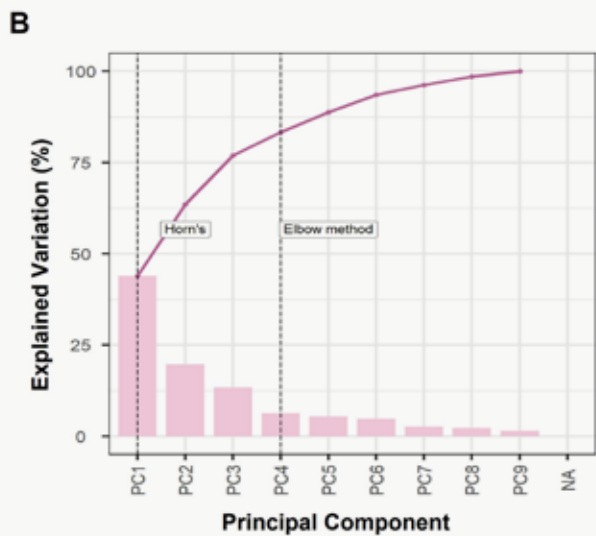
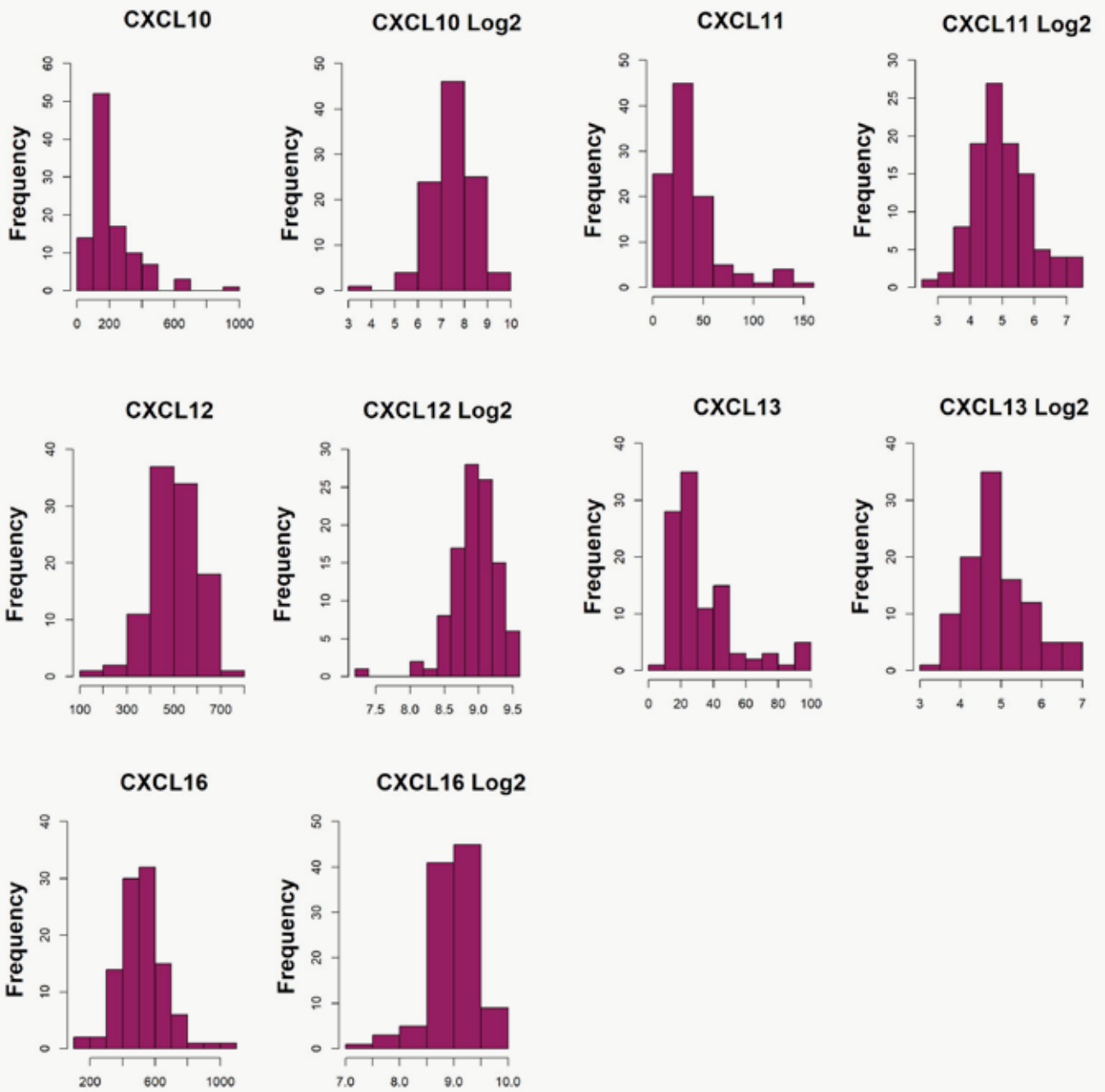
Additionally, as can be observed in **Figure 19.A-C.** all CXC chemokines were logarithmically transformation (Log2). This was necessary for the principal component analysis (PCA), aiming to achieve normality and reduce skewness.

Exploratory data analysis was carried out by using principal component analysis (PCA). Although in this project we are studying eleven variables instead of a large dataset of possible biomarkers, we still performed the PCA with the objective of reducing the number of variables (chemokines), while preserving as much information as possible. This method could allow us to simplify our subsequent analysis. We grouped our CXC chemokines based on their variability according to the dimensional-reduction method, the PCA.

The SCREE plot (**Figure 19.B**) consists of a simple line segment plot that shows the eigenvalues for each individual PC. It looks for the “elbow” in the curve and selects all components just before the line flattens out. In our 11 CXC chemokine model, PC1 starts high on the left, falling rather quickly and then flattening out at the fourth dimension (PC4). This is because the first component usually explains much of the overall variability.

lity, in our study, as much as 43.9%; the next components PC2, PC3 and PC4 explained only a moderate amount of this variability (19.64%, 12.8% and 6.25%, respectively). Also, we wanted to analyze the importance of each variable individually, by studying their loading (Figure 19.C). The loading equals to variables coefficients and explains which variable gives the largest contribution to the component. It is numerical and goes from -1 to 1 absolute values. In the first component (PC1) we can see how CXCL8, alongside to the absolute value, correlates positively (+ sign) and strongly influences the component. Nevertheless, it is closely followed by other 6 CXCs. Similar results were found in PC2 regarding CXCL8; in the other two dimensions (PC3 and PC4), some CXCs are negatively correlated with the components (negative signs). In summary, since the elbow values do not recall most of the variability in our model, and because every CXC recall similar loadings of the variation along the PCs, the clustering of CXCs is not a good way to describe and analyze the data. Therefore, each CXC will be further analyzed individually.





**Figure 19.A. Histograms of all eleven CXC chemokines levels at PRET.** **Left.** Histograms of the distribution. **Right.** Histogram of the Log2-transformed distribution. B. Scree plot of Principal Component Analysis (PCA) of all 11 CXC chemokines showing the total variance explained for each component (PC). Eigenvalue (bars) and cumulative variability (red line connecting dots, %) are presented for the first 9 factors. C. Computing of all variables on the first four PCs and their corresponding loadings.

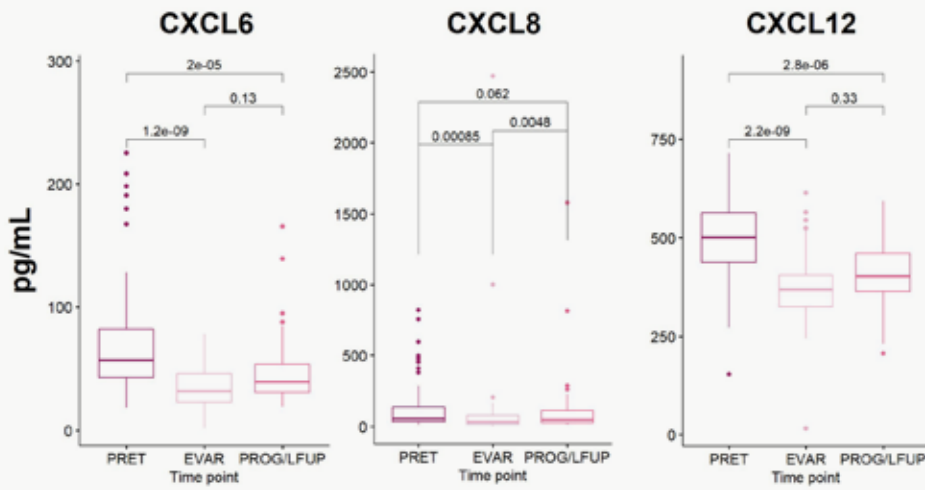
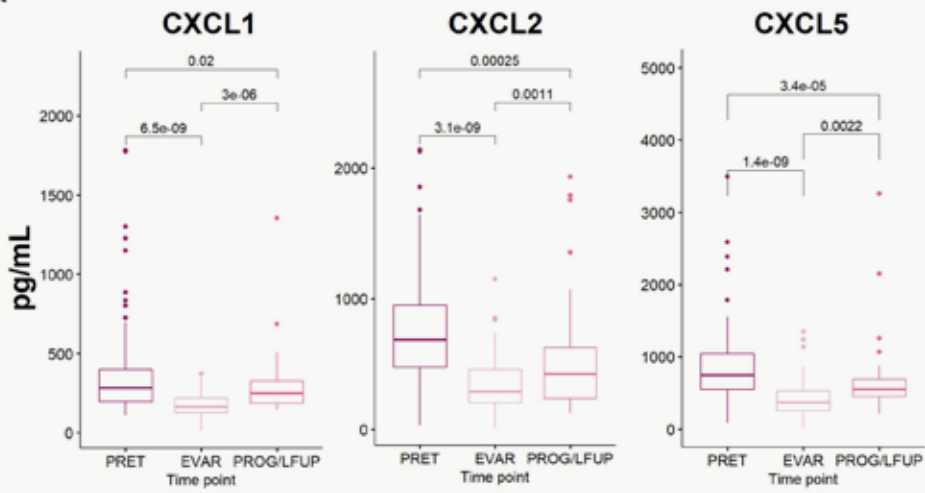
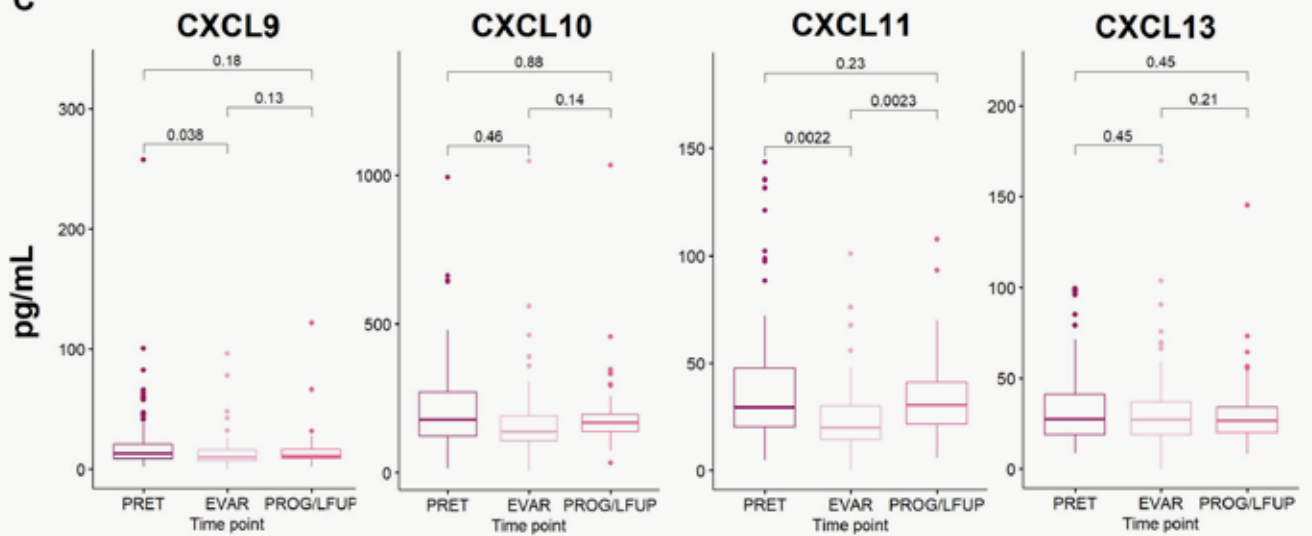
## 2.2. Time-point dynamics of CXC chemokines along the treatment

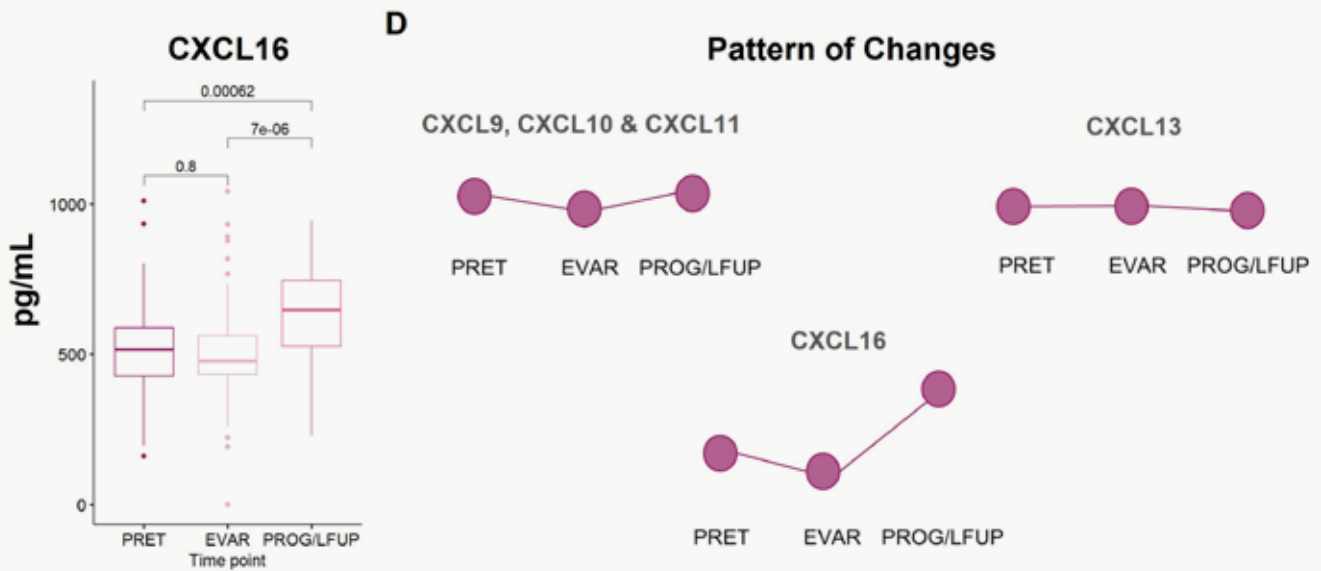
We hypothesized that the levels of the studied chemokines may vary according to the time-point at which the sample of blood was obtained. We compared the basal levels (PRET) with the ones found after a median of three months of first-line treatment (EVAR) and those taken at the time of tumor progression or end of study (PROG/LFUP). Values of each time-point corresponding to each of the studied chemokines are shown in **Table 11** and in the box plots of **Figure 20**. As it can be observed, the highest CXC levels were found in the PRET samples; in general, there was a decrease in the EVAR samples that was followed by an increase at PROG/LFUP; nevertheless, the levels at this time-point never reached the ones found in PRET samples.

CHEMOKINES	TIME-POINTS			P VALUE		
	PRET	EVAR	PROG/LFUP	PRET-EVAR	EVAR-PROG	PRET-PROG
<b>Angiogenic</b>						
<b>CXCL1</b>	283.3 [196.7;397.2]	162.8 [124.6;217.7]	242.7 [182.8;286.7]	<b>6.5e-09</b>	<b>3.1e-08</b>	<b>0.036</b>
<b>CXCL2</b>	686.9 [475.2;950.6]	291.0 [204.1;456.5]	408.7 [254.5;612.2]	<b>3.1e-09</b>	<b>3.3e-05</b>	<b>0.00055</b>
<b>CXCL5</b>	745.7 [547.4;1041.6]	373.3 [254.5;529.3]	518.7 [441.2;664.5]	<b>1.4e-09</b>	<b>0.00029</b>	<b>8,00E-06</b>
<b>CXCL6</b>	57.0 [42.7;82.1]	32.0 [22.9;46.1]	38.6 [28.3;50.8]	<b>1.2e09</b>	0.12	<b>1.5e-05</b>
<b>CXCL8</b>	54.9 [30.5;135.7]	32.2 [15.4;79.2]	33.5 [20.7;95.2]	<b>0.00085</b>	<b>0.0066</b>	<b>0.021</b>
<b>CXCL12</b>	500.8 [437.4;563.1]	368.0 [325.1;404.4]	402.1 [363.4;451.2]	<b>2.2e-09</b>	0.2	<b>8.6e-06</b>
<b>Angiostatic</b>						
<b>CXCL9</b>	12.9 [8.9;21.1]	10.0 [6.9;16.0]	10.5 [8.4;14.5]	<b>0.038</b>	0.21	<b>0.033</b>
<b>CXCL10</b>	178.8 [123.3;271.2]	139.6 [106.8;191.4]	160.1 [129.8;198.1]	0.46	0.14	0.78
<b>CXCL11</b>	29.6 [20.4;47.5]	20.0 [14.4;30.0]	28.1 [20.1;40.5]	<b>0.0022</b>	<b>0.00071</b>	0.36
<b>CXCL13</b>	27.4 [19.0;41.1]	27.1 [18.9;36.9]	24.9 [18.0;34.2]	0.45	0.26	0.64
<b>CXCL16</b>	516.0 [427.0;588.8]	478.6 [431.9;561.1]	646.7 [525.5;739.5]	<b>9.6-05</b>	0.8	<b>2.0e-05</b>

**Table 11. Comparison of the median levels (pg/mL) of the eleven CXCs under study found in serum obtained at specified time-points.** P values correspond to paired t-test. [IQR] interquartile range. In bold, all statistically significant results (p <0.05).

However, we observed these patterns were different if we took into account the CXC role as angiogenic or angiostatic factors. All angiogenic chemokines displayed a similar pattern of changes during the study course: levels were high at baseline, followed by a reduction at EVAR and an increase at PROG/FOLLOW-UP (**Figure 20.A**). Most of these differences were statistically significant (**Table 11**, angiogenic). On the other hand, the pattern of changes corresponding to angiostatic CXCs (**Figure 20.B**) was very heterogeneous with almost a different one observed for each angiostatic CXC (**Figure 20.D**; **Table 11**, angiostatic).

**A****B****Pattern of Changes****C**



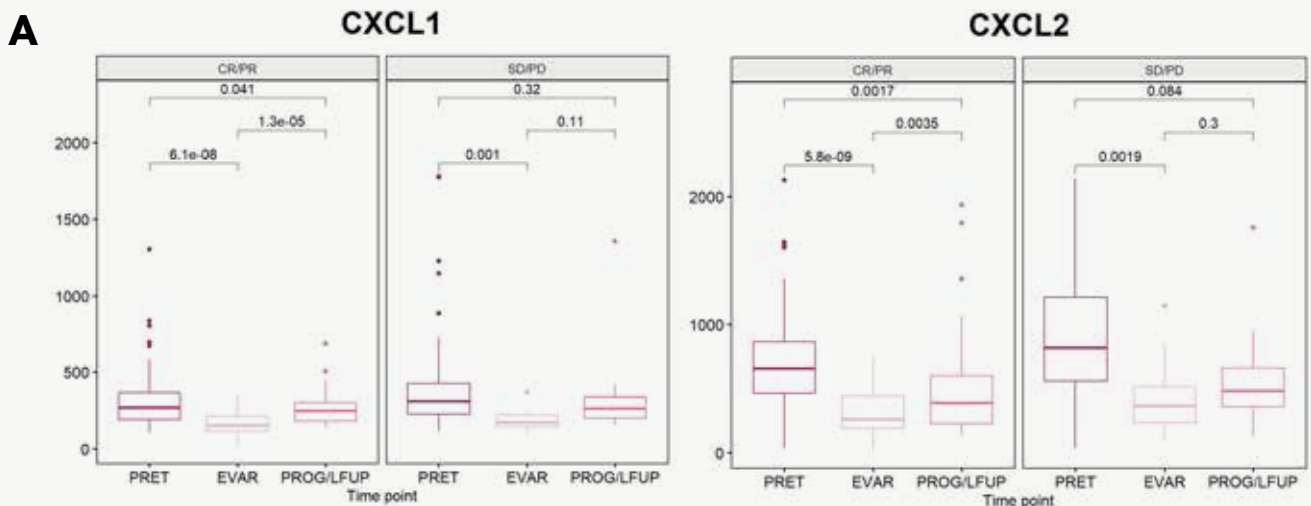
**Figure 20. Dynamics of the levels of specified CXC chemokines along the study.** Figure A and B: angiogenic (CXCL1, 2, 5, 6, 8 & 12) chemokines. Figure C and D: angiostatic (CXCL9, 10, 11, 13 & 16) chemokines. The horizontal line in each data cluster represents the median value.

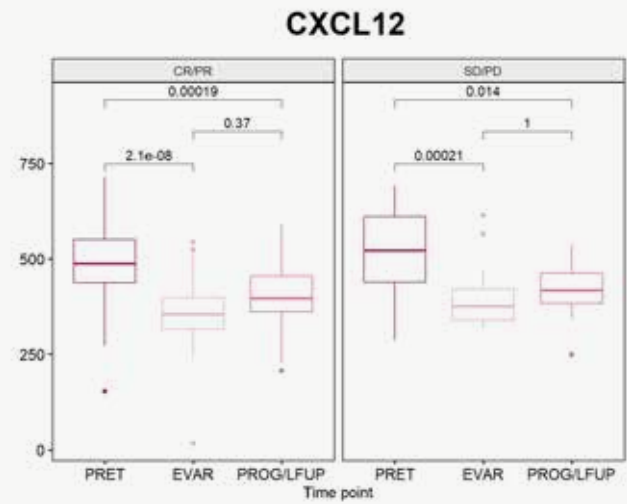
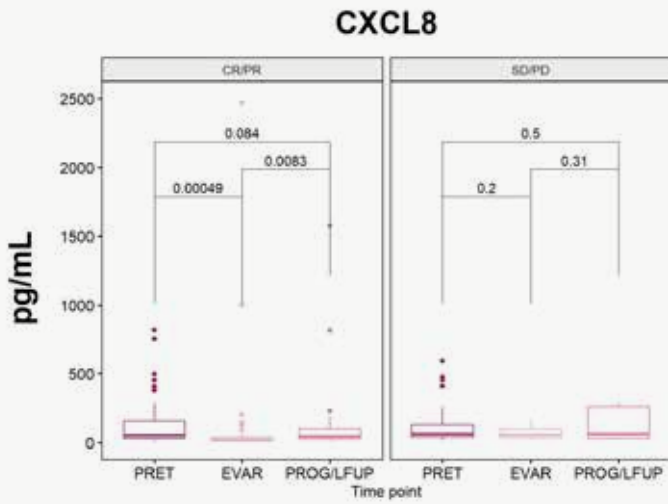
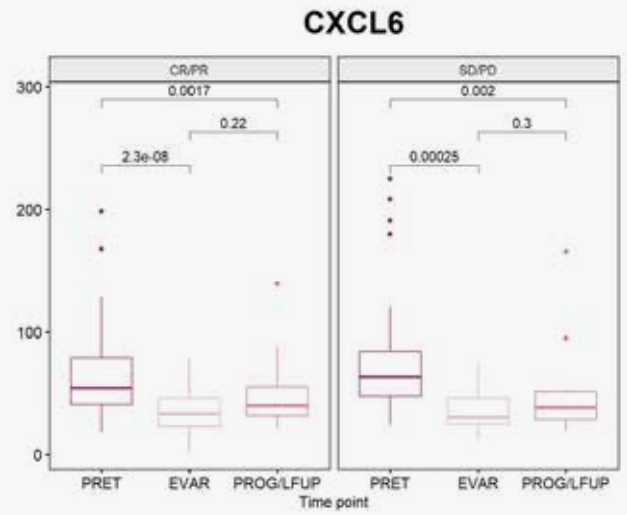
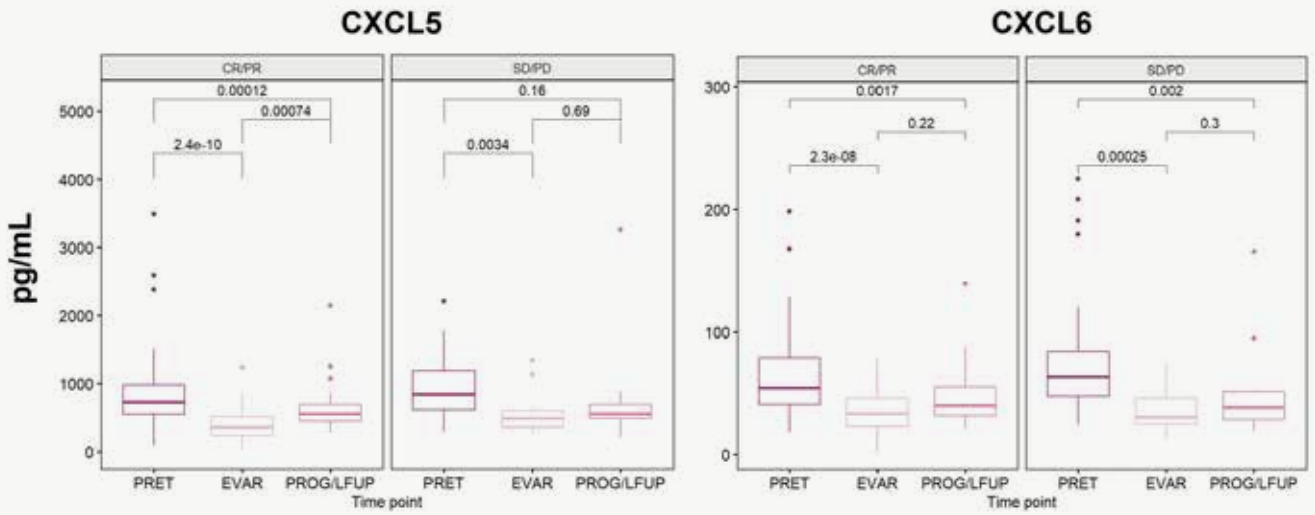
We wonder whether these patterns were different according to the patients' response to treatment. We therefore divided the patients in responders (R = CR/PR) and non-responders (NR = SD/PD) and studied their CXC pattern of changes. Values of each time-point corresponding to each CXC based on patients' response are shown in **Table 12** and in the box plots of **Figure 21**.

Interestingly, we observed the same pattern of changes among angiogenic **Figure 21.A** and angiostatic **Figure 21.B** CXCs regardless of the response to treatment.

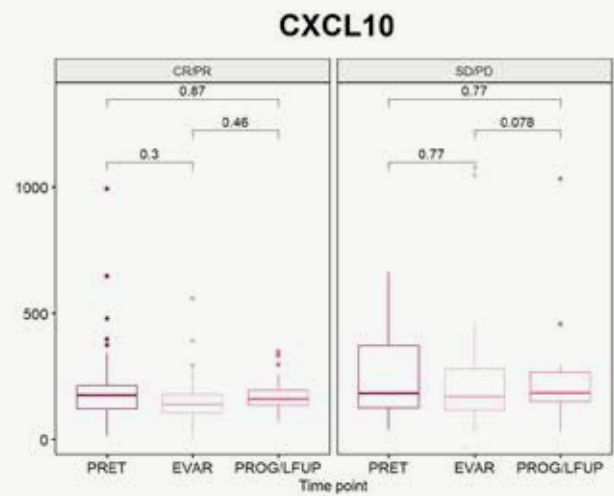
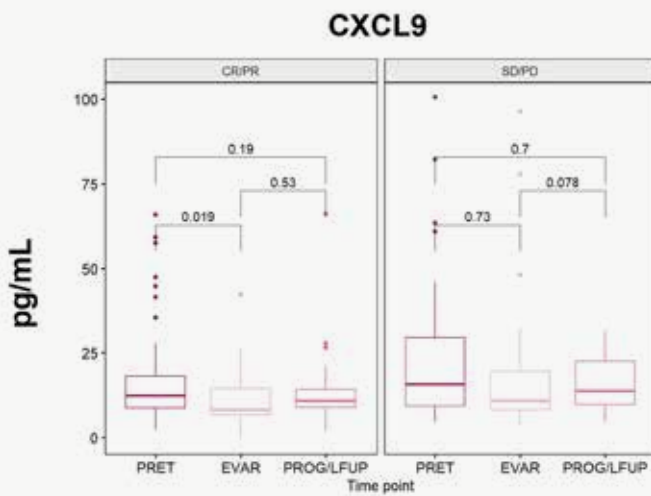
CHEMOKINES	TIME-POINTS						P VALUE					
	PRET		EVAR		PROG/LFUP		PRET-EVAR		EVAR-PROG		PRET-PROG	
	R N = 68	NR N = 36	R N = 45	NR N = 18	R N = 33	NR N = 10	R	NR	R	NR	R	NR
<b>Angiogenic</b>												
<b>CXCL1</b>	270.4 [191.;367.0]	311.5 [227.9;426.8]	155.8 [117.1;213.6]	174.9 [145.3;219.8]	248.8 [183.2;302.6]	263.8 [201.5;337.4]	<b>6.1e-08</b>	<b>0.001</b>	<b>1.3e-05</b>	0.11	<b>0.041</b>	0.32
<b>CXCL2</b>	655.5 [463.1;865.5]	818.7 [556.4;1213.6]	260.3 [188.3;440.5]	369.5 [234.8;510.8]	389.2 [229.1;599.9]	480.4 [360.8;659.6]	<b>5.8e-09</b>	<b>0.0019</b>	<b>0.0035</b>	0.3	<b>0.0017</b>	0.084
<b>CXCL5</b>	729.7 [546.0;977.2]	842.3 [614.0;1189.2]	356.8 [237.5;508.0]	489.3 [359.6;599.6]	551.7 [445.9;690.4]	554.6 [492.4;692.8]	<b>2.4e-10</b>	<b>0.0034</b>	<b>7.4e-04</b>	0.69	<b>1.2e-04</b>	0.16
<b>CXCL6</b>	54.2 [40.5;78.8]	63.3 [47.3;83.9]	32.8 [22.8;45.7]	30.1 [24.8;45.8]	39.6 [31.2;55.0]	38.0 [28.1;51.0]	<b>2.3e-08</b>	<b>2.5e-04</b>	0.22	0.3	<b>0.0017</b>	<b>0.002</b>
<b>CXCL8</b>	52.0 [29.4;159.3]	61.4 [37.1;131.0]	23.6 [12.4;40.7]	56.6 [32.2;97.7]	43.7 [24.6;99.5]	61.8 [30.4;258.5]	<b>4.9e-04</b>	0.2	<b>0.0083</b>	0.31	0.084	0.5
<b>CXCL12</b>	488.1 [437.4;551.4]	522.8 [438.7;611.4]	354.9 [316.0;398.3]	376.1 [338.5;419.6]	398.0 [361.7;454.7]	417.6 [383.8;462.2]	<b>2.1e-08</b>	<b>2.1e-04</b>	0.37	1	<b>1.9e-04</b>	<b>0.014</b>
<b>Angiostatic</b>												
<b>CXCL9</b>	12.5 [8.9;18.1]	15.8 [9.2;29.6]	8.1 [6.6;14.5]	11.0 [8.2;19.6]	10.9 [8.9;14.3]	13.8 [9.9;22.5]	<b>0.019</b>	0.73	0.53	0.078	0.19	0.7
<b>CXCL10</b>	177.3 [122.0;214.9]	183.8 [124.5;372.1]	139.0 [103.7;178.9]	171.3 [115.9;280.2]	162.5 [136.3;195.6]	186.3 [150.3;267.5]	0.3	0.77	0.46	0.078	0.87	0.77
<b>CXCL11</b>	28.3 [20.3;43.4]	30.8 [21.2;59.0]	16.8 [14.2;23.5]	25.0 [19.8;35.3]	28.0 [20.5;37.7]	38.9 [29.4;67.1]	<b>0.0046</b>	0.17	0.06	<b>0.016</b>	0.28	0.77
<b>CXCL13</b>	26.0 [18.2;39.1]	28.0 [22.2;45.9]	28.4 [18.9;40.2]	24.2 [18.4;34.8]	25.8 [20.2;32.1]	28.4 [20.0;53.8]	0.24	0.64	0.15	0.94	0.78	0.28
<b>CXCL16</b>	498.4 [427.0;581.2]	528.7 [427.2;598.6]	473.4 [423.1;539.1]	548.7 [452.1;619.8]	650.5 [550.7;736.2]	564.1 [476.0;813.7]	0.39	0.39	<b>4.4e-05</b>	0.078	<b>4.4e-04</b>	0.62

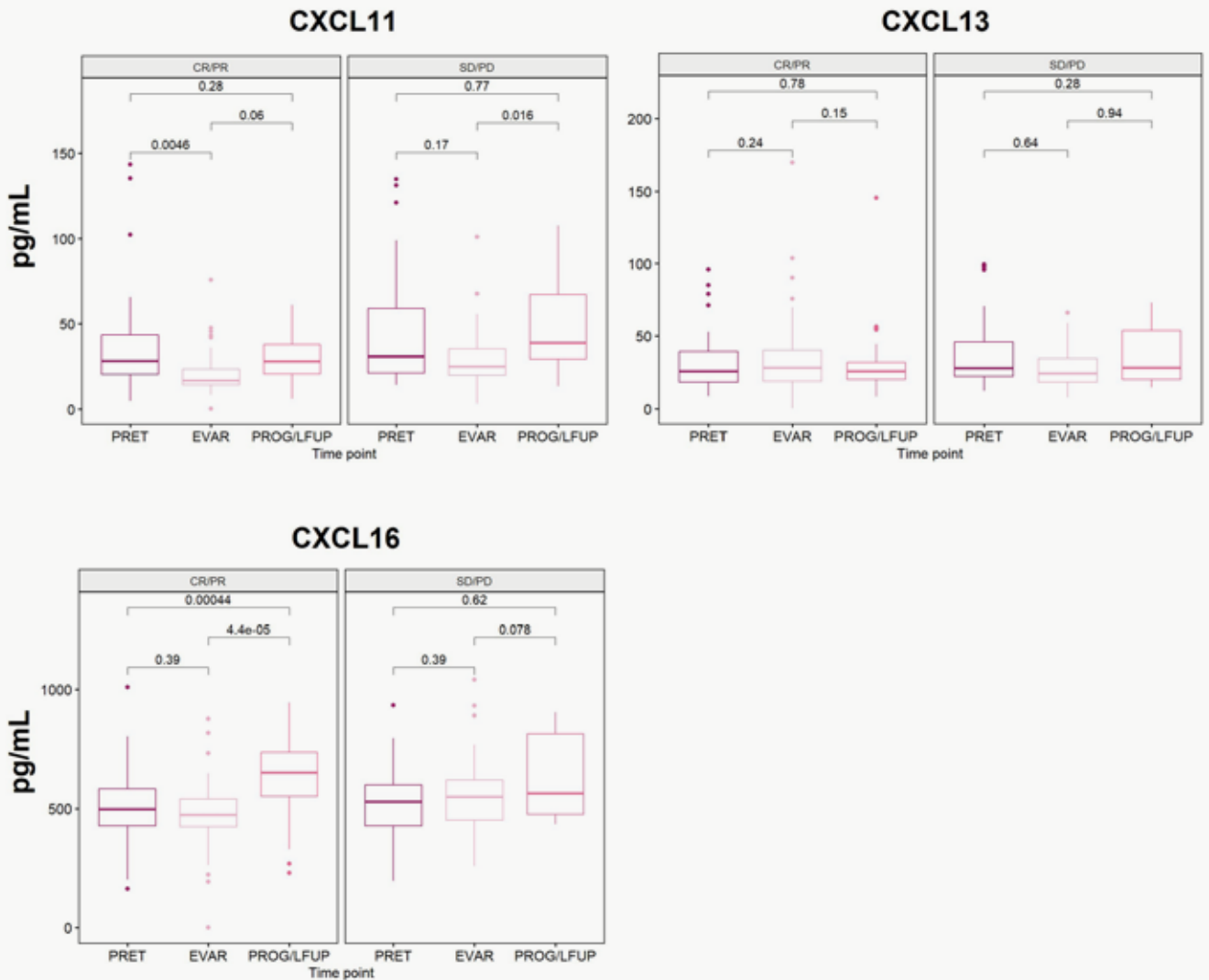
**Table 12. Comparison of the median levels (pg/mL) of the eleven CXCs under study found in serum obtained at specified time-points in responders (R) and non-responders (NR).** P values correspond to paired t-test. [IQR] interquartile range. In bold, all statistically significant results ( $p < 0.05$ ).





**B**

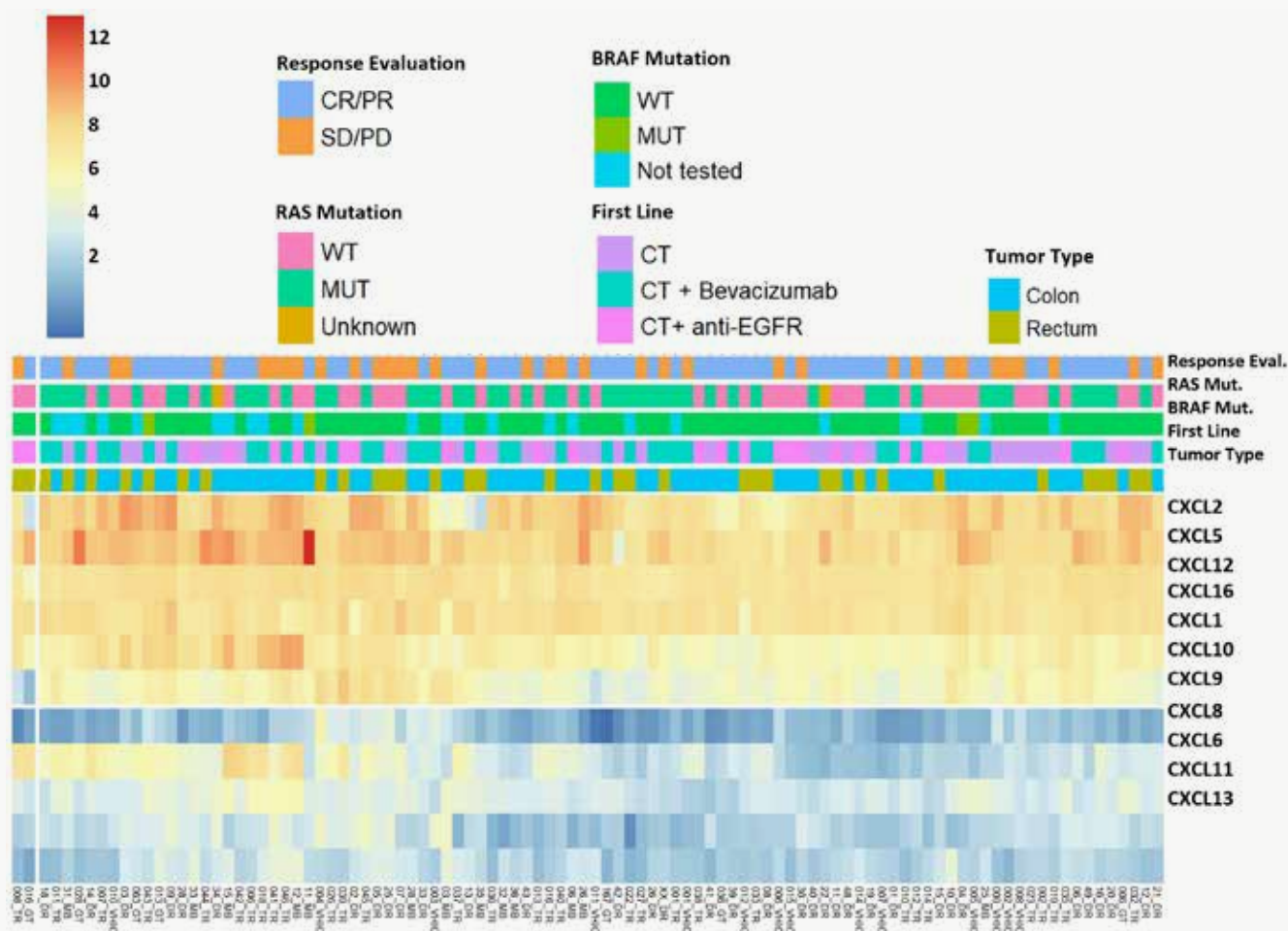




**Figure 21. Dynamics of all CXC chemokine levels along the study comparing responder and non-responder patients.** A: angiogenic (CXCL1, 2, 5, 6, 8 & 12) chemokines. B: angiostatic (CXCL9, 10, 11, 13 & 16) chemokines. The horizontal line in each data cluster represents the median value.

### 2.3. Multidimensional analysis of CXC PRET levels with clinicopathological and molecular patients' features

We performed a multidimensional analysis to study the distribution of the basal levels of the different CXC and according to the patients' clinicopathological characteristics. The heatmap in **Figure 22** shows the unsupervised distribution of the CXC chemokines. There was no evident association of any CXC cluster with the clinicopathological characteristics. However, we observed two well-differentiated groups that corresponded to highly and lowly abundant CXCs at PRET. The highly abundant group, depicted in yellow-orange in the heatmap, included CXCL1, 2, 5, 10, 12, and 16; interestingly, except for CXCL10 and 16 which are angiostatic, the rest are classified as angiogenic. In contrast, the low levels group, depicted in blue tones, mostly includes angiostatic chemokines (CXCL6, 9, 10, 11, and 13) with the exception of CXCL8.



**Figure 22.** Heatmap showing the unsupervised distribution of CXC chemokines' levels in PRET samples and according to clinicopathological variables.

#### 2.4. Association of PRET, EVAR and PROG CXC chemokines levels with patients' clinicopathological and molecular characteristics and with response to treatment

We then investigated the possible associations between the CXC levels at the three time-points and the clinicopathological and molecular characteristics of patients as well as their association with response to first-line treatment. All results can be found in the **Annex VI** and here we only show statistically significant associations (**Table 13** and **Figure 23**).

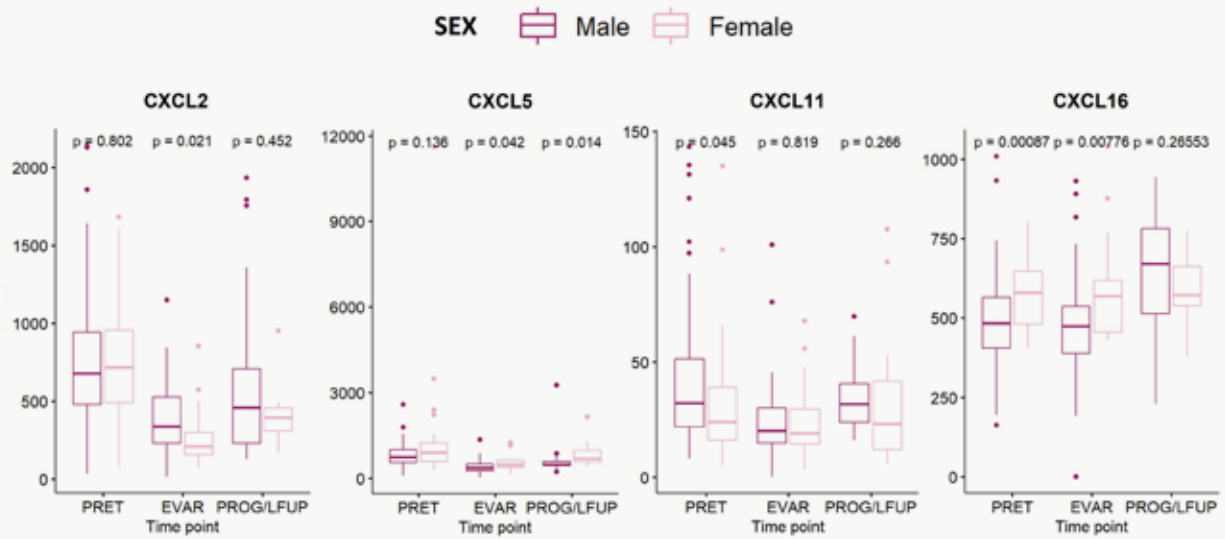
The majority of statistically significant associations were found in PRET samples. Of all CXC studied, CXCL1, CXCL2, CXCL5, CXCL8 and CXCL16 were the most frequently associated with the features investigated here. All these chemokines were associated with number and/or target organ of metastasis; specifically, in PRET samples, high levels of CXCL1, CXCL5 and CXCL16 were associated with lung metastasis and liver and lung metastasis while higher levels of CXCL8 and CXCL12 were found in samples from patients with liver metastasis only. High CXCL8 was also associated with liver and lung metastasis; however, patients with peritoneum metastasis had lower levels of CXCL8. Patients with multiple metastasis had higher levels of CXCL1, 2, 6, 8 and 9 at PRET and of CXCL8 at EVAR samples. Patients whose primary tumour was located at the colon,

displayed higher levels of CXCL2 at PRET and PROG/LFUP samples. Females had higher levels of CXCL16 than males at PRET and EVAR samples; higher levels of CXCL5 at EVAR were also found in females. Regarding RAS and BRAF mutations, we found higher levels of CXCL16 in samples obtained after treatment (EVAR) and at PROG/LFUP of patients harbouring RAS mutations; patients harbouring BRAF mutant-tumours had higher basal levels of CXCL5 and CXCL6. We did not find clear associations with first-line treatment schedules. Finally, patients who basally presented higher levels of CXCL16 and CXCL6 underwent surgery during the study more frequently.

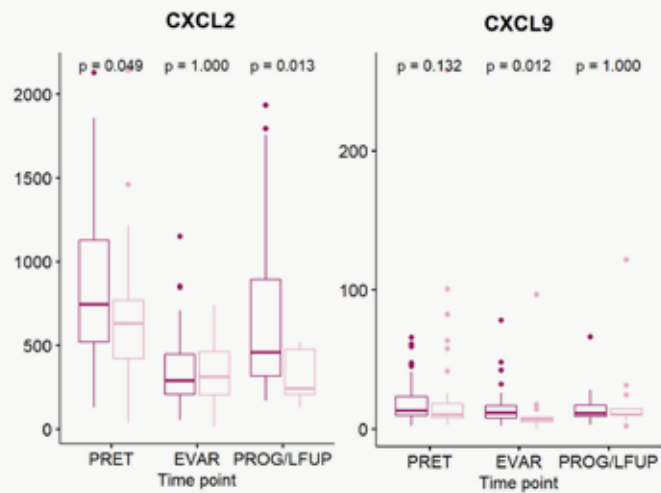
One of our objectives was to demonstrate the possible predictive value of the chemokines under study. In this regard, we studied their possible association with response to first-line treatment. We found that patients who did not respond to treatment had higher CXCL2 basal levels and higher CXCL5, 8 and 11 at the time of response evaluation.

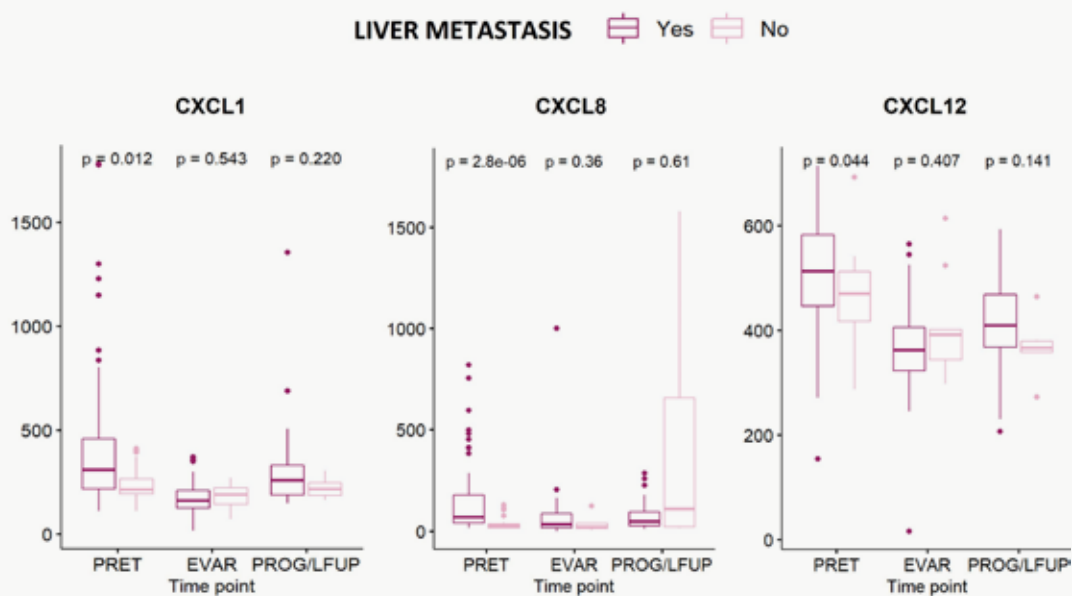
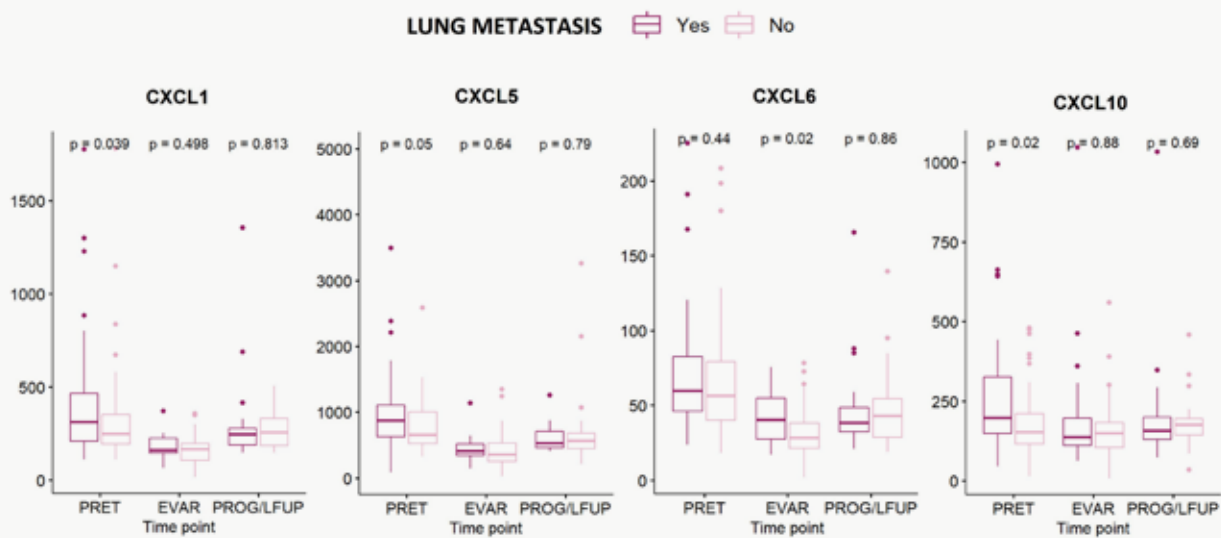
CLINICOPATHOLOGICAL CHARACTERISTICS	TIME-POINT SAMPLE	CXC CHEMOKINE	CXC LEVELS ASSOCIATION	P VALUE
Sex (Female)	PRET	CXCL11	Low	0.045
		CXCL16	High	0.001
	EVAR	CXCL2	Low	0.021
		CXCL5, 16	High	<0.05
	PROG	CXCL5	High	0.014
Primary Tumor Site (Colon)	PRET	CXCL2	High	0.049
	EVAR	CXCL9	High	0.012
	PROG	CXCL2	High	0.013
Liver Metastasis	PRET	CXCL1, 8, 12	High	<0.04
Lung Metastasis	PRET	CXCL1, 5, 10, 16	High	≤0.05
	EVAR	CXCL6, CXCL13	High	<0.03
Peritoneum Metastasis	PRET	CXCL8	Low	0.01
Metastatic Site (Liver + Lung Metastasis)	PRET	CXCL1, 5, 8, 16	High	≤0.04
Oligo/Multiple Metastasis (Multiple Metastasis)	PRET	CXCL1, 2, 6, 8, 9	High	<0.04
	EVAR	CXCL8	High	0.045
	PROG	CXCL12	High	0.036
First Line Treatment Type (Chemotherapy Alone)	EVAR	CXCL16	High	0.042
	PROG	CXCL6	Low	0.027
Response Evaluation (Non-Responders)	PRET	CXCL2	High	0.026
	EVAR	CXCL5, 8, 11	High	<0.03
Radical Surgery	PRET	CXCL6, 16	Low	≤0.04
	PROG	CXCL8, 9	Low	<0.04
BRAF Mutation	PRET	CXCL5, 6	High	<0.02
RAS Mutation	EVAR	CXCL16	High	0.001
	PROG	CXCL10, 12	Low	≤0.05
		CXCL16	High	0.025

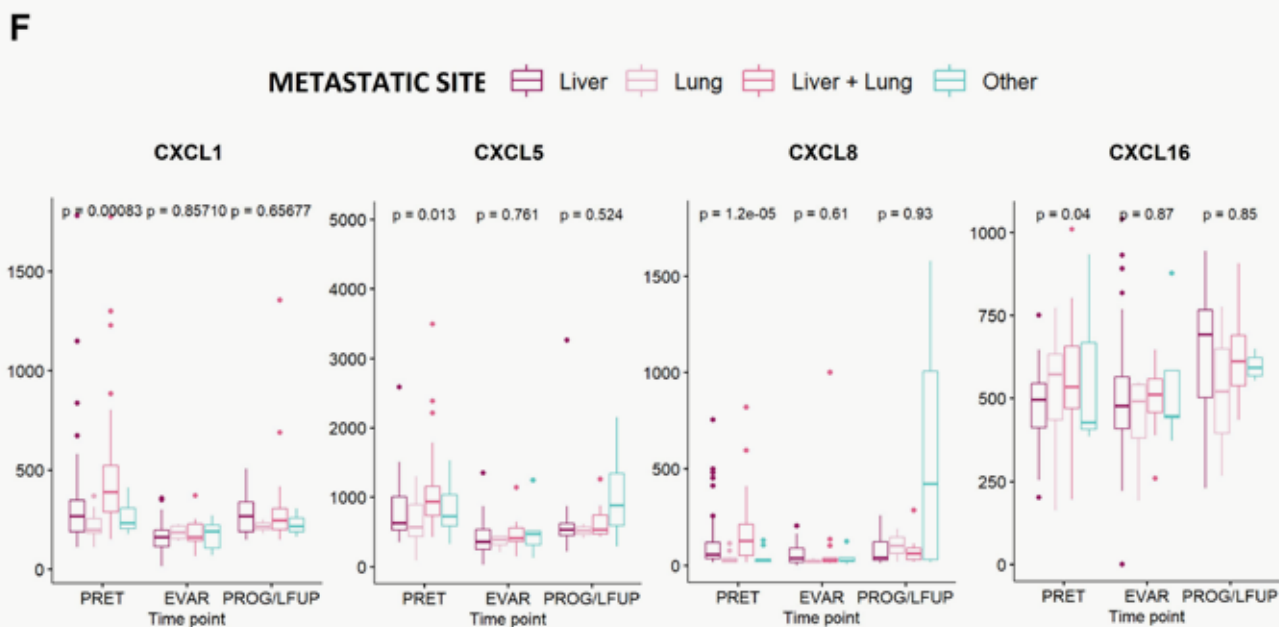
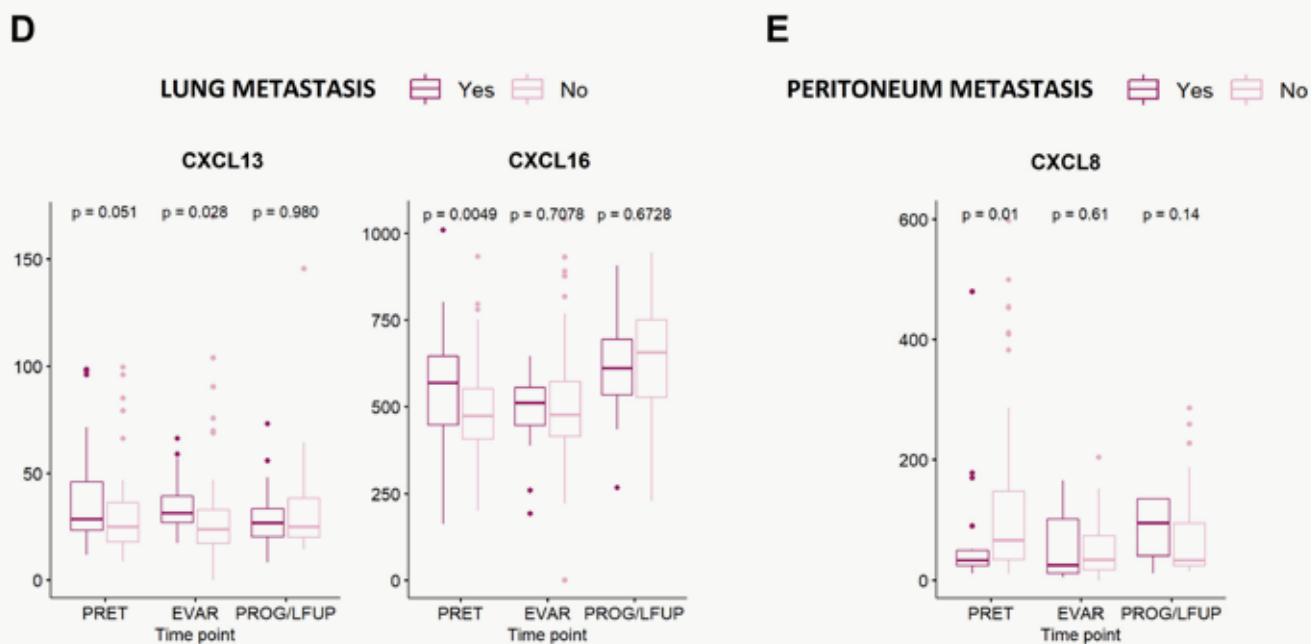
**Table 13. Associations of chemokines' levels with clinico-pathological and molecular variables as well as with response to treatment, according to the different time-points studied.** P values correspond to the Kruskal-Wallis test; Grouped p values for more than one statistically significant CXC. The exact low/high values for each chemokine are shown in **Annex VI**.

**A****B**

PRIMARY TUMOR SITE  Colon  Rectum

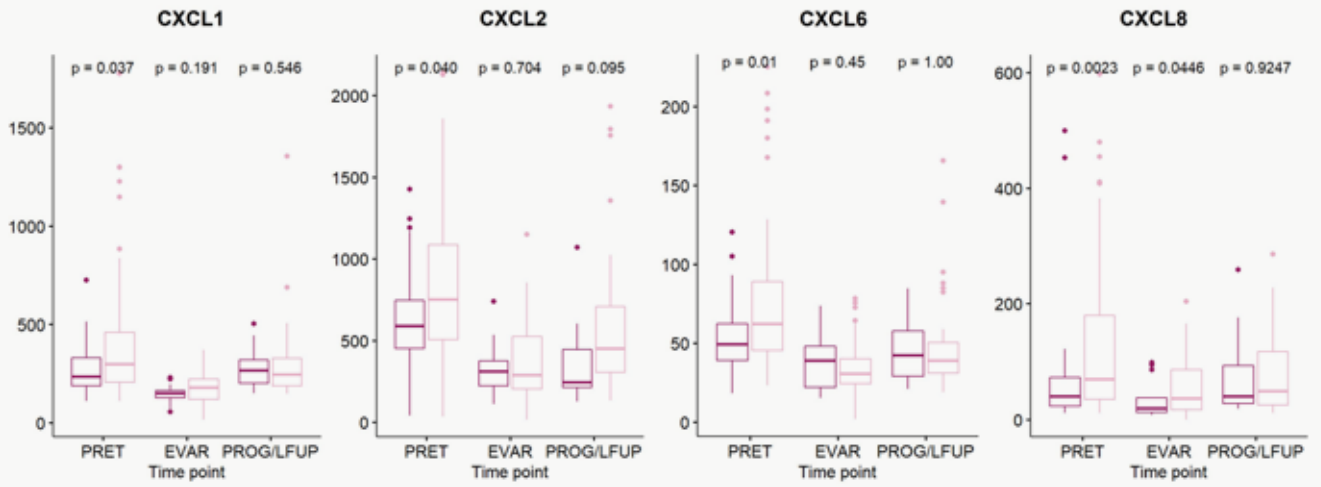


**C****D**

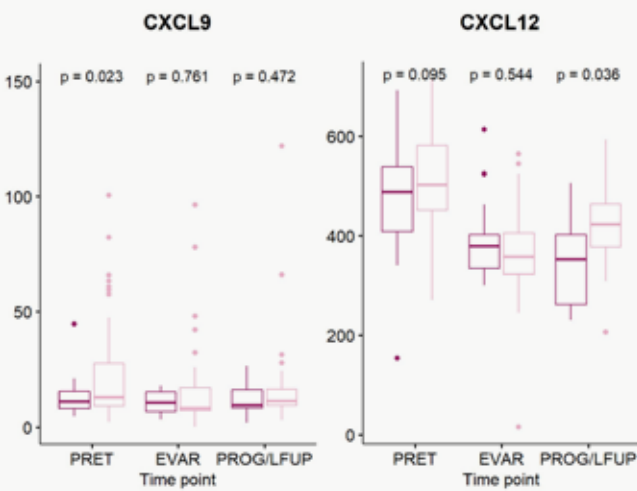


**G****OLIGO/MULTIPLE METASTASIS**

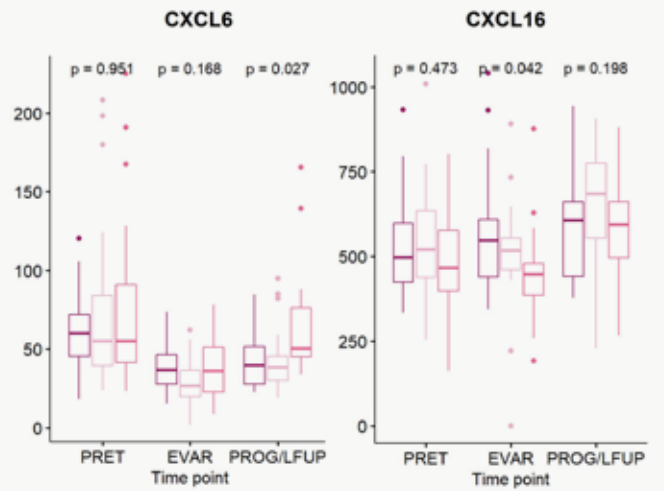
 < 5 Metastasis  
 ≥ 5 Metastasis

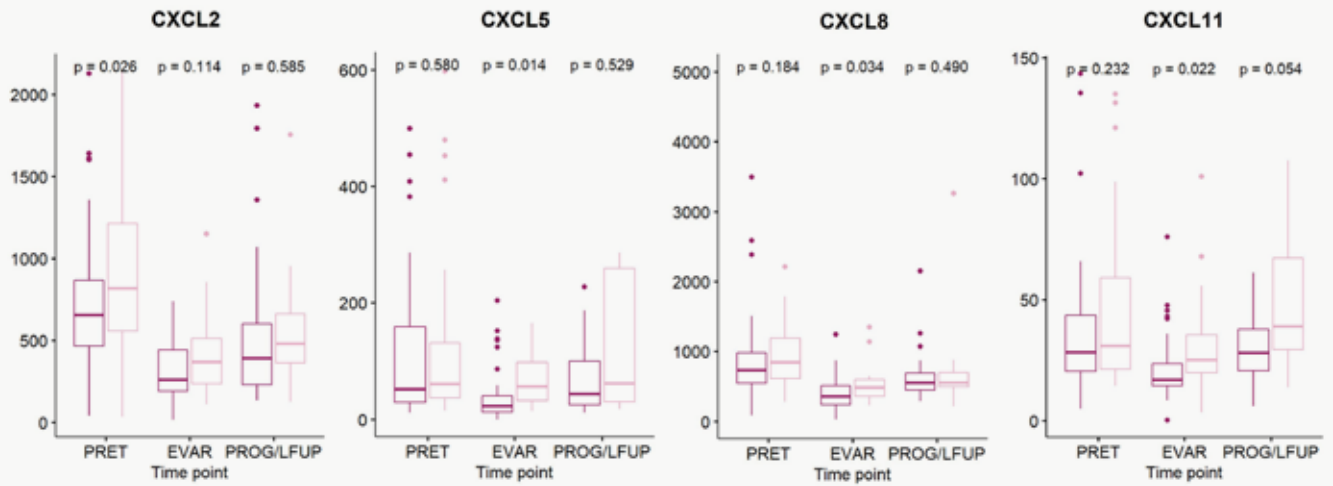
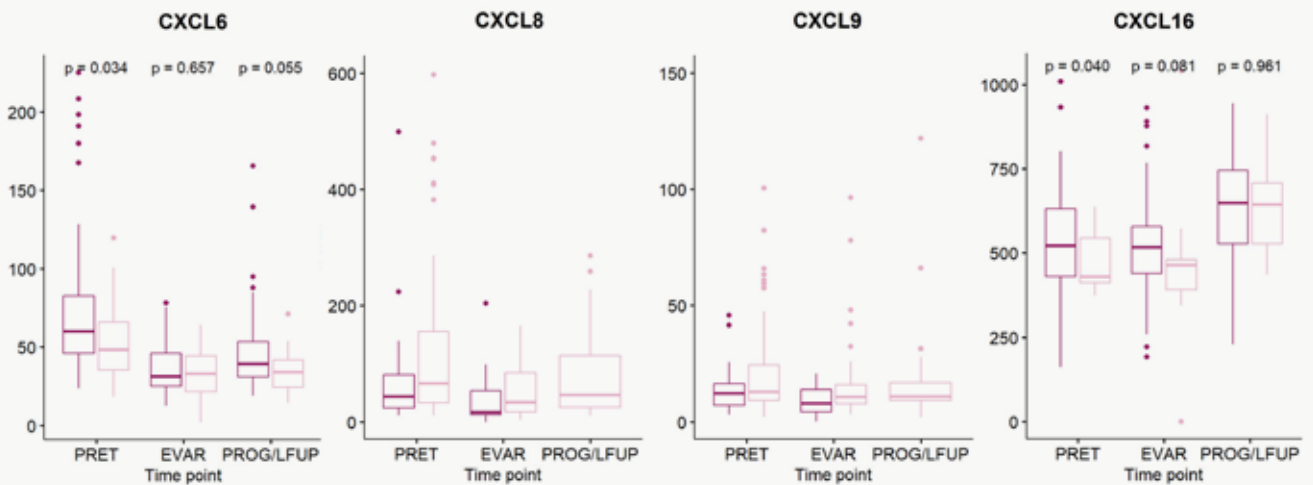
**G****OLIGO/MULTIPLE METASTASIS**

 < 5 Metastasis  
 ≥ 5 Metastasis

**H****FIRST LINE TREATMENT TYPE**

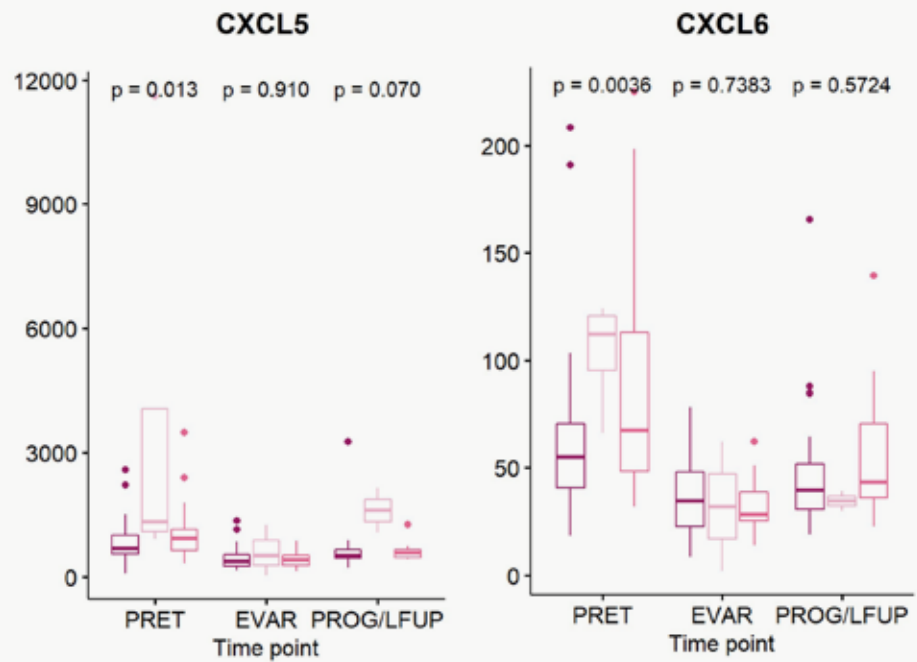
 CT    CT + Bevacizumab  
 CT+ anti-EGFR



**I****RESPONSE EVALUATION**
**J****RADICAL SURGERY**


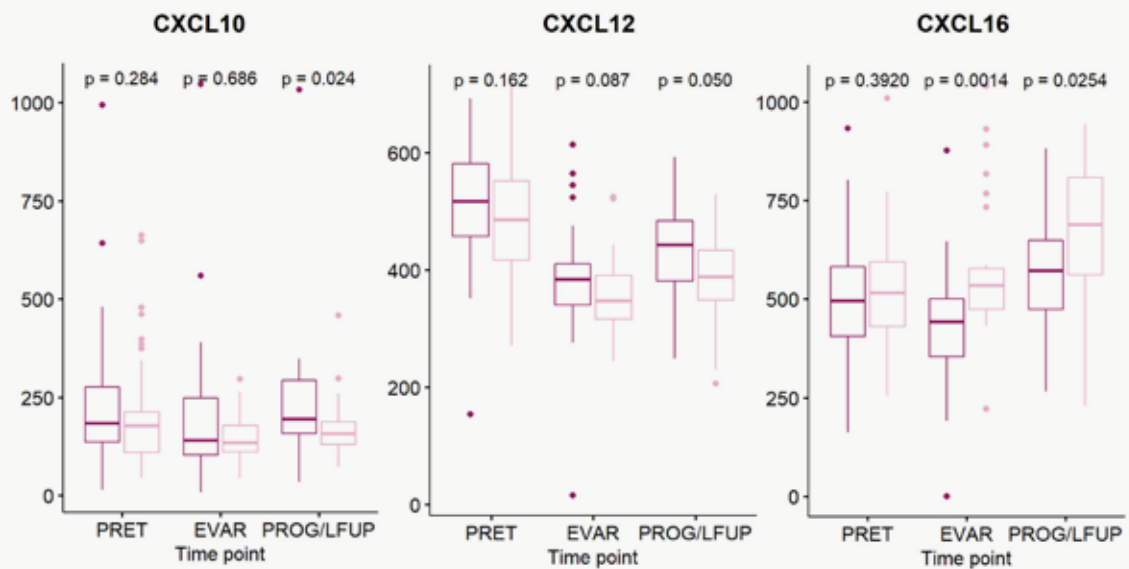
K

**BRAF MUTATION**  WT  MUT  Not tested



L

**RAS MUTATION**  WT  MUT



**Figure 23. Serum levels of the statistically significant chemokines along the time-points PRET, EVAR and PROG/FLUP and their association with the indicated features.** The horizontal line in each boxplot represents the median value. P values correspond to the Kruskal-Wallis test.

## 2.5. CXC chemokines serum levels and their association with OS and PFS

We investigated the possible role of the CXC chemokines under study as prognostic markers of PFS and OS. Here, we only show results concerning PRET samples and changes between PRET and EVAR samples. Results taking into account CXC levels at EVAR and PROG are shown in the **Annex VII**.

As commented before, we found that 22% of our patients had a radical surgery during the study and that this had a clear impact in survival. We considered that the fact of removing a tumor mass could strongly affect the amount of CXC found in blood as it can be considered as a source of releasing them<sup>314</sup>, having an impact in our results. We therefore proceeded to study the prognostic role of our chemokines following two different strategies:

1. To study OS and PFS in all 104 patients considering radical surgery, performance status, age, and sex in the OS multivariate model since they have prognostic value. In the case of PFS, patients who underwent surgery before tumour progression were censored at the date of surgery. PS, age and sex were taken into account in the multivariate models.
2. To study OS and PFS in 81 patients that did not undergo radical surgery (from now onwards, non-operated patients). PS, age, and sex were considered in the multivariate models.

### 2.5.1. CXC chemokines serum levels and their association with OS and PFS in all patients

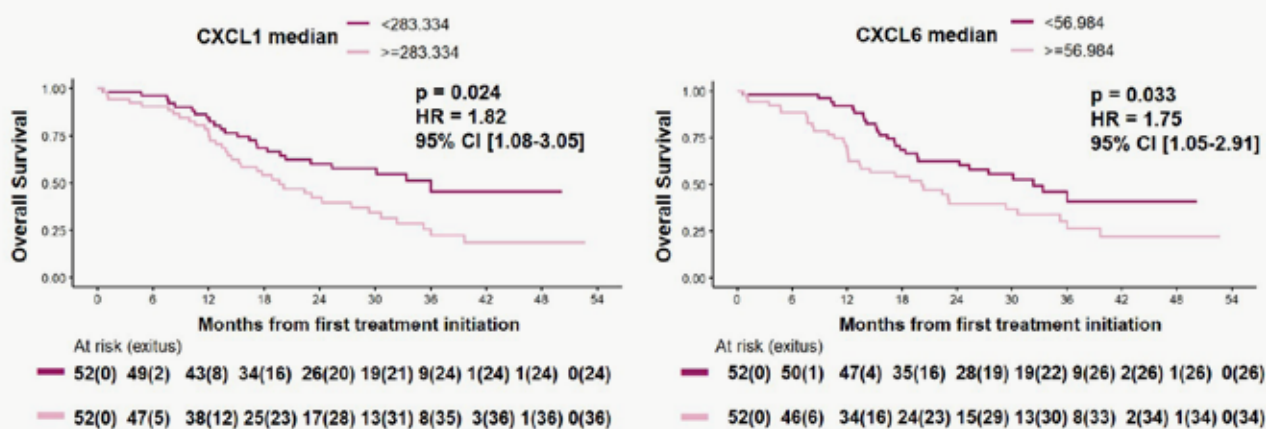
#### 2.5.1.1. Basal CXC levels and their association with OS and PFS

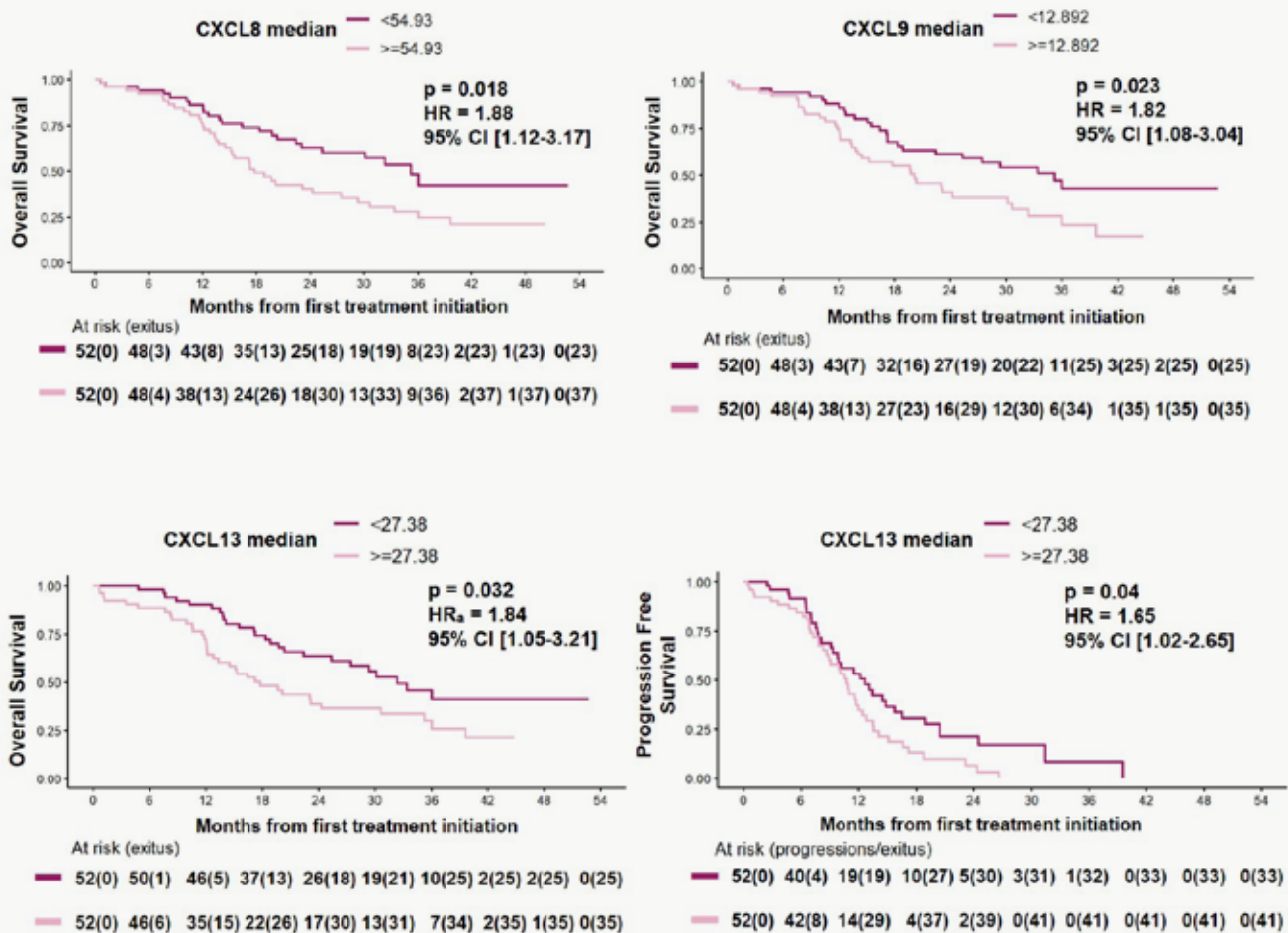
To study the association of PRET CXC levels with OS and PFS, we chose to categorize the variable according to the median value of each CXC (above and below values). Univariate and adjusted multivariate COX models were performed. A summary of the results is shown in **Table 14**.

Median OS and PFS of our cohort were 25 and 11 months, respectively; According to the univariate Kaplan-Meier and COX regression analysis we found that patients with high PRET levels of CXCL1, 6, 8, and 9 had a worse OS. Of note, patients with high PRET levels of CXCL13 displayed worse PFS and OS, being the latter statistically significant also in the multivariate analysis (**Figure 24**).

BASAL LEVELS ASSOCIATION WITH RISK OF DEATH OR PROGRESSION. N = 104							
		OVERALL SURVIVAL			PROGRESSION FREE SURVIVAL		
CHEMOKINES	MEDIAN LEVELS	MEDIAN OS (95% CI)	HR (95% CI, p value) <sup>1</sup>	HRa (95% CI, p value) <sup>2</sup>	MEDIAN PFS (95% CI)	HR (95% CI, p value) <sup>1</sup>	HRa (95% CI, p value) <sup>2</sup>
CXCL1	<283.334	36.0 (23-NA)	<b>1.82 (1.08-3.05, p=0.024)</b>	1.17 (0.67-2.05, p=0.583)	11.7 (9.3-15.1)	1.16 (0.73-1.85, p=0.529)	0.93 (0.57-1.57, p=0.568)
	≥283.334	<b>19.6 (15.3-30.6)</b>			10.9 (9.1-13.6)		
CXCL2	<686.872	30.1 (18.8-NA)	1.34 (0.81-2.23, p=0.259)	0.97 (0.57-1.65, p=0.924)	12 (9.3-14.8)	1.07 (0.67-1.70, p=0.777)	0.90 (0.51-1.56, p=0.699)
	≥686.872	23.1 (17.8-33.4)			10.9 (9.1-13.5)		
CXCL5	<745.744	32.4 (23-NA)	1.51 (0.90-2.52, p=0.118)	0.93 (0.53-1.66, p=0.815)	11.7 (8.1-18.7)	1.30 (0.82-2.08, p=0.267)	1.67 (0.86-3.23, p=0.129)
	≥745.744	20.1 (15.3-35.2)			10.9 (9.8-13.4)		
CXCL6	<56.984	32.4 (24.3-NA)	<b>1.75 (1.05-2.91, p=0.033)</b>	1.50 (0.88-2.57, p=0.138)	11.7 (9.3-15.7)	1.24 (0.78-1.96, p=0.372)	1.23 (0.73-2.06, p=0.433)
	≥56.984	<b>20.1 (13.3-35.2)</b>			10.7 (8.9-12.8)		
CXCL8	<54.93	35.2 (25.3-NA)	<b>1.88 (1.12-3.17, p=0.018)</b>	1.59 (0.93-2.71, p=0.088)	11.7 (9.3-14.8)	1.12 (0.70-1.77, p=0.639)	0.81 (0.45-1.46, p=0.483)
	≥54.93	<b>17.8 (15.1-29.4)</b>			10.9 (9.1-13.5)		
CXCL9	<12.892	35.2 (22.4-NA)	<b>1.82 (1.08-3.04, p=0.023)</b>	1.68 (0.93-3.04, p=0.087)	12.2 (9.8-16.5)	1.50 (0.93-2.40, p=0.094)	1.63 (0.85-3.12, p=0.140)
	≥12.892	20.1 (14.1-30.6)			10.6 (8.9-12.8)		
CXCL10	<178.788	23 (17.2-NA)	1.23 (0.74-2.05, p=0.432)	0.95 (0.56-1.63, p=0.853)	11.6 (8.9-15.1)	1.18 (0.74-1.87, p=0.492)	0.65 (0.34-1.24, p=0.194)
	≥178.788	25.3 (19.6-36)			10.9 (9.8-13.5)		
CXCL11	<29.606	30.6 (20.3-NA)	1.46 (0.88-2.44, p=0.145)	1.16 (0.68-1.98, p=0.575)	11.6 (9.8-15.7)	1.42 (0.89-2.27, p=0.143)	1.46 (0.80-2.66, p=0.213)
	≥29.606	20.1 (16.4-33.4)			10.9 (8.1-13.4)		
CXCL12	<500.828	32.4 (20.3-NA)	1.39 (0.84-2.32, p=0.201)	1.54 (0.90-2.66, p=0.119)	11.5 (9.3-15.7)	1.30 (0.82-2.08, p=0.267)	0.69 (0.37-1.28, p=0.242)
	≥500.828	20.1 (15.1-39.7)			10.9 (9.1-13.5)		
CXCL13	<27.38	32.4 (25.3-NA)	<b>1.87 (1.12-3.12, p=0.017)</b>	<b>1.84 (1.05-3.21, p=0.032)</b>	12.7 (9.8-18.9)	<b>1.65 (1.02-2.65, p=0.040)</b>	1.43 (0.80-2.53, p=0.225)
	≥27.38	<b>17.8 (13.3-35.2)</b>			<b>10.7 (8.9-12.8)</b>		
CXCL16	<515.97	35.2 (20.3-NA)	1.63 (0.97-2.73, p=0.064)	1.46 (0.84-2.54, p=0.181)	10.6 (9.3-17.2)	1.52 (0.94-2.46, p=0.085)	1.66 (0.97-2.84, p=0.065)
	≥515.97	20.1 (15.3-33.4)			11 (9.1-13.4)		

**Table 14. Serum PRET median levels of the eleven CXCs studied and the association with OS and PFS.** Median OS and PFS (in months), P values, HR, and 95% CI correspond to univariate<sup>1</sup> and multivariate<sup>2</sup> COX models. HR correspond to the category above the median respect to category below the median (by default = 1). The variables: PS, radical surgery, age and sex were considered in the OS multivariate analysis; PS, age and sex in the PFS multivariate analysis. In bold, all statistically significant results with a p < 0.05.





**Figure 24. Kaplan-Meier survival curves showing OS and PFS of patients split according to the median values of the indicated CXCs at PRET.** P values, HR, and 95% CI shown correspond to univariate COX regression analysis, except for OS in the case of CXCL13 for which values of the multivariate analysis are shown.

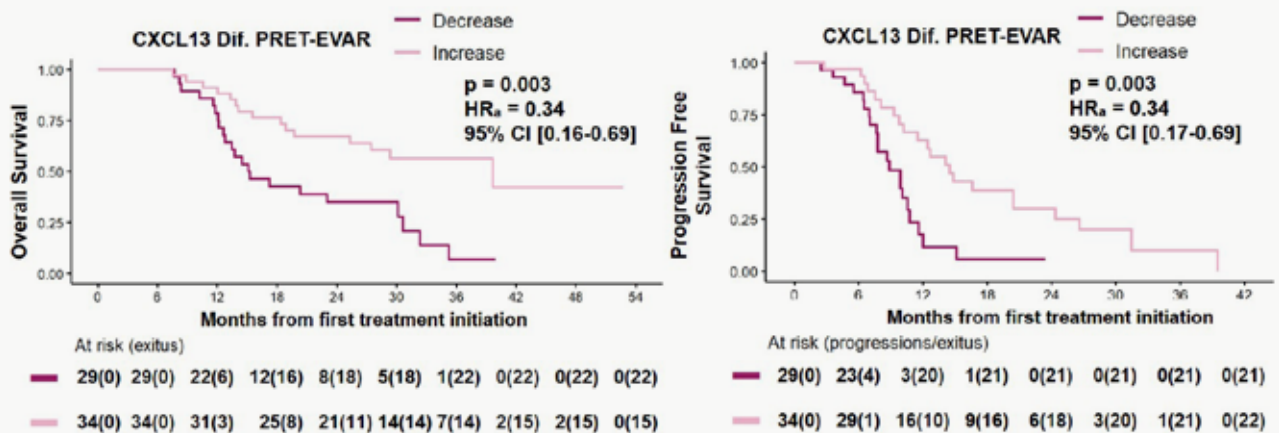
### 2.5.1.2 Dynamic changes of CXC levels between PRET and EVAR samples and their association with OS and PFS

We observed that some chemokines decreased or increased at the time of response evaluation (see section 2.2); this could be due to the influence of chemotherapy not only on the tumour but also on the host itself. Therefore, we wanted to investigate how dynamic changes between PRET and EVAR levels could affect PFS and OS of patients. The dynamic changes were evaluated as increase (higher in EVAR) or decrease (lower in EVAR) of the CXC of interest. Univariate and adjusted multivariate COX models were performed. Results are shown in **Table 15**. Dynamic changes of CXC levels between PRET-PROG and EVAR-PROG are shown in **Annex VIII**.

		DYNAMIC CHANGES ASSOCIATION WITH RISK OF DEATH OR PROGRESSION. N = 63					
		OVERALL SURVIVAL			PROGRESSION FREE SURVIVAL		
CHEMOKINES	DYNAMIC CHANGE	MEDIAN (95% CI)	HR (95%CI, p value) <sup>1</sup>	HRa (95%CI, p value) <sup>2</sup>	MEDIAN (95% CI)	HR (95%CI, p value) <sup>1</sup>	HRa (95%CI, p value) <sup>2</sup>
CXCL1 MEDIAN	Decrease	27.4 (17.2-NA)	1.10 (0.43-2.84, p=0.843)	<b>3.64 (1.11-11.91, p=0.033)</b>	11.5 (9.9-14.8)	1.73 (0.67-4.48, p=0.257)	2.81 (0.99-7.94, p=0.052)
	Increase	<b>26.6 (12.6-NA)</b>			7.5 (6.5-NA)		
CXCL2 MEDIAN	Decrease	27.4 (15.5-NA)	1.10 (0.45-2.65, p=0.835)	0.53 (0.20-1.39, p=0.194)	11.5 (9.9-14.8)	1.24 (0.52-2.97, p=0.628)	1.79 (0.69-4.63, p=0.230)
	Increase	30.1 (18.4-NA)			8.1 (7-NA)		
CXCL5 MEDIAN	Decrease	25.3 (17.2-NA)	1.39 (0.33-5.82, p=0.653)	1.05 (0.22-4.95, p=0.947)	10.6 (9.8-14.1)	1.81 (0.43-7.57, p=0.419)	1.41 (0.31-6.44, p=0.656)
	Increase	-			-		
CXCL6 MEDIAN	Decrease	20.3 (15.1-35.2)	4.07 (0.98-16.98, p=0.054)	2.56 (0.6-10.96, p=0.207)	10.6 (8.7-14.5)	1.33 (0.47-3.74, p=0.594)	1.24 (0.43-3.56, p=0.695)
	Increase	-			14.1 (10.1-NA)		
CXCL8 MEDIAN	Decrease	29.4 (17.2-NA)	1.42 (0.71-2.87, p=0.323)	1.82 (0.88-3.78, p=0.107)	11.5 (9.8-16.6)	1.45 (0.71-2.93, p=0.307)	1.44 (0.7-2.96, p=0.316)
	Increase	20.3 (13.3-NA)			9.8 (7-NA)		
CXCL9 MEDIAN	Decrease	20.3 (13.8-35.2)	1.76 (0.88-3.53, p=0.111)	1.32 (0.61-2.86, p=0.478)	10.6 (7.7-16.6)	1.25 (0.66-2.34, p=0.494)	1.16 (0.58-2.30, p=0.672)
	Increase	-			10.2 (8.9-20.4)		
CXCL10 MEDIAN	Decrease	20.3 (14.5-32.4)	1.74 (0.87-3.50, p=0.117)	1.67 (0.81-3.43, p=0.166)	10.6 (9.3-12.7)	1.52 (0.80-2.88, p=0.203)	1.74 (0.90-3.37, p=0.101)
	Increase	39.7 (15.5-NA)			10.2 (8.7-NA)		
CXCL11 MEDIAN	Decrease	30.1 (19.7-NA)	1.68 (0.85-3.33, p=0.133)	1.48 (0.70-3.14, p=0.301)	11.5 (9.8-20.4)	1.52 (0.80-2.89, p=0.203)	1.33 (0.66-2.72, p=0.426)
	Increase	15.5 (13.3-NA)			10.2 (7.5-16.6)		
CXCL12 MEDIAN	Decrease	20.3 (15.3-NA)	2.05 (0.63-6.7, p=0.235)	1.68 (0.49-5.81, p=0.413)	10.6 (9.3-14.5)	1.03 (0.4-2.65, p=0.949)	0.96 (0.36-2.54, p=0.935)
	Increase	-			14.1 (9.8-NA)		
CXCL13 MEDIAN	Decrease	15.3 (12.8-32.4)	<b>0.34 (0.17-0.67, p=0.002)</b>	<b>0.34 (0.16-0.69, p=0.003)</b>	8.9 (7.7-11.6)	<b>0.34 (0.17-0.67, p=0.002)</b>	<b>0.34 (0.17-0.69, p=0.003)</b>
	Increase	<b>39.7 (25.3-NA)</b>			<b>14.5 (11.5-26.6)</b>		
CXCL16 MEDIAN	Decrease	27.4 (14.5-NA)	1.19 (0.61-2.32, p=0.603)	1.38 (0.70-2.73, p=0.350)	10.2 (7.8-14.1)	1.50 (0.80-2.80, p=0.205)	1.58 (0.81-3.10, p=0.181)
	Increase	23 (18.4-NA)			11.5 (9.8-26.6)		

**Table 15. Dynamic changes of CXC chemokines and their association with OS and PFS.** Median OS and PFS (in months; p values, HR, and 95% CI correspond to univariate<sup>1</sup> and multivariate<sup>2</sup> COX models. HR correspond to the increase category respect to decrease category (by default = 1). The variables: PS, radical surgery, age and sex were considered in the OS multivariate analysis; PS, age and sex in the PFS multivariate analysis. Statistically significant results (p < 0.05) are highlighted in bold.

In the analysis of the dynamic changes, we found that patients with increased levels of CXCL13 at EVAR, had better OS and PFS according to both, univariate and multivariate models (**Figure 25**).



**Figure 25. Kaplan-Meier plots showing OS and PFS of patients split according to CXCL13 increase or decrease at EVAR.** P values, HRa, and 95%CI correspond to COX multivariate analysis.

So far, CXCL13 levels appear to be robustly associated with prognostic in our patients' cohort. However, while with PRET samples levels above the median were a bad prognostic factor, in the case of dynamic changes, it appears that those patients in which CXCL13 increases after 3 months of treatment are the ones with the best prognostic. In view of these apparently contradictory results, we wanted to analyse further our results. First, we have to take into account that 40% of the patients are lost in the analysis of dynamic changes as we did not have an EVAR sample. This 40% represents a big group of patients, and we had to discard the possibility that by only being able to analyse the 60%, we are selecting a population with some clinical characteristic that could be influencing our results. In order to do that we explore possible correlations among the sex, performance status, first-line treatment, response to treatment and radical surgery (**Table 16**). No statistically significant associations were found, except for the proportion of patients with disease progression as response to treatment. This was significantly lower in the group of patients with an EVAR sample (2.9% vs 8.7%  $p = 0.027$ ). Therefore, based on the results, it seems like we are not favoring any clinical feature in the analysis of our patients with available EVAR samples.

Contingency Table		PATIENTS WITH AND WITHOUT EVAR SAMPLE				
SEX		NO EVAR	YES EVAR	TOTAL		
MALE	COUNT	29	45	74		
	% from the total	27.9%	43.3%	71.2%		
FEMALE	COUNT	12	18	30	X <sup>2</sup> Pearson test	P value
	% from the total	11.5%	17.3%	28.8%		
TOTAL	COUNT	41	63	104	Fisher's test	1.000
	% from the total	39.4%	60.6%	100%	Valid Cases	104
PERFORMANCE STATUS		NO EVAR	YES EVAR	TOTAL		
WITHOUT LIMITATIONS	COUNT	14	27	41		
	% from the total	13.5%	26.0%	39.4%		
MINIMAL LIMITATIONS	COUNT	24	35	59		
	% from the total	23.1%	33.7%	56.7%		
LIMITATIONS	COUNT	3	1	4	X <sup>2</sup> Pearson test	P value
	% from the total	2.9%	1.0%	3.8%		
TOTAL	COUNT	41	63	104	Fisher's test	0.268
	% from the total	39.4%	60.6%	100%	Valid Cases	104

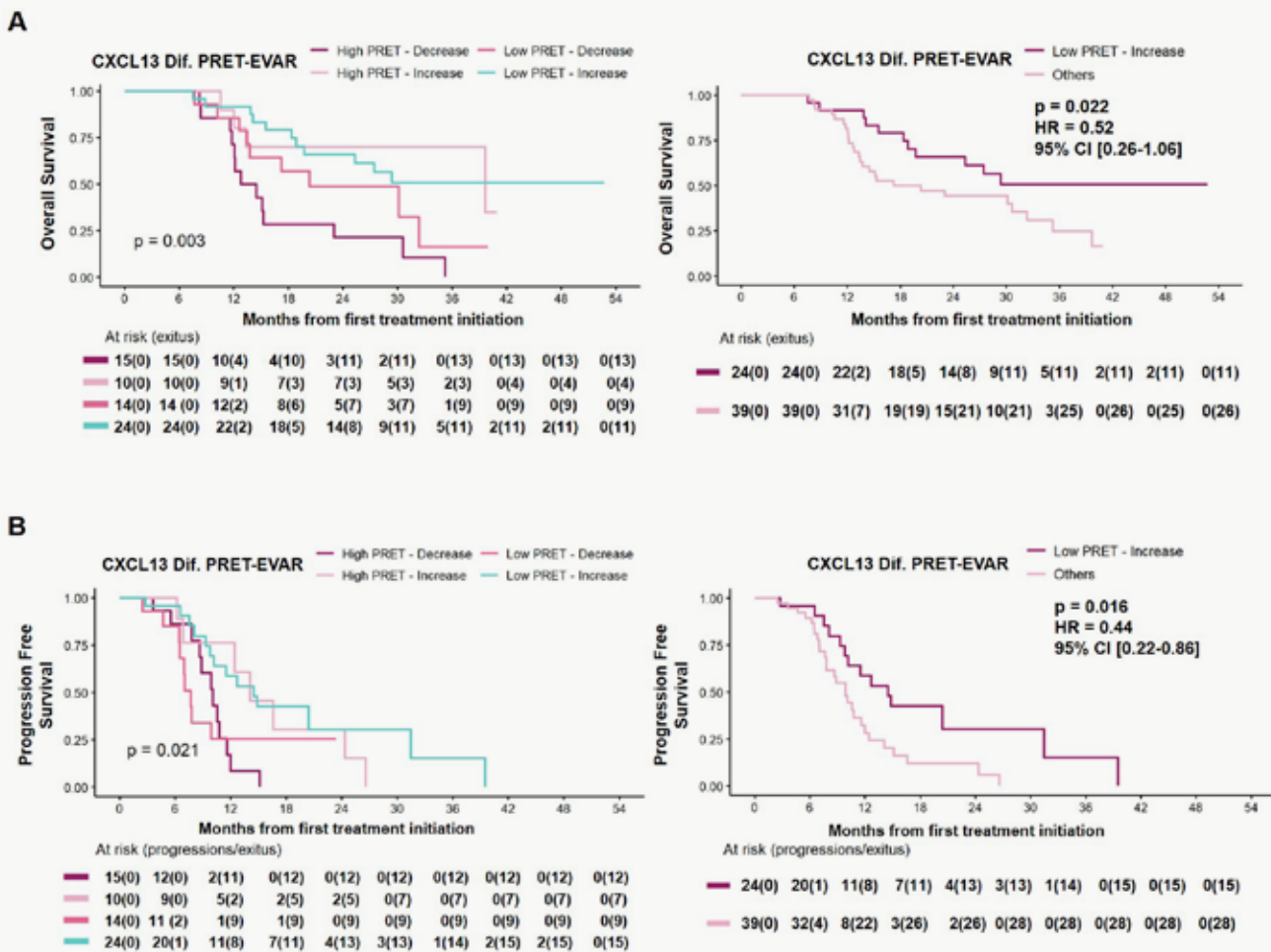
Contingency Table		PATIENTS WITH AND WITHOUT EVAR SAMPLE				
FIRST LINE TREATMENT		NO EVAR	YES EVAR	TOTAL		
CHEMOTHERAPY ALONE	COUNT % from the total	18 40%	20 19.2%	38 36.5%		
CHEMOTHERAPY + BEVACIZUMAB	COUNT % from the total	16 15.4%	23 22.1%	39 37.5%		
CHEMOTHERAPY + ANTI-EGFR	COUNT % from the total	7 6.7%	20 19.2%	27 26.0%	X <sup>2</sup> Pearson test	P value
TOTAL	COUNT % from the total	41 39.4%	63 60.6%	104 100%	Fisher's test	0.212
					Valid Cases	0.207
						104
RESPONSE TO TREATMENT		NO EVAR	YES EVAR	TOTAL		
COMPLETE RESPONSE (CD)	COUNT % from the total	1 1.0%	0 0.0%	1 1.0%		
PARTIAL RESPONSE (PR)	COUNT % from the total	22 21.2%	45 43.3%	67 64.4%		
STABLE DISEASE (SD)	COUNT % from the total	9 8.7%	15 14.4%	24 23.1%		
PROGRESSIVE DISEASE (PD)	COUNT % from the total	9 8.7%	3 2.9%	12 11.5%	X <sup>2</sup> Pearson test	P value
TOTAL	COUNT % from the total	41 39.4%	63 60.6%	104 100%	Fisher's test	0.027
					Valid Cases	0.019
						104
RESPONSE TO TREATMENT GROUPED		NO EVAR	YES EVAR	TOTAL		
RESPONDERS (CR, PR)	COUNT % from the total	23 22.1%	45 43.3%	68 65.4%		
NON RESPONDERS (SD, PD)	COUNT % from the total	18 17.3%	18 17.3%	36 34.6%	X <sup>2</sup> Pearson test	P value
TOTAL	COUNT % from the total	41 39.4%	63 60.6%	104 100%	Fisher's test	0.108
					Valid Cases	0.140
						104
RADICAL SURGERY		NO EVAR	YES EVAR	TOTAL		
NO RADICAL SURGERY	COUNT % from the total	33 31.7%	48 46.2%	81 77.9%		
RADICAL SURGERY	COUNT % from the total	8 7.7%	15 14.4%	23 22.1%	X <sup>2</sup> Pearson test	P value
TOTAL	COUNT % from the total	41 39.4%	63 60.6%	104 100%	Fisher's test	0.606
					Valid Cases	0.639
						104

**Table 16.** Associations of clinical variables in patients with and without EVAR sample.

To further explore our results, we created the 4 categories as indicated in **Table 17**. Patients whose CXCL13 levels increased after 3 months of treatment had the best OS (**Figure 26.A**, left panel) and PFS (**Figure 26.B**, left panel), regardless of whether their PRET levels were high or low. However, it is noteworthy that it was those patients with low PRET levels that increased in the EVAR sample that had a clearly better prognosis (**Table 17** and **Figure 26.A-B**, right panels).

CXCL13 LEVELS ALL PATIENTS						
PRET LEVELS	DYNAMIC CHANGE	CATEGORY	OS		PFS	
			MEDIAN	HR (95% CI, p value)	MEDIAN	HR (95% CI, p value)
HIGH	Decrease	HIGH PRET - Decrease	13.6	-	10.1	-
	Increase	HIGH PRET - Increase	39.7	0.16 (0.05-0.58, p=0.005)	14.1	0.41 (0.15-1.16, p=0.093)
LOW	Decrease	LOW PRET - Decrease	20.3	0.49 (0.21-1.15, p=0.099)	7.6	1.13 (0.47-2.71, p=0.790)
	Increase	LOW PRET - Increase	Not reached	0.27 (0.12-0.60, p=0.002)	14.6	0.33 (0.14-0.78, p=0.011)

**Table 17. The dynamic changes (increase-decrease) were divided in 4 categories as described in the table.** For each category: median OS and PFS in months; HR correspond to the increase category respect to decrease category (by default = 1). HR, 95% CI and p value correspond to univariate analysis.



## 2.5.2. CXC chemokines serum levels and their association with OS and PFS in patients who did not undergo radical surgery during the study

As explained before, we wanted to specifically investigate the role of our selected CXC chemokines in the subgroup of patients that did not undergo radical surgery during the study (N = 81). This group would represent our ideal study population since the fact that they did not undergo surgery eliminates a clear confounding factor and allows us to analyse results without statistical bias. Nevertheless, the reduction in the total number of patients has to be taken into account as it can also affect the outcome.

The following sections show the same analysis we performed in all samples but in this case, only in the non-operated patients.

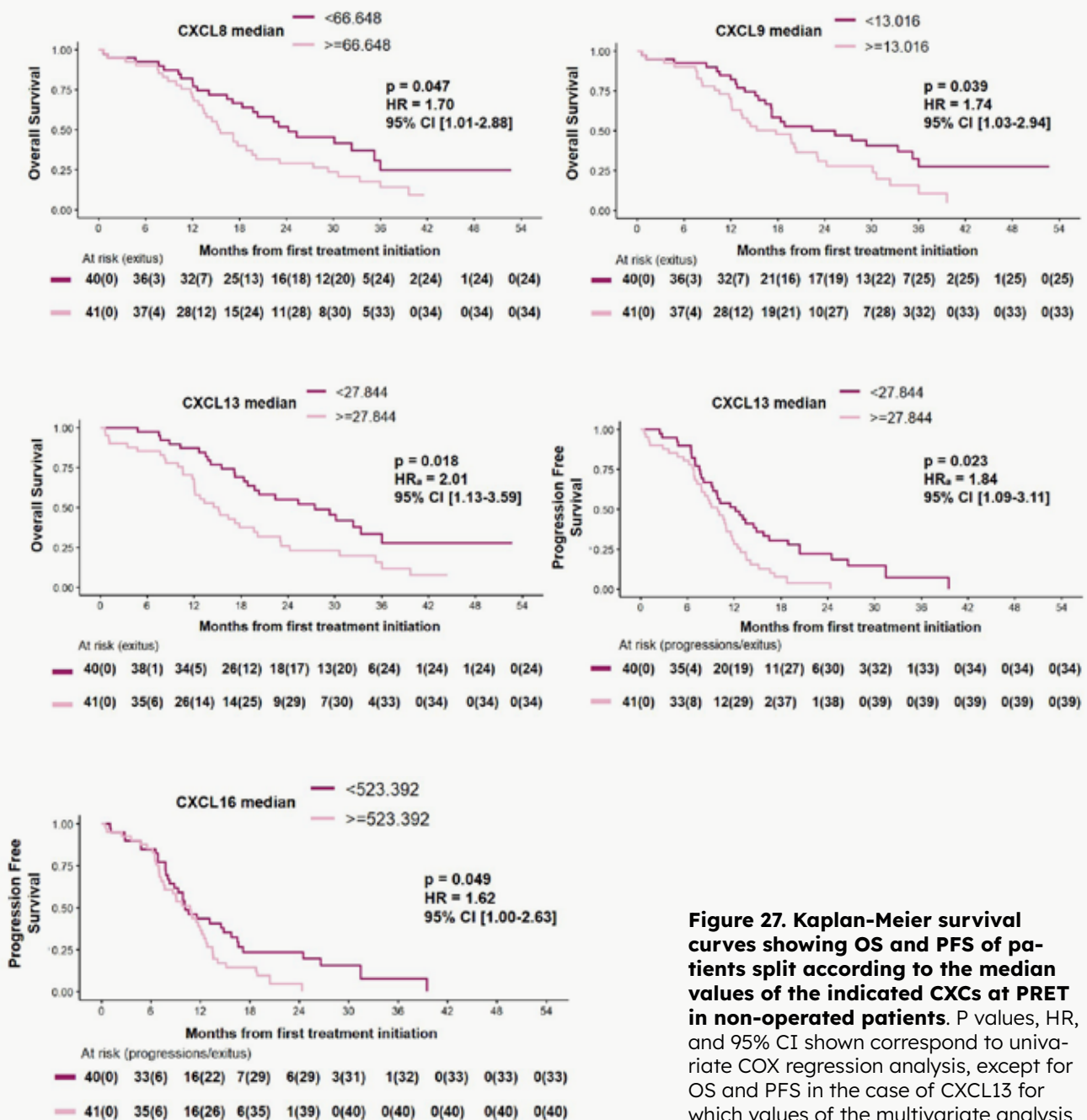
### 2.5.2.1. Basal CXC levels and their association with OS and PFS in non-operated patients

We studied the association of PRET CXC levels with OS and PFS. Following the same methodology as before, we chose to categorize the variable according to the median value of each CXC. Univariate and adjusted multivariate COX models were performed. Results are shown in **Table 18**.

BASAL LEVELS ASSOCIATION WITH RISK OF DEATH OR PROGRESSION. N = 81																																																																																																																
		MEDIAN OS (95% CI)	19.64 (15.5-27.4)		MEDIAN PFS (95% CI)	10.58 (9.1-12.4)																																																																																																										
OVERALL SURVIVAL				PROGRESSION FREE SURVIVAL																																																																																																												
CHEMOKINES	MEDIAN LEVELS	MEDIAN OS (95% CI)	HR (95% CI, p value) <sup>1</sup>	HRa (95% CI, p value) <sup>2</sup>	MEDIAN PFS (95% CI)	HR (95% CI, p value) <sup>1</sup>	HRa (95% CI, p value) <sup>2</sup>																																																																																																									
CXCL1	<298.044	20.3 (16.4-33.4)	1.20 (0.72-2.02, p=0.484)	0.93 (0.52-1.64, p=0.792)	10.6 (8.9-14.1)	1.15 (0.72-1.83, p=0.560)	0.90 (0.55-1.49, p=0.693)																																																																																																									
	≥298.044	17.8 (14.1-30.6)			10.2 (7.8-13.4)			CXCL2	<695.772	19.7 (14.1-36)	1.06 (0.63-1.78, p=0.833)	0.97 (0.57-1.66, p=0.916)	11.7 (7.8-14.5)	1.14 (0.72-1.82, p=0.570)	1.03 (0.64-1.67, p=0.896)	≥695.772	18.4 (15.1-30.6)	10.1 (8.7-12.2)	CXCL5	<794.052	18.8 (16.4-32.4)	1.02 (0.61-1.72, p=0.932)	0.86 (0.48-1.56, p=0.624)	9.5 (7.7-14.1)	1.11 (0.70-1.77, p=0.653)	1.42 (0.88-2.29, p=0.153)	≥794.052	19.6 (13.4-30.6)	10.7 (9.1-13.5)	CXCL6	<60.176	19.7 (17.2-32.4)	1.16 (0.69-1.96, p=0.577)	1.44 (0.82-2.51, p=0.203)	10.2 (8.7-14.1)	1.21 (0.76-1.95, p=0.419)	1.42 (0.88-2.29, p=0.153)	≥60.176	18.8 (12-30.6)	10.6 (7.8-12.7)	CXCL8	<66.648	24.3 (19.7-NA)	<b>1.70 (1.01-2.88, p=0.047)</b>	1.54 (0.90-2.65, p=0.117)	10.6 (9.1-14.1)	1.12 (0.70-1.78, p=0.633)	0.96 (0.59-1.54, p=0.851)	≥66.648	<b>15.5 (13.3-23.1)</b>	10.2 (7.8-12.4)	CXCL9	<13.016	25.3 (17.2-NA)	<b>1.74 (1.03-2.94, p=0.039)</b>	1.60 (0.87-2.94, p=0.128)	11.7 (9.1-15.1)	1.57 (0.98-2.52, p=0.062)	1.54 (0.90-2.63, p=0.117)	≥13.016	<b>17.8 (12.1-23.1)</b>	9.8 (7.7-12)	CXCL10	<180.744	18.4 (15.1-NA)	1.14 (0.67-1.91, p=0.632)	1.05 (0.60-1.82, p=0.869)	10.2 (8.7-14.5)	1.26 (0.79-2.02, p=0.327)	1.25 (0.76-2.04, p=0.373)	≥180.744	20.3 (14.1-30.1))	10.6 (8.3-12.8)	CXCL11	<30.724	19.7 (16.4-35.2)	1.15 (0.69-1.93, p=0.598)	1.12 (0.66-1.92, p=0.670)	10.7 (9.1-14.5)	1.29 (0.81-2.07, p=0.281)	1.35 (0.84-2.19, p=0.216)	≥30.724	19.6 (13.4-30.1)	10.1 (7.8-13.4)	CXCL12	<501.576	25.3 (18.4-36)	1.44 (0.86-2.43, p=0.167)	1.57 (0.90-2.75, p=0.111)	10.2 (8.9-14.8)	1.35 (0.85-2.17, p=0.207)	1.37 (0.85-2.22, p=0.201)	≥501.576	16.4 (12.1-24.3)	10.6 (8.3-12.7)	CXCL13	<27.844	27.4 (19.7-NA)	<b>2.04 (1.21-3.45, p=0.008)</b>	<b>2.01 (1.13-3.59, p=0.018)</b>	12.2 (9.3-16.5)	<b>1.94 (1.19-3.18, p=0.008)</b>	<b>1.84 (1.09-3.11, p=0.023)</b>	≥27.844	<b>15.1 (12-23)</b>	9.9 (7.8-11.7)	CXCL16	<523.392	19.7 (17.2-NA)	1.18 (0.70-1.99, p=0.540)	1.39 (0.80-2.41, p=0.243)	10.2 (8.9-16.5)
CXCL2	<695.772	19.7 (14.1-36)	1.06 (0.63-1.78, p=0.833)	0.97 (0.57-1.66, p=0.916)	11.7 (7.8-14.5)	1.14 (0.72-1.82, p=0.570)	1.03 (0.64-1.67, p=0.896)																																																																																																									
	≥695.772	18.4 (15.1-30.6)			10.1 (8.7-12.2)			CXCL5	<794.052	18.8 (16.4-32.4)	1.02 (0.61-1.72, p=0.932)	0.86 (0.48-1.56, p=0.624)	9.5 (7.7-14.1)	1.11 (0.70-1.77, p=0.653)	1.42 (0.88-2.29, p=0.153)	≥794.052	19.6 (13.4-30.6)	10.7 (9.1-13.5)	CXCL6	<60.176	19.7 (17.2-32.4)	1.16 (0.69-1.96, p=0.577)	1.44 (0.82-2.51, p=0.203)	10.2 (8.7-14.1)	1.21 (0.76-1.95, p=0.419)	1.42 (0.88-2.29, p=0.153)	≥60.176	18.8 (12-30.6)	10.6 (7.8-12.7)	CXCL8	<66.648	24.3 (19.7-NA)	<b>1.70 (1.01-2.88, p=0.047)</b>	1.54 (0.90-2.65, p=0.117)	10.6 (9.1-14.1)	1.12 (0.70-1.78, p=0.633)	0.96 (0.59-1.54, p=0.851)	≥66.648	<b>15.5 (13.3-23.1)</b>	10.2 (7.8-12.4)	CXCL9	<13.016	25.3 (17.2-NA)	<b>1.74 (1.03-2.94, p=0.039)</b>	1.60 (0.87-2.94, p=0.128)	11.7 (9.1-15.1)	1.57 (0.98-2.52, p=0.062)	1.54 (0.90-2.63, p=0.117)	≥13.016	<b>17.8 (12.1-23.1)</b>	9.8 (7.7-12)	CXCL10	<180.744	18.4 (15.1-NA)	1.14 (0.67-1.91, p=0.632)	1.05 (0.60-1.82, p=0.869)	10.2 (8.7-14.5)	1.26 (0.79-2.02, p=0.327)	1.25 (0.76-2.04, p=0.373)	≥180.744	20.3 (14.1-30.1))	10.6 (8.3-12.8)	CXCL11	<30.724	19.7 (16.4-35.2)	1.15 (0.69-1.93, p=0.598)	1.12 (0.66-1.92, p=0.670)	10.7 (9.1-14.5)	1.29 (0.81-2.07, p=0.281)	1.35 (0.84-2.19, p=0.216)	≥30.724	19.6 (13.4-30.1)	10.1 (7.8-13.4)	CXCL12	<501.576	25.3 (18.4-36)	1.44 (0.86-2.43, p=0.167)	1.57 (0.90-2.75, p=0.111)	10.2 (8.9-14.8)	1.35 (0.85-2.17, p=0.207)	1.37 (0.85-2.22, p=0.201)	≥501.576	16.4 (12.1-24.3)	10.6 (8.3-12.7)	CXCL13	<27.844	27.4 (19.7-NA)	<b>2.04 (1.21-3.45, p=0.008)</b>	<b>2.01 (1.13-3.59, p=0.018)</b>	12.2 (9.3-16.5)	<b>1.94 (1.19-3.18, p=0.008)</b>	<b>1.84 (1.09-3.11, p=0.023)</b>	≥27.844	<b>15.1 (12-23)</b>	9.9 (7.8-11.7)	CXCL16	<523.392	19.7 (17.2-NA)	1.18 (0.70-1.99, p=0.540)	1.39 (0.80-2.41, p=0.243)	10.2 (8.9-16.5)	<b>1.62 (1.00-2.63, p=0.049)</b>	1.65 (1.00-2.74, p=0.052)	≥523.392	17.2 (13.4-30.1)	10.7 (7.6-12.4)						
CXCL5	<794.052	18.8 (16.4-32.4)	1.02 (0.61-1.72, p=0.932)	0.86 (0.48-1.56, p=0.624)	9.5 (7.7-14.1)	1.11 (0.70-1.77, p=0.653)	1.42 (0.88-2.29, p=0.153)																																																																																																									
	≥794.052	19.6 (13.4-30.6)			10.7 (9.1-13.5)			CXCL6	<60.176	19.7 (17.2-32.4)	1.16 (0.69-1.96, p=0.577)	1.44 (0.82-2.51, p=0.203)	10.2 (8.7-14.1)	1.21 (0.76-1.95, p=0.419)	1.42 (0.88-2.29, p=0.153)	≥60.176	18.8 (12-30.6)	10.6 (7.8-12.7)	CXCL8	<66.648	24.3 (19.7-NA)	<b>1.70 (1.01-2.88, p=0.047)</b>	1.54 (0.90-2.65, p=0.117)	10.6 (9.1-14.1)	1.12 (0.70-1.78, p=0.633)	0.96 (0.59-1.54, p=0.851)	≥66.648	<b>15.5 (13.3-23.1)</b>	10.2 (7.8-12.4)	CXCL9	<13.016	25.3 (17.2-NA)	<b>1.74 (1.03-2.94, p=0.039)</b>	1.60 (0.87-2.94, p=0.128)	11.7 (9.1-15.1)	1.57 (0.98-2.52, p=0.062)	1.54 (0.90-2.63, p=0.117)	≥13.016	<b>17.8 (12.1-23.1)</b>	9.8 (7.7-12)	CXCL10	<180.744	18.4 (15.1-NA)	1.14 (0.67-1.91, p=0.632)	1.05 (0.60-1.82, p=0.869)	10.2 (8.7-14.5)	1.26 (0.79-2.02, p=0.327)	1.25 (0.76-2.04, p=0.373)	≥180.744	20.3 (14.1-30.1))	10.6 (8.3-12.8)	CXCL11	<30.724	19.7 (16.4-35.2)	1.15 (0.69-1.93, p=0.598)	1.12 (0.66-1.92, p=0.670)	10.7 (9.1-14.5)	1.29 (0.81-2.07, p=0.281)	1.35 (0.84-2.19, p=0.216)	≥30.724	19.6 (13.4-30.1)	10.1 (7.8-13.4)	CXCL12	<501.576	25.3 (18.4-36)	1.44 (0.86-2.43, p=0.167)	1.57 (0.90-2.75, p=0.111)	10.2 (8.9-14.8)	1.35 (0.85-2.17, p=0.207)	1.37 (0.85-2.22, p=0.201)	≥501.576	16.4 (12.1-24.3)	10.6 (8.3-12.7)	CXCL13	<27.844	27.4 (19.7-NA)	<b>2.04 (1.21-3.45, p=0.008)</b>	<b>2.01 (1.13-3.59, p=0.018)</b>	12.2 (9.3-16.5)	<b>1.94 (1.19-3.18, p=0.008)</b>	<b>1.84 (1.09-3.11, p=0.023)</b>	≥27.844	<b>15.1 (12-23)</b>	9.9 (7.8-11.7)	CXCL16	<523.392	19.7 (17.2-NA)	1.18 (0.70-1.99, p=0.540)	1.39 (0.80-2.41, p=0.243)	10.2 (8.9-16.5)	<b>1.62 (1.00-2.63, p=0.049)</b>	1.65 (1.00-2.74, p=0.052)	≥523.392	17.2 (13.4-30.1)	10.7 (7.6-12.4)																	
CXCL6	<60.176	19.7 (17.2-32.4)	1.16 (0.69-1.96, p=0.577)	1.44 (0.82-2.51, p=0.203)	10.2 (8.7-14.1)	1.21 (0.76-1.95, p=0.419)	1.42 (0.88-2.29, p=0.153)																																																																																																									
	≥60.176	18.8 (12-30.6)			10.6 (7.8-12.7)			CXCL8	<66.648	24.3 (19.7-NA)	<b>1.70 (1.01-2.88, p=0.047)</b>	1.54 (0.90-2.65, p=0.117)	10.6 (9.1-14.1)	1.12 (0.70-1.78, p=0.633)	0.96 (0.59-1.54, p=0.851)	≥66.648	<b>15.5 (13.3-23.1)</b>	10.2 (7.8-12.4)	CXCL9	<13.016	25.3 (17.2-NA)	<b>1.74 (1.03-2.94, p=0.039)</b>	1.60 (0.87-2.94, p=0.128)	11.7 (9.1-15.1)	1.57 (0.98-2.52, p=0.062)	1.54 (0.90-2.63, p=0.117)	≥13.016	<b>17.8 (12.1-23.1)</b>	9.8 (7.7-12)	CXCL10	<180.744	18.4 (15.1-NA)	1.14 (0.67-1.91, p=0.632)	1.05 (0.60-1.82, p=0.869)	10.2 (8.7-14.5)	1.26 (0.79-2.02, p=0.327)	1.25 (0.76-2.04, p=0.373)	≥180.744	20.3 (14.1-30.1))	10.6 (8.3-12.8)	CXCL11	<30.724	19.7 (16.4-35.2)	1.15 (0.69-1.93, p=0.598)	1.12 (0.66-1.92, p=0.670)	10.7 (9.1-14.5)	1.29 (0.81-2.07, p=0.281)	1.35 (0.84-2.19, p=0.216)	≥30.724	19.6 (13.4-30.1)	10.1 (7.8-13.4)	CXCL12	<501.576	25.3 (18.4-36)	1.44 (0.86-2.43, p=0.167)	1.57 (0.90-2.75, p=0.111)	10.2 (8.9-14.8)	1.35 (0.85-2.17, p=0.207)	1.37 (0.85-2.22, p=0.201)	≥501.576	16.4 (12.1-24.3)	10.6 (8.3-12.7)	CXCL13	<27.844	27.4 (19.7-NA)	<b>2.04 (1.21-3.45, p=0.008)</b>	<b>2.01 (1.13-3.59, p=0.018)</b>	12.2 (9.3-16.5)	<b>1.94 (1.19-3.18, p=0.008)</b>	<b>1.84 (1.09-3.11, p=0.023)</b>	≥27.844	<b>15.1 (12-23)</b>	9.9 (7.8-11.7)	CXCL16	<523.392	19.7 (17.2-NA)	1.18 (0.70-1.99, p=0.540)	1.39 (0.80-2.41, p=0.243)	10.2 (8.9-16.5)	<b>1.62 (1.00-2.63, p=0.049)</b>	1.65 (1.00-2.74, p=0.052)	≥523.392	17.2 (13.4-30.1)	10.7 (7.6-12.4)																												
CXCL8	<66.648	24.3 (19.7-NA)	<b>1.70 (1.01-2.88, p=0.047)</b>	1.54 (0.90-2.65, p=0.117)	10.6 (9.1-14.1)	1.12 (0.70-1.78, p=0.633)	0.96 (0.59-1.54, p=0.851)																																																																																																									
	≥66.648	<b>15.5 (13.3-23.1)</b>			10.2 (7.8-12.4)			CXCL9	<13.016	25.3 (17.2-NA)	<b>1.74 (1.03-2.94, p=0.039)</b>	1.60 (0.87-2.94, p=0.128)	11.7 (9.1-15.1)	1.57 (0.98-2.52, p=0.062)	1.54 (0.90-2.63, p=0.117)	≥13.016	<b>17.8 (12.1-23.1)</b>	9.8 (7.7-12)	CXCL10	<180.744	18.4 (15.1-NA)	1.14 (0.67-1.91, p=0.632)	1.05 (0.60-1.82, p=0.869)	10.2 (8.7-14.5)	1.26 (0.79-2.02, p=0.327)	1.25 (0.76-2.04, p=0.373)	≥180.744	20.3 (14.1-30.1))	10.6 (8.3-12.8)	CXCL11	<30.724	19.7 (16.4-35.2)	1.15 (0.69-1.93, p=0.598)	1.12 (0.66-1.92, p=0.670)	10.7 (9.1-14.5)	1.29 (0.81-2.07, p=0.281)	1.35 (0.84-2.19, p=0.216)	≥30.724	19.6 (13.4-30.1)	10.1 (7.8-13.4)	CXCL12	<501.576	25.3 (18.4-36)	1.44 (0.86-2.43, p=0.167)	1.57 (0.90-2.75, p=0.111)	10.2 (8.9-14.8)	1.35 (0.85-2.17, p=0.207)	1.37 (0.85-2.22, p=0.201)	≥501.576	16.4 (12.1-24.3)	10.6 (8.3-12.7)	CXCL13	<27.844	27.4 (19.7-NA)	<b>2.04 (1.21-3.45, p=0.008)</b>	<b>2.01 (1.13-3.59, p=0.018)</b>	12.2 (9.3-16.5)	<b>1.94 (1.19-3.18, p=0.008)</b>	<b>1.84 (1.09-3.11, p=0.023)</b>	≥27.844	<b>15.1 (12-23)</b>	9.9 (7.8-11.7)	CXCL16	<523.392	19.7 (17.2-NA)	1.18 (0.70-1.99, p=0.540)	1.39 (0.80-2.41, p=0.243)	10.2 (8.9-16.5)	<b>1.62 (1.00-2.63, p=0.049)</b>	1.65 (1.00-2.74, p=0.052)	≥523.392	17.2 (13.4-30.1)	10.7 (7.6-12.4)																																							
CXCL9	<13.016	25.3 (17.2-NA)	<b>1.74 (1.03-2.94, p=0.039)</b>	1.60 (0.87-2.94, p=0.128)	11.7 (9.1-15.1)	1.57 (0.98-2.52, p=0.062)	1.54 (0.90-2.63, p=0.117)																																																																																																									
	≥13.016	<b>17.8 (12.1-23.1)</b>			9.8 (7.7-12)			CXCL10	<180.744	18.4 (15.1-NA)	1.14 (0.67-1.91, p=0.632)	1.05 (0.60-1.82, p=0.869)	10.2 (8.7-14.5)	1.26 (0.79-2.02, p=0.327)	1.25 (0.76-2.04, p=0.373)	≥180.744	20.3 (14.1-30.1))	10.6 (8.3-12.8)	CXCL11	<30.724	19.7 (16.4-35.2)	1.15 (0.69-1.93, p=0.598)	1.12 (0.66-1.92, p=0.670)	10.7 (9.1-14.5)	1.29 (0.81-2.07, p=0.281)	1.35 (0.84-2.19, p=0.216)	≥30.724	19.6 (13.4-30.1)	10.1 (7.8-13.4)	CXCL12	<501.576	25.3 (18.4-36)	1.44 (0.86-2.43, p=0.167)	1.57 (0.90-2.75, p=0.111)	10.2 (8.9-14.8)	1.35 (0.85-2.17, p=0.207)	1.37 (0.85-2.22, p=0.201)	≥501.576	16.4 (12.1-24.3)	10.6 (8.3-12.7)	CXCL13	<27.844	27.4 (19.7-NA)	<b>2.04 (1.21-3.45, p=0.008)</b>	<b>2.01 (1.13-3.59, p=0.018)</b>	12.2 (9.3-16.5)	<b>1.94 (1.19-3.18, p=0.008)</b>	<b>1.84 (1.09-3.11, p=0.023)</b>	≥27.844	<b>15.1 (12-23)</b>	9.9 (7.8-11.7)	CXCL16	<523.392	19.7 (17.2-NA)	1.18 (0.70-1.99, p=0.540)	1.39 (0.80-2.41, p=0.243)	10.2 (8.9-16.5)	<b>1.62 (1.00-2.63, p=0.049)</b>	1.65 (1.00-2.74, p=0.052)	≥523.392	17.2 (13.4-30.1)	10.7 (7.6-12.4)																																																		
CXCL10	<180.744	18.4 (15.1-NA)	1.14 (0.67-1.91, p=0.632)	1.05 (0.60-1.82, p=0.869)	10.2 (8.7-14.5)	1.26 (0.79-2.02, p=0.327)	1.25 (0.76-2.04, p=0.373)																																																																																																									
	≥180.744	20.3 (14.1-30.1))			10.6 (8.3-12.8)			CXCL11	<30.724	19.7 (16.4-35.2)	1.15 (0.69-1.93, p=0.598)	1.12 (0.66-1.92, p=0.670)	10.7 (9.1-14.5)	1.29 (0.81-2.07, p=0.281)	1.35 (0.84-2.19, p=0.216)	≥30.724	19.6 (13.4-30.1)	10.1 (7.8-13.4)	CXCL12	<501.576	25.3 (18.4-36)	1.44 (0.86-2.43, p=0.167)	1.57 (0.90-2.75, p=0.111)	10.2 (8.9-14.8)	1.35 (0.85-2.17, p=0.207)	1.37 (0.85-2.22, p=0.201)	≥501.576	16.4 (12.1-24.3)	10.6 (8.3-12.7)	CXCL13	<27.844	27.4 (19.7-NA)	<b>2.04 (1.21-3.45, p=0.008)</b>	<b>2.01 (1.13-3.59, p=0.018)</b>	12.2 (9.3-16.5)	<b>1.94 (1.19-3.18, p=0.008)</b>	<b>1.84 (1.09-3.11, p=0.023)</b>	≥27.844	<b>15.1 (12-23)</b>	9.9 (7.8-11.7)	CXCL16	<523.392	19.7 (17.2-NA)	1.18 (0.70-1.99, p=0.540)	1.39 (0.80-2.41, p=0.243)	10.2 (8.9-16.5)	<b>1.62 (1.00-2.63, p=0.049)</b>	1.65 (1.00-2.74, p=0.052)	≥523.392	17.2 (13.4-30.1)	10.7 (7.6-12.4)																																																													
CXCL11	<30.724	19.7 (16.4-35.2)	1.15 (0.69-1.93, p=0.598)	1.12 (0.66-1.92, p=0.670)	10.7 (9.1-14.5)	1.29 (0.81-2.07, p=0.281)	1.35 (0.84-2.19, p=0.216)																																																																																																									
	≥30.724	19.6 (13.4-30.1)			10.1 (7.8-13.4)			CXCL12	<501.576	25.3 (18.4-36)	1.44 (0.86-2.43, p=0.167)	1.57 (0.90-2.75, p=0.111)	10.2 (8.9-14.8)	1.35 (0.85-2.17, p=0.207)	1.37 (0.85-2.22, p=0.201)	≥501.576	16.4 (12.1-24.3)	10.6 (8.3-12.7)	CXCL13	<27.844	27.4 (19.7-NA)	<b>2.04 (1.21-3.45, p=0.008)</b>	<b>2.01 (1.13-3.59, p=0.018)</b>	12.2 (9.3-16.5)	<b>1.94 (1.19-3.18, p=0.008)</b>	<b>1.84 (1.09-3.11, p=0.023)</b>	≥27.844	<b>15.1 (12-23)</b>	9.9 (7.8-11.7)	CXCL16	<523.392	19.7 (17.2-NA)	1.18 (0.70-1.99, p=0.540)	1.39 (0.80-2.41, p=0.243)	10.2 (8.9-16.5)	<b>1.62 (1.00-2.63, p=0.049)</b>	1.65 (1.00-2.74, p=0.052)	≥523.392	17.2 (13.4-30.1)	10.7 (7.6-12.4)																																																																								
CXCL12	<501.576	25.3 (18.4-36)	1.44 (0.86-2.43, p=0.167)	1.57 (0.90-2.75, p=0.111)	10.2 (8.9-14.8)	1.35 (0.85-2.17, p=0.207)	1.37 (0.85-2.22, p=0.201)																																																																																																									
	≥501.576	16.4 (12.1-24.3)			10.6 (8.3-12.7)			CXCL13	<27.844	27.4 (19.7-NA)	<b>2.04 (1.21-3.45, p=0.008)</b>	<b>2.01 (1.13-3.59, p=0.018)</b>	12.2 (9.3-16.5)	<b>1.94 (1.19-3.18, p=0.008)</b>	<b>1.84 (1.09-3.11, p=0.023)</b>	≥27.844	<b>15.1 (12-23)</b>	9.9 (7.8-11.7)	CXCL16	<523.392	19.7 (17.2-NA)	1.18 (0.70-1.99, p=0.540)	1.39 (0.80-2.41, p=0.243)	10.2 (8.9-16.5)	<b>1.62 (1.00-2.63, p=0.049)</b>	1.65 (1.00-2.74, p=0.052)	≥523.392	17.2 (13.4-30.1)	10.7 (7.6-12.4)																																																																																			
CXCL13	<27.844	27.4 (19.7-NA)	<b>2.04 (1.21-3.45, p=0.008)</b>	<b>2.01 (1.13-3.59, p=0.018)</b>	12.2 (9.3-16.5)	<b>1.94 (1.19-3.18, p=0.008)</b>	<b>1.84 (1.09-3.11, p=0.023)</b>																																																																																																									
	≥27.844	<b>15.1 (12-23)</b>			9.9 (7.8-11.7)			CXCL16	<523.392	19.7 (17.2-NA)	1.18 (0.70-1.99, p=0.540)	1.39 (0.80-2.41, p=0.243)	10.2 (8.9-16.5)	<b>1.62 (1.00-2.63, p=0.049)</b>	1.65 (1.00-2.74, p=0.052)	≥523.392	17.2 (13.4-30.1)	10.7 (7.6-12.4)																																																																																														
CXCL16	<523.392	19.7 (17.2-NA)	1.18 (0.70-1.99, p=0.540)	1.39 (0.80-2.41, p=0.243)	10.2 (8.9-16.5)	<b>1.62 (1.00-2.63, p=0.049)</b>	1.65 (1.00-2.74, p=0.052)																																																																																																									
	≥523.392	17.2 (13.4-30.1)			10.7 (7.6-12.4)																																																																																																											

**Table 18. Serum PRET median levels of the eleven CXCs studied and the association with OS and PFS in non-operated patients.** Median OS and PFS (in months), P values, HR, and 95% CIs correspond to univariate<sup>1</sup> and multivariate<sup>2</sup> COX models. HR correspond to the category above the median respect to category below the median (by default = 1). The variables: PS, radical surgery, age and sex were considered in the OS multivariate analysis; PS, age and sex in the PFS multivariate analysis. In bold, all statistically significant results with a p < 0.05.

From the univariate Kaplan-Meier and COX regression models we found that patients with high PRET levels of CXCL8 and 9 had a worse OS, while those with high levels of CXCL16 had a worse PFS. Noteworthy, patients with low levels of CXCL13 in PRET samples were again found to have better OS and PFS in both, univariate and multivariate models. Even in this case, the differences between groups appeared to be higher (**Figure 27**).



**Figure 27. Kaplan-Meier survival curves showing OS and PFS of patients split according to the median values of the indicated CXCs at PRET in non-operated patients.** P values, HR, and 95% CI shown correspond to univariate COX regression analysis, except for OS and PFS in the case of CXCL13 for which values of the multivariate analysis are shown.

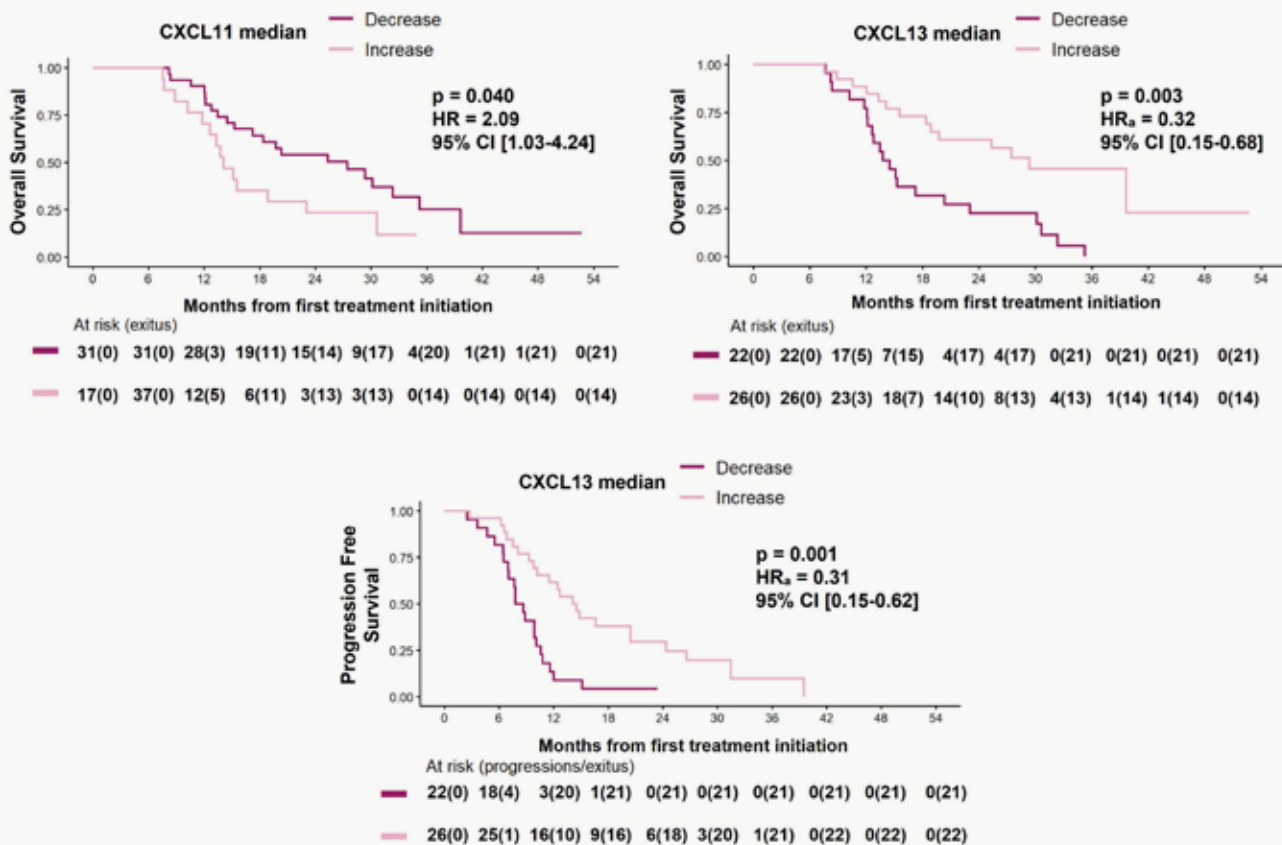
### 2.5.2.2. Dynamic changes of CXC levels between PRET and EVAR samples and their association with OS and PFS in non-operated patients

We repeated the analysis of dynamic changes comparing PRET and EVAR samples in the non-operated patient's cohort. Univariate and adjusted multivariate COX models were performed. Results are shown in **Table 19**.

		DYNAMIC CHANGES ASSOCIATION WITH RISK OF DEATH OR PROGRESSION. N = 48					
		OVERALL SURVIVAL			PROGRESSION FREE SURVIVAL		
CHEMOKINES	DYNAMIC CHANGE	MEDIAN (95% CI)	HR (95%CI, p value) <sup>1</sup>	HRa (95%CI, p value) <sup>2</sup>	MEDIAN (95% CI)	HR (95%CI, p value) <sup>1</sup>	HRa (95%CI, p value) <sup>2</sup>
CXCL1 MEDIAN	Decrease	18.8 (15.1-32.4)	1.62 (0.62-4.24, p=0.328)	3.92 (1.20-12.84, p=0.084)	10.7 (9.8-14.5)	1.65 (0.64-4.27, p=0.300)	2.57 (0.92-7.23, p=0.073)
	Increase	17.8 (7.6-NA)			7.3 (6.5-NA)		
CXCL2 MEDIAN	Decrease	18.8 (14.5-32.4)	0.69 (0.28-1.70, p=0.425)	0.43 (0.16-1.16, p=0.095)	10.7 (9.8-14.5)	1.19 (0.50-2.85, p=0.698)	1.69 (0.65-4.37, p=0.279)
	Increase	19 (8.8-NA)			7.8 (7-NA)		
CXCL5 MEDIAN	Decrease	18.4 (14.5-30.6)	1.38 (0.33-5.82, p=0.659)	0.96 (0.20-4.63, p=0.958)	10.1 (8.9-12.7)	1.88 (0.45-7.86, p=0.389)	1.51 (0.33-6.90, p=0.598)
	Increase	30.1 (7.6-NA)			7 (2.5-NA)		
CXCL6 MEDIAN	Decrease	18.4 (13.8-30.1)	2.21 (0.53-9.31, p=0.279)	2.12 (0.49-9.16, p=0.312)	9.9 (7.8-12.7)	1.36 (0.48-3.83, p=0.565)	1.25 (0.43-3.60, p=0.677)
	Increase	-			14.1 (10.1-NA)		
CXCL8 MEDIAN	Decrease	23 (15.3-NA)	1.99 (0.96-4.12, p=0.065)	1.87 (0.88-3.97, p=0.104)	10.7 (9.3-15.1)	1.56 (0.77-3.15, p=0.219)	1.53 (0.75-3.13, p=0.246)
	Increase	13.3 (12-NA)			8.1 (6.8-NA)		
CXCL9 MEDIAN	Decrease	18.8 (13.4-32.4)	1.43 (0.71-2.89, p=0.322)	1.08 (0.48-2.42, p=0.858)	10.1 (7.6-14.5)	1.31 (0.70-2.47, p=0.394)	1.21 (0.61-2.41, p=0.586)
	Increase	23 (14.5-NA)			10.2 (8.7-20.4)		
CXCL10 MEDIAN	Decrease	19.7 (14.1-30.6)	1.23 (0.61-2.49, p=0.562)	1.39 (0.67-2.87, p=0.376)	9.9 (8.1-12.4)	1.59 (0.84-3.01, p=0.157)	1.79 (0.93-3.47, p=0.083)
	Increase	17.2 (12.8-NA)			10.2 (7.8-NA)		
CXCL11 MEDIAN	Decrease	27.4 (17.2-NA)	<b>2.09 (1.03-4.24, p=0.040)</b>	1.84 (0.87-3.92, p=0.113)	10.6 (9.3-20.4)	1.44 (0.76-2.74, p=0.264)	1.25 (0.61-2.56, p=0.537)
	Increase	<b>14.1 (12.6-NA)</b>			8.9 (6.6-15.1)		
CXCL12 MEDIAN	Decrease	17.2 (14.1-30.6)	1.62 (0.49-5.36, p=0.433)	1.56 (0.44-5.44, p=0.489)	10.1 (8.1-12.7)	0.99 (0.39-2.55, p=0.986)	0.95 (0.36-2.51, p=0.919)
	Increase	27.4 (25.3-NA)			14.1 (9.8-NA)		
CXCL13 MEDIAN	Decrease	14.1 (12.6-23)	<b>0.31 (0.15-0.63, p=0.001)</b>	<b>0.32 (0.15-0.68, p=0.003)</b>	8.2 (7-10.6)	<b>0.31 (0.16-0.6, p=0.001)</b>	<b>0.31 (0.15-0.62, p=0.001)</b>
	Increase	<b>29.4 (18.8-NA)</b>			<b>14.3 (10.2-24.4)</b>		
CXCL16 MEDIAN	Decrease	15.5 (13.3-30.6)	1.40 (0.70-2.80, p=0.342)	1.40 (0.69-2.85, p=0.346)	9.8 (7.6-12.7)	1.63 (0.87-3.03, p=0.125)	1.73 (0.88-3.39, p=0.111)
	Increase	20.3 (15.3-NA)			11.5 (9.3-26.6)		

**Table 19. Dynamic changes of CXC chemokines and their association with OS and PFS in non-operated patients.** Median OS and PFS (in months); p values, HR, and 95% CI correspond to univariate<sup>1</sup> and multivariate<sup>2</sup> COX models. HR correspond to the increase category respect to decrease category (by default = 1). The variables: PS, radical surgery, age and sex were considered in the OS multivariate analysis; PS, age and sex in the PFS multivariate analysis. Statistically significant results (p <0.05) are highlighted in bold.

By far, the most interesting result here is the strong correlation between the increase of CXCL13 levels at the EVAR sample and the better OS and PFS in both the univariate and multivariate analysis; again, differences between groups appear to be higher than when studying the whole cohort of patients. It is worth mentioning that, apart from CXCL13, increased levels of CXCL11 at EVAR were associated with OS, but only in the univariate analysis (**Figure 28**).



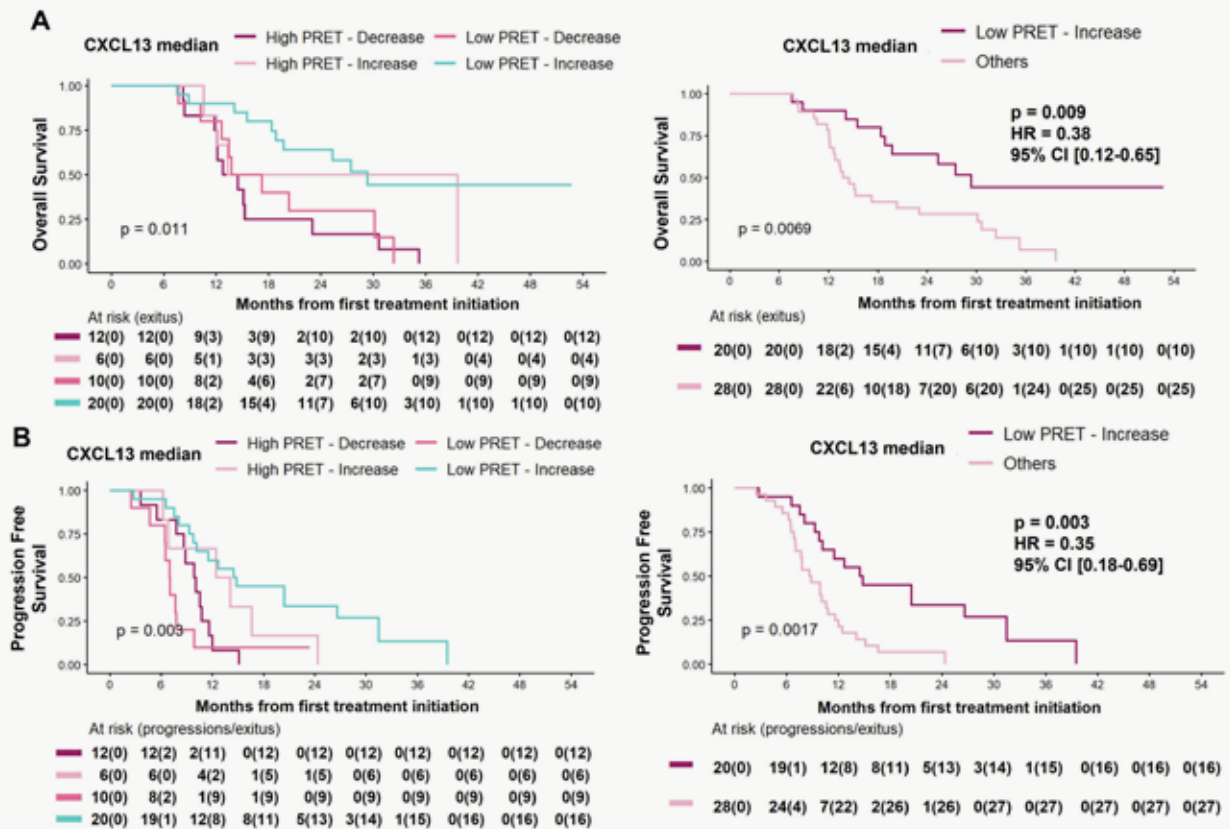
**Figure 28. Kaplan-Meier plots showing OS and PFS of CXCL11 and CXCL13 of patients split according to increase or decrease at EVAR.** P values, HRs, and 95%CI correspond to COX multivariate analysis, except for OS in CXCL11 for which values of the univariate analysis are shown.

We followed the same methodology as we used for the whole cohort of patients and split the patients into 4 categories according to the PRET and Dynamic changes of CXCL13 (**Table 20**):

CXCL13 LEVELS NON-OPERATED						
PRET LEVELS	DYNAMIC CHANGE	CATEGORY	OS		PFS	
			MEDIAN	HR (95% CI, p value)	MEDIAN	HR (95% CI, p value)
HIGH	Decrease	HIGH PRET - Decrease	13.6	-	10.8	-
	Increase	HIGH PRET - Increase	26.5	0.38 (0.12-1.25, p=0.112)	13.2	0.60 (0.22-1.64, p=0.316)
LOW	Decrease	LOW PRET - Decrease	15.5	0.79 (0.33-1.88, p=0.588)	7	1.45 (0.59-3.52, p=0.417)
	Increase	LOW PRET - Increase	29.4	0.28 (0.12-0.65, p=0.003)	14.6	0.33 (0.14-0.75, p=0.008)

**Table 20. The dynamic changes (increase-decrease) were divided in 4 categories as described in the table.** For each category: median OS and PFS in months; HR correspond to the increase category respect to decrease category (by default = 1). HR, 95% CI and p value correspond to univariate analysis.

Similar results were obtained as with the whole cohort of patients and here even the differences appeared to be stronger (**Figure 29**).



**Figure 29. Kaplan-Meier plots showing OS (A) and PFS (B) of patients split according to PRET CXCL13 levels and Dynamic change at EVAR.** P value, HRa, and 95% CI correspond to COX multivariate analysis.

## 2.6 Analysis of the specificity and sensitivity of CXCL13 as a prognostic biomarker: ROC curve.

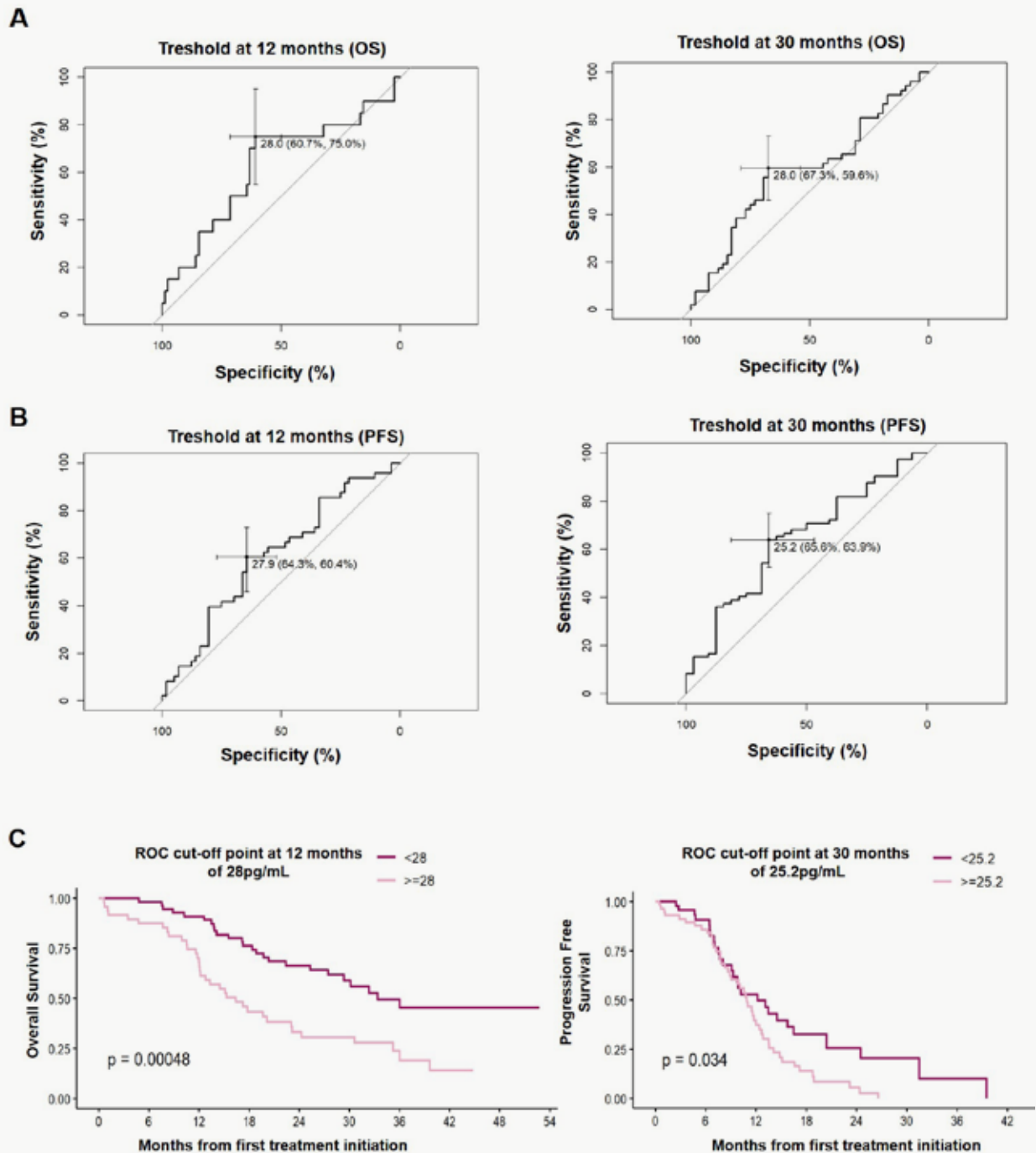
Based on the results obtained from the analysis of the eleven selected chemokines and their association with outcome of patients, CXCL13 stands as the one showing most robust results suggesting it could be used as a prognostic biomarker. We evaluated the specificity and sensitivity of CXCL13 baseline levels when predicting risk of death and progression at 12 and 30 months, in the whole cohort of patients. To evaluate its potential as a biomarker, a receiver operator characteristic (ROC) curve analysis was performed (Figure A-B).

The estimation cut-off value of CXCL13 PRET levels for the risk of death at 12 or 30 months was 28pg/mL (**Figure 30.A**). Similar cut-off points were obtained for the risk of progression, at 12 and 30 months, 27.9pg/mL and 25.2pg/mL at 12 and 30 months, respectively (**Figure 30.B**).

In the evaluation of risk of death, at 12 and 30 months, the specificity was 60.7% and 67.3% while sensitivity was 75% and 59.6%, respectively (**Figure 30.A**). In the case of the evaluation of risk of progression at 12 and 30 months, specificity was 64.3% and 65.6% and sensitivity 60.4% and 63.9% respectively (**Figure 30.B**). These moderate specificity and sensitivity results on the CXCL13 cut-off values, suggest a limited prognostic

effectiveness. Noteworthy, this CXCL13 cut-off value is close to the median CXCL13 value obtained in our study that was 27.38pg/mL.

Further a survival analysis was performed with those CXCL13 PRET level cut-off values that displayed higher sensitivity and specificity, 28pg/mL at 12months and 25.2pg/mL at 30months. Evaluating risk of death, patients with CXCL13 PRET levels lower than 28pg/mL, were associated with better OS, p value = 0.0048 (**Figure 30.C**, left). Regarding risk of progression, patients with lower levels than 25.2pg/mL were associated with better PFS, p value = 0.034, (**Figure 30.C**, right).



**Figure 30. Receiver operating characteristic (ROC) curves and Kaplan-Meier plots.** ROC curves evaluating risk of death and risk of progression at the thresholds of 12 and 30 months. Kaplan-Meier survival curves for the CXCL13 PRET levels cut-off points with better specificity/sensitivity are shown. P value according to COX univariate analysis.

## OBJECTIVE 3

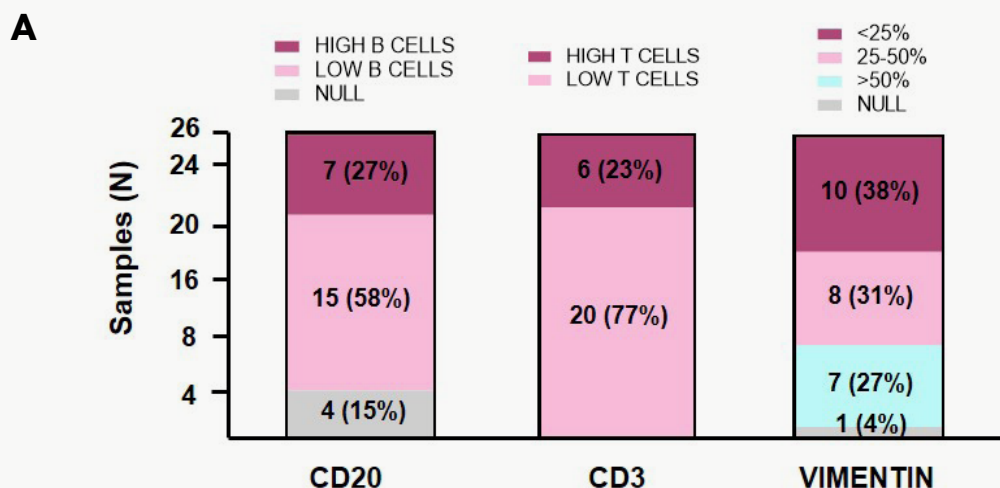
### 3.1. Study of CD20, CD3 and Vimentin in primary CRC tumors, presence of TLS structures and their correlation to CXCL13 serum levels

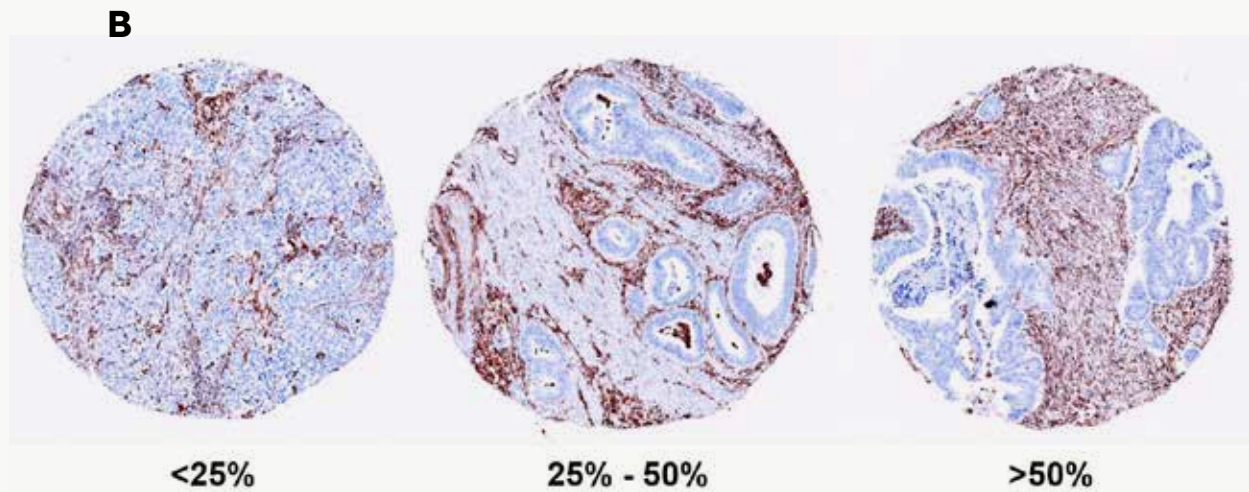
For the IHC study we elaborated a TMA with primary tumor samples from a total of 26 patients (as explained before on material and methods, section 2.2) tissue in the paraffin blocks. Although performing this analysis in the metastases would have been more appropriate, there was not metastatic tissue available from our patients.

Taking into account our results, the study of CXCL13 in patients' tumors was the next thing to do; however, the study of soluble factors by IHC is not trivial and in our experience, results are difficult to interpret.

Interestingly, CXCL13 is a chemokine that facilitates lymphoid neogenesis leading to the formation of ectopic lymphoid-like structures in nonlymphoid organs, also referred to as TLSs<sup>279-281</sup>. These TLSs are commonly found under chronic inflammation (infection, cancer, and autoimmune diseases) in non-lymphoid tissues<sup>282</sup>. In CRC, the presence of these TLS is associated with TFH cells infiltration, which together with B cells, have shown protection against tumor recurrence<sup>140</sup> and correlation with better outcome<sup>224</sup>. Based on these CXCL13-TLS associations, we aimed to correlate the PRET CXCL13 serum levels with the presence of TLS in the primary tumors of 26 patients included in our study. Although there is lack of consensus on how to determine TLS, here we identified them by studying B and T lymphocyte aggregates as in (PMID: 32947928). B and T lymphocytes were identified by CD20<sup>+</sup> and CD3<sup>+</sup> stainings, respectively. An antibody against vimentin was used to identify inflammatory regions.

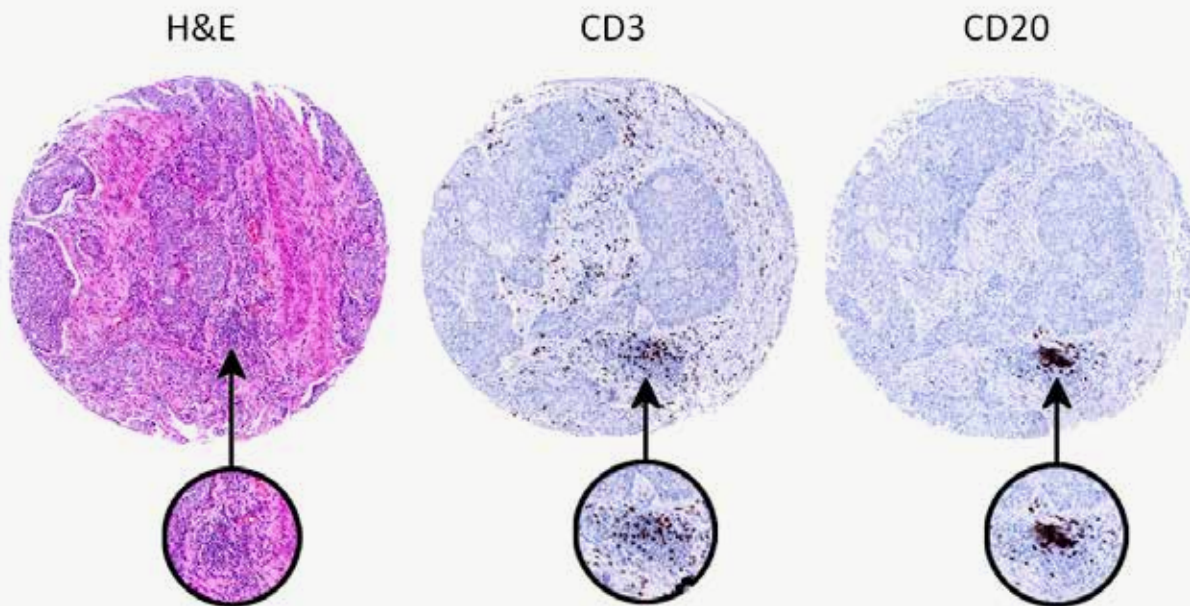
Positive staining for anti-human CD3 and anti-human CD20cy antibody was localized to the lymphocyte membrane. As shown in **Figure 31.A**, we detected CD20 in 22 samples, 7 of which being classified as having more than 5 B lymphocytes. CD3 was detected in all samples; of them, 6 presented staining of more than 10 T lymphocytes. For vimentin, positive staining was localized in the cytoplasm of stromal cells. Positivity was assessed in three different categories, less than 25% positivity was identified, between 25 and 50%, and more than 50%. Most representative immunohistochemistry images for vimentin staining are shown in **Figure 31.B**.





**Figure 31. CD20, CD3 and vimentin IHC staining.** A. Staining positivity quantification of each category in our patients samples (N=26). B. Representative example of all three vimentin staining categories in our samples.

We could only clearly identify an aggregate of CD20<sup>+</sup> and CD3<sup>+</sup> cells in the tumor stroma region of the TR\_18 case which was considered to be a TLS (**Figure 32**).



**Figure 32.** Identification of a TLS by hematoxylin and eosin (H&E) staining and by IHC staining of lymphocyte aggregates, T cell CD3<sup>+</sup> and B cells, CD20<sup>+</sup>.

We also studied possible associations between the immune biomarkers CD3 and CD20 (**Table 21**). No significant associations between both markers were observed.

Contingency Table		CD3 STAINING				
CD20 STAINING		LOW T CELLS	HIGH T CELLS	TOTAL		
LOW B CELLS	COUNT	11	4	15		
	% from the total	50.0%	18.2%	68.2%		
HIGH B CELLS	COUNT	6	1	7		
	% from the total	27.3%	4.5%	31.8%	X <sup>2</sup> Pearson test	0.519
TOTAL	COUNT	17	5	22	Fisher's test	1.000
	% from the total	77.3%	22.7%	100%	Valid Cases	22

**Table 21.** Associations between CD20 and CD3 IHC staining.

As CXCL13 is a key chemoattractant orchestrating the cellular composition of TLS, we wanted to explore possible correlations among CXCL13 serum levels in PRET samples and staining of CD20, CD3 and Vimentin in the corresponding primary tumors. Of course, we would have liked to perform this analysis with metastasis samples but as explained above, this was not possible. No statistically significant associations were found; however, a trend towards a higher presence of CD20<sup>+</sup> and CD3<sup>+</sup> cells was observed in those cases whose PRET samples had CXCL13 levels above the median. Interestingly, this trend was the opposite in the case of vimentin (**Table 20**). These results must be interpreted with caution because of the reasons explained above.

Contingency Table		MEDIAN CXCL13 SERUM PRET LEVELS				
CD20 STAINING		< MEDIAN CXCL13	> MEDIAN CXCL13	TOTAL		
LOW B CELLS	COUNT	7	8	15		
	% from the total	31.8%	36.4%	68.2%		
HIGH B CELLS	COUNT	2	5	7		
	% from the total	9.1%	22.7%	31.8%	X <sup>2</sup> Pearson test	0.421
TOTAL	COUNT	9	13	22	Fisher's test	0.648
	% from the total	40.9%	59.1%	100%	Valid Cases	22
CD3 STAINING		< MEDIAN CXCL13	> MEDIAN CXCL13	TOTAL		
LOW T CELLS	COUNT	11	9	20		
	% from the total	42.3%	34.6%	76.9%		
HIGH T CELLS	COUNT	2	4	6		
	% from the total	7.7%	15.4%	23.1%	X <sup>2</sup> Pearson test	0.352
TOTAL	COUNT	13	13	26	Fisher's test	0.645
	% from the total	50%	50%	100%	Valid Cases	26
VIMENTIN STAINING		< MEDIAN CXCL13	> MEDIAN CXCL13	TOTAL		
<25-50% VIMENTIN	COUNT	10	8	18		
	% from the total	40%	32%	72%		
>50% VIMENTIN	COUNT	2	5	7		
	% from the total	28.6%	4.8%	33.3%	X <sup>2</sup> Pearson test	0.306
TOTAL	COUNT	15	6	21	Fisher's test	0.613
	% from the total	71.4%	28.6%	100%	Valid Cases	21

**Table 22.** Associations of CXCL13 serum levels in PRET samples with CD20, CD3 and Vimentin staining in the corresponding primary tumors. Median of CXCL13 was 27,38pg/mL.

### 3.2. CXCL13 *in Silico* analysis. Study of CXCL13 gene expression and correlation with immune-cells infiltration, TLS and survival in metastases from CRC patients.

In view of the few primary tumor samples that we were able to collect and the lack of clear results of the IHC analysis we decided to take advantage of the hundreds of public databases containing relevant genomic data to perform an *in silico* study. Taking into account our patients cohort's characteristics, we chose the dataset from <https://doi.org/10.1038/s41525-021-00223-7> as this cohort consisted of samples from liver metastasis from 119 mCRC patients. Of them, 104 received OXA-based neoadjuvant treatment) while only 15 patients did not receive any previous systemic treatment (Naive). The available clinico-pathological characteristics of patients are summarized in **Table 7** (see material and methods, section 5).

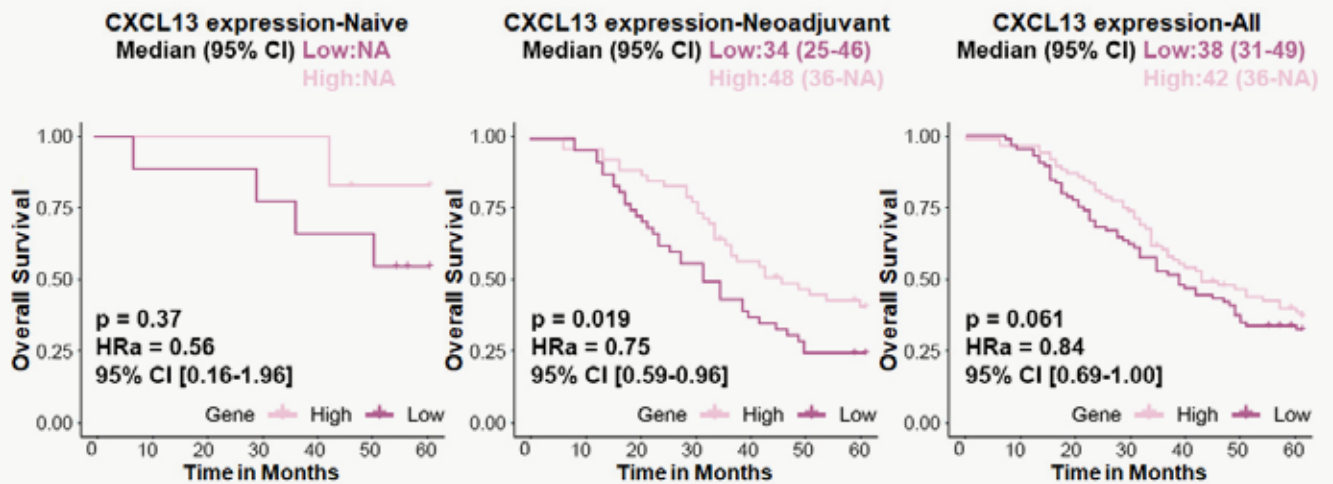
We investigated the correlation of CXCL13 gene expression with the presence of infiltrated immune cells as well as with other cells often found in the tumor microenvironment. To do so, we deconvoluted gene expression data using the MCP-counter method (<https://doi.org/10.1186/s13059-016-1070-5>). Although other available transcriptome-based computational methods exist such as the CIBERSORTx (<https://cibersortx.stanford.edu/>)(<https://doi.org/10.1038/s41587-019-0114-2>), we selected the MCP-counter as it robustly quantifies the abundance of immune and non-immune stromal cell populations in a heterogeneous tissue sample, while CIBERSORT estimates percentages of cells among the screened populations only, regardless of the total infiltration in the sample.

Globally (All), CXCL13 positively correlated with all studied cell types being the strongest associations with B and cytotoxic cells; however, if we studied non-treated (naive) and treated (neoadjuvant) patients separately, we observed that although the strength of the association by means of the R coefficient was in general higher in naive samples, only associations with T, cytotoxic, fibroblasts and monocyte cells remained statistically significant. This was probably due to the small sample size (N= 15). In contrast, despite the correlations in the neoadjuvant group were weaker they were in general statistically significant. In this case, it is worth to highlight the positive correlations with B cells, cytotoxic cells and T cells with an R coefficient above 0.4 but not reaching 0.5 (**Table 23**).

CXCL13 CORRELATION WITH DIFFERENT CELL POPULATIONS IN METASTATIC CRC TUMORS – MCP COUNTER			
CELL TYPE	NAIVE (R, p value; N=15)	NEOADJUVANT (R, p value; N=104)	ALL (R, p value; 119)
B CELLS	0.499	<b>0.499 ***</b>	<b>0.432***</b>
CYTOTOXIC CELLS	<b>0.666 *</b>	<b>0.442 ***</b>	<b>0.402 ***</b>
DENDRITIC CELLS	0.575	0.303 ***	0.290 ***
NK CELLS	0.501	0.156	0.146 *
NEUTROPHILS	0.532	0.151	0.162 **
T CELLS	<b>0.735 *</b>	0.402 ***	0.385 ***
T CELLS CD8	0.546	0.276 ***	0.246 ***
ENDOTHELIAL	0.444	0.163 *	0.186 ***
FIBROBLASTS	<b>0.684*</b>	0.187 *	0.208 **
MONOCYTES	<b>0.610*</b>	0.227**	0.232 ***

**Table 23. MCP counter-based CXCL13 gene expression correlation with immune and non-immune cell infiltrates in liver metastasis of treated (neoadjuvant), non-treated (naive) and in all patients.** For comparisons, Pearson correlation analysis was undertaken, R > 0.4 marked in bold whether there is statistical significance; p value <0.01 (\*); p <0.001 (\*\*); p <0.0001 (\*\*\*).

Taking advantage of the available survival data, we investigated the association of CXCL13 gene expression levels with OS. Patients were split according to the median value of CXCL13 gene expression. As it is shown in **Figure 33**, patients receiving neoadjuvant treatment (N=104) and with CXCL13 gene expression above the median had a better and statistically significant OS. The same non-statistically significant trend was however observed in the naive patients (N=15), and all together (N=119).



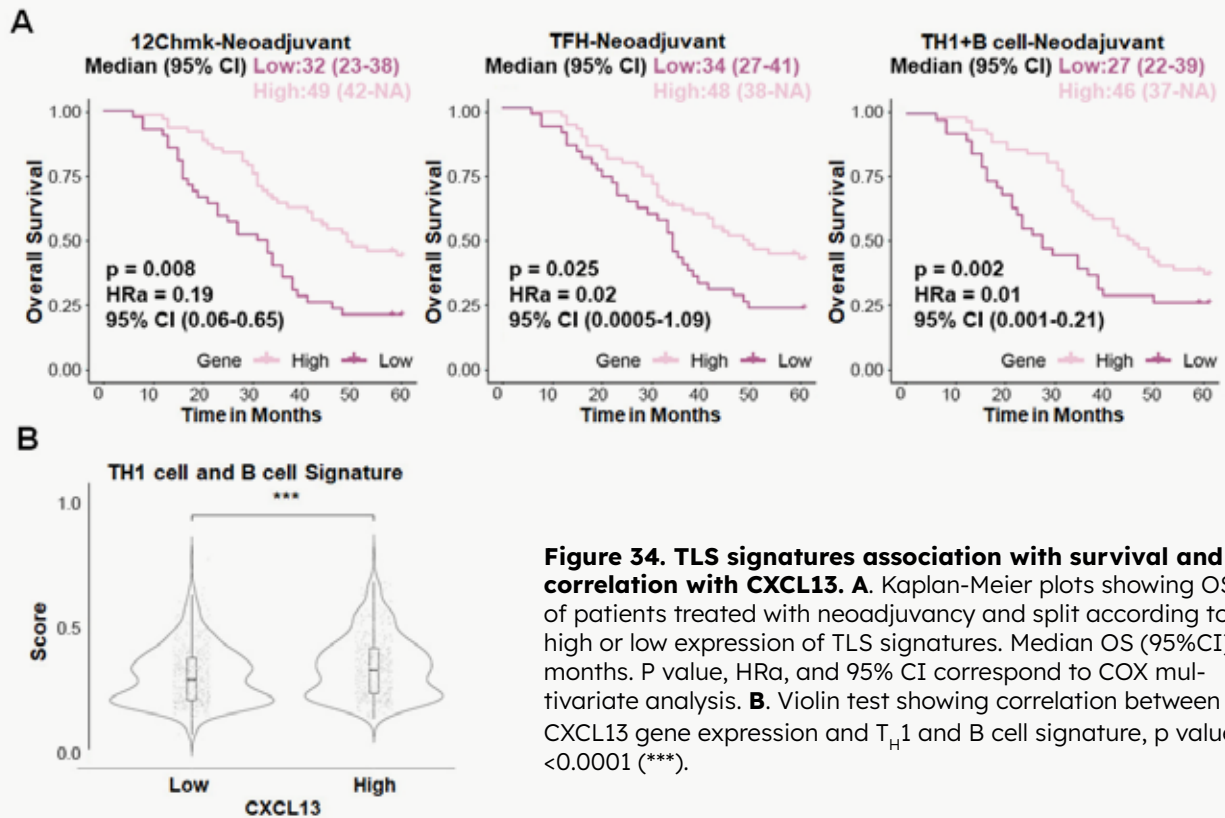
**Figure 33. Kaplan-Meier plots showing OS of patients according to the median CXCL13 gene expression.** Median OS (95%CI) in months. P value, HRa, and 95% CI correspond to COX multivariate analysis.

We then wanted to investigate the correlation of CXCL13 gene expression with the presence or absence of TLSs in these cohort; in this case though, we only had genomic data what made us look for gene signatures that were previously associated with the presence of TLSs. In this regard, we found 3 different gene signatures that have been proposed to identify TLS, all related to their neogenesis: A 12-chemokine gene signature (including CXCL13), an 8-gene signature representing TFH cells (including CXCL13) and a 19-gene signature associated to  $T_H1$  and B cells (not including CXCL13) (Sautès-Fridman et al., 2019 (<https://doi.org/10.1038/s41568-019-0144-6>) (**Table 24**).

TLS GENE SIGNATURES		
12-CHEMOKINE CELL SIGNATURE	TFH CELL SIGNATURE	TH1 AND B CELL SIGNATURE
CCL2	<b>CXCL13</b>	CD4
CCL3	CD200	CCR5
CCL4	FBLN7	CXCR3
CCL5	ICOS	CSF2
CCL8	SGPP2	IGSF6
CCL18	SH2D1A	IL2RA
CCL19	TIGIT	CD38
CCL21	PDCD1	CD40
CXCL9		CD5
CXCL10		MS4A1
CXCL11		SDC1
<b>CXCL13</b>		GFI1
		IL1R1
		IL1R2
		IL10
		CCL20
		IRF4
		TRAF6
		STAT5A

**Table 24.** TLS-associated gene signatures.

First, we studied how these signatures correlated with survival in the cohort of patients that received neoadjuvant treatment. Patients were split according to high or low TLS gene signature expression levels and as it can be seen in **Figure 34**, patients with TLS-related high gene expression levels were found to have statistically significant better OS, median OS for each TLS signature is shown in **Table 25**. It has to be taken into account that the 12-chemokine and THF signatures did include CXCL13 among the genes studied which of course, could have affected our results. However, as explained above, the T<sub>H</sub>1 and B cells signature did not include CXCL13. Therefore, we checked if this signature correlated with CXCL13 gene expression, and we found that they were indeed positively correlated (**Figure 34.B**)

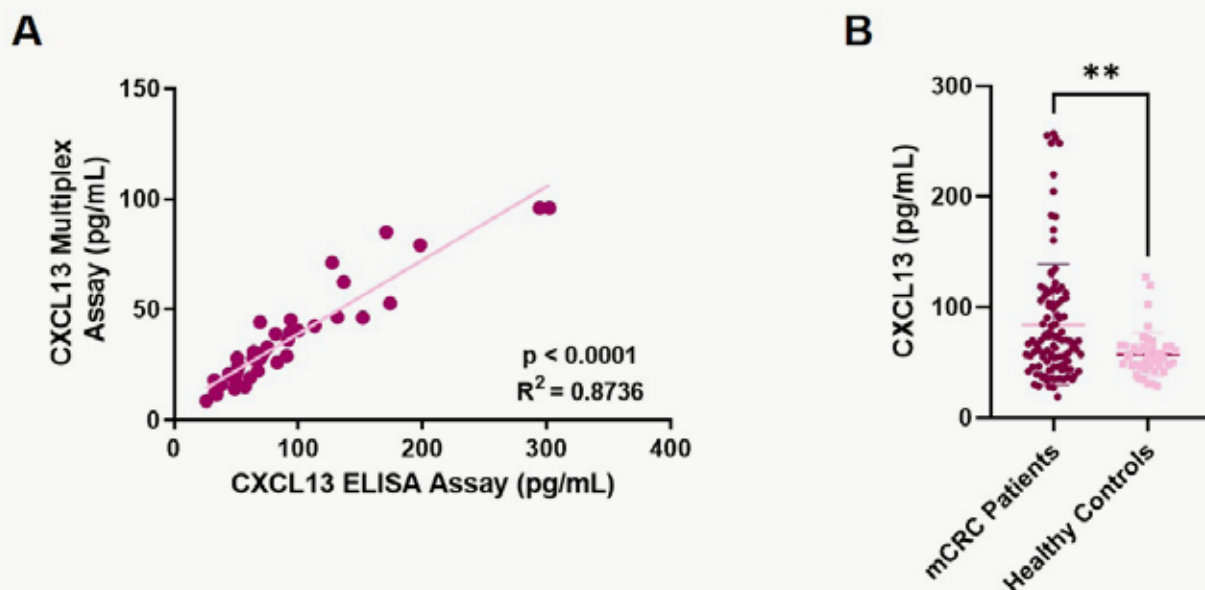


**Figure 34. TLS signatures association with survival and correlation with CXCL13.** **A.** Kaplan-Meier plots showing OS of patients treated with neoadjuvancy and split according to high or low expression of TLS signatures. Median OS (95%CI) in months. P value, HRa, and 95% CI correspond to COX multivariate analysis. **B.** Violin test showing correlation between CXCL13 gene expression and T<sub>H</sub>1 and B cell signature, p value <0.0001 (\*\*\*).

## OBJECTIVE 4

### 4. Study of CXCL13 serum levels in a healthy controls cohort

So far, we have observed that levels of CXCL13 below the median in PRET samples of our metastatic CRC patients' cohort were associated with a better prognostic and that it was in those cases in which CXCL13 increased after 3 months of treatment that the prognostic was the best. However, we did not know how these basal levels compare to let's say a non-cancer situation. Therefore, we compared the CXCL13 serum levels in our PRET samples to the CXCL13 levels in serum samples from a healthy-donors cohort (HMar cohort n=45) by a single-parameter assay (Quantikine® ELISA Kit). The characteristics of the healthy donors can be found in the material and methods, section 4.1. All controls were older than 40 years with no chronic or acute pathologies of note. We firstly evaluated how the values of CXCL13 obtained by Luminex analysis compared to the values of CXCL13 obtained by ELISA in a subset of 39 PRET samples. As seen in **Figure 35. A**, there was a linear positive correlation among the values obtained through both methods. In average, CXCL13 values (92.59pg/mL) obtained by ELISA were 2.5 times higher as the ones obtained by LUMINEX (36.65pg/mL). Based on that linear correlation, the remaining CXCL13 values from the PRET samples (65) obtained by LUMINEX, were interpolated. In the healthy controls, the median for CXCL13 was 53.97pg/mL; as it can be observed in **Figure 32.B**, this value was statistically significantly lower than that of the metastatic CRC patients (p=0.0034).



**Figure 35.** A. Scatter plot showing the correlation between CXCL13 levels measured by LUMINEX and CXCL13 levels measured by ELISA in 39 PRET samples from our patients' cohort. P and R values correspond to the Pearson correlation analysis B. Scatter dot plot showing comparison of CXCL13 levels in serum samples from our mCRC (N = 104) patients and those from samples of healthy controls (N = 45). P values correspond to Non-parametric, Mann-Whitney test p value = 0.0034 (\*\*). The median CXCL13 values were 68.27pg/mL in the mCRC cohort and 53.97pg/mL in the healthy donors cohort: The horizontal line in each boxplot represents the median value.

## OBJECTIVE 5

### 5. Study of serum CXCL13 as a prognostic marker in an independent cohort of mCRC patients

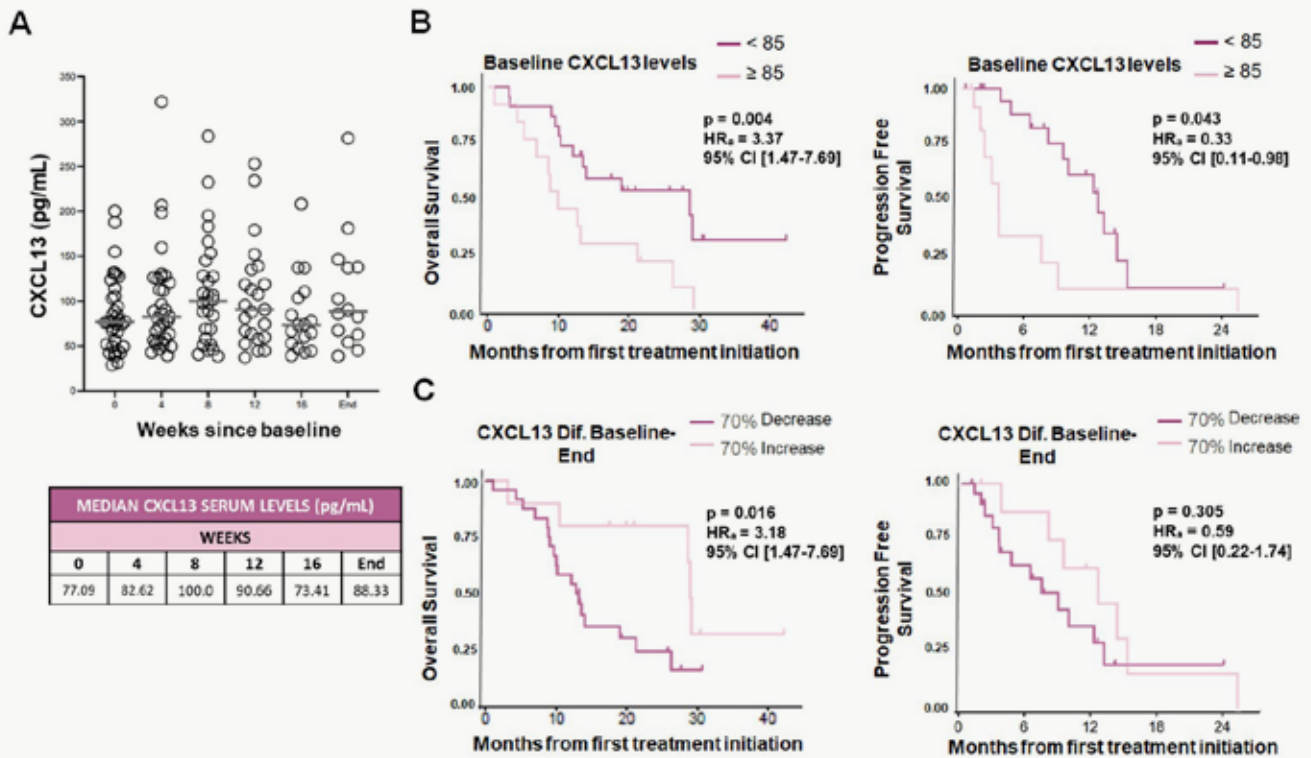
We finally wanted to check whether our results could be replicated in a similar cohort of patients. We were lucky to find out that researchers from the Akershus University Hospital, Lørenskog and from the University of Oslo performed a clinical trial in which patients included in the control arm (N=36), received the Nordic FLOX regimen (oxaliplatin + 5FU + LV) (see material and methods section 7.1, **Table 6**, for more information about the clinical trial and the clinicopathological characteristics of patients). In similar way, they collected serum samples at different time-points (see **Table 23**) along the treatment. We therefore asked them to analyse in these samples the CXCL13 levels by using the ELISA technique (**Figure 36.A**). CXCL13 median levels at baseline were 77.09pg/mL which was similar to ours (68.27pg/mL); we considered the samples taken after 3 months of treatment corresponded to our EVAR time-point. Here, the median CXCL13 value was 90.66pg/mL.

Aiming to replicate here our results, we studied basal and dynamic changes of CXCL13 levels and their association with survival (**Table 23**). As it can be observed, a non-statistically significant trend towards a better OS and PFS was found in those patients with low CXCL13 at baseline samples which is in agreement with our findings. This lack of statistical significance may be caused by the small sample size (N=36). We then explored a different cut-off point that was set up at 85pg/mL; patients with basal CXCL13 levels below this value had statistically significant better outcomes (OS and PFS) than those with values above (**Figure 36.B**).

When analysing CXCL13 dynamic changes, we observed that a great number of patients stopped treatment early, due to progression or toxicity at 8, 12 and 13 weeks, making the sample size smaller as the weeks passed. We thus considered “change at end of treatment” as best time-point to look at CXCL13 differences, as it includes all 33 patients. In agreement with our results, patients with increased levels of CXCL13 at this time-point, had better OS in the multivariate analysis (**Table 23**). In addition to that, we also explored outcomes according to a an increase or decrease of 70% in CXCL13 levels. Interestingly, patients in which there was an increase of CXCL13 levels of more than 70% after treatment had a statistically significant better OS (**Figure 36.C**).

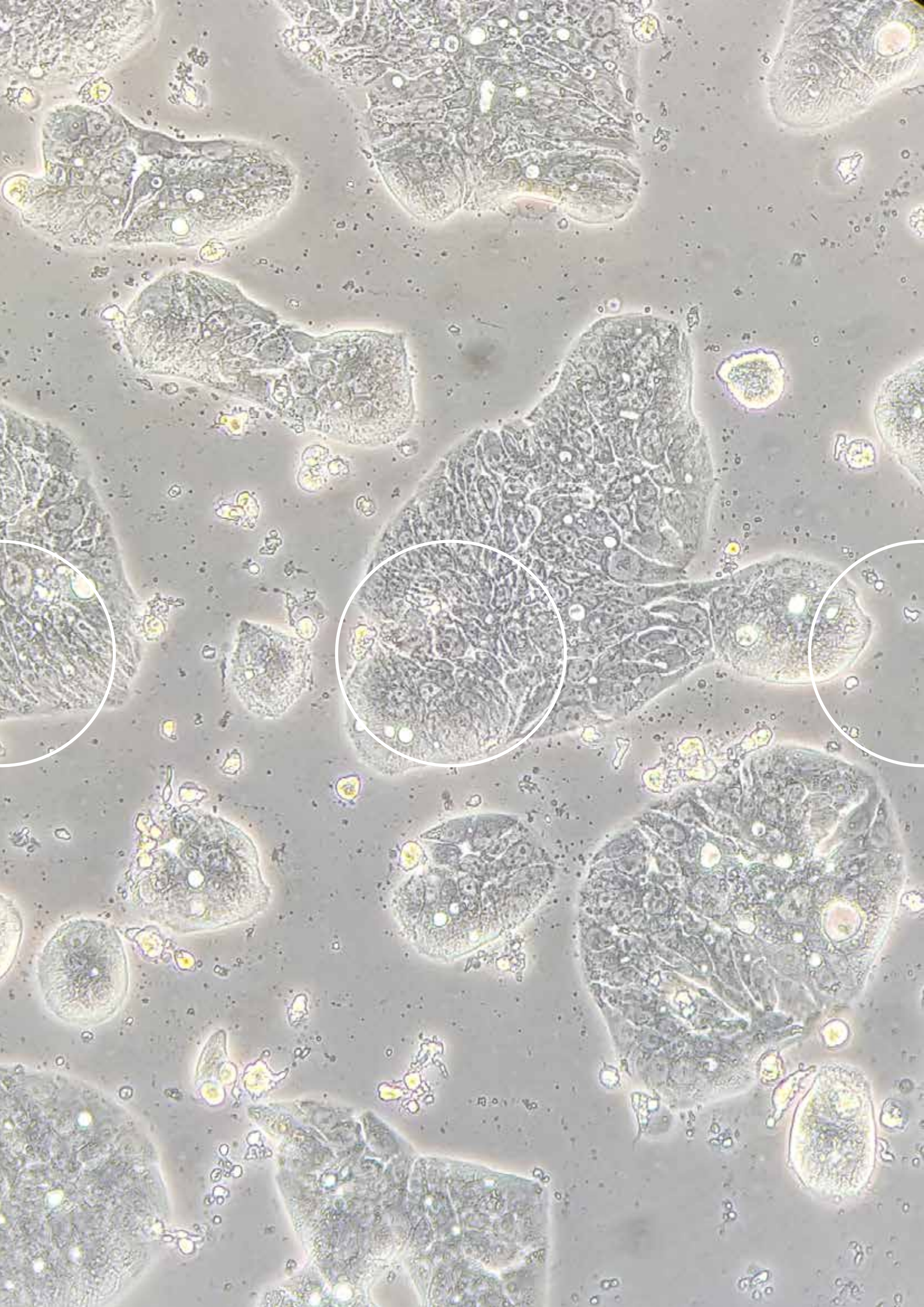
		OVERALL SURVIVAL		PROGRESSION FREE SURVIVAL		
T TIME-POINT	MEDIAN CXCL13 LEVELS	HR (95%CI, p value) <sup>1</sup>	HRa (95%CI, p value) <sup>2</sup>	HR (95%CI, p value) <sup>1</sup>	HRa (95%CI, p value) <sup>2</sup>	ALL N = 36
<b>CXCL13 SERUM LEVELS ALONG THE TREATMENT</b>						
BASELINE	<77.09	1.01 (0.99-1.02, p=0.078)	1.01 (0.99-1.02, p=0.113)	1.01 (0.99-1.02, p=0.079)	1.01 (0.99-1.02, p=0.135)	36
	≥77.09					
4 WEEKS	<82.62	1.00 (0.99-1.01, p=0.385)	1.00 (0.99-1.01, p=0.928)	1.00 (0.99-1.01, p=0.347)	1.00 (0.99-1.01, p=0.780)	33
	≥82.62					
6 WEEKS	<100.00	1.00 (0.99-1.01, p=0.494)	1.00 (0.99-1.01, p=0.815)	1.00 (0.99-1.01, p=0.850)	0.99 (0.99-1.01, p=0.870)	28
	≥100.00					
12 WEEKS	<90.66	1.00 (0.99-1.01, p=0.908)	0.99 (0.99-1.01, p=0.443)	0.99 (0.99-1.00, p=0.468)	0.99 (0.99-1.00, p=0.155)	23
	≥90.66					
16 WEEKS	<73.41	1.01 (0.99-1.02, p=0.301)	1.01 (0.99-1.02, p=0.457)	1.01 (0.99-1.01, p=0.471)	1.00 (0.98-1.02, p=0.913)	17
	≥73.41					
END OF TREATMENT	<88.33	1.00 (0.99-1.01, p=0.658)	0.99 (0.99-1.00, p=0.300)	0.99 (0.99-1.01, p=0.854)	0.99 (0.99-1.00, p=0.328)	33
	≥88.33					
<b>CXCL13 SERUM DYNAMIC CHANGES</b>						
CHANGE AT 4 WEEKS	Decrease	0.91 (0.32-2.62, p=0.861)	0.64 (0.19-2.21, p=0.483)	0.69 (0.20-2.41, p=0.687)	0.53 (0.12-2.25, p=0.390)	33
	Increase					
CHANGE AT 8 WEEKS	Decrease	0.96 (0.47-1.97, p=0.918)	0.75 (0.282-1.99, p=0.561)	0.88 (0.45-1.73, p=0.720)	0.85 (0.39-1.87, p=0.692)	28
	Increase					
CHANGE AT 12 WEEKS	Decrease	0.83 (0.38-1.82, p=0.643)	0.49 (0.14-1.68, p=0.256)	0.84 (0.45-1.55, p=0.573)	0.69 (0.34-1.42, p=0.319)	23
	Increase					
CHANGE AT 16 WEEKS	Decrease	1.60 (0.44-5.84, p=0.479)	1.33 (0.32-5.48, p=0.694)	3.88 (0.71-21.16, p=0.117)	2.64 (0.43-16.25, p=0.295)	17
	Increase					
CHANGE AT END OF TREATMENT	Decrease	0.55 (0.26-1.16, p=0.119)	<b>0.29 (0.11-1.75, p=0.011)</b>	0.73 (0.36-1.46, p=0.375)	0.48 (0.19-1.17, p=0.107)	33
	Increase					

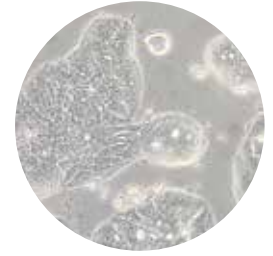
**Table 23. Association of CXCL13 levels with OS and PFS in the Oslo’s cohort.** HR correspond to categories above CXCL13 median and to increase; HR correspond to the increase category respect to decrease category (by default = 1). P values, HR, and 95% CI correspond to univariate<sup>1</sup> and multivariate<sup>2</sup> COX regression models (adjusted by age, sex, and performance status). Values in bold, correspond to statistically significant results p <0.05.



**Figure 36. A. Scatter dot plot of CXCL13 serum levels at baseline, 4, 8, 12, 16 weeks and at the end of treatment in the Oslo's cohort.** Below, table with median CXCL13 levels at each time-point. **B.** Kaplan-Meier plots showing OS and PFS of patients split according to the baseline cut-off of 85pg/mL; **C.** Kaplan-Meier plots showing OS and PFS of patients split according to an increase or decrease of 70% CXCL13 at the end of treatment. P values, HR, and 95% CI correspond to multivariate COX regression analysis (adjusted by age, sex, and performance status).







## 05 Discussion

CRC remains one of the leading causes of cancer-related death worldwide. The more advanced the disease, the poorer the prognosis. Despite advances in recent years in terms of molecular classification, diagnosis and the introduction of new treatment regimens, there is still a clear need for new therapeutic options and biomarkers, that may allow us to develop more personalized approaches and help us to improve patients' clinical outcomes. In the last years, chemokines have been in the spotlight of several studies as possible cancer biomarkers and therapeutic targets. This is because they have been demonstrated to either promote or suppress tumor growth and to predict the outcome of cancer patients. In CRC, their deregulation is related to intestinal inflammation, chemoresistance, EMT and immunosuppression. In a previous work, we demonstrated that the acquisition of resistance to oxaliplatin was associated with an hyperactivation of the NF- $\kappa$ B pathway that in turn promoted the expression and secretion of CXCL1, CXCL2, CXCL5, and CXCL8<sup>104</sup>. Moreover, the fact that they are secreted factors present in the peripheral blood makes them excellent candidates for biomarker development.

In this project, we wanted to specifically study chemokines from the CXC family and their possible role as novel predictive and/or prognostic biomarkers in metastatic CRC. In order to do that, we prospectively collected consecutive serum samples from 104 metastatic CRC patients that were candidates to be treated with first-line OXA-based regimens, in which we analyzed a custom panel of 11 chemokines by Luminex®, a bead-based immu-

noassay that allows for multiplex analytes detection. Our most relevant finding reveals that in our cohort, low pre-treatment CXCL13 serum levels were an independent factor of good prognostic; this was especially observed in those patients in which CXCL13 increases at the time of response evaluation after treatment with oxaliplatin-based first-line schedules. We also found higher levels of CXCL13 in the serum of CRC patients as compared to healthy individuals. Finally, in an *in silico* analysis using data from CRC liver metastasis specimens obtained after neoadjuvant treatment with OXA-containing regimens, high CXCL13 expression was associated with the presence of immune populations with anti-tumor properties and tertiary lymphoid structures; the latter was in turn associated with better overall and progression-free survival.

The median OS of metastatic CRC patients is about 2 years<sup>315</sup>. In our cohort, the Median OS was 23.32 months and the median PFS was 11.01 months which is in agreement with data from a Real World study presented at the European Society for Medical Oncology (ESMO) World Congress on Gastrointestinal Cancer in 2018<sup>316</sup>. The overall response rate was about 64% and 11.5% of patients had disease progression. These results are similar to previous reported ones, although a bit higher, as FOLFOX mCRC responses are around 50% to 56%, usually with more progressors, around 20%<sup>317-322</sup>.

We found that about half of the cases (52.9%) had RAS-mutated tumors (44.2% NRAS, 8.7% NRAS) while only 3.8%, were BRAF mutant. Less than 5% of patients harbored MSI tumors. While these numbers were as expected<sup>111</sup> we found that none of these alterations were significantly associated with patients' prognosis. This could be due to the sample size, especially in the case of low-frequency alterations. In the case of KRAS mutations, it is still not clear whether they have a role as prognostic factors with some works assigning them a negative effect, while others suggesting a lack of influence or giving more weight to some variants than to others<sup>323</sup>; this lack of consensus might be due to differences among the studies, including the cohorts' size, tumor subtyping, tumor staging, genetic background or the different methods of collecting mutational data.

Among all clinical characteristics, performance status (ECOG), the number of metastases, objective response to treatment and undergoing radical surgery had an impact in patients' prognostic. Prognostic factors are defined as those available measurements at diagnosis that are associated with disease-free or overall survival, becoming essential in the management of the disease<sup>324</sup>. Recently, the GERCOR group showed from a multivariate analysis that, in patients receiving oxaliplatin or irinotecan-based first-line combinations, ECOG and the number of metastatic sites were the independent and most important clinical prognostic factors<sup>325</sup>. Also, in a South-Australian registry of 1207 mCRC patients it was reported that patients with multisite metastatic disease had a worse overall survival<sup>315</sup>. Moreover, it is known that response to systemic therapy is a strong prognostic indicator (SEOM 2018) as it has been shown to be associated with a better survival in patients, and consequently, it has been integrated as an endpoint in several studies<sup>326</sup>. Altogether, our results are in line with what has been reported previously, indicating that we are not selecting any relevant characteristic in our cohort.

Despite the advances in treatment strategies that have lengthened the survival of mCRC patients, curative resection of the metastasis is the main factor leading to long-term survival<sup>327</sup>. In particular, the 5-year OS rates after lung or liver metastasis resections are known to be 35 to 68%. Hepatic and pulmonary metastasis are the most frequently resected, in contrast, reports on peritoneal resection are a minority and there are almost no reports of other organs<sup>327-330</sup>. In our study, 23 patients underwent radical resection

at some point after the first response evaluation, most of them of their liver metastasis (78%). Before starting first-line treatment 1 patient was considered unresectable, 13 potentially resectable and 9 resectable; therefore, about 13% of patients became resectable after initiating the treatment which is in line with other data reported previously<sup>331</sup>. As expected, these 23 patients presented better overall survival as compared to those that did not undergo surgery and consequently, we considered the radical surgery as a strong prognostic factor to be taken into account in the multivariate analysis. Nevertheless, we performed a sub-analysis by only considering the non-operated patients (N= 81). This group actually represents our initially ideal study population and importantly, the fact that these patients have not had their metastases removed makes them a purer population, free of confounding factors and statistical bias. Nevertheless, the reduction in the total number of patients needs to be taken into consideration when analyzing results.

Finally, we also collected information related to possible immune alterations as they could directly affect our results if we take into account that chemokines also provide the context for innate and adaptive immune systems responses<sup>332-334</sup>. Given that only 5.8% of patients presented some situation that could lead to immune alteration, and no statistically significant results were found in CXC PRET levels in these patients as compared to the rest of the cohort, we can consider that the circulating levels of the studied chemokines are related to the oncologic disease.

CXC chemokines and their corresponding receptors can be expressed by immune and non-immune cells such as tumor and stromal cells, including vascular endothelial cells. Based on a chemotactic gradient, CXC chemokines may directly and indirectly modulate the immune cell subsets found in the TME, promoting or inhibiting tumor growth. In this regard and together with the presence or absence of their ELR motif, they are respectively classified as angiogenic (pro-tumoral) or angiostatic (anti-tumoral)<sup>158,166,335,336</sup>. We found that in general, angiogenic CXC chemokines (ELR<sup>+</sup>) were more abundant than the angiostatic ones (ELR<sup>-</sup>) in PRET samples; in fact, the highest value was for CXCL5 and the lowest for CXCL9. However, this was not a perfect rule as levels of pro-tumoral chemokines CXCL8 and 6 were more similar to those of the angiostatic chemokines while in the case of CXCL10 and 16 the opposite happened.

Other authors also reported higher serum levels of CXCL5 in patients with metastatic cancer of the biliary tract<sup>337</sup> in comparison to healthy donors; in serum samples from patients with distant metastasis from gastric cancer<sup>338</sup> when compared to early gastric cancer patients; in advanced nasopharyngeal carcinoma patients versus early nasopharyngeal carcinoma patients<sup>339</sup> and in renal cell carcinoma patients in comparison with healthy blood donors<sup>340</sup>, among others. In the case of CXCL10, its serum levels are usually reported to be lower in cancer patients than in healthy donors, such as in glioblastoma (105.4pg/mL vs. 34.2pg/mL, respectively)<sup>341</sup> and acute myeloid leukemia (200pg/mL vs. 125pg/mL, respectively)<sup>342</sup>. However, high serum levels of CXCL10 analyzed by ELISA were associated with liver metastasis in CRC patients when compared to healthy controls (162pg/mL vs. 103pg/mL, respectively)<sup>343</sup>. Actually, these values were similar to ours (178.8pg/mL at baseline), although in our case were obtained through the LUMINEX technique. Also, increased CXCL16 serum levels were found in the preoperative serum of CRC patients with liver metastasis as compared to healthy volunteers; in addition, these authors reported that CXCL16 increased along with the tumor stage<sup>307</sup>. In the case of CXCL9, as it is an angiostatic chemokine<sup>344</sup>, we would have expected lower levels as compared to the angiogenic ones. However, in agreement with our findings, in CRC, increased CXCL9 gene and protein expression was found in tu-

mor tissues compare to matched non-cancerous (normal) tissues samples<sup>345</sup>. Also, high CXCL9 serum levels were reported in two different cohorts of patients with advanced hepatocellular carcinoma<sup>346</sup>. Discrepancies regarding the association of CXCL9 levels with colorectal and other cancers have been reported elsewhere<sup>343</sup>. Regarding CXCL8, similar results were reported in a cohort of 32 mCRC patients with median serum values close to ours (43.4 pg/mL vs 54 pg/mL in our study)<sup>347</sup> and in a study in advanced hepatocellular carcinoma where the LUMINEX technique was also used (40pg/mL)<sup>346</sup>. Multiple associations were observed between chemokine levels and the clinicopathological variables of interest at different time-points. Interestingly, high levels of most of the pro-tumoral chemokines, including CXCL1, 2, 5, 8 and 12, were found to be associated with the primary tumor or metastatic location or with multiple metastases. In this regard, CXCL1, 2, 5, and 8 signal through the CXCR2 axis. Several reports have demonstrated that the upregulation of these chemokines in CRC favors the development of the disease<sup>159,238,239</sup>. In mCRC patients, CXCL1 overexpression was associated with cell seeding of metastases at distant sites, such as the lung<sup>241</sup>. Signaling through the CXCR2 promotes inflammation by recruiting tumor-promoting leukocytes in many cancers, such as CRC. Also, CXCR2 is involved in tumor growth, migration and metastasis, mostly in the liver<sup>156,348-351</sup>. Overexpression of CXCL5 in tumor tissues was associated with advanced tumor stage and with poor prognosis in CRC patients<sup>352</sup>. Also, high serum levels of CXCL5 in gastric cancer were associated with distant metastasis<sup>338</sup>.

The case of CXCL16 is however controversial; while it has been classified as angiostatic due to the absence of the ELR motif and the ability to attract cytotoxic T lymphocytes and NK cells<sup>353</sup>, some authors have shown it may also promote tumor progression probably by guiding the recruitment of immunosuppressive cells such as myeloid cells and fibroblasts<sup>354</sup>. We found that patients with liver and lung metastasis had higher levels of CXCL16; interestingly, low pre-treatment levels of CXCL16 were correlated with a higher probability of undergoing radical surgery. In line with this, CXCL16 has previously been associated with metastatic potential<sup>355</sup>, distant metastasis, and bad prognosis in CRC<sup>356</sup>. Finally, it is worth mentioning that we observed higher PRET levels of this chemokine in women as compared to men. We don't know if there is any causal explanation to this observation, but in another study aimed to investigate the association of CXCL16 with clinical outcomes in patients with acute coronary syndrome, similar results were reported<sup>357</sup>.

With regard to the angiostatic chemokines, we observed that those patients with multiple metastatic disease and those with metastasis in the lungs, had higher PRET levels of CXCL9 and 10, respectively. This result is somehow surprising as these chemokines signal through the CXCR3 receptor and are mainly known for their angiostatic effect, mediating the tumor infiltration of CD8 T cells, NK cells, and B cells). Interestingly, other authors showed that high expression of CXCL9 in CRC tissue was significantly associated with tumor differentiation, tumor invasion, lymph node metastasis, distant metastasis, and vascular invasion<sup>345</sup>. Additionally, CXCL9 and 10 are upregulated by interferon-gamma (IFN- $\gamma$ ) and can exert an important role in inflammation initiation and cancer<sup>267,358,359</sup>. Thus, in agreement with our results, Kawada et al., demonstrated that CXCR3 and its ligands promoted colon cancer metastasis to lymph nodes<sup>264</sup>. In another study, CXCL10 promoted the proliferation and invasion of CRC cells resulting in a worse prognosis and its expression correlated with CRC metastasis and recurrence<sup>358</sup>.

CRC patients' survival is related to the tumor stage at the time of diagnosis and the 5-year survival is lower than 10% in metastatic cases; moreover, resistance to thera-

pies represents a common event that negatively affects prognosis. Therefore, the early identification of responders and non-responders may represent a game-changer in CRC treatment helping to avoid unnecessary prolonged treatments as well as reducing considerable toxicities and costs. In our cohort, few chemokines were associated with response to first-line treatment; specifically, we found that non-responder patients had higher basal levels of CXCL2 as compared to responders. This result is in agreement with ours and other groups' previous observations showing that this chemokine was upregulated in OXA-resistant CRC cell lines as a consequence of the NF- $\kappa$ B pathway hyperactivation<sup>104,360</sup>. Similarly, Joan Massagué's group reported high levels of CXCL2 in breast cancer patients after treatment with chemotherapeutic agents, 5-FU among others<sup>156</sup>. Interestingly, 93% of our patients received 5-FU. Although little information exists about CXCL11 and its role in response to chemotherapy, Lu et al. demonstrated in vitro that CXCL11 mRNA, protein and soluble levels were increased in cancer-associated fibroblasts (CAFs). The conditioned media obtained from these CAFs promoted cell proliferation and epithelial to mesenchymal transition in CRC cell lines. Interestingly, CXCL11 levels were reduced after oxaliplatin administration, restricting CAF-secreted CXCL11 and consequently, the tumor volume in a xenograft model. In contrast, in mice injected with CXCL11-overexpressing CAFs the OXA effect was partially evaded<sup>361</sup>. Nevertheless, these results must be taken with caution as they were only statistically significant in the univariate models. Therefore, further studies with an increased number of patients are needed to confirm them.

After adjusting by age, sex, PS and radical surgery, the only chemokine that was associated with OS and PFS was CXCL13. Even, its prognostic value was maintained when only non-operated patients were taken into account. Therefore, we consider this chemokine has the potential of becoming a reliable independent prognostic biomarker. In particular, we found that on one hand, patients who at baseline had CXCL13 levels below the median had better OS and PFS and on the other hand, an increase in CXCL13 levels at the time of response evaluation was also associated with a better clinical outcome. These results appeared to be contradictory: why high pre-treatment levels of CXCL13 were of bad prognostic but an elevation after 3 months of treatment resulted in a better outcome?

If we take a closer look at these data, we observe that as high as 71% of patients with PRET CXCL13 levels below the median (the ones with the best prognostic) have increased CXCL13 levels at EVAR; although there is only a statistically trend ( $p=0.071$ ), this association may explain at least in part, our results. Also, it is important to remark that when analyzing PRET-EVAR dynamic changes, we are only considering patients that had a sample at the EVAR time-point, being 63 out of 104 patients; therefore, it would be possible that we had selected a subpopulation with specific features affecting our results. We thus compared these 63 patients to the 41 without EVAR sample and found that both subsets were indeed very similar with the exception of the proportion of patients with disease progression as response to first-line treatment as this was significantly lower in the group of patients with an EVAR sample (5% vs 22%  $p = 0.027$ ). Importantly, there were no differences in PFS or OS and therefore, the difference in the number of progressions could indeed be indicating that in a high proportion of patients that progressed the EVAR sample was lost. These results, along with the fact that the predictive role of CXCL13 was maintained in both groups of patients, reinforce the concept that the basal levels of CXCL13 may be indicative of the presence of metastatic disease, maybe related with a host response against the tumor, while the good prognostic value of increasing levels after treatment maybe associated with a long-

term immune response induced by the treatment. While this is only an hypothesis, other studies reported an association between high basal levels of CXCL13 and worse prognosis; in CRC high levels of CXCL13 (and also CXCL8 and CXCL1) proved to modulate the tumor-specific immune response, angiogenesis, and metastasis, displaying an overall association with poor prognosis<sup>362,363</sup>; In gastric cancer, high levels of CXCL13 were significantly associated with worse 5-year OS<sup>364</sup>; in penile cancer, higher preoperative CXCL13 serum level was an independent prognostic factor for shorter disease-free survival<sup>365</sup>; In prostate cancer, the CXCL13-CXCR5 axis was significantly associated with disease progression<sup>366</sup>; finally, increased CXCL13 serum levels pointed out a role in the progression of breast cancer and advanced hepatocellular carcinoma<sup>367,368</sup>.

Finally, our hypothesis is also reinforced by the fact that CXCL13 levels in baseline samples of our patients were statistically significantly higher than in a cohort of healthy controls. In consonance with these findings, a number of studies focusing on circulating inflammation biomarkers in cancer, found increased baseline CXCL13 levels in serum samples from breast<sup>367</sup>, NSCLC<sup>369</sup>, prostate<sup>366</sup> and penile cancer<sup>365</sup>.

So far, we have shown here that high PRET serum levels of CXCL13 correlate with worse outcome in mCRC patients. We would have liked to study whether the levels of CXCL13 detected in serum correlated with tumor levels; unfortunately, we only had samples of the patients' primary tumor, obtained in most cases at the time of diagnosis and therefore far removed from the time when we carried out our study. Therefore, we cannot know whether the CXCL13 assessed in the serum was related to that which could have been released by the metastasis. Nevertheless, other authors described a correlation between CXCL13 serum levels and that found in tumor samples of different cancer types<sup>370-372</sup>.

We however found that an increase in CXCL13 levels at the time of response evaluation was associated with better OS and PFS in an independent manner. In this case, all these samples were taken at the same time-point and after the same therapeutic intervention, i.e. after patients received 4 to 6 cycles of an oxaliplatin-based chemotherapy schedule. Thus, we may hypothesize that this finding is related to treatment. In fact, we also observed that patients who responded to treatment tended to have increased levels of CXCL13 at EVAR samples while the non-responders tended to have a decrease (**Table 12**).

The strong association with PFS and OS, even greater in the non-operated patients, may be reflecting an anti-tumor immune response (by means of CXCL13 increase) which is known to induce a long-lasting clinical benefit<sup>373</sup>.

As previously mentioned, all patients included in this study were treated with OXA-based first-line treatment, and OXA is a well-known immunogenic cell death (ICD) inducer<sup>374</sup>. ICD consists of the stimulation and up-regulation of some protein molecules, like calreticulin (CRT), on the surface of apoptotic cells<sup>374</sup>. CRT may induce the maturation of DCs and activate tumor-specific cytotoxic T lymphocytes (CTLs) to get rid of the tumor cells<sup>375</sup>. The activation of recruited DCs in the TME turns on their migration to the secondary lymphoid organs (or corresponding TLS within the tumor). There, DCs present tumor antigens to T cells, thus initiating an antitumor response<sup>376</sup>. Of note, one of the chemokines involved in the generation of the immune response in the secondary or TLSs is CXCL13<sup>150</sup>. It attracts B and T follicular helper (TFH) cells as well as induces TLS formation (Bruni et al 2020 Nat. Rev). In CRC tumors, the presence of TFH cells together

with B cells have shown protection against tumor recurrence, due to an acquisition of a memory phenotype against the tumor cells. Also, T helper 1 and infiltration of cytotoxic immune cells are associated with a better prognosis, while low levels of T cells are associated with worse survival<sup>149,284</sup>. TLSs are usually associated with favorable patients' outcome, in most cancer types including CRC<sup>284</sup>.

Whether treatment is stimulating the formation of TLSs and whether the increase of CXCL13 levels is a cause or a consequence of these phenomenon requires further investigation. For instance, a similar study should be performed in patients receiving first-line regimens based on irinotecan to elucidate if our observations are specifically associated with OXA or are otherwise independent of the CT drug used in first-line treatment. To our knowledge, there are no previous reports associating irinotecan treatments with CXCL13 or with the formation of TLSs, which may be due to the fact that this drug has not been as clearly associated with the induction of ICD as oxaliplatin<sup>377</sup>. Interestingly, Mocrette G et al, identified massive intratumor TLS containing both lymphocytes and antigen-presenting cells in 11 APC germline hepatoblastomas who received cisplatin-based neoadjuvant chemotherapy but not in five pre-chemotherapy samples<sup>378</sup>. We wish we could have validated these observations in the post-treatment metastases of our patients but this was not possible. Instead, we looked for public datasets that could fit our requirements and could help us to answer these questions. We were lucky to find a dataset consisting of genomic data from liver metastasis of 119 mCRC patients that received neoadjuvant treatment based on an OXA schedule. By using this data, we found that high CXCL13 correlated with abundant B Cells, cytotoxic, and T cells in the TME of treated metastases as well as with the presence of TLSs by using 3 different gene-associated signatures. Both high CXCL13 and TLSs-signatures were associated with better prognostic of patients which is in line with our results and with data reported by other investigators<sup>284,379</sup>. In any case, it should be noted that, unlike our study, which was carried out on peripheral blood samples, the data we have just discussed comes from a transcriptomic analysis.

As I complete this thesis, we are conducting a gene expression study using NanoString that will allow us to know the levels of CXCL13 and a set of genes related to TLSs in a subset of our patients' primary tumors and correlate them with our findings in the blood of the same patients. What we have indeed been able to study is the presence of TLSs in these tumors by IHC staining. We could not observe more than one clear TLSs and no statistical associations were found between CD20 or CD3 staining and the levels of CXCL13 in PRET samples.

In order to demonstrate that our results were reproducible, we investigated CXCL13 levels in serum samples from a cohort similar to ours (Oslo's cohort). Samples came from patients included in the control arm from the METIMMOX clinical trial (NCT03388190, see details in the material and methods section 6.1, mCRC patients' cohort). Although patients from both cohorts were treated with OXA (same regimen, 85mg/m<sup>2</sup> day 1), the regimen here administered was the Nordic FLOX. The main difference between FLOX and FOLFOX is the way 5-FU is administered. In the Nordic FLOX, 5-FU is administered as a bolus of 500mg/m<sup>2</sup>, same dosage on two consecutive days, while FOLFOX consists of a bolus of 400mg/m<sup>2</sup> on day 1 followed by a 5-FU infusion of 2400mg/m<sup>2</sup> during 46 to 48-hours.

We tried to replicate our analysis and we found that similarly, patients with pre-treatment higher CXCL13 serum levels showed a trend towards a worse OS and PFS that

did not reach statistical differences probably due to the small sample size (N=36); it is worth mentioning that by slightly increasing the cut point at which patients were split into 2 groups (85pg/mL), the differences increased, being this time statistically significant. Also, we tried to validate the prognostic value of increased levels of CXCL13 after treatment. To make the analysis comparable, we chose the sample taken after 12 weeks of treatment. Importantly, the sample size became smaller as weeks passed, due to progression or toxicity with only 23 patients having a sample at the mentioned time-point; therefore, to keep the sample size, we considered the last sample taken from each case. Patients with a 70% increase in CXCL13 levels, displayed statistically significantly better OS and a trend towards a better PFS. Whether differences in the administration of 5-FU may have influenced our results remains to be demonstrated. Nevertheless, it should be noted that the way 5-FU is administered has been reported to differently affect toxicity<sup>380,381</sup>; in another study it was demonstrated that a single cycle of 5-FU treatment promoted an anti-tumor immune response, whereas repeated chemotherapy cycles impaired anti-tumor immune functions in a syngeneic mouse model of colon cancer<sup>382</sup>. Despite the differences in treatment schedules and the small sample size, these results are encouraging and we are indeed planning to validate them in additional similar cohorts.

Finally, we tried to assess the prognostic ability of CXCL13 basal levels. To do that, we created a ROC curve for OS and PFS. The best cut-off point was very close to the median value of PRET CXCL13 and although the model did not show either high sensitivity or specificity, these were, in all studied situations, above 60%. Of course, further investigation in larger cohorts is needed but one can speculate that patients with basal levels of CXCL13 above the cut-off should be monitored frequently; moreover, in those cases in which CXCL13 decreases at the time of response evaluation after an oxaliplatin first-line schedule, a change in the chemotherapy regimen should be considered.

Besides CXCL13, which we consider our main finding, a few other chemokines were also associated with clinical outcomes. PRET CXCL1 levels above the median as well as an increase at EVAR were statistically associated with worse OS. These results are similar to those reported by other authors in CRC as well as in other cancers. Thus, high CXCL1 mRNA levels in primary CRC tissues were associated with poor overall survival in advanced CRC patients<sup>383</sup> and elevated CXCL1 serum levels at the time of diagnosis were indicative of a worse prognosis<sup>241</sup>. In ovarian cancer, high levels of CXCL1 in serum correlated with a poor overall survival<sup>384</sup>.

We also found that high PRET levels of CXCL8 and CXCL9 were associated with worse OS in the multivariate analysis in the non-operated subgroup; while we could expect these results for CXCL8 as they are in line with multiple reports, the case of CXCL9 is somehow surprising. As previously discussed in this thesis, CXCL9 is usually associated with a good prognosis due to its ability to recruit cytotoxic T and B cells to the TME in different cancers, such as CRC, although a dual anti-tumor and pro-tumor effect have been described<sup>159,385</sup>. Apparently, it depends on which CXCR3 variant (CXCR3-A, and CXCR3-B) is CXCL9 binding to, since they play different roles associated with tumorigenesis, tumor immunity, and metastasis<sup>336,386</sup>. In vitro activation of CXCR3 by CXCL9 and other cognate ligands, facilitates migration, invasion and CRC progression<sup>386</sup>. Moreover, high levels of CXCL9 in the serum of patients with follicular lymphoma were associated with higher lung cancer risk<sup>369</sup> and with poor prognosis<sup>387</sup>; similar results were reported in patients with nasopharyngeal carcinoma<sup>388</sup>.

As commented above, a series of publications demonstrated that CXCL8 promotes tumor progression and resistance to different treatments. Previous findings from our group showed that the NF- $\kappa$ B-induced CXCL8 release by CRC cells, promotes proliferation and survival through the autocrine activation of the CXCR1/2 receptors, leading to oxaliplatin resistance<sup>247,389</sup>. CXCL8 has been also shown to activate AKT and ERK pathways, induce resistance to apoptosis<sup>390</sup> and EMT<sup>391</sup>. Several authors have studied its prognostic value in CRC with the vast majority showing that increased CXCL8 levels in the serum of CRC patients were associated with poor prognosis, especially in advanced stages<sup>118,247,392,393</sup>.

With the results of this thesis, we have demonstrated that chemokines in the serum from mCRC treated with OXA-based first-line treatment can be measured by the LUMINEX technique. Among all the analyzed chemokines, CXCL13 appears to be the one with the strongest potential to become a prognostic biomarker. Further investigations are warranted to demonstrate our hypothesis and thus help oncologists in decision-making with the aim to improve our patients' survival and quality of life.



# 06

## Conclusions



1. The Luminex-based analysis is a feasible and suitable technique to evaluate the levels of multiple CXC-chemokines in serum samples taken along the first-line treatment with OXA-based schedules in mCRC patients. In the case of CXCL13, we found a strong correlation between values obtained by Luminex and ELISA. In general terms, all chemokines here studied follow a pattern of increase-decrease along the treatment, with increasing values at the time of response evaluation, especially in the case of angiogenic chemokines.
2. With some exceptions, at baseline time-point, angiogenic chemokines are more abundant in mCRC patients' serum than the angiostatic ones. Interestingly, most of these angiogenic chemokines are significantly associated with clinicopathological characteristics related to the number of metastasis and the metastatic site.
3. Among all chemokines studied, only CXCL2 is associated with response to treatment. Specifically, increased levels of CXCL2 at baseline predicted a worse response to OXA-based first-line chemotherapy. Nevertheless, the predictive value of CXCL2 should be further validated.
4. CXCL13 appears to be an independent factor of prognosis in mCRC patients treated with first-line OXA-based schedules as follows:
  - On one hand, low pre-treatment CXCL13 serum levels predict better OS and PFS, which may be related with the fact that levels of CXCL13 are higher in patients than in healthy controls.
  - On the other hand, an increase of CXCL13 at the time of response evaluation predicts better OS and PFS; those patients with low basal CXCL13 and an increase in its levels at the time of response evaluation are indeed the ones with the best prognostic. Our results were confirmed in part in a similar independent cohort of CRC patients.
5. According to the results of the *in silico* analysis in liver metastasis samples from CRC patients, increased levels of CXCL13 after treatment with OXA-containing schedules may be indicative of a long-term induced immune response, as CXCL13 expression correlates with a more immunogenic TME as well as with the presence of TLSs. Both CXCL13 expression and TLSs-associated signatures are associated with better prognosis in the studied cohort.

In summary, we have demonstrated that the serum levels of most of the CXC here studied are altered along the OXA-based first-line treatment in mCRC patients and that specifically, CXCL2 and CXCL13 may be useful predictive and prognostic biomarkers in this setting. Nevertheless, these results may be further validated in larger cohorts of patients.





# 07

## Bibliography

- o1 Global Cancer Observatory. <https://gco.iarc.fr/>.
- o2 Sung, H. et al. Global Cancer Statistics 2020: GLOBOCAN Estimates of Incidence and Mortality Worldwide for 36 Cancers in 185 Countries. *CA Cancer J Clin* 71, 209–249 (2021).
- o3 Kuipers, E. J. et al. Colorectal cancer. *Nat Rev Dis Primers* 1, 15065 (2015).
- o4 Mazidimoradi, A., Tiznobaik, A. & Salehiniya, H. Impact of the COVID-19 Pandemic on Colorectal Cancer Screening: a Systematic Review. *J Gastrointest Cancer* (2021) doi:10.1007/s12029-021-00679-x.
- o5 Sharpless, N. E. COVID-19 and cancer. *Science* (1979) 368, 1290–1290 (2020).
- o6 American Cancer Society. <https://www.cancer.org/>.
- o7 Mattiuzzi, C., Sanchis-Gomar, F. & Lippi, G. Concise update on colorectal cancer epidemiology. *Ann Transl Med* 7, 609–609 (2019).
- o8 Ma, H. et al. Pathology and genetics of hereditary colorectal cancer. *Pathology* 50, 49–59 (2018).

09. Fleming, M., Ravula, S., Tatishchev, S. F. & Wang, H. L. Colorectal carcinoma: Pathologic aspects. *J Gastrointest Oncol* 3, 153–73 (2012).
10. Hanahan, D. & Weinberg, R. A. Hallmarks of Cancer: The Next Generation. *Cell* 144, 646–674 (2011).
11. Brenner, H., Kloor, M. & Pox, C. P. Colorectal cancer. *The Lancet* 383, 1490–1502 (2014).
12. Lao, V. V. & Grady, W. M. Epigenetics and colorectal cancer. *Nat Rev Gastroenterol Hepatol* 8, 686–700 (2011).
13. Pino, M. S. & Chung, D. C. The chromosomal instability pathway in colon cancer. *Gastroenterology* 138, 2059–72 (2010).
14. Tariq, K. & Ghias, K. Colorectal cancer carcinogenesis: a review of mechanisms. *Cancer Biol Med* 13, 120–35 (2016).
15. Nojadeh, J. N., Behrouz Sharif, S. & Sakhinia, E. Microsatellite instability in colorectal cancer. *EXCLI J* 17, 159–168 (2018).
16. De' Angelis, G. L. et al. Microsatellite instability in colorectal cancer. *Acta Biomed* 89, 97–101 (2018).
17. Comprehensive molecular characterization of human colon and rectal cancer. *Nature* 487, 330–337 (2012).
18. Jenkins, M. A. et al. Pathology Features in Bethesda Guidelines Predict Colorectal Cancer Microsatellite Instability: A Population-Based Study. *Gastroenterology* 133, 48–56 (2007).
19. Benatti, P. et al. Microsatellite Instability and Colorectal Cancer Prognosis. *Clinical Cancer Research* 11, 8332–8340 (2005).
20. Fearon, E. R. & Vogelstein, B. A genetic model for colorectal tumorigenesis. *Cell* 61, 759–67 (1990).
21. de Palma, F. et al. The Molecular Hallmarks of the Serrated Pathway in Colorectal Cancer. *Cancers (Basel)* 11, 1017 (2019).
22. Murcia, O. et al. Serrated colorectal cancer: Molecular classification, prognosis, and response to chemotherapy. *World J Gastroenterol* 22, 3516 (2016).
23. Bardelli, A. & Siena, S. Molecular Mechanisms of Resistance to Cetuximab and Panitumumab in Colorectal Cancer. *Journal of Clinical Oncology* 28, 1254–1261 (2010).
24. Huang, L., Guo, Z., Wang, F. & Fu, L. KRAS mutation: from undruggable to druggable in cancer. *Signal Transduct Target Ther* 6, 386 (2021).
25. Scheffzek, K. et al. The Ras-RasGAP Complex: Structural Basis for GTPase Activa-

- tion and Its Loss in Oncogenic Ras Mutants. *Science* (1979) 277, 333–339 (1997).
26. Kasi, A. et al. Molecular Pathogenesis and Classification of Colorectal Carcinoma. *Curr Colorectal Cancer Rep* 16, 97–106 (2020).
  27. Li, H. et al. Targeting the Oncogenic p53 Mutants in Colorectal Cancer and Other Solid Tumors. *Int J Mol Sci* 20, 5999 (2019).
  28. Fodde, R. The APC gene in colorectal cancer. *Eur J Cancer* 38, 867–871 (2002).
  29. Zlobec, I. & Lugli, A. Tumour budding in colorectal cancer: molecular rationale for clinical translation. *Nat Rev Cancer* 18, 203–204 (2018).
  30. Trinh, A. et al. Tumour budding is associated with the mesenchymal colon cancer subtype and RAS/RAF mutations: a study of 1320 colorectal cancers with Consensus Molecular Subgroup (CMS) data. *Br J Cancer* 119, 1244–1251 (2018).
  31. Lugli, A. et al. Recommendations for reporting tumor budding in colorectal cancer based on the International Tumor Budding Consensus Conference (ITBCC) 2016. *Modern Pathology* 30, 1299–1311 (2017).
  32. Amin, M. B. et al. The Eighth Edition AJCC Cancer Staging Manual: Continuing to build a bridge from a population-based to a more “personalized” approach to cancer staging. *CA Cancer J Clin* 67, 93–99 (2017).
  33. de Sousa E Melo, F. et al. Poor-prognosis colon cancer is defined by a molecularly distinct subtype and develops from serrated precursor lesions. *Nat Med* 19, 614–618 (2013).
  34. Roepman, P. et al. Colorectal cancer intrinsic subtypes predict chemotherapy benefit, deficient mismatch repair and epithelial-to-mesenchymal transition. *Int J Cancer* 134, 552–562 (2014).
  35. Schlicker, A. et al. Subtypes of primary colorectal tumors correlate with response to targeted treatment in colorectal cell lines. *BMC Med Genomics* 5, 66 (2012).
  36. Budinska, E. et al. Gene expression patterns unveil a new level of molecular heterogeneity in colorectal cancer. *J Pathol* 231, 63–76 (2013).
  37. Sadanandam, A. et al. A colorectal cancer classification system that associates cellular phenotype and responses to therapy. *Nat Med* 19, 619–25 (2013).
  38. Marisa, L. et al. Gene Expression Classification of Colon Cancer into Molecular Subtypes: Characterization, Validation, and Prognostic Value. *PLoS Med* 10, e1001453 (2013).
  39. Guinney, J. et al. The consensus molecular subtypes of colorectal cancer. *Nat Med* 21, 1350–6 (2015).
  40. Picard, E., Verschoor, C. P., Ma, G. W. & Pawelec, G. Relationships Between Immune Landscapes, Genetic Subtypes and Responses to Immunotherapy in Colorectal

Cancer. *Front Immunol* 11, (2020).

41. Llosa, N. J. et al. The vigorous immune microenvironment of microsatellite instable colon cancer is balanced by multiple counter-inhibitory checkpoints. *Cancer Discov* 5, 43–51 (2015).
42. Tran, B. et al. Impact of BRAF mutation and microsatellite instability on the pattern of metastatic spread and prognosis in metastatic colorectal cancer. *Cancer* 117, 4623–32 (2011).
43. Popovici, V. et al. Context-dependent interpretation of the prognostic value of BRAF and KRAS mutations in colorectal cancer. *BMC Cancer* 13, 439 (2013).
44. Wang, W. et al. Molecular subtyping of colorectal cancer: Recent progress, new challenges and emerging opportunities. *Semin Cancer Biol* 55, 37–52 (2019).
45. Sveen, A. et al. Colorectal Cancer Consensus Molecular Subtypes Translated to Pre-clinical Models Uncover Potentially Targetable Cancer Cell Dependencies. *Clinical Cancer Research* 24, 794–806 (2018).
46. Menter, D. G. et al. Back to the Colorectal Cancer Consensus Molecular Subtype Future. *Curr Gastroenterol Rep* 21, 5 (2019).
47. Kwon, Y. et al. Prognosis of stage III colorectal carcinomas with FOLFOX adjuvant chemotherapy can be predicted by molecular subtype. *Oncotarget* 8, 39367–39381 (2017).
48. ten Hoorn, S., Trinh, A., de Jong, J., Koens, L. & Vermeulen, L. Classification of Colorectal Cancer in Molecular Subtypes by Immunohistochemistry. *Methods Mol Biol* 1765, 179–191 (2018).
49. de Falco, V. et al. How we treat metastatic colorectal cancer. *ESMO Open* 4, e000813 (2019).
50. Biller, L. H. & Schrag, D. Diagnosis and Treatment of Metastatic Colorectal Cancer. *JAMA* 325, 669 (2021).
51. Silberhumer, G. R. et al. Long-term oncologic outcomes for simultaneous resection of synchronous metastatic liver and primary colorectal cancer. *Surgery* 160, 67–73 (2016).
52. Feo, L., Polcino, M. & Nash, G. M. Resection of the Primary Tumor in Stage IV Colorectal Cancer. *Surgical Clinics of North America* 97, 657–669 (2017).
53. Tan, K. K., Lopes Jr, G. de L. & Sim, R. How Uncommon are Isolated Lung Metastases in Colorectal Cancer? A Review from Database of 754 Patients Over 4 Years. *Journal of Gastrointestinal Surgery* 13, 642–648 (2009).
54. Franko, J. et al. Prognosis of patients with peritoneal metastatic colorectal cancer given systemic therapy: an analysis of individual patient data from prospective randomised trials from the Analysis and Research in Cancers of the Digestive System

- (ARCAD) database. *Lancet Oncol* 17, 1709–1719 (2016).
55. Sugarbaker, P. H. Peritonectomy Procedures. *Ann Surg* 221, 29–42 (1995).
  56. Gómez-España, M. A. et al. SEOM clinical guidelines for diagnosis and treatment of metastatic colorectal cancer (2018). *Clinical and Translational Oncology* 21, 46–54 (2019).
  57. Dromain, C. et al. Liver, lung and peritoneal metastases in colorectal cancers: Is the patient still curable? What should the radiologist know. *Diagn Interv Imaging* 95, 513–523 (2014).
  58. Fenocchio, E. et al. Improvement of Metastatic Colorectal Cancer Patient Survival: Single Institution Experience. *Cancers (Basel)* 11, 369 (2019).
  59. van Cutsem, E. et al. ESMO consensus guidelines for the management of patients with metastatic colorectal cancer. *Annals of Oncology* 27, 1386–1422 (2016).
  60. Argilés, G. et al. Localised colon cancer: ESMO Clinical Practice Guidelines for diagnosis, treatment and follow-up. *Annals of Oncology* 31, 1291–1305 (2020).
  61. Parseghian, C. M. et al. Anti-EGFR-resistant clones decay exponentially after progression: implications for anti-EGFR re-challenge. *Annals of Oncology* 30, 243–249 (2019).
  62. Kim, J. H. Chemotherapy for colorectal cancer in the elderly. *World J Gastroenterol* 21, 5158 (2015).
  63. Longley, D. B., Harkin, D. P. & Johnston, P. G. 5-Fluorouracil: mechanisms of action and clinical strategies. *Nat Rev Cancer* 3, 330–338 (2003).
  64. Crea, F. et al. Epigenetics and chemoresistance in colorectal cancer: An opportunity for treatment tailoring and novel therapeutic strategies. *Drug Resistance Updates* 14, 280–296 (2011).
  65. de Mattia, E., Cecchin, E. & Toffoli, G. Pharmacogenomics of intrinsic and acquired pharmacoresistance in colorectal cancer: Toward targeted personalized therapy. *Drug Resistance Updates* 20, 39–70 (2015).
  66. Chintala, L., Vaka, S., Baranda, J. & Williamson, S. K. Capecitabine versus 5-fluorouracil in colorectal cancer: where are we now? *Oncol Rev* 5, 129–140 (2011).
  67. Ahmad, S. Platinum-DNA Interactions and Subsequent Cellular Processes Controlling Sensitivity to Anticancer Platinum Complexes. *Chem Biodivers* 7, 543–566 (2010).
  68. Martinez-Balibrea, E. et al. Tumor-Related Molecular Mechanisms of Oxaliplatin Resistance. *Mol Cancer Ther* 14, 1767–1776 (2015).
  69. Colucci, G. et al. Phase III Randomized Trial of FOLFIRI Versus FOLFOX4 in the Treatment of Advanced Colorectal Cancer: A Multicenter Study of the Gruppo On-

- cologico Dell'Italia Meridionale. *Journal of Clinical Oncology* 23, 4866–4875 (2005).
70. Bailly, C. Irinotecan: 25 years of cancer treatment. *Pharmacol Res* 148, 104398 (2019).
  71. Herbst, R. S. Review of epidermal growth factor receptor biology. *International Journal of Radiation Oncology\*Biophysics* 59, S21–S26 (2004).
  72. Hurwitz, H. et al. Bevacizumab plus Irinotecan, Fluorouracil, and Leucovorin for Metastatic Colorectal Cancer. *New England Journal of Medicine* 350, 2335–2342 (2004).
  73. Ferrara, N., Gerber, H.-P. & LeCouter, J. The biology of VEGF and its receptors. *Nat Med* 9, 669–676 (2003).
  74. Saltz, L. B. et al. Bevacizumab in Combination With Oxaliplatin-Based Chemotherapy As First-Line Therapy in Metastatic Colorectal Cancer: A Randomized Phase III Study. *Journal of Clinical Oncology* 26, 2013–2019 (2008).
  75. Loupakis, F. et al. Initial Therapy with FOLFOXIRI and Bevacizumab for Metastatic Colorectal Cancer. *New England Journal of Medicine* 371, 1609–1618 (2014).
  76. Colucci, G. et al. Phase III Randomized Trial of FOLFIRI Versus FOLFOX4 in the Treatment of Advanced Colorectal Cancer: A Multicenter Study of the Gruppo Oncologico Dell'Italia Meridionale. *Journal of Clinical Oncology* 23, 4866–4875 (2005).
  77. National Comprehensive Cancer Network.
  78. Xie, Y.-H., Chen, Y.-X. & Fang, J.-Y. Comprehensive review of targeted therapy for colorectal cancer. *Signal Transduct Target Ther* 5, 22 (2020).
  79. Kopetz, S. et al. Encorafenib, Binimetinib, and Cetuximab in BRAF V600E-Mutated Colorectal Cancer. *New England Journal of Medicine* 381, 1632–1643 (2019).
  80. Markman, J. L. & Shiao, S. L. Impact of the immune system and immunotherapy in colorectal cancer. *J Gastrointest Oncol* 6, 208–23 (2015).
  81. André, T., Cohen, R. & Salem, M. E. Immune Checkpoint Blockade Therapy in Patients With Colorectal Cancer Harboring Microsatellite Instability/Mismatch Repair Deficiency in 2022. *American Society of Clinical Oncology Educational Book* 233–241 (2022) doi:10.1200/EDBK\_349557.
  82. Cohen, R. et al. RECIST and iRECIST criteria for the evaluation of nivolumab plus ipilimumab in patients with microsatellite instability-high/mismatch repair-deficient metastatic colorectal cancer: the GERCOR NIPICOL phase II study. *J Immunother Cancer* 8, e001499 (2020).
  83. Andre, T. et al. Pembrolizumab versus chemotherapy for microsatellite instability-high/mismatch repair deficient metastatic colorectal cancer: The phase 3 KEYNOTE-177 Study. *Journal of Clinical Oncology* 38, LBA4–LBA4 (2020).

84. Zhang, X. et al. Neoadjuvant Immunotherapy for MSI-H/dMMR Locally Advanced Colorectal Cancer: New Strategies and Unveiled Opportunities. *Front Immunol* 13, 795972 (2022).
85. Morse, M. A., Hochster, H. & Benson, A. Perspectives on Treatment of Metastatic Colorectal Cancer with Immune Checkpoint Inhibitor Therapy. *Oncologist* 25, 33–45 (2020).
86. Sinicrope, F. A. et al. Prognostic impact of deficient DNA mismatch repair in patients with stage III colon cancer from a randomized trial of FOLFOX-based adjuvant chemotherapy. *J Clin Oncol* 31, 3664–72 (2013).
87. Sveen, A., Kopetz, S. & Lothe, R. A. Biomarker-guided therapy for colorectal cancer: strength in complexity. *Nat Rev Clin Oncol* 17, 11–32 (2020).
88. Jeught, K. van der, Xu, H.-C., Li, Y.-J., Lu, X.-B. & Ji, G. Drug resistance and new therapies in colorectal cancer. *World J Gastroenterol* 24, 3834–3848 (2018).
89. Bettegowda, C. et al. Detection of Circulating Tumor DNA in Early- and Late-Stage Human Malignancies. *Sci Transl Med* 6, (2014).
90. Undevia, S. D., Gomez-Abuin, G. & Ratain, M. J. Pharmacokinetic variability of anti-cancer agents. *Nat Rev Cancer* 5, 447–458 (2005).
91. Gottesman, M. M., Fojo, T. & Bates, S. E. Multidrug resistance in cancer: role of ATP-dependent transporters. *Nat Rev Cancer* 2, 48–58 (2002).
92. Dive, C. & Hickman, J. Drug-target interactions: only the first step in the commitment to a programmed cell death? *Br J Cancer* 64, 192–196 (1991).
93. Misale, S. et al. Blockade of EGFR and MEK Intercepts Heterogeneous Mechanisms of Acquired Resistance to Anti-EGFR Therapies in Colorectal Cancer. *Sci Transl Med* 6, (2014).
94. Martinez-Cardús, A. et al. Pharmacogenomic approach for the identification of novel determinants of acquired resistance to oxaliplatin in colorectal cancer. *Mol Cancer Ther* 8, 194–202 (2009).
95. Ruiz de Porras, V. et al. Curcumin mediates oxaliplatin-acquired resistance reversion in colorectal cancer cell lines through modulation of CXC-Chemokine/NF- $\kappa$ B signalling pathway. *Sci Rep* 6, 24675 (2016).
96. Langan, R. C. et al. Colorectal Cancer Biomarkers and the Potential Role of Cancer Stem Cells. *J Cancer* 4, 241–250 (2013).
97. Lech, G. Colorectal cancer tumour markers and biomarkers: Recent therapeutic advances. *World J Gastroenterol* 22, 1745 (2016).
98. Ludwig, J. A. & Weinstein, J. N. Biomarkers in Cancer Staging, Prognosis and Treatment Selection. *Nat Rev Cancer* 5, 845–856 (2005).

99. Petrelli, F. et al. Microsatellite Instability and Survival in Stage II Colorectal Cancer: A Systematic Review and Meta-analysis. *Anticancer Res* 39, 6431–6441 (2019).
100. de Roock, W. et al. Effects of KRAS, BRAF, NRAS, and PIK3CA mutations on the efficacy of cetuximab plus chemotherapy in chemotherapy-refractory metastatic colorectal cancer: a retrospective consortium analysis. *Lancet Oncol* 11, 753–762 (2010).
101. Biller, L. H. & Schrag, D. Diagnosis and Treatment of Metastatic Colorectal Cancer. *JAMA* 325, 669 (2021).
102. Yoon, H. H. et al. KRAS Codon 12 and 13 Mutations in Relation to Disease-Free Survival in BRAF –Wild-Type Stage III Colon Cancers from an Adjuvant Chemotherapy Trial (N0147 Alliance). *Clinical Cancer Research* 20, 3033–3043 (2014).
103. Modest, D. P. et al. Outcome according to KRAS-, NRAS- and BRAF-mutation as well as KRAS mutation variants: pooled analysis of five randomized trials in metastatic colorectal cancer by the AIO colorectal cancer study group. *Annals of Oncology* 27, 1746–1753 (2016).
104. Kopetz, S. et al. Encorafenib, Binimetinib, and Cetuximab in BRAF V600E–Mutated Colorectal Cancer. *New England Journal of Medicine* 381, 1632–1643 (2019).
105. Loupakis, F. et al. Primary tumor location as a prognostic factor in metastatic colorectal cancer. *J Natl Cancer Inst* 107, (2015).
106. Tejpar, S. et al. Prognostic and Predictive Relevance of Primary Tumor Location in Patients With RAS Wild-Type Metastatic Colorectal Cancer: Retrospective Analyses of the CRYSTAL and FIRE-3 Trials. *JAMA Oncol* 3, 194–201 (2017).
107. Lee, M. K. C. & Loree, J. M. Current and emerging biomarkers in metastatic colorectal cancer. *Curr Oncol* 26, S7–S15 (2019).
108. Singh, S., Kumar, R., Kumar, U. & kumari, R. Clinical Significance and Role of TK1, CEA, CA 19-9 and CA 72-4 levels in Diagnosis of Colorectal Cancers. *Asian Pacific Journal of Cancer Prevention* 21, 3133–3136 (2020).
109. Bhardwaj, M., Gies, A., Werner, S., Schrotz-King, P. & Brenner, H. Blood-Based Protein Signatures for Early Detection of Colorectal Cancer: A Systematic Review. *Clin Transl Gastroenterol* 8, e128 (2017).
110. Voronova, V. et al. Diagnostic Value of Combinatorial Markers in Colorectal Carcinoma. *Front Oncol* 10, 832 (2020).
111. Pączek, S., Łukaszewicz-Zajęc, M. & Mroczko, B. Chemokines-What Is Their Role in Colorectal Cancer? *Cancer Control* 27, 1073274820903384.
112. Reece, M. et al. The Use of Circulating Tumor DNA to Monitor and Predict Response to Treatment in Colorectal Cancer. *Front Genet* 10, 1118 (2019).
113. Pascual, J. et al. ESMO recommendations on the use of circulating tumour DNA as-

says for patients with cancer: a report from the ESMO Precision Medicine Working Group. *Ann Oncol* 33, 750–768 (2022).

114. Vidal, J. et al. Liquid biopsy detects early molecular response and predicts benefit to first-line chemotherapy plus cetuximab in metastatic colorectal cancer: PLATFORM-B study. *Clin Cancer Res* (2022) doi:10.1158/1078-0432.CCR-22-1696.
115. Balkwill, F. & Mantovani, A. Inflammation and cancer: back to Virchow? *The Lancet* 357, 539–545 (2001).
116. Schreiber, R. D., Old, L. J. & Smyth, M. J. Cancer Immunoediting: Integrating Immunity's Roles in Cancer Suppression and Promotion. *Science* (1979) 331, 1565–1570 (2011).
117. Shankaran, V. et al. IFN $\gamma$  and lymphocytes prevent primary tumour development and shape tumour immunogenicity. *Nature* 410, 1107–1111 (2001).
118. Galon, J. et al. Type, Density, and Location of Immune Cells Within Human Colorectal Tumors Predict Clinical Outcome. *Science* (1979) 313, 1960–1964 (2006).
119. Mascaux, C. et al. Immune evasion before tumour invasion in early lung squamous carcinogenesis. *Nature* 571, 570–575 (2019).
120. Galon, J. & Bruni, D. Tumor Immunology and Tumor Evolution: Intertwined Histories. *Immunity* 52, 55–81 (2020).
121. Colotta, F., Allavena, P., Sica, A., Garlanda, C. & Mantovani, A. Cancer-related inflammation, the seventh hallmark of cancer: links to genetic instability. *Carcinogenesis* 30, 1073–1081 (2009).
122. Gao, R., Gao, Z., Huang, L. & Qin, H. Gut microbiota and colorectal cancer. *European Journal of Clinical Microbiology & Infectious Diseases* 36, 757–769 (2017).
123. Johnson, S., de Costa, A.-M. & Young, M. Effect of the Premalignant and Tumor Microenvironment on Immune Cell Cytokine Production in Head and Neck Cancer. *Cancers (Basel)* 6, 756–770 (2014).
124. Xia, J. et al. Expressions of CXCL12/CXCR4 in Oral Premalignant and Malignant Lesions. *Mediators Inflamm* 2012, 1–5 (2012).
125. Ao, M. et al. Cross-talk between Paracrine-Acting Cytokine and Chemokine Pathways Promotes Malignancy in Benign Human Prostatic Epithelium. *Cancer Res* 67, 4244–4253 (2007).
126. Erez, N., Truitt, M., Olson, P. & Hanahan, D. Cancer-Associated Fibroblasts Are Activated in Incipient Neoplasia to Orchestrate Tumor-Promoting Inflammation in an NF- $\kappa$ B-Dependent Manner. *Cancer Cell* 17, 135–147 (2010).
127. Vicent, S. et al. Cross-Species Functional Analysis of Cancer-Associated Fibroblasts Identifies a Critical Role for CLCF1 and IL-6 in Non-Small Cell Lung Cancer In Vivo. *Cancer Res* 72, 5744–5756 (2012).

128. Jiang, D. & Lim, S. Y. Influence of Immune Myeloid Cells on the Extracellular Matrix During Cancer Metastasis. *Cancer Microenvironment* 9, 45–61 (2016).
129. Galon, J., Angell, H. K., Bedognetti, D. & Marincola, F. M. The Continuum of Cancer Immunosurveillance: Prognostic, Predictive, and Mechanistic Signatures. *Immunity* 39, 11–26 (2013).
130. Oliver, A. J. et al. Tissue-Dependent Tumor Microenvironments and Their Impact on Immunotherapy Responses. *Front Immunol* 9, (2018).
131. Santegoets, S. J. et al. The Anatomical Location Shapes the Immune Infiltrate in Tumors of Same Etiology and Affects Survival. *Clinical Cancer Research* 25, 240–252 (2019).
132. Gopalakrishnan, V., Helmink, B. A., Spencer, C. N., Reuben, A. & Wargo, J. A. The Influence of the Gut Microbiome on Cancer, Immunity, and Cancer Immunotherapy. *Cancer Cell* 33, 570–580 (2018).
133. Bindea, G., Mlecnik, B., Angell, H. K. & Galon, J. The immune landscape of human tumors. *Oncoimmunology* 3, e27456 (2014).
134. Galon, J. & Bruni, D. Approaches to treat immune hot, altered and cold tumours with combination immunotherapies. *Nat Rev Drug Discov* 18, 197–218 (2019).
135. Hanahan, D. & Weinberg, R. A. The Hallmarks of Cancer. *Cell* 100, 57–70 (2000).
136. Hanahan, D. Hallmarks of Cancer: New Dimensions. *Cancer Discov* 12, 31–46 (2022).
137. Sánchez-Paulete, A. R. et al. Antigen cross-presentation and T-cell cross-priming in cancer immunology and immunotherapy. *Annals of Oncology* 28, xii44–xii55 (2017).
138. Zhu, W. et al. A high density of tertiary lymphoid structure B cells in lung tumors is associated with increased CD4 + T cell receptor repertoire clonality. *Oncoimmunology* 4, e1051922 (2015).
139. Gardner, A. & Ruffell, B. Dendritic Cells and Cancer Immunity. *Trends Immunol* 37, 855–865 (2016).
140. Chen, D. S. & Mellman, I. Oncology Meets Immunology: The Cancer-Immunity Cycle. *Immunity* 39, 1–10 (2013).
141. Dunn, G. P., Bruce, A. T., Ikeda, H., Old, L. J. & Schreiber, R. D. Cancer immunoediting: from immunosurveillance to tumor escape. *Nat Immunol* 3, 991–998 (2002).
142. Abbott, M. & Ustoyev, Y. Cancer and the Immune System: The History and Background of Immunotherapy. *Semin Oncol Nurs* 35, 150923 (2019).
143. Hanahan, D. & Weinberg, R. A. Hallmarks of Cancer: The Next Generation. *Cell* 144, 646–674 (2011).
144. Pagès, F. et al. Effector Memory T Cells, Early Metastasis, and Survival in Colorectal

- Cancer. *New England Journal of Medicine* 353, 2654–2666 (2005).
145. Zhang, L. et al. Intratumoral T Cells, Recurrence, and Survival in Epithelial Ovarian Cancer. *New England Journal of Medicine* 348, 203–213 (2003).
  146. Galon, J., Fridman, W.-H. & Pagès, F. The Adaptive Immunologic Microenvironment in Colorectal Cancer: A Novel Perspective. *Cancer Res* 67, 1883–1886 (2007).
  147. Fridman, W. H., Pagès, F., Sautès-Fridman, C. & Galon, J. The immune contexture in human tumours: impact on clinical outcome. *Nat Rev Cancer* 12, 298–306 (2012).
  148. Remark, R. et al. The Non-Small Cell Lung Cancer Immune Contexture. A Major Determinant of Tumor Characteristics and Patient Outcome. *Am J Respir Crit Care Med* 191, 377–390 (2015).
  149. Tazzari, M. et al. Complex Immune Contextures Characterise Malignant Peritoneal Mesothelioma: Loss of Adaptive Immunological Signature in the More Aggressive Histological Types. *J Immunol Res* 2018, 1–13 (2018).
  150. Pagès, F. et al. International validation of the consensus Immunoscore for the classification of colon cancer: a prognostic and accuracy study. *The Lancet* 391, 2128–2139 (2018).
  151. Yu, L. et al. Comprehensive analysis of the expression and prognostic value of CXC chemokines in colorectal cancer. *Int Immunopharmacol* 89, 107077 (2020).
  152. Nagarsheth, N., Wicha, M. S. & Zou, W. Chemokines in the cancer microenvironment and their relevance in cancer immunotherapy. *Nat Rev Immunol* 17, 559–572 (2017).
  153. Heras, S. C. Ias & Martínez-Balibrea, E. CXC family of chemokines as prognostic or predictive biomarkers and possible drug targets in colorectal cancer. *World J Gastroenterol* 24, 4738–4749 (2018).
  154. Chemokines structure. [https://www.biolegend.com/chemokine\\_receptors](https://www.biolegend.com/chemokine_receptors).
  155. Zlotnik, A., Yoshie, O. & Nomiya, H. The chemokine and chemokine receptor superfamilies and their molecular evolution. *Genome Biol* 7, 243 (2006).
  156. Zlotnik, A., Burkhardt, A. M. & Homey, B. Homeostatic chemokine receptors and organ-specific metastasis. *Nat Rev Immunol* 11, 597–606 (2011).
  157. Janssens, R., Struyf, S. & Proost, P. Pathological roles of the homeostatic chemokine CXCL12. *Cytokine Growth Factor Rev* 44, 51–68 (2018).
  158. D’Agostino, G., Cecchinato, V. & Uguccioni, M. Chemokine Heterocomplexes and Cancer: A Novel Chapter to Be Written in Tumor Immunity. *Front Immunol* 9, (2018).
  159. Nagarsheth, N., Wicha, M. S. & Zou, W. Chemokines in the cancer microenvironment and their relevance in cancer immunotherapy. *Nat Rev Immunol* 17, 559–572 (2017).
  160. Balkwill, F. Cancer and the chemokine network. *Nat Rev Cancer* 4, 540–550 (2004).

161. Gabrilovich, D. I. & Nagaraj, S. Myeloid-derived suppressor cells as regulators of the immune system. *Nat Rev Immunol* 9, 162–174 (2009).
162. Wan, S. et al. Tumor-Associated Macrophages Produce Interleukin 6 and Signal via STAT3 to Promote Expansion of Human Hepatocellular Carcinoma Stem Cells. *Gastroenterology* 147, 1393–1404 (2014).
163. Cui, T. X. et al. Myeloid-Derived Suppressor Cells Enhance Stemness of Cancer Cells by Inducing MicroRNA101 and Suppressing the Corepressor CtBP2. *Immunity* 39, 611–621 (2013).
164. Panni, R. Z. et al. Tumor-induced STAT3 activation in monocytic myeloid-derived suppressor cells enhances stemness and mesenchymal properties in human pancreatic cancer. *Cancer Immunology, Immunotherapy* 63, 513–528 (2014).
165. Peng, D. et al. Myeloid-Derived Suppressor Cells Endow Stem-like Qualities to Breast Cancer Cells through IL6/STAT3 and NO/NOTCH Cross-talk Signaling. *Cancer Res* 76, 3156–3165 (2016).
166. Kitamura, T. et al. CCL2-induced chemokine cascade promotes breast cancer metastasis by enhancing retention of metastasis-associated macrophages. *Journal of Experimental Medicine* 212, 1043–1059 (2015).
167. Pollard, J. W. Trophic macrophages in development and disease. *Nat Rev Immunol* 9, 259–270 (2009).
168. Waugh, D. J. J. & Wilson, C. The Interleukin-8 Pathway in Cancer. *Clinical Cancer Research* 14, 6735–6741 (2008).
169. de Larco, J. E., Wuertz, B. R. K. & Furcht, L. T. The Potential Role of Neutrophils in Promoting the Metastatic Phenotype of Tumors Releasing Interleukin-8. *Clinical Cancer Research* 10, 4895–4900 (2004).
170. Kryczek, I. et al. IL-22+CD4+ T Cells Promote Colorectal Cancer Stemness via STAT3 Transcription Factor Activation and Induction of the Methyltransferase DOT1L. *Immunity* 40, 772–784 (2014).
171. Perusina Lanfranca, M., Lin, Y., Fang, J., Zou, W. & Frankel, T. Biological and pathological activities of interleukin-22. *J Mol Med* 94, 523–534 (2016).
172. Kirchberger, S. et al. Innate lymphoid cells sustain colon cancer through production of interleukin-22 in a mouse model. *Journal of Experimental Medicine* 210, 917–931 (2013).
173. Huber, S. et al. IL-22BP is regulated by the inflammasome and modulates tumorigenesis in the intestine. *Nature* 491, 259–263 (2012).
174. Zou, W. Regulatory T cells, tumour immunity and immunotherapy. *Nat Rev Immunol* 6, 295–307 (2006).
175. Curiel, T. J. et al. Specific recruitment of regulatory T cells in ovarian carcinoma fos-

- ters immune privilege and predicts reduced survival. *Nat Med* 10, 942–949 (2004).
176. Facciabene, A. et al. Tumour hypoxia promotes tolerance and angiogenesis via CCL28 and Treg cells. *Nature* 475, 226–230 (2011).
  177. Zou, L. et al. Bone Marrow Is a Reservoir for CD4+CD25+ Regulatory T Cells that Traffic through CXCL12/CXCR4 Signals. *Cancer Res* 64, 8451–8455 (2004).
  178. Kryczek, I. et al. Inflammatory regulatory T cells in the microenvironments of ulcerative colitis and colon carcinoma. *Oncoimmunology* 5, e1105430 (2016).
  179. Kryczek, I. et al. IL-17 + Regulatory T Cells in the Microenvironments of Chronic Inflammation and Cancer. *The Journal of Immunology* 186, 4388–4395 (2011).
  180. Reizis, B. Plasmacytoid Dendritic Cells: Development, Regulation, and Function. *Immunity* 50, 37–50 (2019).
  181. Zou, W. et al. Stromal-derived factor-1 in human tumors recruits and alters the function of plasmacytoid precursor dendritic cells. *Nat Med* 7, 1339–1346 (2001).
  182. Wei, S. et al. Plasmacytoid Dendritic Cells Induce CD8+ Regulatory T Cells In Human Ovarian Carcinoma. *Cancer Res* 65, 5020–5026 (2005).
  183. Qian, B.-Z. et al. CCL2 recruits inflammatory monocytes to facilitate breast-tumour metastasis. *Nature* 475, 222–225 (2011).
  184. Kryczek, I. et al. B7-H4 expression identifies a novel suppressive macrophage population in human ovarian carcinoma. *Journal of Experimental Medicine* 203, 871–881 (2006).
  185. Wu, K., Kryczek, I., Chen, L., Zou, W. & Welling, T. H. Kupffer Cell Suppression of CD8+ T Cells in Human Hepatocellular Carcinoma Is Mediated by B7-H1/Programmed Death-1 Interactions. *Cancer Res* 69, 8067–8075 (2009).
  186. Li, H. et al. Tim-3/galectin-9 signaling pathway mediates T-cell dysfunction and predicts poor prognosis in patients with hepatitis B virus-associated hepatocellular carcinoma. *Hepatology* 56, 1342–1351 (2012).
  187. Kuang, D.-M. et al. Activated monocytes in peritumoral stroma of hepatocellular carcinoma foster immune privilege and disease progression through PD-L1. *Journal of Experimental Medicine* 206, 1327–1337 (2009).
  188. DeNardo, D. G. et al. Leukocyte Complexity Predicts Breast Cancer Survival and Functionally Regulates Response to Chemotherapy. *Cancer Discov* 1, 54–67 (2011).
  189. Kryczek, I. et al. Phenotype, distribution, generation, and functional and clinical relevance of Th17 cells in the human tumor environments. *Blood* 114, 1141–1149 (2009).
  190. Acosta-Rodriguez, E. v et al. Surface phenotype and antigenic specificity of human interleukin 17-producing T helper memory cells. *Nat Immunol* 8, 639–646 (2007).

191. Kryczek, I. et al. Induction of IL-17 + T Cell Trafficking and Development by IFN- $\gamma$ : Mechanism and Pathological Relevance in Psoriasis. *The Journal of Immunology* 181, 4733–4741 (2008).
192. Kryczek, I. et al. Human T H 17 Cells Are Long-Lived Effector Memory Cells. *Sci Transl Med* 3, (2011).
193. Muranski, P. et al. Tumor-specific Th17-polarized cells eradicate large established melanoma. *Blood* 112, 362–373 (2008).
194. Martin-Orozco, N. et al. T Helper 17 Cells Promote Cytotoxic T Cell Activation in Tumor Immunity. *Immunity* 31, 787–798 (2009).
195. Kryczek, I., Wei, S., Szeliga, W., Vatan, L. & Zou, W. Endogenous IL-17 contributes to reduced tumor growth and metastasis. *Blood* 114, 357–359 (2009).
196. Sato, E. et al. Intraepithelial CD8 + tumor-infiltrating lymphocytes and a high CD8 + /regulatory T cell ratio are associated with favorable prognosis in ovarian cancer. *Proceedings of the National Academy of Sciences* 102, 18538–18543 (2005).
197. Zhao, E. et al. Cancer mediates effector T cell dysfunction by targeting microRNAs and EZH2 via glycolysis restriction. *Nat Immunol* 17, 95–103 (2016).
198. Bell, D. et al. In Breast Carcinoma Tissue, Immature Dendritic Cells Reside within the Tumor, Whereas Mature Dendritic Cells Are Located in Peritumoral Areas. *Journal of Experimental Medicine* 190, 1417–1426 (1999).
199. Pedroza-Gonzalez, A. et al. Thymic stromal lymphopoietin fosters human breast tumor growth by promoting type 2 inflammation. *Journal of Experimental Medicine* 208, 479–490 (2011).
200. Fushimi, T., Kojima, A., Moore, M. A. S. & Crystal, R. G. Macrophage inflammatory protein 3 $\alpha$  transgene attracts dendritic cells to established murine tumors and suppresses tumor growth. *Journal of Clinical Investigation* 105, 1383–1393 (2000).
201. Banchereau, J. & Palucka, A. K. Dendritic cells as therapeutic vaccines against cancer. *Nat Rev Immunol* 5, 296–306 (2005).
202. Liu, X. et al. NK and NKT cells have distinct properties and functions in cancer. *Oncogene* 40, 4521–4537 (2021).
203. Singh, A. K., Tripathi, P. & Cardell, S. L. Type II NKT Cells: An Elusive Population With Immunoregulatory Properties. *Front Immunol* 9, (2018).
204. Berzofsky, J. A. & Terabe, M. NKT Cells in Tumor Immunity: Opposing Subsets Define a New Immunoregulatory Axis. *The Journal of Immunology* 180, 3627–3635 (2008).
205. Dhodapkar, M. v. & Kumar, V. Type II NKT Cells and Their Emerging Role in Health and Disease. *The Journal of Immunology* 198, 1015–1021 (2017).

206. Kim, C. H., Johnston, B. & Butcher, E. C. Trafficking machinery of NKT cells: shared and differential chemokine receptor expression among Va24+Vβ11+ NKT cell subsets with distinct cytokine-producing capacity. *Blood* 100, 11–16 (2002).
207. Germain, C., Gnjatic, S. & Dieu-Nosjean, M.-C. Tertiary Lymphoid Structure-Associated B Cells are Key Players in Anti-Tumor Immunity. *Front Immunol* 6, (2015).
208. Sautès-Fridman, C., Petitprez, F., Calderaro, J. & Fridman, W. H. Tertiary lymphoid structures in the era of cancer immunotherapy. *Nat Rev Cancer* 19, 307–325 (2019).
209. Schmidt, M. et al. The Humoral Immune System Has a Key Prognostic Impact in Node-Negative Breast Cancer. *Cancer Res* 68, 5405–5413 (2008).
210. Milne, K. et al. Systematic Analysis of Immune Infiltrates in High-Grade Serous Ovarian Cancer Reveals CD20, FoxP3 and TIA-1 as Positive Prognostic Factors. *PLoS One* 4, e6412 (2009).
211. Nedergaard, B. S., Ladekarl, M., Nyengaard, J. R. & Nielsen, K. A comparative study of the cellular immune response in patients with stage IB cervical squamous cell carcinoma. Low numbers of several immune cell subtypes are strongly associated with relapse of disease within 5 years. *Gynecol Oncol* 108, 106–111 (2008).
212. Mizoguchi, A. & Bhan, A. K. A Case for Regulatory B Cells. *The Journal of Immunology* 176, 705–710 (2006).
213. Andreu, P. et al. FcRγ Activation Regulates Inflammation-Associated Squamous Carcinogenesis. *Cancer Cell* 17, 121–134 (2010).
214. Yang, C. et al. B Cells Promote Tumor Progression via STAT3 Regulated-Angiogenesis. *PLoS One* 8, e64159 (2013).
215. Affara, N. I. et al. B Cells Regulate Macrophage Phenotype and Response to Chemotherapy in Squamous Carcinomas. *Cancer Cell* 25, 809–821 (2014).
216. Korbecki, J. et al. The Effect of Hypoxia on the Expression of CXC Chemokines and CXC Chemokine Receptors—A Review of Literature. *Int J Mol Sci* 22, 843 (2021).
217. Denisov, S. S. CXCL17: The Black Sheep in the Chemokine Flock. *Front Immunol* 12, (2021).
218. Rajagopal, S., Rajagopal, K. & Lefkowitz, R. J. Teaching old receptors new tricks: biasing seven-transmembrane receptors. *Nat Rev Drug Discov* 9, 373–386 (2010).
219. Meyrath, M. et al. The atypical chemokine receptor ACKR3/CXCR7 is a broad-spectrum scavenger for opioid peptides. *Nat Commun* 11, 3033 (2020).
220. Medzhitov, R. Origin and physiological roles of inflammation. *Nature* 454, 428–435 (2008).
221. Raman, D., Baugher, P. J., Thu, Y. M. & Richmond, A. Role of chemokines in tumor

- growth. *Cancer Lett* 256, 137–165 (2007).
222. Speyer, C. L. & Ward, P. A. Role of Endothelial Chemokines and Their Receptors during Inflammation. *Journal of Investigative Surgery* 24, 18–27 (2011).
  223. Dufies, M. et al. New CXCR1/CXCR2 inhibitors represent an effective treatment for kidney or head and neck cancers sensitive or refractory to reference treatments. *Theranostics* 9, 5332–5346 (2019).
  224. Zboralski, D., Hoehlig, K., Eulberg, D., Frömming, A. & Vater, A. Increasing Tumor-Infiltrating T Cells through Inhibition of CXCL12 with NOX-A12 Synergizes with PD-1 Blockade. *Cancer Immunol Res* 5, 950–956 (2017).
  225. Scala, S. Molecular Pathways: Targeting the CXCR4–CXCL12 Axis—Untapped Potential in the Tumor Microenvironment. *Clinical Cancer Research* 21, 4278–4285 (2015).
  226. Tokunaga, R. et al. CXCL9, CXCL10, CXCL11/CXCR3 axis for immune activation – A target for novel cancer therapy. *Cancer Treat Rev* 63, 40–47 (2018).
  227. Hussain, M. et al. CXCL13/CXCR5 signaling axis in cancer. *Life Sci* 227, 175–186 (2019).
  228. Kazanietz, M. G., Durando, M. & Cooke, M. CXCL13 and Its Receptor CXCR5 in Cancer: Inflammation, Immune Response, and Beyond. *Front Endocrinol (Lausanne)* 10, (2019).
  229. Korbecki, J. et al. The Role of CXCL16 in the Pathogenesis of Cancer and Other Diseases. *Int J Mol Sci* 22, 3490 (2021).
  230. Gowhari Shabgah, A. et al. A comprehensive review of chemokine CXCL17 (VCC1) in cancer, infection, and inflammation. *Cell Biol Int* 46, 1557–1570 (2022).
  231. Mollica Poeta, V., Massara, M., Capucetti, A. & Bonocchi, R. Chemokines and Chemokine Receptors: New Targets for Cancer Immunotherapy. *Front Immunol* 10, (2019).
  232. Itatani, Y. et al. The Role of Chemokines in Promoting Colorectal Cancer Invasion/Metastasis. *Int J Mol Sci* 17, 643 (2016).
  233. Yildirim, K. et al. Clinical Value of CXCL5 for Determining of Colorectal Cancer. *Asian Pac J Cancer Prev* 19, 2481–2484 (2018).
  234. Holmgren, K. et al. Preoperative biomarkers related to inflammation may identify high-risk anastomoses in colorectal cancer surgery: explorative study. *BJS Open* 6, (2022).
  235. Li, L. et al. Serum Chemokine CXCL7 as a Potential Novel Biomarker for Obstructive Colorectal Cancer. *Front Oncol* 10, (2021).
  236. DIVELLA, R. et al. Circulating Levels of VEGF and CXCL1 Are Predictive of Metastatic Organotropism in Patients with Colorectal Cancer. *Anticancer Res* 37, 4867

- (2017).
237. Chen, B. et al. CXCL1 Regulated by miR-302e Is Involved in Cell Viability and Motility of Colorectal Cancer via Inhibiting JAK-STAT Signaling Pathway. *Front Oncol* 10, (2021).
  238. Łukaszewicz-Zajęc, M., Pęczek, S., Mroczko, P. & Kulczyńska-Przybik, A. <p>The Significance of CXCL1 and CXCL8 as Well as Their Specific Receptors in Colorectal Cancer</p>. *Cancer Manag Res Volume* 12, 8435–8443 (2020).
  239. Alfaro, C. et al. Interleukin-8 in cancer pathogenesis, treatment and follow-up. *Cancer Treat Rev* 60, 24–31 (2017).
  240. Waugh, D. J. J. & Wilson, C. The Interleukin-8 Pathway in Cancer. *Clinical Cancer Research* 14, 6735–6741 (2008).
  241. Park, J. W. et al. The relationships between systemic cytokine profiles and inflammatory markers in colorectal cancer and the prognostic significance of these parameters. *Br J Cancer* 123, 610–618 (2020).
  242. Xie, K. Interleukin-8 and human cancer biology. *Cytokine Growth Factor Rev* 12, 375–391 (2001).
  243. Ning, Y. et al. Interleukin-8 is associated with proliferation, migration, angiogenesis and chemosensitivity in vitro and in vivo in colon cancer cell line models. *Int J Cancer* 128, 2038–2049 (2011).
  244. Ha, H., Debnath, B. & Neamati, N. Role of the CXCL8-CXCR1/2 Axis in Cancer and Inflammatory Diseases. *Theranostics* 7, 1543–1588 (2017).
  245. Lee, Y. S. et al. Interleukin-8 and its receptor CXCR2 in the tumour microenvironment promote colon cancer growth, progression and metastasis. *Br J Cancer* 106, 1833–1841 (2012).
  246. Varney, M. L. et al. Small molecule antagonists for CXCR2 and CXCR1 inhibit human colon cancer liver metastases. *Cancer Lett* 300, 180–188 (2011).
  247. Johdi, N. A., Mazlan, L., Sagap, I. & Jamal, R. Profiling of cytokines, chemokines and other soluble proteins as a potential biomarker in colorectal cancer and polyps. *Cytokine* 99, 35–42 (2017).
  248. Müller, A. et al. Involvement of chemokine receptors in breast cancer metastasis. *Nature* 410, 50–56 (2001).
  249. Zlotnik, A., Burkhardt, A. M. & Homey, B. Homeostatic chemokine receptors and organ-specific metastasis. *Nat Rev Immunol* 11, 597–606 (2011).
  250. Darash-Yahana, M. et al. Role of high expression levels of CXCR4 in tumor growth, vascularization, and metastasis. *The FASEB Journal* 18, 1240–1242 (2004).
  251. Matsusue, R. et al. Hepatic Stellate Cells Promote Liver Metastasis of Colon Cancer

Cells by the Action of SDF-1/CXCR4 Axis. *Ann Surg Oncol* 16, 2645–2653 (2009).

252. Kim, J. et al. Chemokine Receptor CXCR4 Expression in Colorectal Cancer Patients Increases the Risk for Recurrence and for Poor Survival. *Journal of Clinical Oncology* 23, 2744–2753 (2005).
253. Ottaiano, A. et al. Overexpression of Both CXC Chemokine Receptor 4 and Vascular Endothelial Growth Factor Proteins Predicts Early Distant Relapse in Stage II-III Colorectal Cancer Patients. *Clinical Cancer Research* 12, 2795–2803 (2006).
254. Mitchell, A. et al. A chemokine/chemokine receptor signature potentially predicts clinical outcome in colorectal cancer patients. *Cancer Biomarkers* 26, 291–301 (2019).
255. Li, Y. et al. Role of CXCR4 and SDF1 as prognostic factors for survival and the association with clinicopathology in colorectal cancer: A systematic meta-analysis. *Tumor Biology* 39, 101042831770620 (2017).
256. Li, X., Wang, X., Li, Z., Zhang, Z. & Zhang, Y. Chemokine receptor 7 targets the vascular endothelial growth factor via the AKT/ERK pathway to regulate angiogenesis in colon cancer. *Cancer Med* 8, 5327–5340 (2019).
257. Wang, M., Yang, X., Wei, M. & Wang, Z. The Role of CXCL12 Axis in Lung Metastasis of Colorectal Cancer. *J Cancer* 9, 3898–3903 (2018).
258. Kaplan, R. N. et al. VEGFR1-positive haematopoietic bone marrow progenitors initiate the pre-metastatic niche. *Nature* 438, 820–827 (2005).
259. Braoudaki, M. et al. Chemokines and chemokine receptors in colorectal cancer; multifarious roles and clinical impact. *Semin Cancer Biol* 86, 436–449 (2022).
260. Murakami, T. et al. The role of CXCR3 and CXCR4 in colorectal cancer metastasis. *Int J Cancer* 132, 276–287 (2013).
261. Kawada, K. et al. Chemokine receptor CXCR3 promotes colon cancer metastasis to lymph nodes. *Oncogene* 26, 4679–4688 (2007).
262. Jiang, Z., Xu, Y. & Cai, S. CXCL10 expression and prognostic significance in stage II and III colorectal cancer. *Mol Biol Rep* 37, 3029–3036 (2010).
263. Wightman, S. C. et al. Oncogenic CXCL10 signalling drives metastasis development and poor clinical outcome. *Br J Cancer* 113, 327–335 (2015).
264. Toiyama, Y. Evaluation of CXCL10 as a novel serum marker for predicting liver metastasis and prognosis in colorectal cancer. *Int J Oncol* (2011) doi:10.3892/ijo.2011.1247.
265. Legler, D. F. et al. B Cell-attracting Chemokine 1, a Human CXC Chemokine Expressed in Lymphoid Tissues, Selectively Attracts B Lymphocytes via BLR1/CXCR5. *Journal of Experimental Medicine* 187, 655–660 (1998).

266. Cyster, J. G. et al. Follicular stromal cells and lymphocyte homing to follicles. *Immunol Rev* 176, (2000).
267. Ansel, K. M. et al. A chemokine-driven positive feedback loop organizes lymphoid follicles. *Nature* 406, 309–314 (2000).
268. Shi, K. et al. Lymphoid Chemokine B Cell-Attracting Chemokine-1 (CXCL13) Is Expressed in Germinal Center of Ectopic Lymphoid Follicles Within the Synovium of Chronic Arthritis Patients. *The Journal of Immunology* 166, 650–655 (2001).
269. Bruni, D., Angell, H. K. & Galon, J. The immune contexture and Immunoscore in cancer prognosis and therapeutic efficacy. *Nat Rev Cancer* 20, 662–680 (2020).
270. Jenh, C.-H. et al. HUMAN B CELL-ATTRACTING CHEMOKINE 1 (BCA-1; CXCL13) IS AN AGONIST FOR THE HUMAN CXCR3 RECEPTOR. *Cytokine* 15, 113–121 (2001).
271. Gunn, M. D. et al. A B-cell-homing chemokine made in lymphoid follicles activates Burkitt's lymphoma receptor-1. *Nature* 391, 799–803 (1998).
272. Sáez de Guinoa, J., Barrio, L., Mellado, M. & Carrasco, Y. R. CXCL13/CXCR5 signaling enhances BCR-triggered B-cell activation by shaping cell dynamics. *Blood* 118, 1560–1569 (2011).
273. Ohmatsu, H., Sugaya, M., Kadono, T. & Tamaki, K. CXCL13 and CCL21 Are Expressed in Ectopic Lymphoid Follicles in Cutaneous Lymphoproliferative Disorders. *Journal of Investigative Dermatology* 127, 2466–2468 (2007).
274. Schaeferli, P. et al. Cxc Chemokine Receptor 5 Expression Defines Follicular Homing T Cells with B Cell Helper Function. *Journal of Experimental Medicine* 192, 1553–1562 (2000).
275. Förster, R. et al. A Putative Chemokine Receptor, BLR1, Directs B Cell Migration to Defined Lymphoid Organs and Specific Anatomic Compartments of the Spleen. *Cell* 87, 1037–1047 (1996).
276. Coelho, F. M. et al. Naive B-cell trafficking is shaped by local chemokine availability and LFA-1-independent stromal interactions. *Blood* 121, 4101–4109 (2013).
277. Luther, S. A., Lopez, T., Bai, W., Hanahan, D. & Cyster, J. G. BLC Expression in Pancreatic Islets Causes B Cell Recruitment and Lymphotoxin-Dependent Lymphoid Neogenesis. *Immunity* 12, 471–481 (2000).
278. Dieu-Nosjean, M.-C., Goc, J., Giraldo, N. A., Sautès-Fridman, C. & Fridman, W. H. Tertiary lymphoid structures in cancer and beyond. *Trends Immunol* 35, 571–580 (2014).
279. Nerviani, A. & Pitzalis, C. Role of chemokines in ectopic lymphoid structures formation in autoimmunity and cancer. *J Leukoc Biol* 104, 333–341 (2018).
280. Schumacher, T. N. & Thommen, D. S. Tertiary lymphoid structures in cancer. *Science*

(1979) 375, (2022).

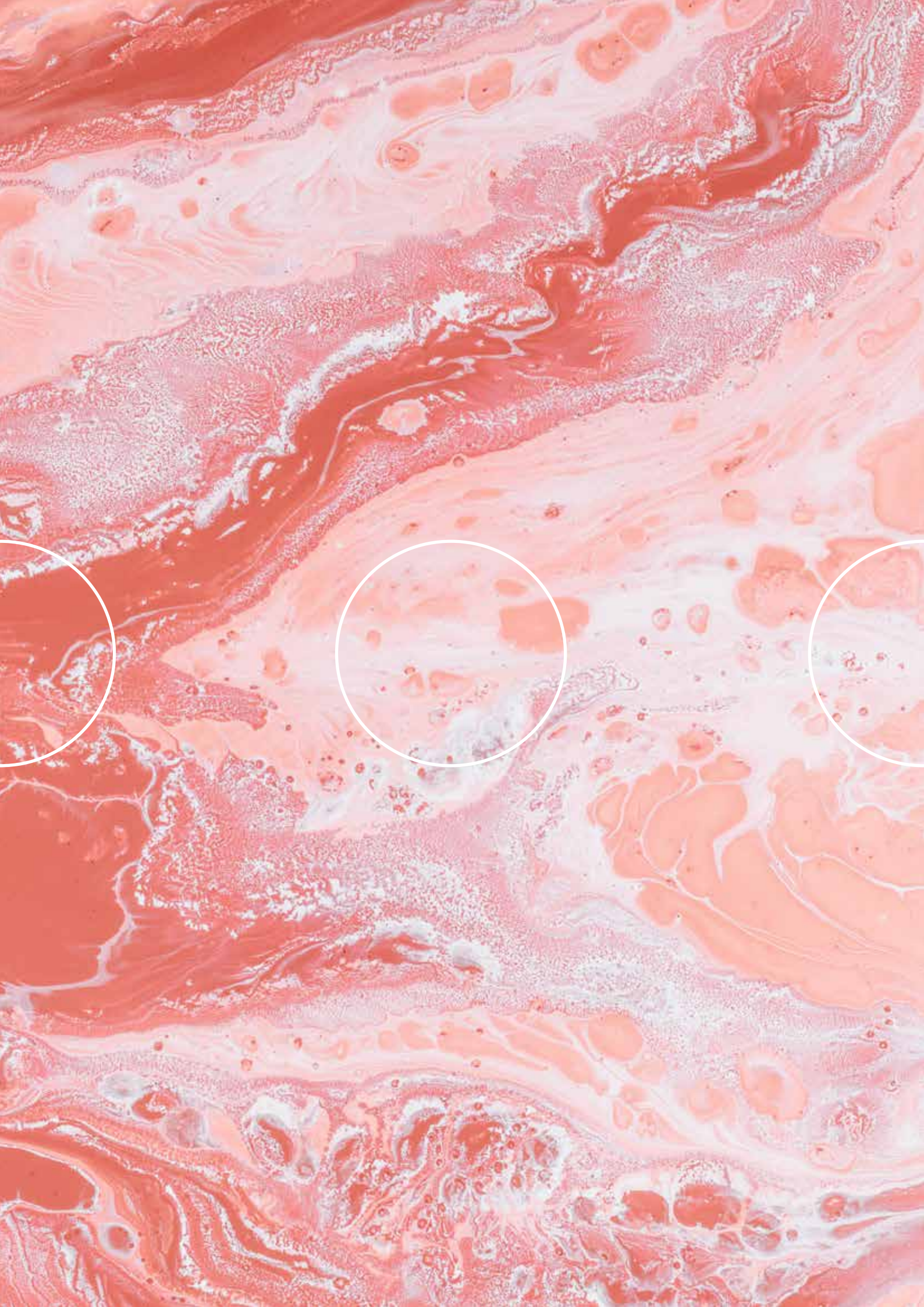
281. Aloisi, F. & Pujol-Borrell, R. Lymphoid neogenesis in chronic inflammatory diseases. *Nat Rev Immunol* 6, 205–217 (2006).
282. Bindea, G. et al. Spatiotemporal Dynamics of Intratumoral Immune Cells Reveal the Immune Landscape in Human Cancer. *Immunity* 39, 782–795 (2013).
283. Galon, J. et al. Type, Density, and Location of Immune Cells Within Human Colorectal Tumors Predict Clinical Outcome. *Science* (1979) 313, 1960–1964 (2006).
284. Ågesen, T. H. et al. ColoGuideEx: a robust gene classifier specific for stage II colorectal cancer prognosis. *Gut* 61, 1560–1567 (2012).
285. Rachidi, S. M., Qin, T., Sun, S., Zheng, W. J. & Li, Z. Molecular Profiling of Multiple Human Cancers Defines an Inflammatory Cancer-Associated Molecular Pattern and Uncovers KPNA2 as a Uniform Poor Prognostic Cancer Marker. *PLoS One* 8, e57911 (2013).
286. Xing, J. et al. CXCR5 + CD8 + T cells infiltrate the colorectal tumors and nearby lymph nodes, and are associated with enhanced IgG response in B cells. *Exp Cell Res* (2017) doi:10.1016/j.yexcr.2017.04.014.
287. Zhu, Z. et al. CXCL13-CXCR5 axis promotes the growth and invasion of colon cancer cells via PI3K/AKT pathway. *Mol Cell Biochem* 400, 287–295 (2015).
288. Olsen, R. S., Nijm, J., Andersson, R. E., Dimberg, J. & Wågsäter, D. Circulating inflammatory factors associated with worse long-term prognosis in colorectal cancer. *World J Gastroenterol* 23, 6212 (2017).
289. Qi, X.-W. et al. Expression features of CXCR5 and its ligand, CXCL13 associated with poor prognosis of advanced colorectal cancer. *Eur Rev Med Pharmacol Sci* 18, 1916–24 (2014).
290. Matloubian, M., David, A., Engel, S., Ryan, J. E. & Cyster, J. G. A transmembrane CXC chemokine is a ligand for HIV-coreceptor Bonzo. *Nat Immunol* 1, 298–304 (2000).
291. Wilbanks, A. et al. Expression Cloning of the STRL33/BONZO/TYMSTR Ligand Reveals Elements of CC, CXC, and CX3C Chemokines. *The Journal of Immunology* 166, 5145–5154 (2001).
292. Schulte, A. et al. Sequential processing of the transmembrane chemokines CX-3CL1 and CXCL16 by  $\alpha$ - and  $\gamma$ -secretases. *Biochem Biophys Res Commun* 358, 233–240 (2007).
293. Gutwein, P. et al. Tumoural CXCL16 expression is a novel prognostic marker of longer survival times in renal cell cancer patients. *Eur J Cancer* 45, 478–489 (2009).

294. Abel, S. et al. The Transmembrane CXC-Chemokine Ligand 16 Is Induced by IFN- $\gamma$  and TNF- $\alpha$  and Shed by the Activity of the Disintegrin-Like Metalloproteinase ADAM10. *The Journal of Immunology* 172, 6362–6372 (2004).
295. Gutwein, P. et al. CXCL16 Is Expressed in Podocytes and Acts as a Scavenger Receptor for Oxidized Low-Density Lipoprotein. *Am J Pathol* 174, 2061–2072 (2009).
296. Shimaoka, T. et al. Cell surface-anchored SR-PSOX/CXC chemokine ligand 16 mediates firm adhesion of CXC chemokine receptor 6-expressing cells. *J Leukoc Biol* 75, 267–274 (2004).
297. Hofnagel, O., Engel, T., Severs, N. J., Robenek, H. & Buers, I. SR-PSOX at sites predisposed to atherosclerotic lesion formation mediates monocyte-endothelial cell adhesion. *Atherosclerosis* 217, 371–378 (2011).
298. Adamski, V. et al. The Chemokine Receptor CXCR6 Evokes Reverse Signaling via the Transmembrane Chemokine CXCL16. *Int J Mol Sci* 18, 1468 (2017).
299. Hattermann, K. et al. “Inverse signaling” of the transmembrane chemokine CXCL16 contributes to proliferative and anti-apoptotic effects in cultured human meningioma cells. *Cell Communication and Signaling* 14, 26 (2016).
300. Hattermann, K. et al. Transmembrane chemokines act as receptors in a novel mechanism termed inverse signaling. *Elife* 5, (2016).
301. Hojo, S. et al. High-Level Expression of Chemokine CXCL16 by Tumor Cells Correlates with a Good Prognosis and Increased Tumor-Infiltrating Lymphocytes in Colorectal Cancer. *Cancer Res* 67, 4725–4731 (2007).
302. Chen, Z. et al. Elevated expression of CXCL16 correlates with poor prognosis in patients with colorectal cancer. *Cancer Manag Res Volume* 11, 4691–4697 (2019).
303. AbdelMageed, M. et al. The Chemokine CXCL16 Is a New Biomarker for Lymph Node Analysis of Colon Cancer Outcome. *Int J Mol Sci* 20, 5793 (2019).
304. Matsushita, K. et al. Soluble CXCL16 in Preoperative Serum is a Novel Prognostic Marker and Predicts Recurrence of Liver Metastases in Colorectal Cancer Patients. *Ann Surg Oncol* 19, 518–527 (2012).
305. Bikfalvi, A. & Billottet, C. The CC and CXC chemokines: major regulators of tumor progression and the tumor microenvironment. *American Journal of Physiology-Cell Physiology* 318, C542–C554 (2020).
306. Schott, A. F. et al. Phase Ib Pilot Study to Evaluate Reparixin in Combination with Weekly Paclitaxel in Patients with HER-2-Negative Metastatic Breast Cancer. *Clinical Cancer Research* 23, 5358–5365 (2017).
307. Galsky, M. D. et al. A Phase I Trial of LY2510924, a CXCR4 Peptide Antagonist, in Patients with Advanced Cancer. *Clinical Cancer Research* 20, 3581–3588

(2014).

308. Li, H., Wu, M. & Zhao, X. Role of chemokine systems in cancer and inflammatory diseases. *MedComm (Beijing)* 3, (2022).
309. Li, G. et al. CXCR5 guides migration and tumor eradication of anti-EGFR chimeric antigen receptor T cells. *Mol Ther Oncolytics* 22, 507–517 (2021).
310. Xu, C., Ju, D. & Zhang, X. Chimeric antigen receptor T-cell therapy: challenges and opportunities in lung cancer. *Antib Ther* 5, 73–83 (2022).
311. Clinical Trials Gov. <https://clinicaltrials.gov>.
312. COLONOMICS. <https://www.colonomics.org/data-browser/dashboard/>.







# 08

## Annexes

### **ANNEX I**

Review

### **ANNEX II**

Newsletter (e.g. November 2019)

### **ANNEX III**

Luminex-Biorad user manual

### **ANNEX IV**

PRET CXC chemokines serum levels in patients with known immune system alterations vs. patients with non-reported alterations

### **ANNEX V**

CXC chemokines distribution at EVAR and PROG time-points

### **ANNEX VI**

PRET, EVAR and PROG CXC chemokines serum levels association with response to treatment and patients' clinicopathological and molecular characteristics

### **ANNEX VII**

CXC chemokines serum levels at EVAR and PROG time-points association with survival

### **ANNEX VIII**

CXC chemokines dynamic changes along PRET-PROG and EVAR-PROG association with survival

## Contents

Weekly Volume 24 Number 42 November 14, 2018

### EDITORIAL

- 4721 Increased susceptibility of aging gastric mucosa to injury and delayed healing: Clinical implications  
*Tarnawski AS, Ahluwalia A*

### REVIEW

- 4728 Liver as a target of human immunodeficiency virus infection  
*Ganesan M, Poluektova LY, Kharbanda KK, Osna NA*

### MINIREVIEWS

- 4738 CXC family of chemokines as prognostic or predictive biomarkers and possible drug targets in colorectal cancer  
*Cabrero-de las Heras S, Martinez-Balibrea E*
- 4750 Gut microbiota in common elderly diseases affecting activities of daily living  
*Shimizu Y*

### ORIGINAL ARTICLE

#### Basic Study

- 4759 Yiguanjian decoction enhances fetal liver stem/progenitor cell-mediated repair of liver cirrhosis through regulation of macrophage activation state  
*Xu Y, Fan WW, Xu W, Jiang SL, Chen GF, Liu C, Chen JM, Zhang H, Liu P, Mu YP*
- 4773 Ubiquitin-like modifier activating enzyme 2 promotes cell migration and invasion through Wnt/ $\beta$ -catenin signaling in gastric cancer  
*Li J, Sun X, He P, Liu WQ, Zou YB, Wang Q, Meng XW*

#### Case Control Study

- 4787 Mode of delivery by an ulcerative colitis mother in a case of twins: Immunological differences in cord blood and placenta  
*Dunsmore G, Koleva P, Sutton RT, Ambrosio L, Huang V, Elahi S*

#### Retrospective Cohort Study

- 4798 Increased end-stage renal disease risk in patients with inflammatory bowel disease: A nationwide population-based study  
*Park S, Chun J, Han KD, Soh H, Choi K, Kim JH, Lee J, Lee C, Im JP, Kim JS*

#### Retrospective Study

- 4809 Prediction of colorectal tumor grade and invasion depth through narrow-band imaging scoring  
*Maeyama Y, Mitsuyama K, Noda T, Nagata S, Nagata T, Yoshioka S, Yoshida H, Mukasa M, Sumie H, Kawano H, Akiba J, Araki Y, Kakuma T, Tsuruta O, Torimura T*

### SYSTEMATIC REVIEWS

- 4821 Burden and outcomes for complex perianal fistulas in Crohn's disease: Systematic review  
*Panes J, Reinisch W, Rupniewska E, Khan S, Forns J, Khalid JM, Bojic D, Patel H*

## Contents

*World Journal of Gastroenterology*  
Volume 24 Number 42 November 14, 2018

## ABOUT COVER

Editorial board member of *World Journal of Gastroenterology*, Kazuaki Inoue, MD, PhD, Associate Professor, Department of Internal Medicine, Division of Gastroenterology, Showa University Fujigaoka Hospital, Yokohama 227-8501, Japan

## AIMS AND SCOPE

*World Journal of Gastroenterology* (*World J Gastroenterol*, *WJG*, print ISSN 1007-9327, online ISSN 2219-2840, DOI: 10.3748) is a peer-reviewed open access journal. *WJG* was established on October 1, 1995. It is published weekly on the 7<sup>th</sup>, 14<sup>th</sup>, 21<sup>st</sup>, and 28<sup>th</sup> each month. The *WJG* Editorial Board consists of 642 experts in gastroenterology and hepatology from 59 countries.

The primary task of *WJG* is to rapidly publish high-quality original articles, reviews, and commentaries in the fields of gastroenterology, hepatology, gastrointestinal endoscopy, gastrointestinal surgery, hepatobiliary surgery, gastrointestinal oncology, gastrointestinal radiation oncology, gastrointestinal imaging, gastrointestinal interventional therapy, gastrointestinal infectious diseases, gastrointestinal pharmacology, gastrointestinal pathophysiology, gastrointestinal pathology, evidence-based medicine in gastroenterology, pancreatology, gastrointestinal laboratory medicine, gastrointestinal molecular biology, gastrointestinal immunology, gastrointestinal microbiology, gastrointestinal genetics, gastrointestinal translational medicine, gastrointestinal diagnostics, and gastrointestinal therapeutics. *WJG* is dedicated to become an influential and prestigious journal in gastroenterology and hepatology, to promote the development of above disciplines, and to improve the diagnostic and therapeutic skill and expertise of clinicians.

## INDEXING/ABSTRACTING

*World Journal of Gastroenterology* (*WJG*) is now indexed in Current Contents®/Clinical Medicine, Science Citation Index Expanded (also known as SciSearch®), Journal Citation Reports®, Index Medicus, MEDLINE, PubMed, PubMed Central and Directory of Open Access Journals. The 2018 edition of Journal Citation Reports® cites the 2017 impact factor for *WJG* as 3.300 (5-year impact factor: 3.387), ranking *WJG* as 35<sup>th</sup> among 80 journals in gastroenterology and hepatology (quartile in category Q2).

## EDITORS FOR THIS ISSUE

Responsible Assistant Editor: *Xiang Li*  
Responsible Electronic Editor: *Yao Huang*  
Proofing Editor-in-Chief: *Lian Sheng Ma*

Responsible Science Editor: *Rao-Yu Ma*  
Proofing Editorial Office Director: *Ze-Mao Gong*

## NAME OF JOURNAL

*World Journal of Gastroenterology*

## ISSN

ISSN 1007-9327 (print)  
ISSN 2219-2840 (online)

## LAUNCH DATE

October 1, 1995

## FREQUENCY

Weekly

## EDITORS-IN-CHIEF

**Andrzej S Tarnawski, MD, PhD, DSc (Med),  
Professor of Medicine, Chief Gastroenterology, VA  
Long Beach Health Care System, University of California,  
Irvine, CA, 5901 E. Seventh Str., Long Beach,  
CA 90822, United States**

## EDITORIAL BOARD MEMBERS

All editorial board members resources online at <http://www.wjgnet.com/1007-9327/editorialboard.htm>

## EDITORIAL OFFICE

**Ze-Mao Gong, Director**  
*World Journal of Gastroenterology*  
Baishideng Publishing Group Inc  
7901 Stoneridge Drive, Suite 501,  
Pleasanton, CA 94588, USA  
Telephone: +1-925-2238242  
Fax: +1-925-2238243  
E-mail: [editorialoffice@wjgnet.com](mailto:editorialoffice@wjgnet.com)  
Help Desk: <http://www.bpgpublishing.com/helpdesk>  
<http://www.wjgnet.com>

## PUBLISHER

Baishideng Publishing Group Inc  
7901 Stoneridge Drive, Suite 501,  
Pleasanton, CA 94588, USA  
Telephone: +1-925-2238242  
Fax: +1-925-2238243  
E-mail: [bpgoffice@wjgnet.com](mailto:bpgoffice@wjgnet.com)  
Help Desk: <http://www.bpgpublishing.com/helpdesk>  
<http://www.wjgnet.com>

## PUBLICATION DATE

November 14, 2018

## COPYRIGHT

© 2018 Baishideng Publishing Group Inc. Articles published by this Open-Access journal are distributed under the terms of the Creative Commons Attribution Non-commercial License, which permits use, distribution, and reproduction in any medium, provided the original work is properly cited, the use is non commercial and is otherwise in compliance with the license.

## SPECIAL STATEMENT

All articles published in journals owned by the Baishideng Publishing Group (BPG) represent the views and opinions of their authors, and not the views, opinions or policies of the BPG, except where otherwise explicitly indicated.

## INSTRUCTIONS TO AUTHORS

Full instructions are available online at <http://www.wjgnet.com/bpg/geninfo/204>

## ONLINE SUBMISSION

<http://www.bpgpublishing.com>



## CXC family of chemokines as prognostic or predictive biomarkers and possible drug targets in colorectal cancer

Sara Cabrero-de las Heras, Eva Martínez-Balibrea

Sara Cabrero-de las Heras, Eva Martínez-Balibrea, Program Against Cancer Therapeutic Resistance, Catalan Institute of Oncology, Germans Trias i Pujol health research institute, Badalona, Barcelona 08916, Catalunya, Spain

Sara Cabrero-de las Heras, Eva Martínez-Balibrea, Program of Predictive and Personalized Cancer Medicine, Germans Trias i Pujol health research institute, Badalona, Barcelona 08916, Catalunya, Spain

ORCID number: Sara Cabrero-de las Heras (0000-0002-9364-5371); Eva Martínez-Balibrea (0000-0002-4501-7100).

**Author contributions:** Both authors contributed equally to the conception and design of the study, literature review and analysis, drafting and critical revision and editing, and approval of the final version.

**Supported by** the Institute of Health Carlos III (ISCIII), No. PI16/01800 and PI16/00011 (Co-funded by European Regional Development Fund "A way to make Europe").

**Conflict-of-interest statement:** The authors declare no potential conflicts of interest.

**Open-Access:** This article is an open-access article which was selected by an in-house editor and fully peer-reviewed by external reviewers. It is distributed in accordance with the Creative Commons Attribution Non Commercial (CC BY-NC 4.0) license, which permits others to distribute, remix, adapt, build upon this work non-commercially, and license their derivative works on different terms, provided the original work is properly cited and the use is non-commercial. See: <http://creativecommons.org/licenses/by-nc/4.0/>

**Manuscript source:** Invited manuscript

**Correspondence to:** Eva Martínez-Balibrea, PhD, Senior Scientist, Program Against Cancer Therapeutic Resistance, Catalan Institute of Oncology, Germans Trias i Pujol health research institute, Carretera de Can Ruti, camí de les escoles s/n, Badalona, Barcelona 08916, Catalunya, Spain. [embalibrea@iconcologia.net](mailto:embalibrea@iconcologia.net)

**Telephone:** +34-93-5543069

**Fax:** +34-93-4978654

**Received:** July 5, 2018

**Peer-review started:** July 5, 2018

**First decision:** August 25, 2018

**Revised:** September 27, 2018

**Accepted:** October 16, 2018

**Article in press:** October 16, 2018

**Published online:** November 14, 2018

### Abstract

Colorectal cancer (CRC) is the third most common cancer in men and the second most common cancer in women, worldwide. In the early stages of the disease, biomarkers predicting early relapse would improve survival rates. In metastatic patients, the use of predictive biomarkers could potentially result in more personalized treatments and better outcomes. The CXC family of chemokines (CXCL1 to 17) are small (8 to 10 kDa) secreted proteins that attract neutrophils and lymphocytes. These chemokines signal through chemokine receptors (CXCR) 1 to 8. Several studies have reported that these chemokines and receptors have a role in either the promotion or inhibition of cancer, depending on their capacity to suppress or stimulate the action of the immune system, respectively. In general terms, activation of the CXCR1/CXCR2 pathway or the CXCR4/CXCR7 pathway is associated with tumor aggressiveness and poor prognosis; therefore, the specific inhibition of these receptors is a possible therapeutic strategy. On the other hand, the lesser known CXCR3 and CXCR5 axes are generally considered to be tumor suppressor signaling pathways, and their stimulation has been suggested as a way to fight cancer. These pathways have been studied in tumor tissues (using immunohistochemistry or measuring mRNA levels) or serum [using enzyme-linked immunosorbent assay (ELISA) or multiplexing techniques], among other sample types. Common variants in genes encoding for the CXC chemokines have also been investigated as possible biomarkers of the disease. This review summarizes the

most recent findings on the role of CXC chemokines and their receptors in CRC and discusses their possible value as prognostic or predictive biomarkers as well as the possibility of targeting them as a therapeutic strategy.

**Key words:** Biomarkers; Treatment; Chemotherapy; Oxaliplatin; Irinotecan; Immunotherapy; Colorectal cancer; CXC chemokines; Immune system; Bevacizumab

© **The Author(s) 2018.** Published by Baishideng Publishing Group Inc. All rights reserved.

**Core tip:** The contribution of the immune system to the development and progression of cancer is now fully acknowledged. The specific action of the immune system depends on the type of immune cells that are recruited to the tumor sites. Chemokines from the CXC subfamily are released by tumor cells and cells within the tumor microenvironment, whereupon they attract cells with anti-tumor (*e.g.*, CD4<sup>+</sup> and CD8<sup>+</sup> lymphocytes) or pro-tumor activity (*e.g.*, myeloid-derived suppressor cells). Chemokines have been proposed as prognostic factors, as biomarkers of response to therapy and as drug targets. The present review addresses the most recent findings in the field.

Cabrero-de las Heras S, Martínez-Balibrea E. CXC family of chemokines as prognostic or predictive biomarkers and possible drug targets in colorectal cancer. *World J Gastroenterol* 2018; 24(42): 4738-4749 Available from: URL: <http://www.wjgnet.com/1007-9327/full/v24/i42/4738.htm> DOI: <http://dx.doi.org/10.3748/wjg.v24.i42.4738>

## INTRODUCTION

Colorectal cancer (CRC) is the third most common type of cancer worldwide, representing approximately 10% of all diagnosed cancers, and it is the most frequent cause of cancer-related deaths<sup>[1]</sup>. In Europe, the prognosis of localized disease is quite good; the 5-year overall survival rates are near 90%; however, in patients with regional or distant disease, these rates drop to 70% and down to 20%, respectively (source: Europacoln, <http://www.europacoln.com/colorectalcaner.php?Action=Colorectalcaner>)<sup>[2]</sup>. One of the main reasons behind this poor survival rate is that, in almost all cases, tumors become resistant to therapy. Therefore, it is necessary to find useful and reliable predictive biomarkers that allow physicians to assign effective drugs specific to each case. In general, the current first-line treatment for metastatic CRC (mCRC) is based upon combinations of chemotherapy [fluoropyrimidines, oxaliplatin (OXA) and/or irinotecan], consisting of doublets (FOLFOX or FOLFIRI) or triplets (FOLFOXIRI) in specific cases, and rational molecularly targeting agents [anti-epidermal growth factor receptor (anti-EGFR), cetuximab or panitumumab; anti-vascular

Cabrero-de las Heras S *et al.* CXC chemokines in CRC

endothelial growth factor (anti-VEGF), bevacizumab]<sup>[3]</sup>. Mutations in the RAS and BRAF family of oncogenes are indicative of the inefficacy of anti-EGFR drugs and are the only predictive markers available currently<sup>[4,5]</sup>. The recent classification of CRC into four molecular subtypes has shed light on the biology of this tumor. However, the clinical usefulness and application of this classification is still under discussion<sup>[6,7]</sup>.

It has been proposed that serum levels of certain chemokines may be used as predictive markers for the response to chemotherapy. The CXC family of chemokines and their receptors are crucial for inflammation and antitumor immunity, which are key factors in CRC progression. These small proteins are secreted not only by tumor cells but also by leukocytes, fibroblasts, endothelial cells and epithelial cells. They modulate tumor behavior by regulating angiogenesis, activating tumor-specific immune responses and directly stimulating tumor proliferation in an autocrine or paracrine fashion. The CXC family of chemokines and receptors have been associated with metastasis and resistance to treatment. Several studies have reported the expression of CXC chemokines and/or their receptors in tumors (in epithelial tumor cells, fibroblasts or infiltrating leukocytes) or in plasma/serum samples from CRC patients, and this expression has been associated with patient outcomes. Furthermore, the CXC genes are highly polymorphic, and certain genetic variants have been associated with prognosis and response to treatment. The aim of the present work is to review the literature and discuss the possible use of the CXC family of chemokines as predictive or prognostic markers in CRC (Table 1). We will focus on the main pathways that are activated after the appropriate chemokines bind to the receptors CXCR1, CXCR2, CXCR4, CXCR7, CXCR3, CXCR5, CXCR6 and CXCR8.

## LITERATURE SEARCH

We established the work of Verbeke *et al.*<sup>[8]</sup> as reference from which we searched the literature. We used PubMed as the primary source to find all of the articles published on this topic. The following keywords were employed in the search: chemokine/s, resistance, CRC, chemotherapy, 5 fluorouracil, OXA, cetuximab, bevacizumab, CXCL1, CXCL2, CXCL3, CXCL4, CXCL5, CXCL6, CXCL7, CXCL8, CXCL9, CXCL10, CXCL11, CXCL12, CXCL13, CXCL16, CXCL17, CXCR1, CXCR2, CXCR4, CXCR2 inhibitor, CXCR4 inhibitor, reparixin, cancer, repertaxin, and plerixafor. In addition to PubMed, we also performed a brief Google search for "Chemokine CRC".

## THE CXC FAMILY OF CHEMOKINES

CXC chemokines are small proteins; CXC refers to the location of the two cysteine residues near the N-terminal, with the X representing any amino acid (cysteine-

Table 1 CXCL chemokines as biomarkers

Biomarker	Cancer type	Expression	Where is it measured?	Treatment	Predictive value	Ref.
CXCL1/2	Breast cancer	High	Paraffin embedded tissue	Chemoresistance 5FU	Poor	[17]
CXCL1	CRC	High	Tumor and cell lines	OXA + CURCUMIN	Poor	[18]
CXCL1/8 CXCR2	CRC, Prostate cancer	High	Cell lines and <i>in vivo</i>	OXA + SCH-527123	Poor	[22,24]
CXCL8	CRC	Low	Serum	Chemotherapy + Bevacizumab	Good	[25,26]
CXCL8	Breast cancer	Polymorphism, TT genotype	Peripheral blood (DNA)	FOLFOX+ Bevacizumab vs FOLFOX alone	Good	[26]
CXCR1	CRC	Polymorphism	Whole blood (DNA)	OXA based + Bevacizumab	Good	[27]
CXCL7/8 CXCR2	CRC	High	mRNA levels tumors	Surgery + ady vs Ady alone	Poor	[28]
CXCR4	CRC	Colocalization-Lgr5	CRC cell lines and tumors		Poor	[35]
CXCR4	CRC	Colocalization-CD133	CRC cell lines and <i>in vivo</i>	5FU; 5FU and OXA	Poor	[36,38]
CXCR4-microbiota	CRC	High	<i>in vivo</i> and <i>in vitro</i>	Lipopolysaccharides	Poor	[39]
CXCL12-visfatin	CRC	Interaction	CRC cells		Poor	[40]
CXCR4	CRC	High	Paraffin embedded tissue	Patients that underwent hepatectomy	Poor	[41]
CXCR4	CRC	High	CRC cells	OXA or 5FU therapies including anti-VEGF	Poor	[46]
CXCL10-KRAS mut	CRC CMS2 and CMS3	Low	TCGA, tumors		Poor	[52]
CXCL10	CRC	High	CRC cells, tumors, <i>in vivo</i>		Good	[53]
CXCL10	CRC	Expression	Post-surgical localized CRC		Good	[53,56]
CXCR3	CRC	High	Protein levels in primary tumors		Poor	[57]
CXCL10/11	CRC	High	Serum		Poor	[58]
CXCL9/10	CRC	High	<i>in vivo</i>	Anthracyclines + STAT KO	Good	[60]
CXCL9/10/11	Rectal cancer	High	mRNA levels tumors	5FU + Radiotherapy	Good	[64,65]
CXCL4	CRC	High	<i>in vivo</i>	5FU	Poor	[66]
CXCL13 CXCR5	CRC	High	Plasma levels and paraffin embedded tissue		Poor	[69,70]
CXCL13-microbiota	CRC	High	Tumors		Good	[71]
CXCR5 <sup>+</sup> CD8 <sup>+</sup> T cell	CRC	Presence	Tumors		Good	[73]
CXCL13	CRC	Low	mRNA levels tumors		Good	[56,74]
CXCL16	CRC	High	Serum		Poor	[81]
CXCL17	CRC	High	mRNA levels cell lines and tumors		Poor	[87]

CRC: Colorectal cancer; OXA: Oxaliplatin; VEGF: Vascular endothelial growth factor; 5FU: 5-fluorouracil; KO: Knock out.

containing motif)<sup>[9]</sup>. These chemokines can be sub-classified based on the presence or absence of the tripeptide motif (Glu-Leu-Arg at the NH2 terminus) as ELR<sup>+</sup> or ELR<sup>-</sup>, respectively. The ELR<sup>+</sup> chemokines are considered to be angiogenic, whereas the ELR<sup>-</sup> chemokines are considered to be angiostatic<sup>[10-12]</sup>. Nevertheless, contradictory results have been published, which we will discuss in the present review.

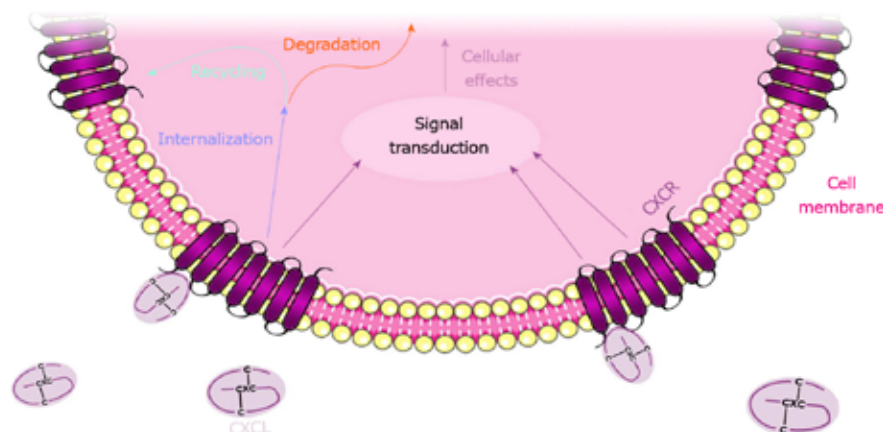
CXCL chemokines are named according to their original function, and they also follow the standard nomenclature CXCLx, where the L stands for "ligand" and the x corresponds to a number (Table 2). To exert their function, chemokines bind to their cognate CXCR

which, in the majority of cases, is a 7-transmembrane G protein-coupled receptor<sup>[13]</sup>. After binding, the receptors change their conformation and activate the coupled G protein, initiating the corresponding signaling pathway. Only a few of the CXCRs are atypical receptors, which are not coupled to a G protein but to beta-arrestins; these receptors include the atypical chemokine receptor 3 (ACKR3) also known as CXCR7<sup>[14]</sup>. Certain chemokines can bind to more than one receptor and *vice versa*, as is the case for the promiscuous CXCR2<sup>[15]</sup> (Table 2). After a given CXCL binds and activates the corresponding CXCR, the receptor is usually internalized through clathrin-mediated endocytosis for further degradation or recycling

Table 2 The CXC chemokines and their receptors

CXC ligand	Chemokine name	Receptor	ELR domain
CXCL1	Growth-regulated oncogene (Gro- $\alpha$ )	CXCR2	ELR <sup>+</sup>
CXCL2	Growth-regulated oncogene (Gro- $\beta$ )	CXCR2	ELR <sup>+</sup>
CXCL3	Growth-regulated oncogene (Gro- $\gamma$ )	CXCR2	ELR <sup>+</sup>
CXCL4	Platelet factor-4 (PF-4)	CXCR3	ELR <sup>-</sup>
CXCL5	Epithelial cell-derived neutrophil-activating peptide-78 (ENA-78)	CXCR2	ELR <sup>+</sup>
CXCL6	Granulocyte chemotactic protein-2 (GCP-2)	CXCR1/2	ELR <sup>+</sup>
CXCL7	Neutrophil-activating peptide-2 (NAP-2)	CXCR2	ELR <sup>+</sup>
CXCL8	Interleukin-8 (IL-8)	CXCR1/2	ELR <sup>+</sup>
CXCL9	Monokine induced by interferon- $\gamma$ (Mig)	CXCR3	ELR <sup>-</sup>
CXCL10	Inducible protein-10 (IP-10)	CXCR3	ELR <sup>-</sup>
CXCL11	Interferon-inducible T cell alpha chemoattractant (I-TAC)	CXCR3/7	ELR <sup>-</sup>
CXCL12	Stromal cell-derived factor-1 (SDF-1)	CXCR4/7	ELR <sup>-</sup>
CXCL13	B cell-attracting chemokine-1 (BCA-1)	CXCR5	ELR <sup>-</sup>
CXCL16	Scavenger receptor that binds phosphatidylserine and oxidized lipoprotein (SR-PSOX)	CXCR6	ELR <sup>-</sup>
CXCL17	VEGF-correlated chemokine-1 (VCC-1)	CXCR8	ELR <sup>+</sup>

VEGF: Vascular endothelial growth factor.



**Figure 1 CXCL and CXCR regulatory mechanisms.** Figure 1 illustrates CXCL binding to the CXCR located at the cellular membrane, internalizing and transducing the signal into the nucleus. CXCR internalization is usually followed by degradation or recycling to the plasma membrane.

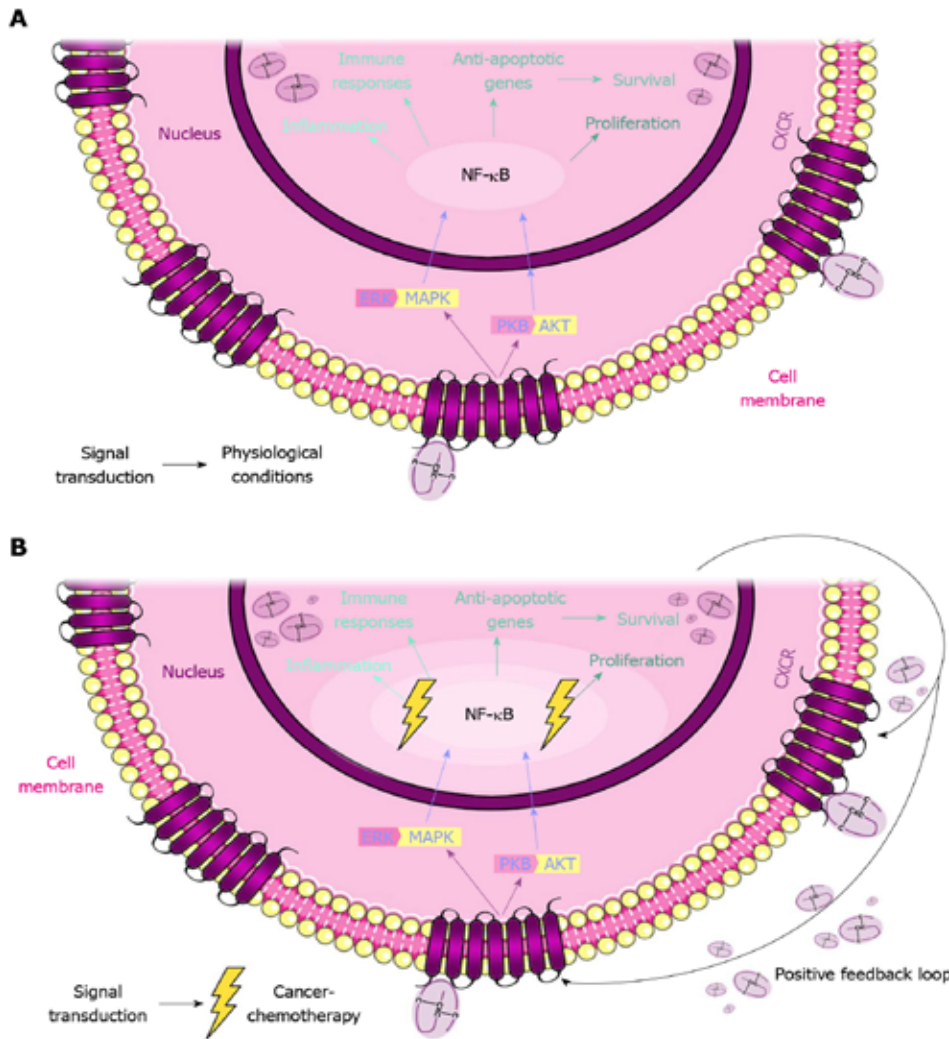
to the plasma membrane<sup>[16]</sup> (Figure 1).

Originally, the role of these chemokines and their receptors was associated with inflammatory processes wherein leukocytes accumulate in injured or infected tissues. Given that inflammation is a hallmark of cancer, it is not surprising that once in the nucleus, the CXC chemokines exert their activity through various pathways, such as tumor necrosis factor alpha (TNF- $\alpha$ )/nuclear factor  $\kappa$ B (NF- $\kappa$ B) and protein kinase B (PKB/AKT)<sup>[17,18]</sup>. These pathways are related to survival, proliferation, angiogenesis, pathological processes such as tumor growth and metastasis<sup>[19,20]</sup>, and even responses to anticancer treatments (Figure 2).

## AXIS 1: CXCR1 AND CXCR2

The CXCR1/CXCR2 pathway is the most widely studied pathway in cancer. CXCL1, 2, 3 and 8 are proangiogenic and chemoattractive chemokines that all bind to the receptor CXCR2, for which CXCL1 has the highest

affinity. All four chemokines have been found to be upregulated in CRC<sup>[21]</sup>. One of the most relevant studies demonstrating the role of CXCL1 and 2 in treatment resistance and metastasis was performed by the group of Joan Massagué. This group showed that CXCL1 and CXCL2 are overexpressed in breast cancer cells that are primed for survival in metastatic sites. These two chemokines attract CD11b<sup>+</sup>Gr1<sup>+</sup> myeloid cells which, in turn, produce more chemokines and enhance cancer cell survival. Regarding chemoresistance, this group found that chemotherapeutic agents, such as 5 Fluorouracil (5FU), doxorubicin hydrochloride, cyclophosphamide monohydrate and paclitaxel trigger a stromal reaction, leading to TNF- $\alpha$  production. TNF- $\alpha$  increases CXCL1/2 expression *via* NF- $\kappa$ B, which results in a feedback loop that promotes cancer cell survival<sup>[17]</sup>. NF- $\kappa$ B is a transcription factor that can be activated downstream of the PKB/AKT and mitogen-activated protein kinase (MAPK) signaling pathways. Increased activity of NF- $\kappa$ B has been associated with the high expression of genes



**Figure 2** CXCL and CXCR network in physiological and cancer conditions. A: The binding of CXCL to CXCR triggers the activation of signaling pathways, such as PKB/AKT and ERK/MAPK. Both pathways share NF-κB as a downstream factor which, in the nucleus, promotes the transcription of the CXCLs. These pathways maintain the physiologic conditions inside the cell. B: In a cancer cell exposed to chemotherapy, the situation is different. The chemotherapeutic treatment promotes the hyperactivation of these pathways. As a result, the CXCLs are also more abundant, promoting an autocrine response and, further, a positive feedback loop. This response results in pathological processes, such as tumor growth and metastasis, and in resistance to anticancer treatments. PKB: Protein kinase B; ERK: Extracellular signal-regulated kinases; MAPK: Mitogen-activated protein kinase; NF-κB: Nuclear factor κB.

related to cancer cell survival, proliferation, angiogenesis, and also the development of resistance to anticancer drugs (Figure 2). As CXCL1 and 2 (and other chemokines that bind to CXCR1 and 2) can activate this pathway, it is not surprising that these chemokines play a role in chemoresistance and may also serve as predictive biomarkers in CRC.

For instance, we reported that CRC cells with acquired resistance to OXA exhibited high intracellular and secreted levels of CXCL1, 2 and 8, which was a consequence of the upregulated activation of NF-κB in the resistant cells. Both the inhibition of NF-κB with curcumin and the silencing of genes encoding for these chemokines led to a partial reversion of the resistance phenotype. The combination of curcumin and OXA was

especially synergistic in resistant cells. Moreover, in experiments with tissue explants derived from hepatic CRC metastasis, we determined that higher levels of CXCL1 led to higher sensitivity of explants to the combination of curcumin + OXA. Thus, the tumor or serum levels of CXCL1 may serve as a useful biomarker for OXA resistance and may be indicative of curcumin + OXA sensitivity<sup>[18]</sup>. In another study, Ning *et al*<sup>[22]</sup> reported that CXCL8 mediated resistance to OXA in CRC cell lines through its binding to CXCR2 and AKT/MAPK/NF-κB signaling. The gene silencing of CXCR2 sensitized cells to the platinum drug. Treatment of CRC cell lines with a CXCR2 antagonist (SCH-527123) resulted in decreased migration and invasion, and increased apoptosis, acting synergistically with OXA. Further work performed *in vivo*

demonstrated similar results<sup>[23]</sup>. These results, together with those reported by Wilson *et al*<sup>[24]</sup> in prostate cancer cells, suggest that the levels of at least CXCL1 and 8 (and also CXCR2) can identify CRC patients who are unlikely to respond to OXA, who may be putative candidates for treatment with CXCR2 inhibitors in combination with this platinum agent.

The role of the CXCR1/CXCR2 pathway in the response and resistance to chemotherapy is not limited to OXA. Due to the role of these chemokines and receptors in promoting angiogenesis, it has been speculated that they can influence the response and resistance to antiangiogenic drugs. Two works reported that low serum levels of CXCL8 in mCRC patients treated with chemotherapy plus bevacizumab had better outcomes. First, in a short communication from Abajo *et al*<sup>[25]</sup>, low levels of CXCL8 measured before treatment with bevacizumab, irinotecan and gemcitabine, were associated with better response rates in a small cohort of patients. This group also reported a general decrease in the levels of CXCL8 in post-treatment samples<sup>[25]</sup>. In another study, Di Salvatore *et al*<sup>[26]</sup> analyzed the serum levels of CXCL8 in 120 RAS mutant patients treated with first-line 5FU + Leucovorin + OXA (known as FOLFOX) + bevacizumab. They found that low levels of CXCL8 were associated with longer progression-free (PFS) and overall survival (OS). The same group also studied a polymorphism (c-251T>A) in the *CXCL8* gene and reported that the TT genotype was associated with longer PFS and OS in the aforementioned patients but not in another cohort that was treated only with FOLFOX. Interestingly, patients carrying the TT genotype had significantly lower serum levels of CXCL8 compared with patients with the AT or AA genotype<sup>[26]</sup>. Another polymorphism (rs2234671) in the *CXCR1* gene was found to be associated with the overall response rate in 132 mCRC patients treated with OXA-based chemotherapy plus bevacizumab. However, the authors did not provide a biological explanation underlying these results<sup>[27]</sup>. Two methods of measuring chemokines and their receptors include the immunohistochemical staining of proteins in tumor tissues and the qPCR evaluation of mRNA levels. Using these techniques, Desurmont *et al*<sup>[28]</sup> determined that high levels of CXCR2 and its ligands, CXCL7 and 8, were associated with worse PFS and OS in CRC patients who underwent neoadjuvant chemotherapy (different schedules) followed by metastatic hepatectomy, but not in those who were treated with surgery alone. CXCR2 and CXCL7 mRNA levels were higher in metastasis from chemotherapy-treated patients compared to metastasis from patients who underwent surgery alone. These data suggest not only the prognostic value of CXCR2 (and CXCL7) but also its involvement in disease aggressiveness. Therefore, targeting the CXCR1/2-mediated signaling pathway has been suggested as a possible therapeutic approach for treating CRC and other tumors.

As the CXCR1/2-mediated signaling pathway is associated with inflammation, several studies have

described how the inhibition of CXCR1 or CXCR2 could potentially be used for preventive purposes<sup>[29-31]</sup>. Notably, the study by Jamieson *et al*<sup>[31]</sup> showed that CXCR2 acts as a potent pro-tumorigenic CXCR which directs the recruitment of tumor-promoting leukocytes into tissues (including the intestines) during tumor-inducing and tumor-driven inflammation. Thus, the deletion or inhibition of this receptor led to the profound suppression of inflammation-driven and spontaneous tumorigenesis in a mouse model of colon cancer, suggesting that CXCR2 antagonists may have therapeutic and prophylactic potential in the treatment of cancer<sup>[31]</sup>. Additionally, in the metastatic setting, it has been shown that treatment with inhibitors of this pathway may be a good strategy<sup>[23,32-34]</sup>. Interestingly, the use of two different inhibitors against CXCR1 and 2 reduced the development of metastasis in mouse models but had no effect on primary tumors. This effect was due, in part, to the capacity of the inhibitors to abrogate neovascularization<sup>[15]</sup>.

## AXIS 2: CXCR4 AND CXCR7

The CXCR4/CXCR7 pathway is activated after the binding of CXCL12 to CXCR4 or 7. Strikingly, although CXCL12 is an ELR<sup>-</sup> chemokine, the activity of this pathway has been primarily associated with stemness, the development of metastasis and poor prognosis. CXCR4 has been shown to co-localize with CRC stem cell markers, such as Lgr5, CD133 and CD44, and this co-localization was associated with epithelial-mesenchymal transition (EMT) processes and resistance to therapy<sup>[35-38]</sup>. Similar to CXCR1/2, the NF- $\kappa$ B transcription factor appears to have a role in the induction of EMT. In this case, it has been shown that lipopolysaccharides can promote the migratory capacity of CRC *in vivo* and *in vitro* by inducing CXCR4 expression and EMT through NF- $\kappa$ B signaling<sup>[39]</sup>. Additionally, the link between obesity and CRC has been attributed to the interaction between the adipokine visfatin and CXCL12<sup>[40]</sup>. CXCR4 expression appears to be increased in tumors compared with normal tissues and in metastasis compared with primary tumors. This increase is associated with poor prognosis, as shown in the work by Yopp *et al*<sup>[41]</sup>. This group assessed CXCR4 (among other factors) expression by immunohistochemical staining in 75 patients who underwent partial hepatectomy with curative intention and found that CXCR4 positivity was negatively associated with disease-specific and recurrence-free survival<sup>[41]</sup>. This finding suggests the possibility of targeting CXCR4 for therapeutic purposes. A lentiviral vector carrying siRNA targeting CXCR4 was used in CRC cell lines and a mouse model; the result was a reduction in cell proliferation, migration and invasion and the formation of hepatic metastasis<sup>[42]</sup>. Other researchers are attempting to exploit the membrane localization of CXCR4 to direct nanoparticles that recognize this receptor, facilitating their entry into the cells to deliver antineoplastic drugs<sup>[43]</sup>. Specific inhibitors, such as plerixafor, have been identified as a possible therapy for CRC and are under investigation in several clinical trials

involving solid and non-solid tumors. Regardless of the strategy, it is important to take into account the biology of CXCR4 and 7. Two studies reported inconsistent regulation and effects between these two receptors. Romain *et al*<sup>[44]</sup> reported elevated levels of both receptors in late stage carcinomas compared to normal mucosa, colon polyps or early carcinomas. However, this group demonstrated that while CXCR4 expression was strongly induced by hypoxia-inducible factor 1 alpha (HIF-1 $\alpha$ ), this was not the case of CXCR7. Moreover, the reduction of CXCR4 expression was associated with a decrease in AKT and extracellular signal-regulated kinases (ERK) activation which, was not observed for CXCR7. The authors conclude that CXCR4 is a more promising target compared to CXCR7 in CRC<sup>[44]</sup>. Similarly, Heckmann and colleagues showed different (and partly antidromic) patterns of expression between CXCR7 and CXCR4 after stimulation with CXCL12 in colon cancer cells. CXCR4 overexpression was associated with increased levels of microRNA-217 and -218 in CXCR4-overexpressing cells, but this was not the case for the overexpression of CXCR7. Additionally, CXCR4 cells were more sensitive to 5FU compared with CXCR7 cells<sup>[45]</sup>. Thus, the clinical application of CXCR4 antagonists, such as plerixafor, should be studied with caution. Finally, the relationship between this pathway and the resistance to treatment of CRC has also been studied. High levels of CXCR4 were found to be associated with resistance to all chemotherapeutic agents used (5FU, irinotecan and OXA), including anti-VEGF therapies. In SW1116 colon cancer cells with acquired resistance to OXA or 5FU, the expression of and signaling through CXCR4 was found to be associated with the chemoresistant phenotype. Specifically, the authors demonstrated that the ERK1/2/MAPK and phosphatidylinositol-3-kinases (PI3K)/AKT pathway was important in CXCR4-mediated chemoresistance<sup>[46]</sup>. The effect of CXCR4 on resistance to OXA can be exploited therapeutically by using endostar, a modified endostatin. When endostar and OXA are administered together, they have a synergistic effect, primarily due to the reduction in CXCR4 levels<sup>[47]</sup>. In two different orthotopic mouse models, treatment with anti-VEGFR2 therapy resulted in the upregulation of both CXCL12 and CXCR4. CXCR4-expressing immunosuppressive innate immune cells (Ly6low monocytes) were recruited to the tumor site upon treatment with anti-VEGFR2, which was abrogated after CXCR4 blockade<sup>[48]</sup>.

### AXIS 3: CXCR3

The chemokines CXCL4, CXCL9, CXCL10 and CXCL11 are considered to exert an angiostatic effect through their binding to CXCR3, although CXCL11 can also bind to CXCR7<sup>[49]</sup>. CXCR3 is found on peripheral blood activated T cells *in vitro* and on a significant fraction of circulating CD4<sup>+</sup> and CD8<sup>+</sup> T cells, B cells and natural killer (NK) cells, but not on monocytes or neutrophils<sup>[50]</sup>. These chemokines are upregulated by interferon gamma (IFN- $\gamma$ )

and, therefore, they have important roles in inflammatory diseases, such as ulcerative colitis<sup>[50]</sup> and active pulmonary tuberculosis<sup>[51]</sup>. However, the infiltration of activated CD4<sup>+</sup> and CD8<sup>+</sup> T cells in tumors is considered to be a good prognostic factor; consequently, most of the research on the expression of these chemokines or their receptors in the context of CRC is focused in that direction. An interesting study by Lal *et al*<sup>[52]</sup> suggests that KRAS mutations are associated with reduced levels of CXCL10 and with the suppression of cytotoxic T cells, neutrophils and the IFN- $\gamma$  pathway, especially in CRC consensus molecular subtype (CMS) 2 and CMS3. Other studies also reported the potential of these chemokines as good prognostic factors, primarily because of their association with the high infiltration of CD8<sup>+</sup> T and CD4<sup>+</sup> T helper 1 (Th1) effector cells<sup>[53-55]</sup>. Mice injected with colonic tumor cells overexpressing CXCL10 were protected against metastasis development<sup>[53]</sup>. Two independent studies demonstrated the post-surgical positive prognostic value of CXCL10 expression in localized colon cancer<sup>[53,56]</sup>. Specifically, in the study by Agesen *et al*<sup>[57]</sup>, CXCL10 levels were part of a 13-gene expression classifier called ColoGuideEX for the prognosis prediction in stage II CRC. Interestingly, some authors have reported the opposite results. For instance, a high level of CXCR3 protein expression in primary CRC tumors was shown to be indicative of a poor prognosis<sup>[57]</sup>. In another study, the authors investigated the molecular factors underlying the poor prognosis of CRC tumor neuroendocrine differentiation and found that neuroendocrine-like cells secreted high levels of CXCL10 and CXCL11 which, in turn, promoted the recruitment of tumor-associated macrophages, thereby promoting the proliferation and invasion of CRC cells and leading to a poor prognosis<sup>[58]</sup>.

Taken together, these findings appear to indicate that targeting CXCR3 or its ligands would not be an effective therapeutic strategy against CRC. However, some authors have speculated otherwise about the possibility of enhancing this pathway indirectly. It is worth commenting on three different papers that address three different strategies. First, Brackett *et al*<sup>[59]</sup> used a Toll-like receptor 5 (TLR5) agonist called entolimod in a murine mCRC model. This group found that entolimod induced the expression of CXCL9 and CXCL10 in tumors which, in turn, led to the recruitment of CXCR3<sup>+</sup> NK cells to the liver, thereby activating dendritic cells (DCs) and stimulating the CD8<sup>+</sup> T cell response. Consequently, the drug exerted an anti-metastatic effect and a tumor-specific and durable immune memory<sup>[59]</sup>. Second, Yang *et al*<sup>[60]</sup> studied the effect of signal transducer and activator transcription 3 (STAT3) inhibition in combination with immunogenic chemotherapy (anthracyclines). This group showed that, when injected in mice, STAT3 KO cells developed tumors with higher infiltration of DCs and cytotoxic T cells after treatment with anthracyclines. These tumors also displayed higher levels of CXCL9 and 10. Consequently, STAT3 inhibition improved the outcome of chemotherapy-treated mice by synergizing with immunogenic chemotherapy<sup>[60]</sup>. Another interesting

approach involved the depletion of regulatory T cells (Treg) in mice bearing CRC tumors. This depletion was associated with an increase in T cell infiltration and proliferation and an increase in CXCL9 and 10, which led to the accumulation of CXCR3<sup>+</sup> T cells and the increased mRNA expression of IFN- $\gamma$ , which suggests Treg cell targeting as a possible anti-tumor immunotherapy<sup>[61]</sup>. It is important to note that some studies have indicated that CXCR3 targeting may be a good strategy against CRC cancer<sup>[62,63]</sup>.

Finally, high mRNA levels of CXCL9 and 11<sup>[64]</sup> as well as CXCL10<sup>[64,65]</sup> appear to be associated with the response to neoadjuvant chemotherapy (5FU) plus radiotherapy in patients with locally advanced rectal cancer; on the other hand, CXCL4 was shown to be upregulated after treatment with 5FU, which was associated with accelerated growth *in vivo*<sup>[66]</sup>. These studies suggest the possibility of using members of this pathway as predictive biomarkers.

#### AXIS 4: MISCELLANY

Finally, it is worth commenting on the lesser known chemokines CXCL13, 16 and 17. Similar to that of the previously mentioned chemokines, the CXCL13-CXCR5 axis is involved in regulating lymphocyte migration and promoting inflammation<sup>[67]</sup>. However, the role of this axis in promoting or inhibiting tumor development or progression is not clear, as the current articles report contradictory results. Zhu *et al.*<sup>[68]</sup> reported that this pathway promotes the growth, migration and invasion of colon cancer cells, likely through the PI3K/AKT pathway. Accordingly, high plasma levels of CXCL13 and positive immunohistochemical staining of CXCL13 and CXCR5 in tumors from CRC patients were associated with clinical and pathological characteristics typically related with a worse prognosis<sup>[69,70]</sup>. In contrast, high levels of CXCL13 in colorectal tumors have also been shown to be associated with the infiltration of follicular Th and B cells and, consequently, with a better prognosis. Cremonesi *et al.*<sup>[71]</sup> attributed the increase in CXCL13 levels to the presence of gut microbiota, whereas in the work of Bindea *et al.*<sup>[72]</sup>, genomic instability affected CXCL13 expression, which led to alterations in T and B cell infiltration and clinical outcomes. In addition, it appears that a significant CD8<sup>+</sup> T cell subset in colorectal tumors that are CXCR5<sup>+</sup> potentially contribute to anti-tumor activity<sup>[73]</sup>. Not surprisingly, low levels of CXCL13 have been reported as a negative prognostic factor in CRC patients<sup>[56,74]</sup>. These contradictory results may be affected by several factors, including tumor stage, treatment, molecular subtype and microsatellite instability.

CXCR6 is expressed on the surface of CD4<sup>+</sup> T cells, CD8<sup>+</sup> T cells, NK cells and plasma cells and is responsible for inducing the chemotactic migration of these cells to inflamed tissues. The ligand of CXCR6, CXCL16, has two forms, the trans-membrane (TM) form and the soluble(s) form. TM-CXCL16 is expressed on macrophages, DCs, monocytes, and B cells where it functions as a cell

adhesion molecule for cells that express CXCR6<sup>[75]</sup>. TM-CXCL16 is also a novel scavenger receptor that binds to phosphatidylserine and oxidized lipoprotein. In the membrane, this chemokine is cleaved by the disintegrin-like metalloproteinases ADAM10 and ADAM17, producing fragments that are released outside the cells<sup>[76]</sup>. sCXCL16 functions as a chemotactic factor for CXCR6-expressing Th1, T cells and NK cells. Interestingly, soluble CXCL16 can promote angiogenesis in human umbilical vein endothelial cells<sup>[77]</sup>. Again, given its capacity to promote tumor immunity, many of the published works describe CXCL16 as a positive prognostic factor<sup>[78-80]</sup>. On the other hand, Matsushita *et al.*<sup>[81]</sup> reported that CRC patients had higher levels of CXCL16 in the serum compared to healthy controls, and these levels increased with tumor stage and were correlated with poor survival. In patients with localized disease, higher serum levels of CXCL16 were associated with a higher probability of metachronous liver recurrence and worse survival. *In vitro*, treatment with recombinant CXCL16 promoted cell growth, migration, invasion and EMT<sup>[81]</sup>. Thus, the exact role of CXCL16 in CRC warrants further investigation.

Finally, CXCL17 is a 119-amino acid CXC chemokine that binds specifically to CXCR8<sup>[82,83]</sup>. This chemokine is expressed in breast and colon cancer and acts as a chemoattractant for monocytes, macrophages and mature and immature DCs, thereby playing an important role in angiogenesis<sup>[84-86]</sup>. CXCL17 expression is co-regulated with VEGF expression<sup>[82,84]</sup> and can attract neutrophils to tumor sites and promote tumorigenesis through angiogenesis in mouse models<sup>[86]</sup>. Very little is known about the role of CXCL17 in CRC. Ohlsson *et al.*<sup>[87]</sup> reported high mRNA levels of CXCL17 in several CRC cell lines as well as very high mRNA and protein levels of CXCL17 in primary CRC tumors compared to normal colon tissue. CXCL17-positive cells measured by immunofluorescence and immunohistochemistry were significantly more abundant in colon cancer tissues (80%) compared with the controls (normal colon samples from proximal or distal resection margin). Interestingly, CXCL17 was more abundant in tumor epithelial cells (17.2%) in comparison with tumor stromal cells (2.7%), and CXCL17 mRNA levels were correlated with the myeloid cell marker CD86, which is primarily expressed in antigen presenting cells (APCs), suggesting that this chemokine may contribute to the infiltration of APCs into the tumor<sup>[87]</sup>. Taken together, these findings indicate that the high expression of CXCL17 in CRC may be an indicator of poor prognosis in colon cancer, although further studies are warranted to elucidate the exact role of this chemokine in this malignancy.

In summary, very little information is available on the role of these less-known chemokines in CRC development or response to treatment.

#### CONCLUSION

The importance of the immune system in the surveillance, prognosis and treatment of cancer is undeniable.

The recent development of immunotherapies and the rapidness of their application to the clinics for several tumor types demonstrate the possibilities of exploiting the immune system as a target for drug development. Moreover, the recent publication of the international validation of the consensus Immunoscore<sup>[88]</sup> as a reliable tool to classify colon cancer and to prognosticate its outcome also reveals the utility of using immune factors [in this case, total tumor-infiltrating T cell (CD3<sup>+</sup>) and cytotoxic T cell counts (CD8<sup>+</sup>)] as biomarkers. Therefore, other immune system-related factors thought to be important in cancer development and/or progression may also serve as prognostic and/or predictive biomarkers. Specially, those soluble factors that are released from tumor cells and are involved in the attraction of tumor-promoting or -killing cells are interesting candidates. In the present review, we have described the potential utility of chemokines from the CXC family as biomarkers of response and prognosis in CRC. Moreover, as these chemokines exert their function through binding to membrane receptors, these receptors also appear to be excellent drug targets. Some challenges still need to be overcome. First, some researchers have doubts about the systemic value of a factor that exerts its function locally. Second, due to certain contradictory reports, a deeper knowledge of the exact roles of each chemokine and its receptor(s) is urgently needed. Nevertheless, we are convinced that in the following years, these small secreted proteins will have a large role in predictive and personalized cancer medicine.

## REFERENCES

- 1 DeSantis CE, Lin CC, Mariotto AB, Siegel RL, Stein KD, Kramer JL, Alteri R, Robbins AS, Jemal A. Cancer treatment and survivorship statistics, 2014. *CA Cancer J Clin* 2014; **64**: 252-271 [PMID: 24890451 DOI: 10.3322/caac.21235]
- 2 Welch HG, Robertson DJ. Colorectal Cancer on the Decline--Why Screening Can't Explain It All. *N Engl J Med* 2016; **374**: 1605-1607 [PMID: 27119236 DOI: 10.1056/NEJMp1600448]
- 3 Van Cutsem E, Cervantes A, Adam R, Sobrero A, Van Krieken JH, Aderka D, Aranda Aguilar E, Bardelli A, Benson A, Bodoky G, Ciardiello F, D'Hoore A, Diaz-Rubio E, Douillard JY, Ducreux M, Falcone A, Grothey A, Gruenberger T, Haustermans K, Heinemann V, Hoff P, Köhne CH, Labianca R, Laurent-Puig P, Ma B, Maughan T, Muro K, Normanno N, Österlund P, Oyen WJ, Papamichael D, Pentheroudakis G, Pfeiffer P, Price TJ, Punt C, Rieke J, Roth A, Salazar R, Scheithauer W, Schmoll HJ, Tabernero J, Taieb J, Tejpar S, Wasan H, Yoshino T, Zaanan A, Arnold D. ESMO consensus guidelines for the management of patients with metastatic colorectal cancer. *Ann Oncol* 2016; **27**: 1386-1422 [PMID: 27380959 DOI: 10.1093/annonc/mdw235]
- 4 Cremolini C, Schirripa M, Antoniotti C, Moretto R, Salvatore L, Masi G, Falcone A, Loupakis F. First-line chemotherapy for mCRC—a review and evidence-based algorithm. *Nat Rev Clin Oncol* 2015; **12**: 607-619 [PMID: 26215044 DOI: 10.1038/nrclinonc.2015.129]
- 5 Dienstmann R, Salazar R, Tabernero J. Overcoming Resistance to Anti-EGFR Therapy in Colorectal Cancer. *Am Soc Clin Oncol Educ Book* 2015; : e149-e156 [PMID: 25993166 DOI: 10.14694/EdBook\_AM.2015.35.e149]
- 6 Guinney J, Dienstmann R, Wang X, de Reyniès A, Schlicker A, Sonesson C, Marisa L, Roepman P, Nyamundanda G, Angelino P, Bot BM, Morris JS, Simon IM, Gerster S, Fessler E, De Sousa E Melo F, Missiaglia E, Ramay H, Barras D, Homicsko K, Maru D, Manyam GC, Broom B, Boige V, Perez-Villamil B, Laderas T, Salazar R, Gray JW, Hanahan D, Tabernero J, Bernards R, Friend SH, Laurent-Puig P, Medema JP, Sadanandam A, Wessels L, Delorenzi M, Kopetz S, Vermeulen L, Tejpar S. The consensus molecular subtypes of colorectal cancer. *Nat Med* 2015; **21**: 1350-1356 [PMID: 26457759 DOI: 10.1038/nm.3967]
- 7 Dienstmann R, Vermeulen L, Guinney J, Kopetz S, Tejpar S, Tabernero J. Consensus molecular subtypes and the evolution of precision medicine in colorectal cancer. *Nat Rev Cancer* 2017; **17**: 79-92 [PMID: 28050011 DOI: 10.1038/nrc.2016.126]
- 8 Verbeke H, Geboes K, Van Damme J, Struyf S. The role of CXC chemokines in the transition of chronic inflammation to esophageal and gastric cancer. *Biochim Biophys Acta* 2012; **1825**: 117-129 [PMID: 22079531 DOI: 10.1016/j.bbcan.2011.10.008]
- 9 Moser B, Wolf M, Walz A, Loetscher P. Chemokines: multiple levels of leukocyte migration control. *Trends Immunol* 2004; **25**: 75-84 [PMID: 15102366 DOI: 10.1016/j.it.2003.12.005]
- 10 Bizzarri C, Beccari AR, Bertini R, Caviechia MR, Giorgini S, Allegretti M. ELR+ CXC chemokines and their receptors (CXC chemokine receptor 1 and CXC chemokine receptor 2) as new therapeutic targets. *Pharmacol Ther* 2006; **112**: 139-149 [PMID: 16720046 DOI: 10.1016/j.pharmthera.2006.04.002]
- 11 Koizumi K, Hojo S, Akashi T, Yasumoto K, Saiki I. Chemokine receptors in cancer metastasis and cancer cell-derived chemokines in host immune response. *Cancer Sci* 2007; **98**: 1652-1658 [PMID: 17894551 DOI: 10.1111/j.1349-7006.2007.00606.x]
- 12 Vandercappellen J, Van Damme J, Struyf S. The role of CXC chemokines and their receptors in cancer. *Cancer Lett* 2008; **267**: 226-244 [PMID: 18579287 DOI: 10.1016/j.canlet.2008.04.050]
- 13 Rajagopal S, Rajagopal K, Lefkowitz RJ. Teaching old receptors new tricks: biasing seven-transmembrane receptors. *Nat Rev Drug Discov* 2010; **9**: 373-386 [PMID: 20431569 DOI: 10.1038/nrd3024]
- 14 Bachelier F, Graham GJ, Locati M, Mantovani A, Murphy PM, Nibbs R, Rot A, Sozzani S, Thelen M. New nomenclature for atypical chemokine receptors. *Nat Immunol* 2014; **15**: 207-208 [PMID: 24549061 DOI: 10.1038/ni.2812]
- 15 Varney ML, Singh S, Li A, Mayer-Ezell R, Bond R, Singh RK. Small molecule antagonists for CXCR2 and CXCR1 inhibit human colon cancer liver metastases. *Cancer Lett* 2011; **300**: 180-188 [PMID: 21035946 DOI: 10.1016/j.canlet.2010.10.004]
- 16 Marchese A. Endocytic trafficking of chemokine receptors. *Curr Opin Cell Biol* 2014; **27**: 72-77 [PMID: 24680433 DOI: 10.1016/j.cceb.2013.11.011]
- 17 Acharyya S, Oskarsson T, Vanharanta S, Malladi S, Kim J, Morris PG, Manova-Todorova K, Leversha M, Hogg N, Seshan VE, Norton L, Brogi E, Massagué J. A CXCL1 paracrine network links cancer chemoresistance and metastasis. *Cell* 2012; **150**: 165-178 [PMID: 22770218 DOI: 10.1016/j.cell.2012.04.042]
- 18 Ruiz de Porras V, Bystrup S, Martínez-Cardús A, Pluvinet R, Sumoy L, Howells L, James MI, Iwuji C, Manzano JL, Layos L, Bugés C, Abad A, Martínez-Balibrea E. Curcumin mediates oxaliplatin-acquired resistance reversion in colorectal cancer cell lines through modulation of CXC-Chemokine/NF-κB signalling pathway. *Sci Rep* 2016; **6**: 24675 [PMID: 27091625 DOI: 10.1038/srep24675]
- 19 Speyer CL, Ward PA. Role of endothelial chemokines and their receptors during inflammation. *J Invest Surg* 2011; **24**: 18-27 [PMID: 21275526 DOI: 10.3109/08941939.2010.521232]
- 20 Raman D, Baugher PJ, Thu YM, Richmond A. Role of chemokines in tumor growth. *Cancer Lett* 2007; **256**: 137-165 [PMID: 17629396 DOI: 10.1016/j.canlet.2007.05.013]
- 21 Bandapalli OR, Ehrmann F, Ehemann V, Gaida M, Macher-Goeppinger S, Wente M, Schirmacher P, Brand K. Down-regulation of CXCL1 inhibits tumor growth in colorectal liver metastasis. *Cytokine* 2012; **57**: 46-53 [PMID: 22129625 DOI: 10.1016/j.cyto.2011.10.019]
- 22 Ning Y, Manegold PC, Hong YK, Zhang W, Pohl A, Lurje G,

- Winder T, Yang D, LaBonte MJ, Wilson PM, Ladner RD, Lenz HJ. Interleukin-8 is associated with proliferation, migration, angiogenesis and chemosensitivity in vitro and in vivo in colon cancer cell line models. *Int J Cancer* 2011; **128**: 2038-2049 [PMID: 20648559 DOI: 10.1002/ijc.25562]
- 23 **Ning Y**, Labonte MJ, Zhang W, Bohanes PO, Gerger A, Yang D, Benhaim L, Paez D, Rosenberg DO, Nagulapalli Venkata KC, Louie SG, Petasis NA, Ladner RD, Lenz HJ. The CXCR2 antagonist, SCH-527123, shows antitumor activity and sensitizes cells to oxaliplatin in preclinical colon cancer models. *Mol Cancer Ther* 2012; **11**: 1353-1364 [PMID: 22391039 DOI: 10.1158/1535-7163.MCT-11-0915]
- 24 **Wilson C**, Purcell C, Seaton A, Oladipo O, Maxwell PJ, O'Sullivan JM, Wilson RH, Johnston PG, Waugh DJ. Chemotherapy-induced CXC-chemokine/CXC-chemokine receptor signaling in metastatic prostate cancer cells confers resistance to oxaliplatin through potentiation of nuclear factor-kappaB transcription and evasion of apoptosis. *J Pharmacol Exp Ther* 2008; **327**: 746-759 [PMID: 18780829 DOI: 10.1124/jpet.108.143826]
- 25 **Abajo A**, Boni V, Lopez I, Gonzalez-Huarriz M, Bitarte N, Rodriguez J, Zarate R, Bandres E, Garcia-Foncillas J. Identification of predictive circulating biomarkers of bevacizumab-containing regimen efficacy in pre-treated metastatic colorectal cancer patients. *Br J Cancer* 2012; **107**: 287-290 [PMID: 22699823 DOI: 10.1038/bjc.2012.242]
- 26 **Di Salvatore M**, Pietrantonio F, Orlandi A, Del Re M, Berenato R, Rossi E, Caporale M, Guarino D, Martinetti A, Basso M, Mennitto R, Santonocito C, Mennitto A, Schinzari G, Bossi I, Capoluongo E, Danesi R, de Braud F, Barone C. IL-8 and eNOS polymorphisms predict bevacizumab-based first line treatment outcomes in RAS mutant metastatic colorectal cancer patients. *Oncotarget* 2017; **8**: 16887-16898 [PMID: 28129643 DOI: 10.18632/oncotarget.14810]
- 27 **Gerger A**, El-Khoueiry A, Zhang W, Yang D, Singh H, Bohanes P, Ning Y, Winder T, Labonte MJ, Wilson PM, Benhaim L, Paez D, El-Khoueiry R, Absenger G, Lenz HJ. Pharmacogenetic angiogenesis profiling for first-line Bevacizumab plus oxaliplatin-based chemotherapy in patients with metastatic colorectal cancer. *Clin Cancer Res* 2011; **17**: 5783-5792 [PMID: 21791631 DOI: 10.1158/1078-0432.CCR-11-1115]
- 28 **Desurmont T**, Skrypek N, Duhamel A, Jonckheere N, Millet G, Leteurte E, Gosset P, Duchene B, Ramdane N, Hebbbar M, Van Seuning I, Pruvot FR, Huet G, Truant S. Overexpression of chemokine receptor CXCR2 and ligand CXCL7 in liver metastases from colon cancer is correlated to shorter disease-free and overall survival. *Cancer Sci* 2015; **106**: 262-269 [PMID: 25580640 DOI: 10.1111/cas.12603]
- 29 **Triener D**, Xue X, Schwartz AJ, Jung I, Colacino JA, Shah YM. Epithelial Hypoxia-Inducible Factor 2 $\alpha$  Facilitates the Progression of Colon Tumors through Recruiting Neutrophils. *Mol Cell Biol* 2017; **37**: [PMID: 27956697 DOI: 10.1128/MCB.00481-16]
- 30 **Lee YS**, Choi D, Kim NY, Yang S, Jung E, Hong M, Yang D, Lenz HJ, Hong YK. CXCR2 inhibition enhances sulindac-mediated suppression of colon cancer development. *Int J Cancer* 2014; **135**: 232-237 [PMID: 24338666 DOI: 10.1002/ijc.28668]
- 31 **Jamieson T**, Clarke M, Steele CW, Samuel MS, Neumann J, Jung A, Huels D, Olson ME, Das S, Nibbs RJ, Sansom OJ. Inhibition of CXCR2 profoundly suppresses inflammation-driven and spontaneous tumorigenesis. *J Clin Invest* 2012; **122**: 3127-3144 [PMID: 22922255 DOI: 10.1172/JCI61067]
- 32 **Kawamura M**, Toiyama Y, Tanaka K, Saigusa S, Okugawa Y, Hiro J, Uchida K, Mohri Y, Inoue Y, Kusunoki M. CXCL5, a promoter of cell proliferation, migration and invasion, is a novel serum prognostic marker in patients with colorectal cancer. *Eur J Cancer* 2012; **48**: 2244-2251 [PMID: 22197219 DOI: 10.1016/j.ejca.2011.11.032]
- 33 **Yamamoto M**, Kikuchi H, Ohta M, Kawabata T, Hiramatsu Y, Kondo K, Baba M, Kamiya K, Tanaka T, Kitagawa M, Konno H. TSU68 prevents liver metastasis of colon cancer xenografts by modulating the premetastatic niche. *Cancer Res* 2008; **68**: 9754-9762 [PMID: 19047154 DOI: 10.1158/0008-5472.CAN-08-1748]
- 34 **Lin SC**, Hsiao KY, Chang N, Hou PC, Tsai SJ. Loss of dual-specificity phosphatase-2 promotes angiogenesis and metastasis via up-regulation of interleukin-8 in colon cancer. *J Pathol* 2017; **241**: 638-648 [PMID: 28026024 DOI: 10.1002/path.4868]
- 35 **Wu W**, Cao J, Ji Z, Wang J, Jiang T, Ding H. Co-expression of Lgr5 and CXCR4 characterizes cancer stem-like cells of colorectal cancer. *Oncotarget* 2016; **7**: 81144-81155 [PMID: 27835894 DOI: 10.18632/oncotarget.13214]
- 36 **Zhu P**, Zhao N, Sheng D, Hou J, Hao C, Yang X, Zhu B, Zhang S, Han Z, Wei L, Zhang L. Inhibition of Growth and Metastasis of Colon Cancer by Delivering 5-Fluorouracil-loaded Pluronic P85 Copolymer Micelles. *Sci Rep* 2016; **6**: 20896 [PMID: 26864651 DOI: 10.1038/srep20896]
- 37 **Cutler MJ**, Lowthers EL, Richard CL, Hajducek DM, Spagnuolo PA, Blay J. Chemotherapeutic agents attenuate CXCL12-mediated migration of colon cancer cells by selecting for CXCR4-negative cells and increasing peptidase CD26. *BMC Cancer* 2015; **15**: 882 [PMID: 26552750 DOI: 10.1186/s12885-015-1702-2]
- 38 **Margolin DA**, Silinsky J, Grimes C, Spencer N, Aycock M, Green H, Cordova J, Davis NK, Driscoll T, Li L. Lymph node stromal cells enhance drug-resistant colon cancer cell tumor formation through SDF-1 $\alpha$ /CXCR4 paracrine signaling. *Neoplasia* 2011; **13**: 874-886 [PMID: 21969820]
- 39 **Liu WT**, Jing YY, Yan F, Han ZP, Lai FB, Zeng JX, Yu GF, Fan QM, Li R, Zhao QD, Wu MC, Wei LX. LPS-induced CXCR4-dependent migratory properties and a mesenchymal-like phenotype of colorectal cancer cells. *Cell Adh Migr* 2017; **11**: 13-23 [PMID: 26745593 DOI: 10.1080/19336918.2015.1134404]
- 40 **Huang WS**, Chen CN, Sze CI, Teng CC. Visfatin induces stromal cell-derived factor-1 expression by  $\beta$ 1 integrin signaling in colorectal cancer cells. *J Cell Physiol* 2013; **228**: 1017-1024 [PMID: 23042611 DOI: 10.1002/jcp.24248]
- 41 **Yopp AC**, Shia J, Butte JM, Allen PJ, Fong Y, Jarnagin WR, DeMatteo RP, D'Angelica MI. CXCR4 expression predicts patient outcome and recurrence patterns after hepatic resection for colorectal liver metastases. *Ann Surg Oncol* 2012; **19** Suppl 3: S339-S346 [PMID: 21584832 DOI: 10.1245/s10434-011-1774-4]
- 42 **Wang TB**, Hu BG, Liu DW, Shi HP, Dong WG. The influence of lentivirus-mediated CXCR4 RNA interference on hepatic metastasis of colorectal cancer. *Int J Oncol* 2014; **44**: 1861-1869 [PMID: 24647809 DOI: 10.3892/ijo.2014.2348]
- 43 **Unzueta U**, Céspedes MV, Ferrer-Mirallès N, Casanova I, Cedano J, Corchero JL, Domingo-Espín J, Villaverde A, Mangues R, Vázquez E. Intracellular CXCR4<sup>+</sup> cell targeting with T22-empowered protein-only nanoparticles. *Int J Nanomedicine* 2012; **7**: 4533-4544 [PMID: 22923991 DOI: 10.2147/IJN.S34450]
- 44 **Romain B**, Hachet-Haas M, Rohr S, Brigand C, Galzi JL, Gaub MP, Peneceach E, Guenet D. Hypoxia differentially regulated CXCR4 and CXCR7 signaling in colon cancer. *Mol Cancer* 2014; **13**: 58 [PMID: 24629239 DOI: 10.1186/1476-4598-13-58]
- 45 **Heckmann D**, Maier P, Laufs S, Li L, Sleeman JP, Trunk MJ, Leupold JH, Wenz F, Zeller WJ, Fruehauf S, Allgayer H. The disparate twins: a comparative study of CXCR4 and CXCR7 in SDF-1 $\alpha$ -induced gene expression, invasion and chemosensitivity of colon cancer. *Clin Cancer Res* 2014; **20**: 604-616 [PMID: 24255072 DOI: 10.1158/1078-0432.CCR-13-0582]
- 46 **Huang WS**, Hsieh MC, Huang CY, Kuo YH, Tung SY, Shen CH, Hsieh YY, Teng CC, Lee KF, Chen TC, Lee KC, Kuo HC. The Association of CXC Receptor 4 Mediated Signaling Pathway with Oxaliplatin-Resistant Human Colorectal Cancer Cells. *PLoS One* 2016; **11**: e0159927 [PMID: 27668882 DOI: 10.1371/journal.pone.0159927]
- 47 **Jin F**, Ji H, Jia C, Brockmeier U, Hermann DM, Metzén E, Zhu Y, Chi B. Synergistic antitumor effects of endostar in combination with oxaliplatin via inhibition of HIF and CXCR4 in the colorectal cell line SW1116. *PLoS One* 2012; **7**: e47161 [PMID: 23071744 DOI: 10.1371/journal.pone.0047161]
- 48 **Jung K**, Heishi T, Incio J, Huang Y, Beech EY, Pinter M, Ho WW, Kawaguchi K, Rahbari NN, Chung E, Kim JK, Clark JW,

- Willett CG, Yun SH, Luster AD, Padera TP, Jain RK, Fukumura D. Targeting CXCR4-dependent immunosuppressive Ly6C<sup>low</sup> monocytes improves antiangiogenic therapy in colorectal cancer. *Proc Natl Acad Sci USA* 2017; **114**: 10455-10460 [PMID: 28900008 DOI: 10.1073/pnas.1710754114]
- 49 **Burns JM**, Summers BC, Wang Y, Melikian A, Berahovich R, Miao Z, Penfold ME, Sunshine MJ, Littman DR, Kuo CJ, Wei K, McMaster BE, Wright K, Howard MC, Schall TJ. A novel chemokine receptor for SDF-1 and I-TAC involved in cell survival, cell adhesion, and tumor development. *J Exp Med* 2006; **203**: 2201-2213 [PMID: 16940167 DOI: 10.1084/jem.20052144]
- 50 **Qin S**, Rottman JB, Myers P, Kassam N, Weinblatt M, Loetscher M, Koch AE, Moser B, Mackay CR. The chemokine receptors CXCR3 and CCR5 mark subsets of T cells associated with certain inflammatory reactions. *J Clin Invest* 1998; **101**: 746-754 [PMID: 9466968 DOI: 10.1172/JCI1422]
- 51 **Sauty A**, Dziejman M, Taha RA, Iarossi AS, Neote K, Garcia-Zepeda EA, Hamid Q, Luster AD. The T cell-specific CXCL chemokines IP-10, Mig, and I-TAC are expressed by activated human bronchial epithelial cells. *J Immunol* 1999; **162**: 3549-3558 [PMID: 10092813]
- 52 **Lal N**, White BS, Goussous G, Pickles O, Mason MJ, Beggs AD, Taniere P, Willcox BE, Guinney J, Middleton GW. KRAS Mutation and Consensus Molecular Subtypes 2 and 3 Are Independently Associated with Reduced Immune Infiltration and Reactivity in Colorectal Cancer. *Clin Cancer Res* 2018; **24**: 224-233 [PMID: 29061646 DOI: 10.1158/1078-0432.CCR-17-1090]
- 53 **Kistner L**, Doll D, Holtorf A, Nitsche U, Janssen KP. Interferon-inducible CXCL-chemokines are crucial immune modulators and survival predictors in colorectal cancer. *Oncotarget* 2017; **8**: 89998-90012 [PMID: 29163806 DOI: 10.18632/oncotarget.21286]
- 54 **Zumwalt TJ**, Arnold M, Goel A, Boland CR. Active secretion of CXCL10 and CCL5 from colorectal cancer microenvironments associates with GranzymeB+ CD8+ T-cell infiltration. *Oncotarget* 2015; **6**: 2981-2991 [PMID: 25671296 DOI: 10.18632/oncotarget.3205]
- 55 **Wu Z**, Huang X, Han X, Li Z, Zhu Q, Yan J, Yu S, Jin Z, Wang Z, Zheng Q, Wang Y. The chemokine CXCL9 expression is associated with better prognosis for colorectal carcinoma patients. *Biomed Pharmacother* 2016; **78**: 8-13 [PMID: 26898419 DOI: 10.1016/j.biopha.2015.12.021]
- 56 **Agesen TH**, Sveen A, Merok MA, Lind GE, Nesbakken A, Skotheim RI, Lothe RA. ColoGuideEx: a robust gene classifier specific for stage II colorectal cancer prognosis. *Gut* 2012; **61**: 1560-1567 [PMID: 22213796 DOI: 10.1136/gutjnl-2011-301179]
- 57 **Wu Z**, Han X, Yan J, Pan Y, Gong J, Di J, Cheng Z, Jin Z, Wang Z, Zheng Q, Wang Y. The prognostic significance of chemokine receptor CXCR3 expression in colorectal carcinoma. *Biomed Pharmacother* 2012; **66**: 373-377 [PMID: 22401929 DOI: 10.1016/j.biopha.2011.12.003]
- 58 **Zeng YJ**, Lai W, Wu H, Liu L, Xu HY, Wang J, Chu ZH. Neuroendocrine-like cells -derived CXCL10 and CXCL11 induce the infiltration of tumor-associated macrophage leading to the poor prognosis of colorectal cancer. *Oncotarget* 2016; **7**: 27394-27407 [PMID: 27034164 DOI: 10.18632/oncotarget.8423]
- 59 **Brackett CM**, Kojouharov B, Veith J, Greene KF, Burdelya LG, Gollnick SO, Abrams SI, Gudkov AV. Toll-like receptor-5 agonist, entolimod, suppresses metastasis and induces immunity by stimulating an NK-dendritic-CD8+ T-cell axis. *Proc Natl Acad Sci USA* 2016; **113**: E874-E883 [PMID: 26831100 DOI: 10.1073/pnas.1521359113]
- 60 **Yang H**, Yamazaki T, Pietrocola F, Zhou H, Zitvogel L, Ma Y, Kroemer G. STAT3 Inhibition Enhances the Therapeutic Efficacy of Immunogenic Chemotherapy by Stimulating Type 1 Interferon Production by Cancer Cells. *Cancer Res* 2015; **75**: 3812-3822 [PMID: 26208907 DOI: 10.1158/0008-5472.CAN-15-1122]
- 61 **Akeus P**, Langenes V, Kristensen J, von Mentzer A, Sparwasser T, Raghavan S, Quiding-Järbrink M. Treg-cell depletion promotes chemokine production and accumulation of CXCR3(+) conventional T cells in intestinal tumors. *Eur J Immunol* 2015; **45**: 1654-1666 [PMID: 25754875 DOI: 10.1002/eji.201445058]
- 62 **Murakami T**, Kawada K, Iwamoto M, Akagami M, Hida K, Nakanishi Y, Kanda K, Kawada M, Seno H, Taketo MM, Sakai Y. The role of CXCR3 and CXCR4 in colorectal cancer metastasis. *Int J Cancer* 2013; **132**: 276-287 [PMID: 22689289 DOI: 10.1002/ijc.27670]
- 63 **Rupertus K**, Sinistra J, Scheuer C, Nickels RM, Schilling MK, Menger MD, Kollmar O. Interaction of the chemokines I-TAC (CXCL11) and SDF-1 (CXCL12) in the regulation of tumor angiogenesis of colorectal cancer. *Clin Exp Metastasis* 2014; **31**: 447-459 [PMID: 24493023 DOI: 10.1007/s10585-014-9639-4]
- 64 **Agostini M**, Janssen KP, Kim JJ, D'Angelo E, Pizzini S, Zangrando A, Zanon C, Pastrello C, Maretto I, Digito M, Bedin C, Jurisica I, Rizzolio F, Giordano A, Bortoluzzi S, Nitti D, Pucciarelli S. An integrative approach for the identification of prognostic and predictive biomarkers in rectal cancer. *Oncotarget* 2015; **6**: 32561-32574 [PMID: 26359356 DOI: 10.18632/oncotarget.4935]
- 65 **Li C**, Wang Z, Liu F, Zhu J, Yang L, Cai G, Zhang Z, Huang W, Cai S, Xu Y. CXCL10 mRNA expression predicts response to neoadjuvant chemoradiotherapy in rectal cancer patients. *Tumour Biol* 2014; **35**: 9683-9691 [PMID: 24969558 DOI: 10.1007/s13277-014-2234-0]
- 66 **Zhang Y**, Gao J, Wang X, Deng S, Ye H, Guan W, Wu M, Zhu S, Yu Y, Han W. CXCL4 mediates tumor regrowth after chemotherapy by suppression of antitumor immunity. *Cancer Biol Ther* 2015; **16**: 1775-1783 [PMID: 26479470 DOI: 10.1080/15384047.2015.1095404]
- 67 **Meijer J**, Zeelenberg IS, Sipos B, Roos E. The CXCR5 chemokine receptor is expressed by carcinoma cells and promotes growth of colon carcinoma in the liver. *Cancer Res* 2006; **66**: 9576-9582 [PMID: 17018614 DOI: 10.1158/0008-5472.CAN-06-1507]
- 68 **Zhu Z**, Zhang X, Guo H, Fu L, Pan G, Sun Y. CXCL13-CXCR5 axis promotes the growth and invasion of colon cancer cells via PI3K/AKT pathway. *Mol Cell Biochem* 2015; **400**: 287-295 [PMID: 25476740 DOI: 10.1007/s11010-014-2285-y]
- 69 **Olsen RS**, Nijm J, Andersson RE, Dimberg J, Wågsäter D. Circulating inflammatory factors associated with worse long-term prognosis in colorectal cancer. *World J Gastroenterol* 2017; **23**: 6212-6219 [PMID: 28974887 DOI: 10.3748/wjg.v23.i34.6212]
- 70 **Qi XW**, Xia SH, Yin Y, Jin LF, Pu Y, Hua D, Wu HR. Expression features of CXCR5 and its ligand, CXCL13 associated with poor prognosis of advanced colorectal cancer. *Eur Rev Med Pharmacol Sci* 2014; **18**: 1916-1924 [PMID: 25010623]
- 71 **Cremonesi E**, Governa V, Garzon JFG, Mele V, Amicarella F, Muraro MG, Trella E, Galati-Fournier V, Oertli D, Däster SR, Droeser RA, Weixler B, Bolli M, Rosso R, Nitsche U, Khanna N, Egli A, Keck S, Slotta-Huspenina J, Terracciano LM, Zajac P, Spagnoli GC, Eppenberger-Castori S, Janssen KP, Borsig L, Izzi G. Gut microbiota modulate T cell trafficking into human colorectal cancer. *Gut* 2018; **67**: 1984-1994 [PMID: 29437871 DOI: 10.1136/gutjnl-2016-313498]
- 72 **Bindea G**, Mlecnik B, Tosolini M, Kirilovsky A, Waldner M, Obenauf AC, Angell H, Fredriksen T, Lafontaine L, Berger A, Bruneval P, Fridman WH, Becker C, Pagès F, Speicher MR, Trajanoski Z, Galon J. Spatiotemporal dynamics of intratumoral immune cells reveal the immune landscape in human cancer. *Immunity* 2013; **39**: 782-795 [PMID: 24138885 DOI: 10.1016/j.immuni.2013.10.003]
- 73 **Xing J**, Zhang C, Yang X, Wang S, Wang Z, Li X, Yu E. CXCR5<sup>+</sup>CD8<sup>+</sup> T cells infiltrate the colorectal tumors and nearby lymph nodes, and are associated with enhanced IgG response in B cells. *Exp Cell Res* 2017; **356**: 57-63 [PMID: 28412245 DOI: 10.1016/j.yexcr.2017.04.014]
- 74 **Rachidi SM**, Qin T, Sun S, Zheng WJ, Li Z. Molecular profiling of multiple human cancers defines an inflammatory cancer-associated molecular pattern and uncovers KPNA2 as a uniform poor prognostic cancer marker. *PLoS One* 2013; **8**: e57911 [PMID: 23536776 DOI: 10.1371/journal.pone.0057911]
- 75 **Griffith JW**, Sokol CL, Luster AD. Chemokines and chemokine receptors: positioning cells for host defense and immunity. *Annu Rev Immunol* 2014; **32**: 659-702 [PMID: 24655300 DOI: 10.1146/annurev-immunol-032713-120145]

- 76 **Schramme A**, Abdel-Bakky MS, Kämpfer-Kolb N, Pfeilschifter J, Gutwein P. The role of CXCL16 and its processing metalloproteinases ADAM10 and ADAM17 in the proliferation and migration of human mesangial cells. *Biochem Biophys Res Commun* 2008; **370**: 311-316 [PMID: 18373975 DOI: 10.1016/j.bbrc.2008.03.088]
- 77 **Yu X**, Zhao R, Lin S, Bai X, Zhang L, Yuan S, Sun L. CXCL16 induces angiogenesis in autocrine signaling pathway involving hypoxia-inducible factor 1 $\alpha$  in human umbilical vein endothelial cells. *Oncol Rep* 2016; **35**: 1557-1565 [PMID: 26707275 DOI: 10.3892/or.2015.4520]
- 78 **Chung S**, Dwabe S, Elshimali Y, Sukhija H, Aroh C, Vadgama JV. Identification of Novel Biomarkers for Metastatic Colorectal Cancer Using Angiogenesis-Antibody Array and Intracellular Signaling Array. *PLoS One* 2015; **10**: e0134948 [PMID: 26258407 DOI: 10.1371/journal.pone.0134948]
- 79 **Kee JY**, Ito A, Hojo S, Hashimoto I, Igarashi Y, Tsuneyama K, Tsukada K, Irimura T, Shibahara N, Takasaki I, Inujima A, Nakayama T, Yoshie O, Sakurai H, Saiki I, Koizumi K. CXCL16 suppresses liver metastasis of colorectal cancer by promoting TNF- $\alpha$ -induced apoptosis by tumor-associated macrophages. *BMC Cancer* 2014; **14**: 949 [PMID: 25495942 DOI: 10.1186/1471-2407-14-949]
- 80 **Kee JY**, Ito A, Hojo S, Hashimoto I, Igarashi Y, Tsukada K, Irimura T, Shibahara N, Nakayama T, Yoshie O, Sakurai H, Saiki I, Koizumi K. Chemokine CXCL16 suppresses liver metastasis of colorectal cancer via augmentation of tumor-infiltrating natural killer T cells in a murine model. *Oncol Rep* 2013; **29**: 975-982 [PMID: 23242131 DOI: 10.3892/or.2012.2185]
- 81 **Matsushita K**, Toiyama Y, Tanaka K, Saigusa S, Hiro J, Uchida K, Inoue Y, Kusunoki M. Soluble CXCL16 in preoperative serum is a novel prognostic marker and predicts recurrence of liver metastases in colorectal cancer patients. *Ann Surg Oncol* 2012; **19** Suppl 3: S518-S527 [PMID: 21845497 DOI: 10.1245/s10434-011-1993-8]
- 82 **Lee WY**, Wang CJ, Lin TY, Hsiao CL, Luo CW. CXCL17, an orphan chemokine, acts as a novel angiogenic and anti-inflammatory factor. *Am J Physiol Endocrinol Metab* 2013; **304**: E32-E40 [PMID: 23115081 DOI: 10.1152/ajpendo.00083.2012]
- 83 **Maravillas-Montero JL**, Burkhardt AM, Hevezi PA, Carnevale CD, Smit MJ, Zlotnik A. Cutting edge: GPR35/CXCR8 is the receptor of the mucosal chemokine CXCL17. *J Immunol* 2015; **194**: 29-33 [PMID: 25411203 DOI: 10.4049/jimmunol.1401704]
- 84 **Weinstein EJ**, Head R, Griggs DW, Sun D, Evans RJ, Swearingen MI, Westlin MM, Mazzarella R. VCC-1, a novel chemokine, promotes tumor growth. *Biochem Biophys Res Commun* 2006; **350**: 74-81 [PMID: 16989774 DOI: 10.1016/j.bbrc.2006.08.194]
- 85 **Mu X**, Chen Y, Wang S, Huang X, Pan H, Li M. Overexpression of VCC-1 gene in human hepatocellular carcinoma cells promotes cell proliferation and invasion. *Acta Biochim Biophys Sin* (Shanghai) 2009; **41**: 631-637 [PMID: 19657564]
- 86 **Matsui A**, Yokoo H, Negishi Y, Endo-Takahashi Y, Chun NA, Kadouchi I, Suzuki R, Maruyama K, Aramaki Y, Semba K, Kobayashi E, Takahashi M, Murakami T. CXCL17 expression by tumor cells recruits CD11b+Gr1 high F4/80- cells and promotes tumor progression. *PLoS One* 2012; **7**: e44080 [PMID: 22952881 DOI: 10.1371/journal.pone.0044080]
- 87 **Ohlsson L**, Hammarström ML, Lindmark G, Hammarström S, Sitohy B. Ectopic expression of the chemokine CXCL17 in colon cancer cells. *Br J Cancer* 2016; **114**: 697-703 [PMID: 26889977 DOI: 10.1038/bjc.2016.4]
- 88 **Pagès F**, Mlecnik B, Marliot F, Bindea G, Ou FS, Bifulco C, Lugli A, Zlobec I, Rau TT, Berger MD, Nagtegaal ID, Vink-Börger E, Hartmann A, Geppert C, Kolwelter J, Merkel S, Grützmann R, Van den Eynde M, Jouret-Mourin A, Kartheuser A, Léonard D, Remue C, Wang JY, Bavi P, Roehrl MHA, Ohashi PS, Nguyen LT, Han S, MacGregor HL, Hafezi-Bakhtiari S, Wouters BG, Masucci GV, Andersson EK, Zavadova E, Vocka M, Spacek J, Petruzella L, Konopasek B, Dunder P, Skalova H, Nemejcova K, Botti G, Tatangelo F, Delrio P, Ciliberto G, Maio M, Laghi L, Grizzi F, Fredriksen T, Buttard B, Angelova M, Vasaturo A, Maby P, Church SE, Angell HK, Lafontaine L, Bruni D, El Sissy C, Haicheur N, Kirilovsky A, Berger A, Lagorce C, Meyers JP, Paustian C, Feng Z, Ballesteros-Merino C, Dijkstra J, van de Water C, van Lent-van Vliet S, Knijn N, Musinà AM, Scripcariu DV, Popivanova B, Xu M, Fujita T, Hazama S, Suzuki N, Nagano H, Okuno K, Torigoe T, Sato N, Furuhashi T, Takemasa I, Itoh K, Patel PS, Vora HH, Shah B, Patel JB, Rajvik KN, Pandya SJ, Shukla SN, Wang Y, Zhang G, Kawakami Y, Marincola FM, Ascierto PA, Sargent DJ, Fox BA, Galon J. International validation of the consensus Immunoscore for the classification of colon cancer: a prognostic and accuracy study. *Lancet* 2018; **391**: 2128-2139 [PMID: 29754777 DOI: 10.1016/S0140-6736(18)30789-X]

**P- Reviewer:** Kim SM, Mastoraki A, Nakayama Y, Popp C  
**S- Editor:** Ma RY **L- Editor:** A **E- Editor:** Huang Y





Published by **Baishideng Publishing Group Inc**  
7901 Stoneridge Drive, Suite 501, Pleasanton, CA 94588, USA  
Telephone: +1-925-223-8242  
Fax: +1-925-223-8243  
E-mail: [bpgoffice@wjgnet.com](mailto:bpgoffice@wjgnet.com)  
Help Desk: <http://www.f6publishing.com/helpdesk>  
<http://www.wjgnet.com>



ISSN 1007-9327



© 2018 Baishideng Publishing Group Inc. All rights reserved.



# N<sub>chemokines</sub>ewsletter

PROYECTO FIS  
QUIMIOCINAS  
CAN RUTI PI16/01800

Estudio de las quimiocinas CXC y sus receptores como biomarcadores pronóstico y/o predictivos de respuesta y como posibles dianas terapéuticas en el cáncer colorrectal

Enlace carpeta google drive: <https://drive.google.com/drive/u/0/folders/0BylgwkcafiFIU2xRR0pRYzFqSmc>

**CRITERIOS DE INCLUSIÓN DE PACIENTES:**

-**Estadios II y III:** cáncer de colon estadios II o III candidatos a tratamiento adyuvante basado en Oxaliplatino

-**Estadio IV:** cáncer colorrectal estadio IV (RAS mt o wt), candidatos a cirugía de metástasis o no, con tratamiento:

Fluoropirimidina + Oxaliplatino con o sin Bevacizumab o Panitumumab

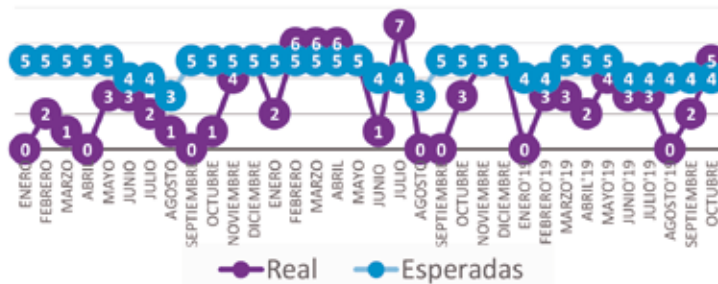
A continuación se muestran los datos hasta la fecha 15/10/19:

**Muestras Recibidas Estadios II y III**



Centro	Pacientes
Dr. JOSEP TRUETA	1
DURAN I REYNALS	10
GERMANS TRIAS I PUJOL	49
MOISES BROGGI	16
VHIO	1

**Muestras Recibidas Estadio IV**



Centro	Pacientes
Dr. JOSEP TRUETA	29
DURAN I REYNALS	28
GERMANS TRIAS I PUJOL	8
MOISES BROGGI	13
VHIO	14



---

# Bio-Plex Pro™ Human Chemokine Assays

## Instruction Manual

For technical support, call your local Bio-Rad office, or in the U.S., call 1-800-424-6723.  
For research use only. Not for diagnostic procedures.



# Table of Contents

<b>Introduction</b>	<b>1</b>
<b>Principle</b>	<b>2</b>
<b>Kit Contents and Storage</b>	<b>4</b>
<b>Recommended Materials</b>	<b>5</b>
<b>Assay Workflow</b>	<b>6</b>
<b>Important Considerations</b>	<b>7</b>
<b>Detailed Instructions</b>	<b>7</b>
1. Plan Plate Layout	<b>8</b>
2. Prepare Instrument	<b>9</b>
3. Prepare Wash Method	<b>10</b>
4. Prepare Wash Buffer	<b>11</b>
5. Prepare Standards and Controls	<b>11</b>
6. Prepare Samples	<b>14</b>
7. Prepare Coupled Beads	<b>16</b>
8. Run Assay	<b>18</b>
9. Read Plate	<b>22</b>
<b>Troubleshooting Guide</b>	<b>29</b>
<b>Appendix: Non-Human Primate (NHP) Cross-Reactivity</b>	<b>34</b>
<b>Plate Layout Template</b>	<b>35</b>
<b>Calculation Worksheet</b>	<b>36</b>
<b>Safety Considerations</b>	<b>38</b>
<b>Legal Notices</b>	<b>38</b>
<b>Ordering Information</b>	<b>39</b>

## Introduction

Chemokines are small molecular weight (8–10 kD) cytokines secreted by various eukaryotic cell types, including those of the immune system. Their main function is to promote and regulate cell migration in both normal and pathological conditions, including immune surveillance, inflammation, angiogenesis, microbial infection, autoimmune diseases, tumor growth, vascular diseases, and transplant rejection (Locati et al. 2005, Slettenaar and Wilson 2006). The regulatory functions of chemokines are exerted via binding and signaling through specific G protein-coupled receptors expressed on the surface of chemokine-responsive cells.

Chemokines are classified into four subfamilies (C, CC, CXC, and CX3C) based on the number and spacing of cysteine residues within the protein sequence. The C chemokines are known as lymphotactins, and are found at high levels in spleen, thymus, intestine, and peripheral blood leukocytes. The CC chemokines have the first two cysteines in adjacent positions and are known to attract granulocytes and lymphocytes, including NK cells. The CXC chemokines have the first two of four cysteines separated by a single amino acid, denoted X. Most CXC chemokines are chemo-attractants for neutrophils and lymphocytes. The CX3C chemokines have three amino acids inserted between the first two cysteines. The only CX3C chemokine discovered to date is fractalkine, which is both a chemo-attractant and adhesion molecule.

### **Multiplexing with Bio-Plex Pro Chemokine Assays**

Bio-Plex Pro chemokine assays enable researchers to quantify multiple protein biomarkers in a single well of a 96-well plate in just 3–4 hours. These robust immunoassays require as little as 12.5 µl of serum or plasma or 50 µl of other biological fluid. The use of magnetic (MagPlex) beads allows researchers to automate wash steps on a Bio-Plex Pro (or similar) wash station. Magnetic separation offers greater convenience and reproducibility compared to vacuum filtration.

For more information please visit [www.bio-rad.com/bio-plex](http://www.bio-rad.com/bio-plex).

# Principle

## Technology

The Bio-Plex® multiplex system is built upon the three core elements of xMAP technology:

- Fluorescently dyed magnetic microspheres (also called beads), each with a distinct color code or spectral address to permit discrimination of individual tests within a multiplex suspension. This allows simultaneous detection of up to 500 different molecules in a single well of a 96-well microplate on the Bio-Plex® 3D system, up to 100 different molecules on the Bio-Plex® 200 system, and up to 50 different molecules on the Bio-Plex® MAGPIX™ system
- A dedicated plate reader. The Bio-Plex 200 and Bio-Plex 3D systems are flow cytometry-based instruments with two lasers and associated optics to measure the different molecules bound to the surface of the beads. In the Bio-Plex MAGPIX system, the sample is injected into a chamber where the beads are imaged using LED and CCD technology
- A high-speed digital signal processor that efficiently manages the fluorescence data

## Assay Format

Bio-Plex Pro™ assays are essentially immunoassays formatted on magnetic beads. The assay principle is similar to that of a sandwich ELISA (Figure 1). Capture antibodies directed against the desired biomarker are covalently coupled to the beads. Coupled beads react with the sample containing the biomarker of interest. After a series of washes to remove unbound protein, a biotinylated detection antibody is added to create a sandwich complex. The final detection complex is formed with the addition of streptavidin-phycoerythrin (SA-PE) conjugate. Phycoerythrin serves as a fluorescent indicator, or reporter.

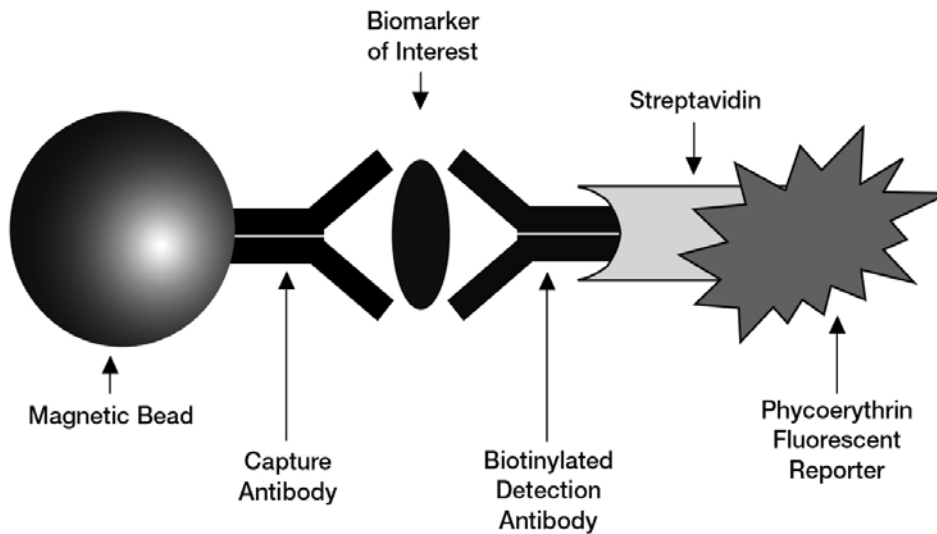


Fig. 1. Bio-Plex sandwich immunoassay.

## Data Acquisition and Analysis

Data from the reactions are acquired using a Bio-Plex system or similar Luminex-based reader. When a multiplex assay suspension is drawn into the Bio-Plex 200 reader, for example, a red (635 nm) laser illuminates the fluorescent dyes within each bead to provide bead classification and thus assay identification. At the same time, a green (532 nm) laser excites PE to generate a reporter signal, which is detected by a photomultiplier tube (PMT). A high-speed digital processor manages data output, and Bio-Plex Manager™ software presents data as median fluorescence intensity (MFI) as well as concentration (pg/ml). The concentration of analyte bound to each bead is proportional to the MFI of reporter signal.

Using Bio-Plex Data Pro™ software, data from multiple instrument runs can be combined into a single project for easy data management, quick visualization of results, and simple statistical analysis.

## Kit Contents and Storage

### Reagents Supplied

Bio-Plex Pro™ human chemokine assays are available in a convenient all-in-one kit format that includes assay, reagent, and diluent components in a single box.

**Table 1. Contents of 1 x 96-well kits.**

Component	Quantity <sup>***</sup>
Coupled magnetic beads (20x)	1 tube
Detection antibodies (20x)	1 tube
Standards	1 vial
Quality control*	1 vial
Sample diluent HB	1 bottle (8 ml)
Detection antibody diluent HB	1 bottle (3.5 ml)
Standard diluent HB	1 bottle (10 ml)
Assay buffer	1 bottle (50 ml)
Wash buffer (10x)	1 bottle (60 ml)
Streptavidin-PE (100x)	1 tube
Assay plate (96-well flat bottom plate)**	1 plate
Sealing tape	1 pack of 4
Assay quick guide	1 booklet
Product data sheet	1 sheet

\* Provided with the 40-plex fixed panel only.

\*\* Filter plate option available with custom x-Plex™ and Express kits.

\*\*\* Volumes shown are approximate.

### Storage and Stability

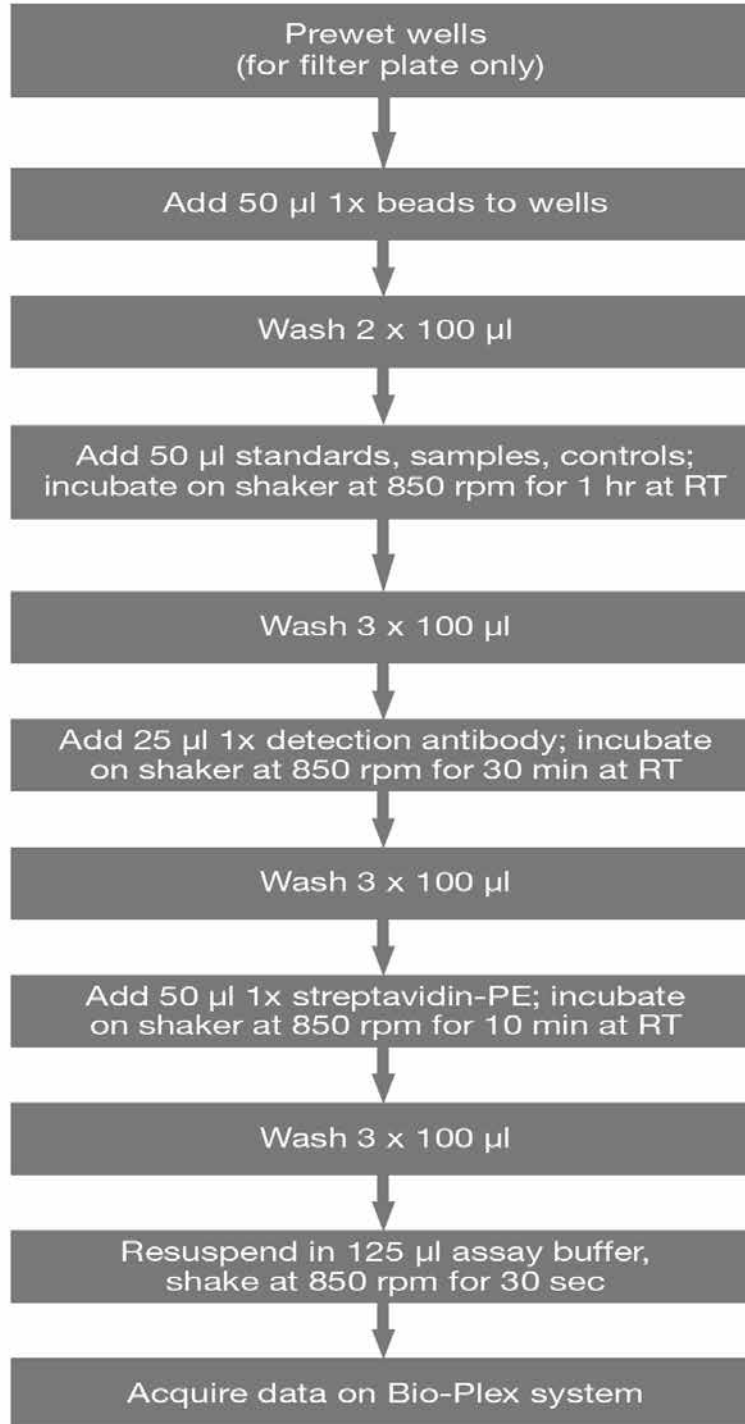
Kit contents should be stored at 4°C and never frozen. Coupled magnetic beads and streptavidin-PE should be stored in the dark. All components are guaranteed for a minimum of six months from the date of purchase when stored as specified.

Table 2. Recommended materials.

Item	Ordering Information
<b>Bio-Plex Pro Chemokine Assays Quick Guide</b>	Bulletin #10031991 (download at <a href="http://www.bio-rad.com/bio-plex">www.bio-rad.com/bio-plex</a> )
<b>Bio-Plex® 200 system or Luminex system with HTF</b>	Bio-Rad catalog #171-000205
<b>Bio-Plex validation kit</b> Note: Run the validation kit monthly to ensure optimal performance of fluidics and optics systems	Bio-Rad catalog #171-203001
<b>Bio-Plex calibration kit</b> Note: Run the calibration kit daily to standardize fluorescence signal	Bio-Rad catalog #171-203060
<b>Bio-Plex Pro wash station</b> For use with magnetic bead-based assays only	Bio-Rad catalog #300-34376
<b>Bio-Plex Pro II wash station</b> For use with both nonmagnetic and magnetic bead-based assays	Bio-Rad catalog #300-34377
<b>Bio-Plex handheld magnetic washer</b> For use with magnetic bead-based assays only	Bio-Rad catalog #170-20100
<b>Bio-Plex Pro flat bottom plates (40 x 96-well)</b> For magnetic separation on the Bio-Plex Pro wash station	Bio-Rad catalog #171-025001
<b>Titertube® micro test tubes</b> For preparing replicate standards, samples, and controls prior to loading the plate	Bio-Rad catalog #223-9390
<b>Microtiter plate shaker</b> IKA MTS 2/4 shaker for 2 or 4 microplates or Barnstead/Lab-Line Model 4625 plate shaker (or equivalent capable of 300–1,100 rpm)	IKA catalog #320-8000  VWR catalog #57019-600
<b>Aurum™ vacuum manifold</b> For vacuum filtration	Bio-Rad catalog #732-6470
<b>BR-2000 vortexer</b>	Bio-Rad catalog #166-0610
<b>Reagent reservoirs, 25 ml</b> For capture beads and detection antibodies	VistaLab catalog #3054-1002 or VistaLab catalog #3054-1004
<b>Reagent reservoir, 50 ml (for reagents and buffers)</b>	VistaLab catalog #3054-1006
<b>Pall Life Science Acrodisc: 25 mm PF syringe filter (0.8/0.2 µm Supor membrane)</b>	Pall Life Sciences catalog #4187
<b>Filter plate, 1 x 96 with clear plastic lid and tray</b>	Bio-Rad catalog #171-304502

**Other:** 15 ml polypropylene tubes for reagent dilutions, calibrated pipets, pipet tips, sterile distilled water, aluminum foil, absorbent paper towels, 1.5 or 2 ml microcentrifuge tubes, and standard flat bottom microplate (for calibrating vacuum manifold).

## Assay Workflow



## Important Considerations

### Instruments and Software

The Bio-Plex Pro™ assays described in this manual are compatible with all currently available Luminex-based life science research instruments. Assays can be read and analyzed with either Bio-Plex Manager™ software or Luminex xPONENT software (see the Run Assay section).

### Assay Procedures

Please pay close attention to vortexing, shaking, and incubation times and to Bio-Plex® reader PMT (RP1) setting, as these have been optimized specifically for each assay panel.

### Assay Quick Guide

Each assay kit comes complete with a printed Bio-Plex Pro™ Assay Quick Guide (bulletin #10031991), which can be used to prepare and run a full 1 x 96-well assay plate. Users can also download a copy at [www.bio-rad.com/bio-plex](http://www.bio-rad.com/bio-plex).

### Bead Regions and Multiplexing Compatibility

- Bead regions for all analytes are listed in the Read Plate section
- Do not mix analytes between different Bio-Plex panels or reagent kits. Resulting standard curves and sample values may be inaccurate

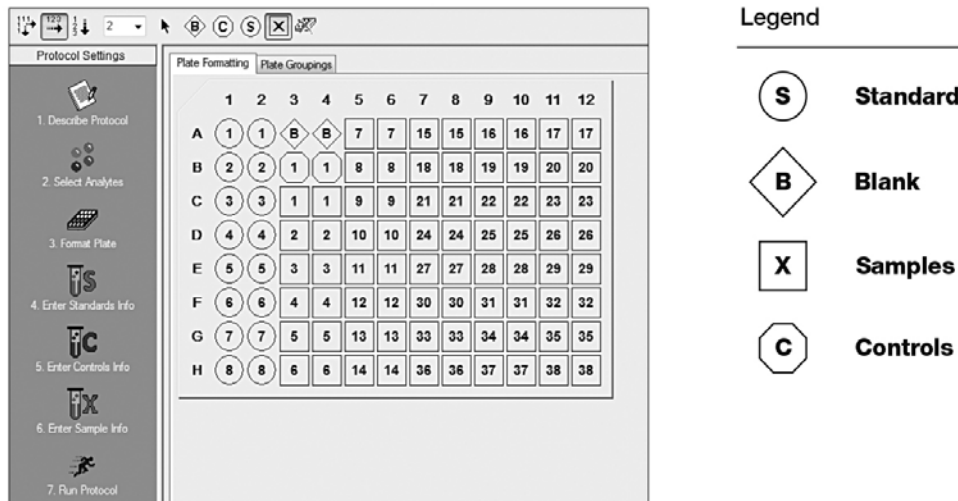
## Detailed Instructions

The following pages provide detailed instructions for each step of the assay procedure, including preparation, running the assay, and reading the plate with Bio-Plex Manager™ and Luminex xPONENT software.

# 1. Plan Plate Layout

Determine the total number of wells in the experiment using the Plate Layout Template on page 35 or the Plate Formatting tab in Bio-Plex Manager™. A suggested plate layout is shown in Figure 2, with all conditions in duplicate.

1. Assign standards to columns 1 and 2, with the highest concentration in row A and the lowest concentration in row H.
2. Assign the blank to wells A3 and A4. The blank should consist of your chosen standard diluent. Note that Bio-Plex Manager automatically subtracts the blank (B) MFI value from all other assay wells.
3. User-specified controls, as well as the quality controls supplied in premixed kits, are assigned to wells in columns 3 and 4.
4. The remainder of the plate is available for samples.
5. Once the total number of wells is known, you can calculate the required volumes of beads, detection antibody, and streptavidin-PE. Use Tables 6–7, 9–10, and 11, respectively, or the Calculation Worksheet on pages 36–37.



**Fig. 2. Suggested plate layout.** For detailed instructions on plate formatting in Bio-Plex Manager, see the Read Plate section.

## 2. Prepare Instrument

These directions are specific for the Bio-Plex® 100/200 reader. To prepare either a Bio-Plex 3D or Bio-Plex® MAGPIX™ reader, consult their respective user manuals.

**Note:** While the instrument is warming up, bring the 10x wash buffer, assay buffer, and diluents to room temperature. Keep other items on ice until needed. Also, begin to thaw frozen samples.

Start up and calibrate the Bio-Plex system with Bio-Plex Manager™ software prior to setting up the assay. The calibration kit should be run daily or before each use of the instrument to standardize the fluorescent signal. For instructions on using other xMAP system software packages, contact Bio-Rad Technical Support.

The validation kit should be run monthly to ensure optimal performance of fluidics and optics systems. Refer to either the software manual or online Help for directions on how to conduct validation.

### Start Up System (Bio-Plex 100, 200, or similar)

1. Empty the waste bottle and fill the sheath fluid bottle before starting if high throughput fluidics (HTF) are not present. This will prevent fluidic system backup and potential data loss.
2. Turn on the reader, XY platform, and HTF (if included). Allow the system to warm up for 30 min (if not already done).
3. Select **Start up**  and follow the instructions. If the system is idle for 4 hr without acquiring data, the lasers will automatically turn off. To reset the 4-hr countdown, select **Warm up**  and wait for the lasers/optics to reach operational temperature.

### Calibrate System

1. Select **Calibrate**  and confirm that the default values for CAL1 and CAL2 are the same as the values printed on the bottle of Bio-Plex calibration beads. Use the Bio-Plex system low RP1 target value.

2. Select **OK** and follow the software prompts for step-by-step instructions for CAL1 and CAL2 calibration.

**Note:** In Bio-Plex Manager version 6.1 and higher, startup, warm up, and calibration can be performed together by selecting the **Start up and calibrate** icon. 

### 3. Prepare Wash Method

Bio-Plex Pro™ assays are compatible with both magnetic separation and vacuum filtration methods. However, for best results, we recommend performing the assays in a flat bottom plate with magnetic separation.

**Table 3. Summary of compatible wash stations and plate types.**

Wash Method	Wash Station	Assay Plate
Magnetic separation	Bio-Plex Pro Bio-Plex Pro II (use MAG programs) Bio-Plex® handheld magnetic washer	Flat bottom plate
Vacuum filtration	Bio-Plex Pro II (use VAC programs) Vacuum manifold (manual)	Filter plate

#### Setting up the Bio-Plex Pro or Bio-Plex Pro II Wash Station

The wash station should be primed before use. For more information, refer to the Bio-Plex Pro Wash Stations Quick Guide (bulletin #5826).

1. Install the appropriate plate carrier on the wash station.
2. Use the Prime procedure to prime channel 1 with 1x wash buffer.

#### Setting up the Bio-Plex Handheld Magnetic Washer

Place an empty flat bottom plate on the magnetic washer by sliding it under the retaining clips. Push the clips inward to secure the plate. Make sure the plate is held securely. If needed, the clips can be adjusted for height and tension. For detailed instructions, refer to the user guide (bulletin #10023087).

## Setting up a Vacuum Manifold

Calibrate the vacuum manifold by placing a standard 96-well flat bottom plate on the unit and adjusting the pressure to -1 to -3" Hg. In general, 100 µl liquid should take 3–4 sec to clear the well. For more detailed instructions, refer to bulletin #10005042.

## 4. Prepare Wash Buffer

1. Bring the 10x stock solution to room temperature.
2. If crystals exist, ensure that they are completely dissolved. Mix the 10x stock solution by inversion before preparing the 1x wash buffer.
3. To prepare 1x wash buffer, dilute 1 part of 10x stock solution with 9 parts of deionized water.

## 5. Prepare Standards and Controls

### General Instructions

- It is essential to prepare standards and quality controls (if included) exactly as described in this section. Incorrect preparation may lead to low signal or variable measurements from plate to plate
- The product data sheet provided with the standards lists the most concentrated point on the standard curve (S1). Enter this information into Bio-Plex Manager™ software as instructed in section 9

### Using the Quality Controls (optional)

A single vial of quality controls is provided with the 40-plex fixed panel only. Their use is intended for monitoring the day-to-day quality of assay results.

## Selecting a Diluent for Standards and Controls

Refer to Table 4 for recommended diluents based on different sample types.

In order to meet the lot-specific control ranges provided on the product data sheet, both the standards and controls should be reconstituted in Bio-Plex® standard diluent HB. If reconstituting in a different diluent, users will need to establish/validate their own control ranges or acceptance criteria.

Table 4. Summary of recommended diluents for standards and controls.

Sample Type	Diluent for Standards and Controls*	Add BSA
Serum and plasma	Standard diluent HB	None
Culture media, with serum	Culture medium	None
Culture media, serum-free	Culture medium	To 0.5% final**
Lavage, sputum, other fluids	Sample diluent HB	To 0.5% final**
Lysate	Sample diluent HB	To 0.5% final**

\* If using diluents other than standard diluent HB, users must establish their own control ranges.

\*\* At least 0.5% final BSA is recommended to stabilize analytes and reduce adsorption to labware.

## Reconstitute Standards and Quality Controls

This procedure prepares enough standard to run each dilution in duplicate.

**Note:** The appearance of the lyophilized standards or controls may vary from a white pellet to clear crystals. Regardless of appearance, the vials have passed QC specifications and perform accordingly.

1. Gently tap the vial containing the lyophilized standards on a solid surface to ensure the pellet is at the bottom of the vial.
2. Reconstitute a single vial of standards with **781 µl** of the appropriate diluent. Optional: at the same time, reconstitute the controls vial with **250 µl** of the appropriate diluent as summarized in Table 4. **Controls do not require further dilution.**
3. **Vortex** the reconstituted standards and controls at medium speed for **5 sec**, then incubate **on ice for 30 min**. It is important that reconstitution of standards and controls is started and ended at the same time. Be consistent with this incubation time to ensure optimal assay performance and reproducibility.

- During the incubation period, prepare the samples as instructed in the Prepare Samples section.

### Prepare the Standard Dilution Series

The following procedure produces an eight-point standard curve with a fourfold dilution between each point. Pipet carefully using calibrated pipets and use a new pipet tip for every volume transfer.

- Label eight 1.5 ml polypropylene tubes S2 through S8 and Blank. Alternatively, using Titer tube<sup>®</sup> micro test tubes may prove to be more convenient if a multichannel pipet will be used to load the plate.
- Add **150 µl** of the appropriate diluent to tubes S2–S8 (Figure 3).
- Vortex** reconstituted standards at medium speed for **5 sec** before removing any volume. Transfer **50 µl** to the S2 tube containing the chosen standard diluent. **Vortex** for **5 sec**.
- Use a new pipet tip to transfer **50 µl** from the S2 tube to the S3 tube. **Vortex** for **5 sec**.
- Continue with 1:4 (fourfold) serial dilutions as shown in Figure 3.
- Use reconstituted and diluted standards and controls immediately. Do not freeze for future use.

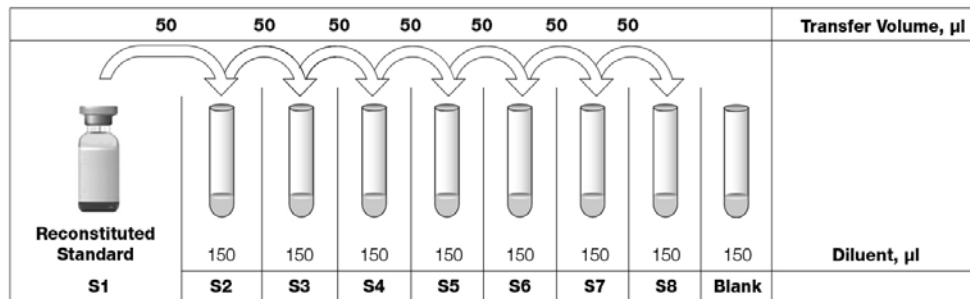


Fig. 3. Preparing a fourfold dilution series with a single reconstituted standard.

## 6. Prepare Samples

General guidelines for preparing different sample types are provided here. For more information, consult publications listed in Bio-Rad bulletin #5297, available for download at [www.bio-rad.com](http://www.bio-rad.com), or contact Bio-Rad Technical Support.

- Once thawed, keep samples on ice. Prepare dilutions just prior to the start of the assay and equilibrate to room temperature before use
- Prepare sample dilutions in microcentrifuge tubes. Alternatively, if a multichannel pipet will be used to load the plate, then aliquot the required volumes into Titer tube® micro test tubes
- Do not freeze diluted samples

**Table 5. Summary of recommended sample diluents and dilution factors.**

Sample Type	Diluent	Add BSA	Sample Dilution*
Serum and plasma	Sample diluent HB	None	Fourfold (1:4)
Culture media, with serum	Culture media	None	User optimized (neat to 1:10)
Culture media, serum-free	Culture media	To 0.5% final*	User optimized (neat to 1:10)
Lavage, sputum, other fluids	Sample diluent HB	To 0.5% final*	User optimized (neat to 1:10)
Lysate	Sample diluent HB	To 0.5% final*	User optimized (at least 1:2 for 200–900 µg/ml final protein)

\* At least 0.5% final BSA is recommended to stabilize analytes and reduce adsorption to labware.

### Serum and Plasma

**Note:** If using plasma, EDTA or citrate is preferred as an anticoagulant. Heparin-treated plasma, while compatible with Bio-Plex Pro™ assays, may absorb certain soluble proteins of interest. Avoid using hemolyzed samples as this may lead to false positive results.

1. Draw whole blood into collection tubes containing anticoagulant. Invert tubes several times to mix.
2. For serum, allow blood to clot at room temperature for **30 to 45 min.** For plasma, proceed directly to the centrifugation steps.

3. Perform centrifugation at 1,000 x g for **15 min** at 4°C and transfer the serum or plasma to a clean polypropylene tube.
4. To completely remove platelets and precipitates, centrifuge again at 10,000 x g for **10 min** at 4°C. Alternatively, filter the samples with a 0.8/0.2 µm dual filter to prevent clogging.
5. Dilute samples fourfold (1:4) by adding 1 volume of sample to 3 volumes of Bio-Plex® sample diluent HB (for example, **40 µl** sample + **120 µl** sample diluent HB).
6. Assay samples immediately or aliquot into single-use tubes and store at -70°C. Avoid repeated freeze-thaw cycles.

### Cell Culture Supernatant

1. Collect supernatants and centrifuge at 1,000 x g for **15 min** at 4°C. For cell lines cultured in serum-free culture media, collect samples and add BSA as a carrier protein to a final concentration of at least 0.5% to stabilize protein analytes and to prevent adsorption to labware.
2. Transfer to a clean polypropylene tube. If cellular debris or precipitates are present, centrifuge again at 10,000 x g for **10 min** at 4°C.
3. We recommend testing undiluted samples first. If high levels of analyte are expected, samples can be further diluted in culture medium. Rarely would samples need to be diluted greater than 1:10.
4. Assay immediately or store samples in single-use aliquots at -70°C. Avoid repeated freeze-thaw cycles.

### Lavage, Sputum, and Other Biological Fluid Samples

Keep all samples on ice until ready for use. The appropriate sample dilution factor should be optimized by the user.

1. If required, dilute the sample in Bio-Plex sample diluent with BSA added to a final concentration of 0.5%.
2. Centrifugation at 10,000 x g for **10 min** at 4°C may be required to clarify the sample.

## Lysates

The Bio-Plex cell lysis kit is required for lysate preparation (available separately, catalog #171-304011 and #171-304012). Refer to bulletin #5297 for a list of published articles on cytokine analysis in tissue samples.

1. Prepare the cell or tissue lysates according to the instructions provided with the Bio-Plex cell lysis kit. The protease inhibitors factor I and factor II are included in the kit. PMSF needs to be added to lysis buffer at a final concentration of 2 mM. The lysates should be free of particulate matter.
2. Determine the total protein concentration of the lysate. It may be necessary to test lyse your samples with different volumes of lysing solution to obtain the specified protein concentration range.
3. Dilute at least 1:2 in sample diluent + 0.5% BSA, to a final protein concentration of 200–900 µg/ml. For analytes with high expression, a lysate protein concentration as low as 50 µg/ml may be sufficient.

**Note:** For optimum antibody binding during sample incubation, it is important to dilute lysates as much as possible to reduce the detergent concentration.

4. If the lysate is not tested immediately, store at –20°C to –70°C. Avoid repeated freeze-thaw cycles.

## 7. Prepare Coupled Beads

1. Use Tables 6–7 or the Calculation Worksheet on page 36 to calculate the volume of coupled beads and assay buffer needed to prepare a 1x stock.
2. Add the required volume of Bio-Plex® assay buffer to a 15 ml polypropylene tube.

3. **Vortex** the 20x stock of coupled beads at medium speed for **30 sec**. Carefully open the cap and pipet any liquid trapped in the cap back into the tube. This is important to ensure maximum bead recovery. **Do not centrifuge the vial**; doing so will cause the beads to pellet.

4. Dilute coupled beads to 1x by pipetting the required volume into the 15 ml tube. **Vortex**.

Each well of the assay requires 2.5  $\mu\text{l}$  of the 20x stock adjusted to a final volume of 50  $\mu\text{l}$  in assay buffer.

5. Protect the beads from light with aluminum foil. Equilibrate to room temperature prior to use.

**Note:** To minimize volume loss, use a 200–300  $\mu\text{l}$  capacity pipet to remove beads from the 20x stock tube. If necessary, perform the volume transfer in two steps. Do not use a 1,000  $\mu\text{l}$  capacity pipet and/or wide bore pipet tip.

Preparing 1x coupled beads from 20x stock (includes 20% excess volume)

Table 6. Premixed panel or one singleplex assay.

# of Wells	20x Beads, $\mu\text{l}$	Assay Buffer, $\mu\text{l}$	Total Volume, $\mu\text{l}$
96	288	5,472	5,760
48	144	2,736	2,880

Table 7. Mixing singleplex assays.

# of Wells	20x Beads, $\mu\text{l}$ Singleplex #1	20x Beads, $\mu\text{l}$ Singleplex #2	Assay Buffer, $\mu\text{l}$	Total Volume, $\mu\text{l}$
96	288	288	5,184	5,760
48	144	144	2,592	2,880

## 8. Run Assay

### Considerations

- Bring all assay components and samples to room temperature before use
- Use calibrated pipets and pipet carefully, avoiding bubbles
- Pay close attention to vortexing, shaking, and incubation instructions. Deviation from the protocol may result in low assay signal and assay variability
- Assay incubations are carried out on a shaker at **850 ± 50 rpm** at room temperature (RT). Cover the plate with sealing tape and **protect from light** with aluminum foil

**Table 8. Summary of wash options and protocols.** After each assay step, select the appropriate Bio-Plex Pro™ wash station program or perform the appropriate manual wash step as summarized below.

Assay Step	Bio-Plex Pro or Pro II Wash Station	Bio-Plex Pro II Wash Station	Handheld Magnet or Vacuum Manifold
	Magnetic Program	Vacuum Program	Manual Wash Steps
Add beads to plate	MAG x2	VAC x2	2 x 100 µl
Sample incubation			
Detection Ab incubation	MAG x3	VAC x3	3 x 100 µl
SA-PE incubation			

### Considerations When Using a Vacuum Manifold

- After each incubation, place the filter plate on a calibrated vacuum apparatus and remove the liquid by vacuum filtration
- To wash, add 100 µl wash buffer to each well and remove the liquid as before. Ensure that all wells are exposed to the vacuum
- Thoroughly blot the bottom of the filter plate with a clean paper towel between each vacuum step to prevent cross contamination
- Place the assay plate on the plastic plate holder/tray as needed
- Before each incubation, gently cover the plate with a new sheet of sealing tape. Avoid pressing down on the wells to prevent leaking from the bottom

## Add Coupled Beads, Samples, Standards, Blank, and Controls

1. Cover unused wells of the assay plate with sealing tape.
2. Prewet the filter plate. Skip this step if using a flat bottom plate.  
Prewet the wells with **100 µl** assay buffer and remove the liquid by vacuum filtration. Dry the bottom of the filter plate thoroughly by blotting on a clean paper towel.
3. **Vortex** the diluted (1x) beads for **30 sec** at medium speed. Pour into a reagent reservoir and transfer **50 µl** to each well of the assay plate.

**Tip:** A multichannel pipet is highly recommended for ease of use and efficiency.

4. **Wash the plate two times** with **100 µl** Bio-Plex® wash buffer per well, using the wash method of choice.
5. **Vortex** the diluted samples, standards, blank, and controls at medium speed for **5 sec**. Transfer **50 µl** of each to the appropriate well of the assay plate, changing the pipet tip after every volume transfer.
6. **Cover** plate with a new sheet of sealing tape and protect from light with aluminum foil. **Incubate** on shaker at **850 ± 50 rpm** for **1 hr** at RT.

**Note:** Be consistent with this incubation time and shaker setting for optimal assay performance and reproducibility.

## Prepare and Add Detection Antibodies

1. While the samples are incubating use Tables 9 and 10 or the Calculation Worksheet on page 36 to calculate the volume of detection antibodies and Bio-Plex detection antibody diluent HB needed to prepare a 1x stock. Detection antibodies should be prepared **10 min before use**.
2. Add the required volume of Bio-Plex detection antibody diluent HB to a 15 ml polypropylene tube.
3. **Vortex** the 20x stock of detection antibodies for **15–20 sec** at medium speed, then perform a **30 sec** spin to collect the entire volume at the bottom of the tube.

4. Dilute detection antibodies to 1x by pipetting the required volume into the 15 ml tube. **Vortex**.

Each well of the assay requires 1.25  $\mu\text{l}$  of the 20x stock adjusted to a final volume of 25  $\mu\text{l}$  in detection antibody diluent.

Preparing 1x detection antibodies from 20x stock (includes 25% excess volume)

Table 9. Premixed panel or one singleplex assay.

# of Wells	20x Detection Antibodies, $\mu\text{l}$	Detection Antibody Diluent, $\mu\text{l}$	Total Volume, $\mu\text{l}$
96	150	2,850	3,000
48	75	1,425	1,500

Table 10. Mixing singleplex assays.

# of Wells	20x Detection Antibodies, $\mu\text{l}$ Singleplex #1	20x Detection Antibodies, $\mu\text{l}$ Singleplex #2	Detection Antibody Diluent, $\mu\text{l}$	Total Volume, $\mu\text{l}$
96	150	150	2,700	3,000
48	75	75	1,500	1,500

5. After incubating the beads, samples, standards, blank, and controls, slowly remove and discard the sealing tape.
6. **Wash the plate three times** with 100  $\mu\text{l}$  wash buffer per well.
7. **Vortex** the diluted (1x) detection antibodies at medium speed for **5 sec**. Pour into a reagent reservoir and transfer **25  $\mu\text{l}$**  to each well of the assay plate using a multichannel pipet.
8. **Cover** plate with a new sheet of sealing tape and protect from light with aluminum foil. **Incubate** on shaker at **850  $\pm$  50 rpm** for **30 min** at RT.

### Prepare and Add Streptavidin-PE (SA-PE)

1. While detection antibodies are incubating, use Table 11 or the Calculation Worksheet on page 36 to calculate the volume of SA-PE and assay buffer needed to prepare a 1x stock. SA-PE should be prepared **10 min before use**.

2. Add the required volume of assay buffer to a 15 ml polypropylene tube.
3. **Vortex** the 100x stock of SA-PE for **5 sec** at medium speed. Perform a **30 sec** spin to collect the entire volume at the bottom of the tube.
4. Dilute SA-PE to 1x by pipetting the required volume into the 15 ml tube. **Vortex** and protect from light until ready to use.

Each well of the assay requires 0.5  $\mu\text{l}$  of the 100x stock adjusted to a final volume of 50  $\mu\text{l}$  in assay buffer.

Table 11. Preparing 1x SA-PE from 100x stock (includes 25% excess volume).

# of Wells	100x SA-PE, $\mu\text{l}$	Assay Buffer, $\mu\text{l}$	Total Volume, $\mu\text{l}$
96	60	5,940	6,000
48	30	2,970	3,000

5. After detection antibody incubation, slowly remove and discard the sealing tape.
6. **Wash the plate three times** with **100  $\mu\text{l}$**  of wash buffer per well.
7. **Vortex** the diluted (1x) SA-PE at medium speed for **5 sec**. Pour into a reagent reservoir and transfer **50  $\mu\text{l}$**  to each well using a multichannel pipet.
8. **Cover** plate with a new sheet of sealing tape and protect from light with aluminum foil. **Incubate** on shaker at **850  $\pm$  50 rpm** for **10 min** at RT.
9. After the streptavidin-PE incubation step, slowly remove and discard the sealing tape.
10. **Wash the plate three times** with **100  $\mu\text{l}$**  of wash buffer per well.
11. To resuspend beads for plate reading, add **125  $\mu\text{l}$**  assay buffer to each well. Cover the plate with a new sheet of sealing tape. Shake at room temperature at **850  $\pm$  50 rpm** for **30 sec**, and slowly remove the sealing tape. Ensure that the plate cover has been removed before placing the plate on the reader.

Table 12. Read the plate using the appropriate instrument settings.

Instrument	RP1 (PMT)	DD Gates	Bead Events
Bio-Plex 100, 200*	Low	5,000 (low), 25,000 (high)	50
Bio-Plex 3D*	Standard	Select MagPlex beads	50
Bio-Plex® MAGPIX™	N/A, use default instrument settings		

\* Or similar Luminex-based system.

## 9. Read Plate

Bio-Plex Manager™ software is recommended for all Bio-Plex Pro™ assay data acquisition and analysis. Instructions for Luminex xPONENT software are also included. For instructions using other xMAP system software packages, contact Bio-Rad Technical Support or your regional Bio-Rad field applications specialist.

### Prepare Protocol in Bio-Plex Manager Software Version 6.0 and Higher

The protocol should be prepared in advance so that the plate is read as soon as the experiment is complete.

A protocol file specifies the analytes in the assay, the plate wells to be read, sample information, the values of standards and controls, and instrument settings.

Bio-Plex Manager software versions 6.0 and higher contain protocols for most Bio-Plex® assays. Choose from available protocols or create a new protocol. To create a new protocol, select **File**, then **New** from the main menu. Locate and follow the steps under **Protocol Settings**.

1. Click **Describe Protocol** and enter information about the assay (optional).
2. Click **Select Analytes** and create a new panel. Visually confirm the selected analytes and proceed to step 3.

- a. Click **Add Panel**  in the **Select Analytes** toolbar. Enter a new panel name. Select **Bio-Plex Pro Assay Magnetic** from the assay dropdown list. If using Bio-Plex Manager version 5.0 or lower, select MagPlex from the assay dropdown list.
- b. Click **Add**. Enter the bead region number and name for the first analyte. Click **Add Continue** to repeat for each analyte in the assay. Refer to the bead regions in parentheses ( ) listed on the peel-off label provided with the standards.

For reference, bead regions are shown in Table 13.

- c. Click **Add** when the last analyte has been added and click **OK** to save the new panel.
- d. Highlight analytes from the **Available** list (left) and move to the **Selected** list (right) using the **Add** button. To move all analytes at once, simply click **Add All**.
- e. If some of the analytes need to be removed from the **Selected** list, highlight them and select **Remove**. If desired, it is possible to rename the panel by clicking **Rename Panel** and entering a new panel name.

Table 13. Bead regions for the human chemokine panel.

Analyte	Bead Region	Analyte	Bead Region	Analyte	Bead Region
6Ckine/CCL21	12	IL-1 $\beta$	39	MDC/CCL22	29
BCA-1/CXCL13	74	IL-2	38	MIF	35
CTACK/CCL27	72	IL-4	52	MIG/CXCL9	14
ENA-78/CXCL5	73	IL-6	19	MIP-1 $\alpha$ /CCL3	55
Eotaxin/CCL11	43	IL-8/CXCL8	54	MIP-1 $\delta$ /CCL15	66
Eotaxin-2/CCL24	30	IL-10	56	MIP-3 $\alpha$ /CCL20	62
Eotaxin-3/CCL26	65	IL-16	27	MIP-3 $\beta$ /CCL19	76
Fractalkine/CX3CL1	77	IP-10/CXCL10	48	MPIF-1/CCL23	37
GCP-2/CXCL6	15	I-TAC/CXCL11	25	SCYB16/CXCL16	64
GM-CSF	34	MCP-1/CCL2	53	SDF-1 $\alpha$ + $\beta$ /CXCL12	22
Gro- $\alpha$ /CXCL1	61	MCP-2/CCL8	57	TARC/CCL17	67
Gro- $\beta$ /CXCL2	78	MCP-3/CCL7	26	TECK/CCL25	46
I-309/CCL1	20	MCP-4/CCL13	28	TNF- $\alpha$	36
IFN- $\gamma$	21				

**Note:** Do not use preset panels found in Bio-Plex Manager software version 5.0 or earlier, as the bead regions are not up to date.

3. Click **Format Plate** and format the plate according to the plate layout created in section 1 (Plan Plate Layout). To modify the plate layout, follow the steps below (see Figure 4).
  - a. Select the **Plate Formatting** tab.
  - b. Select the standards icon (S) and drag the cursor over all the wells that contain standards. Repeat this process for Blanks (B), Controls (C), and Samples (X). Note that Bio-Plex Manager automatically subtracts the blank MFI value from all other assay wells.
4. Click **Enter Standards Info** in the Protocol Settings bar.
  - a. Enter the highest concentration of each analyte in the top row (labeled S1) of the table. S1 concentration information is included with each vial of standards.

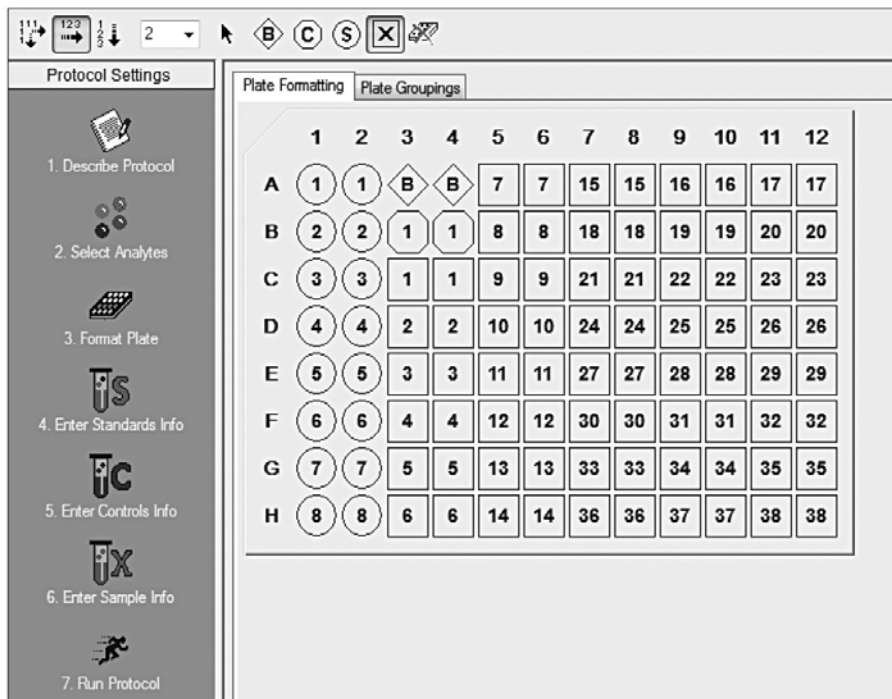


Fig. 4. Plate formatting.

- b. Enter a dilution factor of 4 and click **Calculate**. The concentrations for each standard point will be populated for all analytes in the table.
    - c. Optional: enter the lot number of the vial of standards into the **Standard Lot** box and click **Save**.
  5. Click **Enter Controls Info**.
    - a. For user-specified controls, select an analyte from the dropdown menu, then enter a description and concentration. Repeat for each additional analyte in the assay.
    - b. **For the quality controls supplied with the 40-plex fixed panel only**, format the appropriate wells as controls, enter descriptions, but leave the concentrations blank. Alternatively, the quality controls can be formatted as samples with clear descriptions such as “quality control high” and “quality control low.” In any case, **the expected control ranges provided are not entered into Bio-Plex Manager software version 6.1 and earlier**.
  6. Click **Enter Sample Info** and enter sample information and the appropriate dilution factor.
  7. Click **Run Protocol** and confirm that the assay settings are correct.
    - a. Refer to Table 12 for the recommended RP1 (PMT) setting. Protocols using alternative PMT settings should be validated by the end user.
    - b. Confirm that data acquisition is set to **50 beads per region**. In Advanced Settings, confirm that the bead map is set to **100 region**, the sample size is set to **50 µl**, and the doublet discriminator (DD) gates are set to **5,000 (Low)** and **25,000 (High)**. In Bio-Plex Manager software versions 4.0, 4.1, 4.1.1, and 5.0, check **Override Gates** and set the DD gate values as indicated. Select **Start**, name and save the .rbx file, and begin data acquisition. The Run Protocol pop-up screen will appear. Click **Eject/Retract** to eject the plate carrier.

## Acquire Data

1. Shake the assay plate at **850 ± 50 rpm** for **30 sec**, and visually inspect the plate to ensure that the assay wells are filled with buffer. Slowly remove the sealing tape and any plate cover before placing the plate on the plate carrier.
2. Click **Run Protocol** and on the pop-up screen, select **Load Plate** and click **OK** to start acquiring data.
3. Use the **Wash Between Plates**  command after every plate run to reduce the possibility of clogging the instrument.
4. If acquiring data from more than one plate, empty the waste bottle and refill the sheath bottle after each plate (if HTF are not present). Select **Wash Between Plates** and follow the instructions. Then repeat the Prepare Protocol and Acquire Data instructions.
5. When data acquisition is complete, select **Shut Down**  and follow the instructions.

## Reacquire Data

It is possible to acquire data from a well or plate a second time using the **Rerun/Recovery** mode located below Start in the Run Protocol step. Any previous data will be overwritten.

1. Check the wells from which data will be reacquired.
2. Aspirate the buffer with the wash method of choice, but do not perform the wash step.
3. Add **100 µl** of assay buffer to each well. Cover the plate with a new sheet of sealing tape. Shake the plate at **850 ± 50 rpm** for **30 sec**. Slowly remove the sealing tape before placing the plate on the plate reader.
4. Repeat the **Acquire Data** steps to reacquire data. The data acquired should be similar to those acquired initially; however, the acquisition time will be extended because the wells have fewer beads.

## Data Analysis

### Quality Controls

If the quality controls were run in the assay plate, open the results (.rbx) file, click on **Report Table**, and locate the control wells. Visually compare the observed concentrations of the high and low controls in the Report Table against the lot-specific control ranges shown in the product data sheet.

**Note:** Expected control ranges are provided for reference and should be used as general guidelines. Actual results may vary for some operators. If the controls do not fall within the expected ranges, please refer to the troubleshooting section for possible causes and solutions.

### Removing Outliers

Outliers are identified as standard data points that do not meet accuracy or precision requirements and should be considered invalid when performing curve fitting. As such, they should be removed to generate a more realistic and accurate standard curve. This may result in an extended assay working range and allow quantitation of samples that might otherwise be considered out of range.

In Bio-Plex Manager software version 6.0 and higher, outliers can be automatically removed by selecting the **Optimize** button in the Standard Curve window. In Bio-Plex Manager software 5.0 and earlier versions, outliers also can be manually selected in the Report Table. Visit online Help to learn more about the standard curve optimizer feature and how outliers are determined.

### Previous Versions of Bio-Plex Manager Software

For instructions on using previous versions of Bio-Plex Manager software, please contact Bio-Rad Technical Support.

## Luminex xPONENT Software

Although guidelines are provided here, consult the xPONENT software manual for more details. Perform a system initialization with Luminex's calibration and performance verification kit, as directed by Luminex. Select **Batches** to set up the protocol and follow the information under **Settings**.

**Note:** The instrument settings described below apply to Luminex 100/200 and FLEXMAP 3D or Bio-Plex® 3D instruments. For the Bio-Plex® MAGPIX™ reader, use the default instrument settings.

1. Select **MagPlex** as the bead type for magnetic beads, which automatically sets the DD gates.
2. Volume = 50 µl.
3. Refer to Table 12 to select the appropriate PMT setting for your instrument.
4. Plate name: 96-well plate.
5. Analysis type: Quantitative, 5PL Curve Fit.
6. Number of standards: 8.

Select **Analytes** to set up the panel.

1. Enter **pg/ml** in the Units field.
2. Enter **50** in the **Count** field.
3. Select the bead region and enter the analyte name.
4. Click **Apply all** for Units and Count.

Select **Stds and Ctrl.**

1. Enter standard concentrations, lot number, dilution factor, and other information as applicable.

After the assay is complete, select **Results**, then select **Saved Batches**.

## Troubleshooting Guide

This troubleshooting guide addresses problems that may be encountered with Bio-Plex Pro™ assays. If you experience any of the problems listed below, review the possible causes and solutions provided. Poor assay performance may also be due to the Bio-Plex® suspension array reader. To eliminate this possibility, use the validation kit to assist in determining if the array reader is functioning properly.

### Possible Causes

#### High Inter-Assay CV

Standards and controls were not reconstituted consistently between assays

Reconstituted standards, controls, and diluted samples were not stored properly

Bottom of filter plate not dry

### Possible Solutions

Incubate the reconstituted standards for 30 min on ice. Always be consistent with the incubation time and temperature.

Reconstituted standards and diluted samples should be prepared on ice as instructed. Prior to plating, the reconstituted standards and diluted samples should be equilibrated to room temperature.

Dry the bottom of the filter plate with absorbent paper towel (preferably lint-free) to prevent cross-well contamination.

**Possible Causes**

**High Intra-Assay CV**

Improper pipetting technique

Reagents and assay components not equilibrated to room temperature prior to pipetting

Contamination with wash buffer during wash steps

Slow pipetting of samples and reagents across the plate

Bio-Plex wash station: insufficient washing due to clogged pins

**Possible Solutions**

Pipet carefully when adding standards, controls, samples, detection antibodies, and streptavidin-PE, especially when using a multichannel pipet. Use a calibrated pipet. Change pipet tip after every volume transfer.

All reagents and assay components should be equilibrated to room temperature prior to pipetting.

During the wash steps, be careful not to splash wash buffer from one well to another. Be sure that the wells are filtered completely and that no residual volume remains. Ensure that the microplate shaker setting is not too high. Reduce the microplate shaker speed to minimize splashing

Sample pipetting across the entire plate should take less than 4 min. Reagent pipetting across the entire plate should take less than 1 min.

Clean dispensing pins with the thicker of the two cleaning needles provided with washer. Perform regular rinses to minimize salt buildup.

**Possible Causes****Low Bead Count**

Miscalculation of bead dilution

Beads clumped in multiplex bead stock tube

Vacuum on for too long when aspirating buffer from wells

Assay plate not shaken enough during incubation steps and prior to reading

Reader is clogged

Incorrect needle height of the reader

**Low Signal or Poor Sensitivity**

Standards reconstituted incorrectly

Detection antibody or streptavidin-PE diluted incorrectly

**Possible Solutions**

Check your calculations and be careful to add the correct volumes.

Vortex for 30 sec at medium speed before aliquoting beads.

Do not apply vacuum to the filter plate for longer than 10 sec after the buffer is completely drained from each well.

Shake the plate at  $850 \pm 50$  rpm during incubation steps and for 30 sec immediately before reading the plate.

Refer to the troubleshooting guide in the Bio-Plex System Hardware Instruction Manual (bulletin #10005042).

Adjust the needle height to coincide with the plate type provided in the kit.

Follow the standard preparation instructions carefully.

Check your calculations and be careful to add the correct volumes.

### Possible Causes

#### High Background Signal

Incorrect buffer was used for (example, assay buffer used to dilute standards)

Accidentally spiked blank wells

Detection antibodies or streptavidin-PE incubated too long

#### Poor Recovery

Expired Bio-Plex reagents were used

Incorrect amounts of components were added

Microplate shaker set to an incorrect speed

High end saturation of the standard curve

Quality controls do not fall within expected ranges

### Possible Solutions

Use standard diluent or diluent similar to final sample matrix to dilute standards.

Do not add any antigens to the blank wells.

Follow the procedure incubation time precisely.

Check that reagents have not expired. Use new or nonexpired components.

Check your calculations and be careful to add the correct volumes.

Check the microplate shaker speed and use the recommended setting. Setting the speed too high may cause splashing and contamination. Use the recommended plate shaker. Setting the speed too low may cause low assay signal and false plateau or high end saturation of standard curves.

Make sure that correct shaker speed and incubation times are used. Remove S1 for data analysis if needed.

Make sure that the controls are reconstituted at the same time as standards and in the same diuent (standard diluent HB). Incubate for precisely 30 min.

## Possible Causes

### Poor Recovery

Improper pipetting technique

### Impact of Sample Matrix

Negative MFI values in samples or standards

Poor precision in serum and plasma sample measurements

## Possible Solutions

Pipet carefully when adding standards, samples, detection antibodies, and streptavidin-PE, especially when using a multichannel pipet. Use a calibrated pipet. Change pipet tip after every volume transfer.

If samples contain little or no analyte, negative values observed may be due to statistical variation. If assay drift is suspected, retest the samples by positioning them next to the standards. If contamination of standards is suspected, check the standard replicate value and be careful when adding samples to the wells. Matrix effects could also produce negative sample values.

Bio-Plex Manager™ software automatically subtracts the Blank (B) MFI value from all other assay wells. While this has no impact on observed concentrations of samples within the assay working range, it may result in a negative MFI value if the Blank's MFI value is greater than either the standard or the sample value. If this is undesirable, then reformat the blank wells as Sample (X) or Control (C) in the protocol or results file.

Check if any interfering components, additives, or gel from separators were introduced into the samples. Avoid using hemolyzed and heavily lipemic samples. Remove visible particulate in samples by centrifugation. Avoid multiple freeze-thaw cycles of samples.

## Appendix: Non-Human Primate (NHP) Cross-Reactivity

The human chemokine assays were found to be cross-reactive with two common NHP species, cynomolgus (Cyno) macaque and rhesus macaque. Other NHP species were not tested. The degree of cross-reactivity was determined based on the ability of each assay to detect native analyte in serum, plasma and/or culture media from mitogen stimulated peripheral blood mononuclear cells (PBMC).

Assay signal (MFI) for the most highly cross-reactive samples were compared against the human standard curve and scored as shown in the Table 14.

**Table 14. NHP cross-reactivity of the human chemokine assays.**

Analyte	Cyno	Rhesus	Analyte	Cyno	Rhesus
6Ckine/CCL21	–	–	IL-8	+++	+++
BCA-1/CXCL13	+++	+++	IP-10/CXCL10	+++	+++
CTACK/CCL27	–	–	I-TAC/CXCL11	+++	+++
ENA-78/CXCL5	+	+	MCP-1/CCL2	+++	+++
Eotaxin/CCL11	+	+	MCP-2/CCL8	++	++
Eotaxin-2/CCL24	–	–	MCP-3/CCL7	–	–
Eotaxin-3/CCL-26	–	–	MCP-4/CCL13	+++	+++
Fractalkine/CX3CL1	+++	+	MDC/CCL22	+	–
GCP-2/CXCL6	–	–	MIF	+++	+++
GM-CSF	+++	+++	MIG/CXCL9	–	–
Gro- $\alpha$ /CXCL1	–	–	MIP-1 $\alpha$ /CCL3	+++	+++
Gro- $\beta$ /CXCL2	+	+	MIP-1 $\delta$ /CCL15	–	+
I-309/CCL1	–	–	MIP-3 $\alpha$ /CCL20	–	–
IFN- $\gamma$	–	–	MIP-3 $\beta$ /CCL19	++	++
IL-10	+++	+++	MPIF-1/CCL23	–	–
IL-16	+	+	SCYB16/CXCL16	–	+
IL-1 $\beta$	+++	+++	SDF-1 $\alpha$ + $\beta$ /CXCL12	+	+
IL-2	–	–	TARC/CCL17	–	–
IL-4	++	+	TECK/CCL25	+	+
IL-6	+++	+++	TNF- $\alpha$	+	–

– No NHP cross-reactivity observed. Assay signal below S6 on the standard curve.

+ Some NHP cross-reactivity observed. Assay signal above S6.

++ Moderate NHP cross-reactivity observed. Assay signal above S5.

+++ Strong NHP cross-reactivity observed. Assay signal above S3.



## Calculation Worksheet

If using either a **premixed panel or one singleplex assay**, follow these directions.

Plan the plate layout and enter the number of wells to be used in the assay: \_\_\_\_\_  
1

### 1. Determine the volume of 1x coupled beads needed.

- Each well requires 50  $\mu\text{l}$  of coupled beads (1x): \_\_\_\_\_ x 50  $\mu\text{l}$  = \_\_\_\_\_  $\mu\text{l}$   
1 2
- Include 20% excess to ensure enough volume: \_\_\_\_\_  $\mu\text{l}$  x 0.20 = \_\_\_\_\_  $\mu\text{l}$   
2 3
- Total volume of 1x coupled beads: \_\_\_\_\_  $\mu\text{l}$  + \_\_\_\_\_  $\mu\text{l}$  = \_\_\_\_\_  $\mu\text{l}$   
2 3 4
- Volume of **20x coupled beads** required: \_\_\_\_\_  $\mu\text{l}/20$  = \_\_\_\_\_  $\mu\text{l}$   
4 5
- Volume of **assay buffer** required: \_\_\_\_\_  $\mu\text{l}$  - \_\_\_\_\_  $\mu\text{l}$  = \_\_\_\_\_  $\mu\text{l}$   
4 5 6

### 2. Determine the volume of 1x detection antibody needed.

- Each well requires 25  $\mu\text{l}$  detection antibodies (1x): \_\_\_\_\_ x 25  $\mu\text{l}$  = \_\_\_\_\_  $\mu\text{l}$   
1 7
- Include 25% excess to ensure enough volume: \_\_\_\_\_  $\mu\text{l}$  x 0.25 = \_\_\_\_\_  $\mu\text{l}$   
7 8
- Total volume of 1x detection antibodies: \_\_\_\_\_  $\mu\text{l}$  + \_\_\_\_\_  $\mu\text{l}$  = \_\_\_\_\_  $\mu\text{l}$   
7 8 9
- Volume of **20x detection antibodies** required: \_\_\_\_\_  $\mu\text{l}/20$  = \_\_\_\_\_  $\mu\text{l}$   
9 10
- Volume of **detection antibody diluent** required: \_\_\_\_\_  $\mu\text{l}$  - \_\_\_\_\_  $\mu\text{l}$  = \_\_\_\_\_  $\mu\text{l}$   
9 10 11

### 3. Determine the volume of 1x streptavidin-PE needed.

- Each well requires 50  $\mu\text{l}$  streptavidin-PE (1x): \_\_\_\_\_ x 50  $\mu\text{l}$  = \_\_\_\_\_  $\mu\text{l}$   
1 12
- Include 25% excess to ensure enough volume: \_\_\_\_\_  $\mu\text{l}$  x 0.25 = \_\_\_\_\_  $\mu\text{l}$   
12 13
- Total volume of 1x streptavidin-PE: \_\_\_\_\_  $\mu\text{l}$  + \_\_\_\_\_  $\mu\text{l}$  = \_\_\_\_\_  $\mu\text{l}$   
12 13 14
- Volume of **100x streptavidin-PE** required: \_\_\_\_\_  $\mu\text{l}/100$  = \_\_\_\_\_  $\mu\text{l}$   
14 15
- Volume of **assay buffer** required: \_\_\_\_\_  $\mu\text{l}$  - \_\_\_\_\_  $\mu\text{l}$  = \_\_\_\_\_  $\mu\text{l}$   
14 15 16

If **mixing singleplex assays**, follow these directions.

Enter the number of wells to be used in the assay: \_\_\_\_\_  
1

### 1. Determine the volume of 1x coupled beads needed.

- Each well requires 50  $\mu\text{l}$  coupled beads (1x): \_\_\_\_\_ x 50  $\mu\text{l}$  = \_\_\_\_\_  $\mu\text{l}$   
1 2
- Include 20% excess to ensure enough volume: \_\_\_\_\_  $\mu\text{l}$  x 0.20 = \_\_\_\_\_  $\mu\text{l}$   
2 3
- Total volume of 1x coupled beads: \_\_\_\_\_  $\mu\text{l}$  + \_\_\_\_\_  $\mu\text{l}$  = \_\_\_\_\_  $\mu\text{l}$   
2 3 4
- Enter the number of singleplex sets (or analytes) that will be multiplexed: \_\_\_\_\_  
5
- Volume of **20x coupled beads** required from **each stock tube**:  
\_\_\_\_\_  $\mu\text{l}/20$  = \_\_\_\_\_  $\mu\text{l}$   
4 6
- Total volume of combined bead stocks: \_\_\_\_\_ x \_\_\_\_\_  $\mu\text{l}$  = \_\_\_\_\_  $\mu\text{l}$   
5 6 7
- Volume of **assay buffer** required: \_\_\_\_\_  $\mu\text{l}$  - \_\_\_\_\_  $\mu\text{l}$  = \_\_\_\_\_  $\mu\text{l}$   
4 7 8

### 2. Determine the volume of 1x detection antibody needed.

- Each well requires 25  $\mu\text{l}$  detection antibodies (1x): \_\_\_\_\_ x 25  $\mu\text{l}$  = \_\_\_\_\_  $\mu\text{l}$   
1 9
- Include 25% excess to ensure enough volume: \_\_\_\_\_  $\mu\text{l}$  x 0.25 = \_\_\_\_\_  $\mu\text{l}$   
9 10
- Total volume of 1x detection antibodies: \_\_\_\_\_  $\mu\text{l}$  + \_\_\_\_\_  $\mu\text{l}$  = \_\_\_\_\_  $\mu\text{l}$   
9 10 11
- Enter the number of singleplex sets (or analytes) that will be multiplexed: \_\_\_\_\_  
5
- Volume of **20x detection antibodies** required from **each stock tube**:  
\_\_\_\_\_  $\mu\text{l}/20$  = \_\_\_\_\_  $\mu\text{l}$   
11 12
- Total volume of combined detection antibody stock: \_\_\_\_\_  $\mu\text{l}$  x \_\_\_\_\_ = \_\_\_\_\_  $\mu\text{l}$   
12 5 13
- Volume of **detection antibody diluent** required: \_\_\_\_\_  $\mu\text{l}$  - \_\_\_\_\_  $\mu\text{l}$  = \_\_\_\_\_  $\mu\text{l}$   
11 13 14

### 3. Determine the volume of 1x streptavidin-PE needed.

- Each well requires 50  $\mu\text{l}$  streptavidin-PE (1x): \_\_\_\_\_ x 50  $\mu\text{l}$  = \_\_\_\_\_  $\mu\text{l}$   
1 15
- Include 25% excess to ensure enough volume: \_\_\_\_\_  $\mu\text{l}$  x 0.25 = \_\_\_\_\_  $\mu\text{l}$   
15 16
- Total volume of 1x streptavidin-PE: \_\_\_\_\_  $\mu\text{l}$  + \_\_\_\_\_  $\mu\text{l}$  = \_\_\_\_\_  $\mu\text{l}$   
15 16 17
- Volume of **100x streptavidin-PE** required: \_\_\_\_\_  $\mu\text{l}/100$  = \_\_\_\_\_  $\mu\text{l}$   
17 18
- Volume of **assay buffer** required: \_\_\_\_\_  $\mu\text{l}$  - \_\_\_\_\_  $\mu\text{l}$  = \_\_\_\_\_  $\mu\text{l}$   
17 18 19

## Safety Considerations

Eye protection and gloves are recommended when using these products. Consult the MSDS for additional information. The Bio-Plex Pro™ assays contain components of animal origin. This material should be handled as if capable of transmitting infectious agents. Use universal precautions. These components should be handled at Biosafety Level 2 containment as defined by U.S. government publication, *Biosafety in Microbiological and Biomedical Laboratories* (Centers for Disease Control 1999).

## Legal Notices

Acrodisc and Supor are trademarks of Pall Corporation. MagPlex, xMAP, xPONENT, FLEXMAP 3D, and Luminex are trademarks of Luminex Corporation.

The Bio-Plex® suspension array system includes fluorescently labeled microspheres and instrumentation licensed to Bio-Rad Laboratories, Inc. by the Luminex Corporation.

## References

Page 1, Introduction:

Locati M et al. (2005). Chemokines and their receptors: Roles in specific clinical conditions and measurement in the clinical laboratory. *Am J Clin Pathol* 123, S82–S95.

Slettenaar VIF and Wilson JL (2006). The chemokine network: A target in cancer biology? *Adv Drug Deliv Rev* 58, 962–974.

## Ordering Information

Detailed ordering information can be found at [www.bio-rad.com/bio-plex](http://www.bio-rad.com/bio-plex).

Catalog #	Premixed Multiplex Assay Panel
171-AK99MR2	Bio-Plex Pro Human Chemokine Panel 40-Plex, 1 x 96-well
Singleplex Set	
Various	Bio-Plex Pro Human Chemokine Singleplex Sets, 1 x 96-well (requires reagent kit III and chemokine standards to run an assay)
Individual Components and Accessories	
171-304090	Bio-Plex Pro Reagent Kit III with Filter Plate, 1 x 96-well
171-304090M	Bio-Plex Pro Reagent Kit III with Flat Bottom Plate, 1 x 96-well
171-DK0001	Bio-Plex Pro Human Chemokine Standard, pkg of 1 vial
171-DK0050	Bio-Plex Pro Human Chemokine Standard, pkg of 50 vials
171-304502	Filter Plate, 1 x 96-well with clear plastic lid and tray

### **Bio-Plex® x-Plex™ Assays (We Mix)**

Premium custom assay service using the Bio-Plex Assay Builder ([www.bio-rad.com/bio-plex/assaybuilder](http://www.bio-rad.com/bio-plex/assaybuilder)) to select analytes and plate type of interest. Assays are supplied as premixed coupled beads and detection antibodies in the all-in-one kit format. **Quality controls are not included in chemokine x-Plex kits.**

### **Bio-Plex Express Assays (You Mix)**

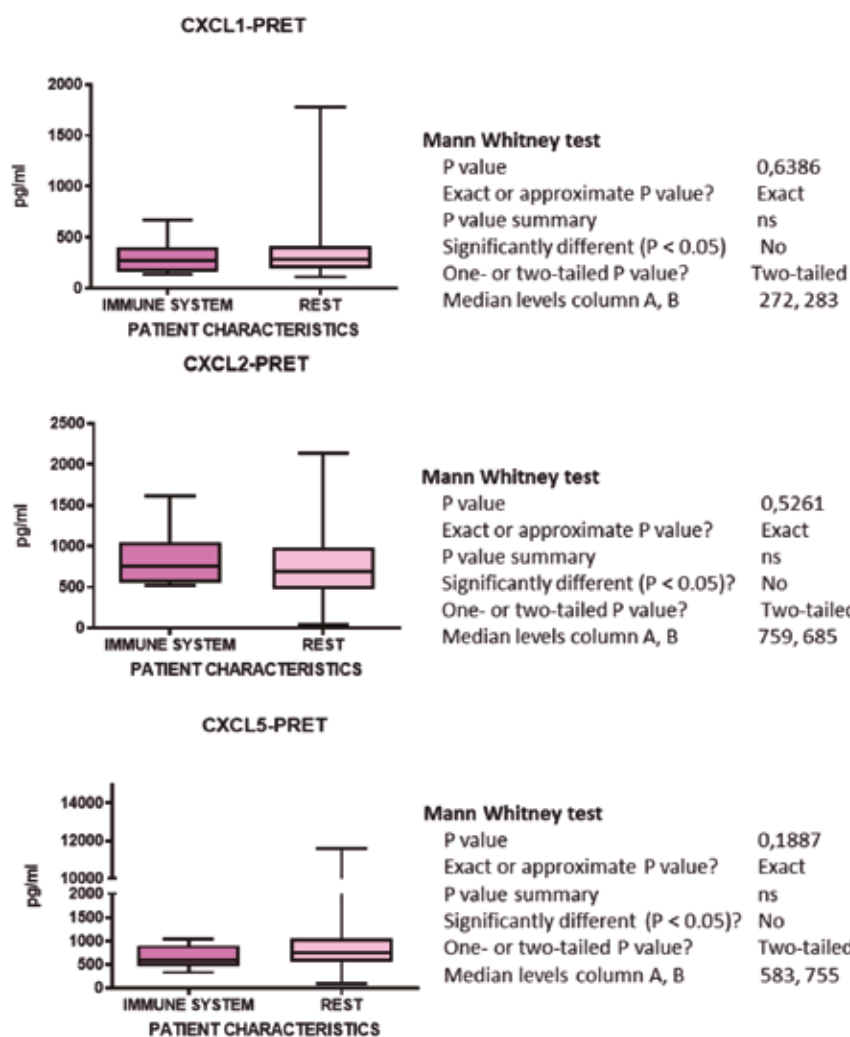
Fast and economical custom assay service using the Bio-Plex Assay Builder ([www.bio-rad.com/bio-plex/assaybuilder](http://www.bio-rad.com/bio-plex/assaybuilder)) to select analytes and plate type of interest. Assays are supplied as individual sets of coupled beads and detection antibodies in the all-in-one kit format. **Quality controls are not included in chemokine Express kits.**

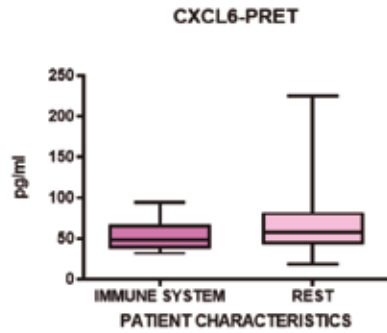
### **Other Components and Accessories**

Bio-Plex software, wash buffer, Bio-Plex Pro flat bottom plates, and streptavidin-PE are also available individually. For more information, go to [www.bio-rad.com/bio-plex](http://www.bio-rad.com/bio-plex).

## Annex IV. PRET CXC chemokines serum levels in patients with known immune system alterations vs. patients with non-reported alterations

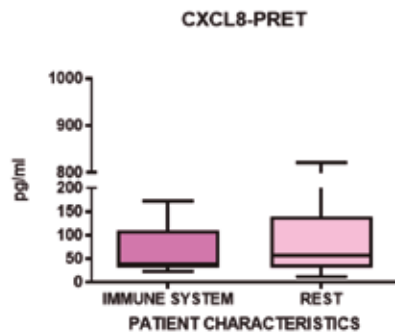
**Mann Whitney test: Non-parametric**, as CXC chemokines do not follow a Normal distribution. **Unpaired**, patients with a known alteration in the immune system [N=6] vs rest of patients with no preported alteration [N=98]





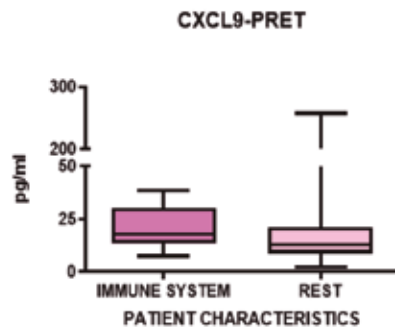
**Mann Whitney test**

P value	0,3785
Exact or approximate P value?	Exact
P value summary	ns
Significantly different (P < 0.05)?	No
One- or two-tailed P value?	Two-tailed
Median levels column A, B	49, 58



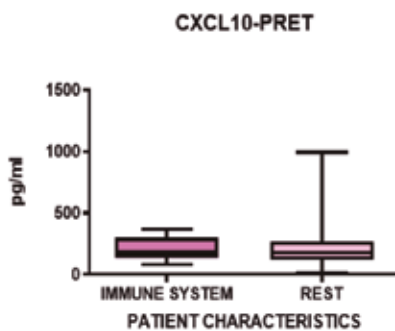
**Mann Whitney test**

P value	0,5442
Exact or approximate P value?	Exact
P value summary	ns
Significantly different (P < 0.05)?	No
One- or two-tailed P value?	Two-tailed
Median levels column A, B	39, 56



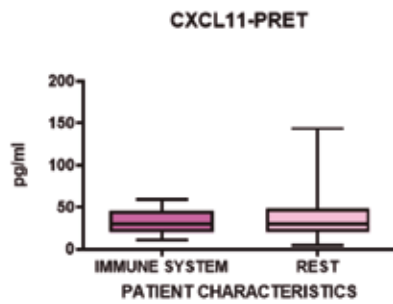
**Mann Whitney test**

P value	0,2513
Exact or approximate P value?	Exact
P value summary	ns
Significantly different (P < 0.05)?	No
One- or two-tailed P value?	Two-tailed
Median levels column A, B	18, 13



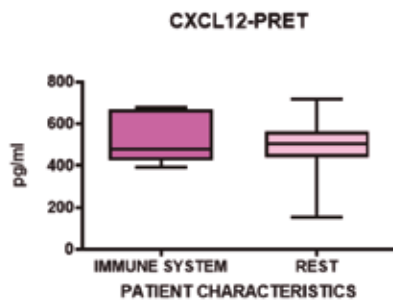
**Mann Whitney test**

P value	0,7909
Exact or approximate P value?	Exact
P value summary	ns
Significantly different (P < 0.05)?	No
One- or two-tailed P value?	Two-tailed
Median levels column A, B	182, 178



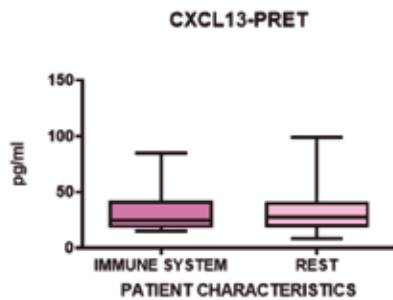
**Mann Whitney test**

P value	0,8966
Exact or approximate P value?	Exact
P value summary	ns
Significantly different (P < 0.05)?	No
One- or two-tailed P value?	Two-tailed
Median levels column A, B	30, 29



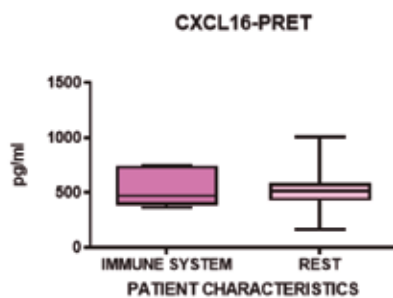
**Mann Whitney test**

P value	>0,9999
Exact or approximate P value?	Exact
P value summary	ns
Significantly different (P < 0.05)?	No
One- or two-tailed P value?	Two-tailed
Median levels column A, B	475, 502



**Mann Whitney test**

P value	0,7287
Exact or approximate P value?	Exact
P value summary	ns
Significantly different (P < 0.05)?	No
One- or two-tailed P value?	Two-tailed
Median levels column A, B	25, 28

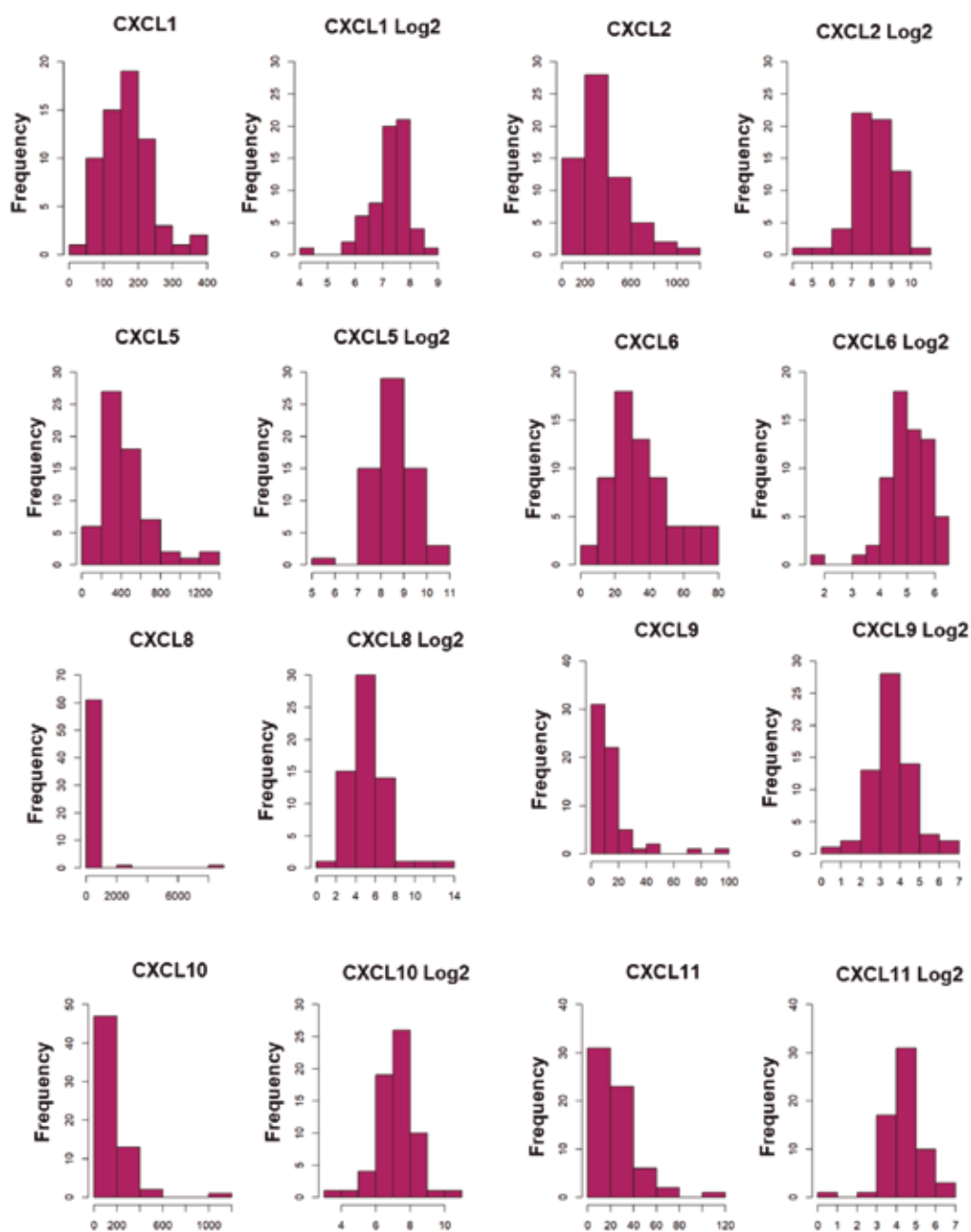


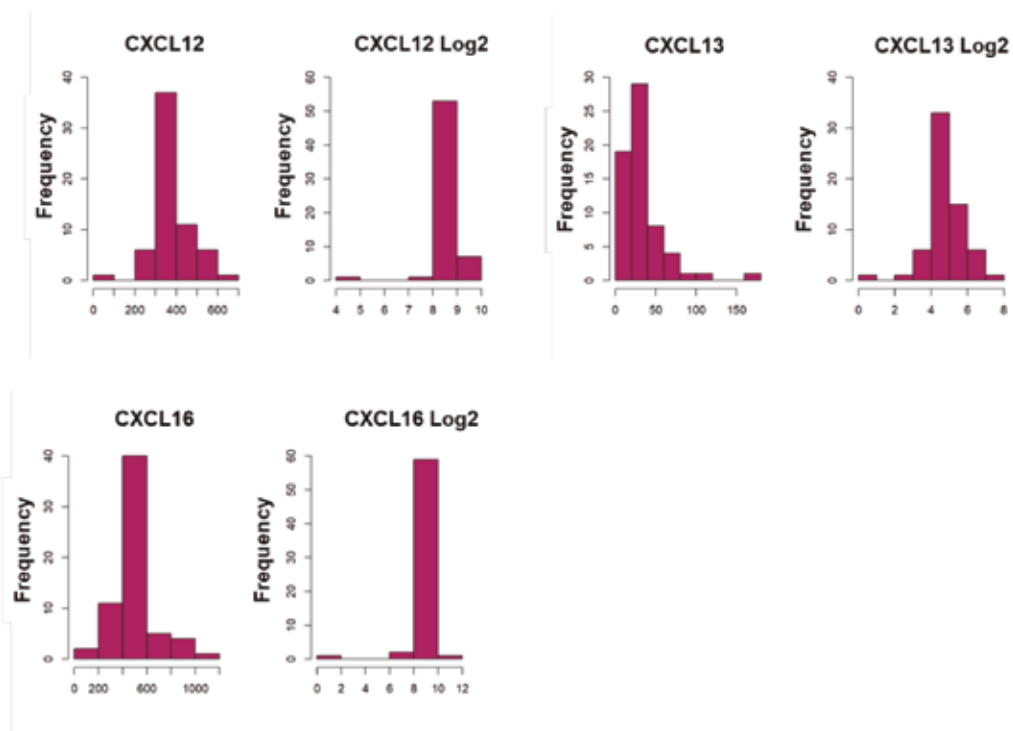
**Mann Whitney test**

P value	0,9296
Exact or approximate P value?	Exact
P value summary	ns
Significantly different (P < 0.05)?	No
One- or two-tailed P value?	Two-tailed
Median levels column A, B	471, 517

## Annex V. CXC chemokines distribution at EVAR and PROG time-points

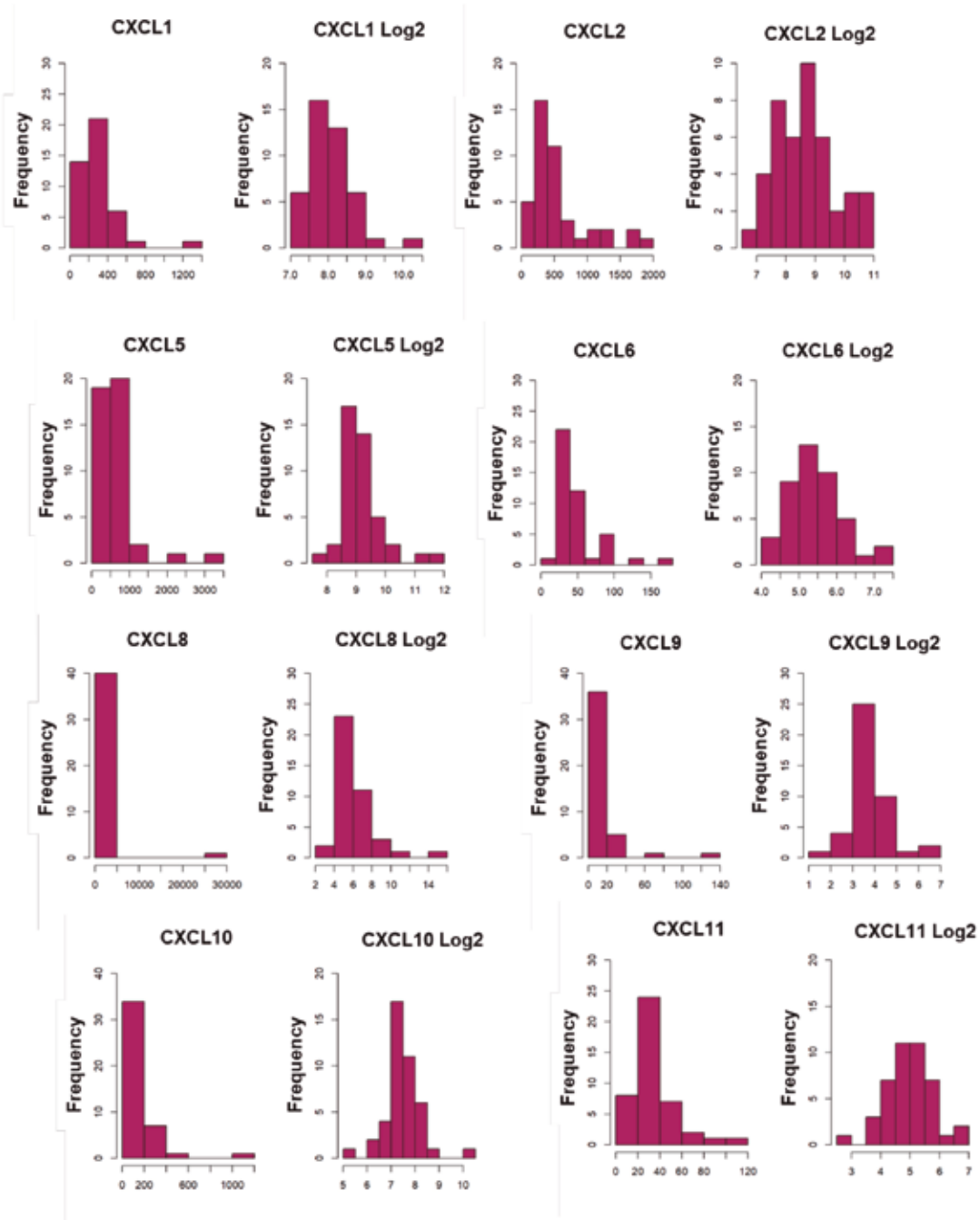
### EVAR - CXC CHEMOKINES DISTRIBUTION

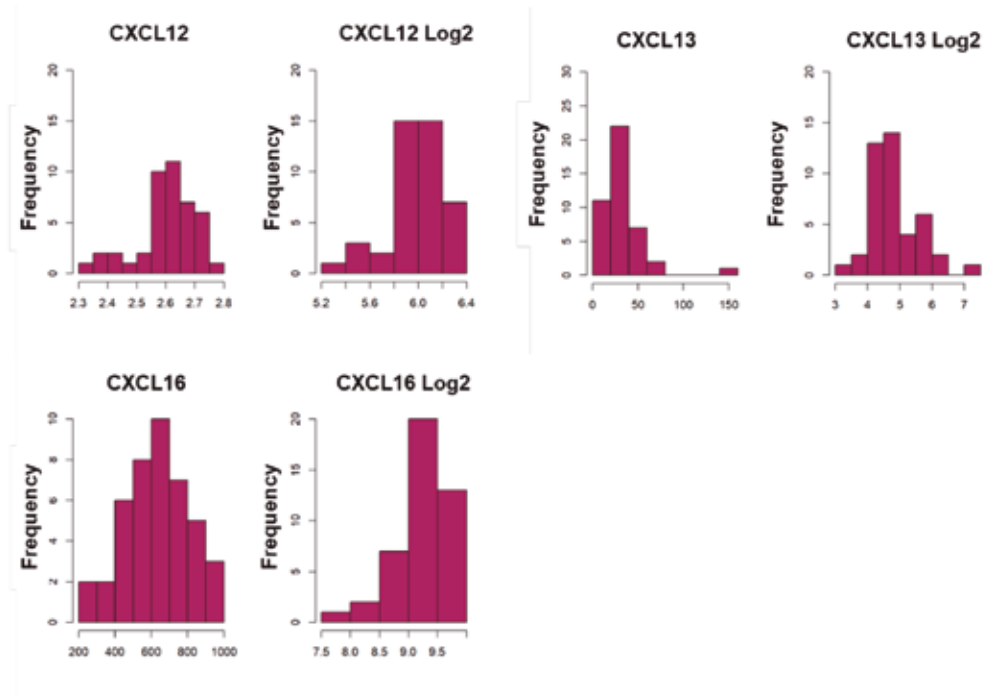




Histograms of all eleven CXC chemokines levels at EVAR time-point. **Left.** Histograms of the distribution. **Right.** Histogram of the Log2-transformed distribution.

## PROG - CXC CHEMOKINES DISTRIBUTION





**Histograms of all eleven CXC chemokines levels at PROG time-point. Left. Histograms of the distribution. Right. Histogram of the Log2-transformed distribution.**

## Annex VI. PRET, EVAR and PROG CXC chemokines serum levels association with response to treatment and patients' clinicopathological and molecular characteristics

### CXC chemokines by time-point and response to treatment

#### Angiogenic:

	Total N=104	CR/PR N=68	SD/PD N=36	p	N
<b>PRET</b>					
CXCL1, Median [IQR]	283.3 [196.7;397.2]	270.4 [191.4;367.0]	311.5 [227.9;426.8]	0.090	104
CXCL2, Median [IQR]	686.9 [475.2;950.6]	655.5 [463.1;865.5]	818.7 [556.4;1213.6]	0.026	104
CXCL5, Median [IQR]	745.7 [547.4;1041.6]	729.7 [546.0;977.2]	842.3 [614.0;1189.2]	0.184	104
CXCL6, Median [IQR]	57.0 [42.7;82.1]	54.2 [40.5;78.8]	63.3 [47.3;83.9]	0.186	104
CXCL8, Median [IQR]	54.9 [30.5;135.7]	52.0 [29.4;159.3]	61.4 [37.1;131.0]	0.580	104
CXCL12, Median [IQR]	500.8 [437.4;563.1]	488.1 [437.4;551.4]	522.8 [438.7;611.4]	0.159	104
<b>EVAR</b>					
CXCL1, Median [IQR]	162.8 [124.6;217.7]	155.8 [117.1;213.6]	174.9 [145.3;219.8]	0.212	63
CXCL2, Median [IQR]	291.0 [204.1;456.5]	260.3 [188.3;440.5]	369.5 [234.8;510.8]	0.114	63
CXCL5, Median [IQR]	373.3 [254.5;529.3]	356.8 [237.5;508.0]	489.3 [359.6;599.6]	0.034	63
CXCL6, Median [IQR]	32.0 [22.9;46.1]	32.8 [22.8;45.7]	30.1 [24.8;45.8]	0.988	63
CXCL8, Median [IQR]	32.2 [15.4;79.2]	23.6 [12.4;40.7]	56.6 [32.2;97.7]	0.014	63
CXCL12, Median [IQR]	368.0 [325.1;404.4]	354.9 [316.0;398.3]	376.1 [338.5;419.6]	0.188	62
<b>PROG/LFUP</b>					
CXCL1, Median [IQR]	248.8 [185.5;326.7]	248.8 [183.2;302.6]	263.8 [201.5;337.4]	0.508	43
CXCL2, Median [IQR]	423.8 [234.7;624.4]	389.2 [229.1;599.9]	480.4 [360.8;659.6]	0.585	43
CXCL5, Median [IQR]	551.7 [445.9;690.8]	551.7 [445.9;690.4]	554.6 [492.4;692.8]	0.490	43
CXCL6, Median [IQR]	39.4 [30.8;53.5]	39.6 [31.2;55.0]	38.0 [28.1;51.0]	0.666	43
CXCL8, Median [IQR]	46.8 [24.9;113.7]	43.7 [24.6;99.5]	61.8 [30.4;258.5]	0.529	41
CXCL12, Median [IQR]	402.8 [363.2;459.6]	398.0 [361.7;454.7]	417.6 [383.8;462.2]	0.527	43

Angiogenic CXC chemokines median levels (pg/mL) and [IQR] obtained at specific time points associated to patients response to treatment. P values correspond to the Kruskal-Wallis test.

*Angiostatic:*

	Total N=104	CR/PR N=68	SD/PD N=36	p	N
<b>PRET</b>					
CXCL9, Median [IQR]	12.9 [8.9;21.1]	12.5 [8.8;18.1]	15.8 [9.2;29.6]	0.088	104
CXCL10, Median [IQR]	178.8 [123.3;271.2]	177.3 [122.0;214.9]	183.8 [124.5;372.1]	0.234	104
CXCL11, Median [IQR]	29.6 [20.4;47.5]	28.3 [20.3;43.4]	30.8 [21.2;59.0]	0.232	104
CXCL13, Median [IQR]	27.4 [19.0;41.1]	26.0 [18.2;39.1]	28.0 [22.2;45.9]	0.183	104
CXCL16, Median [IQR]	516.0 [427.0;588.8]	498.4 [427.0;581.2]	528.7 [427.2;598.6]	0.507	104
<b>EVAR</b>					
CXCL9, Median [IQR]	10.0 [6.9;16.0]	8.1 [6.6;14.5]	11.0 [8.2;19.6]	0.058	63
CXCL10, Median [IQR]	139.6 [106.8;191.4]	139.0 [103.7;178.9]	171.3 [115.9;280.2]	0.178	63
CXCL11, Median [IQR]	20.0 [14.4;30.0]	16.8 [14.2;23.5]	25.0 [19.8;35.3]	0.022	63
CXCL13, Median [IQR]	27.1 [18.9;36.9]	28.4 [18.9;40.2]	24.2 [18.4;34.8]	0.573	63
CXCL16, Median [IQR]	478.6 [431.9;561.1]	473.4 [423.1;539.1]	548.7 [452.1;619.8]	0.073	63
<b>PROG/FUP</b>					
CXCL9, Median [IQR]	11.0 [9.1;16.7]	10.9 [8.9;14.3]	13.8 [9.9;22.5]	0.227	43
CXCL10, Median [IQR]	167.8 [139.4;196.6]	162.5 [136.3;195.6]	186.3 [150.3;267.5]	0.388	43
CXCL11, Median [IQR]	30.6 [21.7;41.1]	28.0 [20.5;37.7]	38.9 [29.4;67.1]	0.054	43
CXCL13, Median [IQR]	26.6 [20.0;34.1]	25.8 [20.2;32.1]	28.4 [20.0;53.8]	0.438	43
CXCL16, Median [IQR]	648.3 [526.7;745.3]	650.5 [550.7;736.2]	564.1 [476.0;813.7]	0.796	43

**Angiostatic CXC chemokines median levels (pg/mL) and [IQR] obtained at specific time points associated to patients response to treatment. P values correspond to the Kruskal-Wallis test.**

### CXC chemokines by time-point and sex

#### Angiogenic:

	Total N=104	Male N=74	Female N=30	p	N
<b>PRET</b>					
CXCL1, Median [IQR]	283.3 [196.7;397.2]	279.0 [196.1;414.1]	286.4 [201.7;368.9]	0.914	104
CXCL2, Median [IQR]	686.9 [475.2;950.6]	677.8 [475.5;942.5]	713.9 [487.6;955.1]	0.802	104
CXCL5, Median [IQR]	745.7 [547.4;1041.6]	733.2 [547.0;1001.5]	892.4 [581.7;1230.4]	0.136	104
CXCL6, Median [IQR]	57.0 [42.7;82.1]	57.6 [42.8;82.3]	56.4 [41.5;80.9]	0.929	104
CXCL8, Median [IQR]	54.9 [30.5;135.7]	58.0 [32.6;151.3]	45.9 [28.7;103.4]	0.315	104
CXCL12, Median [IQR]	500.8 [437.4;563.1]	497.3 [436.2;556.1]	517.4 [452.2;567.0]	0.486	104
CXCL2, Median [IQR]	291.0 [204.1;456.5]	337.0 [229.3;524.7]	207.6 [154.4;298.9]	0.021	63
CXCL5, Median [IQR]	373.3 [254.5;529.3]	356.8 [253.2;505.3]	487.8 [379.3;614.0]	0.042	63
CXCL6, Median [IQR]	32.0 [22.9;46.1]	33.4 [25.1;45.7]	25.8 [20.2;45.1]	0.438	63
CXCL8, Median [IQR]	32.2 [15.4;79.2]	31.1 [13.9;85.9]	38.1 [21.8;54.0]	0.411	63
CXCL12, Median [IQR]	368.0 [325.1;404.4]	374.5 [337.0;403.2]	347.3 [313.2;414.9]	0.429	62
<b>PROG/LFUP</b>					
CXCL1, Median [IQR]	248.8 [185.5;326.7]	250.9 [183.2;327.7]	248.8 [200.2;266.8]	0.978	43
CXCL2, Median [IQR]	423.8 [234.7;624.4]	457.8 [228.8;707.0]	393.6 [308.4;454.7]	0.452	43
CXCL5, Median [IQR]	551.7 [445.9;690.8]	481.4 [444.7;592.1]	690.4 [568.4;974.3]	0.014	43
CXCL6, Median [IQR]	39.4 [30.8;53.5]	44.1 [31.1;59.0]	38.4 [29.1;39.5]	0.290	43
CXCL8, Median [IQR]	46.8 [24.9;113.7]	51.6 [26.4;104.6]	31.5 [24.6;123.4]	0.738	41
CXCL12, Median [IQR]	402.8 [363.2;459.6]	416.9 [374.6;465.3]	372.0 [361.7;412.7]	0.242	43

Angiogenic CXC chemokines median levels (pg/mL) and [IQR] obtained at specific time points associated to patients sex. P values correspond to the Kruskal-Wallis test.

*Angiostatic:*

	Total N=104	Male N=74	Female N=30	p	N
<b>PRET</b>					
CXCL9, Median [IQR]	12.9 [8.9;21.1]	12.0 [8.6;19.2]	15.7 [10.8;26.9]	0.217	104
CXCL10, Median [IQR]	178.8 [123.3;271.2]	175.6 [123.4;217.0]	197.9 [122.4;275.7]	0.571	104
CXCL11, Median [IQR]	29.6 [20.4;47.5]	32.1 [21.9;51.3]	24.0 [16.1;39.0]	0.045	104
CXCL13, Median [IQR]	27.4 [19.0;41.1]	25.7 [18.9;39.5]	31.5 [22.9;44.4]	0.242	104
CXCL16, Median [IQR]	516.0 [427.0;588.8]	483.7 [406.3;565.2]	581.0 [480.0;648.2]	0.001	104
<b>EVAR</b>					
CXCL9, Median [IQR]	10.0 [6.9;16.0]	10.7 [7.8;16.2]	8.2 [6.7;15.4]	0.670	63
CXCL10, Median [IQR]	139.6 [106.8;191.4]	144.3 [114.0;178.9]	134.4 [97.8;217.6]	0.958	63
CXCL11, Median [IQR]	20.0 [14.4;30.0]	20.0 [14.8;29.9]	19.0 [14.2;29.3]	0.819	63
CXCL13, Median [IQR]	27.1 [18.9;36.9]	28.4 [18.9;37.1]	23.9 [18.9;35.5]	0.538	63
CXCL16, Median [IQR]	478.6 [431.9;561.1]	474.0 [388.5;536.3]	569.1 [455.5;617.8]	0.008	63
<b>PROG/LFUP</b>					
CXCL9, Median [IQR]	11.0 [9.1;16.7]	11.0 [9.5;16.0]	11.5 [7.6;16.7]	0.636	43
CXCL10, Median [IQR]	167.8 [139.4;196.6]	166.5 [135.5;196.1]	184.5 [148.5;243.6]	0.656	43
CXCL11, Median [IQR]	30.6 [21.7;41.1]	31.6 [23.8;40.5]	23.2 [12.0;41.6]	0.266	43
CXCL13, Median [IQR]	26.6 [20.0;34.1]	27.2 [20.4;33.8]	21.5 [16.1;38.2]	0.266	43
CXCL16, Median [IQR]	648.3 [526.7;745.3]	670.5 [513.6;781.8]	572.1 [538.5;661.1]	0.266	43

**Angiostatic CXC chemokines median levels (pg/mL) and [IQR] obtained at specific time points associated to patients sex. P values correspond to the Kruskal-Wallis test.**

### CXC chemokines by time-point and primary tumor site

#### Angiogenic:

	Total N=104	Colon N=66	Rectum N=38	p	N
<b>PRET</b>					
CXCL1, Median [IQR]	283.3 [196.7;397.2]	286.4 [201.7;392.0]	258.9 [194.0;404.8]	0.552	104
CXCL2, Median [IQR]	686.9 [475.2;950.6]	743.4 [517.0;1126.3]	629.2 [419.9;767.5]	0.049	104
CXCL5, Median [IQR]	745.7 [547.4;1041.6]	789.6 [548.9;1066.7]	640.7 [550.3;1028.0]	0.333	104
CXCL6, Median [IQR]	57.0 [42.7;82.1]	60.6 [44.8;91.3]	54.1 [42.6;69.4]	0.182	104
CXCL8, Median [IQR]	54.9 [30.5;135.7]	47.8 [29.9;161.9]	64.6 [34.0;129.2]	0.548	104
CXCL12, Median [IQR]	500.8 [437.4;563.1]	505.8 [448.0;559.9]	472.4 [407.9;565.1]	0.217	104
<b>EVAR</b>					
CXCL1, Median [IQR]	162.8 [124.6;217.7]	164.5 [130.2;221.9]	156.7 [85.3;187.8]	0.338	63
CXCL2, Median [IQR]	291.0 [204.1;456.5]	289.3 [205.6;443.9]	310.4 [202.9;461.9]	1.000	63
CXCL5, Median [IQR]	373.3 [254.5;529.3]	397.1 [315.4;529.7]	314.3 [237.5;511.5]	0.382	63
CXCL6, Median [IQR]	32.0 [22.9;46.1]	30.5 [24.1;45.7]	33.1 [20.6;45.9]	0.721	63
CXCL8, Median [IQR]	32.2 [15.4;79.2]	34.3 [17.1;74.0]	19.2 [11.4;74.2]	0.235	63
CXCL12, Median [IQR]	368.0 [325.1;404.4]	374.2 [332.8;416.1]	359.0 [305.4;395.2]	0.356	62
<b>PROG/LFUP</b>					
CXCL1, Median [IQR]	248.8 [185.5;326.7]	259.5 [210.3;329.4]	187.8 [180.5;246.2]	0.059	43
CXCL2, Median [IQR]	423.8 [234.7;624.4]	457.8 [313.2;891.0]	240.3 [205.9;471.8]	0.013	43
CXCL5, Median [IQR]	551.7 [445.9;690.8]	554.0 [465.1;732.8]	445.9 [441.4;629.7]	0.165	43
CXCL6, Median [IQR]	39.4 [30.8;53.5]	39.5 [31.1;57.9]	37.3 [30.8;48.2]	0.475	43
CXCL8, Median [IQR]	46.8 [24.9;113.7]	59.8 [31.7;95.4]	23.0 [19.0;145.0]	0.136	41
CXCL12, Median [IQR]	402.8 [363.2;459.6]	404.6 [365.5;449.3]	402.8 [361.7;467.9]	0.958	43

Angiogenic CXC chemokines median levels (pg/mL) and [IQR] obtained at specific time points associated to patients primary tumor site. P values correspond to the Kruskal-Wallis test.

**Angiostatic:**

	Total N=104	Colon N=66	Rectum N=38	p	N
<b>PRET</b>					
CXCL9, Median [IQR]	12.9 [8.9;21.1]	13.0 [9.6;23.4]	10.3 [8.3;18.1]	0.132	104
CXCL10, Median [IQR]	178.8 [123.3;271.2]	179.1 [123.5;275.7]	178.8 [123.4;217.6]	0.548	104
CXCL11, Median [IQR]	29.6 [20.4;47.5]	28.3 [18.6;43.0]	31.4 [21.5;51.8]	0.458	104
CXCL13, Median [IQR]	27.4 [19.0;41.1]	28.0 [18.9;42.4]	25.5 [20.7;36.5]	0.438	104
CXCL16, Median [IQR]	516.0 [427.0;588.8]	508.3 [426.5;580.4]	527.9 [427.6;630.6]	0.470	104
<b>EVAR</b>					
CXCL9, Median [IQR]	10.0 [6.9;16.0]	11.5 [7.9;16.5]	7.2 [5.0;8.4]	0.012	63
CXCL10, Median [IQR]	139.6 [106.8;191.4]	149.8 [114.0;221.2]	130.1 [78.5;158.6]	0.073	63
CXCL11, Median [IQR]	20.0 [14.4;30.0]	21.4 [14.8;31.0]	15.9 [13.7;21.6]	0.080	63
CXCL13, Median [IQR]	27.1 [18.9;36.9]	28.4 [21.3;44.8]	21.8 [15.6;30.4]	0.074	63
CXCL16, Median [IQR]	478.6 [431.9;561.1]	517.2 [439.3;578.2]	462.2 [371.7;525.9]	0.114	63
<b>PROG/LFUP</b>					
CXCL9, Median [IQR]	11.0 [9.1;16.7]	11.2 [9.0;16.9]	10.7 [9.6;14.3]	1.000	43
CXCL10, Median [IQR]	167.8 [139.4;196.6]	160.1 [143.1;192.4]	187.7 [133.2;297.0]	0.267	43
CXCL11, Median [IQR]	30.6 [21.7;41.1]	28.1 [20.4;37.8]	34.0 [25.1;42.2]	0.341	43
CXCL13, Median [IQR]	26.6 [20.0;34.1]	26.2 [20.0;31.4]	26.7 [20.5;44.4]	0.653	43
CXCL16, Median [IQR]	648.3 [526.7;745.3]	656.7 [544.8;770.3]	594.0 [474.0;708.8]	0.341	43

**Angiostatic CXC chemokines median levels (pg/mL) and [IQR] obtained at specific time points associated to patients primary tumor site. P values correspond to the Kruskal-Wallis test.**

**CXC chemokines by time-point and oligo/multiple metastasis**

*Angiogenic:*

	Total N=103	< 5 Mlx N=32	≥ 5 N=71	p	N
<b>PRET</b>					
CXCL1, Median [IQR]	281.6 [196.3;401.2]	234.2 [188.5;328.9]	298.0 [205.6;459.9]	0.037	103
CXCL2, Median [IQR]	683.6 [475.2;956.1]	587.1 [450.4;743.2]	749.7 [504.4;1085.8]	0.040	103
CXCL5, Median [IQR]	737.0 [547.2;1038.7]	629.9 [522.6;878.5]	852.8 [593.9;1044.0]	0.077	103
CXCL6, Median [IQR]	56.9 [42.6;81.8]	49.5 [39.1;62.2]	62.1 [45.3;89.0]	0.010	103
CXCL8, Median [IQR]	53.7 [30.4;136.9]	39.9 [23.0;73.0]	69.6 [34.8;179.3]	0.002	103
CXCL12, Median [IQR]	500.1 [437.3;564.8]	488.1 [408.8;538.5]	502.5 [451.6;581.7]	0.095	103
<b>EVAR</b>					
CXCL1, Median [IQR]	162.8 [124.6;217.7]	149.9 [127.4;164.5]	178.4 [118.1;221.9]	0.191	63
CXCL2, Median [IQR]	291.0 [204.1;456.5]	310.4 [221.2;373.2]	289.3 [202.6;524.7]	0.704	63
CXCL5, Median [IQR]	373.3 [254.5;529.3]	328.5 [241.4;432.0]	447.6 [308.0;567.4]	0.075	63
CXCL6, Median [IQR]	32.0 [22.9;46.1]	39.1 [22.0;48.0]	30.5 [24.1;40.1]	0.447	63
CXCL8, Median [IQR]	32.2 [15.4;79.2]	20.1 [12.6;37.2]	36.7 [17.0;86.6]	0.045	63
CXCL12, Median [IQR]	368.0 [325.1;404.4]	378.9 [334.0;402.6]	358.1 [323.0;405.1]	0.544	62
<b>PROG/LFUP</b>					
CXCL1, Median [IQR]	248.8 [185.5;326.7]	267.0 [199.6;320.7]	244.5 [187.8;326.6]	0.546	43
CXCL2, Median [IQR]	423.8 [234.7;624.4]	244.1 [211.1;445.5]	451.5 [305.7;705.4]	0.095	43
CXCL5, Median [IQR]	551.7 [445.9;690.8]	513.6 [446.3;607.4]	551.7 [445.9;746.7]	0.328	43
CXCL6, Median [IQR]	39.4 [30.8;53.5]	42.4 [28.9;57.8]	38.9 [30.8;50.4]	1.000	43
CXCL8, Median [IQR]	46.8 [24.9;113.7]	40.6 [28.0;93.0]	49.2 [24.6;117.4]	0.925	41
CXCL12, Median [IQR]	402.8 [363.2;459.6]	353.3 [261.7;402.4]	423.7 [377.3;464.5]	0.036	43

**Angiogenic CXC chemokines median levels (pg/mL) and [IQR] obtained at specific time points associated to patients with oligo/multiple metastasis. P values correspond to the Kruskal-Wallis test.**

**Angiostatic:**

	Total N=103	< 5 Mln N=52	≥ 5 N=71	p	N
<b>PRET</b>					
CXCL9, Median [IQR]	12.9 [8.9;21.1]	11.1 [8.0;15.4]	13.0 [9.2;27.6]	0.023	103
CXCL10, Median [IQR]	179.3 [123.3;271.6]	148.0 [102.9;203.7]	183.4 [127.0;313.6]	0.071	103
CXCL11, Median [IQR]	29.6 [20.4;47.6]	26.3 [18.3;36.0]	31.0 [22.4;53.3]	0.119	103
CXCL13, Median [IQR]	27.2 [19.0;41.3]	24.4 [18.6;30.7]	27.6 [19.9;44.8]	0.097	103
CXCL16, Median [IQR]	516.2 [427.3;589.9]	481.2 [425.6;573.1]	521.0 [428.1;612.1]	0.437	103
<b>EVAR</b>					
CXCL9, Median [IQR]	10.0 [6.9;16.0]	10.8 [6.7;15.2]	8.3 [7.2;17.1]	0.761	63
CXCL10, Median [IQR]	139.6 [106.8;191.4]	161.7 [137.8;196.1]	135.6 [103.7;182.0]	0.338	63
CXCL11, Median [IQR]	20.0 [14.4;30.0]	19.5 [15.4;26.3]	20.0 [14.2;31.0]	0.964	63
CXCL13, Median [IQR]	27.1 [18.9;36.9]	27.2 [21.3;40.7]	27.1 [18.9;36.0]	0.692	63
CXCL16, Median [IQR]	478.6 [431.9;561.1]	478.1 [441.4;538.1]	486.4 [423.1;583.1]	0.831	63
<b>PROG/LFUP</b>					
CXCL9, Median [IQR]	11.0 [9.1;16.7]	9.7 [8.2;16.2]	11.3 [9.4;16.4]	0.472	43
CXCL10, Median [IQR]	167.8 [139.4;196.6]	162.8 [136.1;236.5]	173.8 [142.4;195.6]	0.646	43
CXCL11, Median [IQR]	30.6 [21.7;41.1]	32.6 [26.5;47.0]	28.2 [20.2;40.0]	0.328	43
CXCL13, Median [IQR]	26.6 [20.0;34.1]	25.0 [20.3;28.0]	27.6 [19.6;34.8]	0.818	43
CXCL16, Median [IQR]	648.3 [526.7;745.3]	654.1 [596.3;770.3]	648.3 [496.4;731.5]	0.373	43

**Angiostatic CXC chemokines median levels (pg/mL) and [IQR] obtained at specific time points associated to patients with oligo/multiple metastasis. P values correspond to the Kruskal-Wallis test.**

**CXC chemokines by time-point and liver metastasis**

*Angiogenic:*

	Total <i>N=104</i>	Yes <i>N=82</i>	No <i>N=22</i>	p	N
<b>PRET</b>					
CXCL1, Median [IQR]	283.3 [196.7;397.2]	308.3 [215.5;455.9]	214.0 [192.4;265.1]	0.012	104
CXCL2, Median [IQR]	686.9 [475.2;950.6]	706.2 [475.5;1105.5]	552.7 [476.1;804.5]	0.141	104
CXCL5, Median [IQR]	745.7 [547.4;1041.6]	776.3 [564.2;1039.0]	668.6 [473.9;1020.4]	0.277	104
CXCL6, Median [IQR]	57.0 [42.7;82.1]	57.0 [43.0;85.0]	56.6 [42.8;69.2]	0.445	104
CXCL8, Median [IQR]	54.9 [30.5;135.7]	70.8 [39.7;176.5]	25.5 [16.5;34.3]	<0.001	104
CXCL12, Median [IQR]	500.8 [437.4;563.1]	513.6 [446.7;582.3]	470.5 [416.5;512.3]	0.044	104
<b>EVAR</b>					
CXCL1, Median [IQR]	162.8 [124.6;217.7]	161.0 [124.4;208.9]	189.6 [143.1;222.4]	0.543	63
CXCL2, Median [IQR]	291.0 [204.1;456.5]	278.1 [196.9;462.8]	381.9 [224.1;415.8]	0.455	63
CXCL5, Median [IQR]	373.3 [254.5;529.3]	372.9 [254.1;539.3]	431.6 [315.4;472.4]	0.783	63
CXCL6, Median [IQR]	32.0 [22.9;46.1]	30.3 [22.2;45.3]	36.7 [28.3;48.1]	0.276	63
CXCL8, Median [IQR]	32.2 [15.4;79.2]	33.6 [16.5;85.5]	21.4 [13.9;37.9]	0.356	63
CXCL12, Median [IQR]	368.0 [325.1;404.4]	363.0 [323.0;405.1]	392.0 [343.2;401.1]	0.407	62
<b>PROG/LFUP</b>					
CXCL1, Median [IQR]	248.8 [185.5;326.7]	258.2 [187.8;330.4]	216.2 [183.7;246.4]	0.220	43
CXCL2, Median [IQR]	423.8 [234.7;624.4]	451.5 [253.6;648.9]	273.0 [213.5;368.3]	0.151	43
CXCL5, Median [IQR]	551.7 [445.9;690.8]	529.7 [445.9;655.9]	653.9 [464.8;975.0]	0.494	43
CXCL6, Median [IQR]	39.4 [30.8;53.5]	42.6 [30.8;58.8]	37.5 [31.5;39.3]	0.362	43
CXCL8, Median [IQR]	46.8 [24.9;113.7]	46.8 [25.6;95.1]	110.2 [22.4;657.8]	0.606	41
CXCL12, Median [IQR]	402.8 [363.2;459.6]	410.2 [368.1;467.9]	366.8 [358.7;379.2]	0.141	43

**Angiogenic CXC chemokines median levels (pg/mL) and [IQR] obtained at specific time points associated to patients to liver metastasis. P values correspond to the Kruskal-Wallis test.**

**Angiostatic**

	Total <i>N</i> =104	Yes <i>N</i> =82	No <i>N</i> =22	<i>p</i>	<i>N</i>
<b>PRET</b>					
CXCL9, Median [IQR]	12.9 [8.9;21.1]	12.5 [8.9;20.8]	13.6 [9.4;21.0]	0.702	104
CXCL10, Median [IQR]	178.8 [123.3;271.2]	177.7 [123.4;280.3]	184.5 [119.1;211.5]	0.918	104
CXCL11, Median [IQR]	29.6 [20.4;47.5]	32.1 [20.7;53.4]	25.7 [20.5;30.5]	0.105	104
CXCL13, Median [IQR]	27.4 [19.0;41.1]	27.2 [19.0;41.8]	27.5 [19.5;32.2]	0.650	104
CXCL16, Median [IQR]	516.0 [427.0;588.8]	516.0 [427.6;582.8]	510.8 [412.7;633.8]	0.762	104
<b>EVAR</b>					
CXCL9, Median [IQR]	10.0 [6.9;16.0]	9.2 [6.8;15.4]	13.9 [7.8;18.0]	0.596	63
CXCL10, Median [IQR]	139.6 [106.8;191.4]	141.9 [110.7;181.2]	139.6 [103.7;243.6]	0.543	63
CXCL11, Median [IQR]	20.0 [14.4;30.0]	19.0 [14.2;27.4]	21.4 [14.8;30.8]	0.377	63
CXCL13, Median [IQR]	27.1 [18.9;36.9]	26.2 [18.9;37.0]	30.7 [18.9;35.4]	0.776	63
CXCL16, Median [IQR]	478.6 [431.9;561.1]	481.6 [431.6;561.6]	446.2 [440.8;548.1]	0.814	63
<b>PROG/LFUP</b>					
CXCL9, Median [IQR]	11.0 [9.1;16.7]	11.0 [9.4;17.1]	10.1 [8.1;15.1]	0.528	43
CXCL10, Median [IQR]	167.8 [139.4;196.6]	165.1 [136.3;192.7]	196.2 [157.5;198.9]	0.441	43
CXCL11, Median [IQR]	30.6 [21.7;41.1]	31.1 [20.5;40.0]	25.4 [23.4;42.5]	0.674	43
CXCL13, Median [IQR]	26.6 [20.0;34.1]	27.6 [20.5;40.4]	20.7 [16.5;25.4]	0.099	43
CXCL16, Median [IQR]	648.3 [526.7;745.3]	665.2 [519.3;754.4]	592.9 [558.4;639.6]	0.462	43

**Angiostatic CXC chemokines median levels (pg/mL) and [IQR] obtained at specific time points associated to patients liver metastasis. P values correspond to the Kruskal-Wallis test.**

### CXC chemokines by time-point and lung metastasis

#### Angiogenic

	Total N=104	Yes N=42	No N=62	p	N
<b>PRET</b>					
CXCL1, Median [IQR]	283.3 [196.7;397.2]	311.5 [208.0;463.8]	247.4 [191.4;351.5]	0.039	104
CXCL2, Median [IQR]	686.9 [475.2;950.6]	712.4 [511.8;1139.3]	643.7 [466.5;852.2]	0.152	104
CXCL5, Median [IQR]	745.7 [547.4;1041.6]	878.9 [629.4;1110.1]	660.8 [525.2;1001.5]	0.050	104
CXCL6, Median [IQR]	57.0 [42.7;82.1]	59.6 [46.0;82.3]	56.4 [40.1;79.3]	0.440	104
CXCL8, Median [IQR]	34.9 [30.5;135.7]	83.1 [31.4;172.4]	49.0 [28.6;113.4]	0.241	104
CXCL12, Median [IQR]	500.8 [437.4;563.1]	502.8 [446.7;614.2]	495.6 [425.8;545.9]	0.194	104
<b>EVAR</b>					
CXCL1, Median [IQR]	162.8 [124.6;217.7]	161.0 [143.7;223.8]	165.1 [106.1;194.7]	0.498	63
CXCL2, Median [IQR]	291.0 [204.1;456.5]	290.1 [206.6;523.9]	302.1 [202.6;440.5]	0.762	63
CXCL5, Median [IQR]	373.3 [254.5;529.3]	408.7 [347.0;517.0]	359.6 [253.2;529.7]	0.639	63
CXCL6, Median [IQR]	32.0 [22.9;46.1]	40.4 [27.2;54.6]	28.3 [21.4;38.0]	0.020	63
CXCL8, Median [IQR]	32.2 [15.4;79.2]	23.6 [14.6;38.1]	35.2 [16.5;86.6]	0.313	63
CXCL12, Median [IQR]	368.0 [325.1;404.4]	578.9 [315.1;475.4]	358.1 [329.1;398.3]	0.518	62
<b>PROG-LFUP</b>					
CXCL1, Median [IQR]	248.8 [185.5;326.7]	246.2 [187.8;278.5]	256.9 [185.7;329.5]	0.813	43
CXCL2, Median [IQR]	423.8 [234.7;624.4]	464.2 [240.3;513.9]	340.9 [235.2;679.0]	0.568	43
CXCL5, Median [IQR]	551.7 [445.9;690.8]	529.7 [461.7;713.8]	567.9 [445.9;681.8]	0.794	43
CXCL6, Median [IQR]	39.4 [30.8;53.5]	38.2 [32.2;48.2]	43.0 [28.7;54.2]	0.862	43
CXCL8, Median [IQR]	46.8 [24.9;113.7]	60.4 [25.8;92.2]	40.2 [25.3;133.0]	0.957	41
CXCL12, Median [IQR]	402.8 [363.2;459.6]	429.4 [357.7;454.7]	399.7 [373.3;460.0]	0.980	43

Angiogenic CXC chemokines median levels (pg/mL) and [IQR] obtained at specific time points associated to patients lung metastasis. P values correspond to the Kruskal-Wallis test.

**Angiostatic**

	Total N=104	Yes N=42	No N=62	p	N
<b>PRET</b>					
CXCL9, Median [IQR]	12.9 [8.9;21.1]	14.1 [8.9;27.1]	12.6 [9.0;18.4]	0.311	104
CXCL10, Median [IQR]	178.8 [123.3;271.2]	197.8 [148.1;324.8]	153.4 [115.0;209.8]	0.020	104
CXCL11, Median [IQR]	29.6 [20.4;47.5]	30.1 [21.4;56.2]	29.2 [20.1;42.7]	0.415	104
CXCL13, Median [IQR]	27.4 [19.0;41.1]	28.7 [23.1;45.8]	25.0 [18.0;36.1]	0.051	104
CXCL16, Median [IQR]	516.0 [427.0;588.8]	569.3 [447.0;646.5]	473.7 [407.1;553.0]	0.005	104
<b>EVAR</b>					
CXCL9, Median [IQR]	10.0 [6.9;16.0]	10.5 [7.2;15.1]	8.4 [6.6;16.5]	0.801	63
CXCL10, Median [IQR]	139.6 [106.8;191.4]	137.4 [110.7;196.1]	149.2 [103.7;181.9]	0.880	63
CXCL11, Median [IQR]	20.0 [14.4;30.0]	17.4 [14.2;27.4]	20.4 [15.2;31.0]	0.371	63
CXCL13, Median [IQR]	27.1 [18.9;36.9]	31.3 [26.7;39.3]	23.9 [17.2;32.8]	0.028	63
CXCL16, Median [IQR]	478.6 [431.9;561.1]	511.1 [445.5;554.9]	477.6 [414.3;571.8]	0.708	63
<b>PROG/LFUP</b>					
CXCL9, Median [IQR]	11.0 [9.1;16.7]	10.2 [8.4;12.0]	11.9 [9.6;17.4]	0.285	43
CXCL10, Median [IQR]	167.8 [139.4;196.6]	157.5 [129.9;199.3]	176.2 [143.8;195.4]	0.691	43
CXCL11, Median [IQR]	30.6 [21.7;41.1]	25.9 [20.5;33.5]	31.6 [23.4;50.2]	0.285	43
CXCL13, Median [IQR]	26.6 [20.0;34.1]	26.7 [20.2;33.4]	25.0 [20.0;38.3]	0.980	43
CXCL16, Median [IQR]	648.3 [526.7;745.3]	612.1 [534.1;694.5]	656.7 [528.0;749.8]	0.673	43

**Angiostatic CXC chemokines median levels (pg/mL) and [IQR] obtained at specific time points associated to patients lung metastasis. P values correspond to the Kruskal-Wallis test.**

### CXC chemokines by time-point and peritoneum metastasis

#### Angiogenic

	Total N=102	Yes N=19	No N=83	p	N
<b>PRET</b>					
CXCL1, Median [IQR]	279.0 [195.9;384.9]	237.3 [192.5;341.6]	287.7 [197.5;401.2]	0.484	102
CXCL2, Median [IQR]	681.9 [475.1;930.8]	683.6 [490.5;892.7]	680.3 [475.2;932.2]	0.990	102
CXCL5, Median [IQR]	733.6 [547.0;1039.0]	698.3 [346.3;1087.9]	755.8 [554.2;1028.9]	0.525	102
CXCL6, Median [IQR]	57.0 [42.6;82.3]	56.5 [40.8;66.6]	59.4 [42.8;82.5]	0.476	102
CXCL8, Median [IQR]	53.5 [30.3;133.4]	33.3 [23.7;49.7]	66.6 [33.9;147.2]	0.010	102
CXCL12, Median [IQR]	499.8 [437.2;556.1]	496.1 [477.8;553.9]	500.1 [421.2;555.8]	0.505	102
<b>EVAR</b>					
CXCL1, Median [IQR]	162.8 [124.6;217.7]	154.8 [114.8;207.1]	164.5 [125.0;221.9]	0.522	63
CXCL2, Median [IQR]	291.0 [204.1;456.5]	318.6 [240.9;417.6]	266.9 [202.6;469.1]	0.547	63
CXCL5, Median [IQR]	373.3 [254.5;529.3]	426.2 [280.2;506.8]	372.6 [255.2;542.5]	0.910	63
CXCL6, Median [IQR]	32.0 [22.9;46.1]	33.6 [27.2;47.5]	32.0 [22.8;44.3]	0.686	63
CXCL8, Median [IQR]	32.2 [15.4;79.2]	25.4 [11.4;101.3]	34.3 [16.6;74.0]	0.612	63
CXCL12, Median [IQR]	368.0 [325.1;404.4]	369.8 [352.3;436.9]	368.0 [322.3;401.4]	0.315	62
<b>PROG/LFUP</b>					
CXCL1, Median [IQR]	252.2 [184.4;326.8]	219.7 [183.2;244.5]	258.2 [187.8;326.8]	0.312	42
CXCL2, Median [IQR]	408.7 [231.9;636.6]	393.6 [229.1;705.4]	423.8 [240.3;599.9]	0.818	42
CXCL5, Median [IQR]	551.7 [445.9;691.0]	551.7 [487.4;691.1]	551.7 [441.4;690.4]	0.416	42
CXCL6, Median [IQR]	39.5 [30.8;54.2]	42.6 [30.0;47.6]	39.4 [31.2;55.0]	0.702	42
CXCL8, Median [IQR]	49.2 [26.0;117.4]	95.4 [40.6;134.6]	33.3 [24.4;93.9]	0.141	40
CXCL12, Median [IQR]	404.6 [362.5;462.0]	432.4 [372.0;450.1]	398.0 [361.7;467.9]	0.571	42

Angiogenic CXC chemokines median levels (pg/mL) and [IQR] obtained at specific time points associated to patients peritoneum metastasis. P values correspond to the Kruskal-Wallis test.

**Angiostatic**

	Total	Yes	No	p	N
	N=102	N=19	N=83		
<b>PRET</b>					
CXCL9, Median [IQR]	12.8 [8.9;20.3]	12.4 [9.4;17.2]	12.8 [8.5;22.7]	0.702	102
CXCL10, Median [IQR]	177.9 [123.1;270.3]	177.5 [118.5;214.7]	178.3 [123.4;271.6]	0.806	102
CXCL11, Median [IQR]	29.2 [20.3;44.1]	29.7 [22.4;41.7]	28.8 [20.1;49.8]	0.747	102
CXCL13, Median [IQR]	27.0 [18.9;40.6]	23.6 [16.0;36.2]	27.6 [19.9;41.3]	0.217	102
CXCL16, Median [IQR]	516.0 [426.5;586.5]	535.0 [427.0;579.0]	515.8 [425.9;594.5]	0.787	102
<b>EVAR</b>					
CXCL9, Median [IQR]	10.0 [6.9;16.0]	9.1 [5.2;15.8]	10.0 [7.2;15.8]	0.665	63
CXCL10, Median [IQR]	139.6 [106.8;191.4]	108.9 [101.4;154.2]	149.2 [114.4;200.8]	0.194	63
CXCL11, Median [IQR]	20.0 [14.4;30.0]	20.7 [15.4;31.8]	19.5 [14.3;29.9]	0.498	63
CXCL13, Median [IQR]	27.1 [18.9;36.9]	21.1 [17.2;28.0]	28.4 [19.7;40.9]	0.085	63
CXCL16, Median [IQR]	478.6 [431.9;561.1]	475.0 [401.5;544.9]	478.6 [432.4;571.8]	0.652	63
<b>PROG/LFUP</b>					
CXCL9, Median [IQR]	11.0 [9.0;16.1]	11.3 [9.5;11.6]	10.9 [8.9;17.1]	0.794	42
CXCL10, Median [IQR]	166.5 [137.9;197.2]	187.5 [124.3;197.7]	165.1 [145.1;195.6]	0.771	42
CXCL11, Median [IQR]	29.6 [21.1;41.7]	31.7 [20.2;37.8]	28.2 [22.8;42.2]	0.963	42
CXCL13, Median [IQR]	26.2 [20.0;33.1]	17.9 [15.4;29.1]	26.7 [21.5;33.4]	0.137	42
CXCL16, Median [IQR]	649.4 [536.3;749.8]	694.5 [648.3;841.1]	612.1 [519.3;731.5]	0.122	42

**Angiostatic CXC chemokines median levels (pg/mL) and [IQR] obtained at specific time points associated to patients peritoneum metastasis. P values correspond to the Kruskal-Wallis test.**

## CXC chemokines by time-point and metastatic site

### Angiogenic

	Total N=104	Liver N=31	Lung N=11	Liver + Lung N=31	Other N=21	p	N
<b>PRET</b>							
CXCL1, Median [IQR]	283.3 [196.7;397.2]	265.4 [187.4;346.1]	198.0 [182.4;252.7]	388.9 [287.1;521.3]	233.0 [202.0;305.3]	0.001	104
CXCL2, Median [IQR]	686.9 [475.2;950.6]	646.5 [454.8;851.7]	517.1 [481.0;706.2]	914.1 [615.8;1402.7]	567.4 [494.0;872.3]	0.057	104
CXCL5, Median [IQR]	745.7 [547.4;1041.6]	629.9 [522.9;1001.4]	371.0 [431.7;888.0]	937.2 [733.6;1155.1]	727.1 [583.9;1036.2]	0.013	104
CXCL6, Median [IQR]	57.0 [42.7;82.1]	56.0 [40.1;76.8]	46.3 [42.9;61.9]	84.6 [48.3;89.0]	62.8 [42.2;79.4]	0.335	104
CXCL8, Median [IQR]	34.9 [30.5;135.7]	36.1 [35.8;119.2]	26.5 [16.3;37.7]	127.2 [51.6;211.5]	24.6 [17.2;31.3]	<0.001	104
CXCL12, Median [IQR]	500.8 [437.4;563.1]	501.8 [429.7;551.7]	468.7 [421.4;511.9]	561.5 [464.2;628.0]	472.3 [423.0;505.7]	0.053	104
<b>EVAR</b>							
CXCL1, Median [IQR]	162.8 [124.6;217.7]	180.5 [113.5;194.5]	185.6 [154.0;216.3]	161.0 [142.1;227.2]	189.6 [106.1;232.4]	0.857	63
CXCL2, Median [IQR]	291.0 [204.1;456.3]	316.0 [207.9;457.4]	491.8 [372.5;622.3]	263.6 [192.6;459.2]	224.1 [202.6;381.9]	0.323	63
CXCL5, Median [IQR]	373.3 [234.5;529.3]	335.8 [249.3;532.6]	387.6 [310.8;431.7]	408.7 [357.5;555.8]	472.4 [315.4;508.0]	0.761	63
CXCL6, Median [IQR]	32.0 [22.9;46.1]	28.4 [21.4;38.1]	44.1 [39.3;54.4]	40.0 [23.5;54.6]	28.3 [26.4;32.0]	0.082	63
CXCL8, Median [IQR]	32.2 [15.4;79.2]	36.5 [16.0;88.5]	17.6 [13.8;25.5]	27.0 [16.8;38.4]	23.6 [21.3;40.7]	0.613	63
CXCL12, Median [IQR]	368.0 [325.1;404.4]	339.0 [323.6;399.4]	459.2 [370.3;546.3]	375.3 [315.1;442.7]	358.1 [343.2;392.0]	0.692	62
<b>PROG-LFUP</b>							
CXCL1, Median [IQR]	248.8 [185.5;326.7]	366.0 [186.3;338.3]	214.6 [197.5;231.7]	246.2 [197.5;302.6]	216.2 [186.1;255.0]	0.657	43
CXCL2, Median [IQR]	423.8 [324.7;624.4]	340.9 [235.2;683.7]	222.4 [213.5;231.3]	471.8 [430.7;581.4]	347.4 [271.4;468.3]	0.316	43
CXCL5, Median [IQR]	551.7 [443.9;899.8]	532.0 [445.9;624.0]	515.4 [464.8;566.0]	529.7 [468.5;742.7]	880.4 [590.9;1339.0]	0.524	43
CXCL6, Median [IQR]	39.4 [30.8;53.5]	44.1 [29.0;58.5]	37.7 [26.9;38.6]	38.2 [31.5;53.3]	34.5 [29.4;41.1]	0.811	43
CXCL8, Median [IQR]	46.8 [24.9;113.7]	40.2 [25.3;120.2]	102.8 [60.8;145.0]	60.4 [30.4;89.8]	424.0 [28.7;1005.3]	0.930	41
CXCL12, Median [IQR]	402.8 [363.2;459.6]	404.6 [377.5;474.5]	359.7 [358.7;360.7]	432.4 [354.7;461.3]	376.8 [347.0;402.4]	0.446	43

Angiogenic CXC chemokines median levels (pg/mL) and [IQR] obtained at specific time points associated to patients metastatic site. P values correspond to the Kruskal-Wallis test.

### Angiostatic

	Total N=104	Liver N=31	Lung N=11	Liver + Lung N=31	Other N=11	p	N
<b>PRET</b>							
CXCL9, Median [IQR]	12.9 [8.9;21.1]	12.0 [8.8;18.2]	14.2 [8.7;20.8]	13.8 [9.1;27.7]	12.8 [11.5;19.6]	0.712	104
CXCL10, Median [IQR]	178.8 [123.3;271.2]	152.6 [114.2;209.4]	195.8 [137.1;210.3]	200.1 [148.4;337.0]	177.5 [124.4;200.9]	0.102	104
CXCL11, Median [IQR]	29.6 [20.4;47.3]	30.7 [20.2;45.3]	24.3 [20.7;30.1]	35.2 [22.4;70.6]	27.2 [20.7;33.9]	0.252	104
CXCL13, Median [IQR]	27.4 [19.0;41.1]	25.1 [18.8;38.4]	27.8 [24.2;32.8]	29.5 [22.4;49.4]	24.6 [15.9;31.2]	0.229	104
CXCL16, Median [IQR]	516.0 [427.0;588.8]	495.7 [411.6;545.2]	572.0 [434.8;633.4]	534.4 [469.9;656.2]	427.7 [407.3;667.9]	0.040	104
<b>EVAR</b>							
CXCL9, Median [IQR]	10.0 [6.9;16.0]	9.2 [6.5;16.3]	15.7 [11.7;17.7]	9.3 [7.2;13.6]	7.8 [7.8;19.3]	0.886	63
CXCL10, Median [IQR]	139.6 [106.8;191.4]	149.5 [114.3;179.8]	191.6 [134.8;239.5]	126.2 [103.1;181.2]	103.7 [102.9;206.7]	0.780	63
CXCL11, Median [IQR]	20.0 [14.4;30.0]	20.0 [15.0;30.3]	22.4 [14.7;30.2]	17.4 [13.4;26.6]	21.4 [20.0;43.1]	0.613	63
CXCL13, Median [IQR]	27.1 [18.9;36.9]	24.2 [17.0;33.9]	33.6 [31.5;36.6]	28.8 [24.1;42.8]	18.9 [17.2;28.9]	0.145	63
CXCL16, Median [IQR]	478.6 [431.9;541.1]	477.9 [409.0;564.6]	491.2 [380.5;541.3]	511.1 [457.5;559.2]	446.2 [440.8;584.0]	0.868	63
<b>PROGLFUP</b>							
CXCL9, Median [IQR]	11.0 [9.1;16.7]	11.9 [9.6;17.2]	8.1 [7.7;8.5]	10.7 [8.9;14.5]	13.8 [10.5;16.8]	0.383	43
CXCL10, Median [IQR]	167.8 [139.4;196.6]	166.5 [143.8;192.4]	172.2 [158.6;185.7]	157.5 [129.8;221.5]	196.2 [167.5;231.8]	0.880	43
CXCL11, Median [IQR]	30.6 [21.7;41.1]	31.6 [23.4;48.8]	24.0 [23.4;24.5]	28.0 [20.4;35.6]	36.9 [21.9;49.3]	0.678	43
CXCL13, Median [IQR]	26.6 [20.0;34.1]	27.7 [21.2;43.4]	27.6 [27.2;28.0]	26.6 [18.8;34.1]	17.6 [15.3;20.3]	0.147	43
CXCL16, Median [IQR]	648.3 [526.7;745.3]	692.3 [502.1;765.8]	521.3 [394.1;648.5]	612.1 [538.5;689.8]	592.9 [567.5;622.3]	0.853	43

**Angiostatic CXC chemokines median levels (pg/mL) and [IQR] obtained at specific time points associated to patients metastatic site. P values correspond to the Kruskal-Wallis test.**

## CXC chemokines by time-point and first-line treatment

### Angiogenic

	Total N=103	CT N=37	CT + Bevacirumab N=39	CT+ anti-EGFR N=27	p	N
<b>PRET</b>						
CXCL1, Median [IQR]	281.6 [196.3;401.2]	265.4 [202.9;368.2]	289.1 [204.8;368.1]	270.8 [186.4;459.9]	0.873	103
CXCL2, Median [IQR]	683.6 [475.2;956.1]	701.3 [517.0;1166.1]	693.8 [503.3;932.2]	640.9 [382.7;915.3]	0.260	103
CXCL5, Median [IQR]	737.0 [547.2;1038.7]	698.3 [596.8;1019.6]	863.2 [584.5;1050.8]	629.9 [520.3;1020.4]	0.484	103
CXCL6, Median [IQR]	57.1 [42.6;82.2]	60.2 [45.3;71.7]	54.9 [39.2;83.9]	55.0 [41.2;90.9]	0.951	103
CXCL8, Median [IQR]	53.7 [30.4;132.2]	50.9 [27.9;122.3]	69.6 [34.1;179.3]	50.0 [30.2;126.5]	0.523	103
CXCL12, Median [IQR]	500.1 [437.3;564.8]	502.5 [420.0;555.1]	486.6 [444.8;549.6]	519.5 [436.5;617.4]	0.682	103
<b>EVAR</b>						
CXCL1, Median [IQR]	161.0 [124.4;213.6]	176.3 [140.1;204.2]	143.1 [98.6;186.4]	175.7 [143.8;229.5]	0.175	62
CXCL2, Median [IQR]	290.1 [203.3;443.1]	302.1 [173.5;396.4]	250.8 [206.1;463.7]	334.1 [217.0;450.2]	0.842	62
CXCL5, Median [IQR]	372.9 [254.1;527.5]	456.1 [328.5;569.7]	359.6 [261.7;479.5]	355.2 [253.2;567.9]	0.582	62
CXCL6, Median [IQR]	32.4 [22.9;46.4]	36.7 [27.5;46.2]	26.7 [19.5;36.3]	36.0 [22.6;50.9]	0.168	62
CXCL8, Median [IQR]	32.2 [14.9;70.1]	37.9 [19.2;100.6]	30.0 [12.3;40.6]	33.1 [16.0;44.6]	0.416	62
CXCL12, Median [IQR]	363.0 [323.7;402.6]	359.0 [338.5;397.3]	343.2 [317.7;398.5]	382.9 [335.8;463.7]	0.355	61
<b>PROG-LFUP</b>						
CXCL1, Median [IQR]	248.8 [185.5;326.7]	275.4 [219.0;316.5]	246.2 [183.2;278.5]	239.2 [213.3;458.9]	0.527	43
CXCL2, Median [IQR]	423.8 [234.7;624.4]	311.1 [257.0;439.1]	451.5 [305.7;599.9]	437.6 [199.3;828.1]	0.697	43
CXCL5, Median [IQR]	551.7 [445.9;690.8]	440.6 [396.7;592.8]	551.7 [447.6;616.6]	629.7 [457.6;743.4]	0.250	43
CXCL6, Median [IQR]	39.4 [30.8;53.5]	39.6 [27.5;51.5]	38.2 [30.0;45.3]	50.4 [45.1;76.1]	0.027	43
CXCL8, Median [IQR]	46.8 [24.9;113.7]	33.3 [28.4;46.7]	43.7 [23.3;94.9]	110.7 [37.8;240.7]	0.496	41
CXCL12, Median [IQR]	402.8 [363.2;459.6]	368.1 [307.2;465.2]	398.0 [364.7;432.4]	464.5 [403.8;491.9]	0.163	43

Angiogenic CXC chemokines median levels (pg/mL) and [IQR] obtained at specific time points associated to patients first-line treatment. P values correspond to the Kruskal-Wallis test.

### Angiostatic

	Total N=103	CT N=37	CT + Bevacizumab N=39	CT+ anti-EGFR N=27	p	N
<b>PRET</b>						
CXCL9, Median [IQR]	12.9 [8.9;21.1]	13.8 [8.0;19.7]	12.6 [9.1;22.7]	12.4 [9.1;24.4]	0.960	103
CXCL10, Median [IQR]	179.3 [123.4;271.6]	178.3 [113.9;210.5]	188.3 [116.9;298.7]	169.2 [131.9;278.8]	0.837	103
CXCL11, Median [IQR]	29.6 [20.4;47.6]	29.7 [18.5;42.0]	29.6 [21.9;49.7]	27.1 [21.5;52.5]	0.886	103
CXCL13, Median [IQR]	27.6 [19.1;41.3]	26.8 [22.0;40.9]	25.4 [19.5;38.2]	30.0 [18.2;45.4]	0.714	103
CXCL16, Median [IQR]	516.2 [427.3;589.9]	497.3 [424.5;596.8]	521.0 [437.9;635.4]	466.1 [397.1;577.8]	0.473	103
<b>EVAR</b>						
CXCL9, Median [IQR]	9.2 [6.8;15.7]	8.3 [7.8;14.1]	10.0 [7.3;13.5]	13.0 [6.0;17.3]	0.932	62
CXCL10, Median [IQR]	141.9 [105.3;196.1]	173.5 [126.8;266.2]	120.6 [106.8;164.7]	139.2 [100.3;196.0]	0.162	62
CXCL11, Median [IQR]	19.8 [14.3;29.3]	22.8 [15.4;34.8]	16.8 [12.9;21.5]	20.3 [15.1;30.8]	0.093	62
CXCL13, Median [IQR]	27.7 [18.9;37.0]	25.8 [16.0;43.4]	24.6 [18.9;28.5]	31.4 [25.2;56.3]	0.064	62
CXCL16, Median [IQR]	481.6 [433.7;561.6]	548.1 [439.2;608.6]	518.4 [459.8;554.2]	447.7 [384.5;479.4]	0.042	62
<b>PROG-LFUP</b>						
CXCL9, Median [IQR]	11.0 [9.1;16.7]	8.9 [6.3;11.8]	11.6 [9.7;18.2]	11.0 [9.2;14.5]	0.178	43
CXCL10, Median [IQR]	167.8 [139.4;196.6]	185.1 [133.6;260.6]	165.1 [133.2;191.4]	187.7 [149.9;245.9]	0.525	43
CXCL11, Median [IQR]	30.6 [21.7;41.1]	25.7 [21.7;51.6]	30.6 [19.8;37.8]	31.5 [26.7;49.7]	0.345	43
CXCL13, Median [IQR]	26.6 [20.0;34.1]	23.4 [20.7;40.6]	24.2 [20.2;29.0]	40.4 [21.8;51.1]	0.289	43
CXCL16, Median [IQR]	648.3 [526.7;745.3]	607.0 [441.1;661.2]	685.2 [553.9;775.6]	594.0 [496.7;662.1]	0.198	43

**Angiostatic CXC chemokines median levels (pg/mL) and [IQR] obtained at specific time points associated to patients first-line treatment. P values correspond to the Kruskal-Wallis test.**

## CXC chemokines by time-point and MSI/MSS

### Angiogenic

	Total N=80	MSI N=5	MSS N=75	p	N
<b>PRET</b>					
CXCL1, Median [IQR]	293.6 [197.8;376.9]	310.7 [310.4;393.1]	287.7 [196.3;371.3]	0.335	80
CXCL2, Median [IQR]	685.2 [476.1;978.0]	732.1 [569.2;945.1]	680.3 [475.8;988.9]	0.945	80
CXCL5, Median [IQR]	755.1 [567.2;1041.6]	767.5 [651.4;1230.5]	754.5 [563.4;1038.7]	0.493	80
CXCL6, Median [IQR]	58.8 [42.0;82.1]	45.9 [38.9;82.4]	59.4 [42.8;81.8]	0.743	80
CXCL8, Median [IQR]	53.5 [30.5;139.4]	50.0 [38.3;76.2]	53.7 [30.4;139.4]	0.804	80
CXCL12, Median [IQR]	499.8 [443.6;559.4]	488.1 [473.1;542.2]	500.1 [439.7;562.3]	0.698	80
<b>EVAR</b>					
CXCL1, Median [IQR]	170.4 [137.0;215.7]	213.6 [213.6;213.6]	164.5 [133.0;217.7]	0.411	40
CXCL2, Median [IQR]	336.1 [219.9;476.3]	302.1 [302.1;302.1]	337.0 [219.4;483.5]	0.762	40
CXCL5, Median [IQR]	449.3 [332.3;549.2]	503.2 [503.2;503.2]	447.6 [326.7;555.9]	0.697	40
CXCL6, Median [IQR]	34.7 [24.6;47.3]	15.8 [15.8;15.8]	35.2 [25.8;48.0]	0.153	40
CXCL8, Median [IQR]	32.5 [16.9;95.3]	32.1 [32.1;32.1]	32.9 [16.7;96.5]	0.965	40
CXCL12, Median [IQR]	374.5 [331.3;419.6]	351.4 [351.4;351.4]	376.1 [328.5;419.6]	0.697	40
<b>PROG/LFUP</b>					
CXCL1, Median [IQR]	253.5 [184.4;297.3]	218.3 [203.1;233.5]	258.2 [183.2;309.5]	0.561	30
CXCL2, Median [IQR]	391.4 [231.9;635.4]	359.2 [281.9;436.6]	391.4 [237.5;664.6]	0.618	30
CXCL5, Median [IQR]	551.7 [442.5;708.0]	529.0 [485.2;572.8]	551.7 [444.6;722.0]	0.803	30
CXCL6, Median [IQR]	39.5 [30.2;49.9]	35.1 [33.0;37.3]	41.1 [29.6;51.6]	0.561	30
CXCL8, Median [IQR]	37.1 [21.0;118.9]	20.0 [19.4;20.6]	43.7 [24.2;129.3]	0.153	28
CXCL12, Median [IQR]	388.2 [361.7;443.5]	408.2 [385.0;431.4]	388.2 [360.7;437.0]	0.803	30

Angiogenic CXC chemokines median levels (pg/mL) and [IQR] obtained at specific time points associated to patients MSI-MSS Status. P values correspond to the Kruskal-Wallis test.

**Angiostatic**

	Total N=80	MSI N=5	MSS N=75	p	N
<b>PRET</b>					
CXCL9, Median [IQR]	13.0 [9.0;22.0]	12.5 [11.8;38.3]	13.0 [8.8;21.1]	0.544	80
CXCL10, Median [IQR]	183.4 [123.5;275.8]	195.8 [183.4;272.5]	180.7 [123.2;276.1]	0.376	80
CXCL11, Median [IQR]	31.5 [22.5;53.3]	35.2 [29.6;38.4]	31.0 [22.3;54.1]	0.866	80
CXCL13, Median [IQR]	27.5 [19.7;40.8]	27.9 [23.6;28.1]	27.2 [19.5;41.3]	0.493	80
CXCL16, Median [IQR]	520.0 [427.6;593.3]	647.8 [495.7;695.5]	517.1 [427.5;585.4]	0.186	80
<b>EVAR</b>					
CXCL9, Median [IQR]	9.6 [7.2;16.4]	48.1 [48.1;48.1]	8.4 [7.0;15.8]	0.109	40
CXCL10, Median [IQR]	141.9 [112.3;184.4]	299.9 [299.9;299.9]	139.6 [111.5;176.2]	0.153	40
CXCL11, Median [IQR]	20.5 [15.1;30.8]	55.7 [55.7;55.7]	20.4 [15.0;30.4]	0.153	40
CXCL13, Median [IQR]	26.8 [17.5;35.6]	25.8 [25.8;25.8]	27.1 [17.5;35.7]	0.897	40
CXCL16, Median [IQR]	475.8 [436.0;560.5]	632.0 [632.0;632.0]	474.0 [434.5;554.2]	0.209	40
<b>PROG/LFUP</b>					
CXCL9, Median [IQR]	11.2 [9.4;16.4]	9.0 [8.2;9.8]	11.6 [9.4;17.4]	0.280	30
CXCL10, Median [IQR]	172.9 [134.0;218.0]	126.3 [117.0;135.7]	179.1 [135.5;232.6]	0.183	30
CXCL11, Median [IQR]	28.2 [20.4;37.8]	21.1 [20.2;22.0]	30.9 [20.5;38.4]	0.183	30
CXCL13, Median [IQR]	27.6 [20.3;42.0]	25.7 [24.2;27.1]	27.8 [20.1;45.3]	0.739	30
CXCL16, Median [IQR]	603.8 [502.1;705.2]	713.1 [681.8;744.4]	593.3 [490.8;698.0]	0.280	30

**Angiostatic CXC chemokines median levels (pg/mL) and [IQR] obtained at specific time points associated to patients MSI-MSS Status. P values correspond to the Kruskal-Wallis test.**

## CXC chemokines by time-point and BRAF mutation

### Angiogenic

	Total N=104	WT N=77	MUT N=4	Not tested N=23	p	N
<b>PRET</b>						
CXCL1, Median [IQR]	283.3 [196.7;397.2]	274.2 [191.4;366.6]	401.2 [348.7;515.6]	321.8 [223.6;499.5]	0.144	104
CXCL2, Median [IQR]	686.9 [475.2;950.6]	640.9 [465.1;934.6]	976.8 [755.9;1155.1]	767.5 [645.2;981.5]	0.182	104
CXCL5, Median [IQR]	745.7 [547.4;1041.6]	684.3 [546.8;1001.6]	1333.3 [1079.9;4052.0]	957.2 [644.0;1155.6]	0.013	104
CXCL6, Median [IQR]	57.0 [42.7;82.1]	54.9 [40.5;70.3]	112.3 [95.3;120.6]	67.5 [48.4;112.9]	0.004	104
CXCL8, Median [IQR]	54.9 [30.5;135.7]	53.7 [30.2;116.1]	31.2 [25.0;81.9]	104.6 [36.4;254.5]	0.134	104
CXCL12, Median [IQR]	500.8 [437.4;563.1]	501.6 [441.9;561.5]	552.9 [524.1;599.1]	491.9 [417.1;531.1]	0.268	104
<b>EVAR</b>						
CXCL1, Median [IQR]	162.8 [124.6;217.7]	161.8 [139.4;222.0]	106.1 [61.0;187.6]	173.8 [117.9;190.9]	0.674	63
CXCL2, Median [IQR]	291.0 [204.1;456.5]	331.4 [217.0;450.2]	202.6 [108.9;213.4]	290.1 [189.4;504.6]	0.341	63
CXCL5, Median [IQR]	373.3 [254.5;529.3]	369.6 [254.7;529.0]	508.0 [270.0;873.4]	402.8 [265.7;514.6]	0.910	63
CXCL6, Median [IQR]	32.0 [22.9;46.1]	34.7 [22.5;48.1]	32.0 [16.9;47.0]	28.4 [25.2;38.7]	0.738	63
CXCL8, Median [IQR]	32.2 [15.4;79.2]	27.6 [16.0;51.2]	40.7 [20.4;82.5]	38.3 [15.9;89.7]	0.719	63
CXCL12, Median [IQR]	368.0 [325.1;404.4]	377.6 [338.3;419.6]	343.2 [179.6;367.6]	358.1 [315.2;392.7]	0.300	62
<b>PROG/FUP</b>						
CXCL1, Median [IQR]	248.8 [185.5;326.7]	256.9 [184.4;297.3]	178.9 [171.7;186.1]	244.5 [201.3;335.7]	0.323	43
CXCL2, Median [IQR]	423.8 [254.7;624.4]	437.6 [231.9;574.8]	237.2 [202.9;271.4]	437.6 [324.9;677.1]	0.286	43
CXCL5, Median [IQR]	551.7 [445.9;690.8]	513.7 [442.5;649.4]	1608.4 [1339.0;1877.8]	579.6 [454.6;649.1]	0.070	43
CXCL6, Median [IQR]	39.4 [30.8;53.5]	39.5 [30.8;51.6]	34.5 [32.2;36.7]	43.3 [36.1;70.5]	0.572	43
CXCL8, Median [IQR]	46.8 [24.9;113.7]	35.0 [21.0;93.4]	795.9 [405.4;1186.3]	89.8 [47.0;131.5]	0.174	41
CXCL12, Median [IQR]	402.8 [363.2;439.6]	400.1 [348.0;446.0]	376.8 [374.4;379.2]	446.7 [399.7;508.5]	0.151	43

Angiogenic CXC chemokines median levels (pg/mL) and [IQR] obtained at specific time points associated to patients BRAF mutational status. P values correspond to the Kruskal-Wallis test.

### Angiostatic

	Total N=104	WT N=77	MUT N=4	Not tested N=23	p	N
<b>PRET</b>						
CXCL9, Median [IQR]	12.9 [8.9;21.1]	12.4 [8.5;20.4]	24.2 [12.9;36.9]	13.0 [9.6;19.5]	0.368	104
CXCL10, Median [IQR]	178.8 [123.3;271.2]	163.3 [113.9;270.7]	243.0 [207.1;275.2]	179.3 [139.2;244.2]	0.324	104
CXCL11, Median [IQR]	29.6 [20.4;47.5]	30.0 [20.5;52.0]	37.4 [25.0;49.3]	28.0 [20.4;39.4]	0.646	104
CXCL13, Median [IQR]	27.4 [19.0;41.1]	27.2 [18.9;39.7]	30.4 [27.1;33.8]	26.0 [18.9;45.8]	0.798	104
CXCL16, Median [IQR]	516.0 [427.0;588.8]	515.8 [427.3;587.7]	532.2 [422.4;676.5]	523.4 [430.0;556.3]	0.904	104
<b>EVAR</b>						
CXCL9, Median [IQR]	10.0 [6.9;16.0]	8.4 [6.7;16.3]	7.8 [4.0;16.8]	11.2 [7.7;15.5]	0.798	63
CXCL10, Median [IQR]	159.6 [106.8;191.4]	149.5 [111.0;205.9]	103.7 [55.9;331.7]	152.7 [112.3;170.3]	0.657	63
CXCL11, Median [IQR]	20.0 [14.4;30.0]	21.7 [15.9;33.8]	21.4 [10.8;34.4]	15.8 [13.0;21.6]	0.064	63
CXCL13, Median [IQR]	27.1 [18.9;36.9]	28.3 [17.7;36.8]	18.9 [9.5;32.7]	26.8 [21.9;34.7]	0.657	63
CXCL16, Median [IQR]	478.6 [431.9;561.1]	475.5 [429.3;541.4]	446.2 [223.2;515.1]	539.7 [438.6;580.0]	0.424	63
<b>PROG/LFUP</b>						
CXCL9, Median [IQR]	11.0 [9.1;16.7]	10.0 [8.5;17.6]	17.3 [16.8;17.8]	11.3 [10.6;13.3]	0.364	43
CXCL10, Median [IQR]	167.8 [139.4;196.6]	168.6 [137.9;218.0]	264.4 [229.3;299.2]	156.2 [138.8;189.4]	0.215	43
CXCL11, Median [IQR]	30.6 [21.7;41.1]	31.6 [23.6;41.7]	31.6 [21.0;42.1]	24.2 [20.0;30.0]	0.295	43
CXCL13, Median [IQR]	26.6 [20.0;34.1]	27.2 [20.7;42.0]	18.2 [16.6;19.9]	24.2 [16.9;29.9]	0.178	43
CXCL16, Median [IQR]	648.3 [526.7;745.3]	632.1 [523.0;726.2]	563.0 [558.4;567.3]	683.2 [340.7;848.9]	0.560	43

**Angiostatic CXC chemokines median levels (pg/mL) and [IQR] obtained at specific time points associated to patients BRAF mutational status. P values correspond to the Kruskal-Wallis test.**

## CXC chemokines by time-point and RAS mutation

### Angiogenic

	Total N=102	WT N=47	MUT N=55	p	N
<b>PRET</b>					
CXCL1, Median [IQR]	283.3 [193.9;392.0]	310.7 [206.7;452.8]	265.4 [193.7;360.9]	0.187	102
CXCL2, Median [IQR]	686.9 [475.1;942.5]	675.3 [461.2;1046.1]	692.8 [484.1;885.0]	0.949	102
CXCL5, Median [IQR]	733.6 [547.0;1036.7]	729.3 [546.3;1055.4]	737.0 [563.4;1007.8]	0.799	102
CXCL6, Median [IQR]	57.0 [42.6;81.9]	58.1 [43.7;90.6]	56.4 [40.1;71.2]	0.340	102
CXCL8, Median [IQR]	54.9 [30.6;138.1]	46.8 [28.9;128.5]	59.6 [35.1;166.7]	0.374	102
CXCL12, Median [IQR]	499.8 [437.2;560.3]	518.0 [457.7;581.7]	486.6 [417.1;551.7]	0.162	102
<b>EVAR</b>					
CXCL1, Median [IQR]	164.5 [124.2;221.8]	173.0 [129.8;217.7]	155.6 [117.4;215.1]	0.614	61
CXCL2, Median [IQR]	302.1 [205.6;469.1]	289.3 [207.5;442.2]	334.0 [206.6;518.0]	0.614	61
CXCL5, Median [IQR]	372.6 [253.7;529.7]	366.7 [245.3;568.4]	372.9 [309.9;509.5]	0.885	61
CXCL6, Median [IQR]	30.5 [22.8;44.3]	32.8 [21.4;49.3]	29.3 [24.4;39.2]	0.604	61
CXCL8, Median [IQR]	32.2 [16.5;84.4]	32.1 [14.1;53.6]	32.6 [17.0;86.0]	0.564	61
CXCL12, Median [IQR]	363.0 [323.7;402.6]	384.2 [341.0;411.1]	348.3 [316.5;390.6]	0.087	61
<b>PROG/LFUP</b>					
CXCL1, Median [IQR]	248.8 [185.5;326.7]	239.2 [193.3;326.8]	258.2 [184.4;320.6]	0.882	43
CXCL2, Median [IQR]	423.8 [234.7;624.4]	305.7 [229.1;503.5]	457.8 [322.1;636.6]	0.143	43
CXCL5, Median [IQR]	551.7 [445.9;690.8]	579.6 [440.6;772.9]	540.7 [451.1;614.2]	0.728	43
CXCL6, Median [IQR]	39.4 [30.8;53.5]	47.6 [37.3;59.7]	38.3 [27.9;45.3]	0.066	43
CXCL8, Median [IQR]	46.8 [24.9;113.7]	74.8 [19.8;204.9]	40.6 [30.4;94.7]	0.915	41
CXCL12, Median [IQR]	402.8 [363.2;459.6]	443.7 [381.6;483.7]	388.5 [349.0;433.4]	0.050	43

Angiogenic CXC chemokines median levels (pg/mL) and [IQR] obtained at specific time points associated to patients RAS mutational status. P values correspond to the Kruskal-Wallis test.

*Angiostatic*

	Total N=102	WT N=47	MUT N=55	p	N
<b>PRET</b>					
CXCL9, Median [IQR]	12.9 [8.9;21.1]	13.0 [9.5;25.2]	12.6 [8.0;19.7]	0.252	102
CXCL10, Median [IQR]	178.8 [123.1;272.0]	183.5 [135.5;276.1]	177.1 [108.4;211.6]	0.284	102
CXCL11, Median [IQR]	29.2 [20.3;46.8]	28.8 [21.5;48.4]	29.6 [18.4;43.6]	0.587	102
CXCL13, Median [IQR]	27.4 [18.9;40.9]	29.3 [20.7;45.8]	25.0 [18.9;36.2]	0.077	102
CXCL16, Median [IQR]	514.4 [426.5;591.0]	495.7 [406.3;582.7]	517.1 [431.3;594.5]	0.392	102
<b>EVAR</b>					
CXCL9, Median [IQR]	8.4 [6.7;15.4]	10.9 [6.5;17.6]	8.3 [7.8;13.1]	0.778	61
CXCL10, Median [IQR]	139.5 [103.7;181.9]	139.5 [103.3;247.8]	134.7 [110.7;177.6]	0.686	61
CXCL11, Median [IQR]	20.0 [14.4;30.1]	21.9 [15.0;34.8]	17.6 [14.2;23.3]	0.116	61
CXCL13, Median [IQR]	26.6 [18.9;36.0]	28.8 [18.3;46.5]	24.0 [18.9;29.2]	0.124	61
CXCL16, Median [IQR]	478.1 [431.4;562.2]	443.2 [354.4;500.9]	535.8 [475.0;576.6]	0.001	61
<b>PROG/LFUP</b>					
CXCL9, Median [IQR]	11.0 [9.1;16.7]	12.0 [9.6;17.8]	10.5 [8.6;13.9]	0.264	43
CXCL10, Median [IQR]	167.8 [139.4;196.6]	194.7 [157.7;292.5]	156.9 [129.7;186.9]	0.024	43
CXCL11, Median [IQR]	30.6 [21.7;41.1]	37.7 [25.1;51.3]	26.9 [19.9;33.8]	0.062	43
CXCL13, Median [IQR]	26.6 [20.0;34.1]	34.8 [21.6;54.4]	23.7 [20.0;28.8]	0.143	43
CXCL16, Median [IQR]	648.3 [526.7;745.3]	572.1 [474.0;648.3]	689.8 [561.2;807.5]	0.025	43

**Angiostatic CXC chemokines median levels (pg/mL) and [IQR] obtained at specific time points associated to patients RAS mutational status. P values correspond to the Kruskal-Wallis test.**

## CXC chemokines by time-point and BRAF/RAS mutation

### Angiogenic

	Total N=102	BRAF mut N=4	NRAS mut N=9	KRAS mut N=40	WT N=49	p	N
<b>PRET</b>							
CXCL1, Median [IQR]	283.3 [195.9;392.0]	401.2 [348.7;515.6]	287.7 [226.5;511.9]	263.0 [191.9;349.3]	306.0 [197.5;452.8]	0.240	102
CXCL2, Median [IQR]	686.9 [475.1;942.5]	976.8 [755.9;1155.1]	767.4 [608.1;1166.1]	685.2 [479.4;846.4]	664.4 [451.0;930.8]	0.498	102
CXCL5, Median [IQR]	733.6 [347.0;1036.7]	1333.3 [1079.9;4052.0]	794.1 [754.5;1125.0]	716.8 [530.9;934.3]	684.3 [544.6;1035.3]	0.053	102
CXCL6, Median [IQR]	57.0 [42.6;81.9]	112.3 [95.3;120.6]	67.5 [44.6;91.9]	55.5 [39.1;70.2]	56.5 [42.8;80.1]	0.054	102
CXCL8, Median [IQR]	54.9 [30.6;138.1]	31.2 [25.0;81.9]	122.3 [58.2;178.1]	52.0 [33.4;147.4]	50.0 [30.2;128.5]	0.330	102
CXCL12, Median [IQR]	499.8 [437.2;560.3]	552.9 [324.1;599.1]	551.0 [491.9;568.9]	467.7 [414.5;543.0]	515.4 [445.0;581.7]	0.224	102
<b>EVAR</b>							
CXCL1, Median [IQR]	164.5 [124.2;221.8]	106.1 [61.0;187.6]	272.8 [230.5;315.0]	149.4 [113.5;201.5]	174.6 [141.0;215.7]	0.287	61
CXCL2, Median [IQR]	302.1 [205.6;469.1]	202.6 [108.9;213.4]	263.5 [228.8;298.2]	336.1 [208.6;527.2]	316.0 [217.0;450.2]	0.261	61
CXCL5, Median [IQR]	372.6 [253.7;529.7]	508.0 [270.0;873.4]	465.7 [460.9;470.6]	366.1 [298.4;523.1]	361.7 [249.3;567.9]	0.899	61
CXCL6, Median [IQR]	30.5 [22.8;44.3]	32.0 [16.9;41.0]	34.3 [33.9;34.8]	28.5 [23.8;39.7]	34.1 [21.4;48.5]	0.915	61
CXCL8, Median [IQR]	32.2 [16.5;84.4]	40.7 [20.4;82.5]	120.5 [111.4;129.7]	31.1 [16.9;76.6]	31.6 [14.2;51.2]	0.351	61
CXCL12, Median [IQR]	363.0 [323.7;402.6]	343.2 [179.6;367.6]	357.0 [354.0;360.0]	342.1 [315.3;397.1]	384.3 [341.6;430.4]	0.198	61
<b>PROG/FUP</b>							
CXCL1, Median [IQR]	248.8 [185.5;326.7]	178.9 [171.7;186.1]	443.0 [350.6;565.2]	248.8 [183.2;292.0]	248.2 [213.3;370.9]	0.111	43
CXCL2, Median [IQR]	423.8 [234.7;624.4]	237.2 [202.9;271.4]	351.1 [278.5;1070.8]	464.2 [324.9;624.4]	311.1 [234.7;604.5]	0.337	43
CXCL5, Median [IQR]	551.7 [445.9;690.8]	1608.4 [1339.0;1877.8]	655.9 [603.8;673.2]	507.7 [446.7;593.3]	469.3 [427.4;702.5]	0.117	43
CXCL6, Median [IQR]	39.4 [30.8;53.5]	34.5 [32.2;36.7]	84.6 [56.4;84.7]	38.2 [27.5;45.1]	48.2 [38.5;62.1]	0.071	43
CXCL8, Median [IQR]	46.8 [24.9;113.7]	795.9 [405.4;1186.3]	113.7 [88.8;145.0]	37.1 [30.7;73.7]	74.8 [21.6;172.4]	0.935	41
CXCL12, Median [IQR]	402.8 [363.2;459.6]	376.8 [374.4;379.2]	377.3 [304.1;413.7]	398.0 [353.2;433.1]	464.5 [400.1;498.0]	0.129	43

Angiogenic CXC chemokines median levels (pg/mL) and [IQR] obtained at specific time points associated to patients BRAF/RAS mutational status. P values correspond to the Kruskal-Wallis test.

**Angiostatic**

	Total N=102	BRAF mut N=4	NRAS mut N=9	KRAS mut N=46	WT N=43	p	N
<b>PRET</b>							
CXCL9, Median [IQR]	12.9 [8.9;21.1]	24.2 [12.9;36.9]	13.8 [7.6;19.7]	12.3 [8.3;19.3]	12.9 [9.1;24.7]	0.459	102
CXCL10, Median [IQR]	178.8 [123.1;272.0]	243.0 [207.1;273.2]	179.3 [158.4;270.7]	162.5 [107.6;210.4]	177.5 [131.9;282.7]	0.314	102
CXCL11, Median [IQR]	29.2 [20.3;46.8]	37.4 [25.0;49.3]	47.6 [22.8;58.1]	28.3 [18.1;41.4]	28.8 [21.5;46.2]	0.451	102
CXCL13, Median [IQR]	27.4 [18.9;40.9]	30.4 [27.1;33.8]	26.0 [22.0;40.9]	25.0 [18.8;35.2]	29.3 [18.8;46.2]	0.270	102
CXCL16, Median [IQR]	514.4 [426.5;591.0]	532.2 [422.4;676.5]	517.1 [497.3;592.1]	519.6 [430.8;594.5]	495.7 [401.3;590.8]	0.758	102
<b>EVAR</b>							
CXCL9, Median [IQR]	8.4 [6.7;15.4]	7.8 [4.0;16.8]	14.4 [11.3;17.6]	8.3 [7.7;12.6]	11.5 [6.5;17.3]	0.757	61
CXCL10, Median [IQR]	139.5 [103.7;181.9]	103.7 [55.9;331.7]	234.5 [204.0;264.9]	125.2 [107.6;171.6]	141.9 [116.1;227.2]	0.390	61
CXCL11, Median [IQR]	20.0 [14.4;30.1]	21.4 [10.8;34.4]	25.9 [21.9;29.9]	17.0 [14.2;22.8]	22.3 [15.1;34.3]	0.338	61
CXCL13, Median [IQR]	26.6 [18.9;36.0]	18.9 [9.5;32.7]	49.0 [39.2;58.8]	22.8 [18.5;28.5]	28.9 [19.2;48.8]	0.084	61
CXCL16, Median [IQR]	478.1 [431.4;562.2]	446.2 [223.2;515.1]	874.6 [846.1;903.0]	533.7 [473.8;564.6]	441.3 [354.5;492.8]	0.005	61
<b>PROG-LFUP</b>							
CXCL9, Median [IQR]	11.0 [9.1;16.7]	17.3 [16.8;17.8]	9.5 [5.8;11.1]	10.7 [8.9;14.8]	11.3 [9.2;17.5]	0.371	43
CXCL10, Median [IQR]	167.8 [139.4;196.6]	264.4 [229.5;299.2]	184.5 [154.4;240.8]	156.2 [129.8;186.3]	187.7 [154.9;258.3]	0.087	43
CXCL11, Median [IQR]	30.8 [21.7;41.1]	31.6 [21.0;42.1]	37.8 [34.2;49.5]	25.7 [19.7;32.6]	37.7 [26.7;51.1]	0.074	43
CXCL13, Median [IQR]	26.6 [20.0;34.1]	18.2 [16.6;19.9]	29.1 [24.8;42.8]	23.2 [19.7;28.1]	40.4 [24.6;54.8]	0.070	43
CXCL16, Median [IQR]	648.3 [526.7;745.3]	563.0 [558.4;567.5]	710.2 [570.3;808.2]	685.2 [571.7;796.9]	594.0 [454.3;662.1]	0.170	43

**Angiostatic CXC chemokines median levels (pg/mL) and [IQR] obtained at specific time points associated to patients BRAF/RAS mutational status. P values correspond to the Kruskal-Wallis test.**

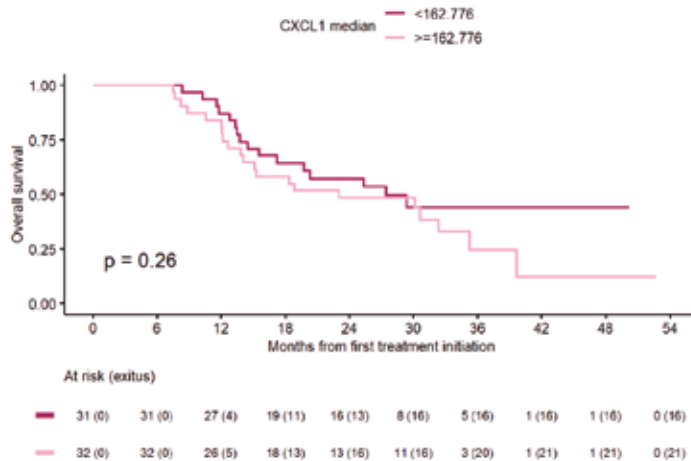
## Annex VII. CXC chemokines serum levels at EVAR and PROG time-points association with survival

### CXC chemokines serum levels association with risk of death and progression at EVAR

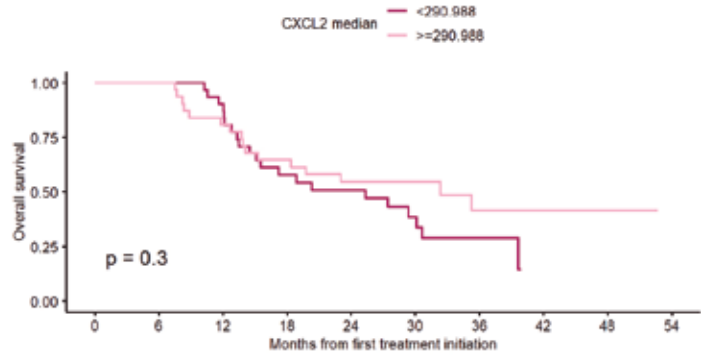
EVAR SERUM ASSOCIATION WITH RISK OF DEATH OR PROGRESSION. N = 63							
CHEMOKINES	MEDIAN LEVELS	OVERALL SURVIVAL			PROGRESSION FREE SURVIVAL		
		MEDIAN OS (95% CI)	HR (95% CI, p value) <sup>1</sup>	HRa (95% CI, p value) <sup>2</sup>	MEDIAN PFS (95% CI)	HR (95% CI, p value) <sup>1</sup>	HRa (95% CI, p value) <sup>2</sup>
CXCL1	<162.776	27.4 (17.2-NA)	1.39 (0.72-2.68, p=0.331)	0.87 (0.42-1.82, p=0.714)	10.2 (9.8-20.4)	1.00 (0.54-1.85, p=0.989)	0.99 (0.50-1.97, p=0.985)
	≥162.776	23 (14.1-NA)			10.7 (8.1-14.8)		
CXCL2	<290.988	25.3 (15.1-NA)	0.74 (0.38-1.42, p=0.363)	1.05 (0.52-2.14, p=0.886)	11.5 (9.9-16.6)	1.04 (0.55-1.94, p=0.911)	1.28 (0.64-2.55, p=0.985)
	≥290.988	32.4 (15.3-NA)			9.3 (7.8-NA)		
CXCL5	<373.324	24.5 (15.5-NA)	1.08 (0.56-2.08, p=0.817)	0.72 (0.29-1.72, p=0.473)	10.6 (9.3-NA)	1.61 (0.84-3.07, p=0.151)	1.54 (0.71-3.36, p=0.278)
	≥373.324	27.4 (15.3-NA)			10.1 (8.7-14.1)		
CXCL6	<31.984	19.7 (14.1-35.2)	0.61 (0.31-1.20, p=0.151)	0.62 (0.31-1.23, p=0.172)	9.3 (7.6-20.4)	0.76 (0.41-1.43, p=0.394)	0.76 (0.40-1.45, p=0.409)
	≥31.984	39.7 (18.8-NA)			12 (9.9-16.6)		
CXCL8	<32.22	32.4 (19.7-NA)	1.79 (0.92-3.49, p=0.087)	1.32 (0.66-2.64, p=0.430)	12.7 (8.1-20.4)	1.00 (0.54-1.86, p=0.997)	0.90 (0.48-1.69, p=0.739)
	≥31.22	19.6 (13.8-NA)			10.6 (9.8-14.5)		
CXCL9	<10.016	30.1 (18.8-NA)	1.29 (0.67-2.50, p=0.443)	0.78 (0.38-1.60, p=0.499)	11.6 (9.8-NA)	1.20 (0.64-2.22, p=0.572)	1.02 (0.52-1.99, p=0.963)
	≥10.016	21.4 (15.1-NA)			9.9 (8.1-15.1)		
CXCL10	<139.58	29.4 (18.8-NA)	0.89 (0.46-1.74, p=0.738)	0.84 (0.42-1.70, p=0.636)	11.6 (9.8-NA)	1.52 (0.81-2.85, p=0.192)	1.42 (0.74-2.72, p=0.286)
	≥139.58	23 (15.1-NA)			9.9 (7.8-14.1)		
CXCL11	<20.004	29.4 (18.4-NA)	1.44 (0.75-2.79, p=0.274)	0.94 (0.45-1.95, p=0.858)	11.5 (9.8-NA)	1.33 (0.72-2.47, p=0.367)	1.33 (0.68-2.61, p=0.408)
	≥20.004	20.3 (13.8-NA)			10.1 (7.8-14.1)		
CXCL12	<368.024	20.3 (15.5-NA)	0.78 (0.40-1.53, p=0.471)	0.72 (0.36-1.42, p=0.338)	11.5 (9.3-20.4)	1.17 (0.63-2.19, p=0.624)	1.02 (0.53-1.96, p=0.949)
	≥368.024	30.6 (15.3-NA)			10.7 (7.8-16.6)		
CXCL13	<27.104	19.7 (14.5-35.2)	0.63 (0.33-1.23, p=0.179)	0.57 (0.29-1.13, p=0.108)	9.8 (7.6-20.4)	0.74 (0.39-1.37, p=0.334)	0.68 (0.36-1.29, p=0.239)
	≥27.104	30.6 (15.3-NA)			12 (10.1-16.6)		
CXCL16	<478.624	32.4 (18.4-NA)	1.72 (0.88-3.37, p=0.113)	1.31 (0.61-2.83, p=0.492)	10.6 (8.1-20.4)	1.01 (0.54-1.89, p=0.966)	0.87 (0.44-1.71, p=0.689)
	≥478.624	21.4 (14.1-35.2)			10.7 (8.9-15.1)		

Serum EVAR median levels of the eleven CXCs studied and the association with OS and PFS. Median OS and PFS (in months), P values, HR, and 95% CI correspond to univariate (<sup>1</sup>) and multivariate (<sup>2</sup>) COX models. HR correspond to the category above the median respect to category below the median (by default = 1). The variables: PS, radical surgery, age and sex were considered in the OS multivariate analysis; PS, age and sex in the PFS multivariate analysis.

### OVERALL SURVIVAL

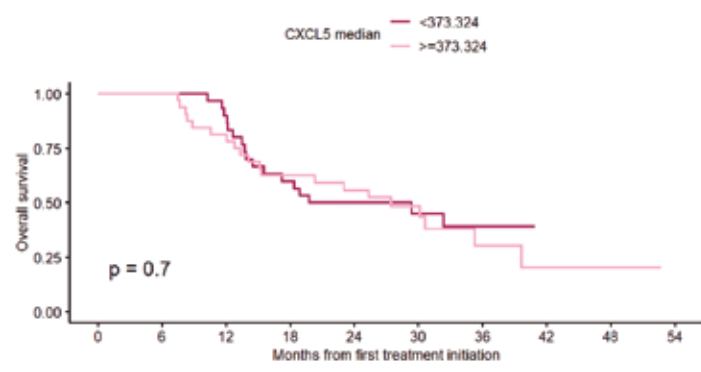


**ANNEX VII: CXC chemokines serum levels at EVAR and PROG time-points association with survival**



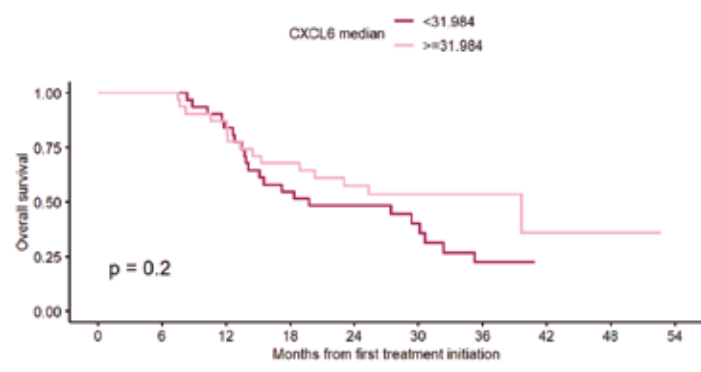
At risk (exitus)

31 (0)	31 (0)	28 (3)	17 (13)	14 (15)	8 (18)	2 (20)	0 (21)	0 (21)	0 (21)
32 (0)	32 (0)	28 (6)	20 (11)	15 (14)	11 (14)	6 (16)	2 (16)	2 (16)	0 (16)



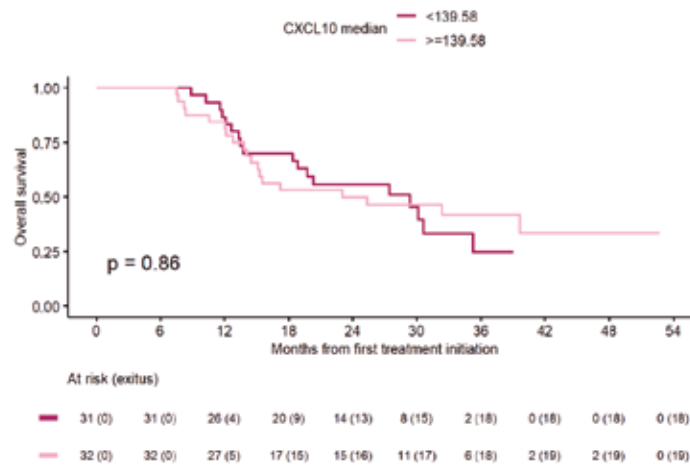
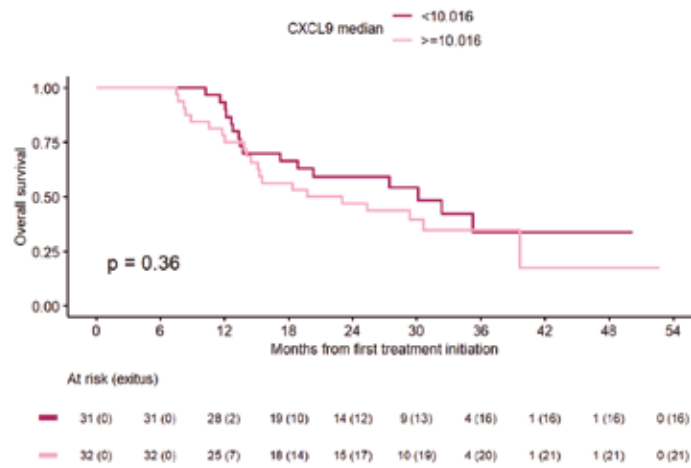
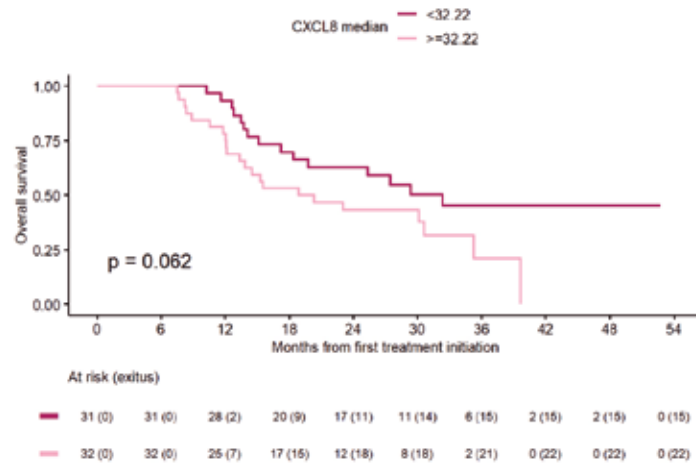
At risk (exitus)

31 (0)	31 (0)	27 (3)	18 (12)	13 (15)	9 (16)	4 (17)	0 (17)	0 (17)	0 (17)
32 (0)	32 (0)	26 (6)	19 (12)	16 (14)	10 (16)	4 (19)	2 (20)	2 (20)	0 (20)

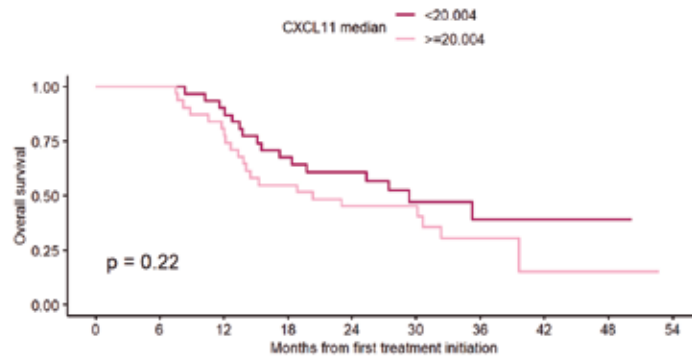


At risk (exitus)

31 (0)	31 (0)	26 (5)	17 (14)	14 (16)	9 (18)	4 (22)	0 (22)	0 (22)	0 (22)
32 (0)	32 (0)	27 (4)	20 (10)	15 (13)	10 (14)	4 (14)	2 (15)	2 (15)	0 (15)

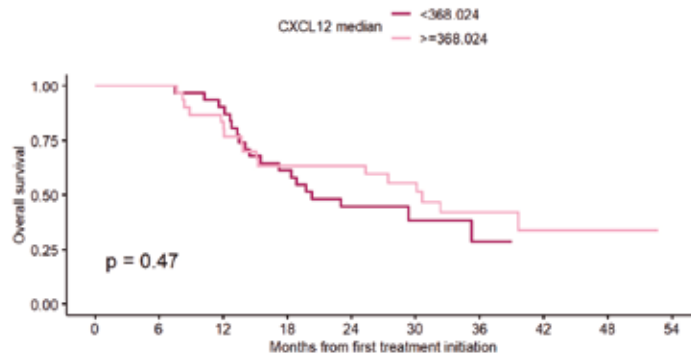


**ANNEX VII: CXC chemokines serum levels at EVAR and PROG time-points association with survival**



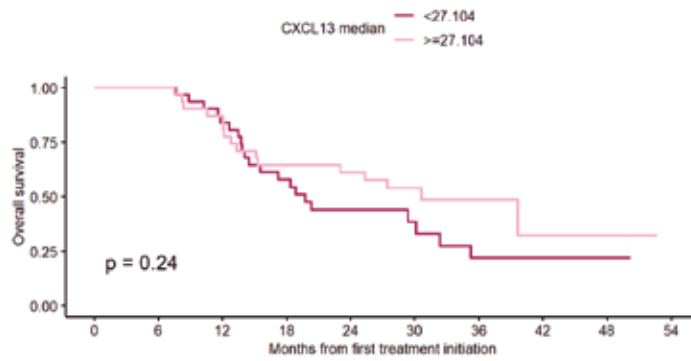
At risk (exitus)

31 (0)	31 (0)	28 (3)	20 (10)	15 (12)	9 (15)	5 (16)	1 (16)	1 (16)	0 (16)
32 (0)	32 (0)	26 (6)	17 (14)	14 (17)	10 (17)	3 (20)	1 (21)	1 (21)	0 (21)



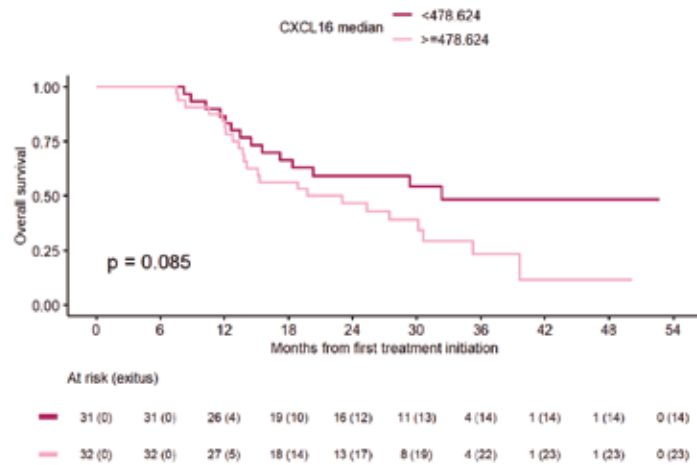
At risk (exitus)

31 (0)	31 (0)	28 (3)	19 (12)	12 (17)	6 (18)	2 (19)	0 (19)	0 (19)	0 (19)
31 (0)	31 (0)	25 (5)	18 (11)	17 (11)	13 (13)	6 (16)	2 (17)	2 (17)	0 (17)



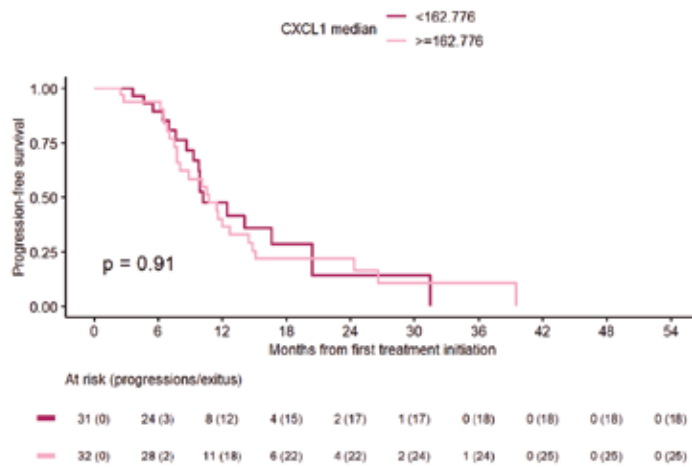
At risk (exitus)

31 (0)	31 (0)	26 (5)	17 (13)	11 (17)	7 (16)	4 (21)	1 (21)	1 (21)	0 (21)
32 (0)	32 (0)	27 (4)	20 (11)	18 (12)	12 (14)	4 (16)	1 (16)	1 (16)	0 (16)

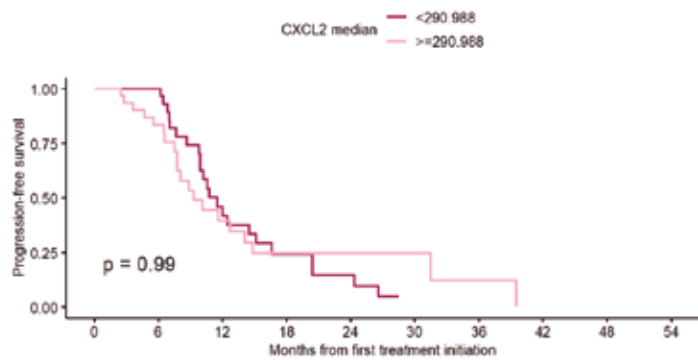


Kaplan-Meier survival curves showing OS of patients split according to the median values of the indicated CXCs at PRET. P values shown correspond to univariate log-rank test.

#### PROGRESSION FREE SURVIVAL

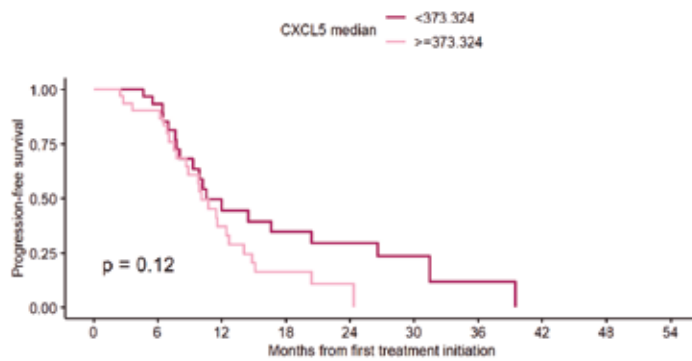


**ANNEX VII: CXCL chemokines serum levels at EVAR and PROG time-points association with survival**



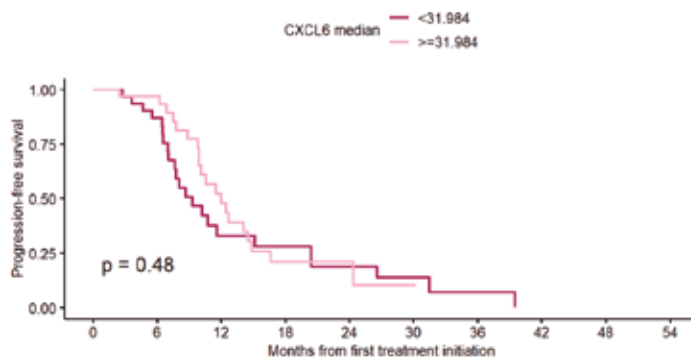
At risk (progressions/exitus)

—	31 (0)	30 (0)	11 (15)	5 (19)	3 (21)	0 (23)	0 (23)	0 (23)	0 (23)	0 (23)
—	32 (0)	22 (5)	8 (15)	5 (18)	3 (18)	3 (18)	1 (19)	0 (20)	0 (20)	0 (20)



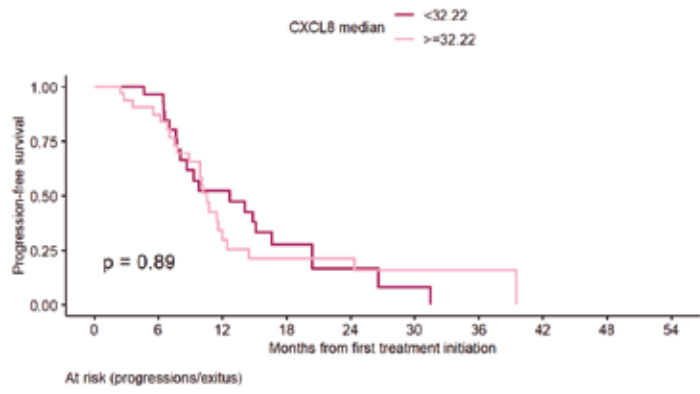
At risk (progressions/exitus)

—	31 (0)	26 (2)	10 (13)	7 (15)	6 (16)	3 (17)	1 (18)	0 (19)	0 (19)	0 (19)
—	32 (0)	26 (3)	9 (17)	3 (22)	1 (23)	0 (24)	0 (24)	0 (24)	0 (24)	0 (24)



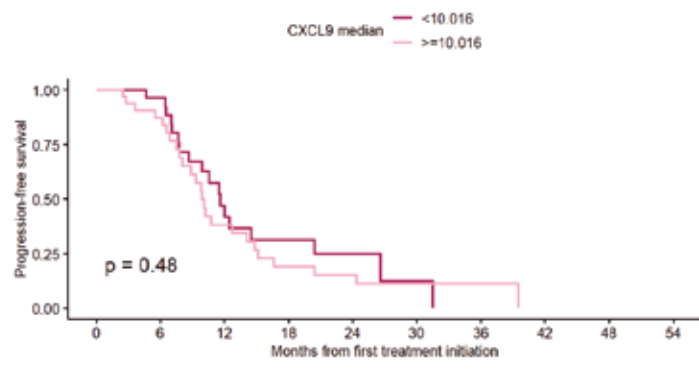
At risk (progressions/exitus)

—	31 (0)	25 (4)	7 (17)	6 (18)	4 (20)	2 (21)	1 (22)	0 (23)	0 (23)	0 (23)
—	32 (0)	27 (1)	12 (13)	4 (19)	2 (19)	1 (20)	0 (20)	0 (20)	0 (20)	0 (20)



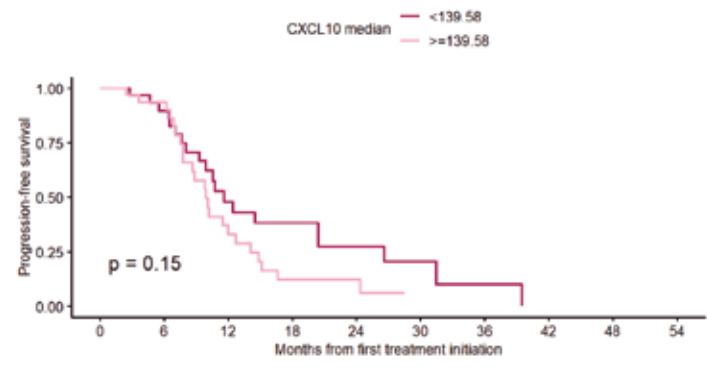
At risk (progressions/exitus)

■	31 (0)	26 (1)	11 (11)	5 (16)	2 (18)	1 (19)	0 (20)	0 (20)	0 (20)	0 (20)
■	32 (0)	26 (4)	8 (19)	5 (21)	4 (21)	2 (22)	1 (22)	0 (23)	0 (23)	0 (23)



At risk (progressions/exitus)

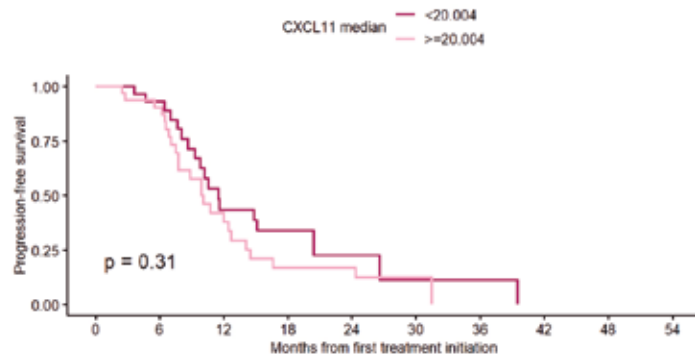
■	31 (0)	26 (1)	9 (13)	5 (15)	2 (16)	1 (17)	0 (18)	0 (18)	0 (18)	0 (18)
■	32 (0)	26 (4)	10 (17)	5 (22)	4 (23)	2 (24)	1 (24)	0 (25)	0 (25)	0 (25)



At risk (progressions/exitus)

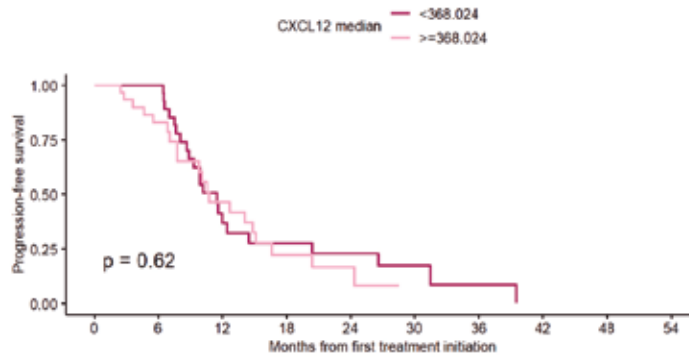
■	31 (0)	25 (3)	10 (13)	7 (15)	4 (17)	3 (18)	1 (19)	0 (20)	0 (20)	0 (20)
■	32 (0)	27 (2)	9 (17)	3 (22)	2 (22)	0 (23)	0 (23)	0 (23)	0 (23)	0 (23)

**ANNEX VII:** CXCL chemokines serum levels at EVAR and PROG time-points association with survival



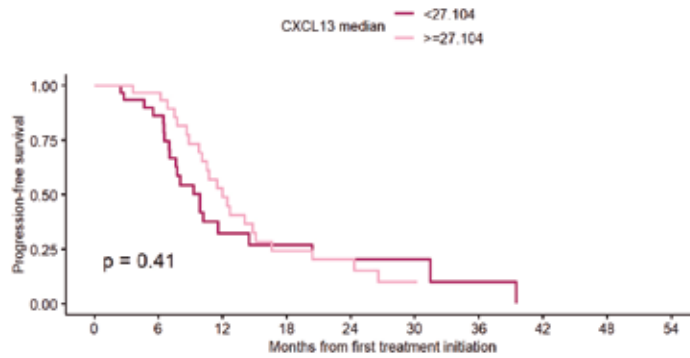
At risk (progressions/exits)

31 (0)	24 (2)	9 (13)	6 (15)	2 (17)	1 (18)	1 (18)	0 (19)	0 (19)	0 (19)
32 (0)	28 (3)	10 (17)	4 (22)	4 (22)	2 (23)	0 (24)	0 (24)	0 (24)	0 (24)



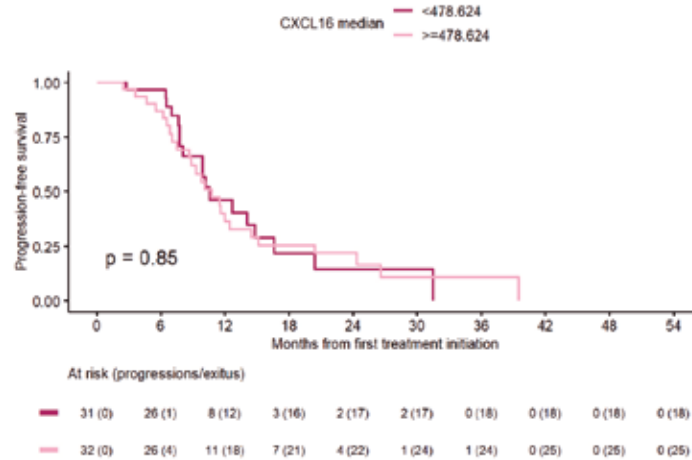
At risk (progressions/exits)

31 (0)	29 (0)	9 (16)	6 (18)	4 (19)	3 (20)	1 (21)	0 (22)	0 (22)	0 (22)
31 (0)	22 (8)	10 (13)	4 (18)	2 (19)	0 (20)	0 (20)	0 (20)	0 (20)	0 (20)



At risk (progressions/exits)

31 (0)	24 (4)	6 (17)	4 (18)	2 (19)	2 (19)	1 (20)	0 (21)	0 (21)	0 (21)
32 (0)	28 (1)	13 (13)	6 (19)	4 (20)	1 (22)	0 (22)	0 (22)	0 (22)	0 (22)



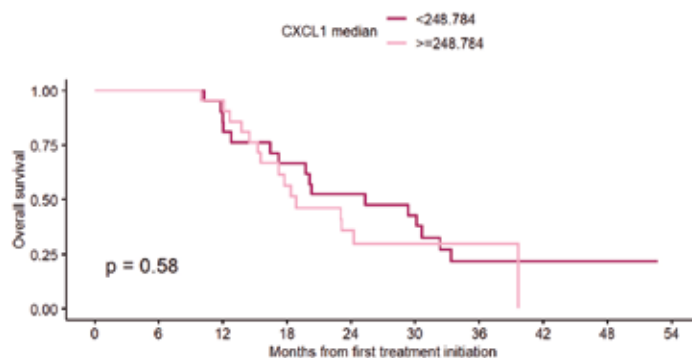
Kaplan-Meier survival curves showing PFS of patients split according to the median values of the indicated CXCs at PRET. P values shown correspond to univariate log-rank test.

CXC chemokines serum levels association with risk of death and progression at PROG

CHEMOKINES	MEDIAN LEVELS	PROG SERUM LEVELS ASSOCIATION WITH RISK OF DEATH OR PROGRESSION, N = 41					
		OVERALL SURVIVAL			PROGRESSION FREE SURVIVAL		
		MEDIAN OS (95% CI)	HR (95% CI, p value) <sup>1</sup>	HRa (95% CI, p value) <sup>2</sup>	MEDIAN PFS (95% CI)	HR (95% CI, p value) <sup>1</sup>	HRa (95% CI, p value) <sup>2</sup>
CXCL1	<248.784	25.3 (17.2-NA)	1.28 (0.62-2.65, p=0.505)	1.13 (0.54-2.38, p=0.744)	9.8 (7.7-13.5)	0.68 (0.35-1.34, p=0.264)	0.56 (0.28-1.14, p=0.110)
	≥248.784	18.8 (15.5-NA)			10.9 (10.1-24.4)		
CXCL2	<423.768	20.3 (16.4-NA)	1.08 (0.52-2.22, p=0.839)	1.36 (0.62-3.00, p=0.446)	10.6 (7.8-17.2)	0.94 (0.48-1.83, p=0.851)	1.23 (0.54-2.77, p=0.623)
	≥423.768	23 (17.2-NA)			10.7 (9.3-20.4)		
CXCL5	<551.736	29.4 (17.2-NA)	1.49 (0.72-3.09, p=0.287)	1.35 (0.64-2.85, p=0.433)	11.7 (8.7-24.4)	1.13 (0.58-2.20, p=0.718)	1.17 (0.59-2.35, p=0.652)
	≥551.736	18.8 (15.5-NA)			10.4 (9.8-14.8)		
CXCL6	<39.396	20.3 (17.2-32.4)	0.49 (0.23-1.04, p=0.064)	0.50 (0.23-1.09, p=0.082)	9.3 (7.6-14.8)	<b>0.50 (0.25-0.99, p=0.047)</b>	<b>0.43 (0.21-0.89, p=0.024)</b>
	≥39.396	23 (16.4-NA)			<b>11.7 (10.6-24.5)</b>		
CXCL8	<46.796	24.3 (18.4-39.7)	1.32 (0.64-2.74, p=0.458)	1.39 (0.66-2.94, p=0.387)	11.4 (8.7-17.2)	0.82 (0.41-1.62, p=0.566)	0.82 (0.40-1.69, p=0.594)
	≥46.796	20.3 (14.5-NA)			10.6 (8.9-20.4)		
CXCL9	<10.992	29.4 (17.2-NA)	1.32 (0.64-2.72, p=0.452)	1.48 (0.70-3.16, p=0.308)	12.2 (10.7-24.5)	1.57 (0.80-3.08, p=0.191)	1.74 (0.85-3.59, p=0.133)
	≥10.992	20.1 (15.3-32.4)			9.9 (8.9-13.5)		
CXCL10	<167.84	23 (17.2-NA)	1.04 (0.51-2.14, p=0.913)	1.13 (0.54-2.39, p=0.745)	11 (10.2-24.5)	1.24 (0.64-2.41, p=0.528)	1.33 (0.67-2.66, p=0.417)
	≥167.84	20.2 (17.2-NA)			9.9 (8.7-14.8)		
CXCL11	<30.596	23 (14.5-NA)	0.95 (0.46-1.94, p=0.8)	1.31 (0.55-3.11, p=0.547)	12.2 (9.9-NA)	1.49 (0.76-2.92, p=0.242)	1.97 (0.90-4.31, p=0.09)
	≥30.596	20.2 (17.2-32.4)			10 (8.1-13.5)		
CXCL12	<402.76	23 (17.2-NA)	0.78 (0.38-1.62, p=0.201)	1.54 (0.90-2.66, p=0.119)	9.9 (8.7-20.4)	0.83 (0.42-1.62, p=0.578)	0.70 (0.31-1.59, p=0.396)
	≥402.76	20.1 (16.4-NA)			10.7 (10.1-16.6)		
CXCL13	<26.62	23.3 (19.7-NA)	1.31 (0.63-2.70, p=0.471)	1.27 (0.57-2.81, p=0.557)	10.7 (8.7-24.5)	1.15 (0.59-2.25, p=0.680)	0.97 (0.45-2.10, p=0.936)
	≥26.62	17.8 (15.5-NA)			10.6 (9.9-13.5)		
CXCL16	<648.3	20.3 (14.5-NA)	1.28 (0.61-2.70, p=0.521)	1.60 (0.71-3.61, p=0.256)	10.6 (8.7-16.6)	0.81 (0.41-1.60, p=0.548)	0.89 (0.44-1.80, p=0.742)
	≥648.3	23 (17.8-33.4)			10.9 (9.3-20.4)		

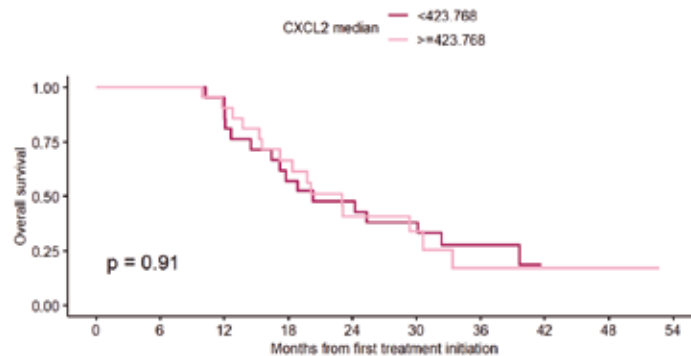
Serum PROG median levels of the eleven CXCs studied and the association with OS and PFS. Median OS and PFS (in months), P values, HR, and 95% CI correspond to univariate (<sup>1</sup>) and multivariate (<sup>2</sup>) COX models. HR correspond to the category above the median respect to category below the median (by default = 1). The variables: PS, radical surgery, age and sex were considered in the OS multivariate analysis; PS, age and sex in the PFS multivariate analysis. In bold, all statistically significant results with a p <0.05.

**OVERALL SURVIVAL**



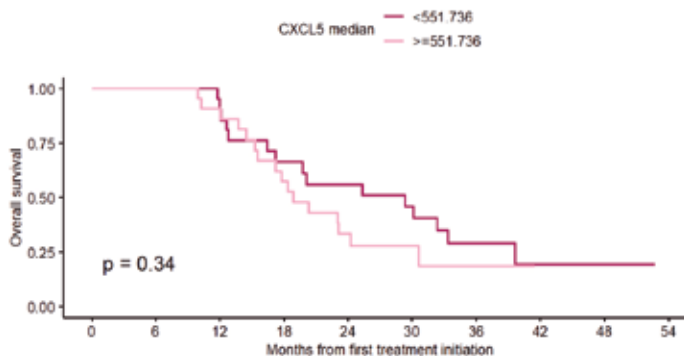
At risk (exitus)

21 (0)	21 (0)	18 (3)	14 (7)	11 (10)	9 (12)	4 (16)	1 (16)	1 (16)	0 (16)
22 (0)	22 (0)	20 (1)	11 (9)	6 (13)	4 (14)	2 (14)	0 (15)	0 (15)	0 (15)



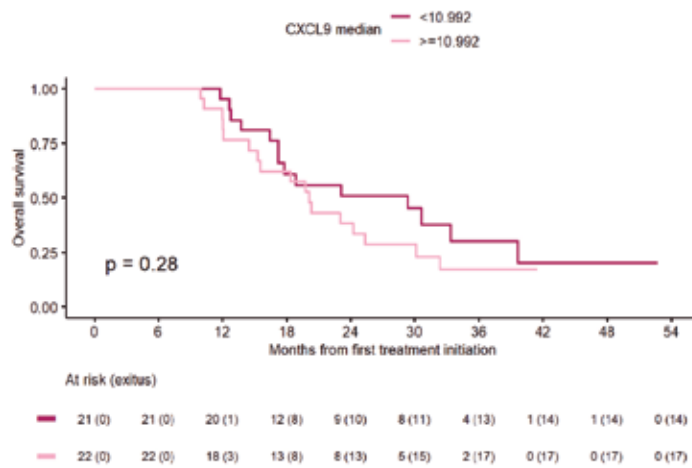
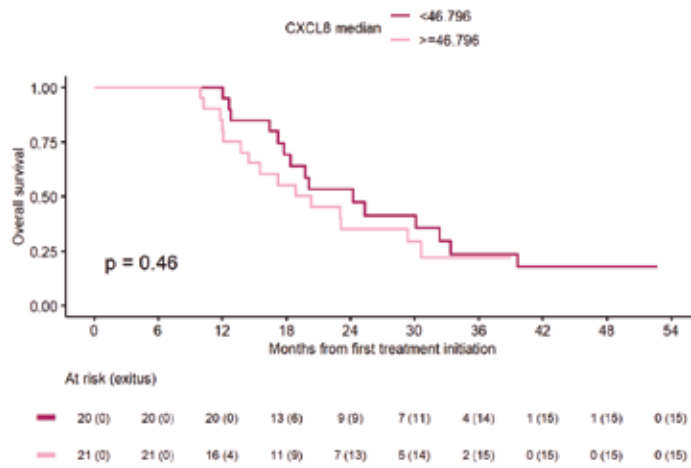
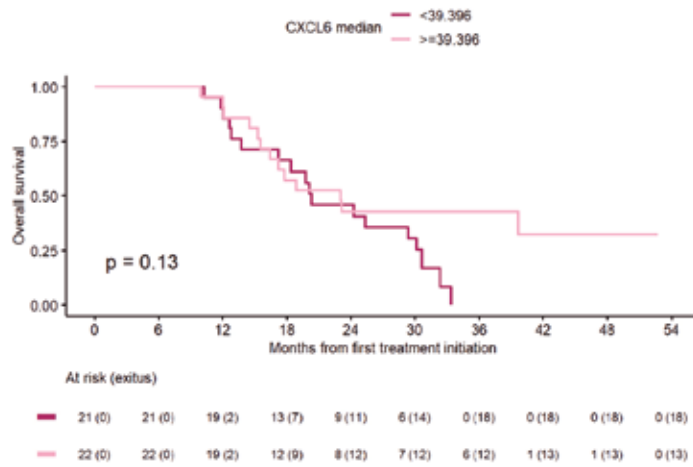
At risk (exitus)

21 (0)	21 (0)	19 (2)	12 (9)	10 (11)	8 (13)	4 (15)	0 (16)	0 (16)	0 (16)
22 (0)	22 (0)	19 (2)	13 (7)	7 (12)	5 (13)	2 (15)	1 (15)	1 (15)	0 (15)

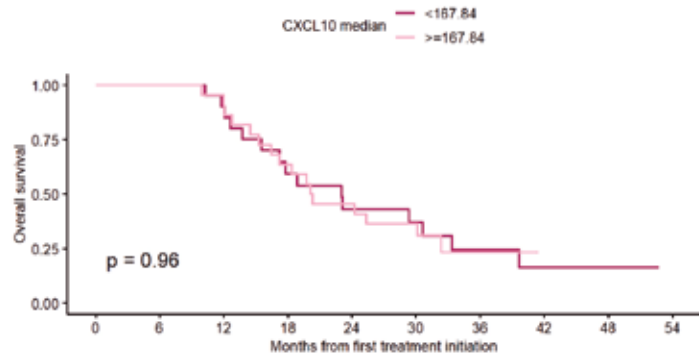


At risk (exitus)

21 (0)	21 (0)	19 (2)	13 (7)	11 (9)	9 (11)	4 (14)	1 (15)	1 (15)	0 (15)
22 (0)	22 (0)	19 (2)	12 (9)	6 (14)	4 (15)	2 (16)	0 (16)	0 (16)	0 (16)

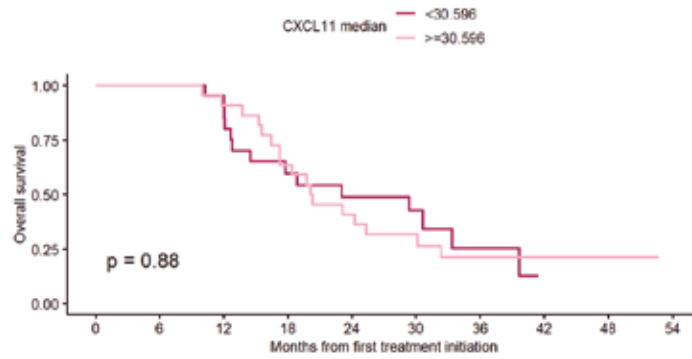


**ANNEX VII: CXCL chemokines serum levels at EVAR and PROG time-points association with survival**



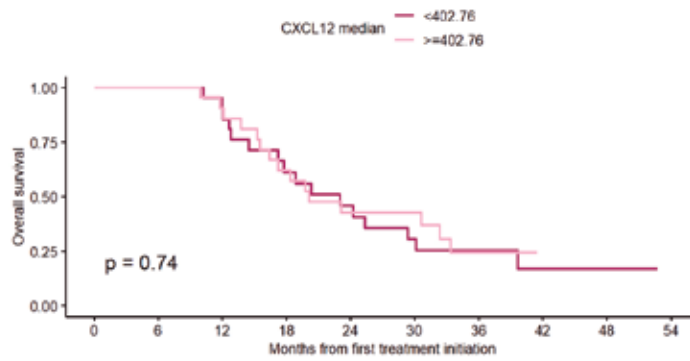
At risk (exitus)

21 (0)	21 (0)	18 (2)	11 (8)	7 (11)	6 (12)	4 (14)	1 (15)	1 (15)	0 (15)
22 (0)	22 (0)	20 (2)	14 (8)	10 (12)	7 (14)	2 (16)	0 (16)	0 (16)	0 (16)



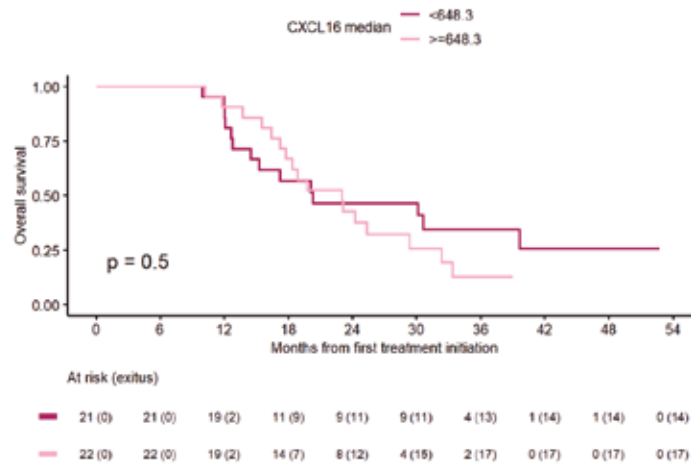
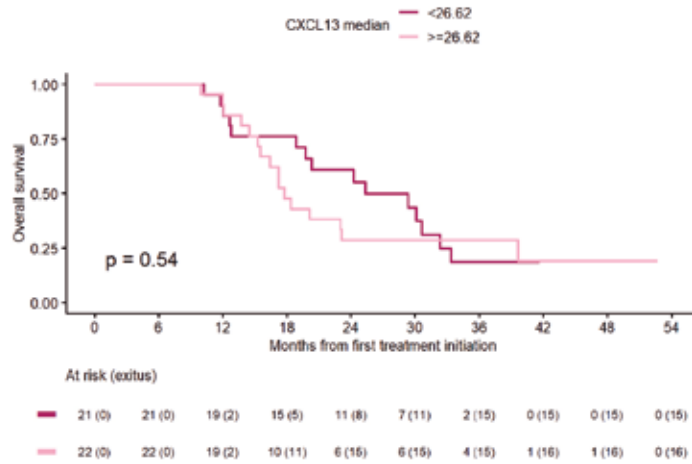
At risk (exitus)

21 (0)	21 (0)	18 (2)	11 (8)	8 (10)	7 (11)	3 (13)	0 (14)	0 (14)	0 (14)
22 (0)	22 (0)	20 (2)	14 (8)	9 (13)	6 (15)	3 (17)	1 (17)	1 (17)	0 (17)



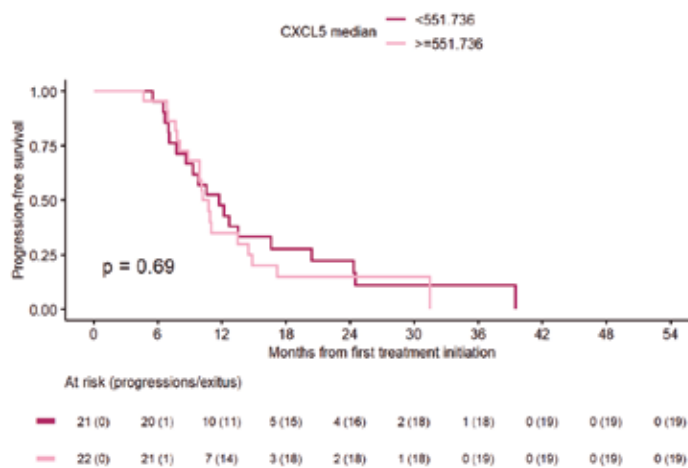
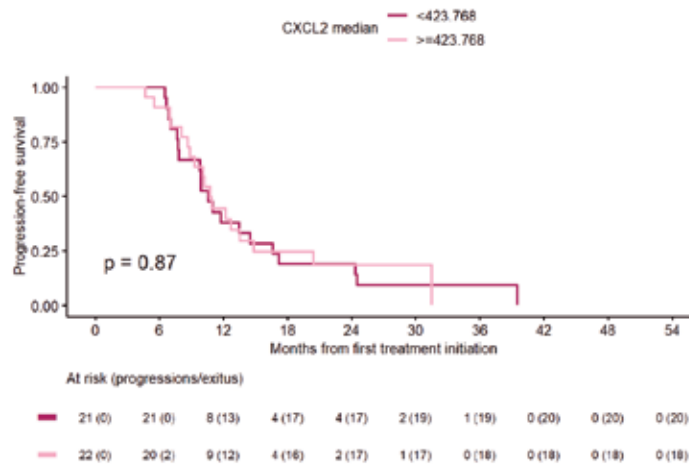
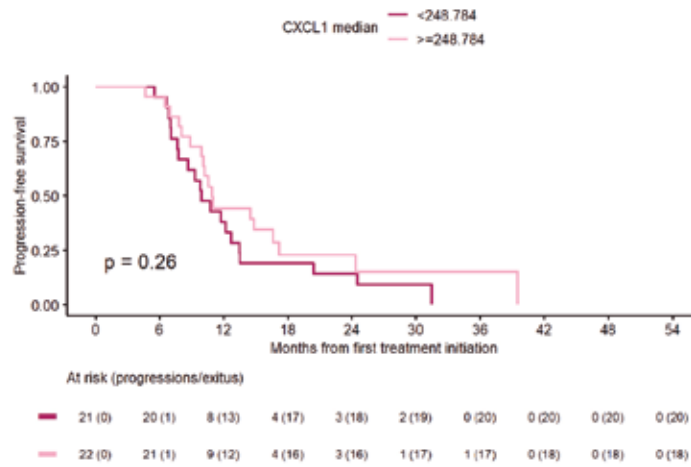
At risk (exitus)

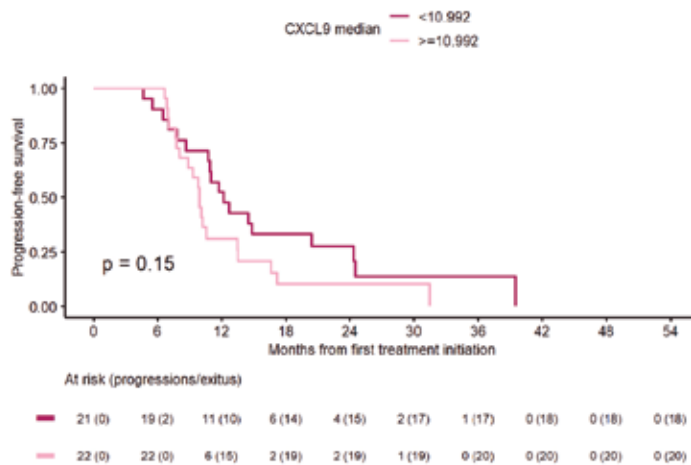
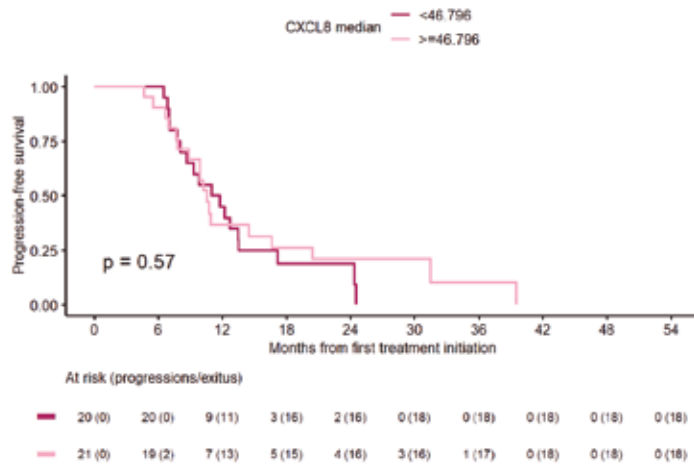
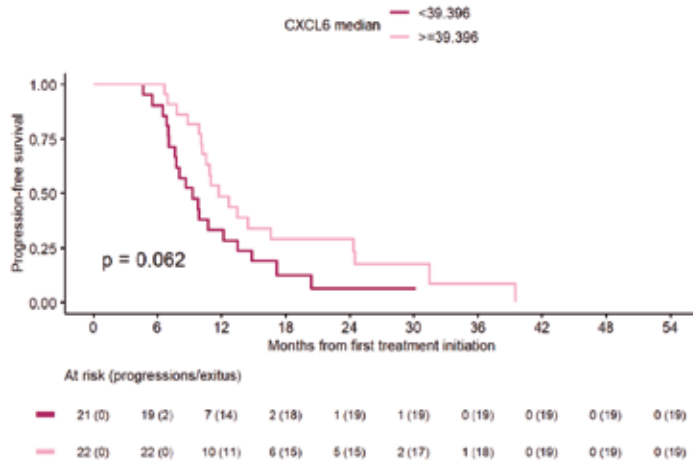
21 (0)	21 (0)	19 (2)	12 (8)	9 (11)	6 (14)	3 (15)	1 (16)	1 (16)	0 (16)
22 (0)	22 (0)	19 (2)	13 (8)	8 (12)	7 (12)	3 (15)	0 (15)	0 (15)	0 (15)



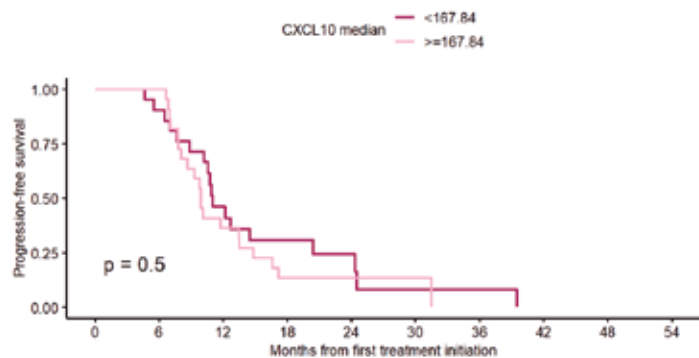
Kaplan-Meier survival curves showing OS of patients split according to the median values of the indicated CXCs at PRET. P values shown correspond to univariate log-rank test.

**PROGRESSION FREE SURVIVAL**



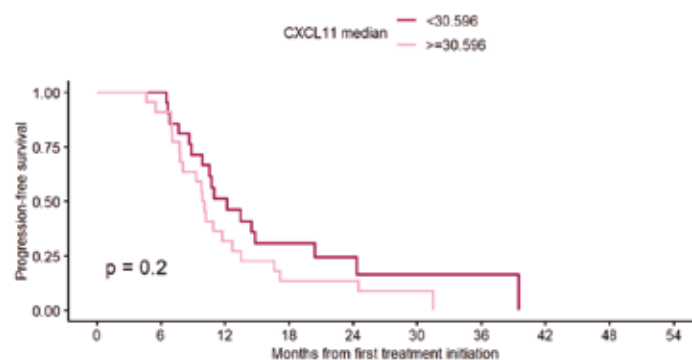


**ANNEX VII: CXC chemokines serum levels at EVAR and PROG time-points association with survival**



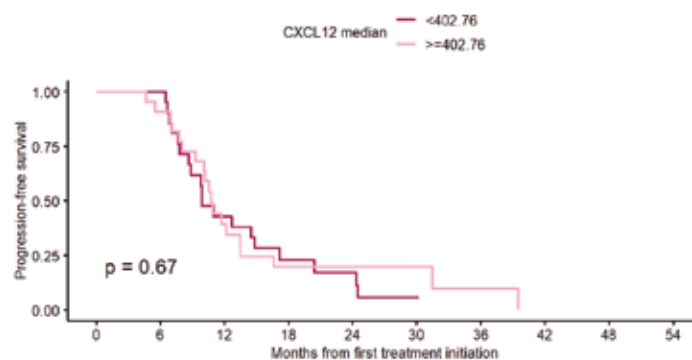
At risk (progressions/exitus)

—	21 (0)	19 (2)	9 (11)	5 (14)	3 (15)	1 (17)	1 (17)	0 (18)	0 (18)	0 (18)
—	22 (0)	22 (0)	8 (14)	3 (19)	3 (19)	2 (19)	0 (20)	0 (20)	0 (20)	0 (20)



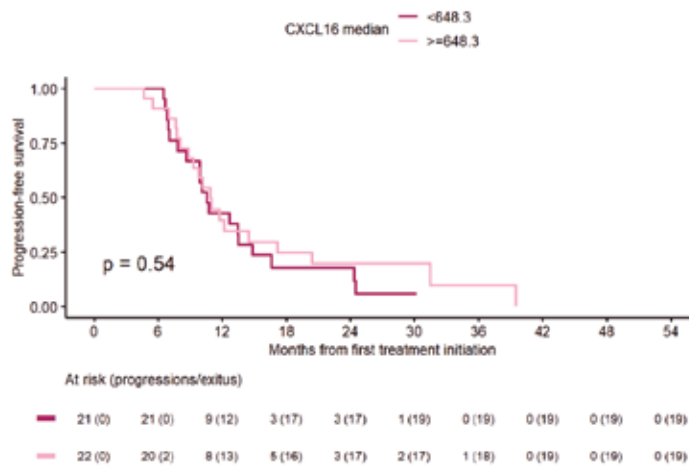
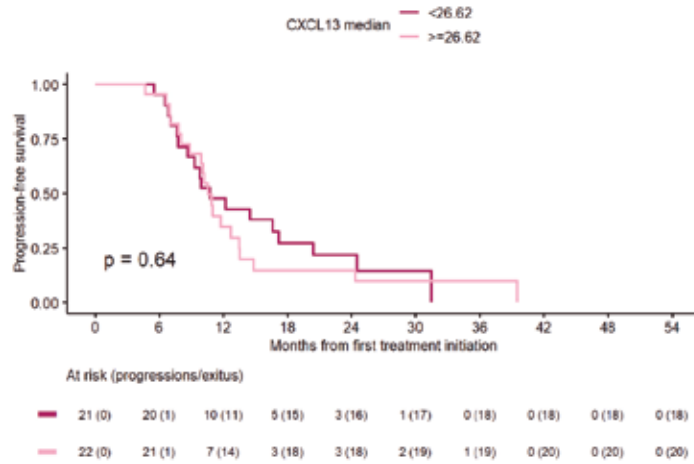
At risk (progressions/exitus)

—	21 (0)	21 (0)	10 (10)	5 (14)	3 (15)	2 (16)	1 (16)	0 (17)	0 (17)	0 (17)
—	22 (0)	20 (2)	7 (15)	3 (19)	3 (19)	1 (20)	0 (21)	0 (21)	0 (21)	0 (21)



At risk (progressions/exitus)

—	21 (0)	21 (0)	9 (12)	4 (16)	3 (17)	1 (19)	0 (19)	0 (19)	0 (19)	0 (19)
—	22 (0)	20 (2)	8 (13)	4 (17)	3 (17)	2 (17)	1 (18)	0 (19)	0 (19)	0 (19)



Kaplan-Meier survival curves showing PFS of patients split according to the median values of the indicated CXCs at PRET. P values shown correspond to univariate log-rank test.

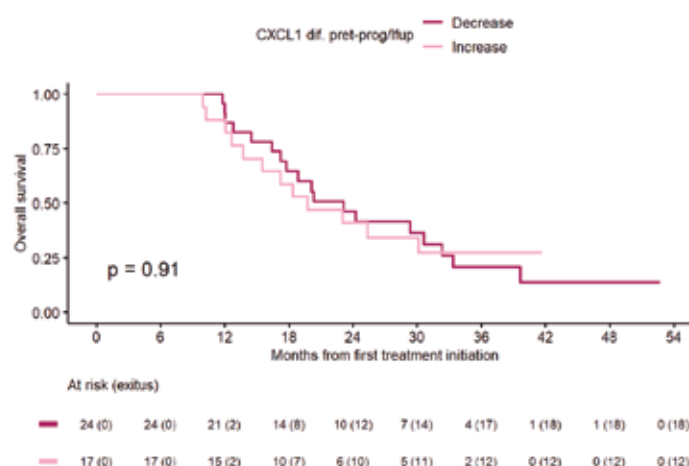
## Annex VIII. CXC chemokines dynamic changes along PRET-PROG and EVAR-PROG association with survival

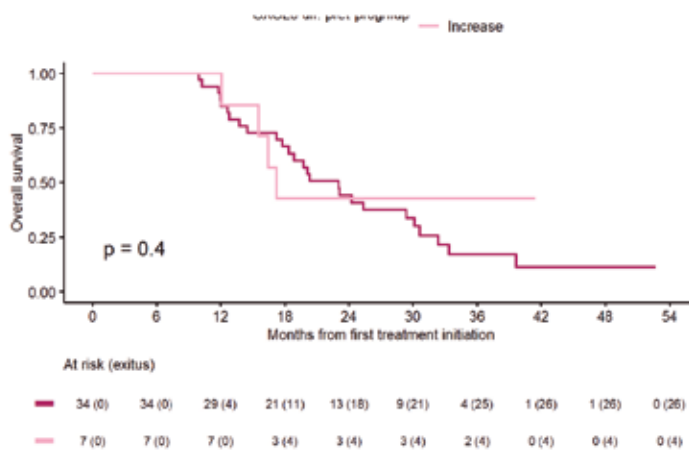
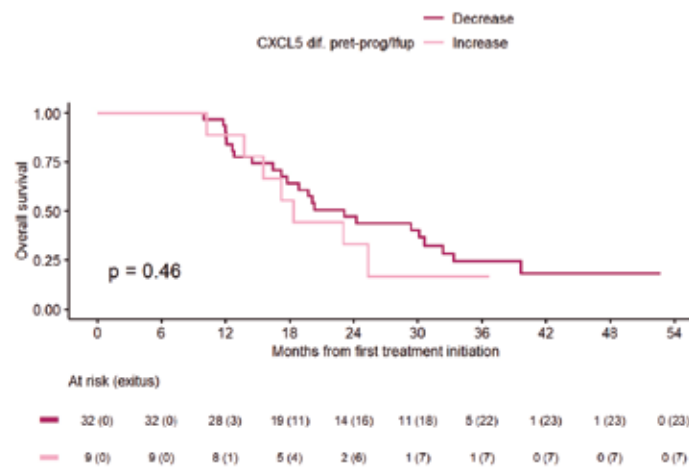
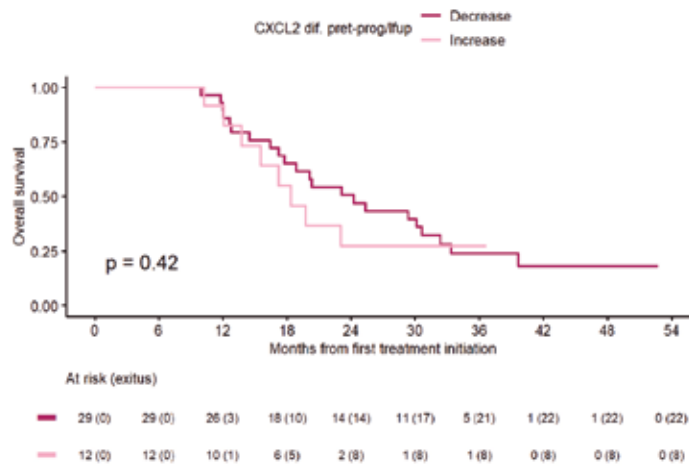
### PRET-PROG dynamic changes association with risk of death and progression

PRET-PROG DYNAMIC CHANGES ASSOCIATION WITH RISK OF DEATH OR PROGRESSION. N = 41								
CHEMOKINES	DYNAMIC CHANGE	OVERALL SURVIVAL			PROGRESSION FREE SURVIVAL			
		MEDIAN (95% CI)	HR (95%CI, p value) <sup>1</sup>	HRa (95%CI, p value) <sup>2</sup>	MEDIAN (95% CI)	HR (95%CI, p value) <sup>1</sup>	HRa (95%CI, p value) <sup>2</sup>	
CXCL1 MEDIAN	Decrease	23.1 (17.8-33.4)	1.04 (0.50-2.17, p=0.908)	1.79 (0.72-4.50, p=0.213)	11.7 (10.7-17.2)	0.26 (0.64-2.49, p=0.500)	1.79 (0.82-3.91, p=0.144)	
	Increase	19.7 (15.5-NA)			9.3 (7.6-NA)			
CXCL2 MEDIAN	Decrease	24.3 (17.8-33.4)	0.71 (0.31-1.63, p=0.422)	0.38 (0.14-1.06, p=0.064)	9.7 (8.1-NA)	0.93 (0.43-2.00, p=0.849)	1.29 (0.53-3.15, p=0.579)	
	Increase	18.4 (15.5-NA)			11 (9.8-14.5)			
CXCL5 MEDIAN	Decrease	23.1 (17.8-33.4)	0.72 (0.31-1.70, p=0.455)	0.52 (0.20-1.32, p=0.170)	8.9 (7.6-NA)	0.74 (0.33-1.64, p=0.454)	0.56 (0.23-1.36, p=0.200)	
	Increase	18.4 (15.5-NA)			11 (9.9-16.6)			
CXCL6 MEDIAN	Decrease	23 (18.4-30.6)	1.56 (0.54-4.51, p=0.412)	1.90 (0.57-6.31, p=0.294)	11.7 (10.2-NA)	1.28 (0.53-3.12, p=0.582)	2.04 (0.70-5.89, p=0.189)	
	Increase	17.2 (15.5-NA)			10.3 (8.9-14.5)			
CXCL8 MEDIAN	Decrease	24.3 (18.8-33.4)	1.34 (0.61-2.94, p=0.473)	1.49 (0.66-3.35, p=0.336)	11 (9.9-14.5)	1.20 (0.58-2.46, p=0.622)	1.34 (0.64-2.78, p=0.437)	
	Increase	18.4 (12.6-NA)			8.9 (7.6-NA)			
CXCL9 MEDIAN	Decrease	20.1 (16.4-39.7)	0.83 (0.40-1.72, p=0.616)	0.94 (0.42-2.08, p=0.875)	10.2 (9.8-NA)	0.65 (0.32-1.29, p=0.216)	0.69 (0.33-1.42, p=0.314)	
	Increase	23 (18.4-NA)			10.7 (7.8-16.6)			
CXCL10 MEDIAN	Decrease	24.3 (17.8-39.7)	1.01 (0.49-2.09, p=0.968)	0.94 (0.41-2.15, p=0.888)	9.8 (8.7-16.6)	0.77 (0.39-1.53, p=0.463)	0.79 (0.37-1.67, p=0.532)	
	Increase	19.7 (17.2-NA)			12.2 (10.7-24.4)			
CXCL11 MEDIAN	Decrease	23.1 (14.5-NA)	1.06 (0.51-2.21, p=0.867)	1.09 (0.51-2.33, p=0.820)	12.2 (9.9-20.4)	1.07 (0.54-2.10, p=0.855)	1.04 (0.51-2.15, p=0.906)	
	Increase	20 (17.2-NA)			9.8 (8.1-16.6)			
CXCL12 MEDIAN	Decrease	20.1 (17.2-29.4)	2.23 (0.89-5.58, p=0.086)	2.97 (1.02-8.68, p=0.047)	12 (9.3-NA)	0.76 (0.34-1.68, p=0.498)	0.61 (0.25-1.49, p=0.276)	
	Increase	32.9 (18.4-NA)			10.6 (8.7-14.5)			
CXCL13 MEDIAN	Decrease	23.1 (20-NA)	0.92 (0.45-1.90, p=0.829)	0.71 (0.29-1.71, p=0.442)	10.6 (9.3-14.5)	0.97 (0.50-1.90, p=0.940)	0.97 (0.45-2.07, p=0.933)	
	Increase	18.6 (17.2-NA)			10.7 (8.7-24.4)			
CXCL16 MEDIAN	Decrease	26.6 (14.5-NA)	0.88 (0.41-1.92, p=0.751)	0.68 (0.29-1.57, p=0.366)	10.6 (9.3-20.4)	1.59 (0.77-3.28, p=0.206)	1.30 (0.58-2.92, p=0.528)	
	Increase	19.7 (17.2-32.4)			10.8 (8.7-NA)			

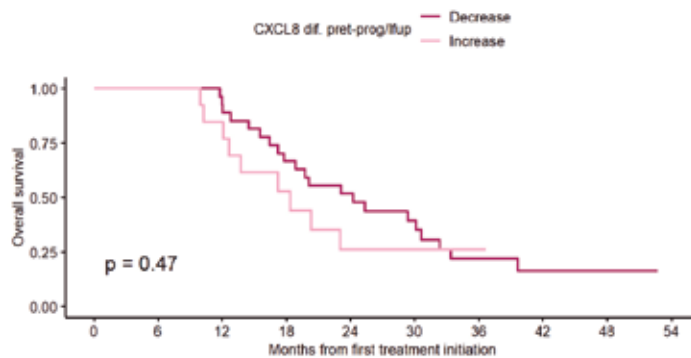
Dynamic changes of CXC chemokines and their association with OS and PFS. Median OS and PFS (in months; p values, HR, and 95% CI correspond to univariate (<sup>1</sup>) and multivariate (<sup>2</sup>) COX models. HR correspond to the increase category respect to decrease category (by default = 1). The variables: PS, radical surgery, age and sex were considered in the OS multivariate analysis; PS, age and sex in the PFS multivariate analysis. Statistically significant results (p < 0.05) are highlighted in bold.

### OVERALL SURVIVAL



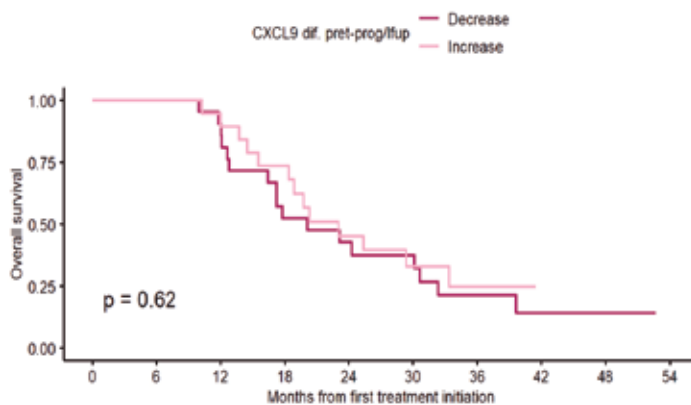


**ANNEX VIII:** CXC chemokines dynamic changes along PRET-PROG and EVAR-PROG association with survival



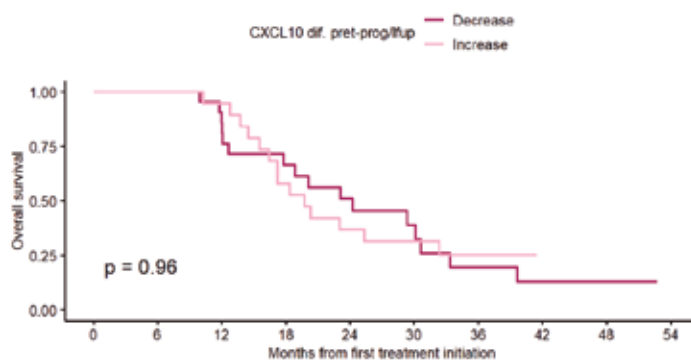
At risk (exitus)

28 (0)	28 (0)	25 (2)	18 (9)	13 (13)	9 (16)	5 (20)	1 (21)	1 (21)	0 (21)
13 (0)	13 (0)	11 (2)	6 (6)	3 (9)	3 (9)	1 (9)	0 (9)	0 (9)	0 (9)



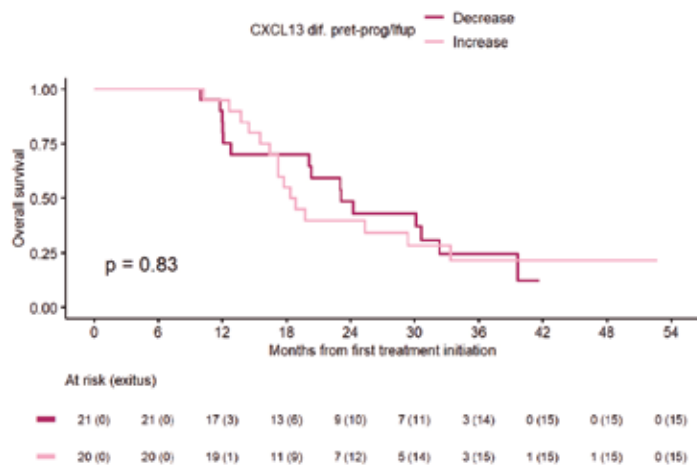
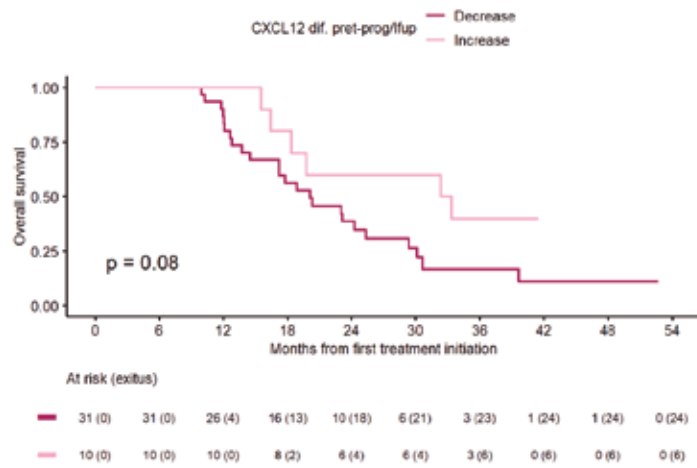
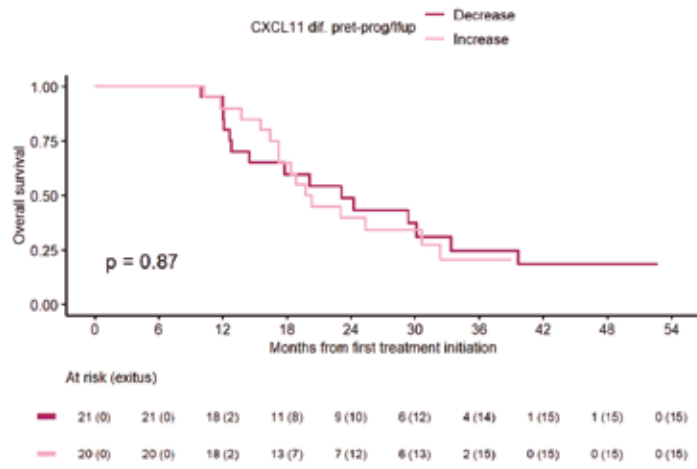
At risk (exitus)

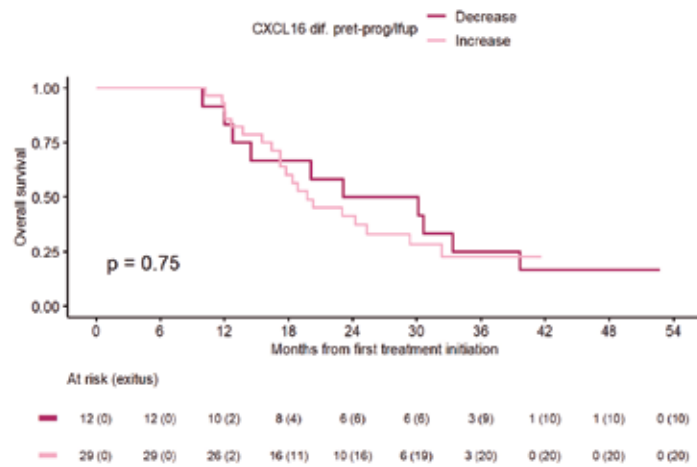
22 (0)	22 (0)	19 (2)	11 (10)	8 (12)	7 (13)	3 (16)	1 (17)	1 (17)	0 (17)
19 (0)	19 (0)	17 (2)	13 (5)	8 (10)	5 (12)	3 (13)	0 (13)	0 (13)	0 (13)



At risk (exitus)

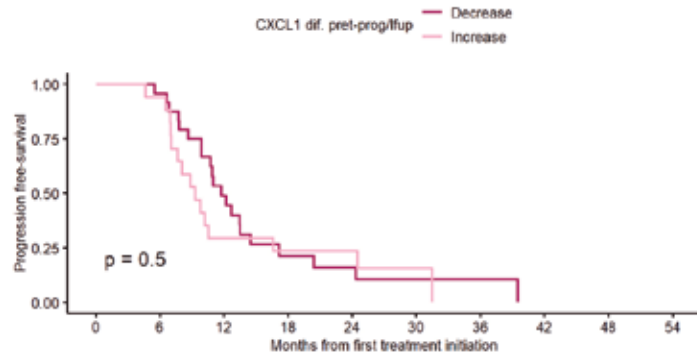
22 (0)	22 (0)	18 (3)	13 (7)	9 (10)	6 (12)	3 (15)	1 (16)	1 (16)	0 (16)
19 (0)	19 (0)	18 (1)	11 (8)	7 (12)	6 (13)	3 (14)	0 (14)	0 (14)	0 (14)





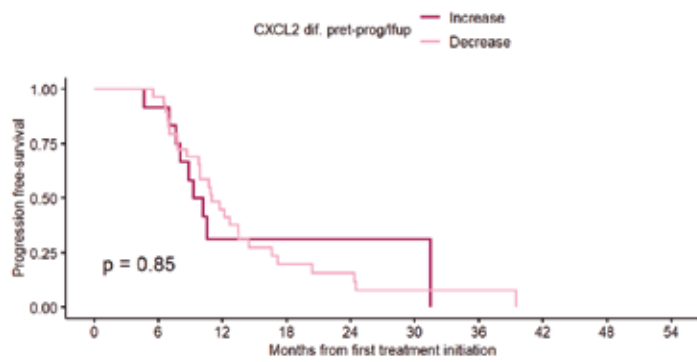
**Kaplan-Meier survival curves showing OS of patients split according to the dynamic changes of all eleven chemokines when comparing PRET-PROG time-points. P values shown correspond to univariate log-rank test.**

## PROGRESSION FREE SURVIVAL



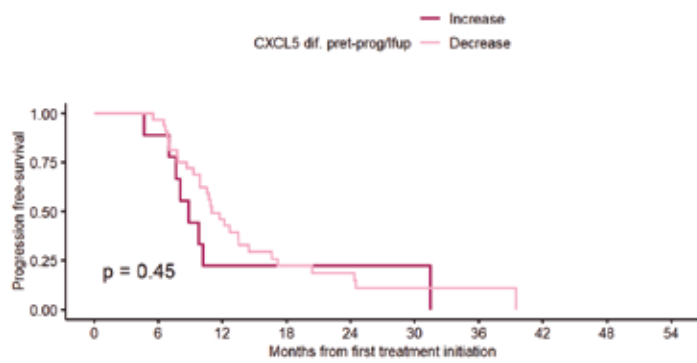
At risk (progressions/exitus)

—	24 (0)	23 (1)	11 (12)	4 (18)	3 (19)	1 (20)	1 (20)	0 (21)	0 (21)	0 (21)
—	17 (0)	16 (1)	6 (12)	4 (13)	3 (13)	2 (14)	0 (15)	0 (15)	0 (15)	0 (15)



At risk (progressions/exitus)

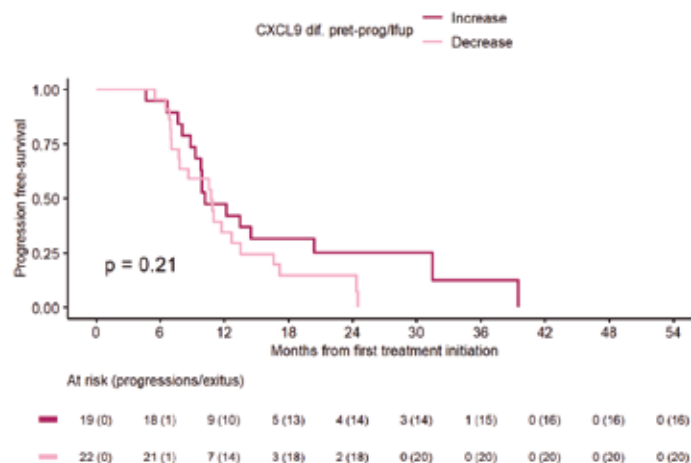
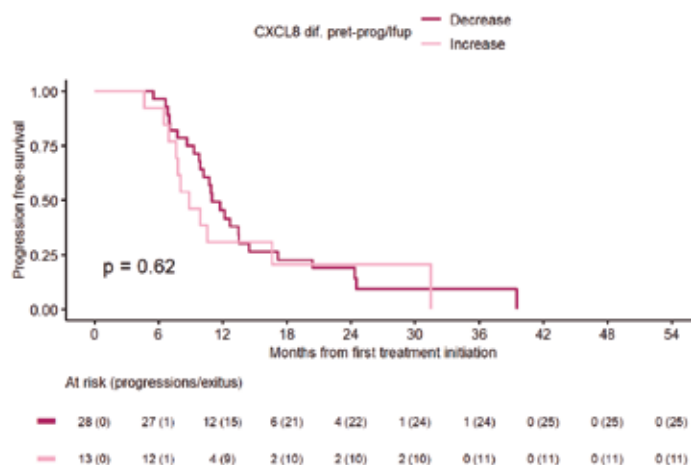
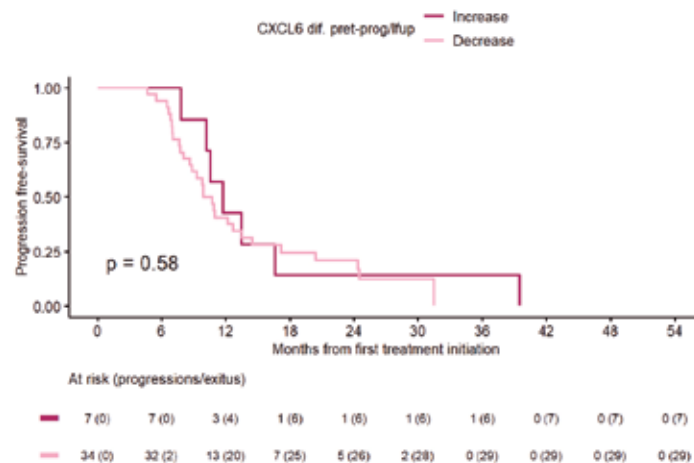
—	12 (0)	11 (1)	3 (8)	3 (8)	2 (8)	1 (8)	0 (9)	0 (9)	0 (9)	0 (9)
—	29 (0)	28 (1)	13 (16)	5 (23)	4 (24)	2 (26)	1 (26)	0 (27)	0 (27)	0 (27)

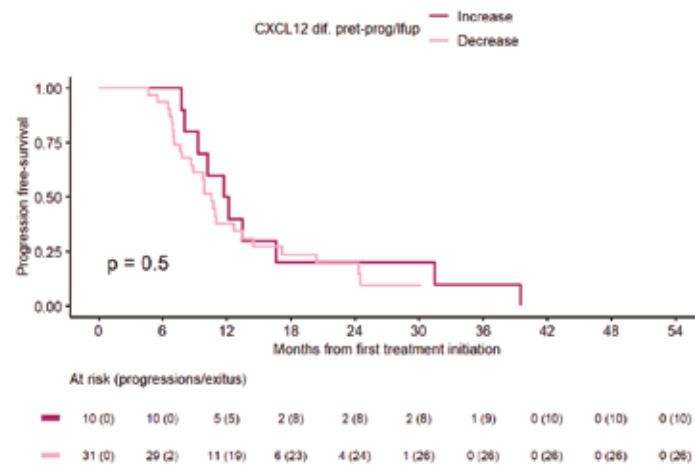
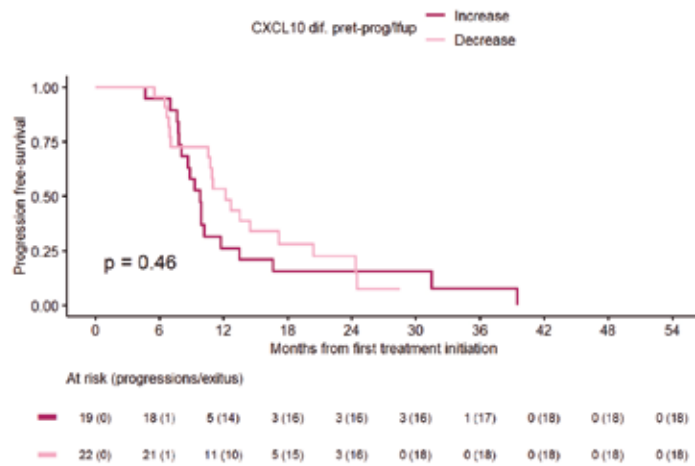
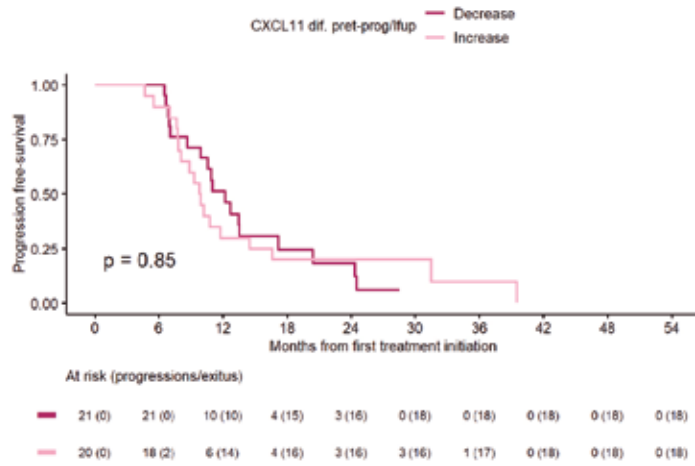


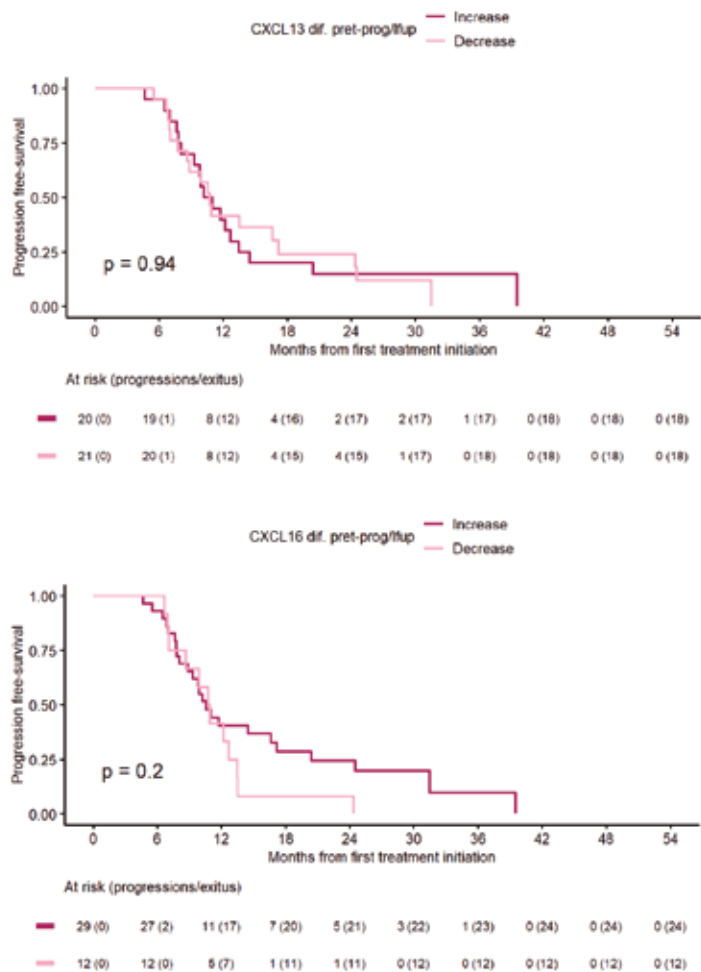
At risk (progressions/exitus)

—	9 (0)	8 (1)	2 (7)	2 (7)	1 (7)	1 (7)	0 (8)	0 (8)	0 (8)	0 (8)
—	32 (0)	31 (1)	14 (17)	6 (24)	5 (25)	2 (27)	1 (27)	0 (28)	0 (28)	0 (28)

**ANNEX VIII: CXCL chemokines dynamic changes along PRET-PROG and EVAR-PROG association with survival**







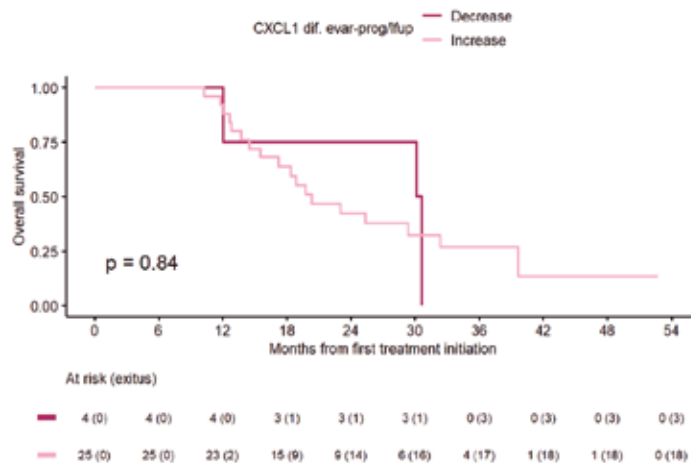
**Kaplan-Meier survival curves showing PFS of patients split according to the dynamic changes of all eleven chemokines when comparing PRET-PROG time-points. P values shown correspond to univariate log-rank test.**

EVAR-PROG dynamic changes association with risk of death and progression

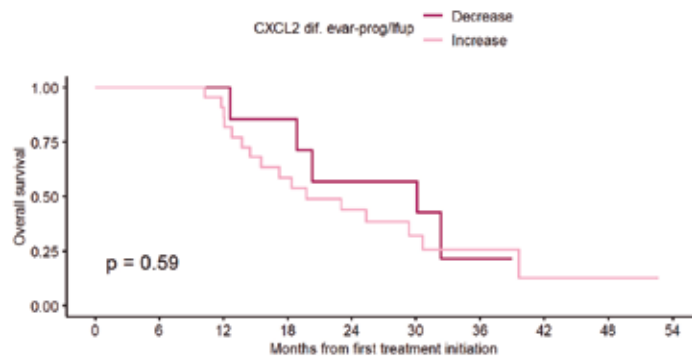
EVAR-PROG DYNAMIC CHANGES ASSOCIATION WITH RISK OF DEATH OR PROGRESSION. N = 29							
CHEMOKINES	DYNAMIC CHANGE	OVERALL SURVIVAL			PROGRESSION FREE SURVIVAL		
		MEDIAN (95% CI)	HR (95%CI, p value) <sup>1</sup>	HRa (95%CI, p value) <sup>2</sup>	MEDIAN (95% CI)	HR (95%CI, p value) <sup>1</sup>	HRa (95%CI, p value) <sup>2</sup>
CXCL1 MEDIAN	Decrease	30.4 (12-NA)	1.14 (0.33-3.95, p=0.841)	1.19 (0.32-4.40, p=0.796)	8.9 (6.8-NA)	1.73 (0.67-4.48, p=0.257)	2.81 (0.99-7.94, p=0.052)
	Increase	20.3 (17.2-NA)			9.9 (8.9-20.4)		
CXCL2 MEDIAN	Decrease	30.1 (18.8-8)	0.76 (0.27-2.10, p=0.592)	0.67 (0.23-1.99, p=0.471)	10 (8.9-20.4)	1.24 (0.52-2.97, p=0.628)	1.79 (0.69-4.63, p=0.230)
	Increase	19.7 (15.5-NA)			9.8 (7-NA)		
CXCL5 MEDIAN	Decrease	39.7 (30.1-NA)	0.37 (0.08-1.59, p=0.179)	0.37 (0.08-1.71, p=0.203)	9.9 (8.9-16.6)	1.81 (0.43-7.57, p=0.419)	1.41 (0.31-6.44, p=0.656)
	Increase	19.7 (17.2-32.4)			12.7 (7-NA)		
CXCL6 MEDIAN	Decrease	32.4 (20.3-NA)	0.45 (0.15-1.37, p=0.160)	0.36 (0.12-1.13, p=0.080)	9.9 (8.1-20.4)	1.33 (0.47-3.74, p=0.594)	1.24 (0.43-3.56, p=0.695)
	Increase	18.8 (14.5-NA)			11.3 (9.8-NA)		
CXCL8 MEDIAN	Decrease	39.7 (30.1-NA)	2.68 (0.62-11.62, p=0.189)	2.74 (0.59-12.68, p=0.198)	12.7 (7-NA)	1.45 (0.71-2.93, p=0.307)	1.44 (0.7-2.96, p=0.316)
	Increase	19.7 (17.2-32.4)			9.9 (8.9-16.6)		
CXCL9 MEDIAN	Decrease	23 (14.5-NA)	0.73 (0.29-1.85, p=0.514)	1.32 (0.61-2.86, p=0.478)	9.8 (8.1-20.4)	1.25 (0.66-2.34, p=0.494)	1.16 (0.58-2.30, p=0.672)
	Increase	20.3 (18.4-NA)			10.2 (8.7-NA)		
CXCL10 MEDIAN	Decrease	39.7 (15.5-NA)	1.74 (0.87-3.50, p=0.117)	1.67 (0.81-3.43, p=0.166)	9.8 (8.1-16.6)	1.52 (0.80-2.88, p=0.203)	1.74 (0.90-3.37, p=0.101)
	Increase	20 (17.2-32.4)			12.7 (8.9-NA)		
CXCL11 MEDIAN	Decrease	18.7 (12.6-NA)	0.64 (0.23-1.81, p=0.402)	0.48 (0.14-1.65, p=0.242)	9.4 (7.6-NA)	1.28 (0.47-3.47, p=0.624)	1.11 (0.38-3.44, p=0.811)
	Increase	25.3 (18.4-NA)			10.2 (8.7-20.4)		
CXCL12 MEDIAN	Decrease	23 (12.6-NA)	1.14 (0.44-2.97, p=0.792)	0.95 (0.33-2.75, p=0.922)	10 (8.7-NA)	1.03 (0.4-2.65, p=0.949)	0.96 (0.36-2.54, p=0.935)
	Increase	24.8 (17.2-NA)			9.8 (6.8-NA)		
CXCL13 MEDIAN	Decrease	29.4 (18.8-NA)	0.34 (0.17-0.67, p=0.002)	0.34 (0.16-0.69, p=0.003)	8.1 (7-NA)	0.34 (0.17-0.67, p=0.002)	0.34 (0.17-0.69, p=0.003)
	Increase	18.4 (14.5-NA)			13.6 (9.8-NA)		
CXCL16 MEDIAN	Decrease	23 (12.8-NA)	1.19 (0.61-2.32, p=0.603)	1.38 (0.70-2.73, p=0.350)	10 (9.3-20.4)	1.52 (0.80-2.80, p=0.205)	1.58 (0.81-3.10, p=0.181)
	Increase	20.3 (17.2-NA)			8.9 (8.7-NA)		

Dynamic changes of CXC chemokines and their association with OS and PFS. Median OS and PFS (in months; p values, HR, and 95% CI correspond to univariate (1) and multivariate (2) COX models. HR correspond to the increase category respect to decrease category (by default = 1). The variables: PS, radical surgery, age and sex were considered in the OS multivariate analysis; PS, age and sex in the PFS multivariate analysis. Statistically significant results (p < 0.05) are highlighted in bold.

OVERALL SURVIVAL

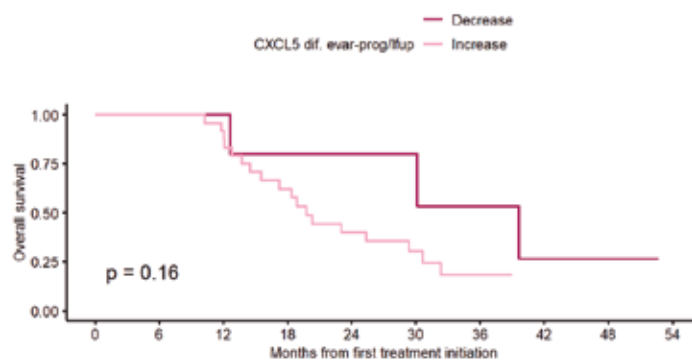


**ANNEX VIII:** CXCL chemokines dynamic changes along PRET-PROG and EVAR-PROG association with survival



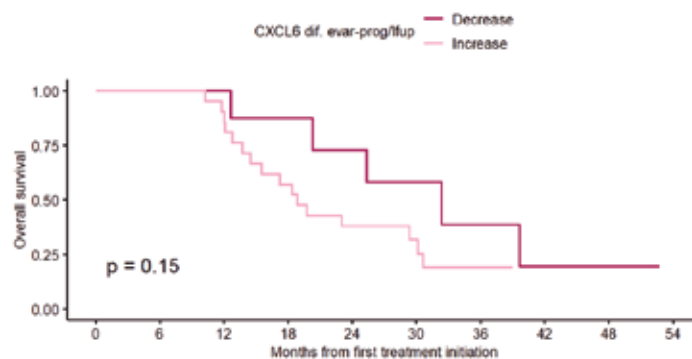
At risk (exitus)

7 (0)	7 (0)	7 (0)	6 (1)	4 (3)	4 (3)	1 (5)	0 (5)	0 (5)	0 (5)
22 (0)	22 (0)	20 (2)	12 (9)	9 (12)	6 (14)	3 (16)	1 (16)	1 (16)	0 (16)



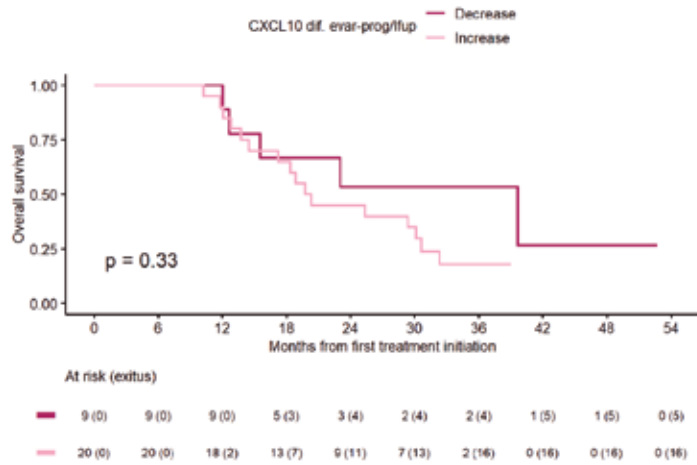
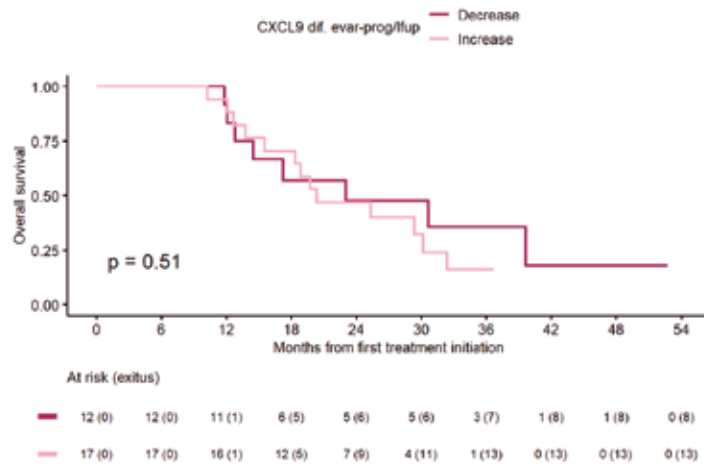
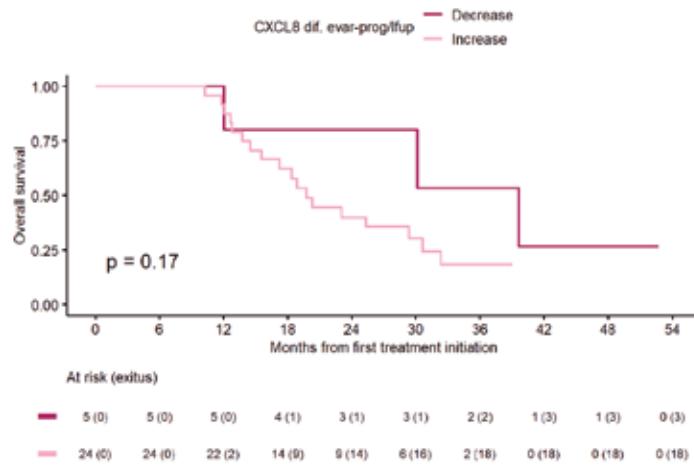
At risk (exitus)

5 (0)	5 (0)	5 (0)	4 (1)	3 (1)	3 (1)	2 (2)	1 (3)	1 (3)	0 (3)
24 (0)	24 (0)	22 (2)	14 (9)	9 (14)	6 (16)	2 (18)	0 (18)	0 (18)	0 (18)

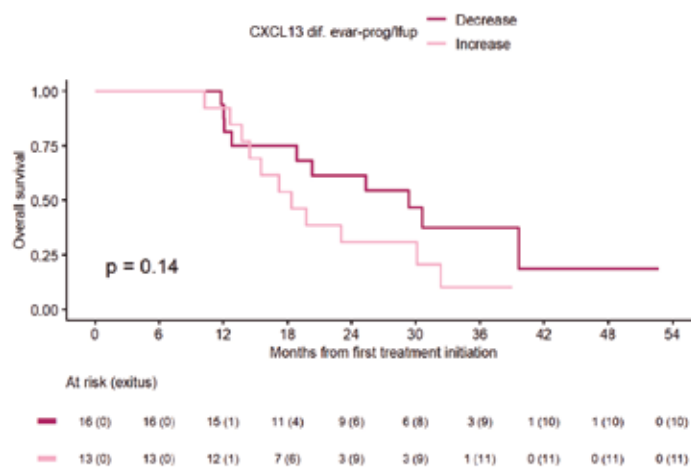
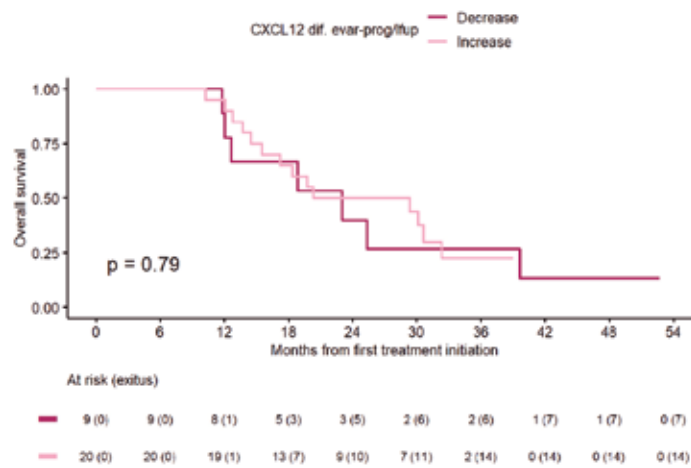
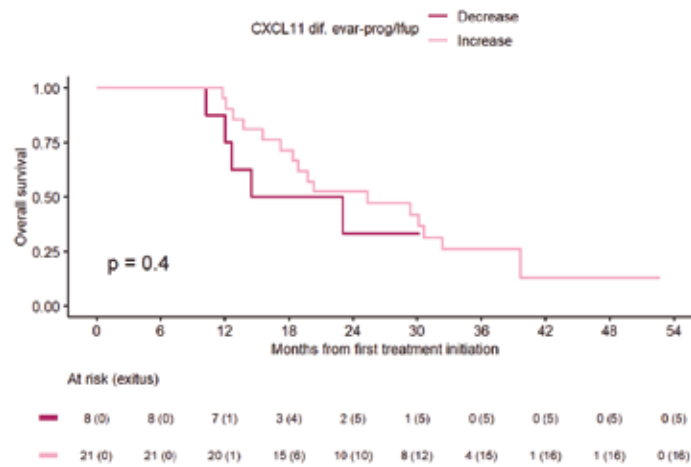


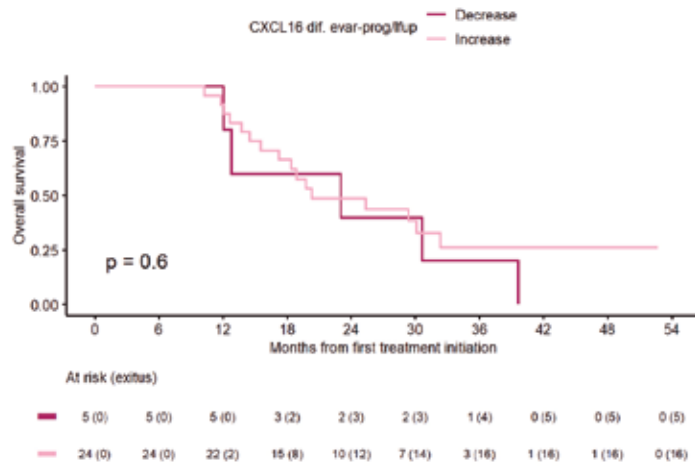
At risk (exitus)

8 (0)	8 (0)	8 (0)	6 (1)	5 (2)	4 (3)	2 (4)	1 (5)	1 (5)	0 (5)
21 (0)	21 (0)	19 (2)	12 (9)	7 (13)	5 (14)	2 (16)	0 (16)	0 (16)	0 (16)



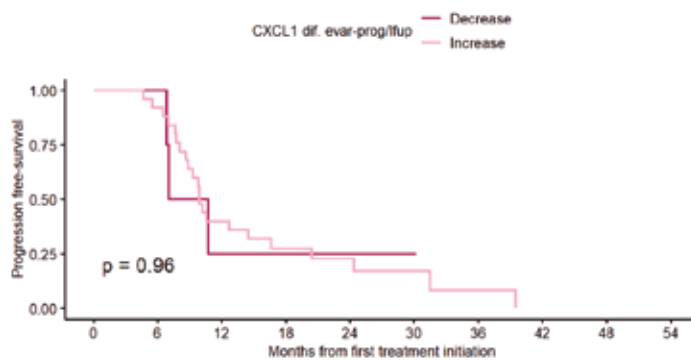
**ANNEX VIII:** CXCL chemokines dynamic changes along PRET-PROG and EVAR-PROG association with survival





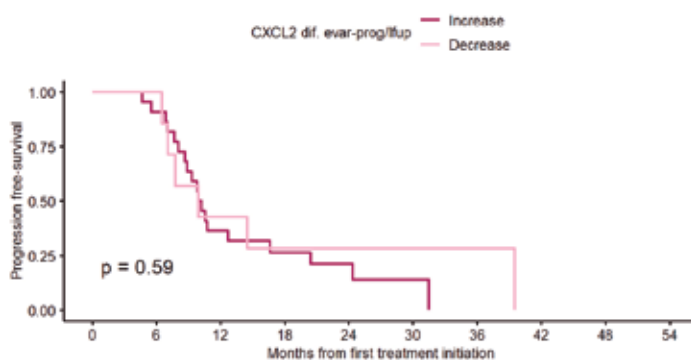
**Kaplan-Meier survival curves showing OS of patients split according to the dynamic changes of all eleven chemokines when comparing EVAR-PROG time-points. P values shown correspond to univariate log-rank test.**

**PROGRESSION FREE SURVIVAL**



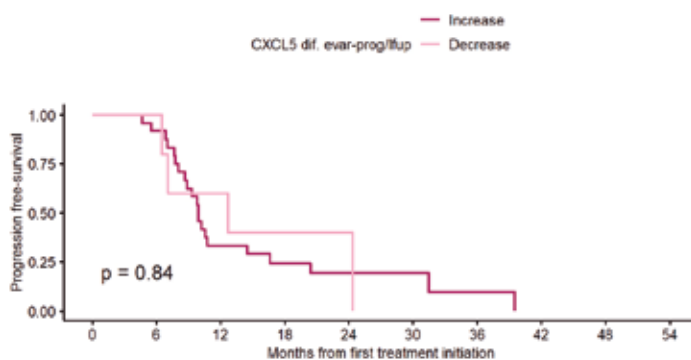
At risk (progressions/exitus)

Decrease	4 (0)	4 (0)	1 (3)	1 (3)	1 (3)	1 (3)	0 (3)	0 (3)	0 (3)	0 (3)
Increase	26 (0)	23 (2)	10 (15)	6 (18)	4 (19)	2 (20)	1 (21)	0 (22)	0 (22)	0 (22)



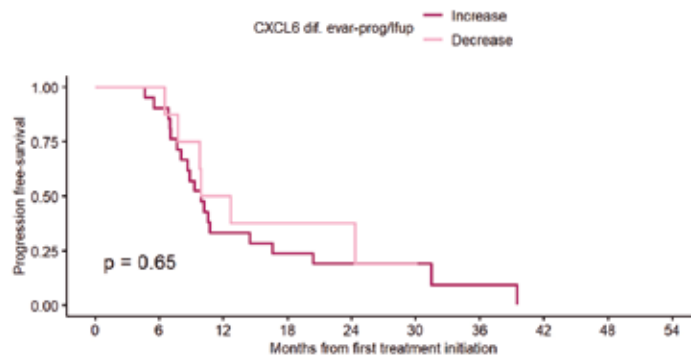
At risk (progressions/exitus)

Increase	22 (0)	20 (2)	8 (14)	5 (16)	3 (17)	1 (18)	0 (19)	0 (19)	0 (19)	0 (19)
Decrease	7 (0)	7 (0)	3 (4)	2 (5)	2 (5)	2 (5)	1 (5)	0 (6)	0 (6)	0 (6)



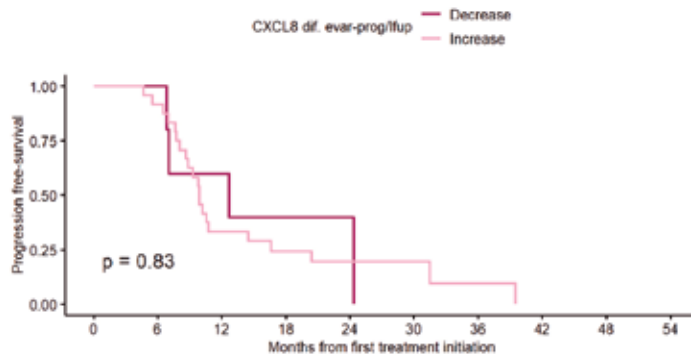
At risk (progressions/exitus)

Increase	24 (0)	22 (2)	8 (16)	5 (18)	4 (19)	3 (19)	1 (20)	0 (21)	0 (21)	0 (21)
Decrease	5 (0)	5 (0)	3 (2)	2 (3)	1 (3)	0 (4)	0 (4)	0 (4)	0 (4)	0 (4)



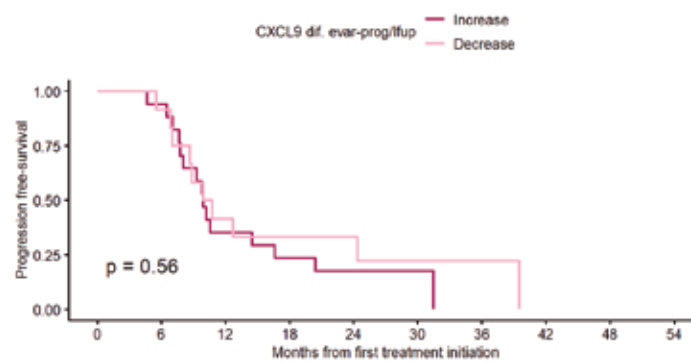
At risk (progressions/exitus)

21 (0)	19 (2)	7 (14)	5 (16)	3 (17)	2 (17)	1 (18)	0 (19)	0 (19)	0 (19)
8 (0)	8 (0)	4 (4)	2 (5)	2 (5)	1 (6)	0 (6)	0 (6)	0 (6)	0 (6)



At risk (progressions/exitus)

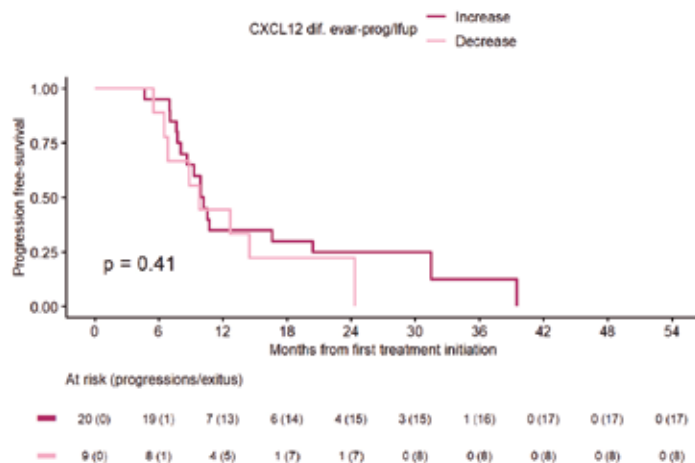
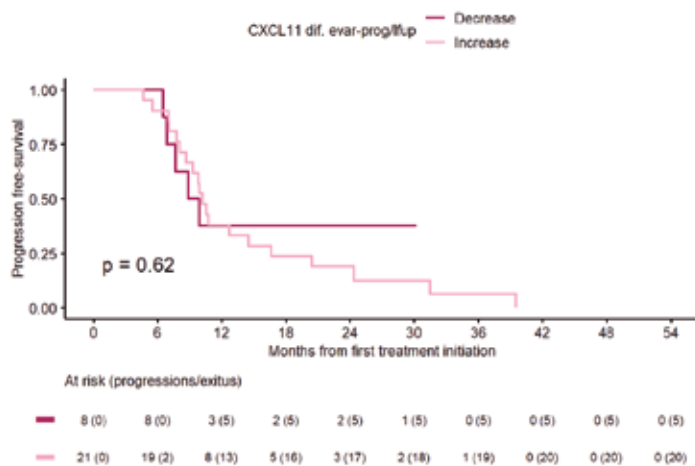
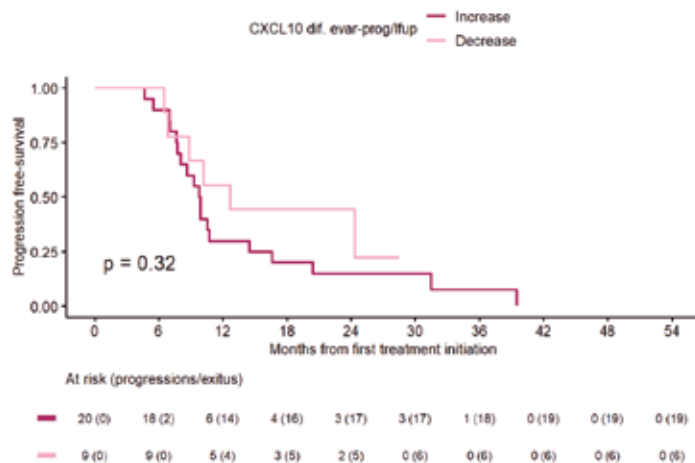
5 (0)	5 (0)	3 (2)	2 (3)	1 (3)	0 (4)	0 (4)	0 (4)	0 (4)	0 (4)
24 (0)	22 (2)	8 (16)	5 (18)	4 (19)	3 (19)	1 (20)	0 (21)	0 (21)	0 (21)

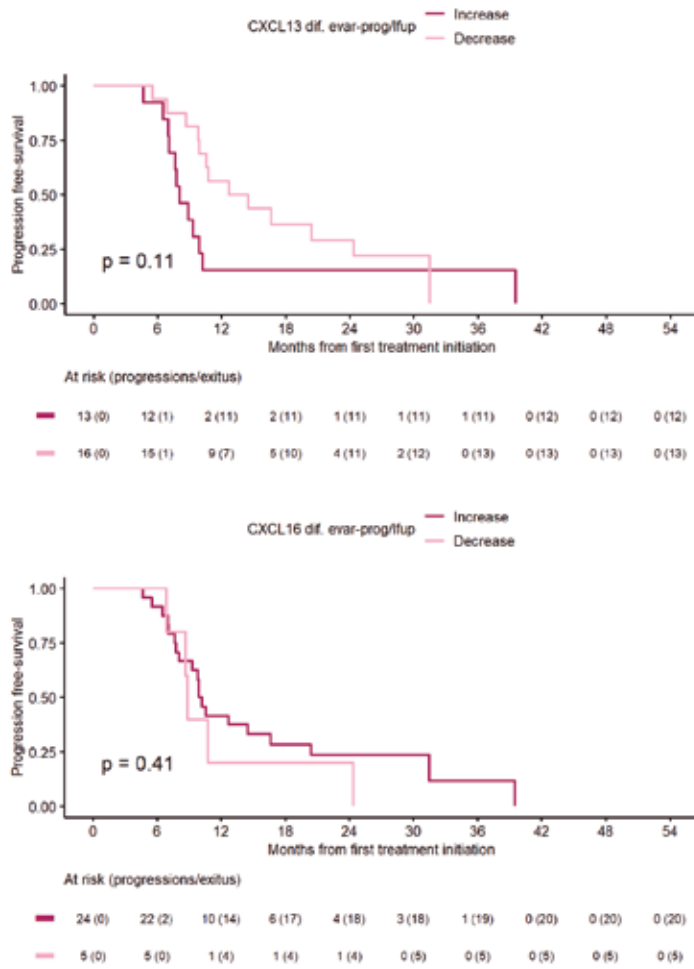


At risk (progressions/exitus)

17 (0)	16 (1)	6 (11)	4 (13)	2 (14)	1 (14)	0 (15)	0 (15)	0 (15)	0 (15)
12 (0)	11 (1)	5 (7)	3 (8)	3 (8)	2 (9)	1 (9)	0 (10)	0 (10)	0 (10)

**ANNEX VIII: CXCL chemokines dynamic changes along PRET-PROG and EVAR-PROG association with survival**





**Kaplan-Meier survival curves showing PFS of patients split according to the dynamic changes of all eleven chemokines when comparing EVAR-PROG time-points. P values shown correspond to univariate log-rank test.**



